Vol. 8 No. 2 2023
ISSN:1390-9347

Bionatura

Ibero American journal of Biotechnology and Life Sciences

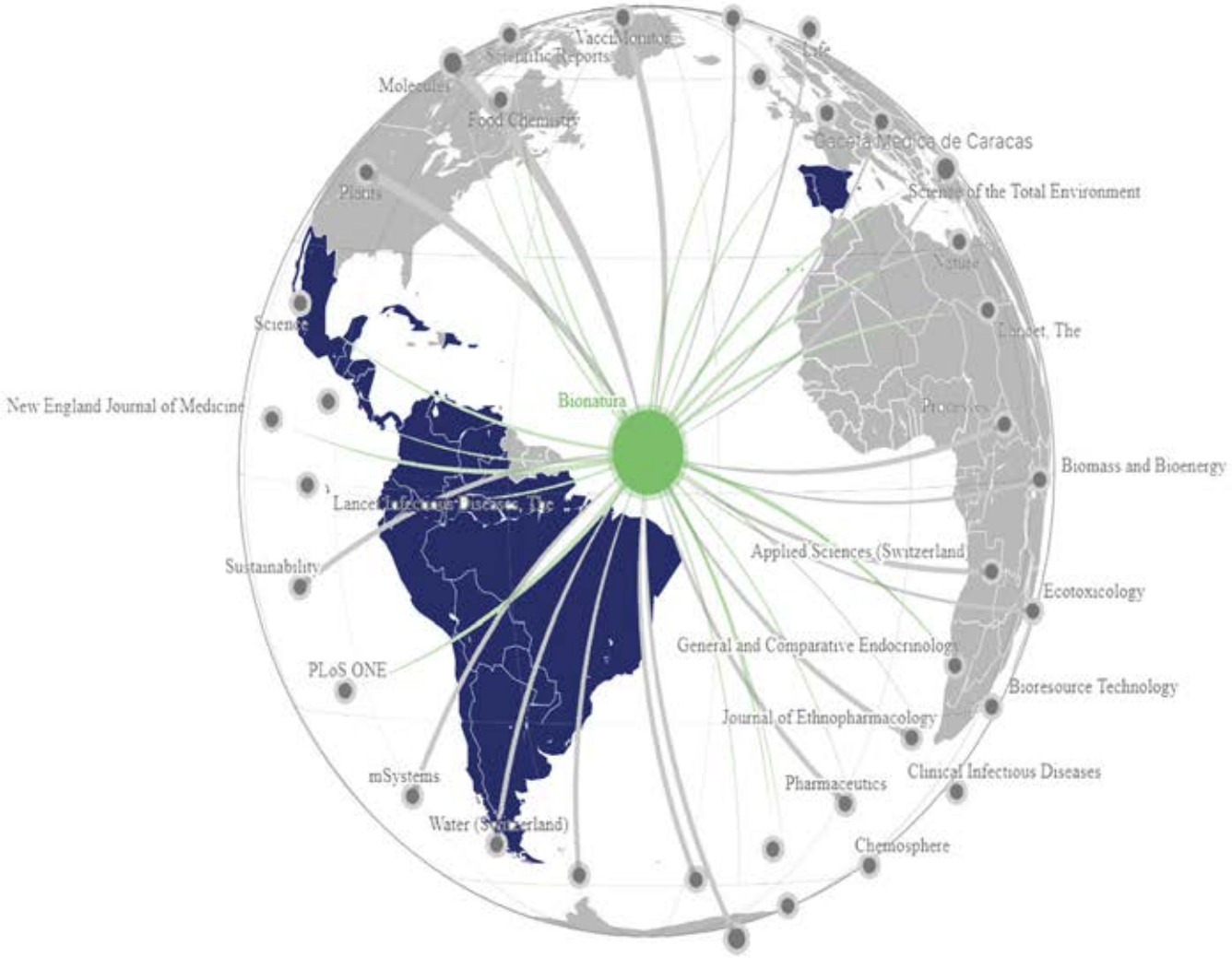

Bionatura journal, published since 2023 from Madrid, Spain., by its partners Clinical Biotec, Universidad Catolica del Oriente (UCO) and Universidad Nacional Autonoma de Honduras (UNAH) .

SJR SCOPUS SCImago Journal Rank

International journals citing Bionatura according to Scimago 2023.

Scopus Publons

UCO Universidad Católica de Oriente

UNAH UNIVERSIDAD NACIONAL AUTÓNOMA DE HONDURAS

clinicalbiotec.com

Es el momento de los que se atreven a soñar y luchan por alcanzar sus metas.

En la UCO te acompañamos

UCO
Universidad Católica de Oriente
Acreditación Institucional en
ALTA CALIDAD

Vigilada Mineducación

Pregrados

Tecnología en Operaciones Financieras
SNIES 104841 Registro Calificado - Res. 12903 del 21-09-2015 M.E.N.
95 créditos - A distancia tradicional - Rionegro Ant.

Contaduría Pública
SNIES 13018 Registro Calificado - Res. 9256 del 07- 05- 2018
Acreditación de Alta Calidad 4610 del 21- 03 - 2018 M.E.N.
166 créditos Presencial - Rionegro

Comercio Exterior
SNIES 1854 Registro Calificado - Res.14314 del 11-12-2019 M.E.N.
159 créditos - Presencial - Rionegro Ant.

Administración de Empresas
SNIES 55096 Registro Calificado - Res. 7656 del 18-04-2017 M.E.N.
152 créditos - Presencial - Rionegro Ant.

Tecnología Agropecuaria
SNIES 1850 Registro Calificado - Res. 8684 del 10-07-2013 M.E.N.
113 créditos - Presencial - Rionegro Ant.

Agronomía
SNIES 4443 Registro Calificado - Res. 8087 del 17-05-2018
Acreditación de Alta Calidad Nº 29149 del 26-12-2017
157 créditos - Presencial - Rionegro Ant.

Zootecnia
SNIES 53037 Registro Calificado - Res. 14466 del 04-09-2014 M.E.N.
156 créditos - Presencial - Rionegro Ant.

Psicología
SNIES 8662 Registro Calificado - Res. 8902 del 31-07-2013 M.E.N.
Acreditación de Alta Calidad Nº 17227 del 24 - 10 - 2018
175 créditos - Presencial - Rionegro Ant.

Comunicación Social
SNIES 53045 Registro Calificado - Res. 14892 del 11-09-2014 M.E.N.
146 créditos - Presencial - Rionegro Ant.

Trabajo Social
SNIES 106586 Registro Calificado - Res. 26741 del 29-11-2017 M.E.N.
141 créditos - Presencial - Rionegro Ant.

Derecho
SNIES 53539 Registro Calificado - Res. 10542 del 14-07-2015 M.E.N.
166 créditos - Presencial - Rionegro Ant.

Nutrición y Dietética
SNIES 104601 Registro Calificado - Res. 7823 del 01-06-2015 M.E.N
166 créditos - Presencial - Rionegro Ant.

Gerontología
SNIES 1853 Registro Calificado - Res. 14839 del 22-10-2013 M.E.N.
138 créditos - A distancia con apoyo virtual - Rionegro Ant.

Enfermería
SNIES 91027 Registro Calificado- Res. 12600 del 03-08-2018 M.E.N.
166 créditos - Presencial - Rionegro Ant.

Licenciatura en Filosofía
SNIES 106542 Registro Calificado - Res. 22108 del 24 - 10 - 2017 M.E.N.
164 créditos - Presencial - Rionegro Ant.

Licenciatura en Lenguas Extranjeras con énfasis en Inglés
SNIES 106947 Registro Calificado - Res. 25629 del 29-12-2017 M.E.N.
164 créditos - Presencial - Rionegro Ant.

Licenciatura en Educación Física, Recreación y Deportes
SNIES 106436 Registro Calificado - Res. 17481 del 31-08-2017 M.E.N.
164 créditos - Presencial - Rionegro Ant.

Licenciatura en Educación para la Primera Infancia
SNIES 105359 Registro Calificado - Res. 03948 del 16-03-2016 M.E.N.
164 créditos - Presencial - Rionegro Ant.

Licenciatura en Ciencias Naturales
SNIES 105898 Registro Calificado - Res.19869 del 18-10-2016 M.E.N.
164 créditos - Presencial - Rionegro Ant.

Licenciatura en Educación Religiosa
SNIES 106705 Registro Calificado - Res. 2084 del 13 - 02 - 2018 M.E.N.
164 créditos - Presencial - Rionegro Ant.

Técnico Profesional en Programación Web
SNIES 103704 Registro Calificado - Res.14454 del 04-09-2014 M.E.N.
67 créditos - Presencial - Rionegro Ant.

Ingeniería Ambiental
SNIES 4361 Registro Calificado - Res. 3654 del 02-03-2018 M.E.N.
Acreditación de Alta Calidad No. 6543 del 18 - 04 - 2018
173 créditos - Presencial - Rionegro Ant.

Ingeniería de Sistemas
SNIES 1855 Registro Calificado - Res. 0178 del 05-01-2019 M.E.N.
164 créditos - Presencial- Rionegro Ant.

Ingeniería Industrial
SNIES 1856 Registro Calificado - Res. 1293 del 04-02-2019 M.E.N.
160 créditos - Presencial- Rionegro Ant.

Ingeniería Electrónica
SNIES 20271 Registro Calificado - Res. 24646 del 14-11-2017 M.E.N.
178 créditos - Presencial- Rionegro Ant.

Teología
SNIES 103450 Registro Calificado - Res. 10638 del 09-07-2014 M.E.N.
130 créditos - A distancia - Rionegro Ant.

¡HAGAMOS QUE PASE!

www.uco.edu.co @uconiano universidad catolica de oriente 322 569 90 90

UNAH RANKING MUNDIAL 2023

RANKING MUNDIAL SCIMAGO UNAH 2022

SOMOS UNA MACROUNIVERSIDAD

RECTORA DEL NIVEL DE EDUCACIÓN SUPERIOR EN HONDURAS

APROXIMADAMENTE:

100,000 Estudiantes
4,000 Docentes
10 Facultades
9 Centros regionales

DICIHT
DIRECCIÓN DE INVESTIGACIÓN CIENTÍFICA, HUMANÍSTICA Y TECNOLÓGICA

UNAH
UNIVERSIDAD NACIONAL AUTÓNOMA DE HONDURAS

ARTICLE / INVESTIGACIÓN

Development of a novel microdevice for sorptive extraction under a green analytical chemistry approach: Application for bioanalytical determination of Ibuprofen

Jessica P. Riera-Williams and H.D. Ponce-Rodríguez*
DOI. 10.21931/RB/2023.08.02.1
Departamento de Control Químico, Facultad de Ciencias Químicas y Farmacia, Universidad Nacional Autónoma de Honduras, Ciudad Universitaria, Tegucigalpa, Honduras.
Corresponding author: henry.ponce@unah.edu.hn

Abstract: This study proposes a novel device called micro polymeric magnetized bar adsorptive extraction (µ-PMBAE), as an extraction and enrichment technique for trace analysis in aqueous samples. These micro-bar absorbent devices were prepared using easily accessible and low-cost materials, incorporating different sorbent materials into a polymer and introducing a small piece of neodymium magnet. Several stability tests were applied to determine their robustness, stability, and weight variation; finally, ibuprofen concentration in urine samples was determined, demonstrating the applicability of extraction devices under a green analytical chemistry approach. The µ-PMBAE showed remarkable advantages since different sorbents can be added to the hot melt glue. This tunes the interaction with the analytes to become more specific in the extraction. Likewise, the magnetic ability makes it possible to carry out extraction without using an extra stir bar, matching its performance with the traditional commercially based on polydimethylsiloxane phase. The proposed analytical method demonstrated excellent performance concerning high recovery percentages, adequate coefficients of variation, and low detection limits.

Key words: Bioanalytics, sample preparation, HPLC, µ-PMBAE, green analytical chemistry.

Introduction

In the last three decades, sample treatment techniques have shown an advance in the green chemistry point of view, searching for new methodologies friendly to the environment, with less waste, toxic solvent volumes, energy consumption and timeless development[1]. The current approach for sample treatment techniques aims to increase the analysis's selectivity and sensitivity, extract, purify, concentrate and/or derivatize the analytes without using laborious and tedious procedures, with a high economic and time cost such a case of conventional extraction techniques[2].

An influential group of microextraction techniques is those that use the mechanism of sorption of the analytes in a solid, which may include absorption (also known as a partition) and adsorption, within which Solid-phase microextraction (SPME) and Stir bar sorptive extraction (SBSE) is found. SBSE, introduced by Pat Sandra in 1999, and marketed under the name of "Twister®" (GERSTEL-GmbH & Co. KG), emerged under the idea of overcoming some of the disadvantages of SPME, including the recovery of analytes with ranges of medium-high volatility present in liquid phase samples[3]. Likewise, SBSE improves the limited recovery that can be achieved in ultra-trace analysis with SPME, especially in unfavorable phase relationships when working with small volumes of sorptive material, usually, polydimethylsiloxane (PDMS), which covers molten silica fiber[4].

In SBSE, stirring bars coated with PDMS is used, with a length of 10 and 40 mm covered with 55 and 219 µL of PDMS, respectively. The stir bars are placed in contact with the liquid sample with stirring times until the analytes are extracted[5]. Subsequently, in the desorption stage, the analytes are released from the bar, either by a thermal desorption mechanism mainly for gas chromatography or liquid desorption for liquid chromatography. In both stages, variables such as solution volume, speed and stirring time, pH, ionic strength, type, and amount of desorption solvent should be optimized[6].

Nowadays, the application of the SBSE has had fundamental advances in using different coating materials, which has achieved the application of the technique for analytes of different polarities[7]. Gorji et al. developed a monolithic auto-magnetic nanocomposite (SMNM) kit, which proved helpful for determining Bisphenol A in liquid samples[8]. Other authors have evaluated polydimethylsiloxane-phenyl siloxane as a coating material for extracting antibiotic compounds in aqueous samples[9]. Along the same lines, W. Fan and collaborators demonstrated the use of coating the bars with an ionic liquid incorporated through the sol-gel route to study naproxen, ketoprofen, and fenbufen in water samples[10].

Despite the problems involved in the study of biological samples, where the analytes are at low levels of concentration with the presence of many impurities, which can influence the determination of analytes, the use of SBSE has demonstrated its application in this field. In that sense, using a monolithic acrylate polymer was satisfactory for determining angiotensin II antagonist receptors in human plasma[11]. Likewise, determining fluoxetine in plasma using

Citation: Riera-Williams J P, Ponce-Rodríguez H D. Development of a novel microdevice for sorptive extraction under a green analytical chemistry approach: Application for bioanalytical determination of Ibuprofe. Revis Bionatura 2023;8 (2) 1. http://dx.doi.org/10.21931/RB/2023.08.02.1
Received: 10 February 2023 / **Accepted:** 15 May 2023 / **Published:** 15 June 2023
Publisher's Note: Bionatura stays neutral with regard to jurisdictional claims in published maps and institutional affiliations.

a homemade bar by Marques *et al.*[12]. Other works have determined several compounds in urine samples, including fluorouracil and phenobarbital[13] and amphetamines[14].

Due to the great popularity of the technique, new devices have been developed following the principle of the SBSE. In 2009 J.M.F. Nogueira and his group introduced the use of an analytical device called bar adsorptive µ-extraction (BAµE), for which hollow cylindrical tubes of polyethylene (15 mm in length and 3 mm in diameter) are coated with adhesive films. Then solids Sorbents are adhered to by manual agitation[15,16]. Likewise, Liu and collaborators developed a device covering a coal pencil mine with a layer of poly luminol by electrochemical polymerization. This obtained good results in extracting residues of β-agonists in pork[17]. Recently, a tube of polyether ether-ketone treated with sulfuric acid and on whose surface polydopamine and p-naphthol benzene molecules were immobilized was used to determine dye contaminants in environmental samples[18].

On the other hand, eight bisphenol compounds were determined by applying a novel cage shell device manufactured in 3D printing consisting of two pieces locked together by a magnetic stirring rod. The authors use nanofibers as adsorbent material[19]. A new extraction mode that combines the principles of SBSE and DSPE, called stir bar sorptive-dispersive microextraction (SBSDE), was proposed by Benede et al. In the procedure, magnetic nanoparticles were physically loaded on the magnetic stir bar to extract UV absorbent in seawater samples[20]. In recent years, new trends in SBSE include advances in developing new adsorbent materials, structural changes, and developments in technical automation[21].

In the present work, we have developed a device called "micro polymeric magnetized bar adsorptive extraction (µ-PMBAE)"[22], using easy and accessible materials such as hot melt glue, commonly called "termocola", which is composed of polymeric mixtures, with the characteristic of melting at temperatures above 80 °C. It returns to its solid state at room temperature. This property allows mixing the hot melt glue with sorbents usually used for the extraction of analytes, and subsequently, said mixture can be molded of desired size and shape to obtain the adsorptive microbars. Finally, during the elaboration of the device, a neodymium magnet is incorporated into it.

To demonstrate the applicability of the developed devices, it was proposed to determine Ibuprofen as a representative molecule in urine samples. Different sorption parameters were optimized, including stirring time, solution pH, volume, and ionic strength. In the liquid desorption, the sonication time, elution solvent, and volume were evaluated to obtain the most excellent recovery of the analyte. As far as the authors know, this work is the first to develop SBSE devices with the proposed materials, which demonstrate advantages in terms of cost, applicability, easy preparation, and versatility.

Materials and methods

Reagents and Materials

Acetonitrile and methanol HPLC grade, ethyl acetate and hexane pesticide grade, sodium chloride, and sodium hydroxide all of them were obtained from JT BAKER (Center Valley, PA) instead of formic acid, glacial acetic acid, hydrochloric acid, activated charcoal and silica from Merck (Darmstadt, Germany). C18, strong cation exchange (SCX) and weak exchange cationic resin (WCX) sorbents of Agilent (Santa Clara, CA). Ibuprofen standard from Sigma-Aldrich (St. Louis, MO) was used. Ultrasonic baths from Branson (Sterling Heights, MI), vortex mixer from Kool Lab Kyrios-Soter Scientific (Miami, FL), and centrifuge from LW Scientific (Lawrenceville, GA) were used. Stir plate and ultra-pure water obtained with Barnstead micro-pure st from Thermo Scientific (Waltham, MA). For pH measurement, a pH meter from Hanna Instruments HI 9829 (Woonsocket, RI) and a convection oven from Quincy Lab (Chicago, IL) were used for heating in the preparation of the microbars. Hot melt glue sticks and wooden molds were obtained at a local store.

Experimental settings

Preparation of polymeric bars

For the preparation of the devices, the following procedure was performed. An amount of hot melt glue, consisting mainly of ethylene-vinyl acetate copolymer, was melted in a water bath. Subsequently, the sorbent and a few milliliters (≈ 2 mL) of methanol were added to ensure a homogeneous mixture. Then the mixture was subjected to manual stirring, and once the methanol evaporated, the mixture was removed and placed in a wooden mold. It is placed in the oven at 100 °C for 5 minutes. Subsequently, the neodymium magnet is incorporated into the molds and compacted to obtain the desired cylindrical shape. Finally, the molds are removed from the oven, and once they are cooled to room temperature, the formed bars are obtained, which are cut to the desired size (Figure 1. A).

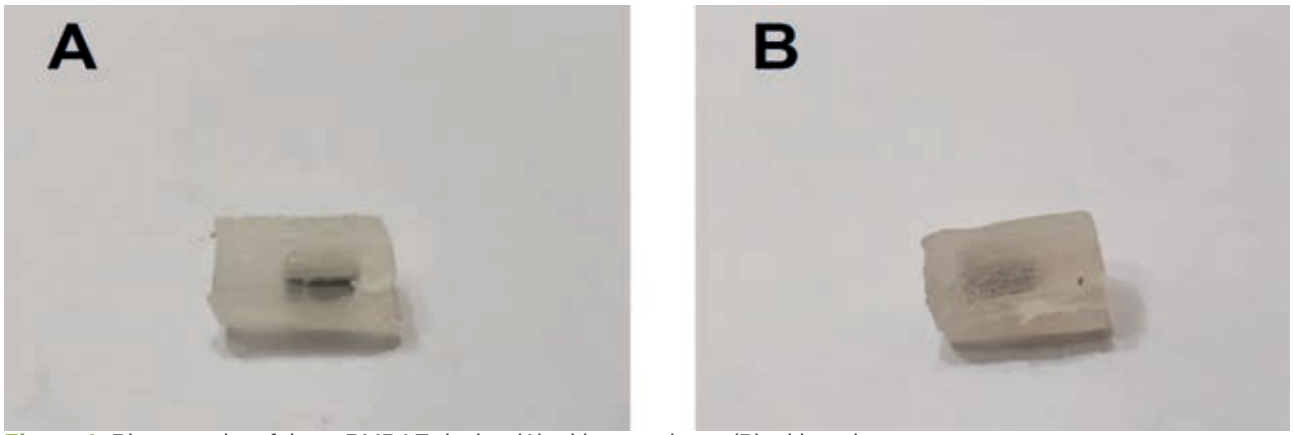

Figure 1. Photography of the µ-PMBAE device (A) without sorbent; (B) with sorbent.

Stability and robustness studies

Once the polymeric microbars were prepared, their robustness, stability, and weight variation were evaluated, for which tests were carried out with different solvents, pH values, temperature, sonication process, and sorbent losses as a function of time. Devices prepared with other sorbents were immersed in HPLC vials containing solvents of broad polarity, including hexane, ethyl acetate, acetonitrile, methanol, and aqueous solutions of formic acid and acetic acid, both at 1 %. The microbars were left in the solvents for 48 hours at room conditions. Likewise, to evaluate the effect of pH on the devices, these were immersed in solutions of 1N hydrochloric acid (pH ≈ 2) and 1 N sodium hydroxide (pH ≈10) and left standing at ambient conditions for 48 hours.

The stability depending on the temperature and sonication process was carried out by placing the micro bars in HPLC vials with ultra-pure water and subjecting sonication with varying times of 30, 60, 90, and 120 minutes, measuring the temperature at each of these times. Finally, the devices were weighed immediately after elaboration for the weight variation test, and the average value, standard deviation, and coefficient of variation were obtained. After thirty days, they were again weighed, and different statistical tests were applied to assess their suitability.

Extraction procedure

Once the parameters of the adsorption and desorption processes, including the agitation time, modifier, ionic strength, type and solvent amount of desorption, and sonication time, were optimized until the optimal recovery conditions, the extraction of urine samples was carried out as follows. 2 mL of urine sample was diluted to 20 mL with ultrapure water in a 25 mL glass flask, then the µ-PMBAE was added. The solution was acidified with a 0.1 % (v/v) formic acid solution, and 600 µL of a 25 % (w/v) sodium chloride solution was added. Then the flask was placed under stirring for 2 hours at room condition. After this time, the device was removed, avoiding contamination, and placed in an HPLC vial, and 1 mL of methanol was added and placed in an ultrasonic bath for 60 minutes. Finally, µ-PMBAE is removed, and an amount of the solution is chromatographed by duplicate. Figure 2 shows the optimized microextraction procedure using the µ-PMBE developed in this work.

Chromatographic conditions

The chromatographic separation was carried out on a Shimadzu Prominence liquid chromatograph, consisting of an LC20-AT pump, CMB-20Alite control system, SIL-20A automatic injector, CTO-A20 column oven, and SPD-M20A detector. The EZ Start software was used to collect all the data obtained. A Thermo scientific Hypersill, C8 column (150 x 4.6 mm, 5 µm) was used. In isocratic mode, the mobile phase was a mixture of acidified water with formic acid (pH = 3) and acetonitrile (70:30). The flow of the mobile phase was 1.5 mL/min and injection volume of 5 µL for standard solutions and samples. The DAD was controlled at 220nm. The analyte identification was performed through retention times and comparing the absorption spectrum obtained from the standard.

Results

Preparation of µ-PMBAE devices

The initial objective was to design and build stir bar extraction devices that were made with simple, cheap, and easily accessible materials and that functionally show similarities and, if possible, some advantages with the "Twister" stir bar device, as well as devices recently reported in the literature. The first issue to be defined as the support to which to incorporate the sorbent solid, which could adhere to the sorbent by itself and an excellent malleability to take the desired cylindrical shape and size. The hot melt glue, commonly referred to as "termocola or silicone glue," is used to adhere various materials; it is easily accessible and has been widely used, and has the characteristic of melting at temperatures above 80 °C, returning to a solid state at room temperature. This glue contains mixtures of polymers, mainly the elastomeric copolymer ethylene vinyl acetate (CAS: 24937-78-81), which has also been used as a drug carrier for 3D printed medical devices of indomethacin due his properties of melting index and flexural[23].

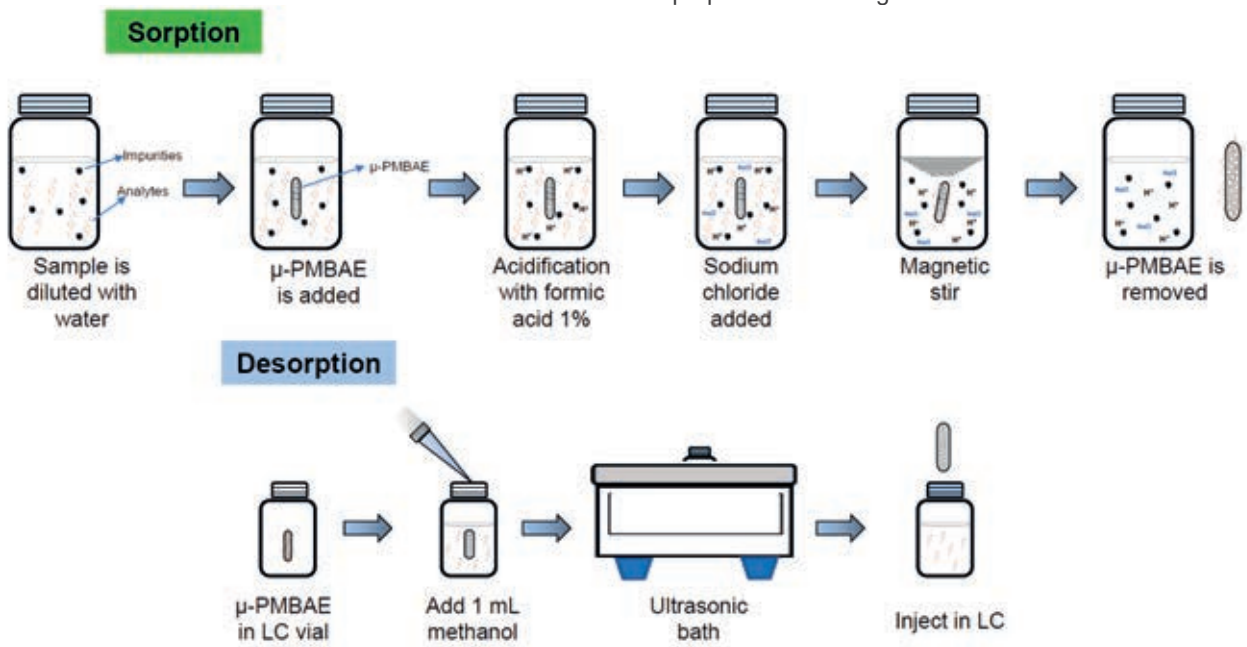

Figure 2. Optimized microextraction procedure using the µ-PMBE to determine Ibuprofen in urine samples.

These characteristics make it an ideal support to incorporate solids on its surface. In the initial tests, modified silica (C18) was integrated, evaluating different percentages of the sorbent, from equal parts of sorbent and hot melt glue to the ratio of 1:0.2. The visual evaluation of the devices obtained showed little homogeneity of the mixture of equal amounts and better with the 1: 0.2 ratio, however, to incorporate a more significant amount of sorbent, which will allow increasing the extraction of the analytes, the amount maximum sorbent with adequate homogeneity was reached when eight parts of the sorbent were mixed in 10 of the glue (ratio 1: 0.8).

To facilitate the homogeneity of the mixture, it was placed at 80 °C under mechanical agitation; here, adding a few milliliters of methanol improved the uniformity. Under these conditions, the organic solvent was evaporated during the heating process. Once this mixture was obtained, giving the devices the appropriate size and shape was necessary. For this, wooden molds with dimensions equal to the size required for the devices were used. Due to the malleability of the polymer, at this stage, an attempt was made to incorporate a magnetic piece so that the use of Teflon-coated magnetic bars could be dispensed with, necessary in other devices reported in the literature, offering this way a similar performance to "Twister stir bar." For this, cylindrical-shaped nickel-plated neodymium magnets (diameter 2 mm, length 4 mm) were purchased through an e-commerce platform.

When this process was standardized, it was repeated with other sorbents of a wide range of polarity, including activated charcoal, silica, strong cation exchange (SCX), and weak cation exchange (WCX) resins, which are typically used for extraction process due to his sorptive properties. Figure 1.B shows a photograph of the µ-PMBAE device with C18 sorbent; as can be seen, there is a uniformity in the composition of the mixture of the hot melt glue with the sorbent, which could qualitatively guarantee the repeatability of the sorption process. Figure 3 shows a diagram of the µ-PMBAE device.

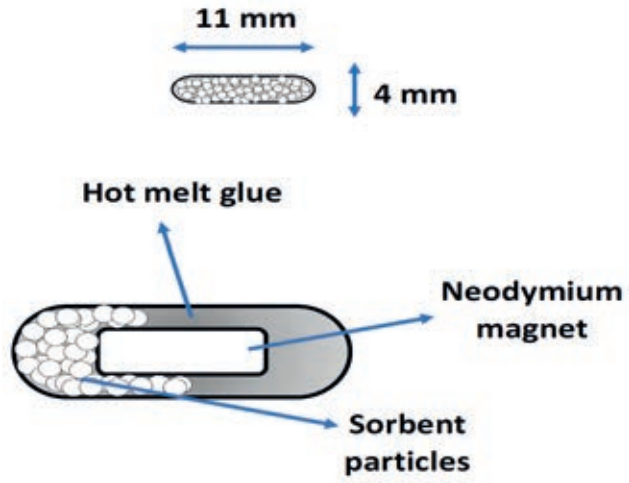

Figure 3. Diagram of the µ-PMBAE device.

Stability tests for µ-PMBAE devices

The next step was to evaluate the stability and robustness of devices developed through appropriate physic-chemical tests based on procedures applied by other authors who report the development of similar devices. This should be done before the application of µ-PMBAE to extract real samples. In the first instance, the µ-PMBAE devices were submitted to the effect of several solvents with a wide range of polarity characteristics, including hexane, acetonitrile, methanol, aqueous solutions of formic and acetic acid at 1 % v/v, regarding the interaction and mainly the occurrence of possible desegregation phenomena of the mixture of hot melt glue and the sorbents. The prepared sorptive bars were immersed for 48 hours in the solvents evaluated under ambient conditions. Then, after this time, a visual examination of the devices was performed. Complete stability in all solvents except for hexane was shown. This can be explained due to the solubility of the copolymer ethylene vinyl acetate in non-polar solvents like hexane.

For the evaluation of the pH effect in the µ-PMBAE devices, these were immersed for two days in solutions of hydrochloric acid (pH > 2) and sodium hydroxide (pH < 10); values outside this range were discarded since they are not usually used to modify the pH of the matrices subjected to extraction. All µ-PMBAE bars showed excellent stability without loss of sorbent particles. The effects of stirring and sonication processes on the stability of the devices were evaluated. For the stirring process, all the prepared µ-PMBAE devices were submitted for 24 hours, showing adequate strength without loss of the sorbents. Likewise, the devices were subjected to an ultrasonic bath for 30 to 120 minutes for sonification tests. A remarkable stability behavior was obtained for all devices. This is especially important for their future application in real samples since both parameters must be optimized to get a high recovery value.

Finally, the variation in the mass of the devices prepared with C18 sorbent was evaluated. For this, a batch of 21 units was prepared and immediately weighed. After 30 days, the mass values were weighted again. The t-test for equal variances showed that there were no significant differences between the initial data with those obtained one month later ($t_{cal} = 0.15 < t_{tab} = 1.68$), therefore stability in the composition of the µ-PMBAE was demonstrated, without losses of the sorbent as a function of time. From the results obtained in the weight variation test, under the preparation conditions of the devices, it is possible to estimate the amount of sorbent present in each microbar, being more significant than 80 milligrams. (Supplementary Materials).

Application of µ-PBAE in urine samples

Since its inception, SBSE has been widely applied for analyzing biological samples in clinical investigations, bioanalysis, and forensic toxicology. Here, the complexity of the matrix represents a significant challenge to overcome, as well as lower concentration levels of analytes and the small amount of sample available[24]. Therefore, once the µ-PMBAE had been produced and its stability had been demonstrated, it was decided to use it for the extraction of Ibuprofen, a nonsteroidal anti-inflammatory drug (NSAID) widely used for the treatment of inflammation and pain, as a representative molecule in real urine samples. For chromatographic separation, the conditions established in some previous works in the literature were taken as a basis[25,26].

Optimization of the extraction process

In general, for all sample treatment techniques, especially those based on the sorption principle, optimization of his parameters to obtain a high extraction efficiency is required. So, the extraction conditions for the sorption and desorption processes were optimized, starting with the sorbent phase in µ-PMBAE. For this, initial conditions with aqueous solutions of Ibuprofen with a concentration equal to 5 µg / mL (10 mL) were tested and subjected to extraction with

the microbars prepared with the five study sorbents. The extraction assemblies were stirred for 6 hours. Subsequently, the devices were removed and desorbed with 1 mL of acetonitrile in an ultrasonic bath for 30 minutes. After this time, the solution was injected. As shown in Figure 4, a higher recovery percentage was obtained with the µ-PMBAE prepared with C18 sorbent, which can be explained due to the low polarity of Ibuprofen (log Kow = 3.97). Under the evaluated conditions, the rest of the sorbents showed recoveries below 25%, so the following tests were performed with the C18 µ-PMBAE.

According to Nogueira[16], the parameters to optimize in SBSE include solution volume, stirring time and speed, salting effect, pH, and addition of organic modifier for the sorption stage. On the other hand, for liquid desorption, solvent type, volume, and sonication time can be optimized. Table 1 shows the parameters and variables optimized in the present study.

The volume of the solution turned out to be an essential parameter, obtaining better results when 20 mL of total volume was used, which can be explained by the greater contact of the analyte with the µ-PMBAE. Since Ibuprofen has a pKa value equal to 5.3, the pH of the extraction solution plays a vital role in its dissociation, so better results were obtained when acidification with a formic acid aqueous solution was performed; in comparison, when the extraction solution had a pH equal to 7. Although Ibuprofen does not show as a completely hydrophilic compound, modification of ionic strength by adding a few microliters of sodium chloride solution favored the salting-out phenomenon, so a lightly better recovery percentage was obtained. Finally, no significant differences were shown for stirring time between 2 and 6 hours, which means that the equilibrium is reached passed that time. In this line, the stirring speed was not tested since the used stirring apparatus only works at a speed of 1000 rpm.

In the liquid desorption stage, a better recovery percentage was obtained using methanol instead of acetonitrile; also, as expected, a better result was observed with 60 minutes of sonication. Other conditions used as a strategy to lower detection limits, such as sample volume and desorption volume, were evaluated. For this, a urine sample taken from a healthy adult volunteer free of ibuprofen intake in the last month was filtered and fortified at three concentrations, 25, 5, and 2.5 µg / mL. Two millimeters of the samples were extracted under optimized conditions and finally desorbed with 1 mL of methanol; the calculated recovery was 96.0 ± 6.5 for high concentration, 87.2 ± 5.4 for the intermediate value, and 79.0 ± 7.7 for the lower (n = 3). Under these conditions, the detection limit was set at 0.5 µg / mL, which can be reduced if the desorption is carried with 0.5 mL of methanol. Figure 5 shows representative chromatograms obtained during the optimization of the method. The specificity of the process was demonstrated by comparing the corresponding UV absorption spectrums for standard solutions and samples (Figure 5).

Reuse of the µ-PMBAE devices

At this point, the possibility of reusing µ-PMBAE was considered. For this, using devices to extract standard solutions was left immersed in methanol for 24 hours and subsequently analyzed, finding the presence of Ibuprofen in a range of 2 - 7 % of the fortified amount. Therefore, the reuse of the devices is not recommended unless they are subjected to thorough cleaning. In any case, the low-cost manufacturing of the µ-PMBAE counteracts its non-reuse. Finally, the interaction of the analyte with micro bars without the sorbent phase, composed solely of the polymer, was

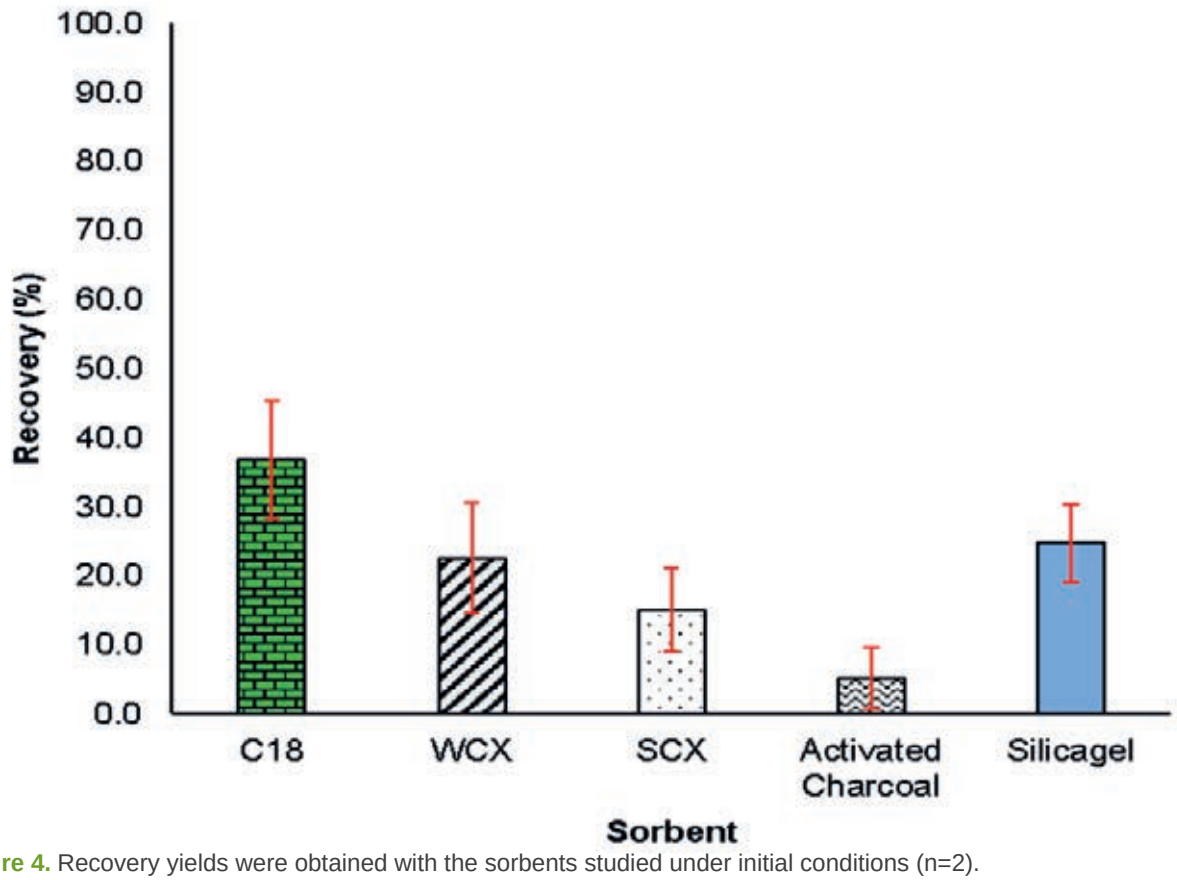

Figure 4. Recovery yields were obtained with the sorbents studied under initial conditions (n=2).

Stage	Factors	Units	Evaluated values	
			Lower value	Upper value
Sorption	Dilution volume	mL	10	**20**
	Stirring time	Hours	**2**	6
	pH modification	Yes/No	No	**Yes**
	Ionic strength	Yes/No	No	**Yes**
Desorption	Solvent	Type	Acetonitrile	**Methanol**
	Sonication time	Min	30	**60**

Table 1. Factors and values were evaluated to optimize the extraction efficiency using a 2^{6-1} factorial design. Bold values represent the optimized values.

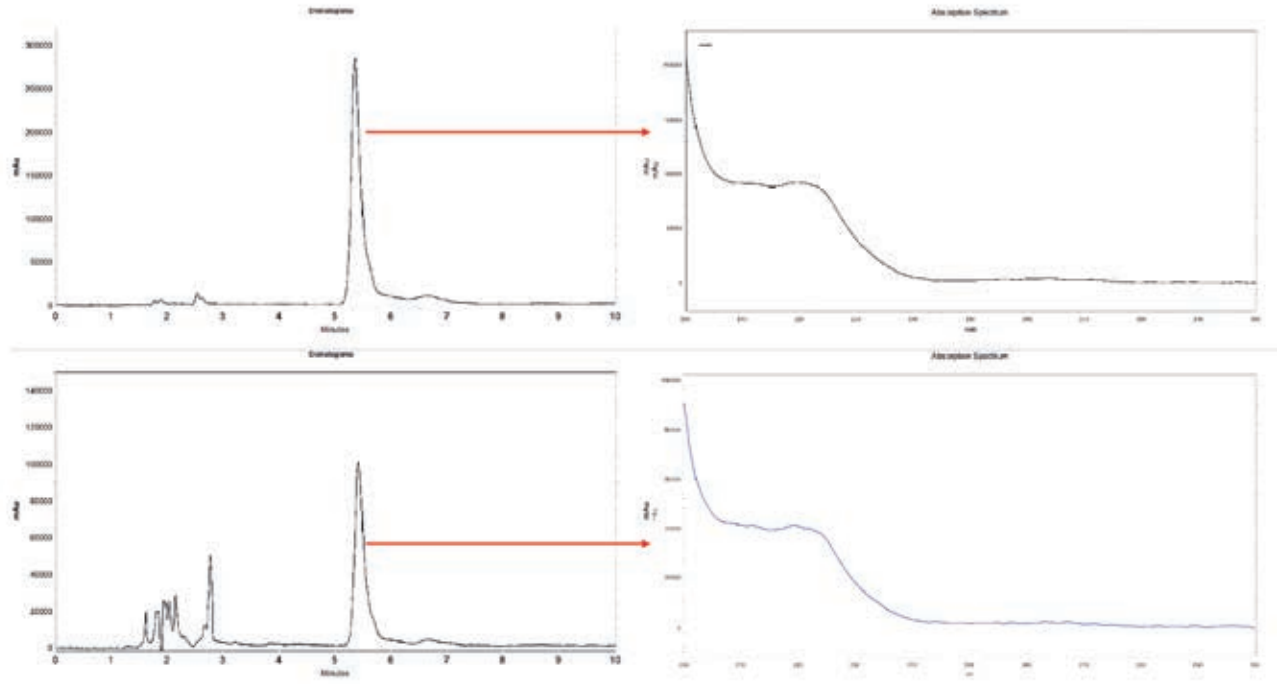

Figure 5. Representative chromatograms. Upper: analysis of standard solution at 50 µg / mL. Lower: analysis of a fortified sample at 25 µg / mL. Images on the right side show the corresponding UV absorption spectrum.

studied by repeating the extraction of standard solutions with a concentration of 25 µg / mL under optimal conditions. The results showed recoveries close to 25 %, so it is possible to establish that there is an interaction of the analyte with the polymer of the hot melt, possibly under an adsorption mechanism in the polymeric walls, which represents an advantage in its use.

Analytical performance

A fast evaluation of the main analytical performance parameters of the developed method was carried out, including linearity, limits of detection and quantification, recovery, precision, specificity, and selectivity. Adequate linearity was shown in the 50 to 2.5 µg / mL concentration range. The limit of detection (LOD) was calculated based on a signal-to-noise (S/N) ratio greater than 3 and the limit of quantification S/N of 10. The obtained values were 0.5 and 1.7 µg / mL, respectively. As mentioned in the previous section, the recovery yield was obtained at three levels of concentration, established from the peak area of the analyte in the urine sample spiked and the calibration equation obtained in the linearity evaluation. The recovery values obtained were between 79 and 96%. Specificity and selectivity were established by analyzing blank and spiked urine samples, which showed the nonappearance of endogenous substances interferences at the Ibuprofen retention time. Furthermore, the absorption spectrum of the peak attributed to Ibuprofen in the sample was compared with that obtained from the standard solution.

Analysis of actual urine sample

A urine sample from a healthy adult volunteer who was

administered a 600 mg dose of Ibuprofen orally was taken three hours after ingestion. The sample was filtered and analyzed in triplicate under the optimized conditions. The concentration found was 23.25 ± 0.51 µg / mL. These results were similar to the findings previously reported[27].

µ-PMBAE performance versus other SBSE devices

µ-PMBAE devices developed in this work demonstrate higher performance under optimized experimental conditions for the extraction of Ibuprofen in real urine samples, and its comparison with other devices, including the traditional stir bar, shows some notable advantages concerning economic cost, preparation, and versatility, as shown in Table 2. It is important to note that incorporating the neodymium magnet in the microbars offers the possibility of dispensing with Teflon-coated magnetic bars as in other works reported in the literature, equating its performance to the traditional stir bar device.

Discussion

Applying microextraction techniques based on the green analytical chemistry approach represents an essential trend for developing bioanalytical methods. In this study, a microdevice able to use different sorbents, which are added to a polymer, was developed, which makes it possible to increase the selectivity of extraction. Some of the advantages of this device compared to other devices reported in the literature include a simple manufacturing process, being able to make up to thirty units in less than 30 minutes; low cost per unit (less than one US dollar); and mainly the ability to add different sorbent materials, which translates into more excellent selectivity in the analysis. On the other hand, it is appropriate to point out that the device cannot be reused since a percentage of the extracted analyte remains in the microbar, as discussed in the results section. However, due to its low cost and considering that the neodymium piece can be recovered and reused to manufacture new devices, the authors consider that it does not represent a significant disadvantage. It should be noted that to ensure the composition of the polymer used in the manufacture of µ-PMBAE, it is recommended to prepare the polymer in the laboratory and not use commercial products. This final consideration should be assessed in the future. The analytical methodology was satisfactory for determining Ibuprofen in urine samples, demonstrating an analytical performance with adequate specificity, linearity, precision, and accuracy. Similarly, µ-PMBAE can be used to determine other bioanalytical molecules for which various sorbents, including metallic and vegetable nanoparticles, are promising. For example, our research group uses black carbon nanoparticles from olive seeds to determine dexamethasone in biological matrices.

Conclusions

The present work reports the development of a new device for sorptive extraction. Using easily accessible and low-cost materials, we developed a novel micro-bar absorbent device, incorporating different sorbent materials into a polymer commonly used as hot melt glue and introducing a small piece of neodymium magnet. The µ-PMBAE device demonstrated excellent stability, robustness, and high extraction efficiency to apply in the preparation of biological samples, following the principles of green analytical chemistry. The developed device has significant advantages compared with other devices reported in the literature. Different sorbents can be stuck on the hot melt glue, which tunes the interaction with the analytes to become more specific in the extraction. Besides, including a piece of a neodymium magnet in the device makes it possible to carry out extraction without needing an extra stir bar, matching its performance with the traditional commercially based on polydimethylsiloxane phase.

Patents

Invention patent Application No.HN/P/2022/001998.

Supplementary Materials

The following are available online at www.revistabionatura.com/xxx/s1, Table S1: Summarized results of stability studies., Table S2: Individual weight of µ-PBAE devices.

Author Contributions

Conceptualization, Jessica P. Riera-Williams, and H.D. Ponce-Rodríguez; methodology, Jessica P. Riera-Williams and H.D. Ponce-Rodríguez; software, Jessica P. Riera-Williams and H.D. Ponce-Rodríguez; validation, Jessica P. Riera-Williams and H.D. Ponce-Rodríguez; formal analysis, Jessica P. Riera-Williams and H.D. Ponce-Rodríguez; investigation, Jessica P. Riera-Williams and H.D. Ponce-Rodríguez; resources, H.D. Ponce-Rodríguez data curation, H.D. Ponce-Rodríguez; writing—original draft preparation, Jessica P. Riera-Williams and H.D. Ponce-Rodríguez; wri-

Characteristic	Twister stir bar[3]	BAµE[16]	Polylumi-nol[17]	µ-PMBAE-This work
Economic cost	High	Low	Low	Low
Preparation	No, apply	Easy	Easy	Easy
Variety of sorbents phases	No	Yes	No	Yes
Magnetism included in the device	Yes	No	No	Yes
Reuse	Yes	Yes	Yes	No

Table 2. Comparison of µ-PMBAE versus other SBSE devices.

ting—review and editing, H.D. Ponce-Rodríguez; visualization, Jessica P. Riera-Williams and H.D. Ponce-Rodríguez; supervision, H.D. Ponce-Rodríguez; project administration, H.D. Ponce-Rodríguez; funding acquisition, H.D. Ponce-Rodríguez. All authors have read and agreed to the published version of the manuscript.

Funding

This research received no external funding

Conflicts of Interest

The authors declare no conflict of interest.

Bibliographic references

1. Gałuszka, A.; Migaszewski, Z.; Namieśnik, J. The 12 principles of green analytical chemistry and the SIGNIFICANCE mnemonic of green analytical practices. TrAC, Trends Anal. Chem., 2013, 50, 78-84. https://doi.org/10.1016/j.trac.2022.116530
2. David, F.; Ochiai, N.; Sandra, P. Two decades of stir bar sorptive extraction: A retrospective and future outlook. TrAC, Trends Anal. Chem., 2019, 112, 102-111. https://doi.org/10.1016/j.trac.2018.12.006
3. Baltussen, E.; Sandra, P.; David, F.; Cramers, C. Stir bar sorptive extraction (SBSE), a novel technique for aqueous sam-ples: Theory and principles. J. Microcolumn Sep., 1999, 11, 737-747. https://doi.org/10.1002/(SICI)1520-667X(1999)11:10<737::AID-MCS7>3.0.CO;2-4
4. Liu, Y.; Liu, Z.; Xu, Z.; Li, g. Stir Bar Sorptive Extraction Technology. Progress in Chemistry, 2020, 32, 1334-1343. http://doi.org/10.7536/PC200101.
5. Mohamed, H.M. Solventless Microextration Techniques for Pharmaceutical Analysis: The Greener Solution. Front. Chem. 2022, 9,785830. http://doi.org/10.3389/fchem.2021.785830.
6. Kabir, A.; Locatelli, M.; Ulusoy, H.I. Recent Trends in Microextraction Techniques Employed in Analytical and Bioanalytical Sample Preparation. Separations, 2017, 4, 36. http://doi.org/10.3390/separations4040036.
7. He, M.; Wang, Y.; Zhang, Q.; Zang, L.; Chen, B.; Hu, B. Stir bar sorptive extraction and its application. J. Chromatogr. A, 2021, 1637, 461810. https://doi.org/10.1016/j.chroma.2020.461810.
8. Gorji, S.; Bahram, M.; Biparva, P. Optimized Stir Bar Sorptive Extraction Based on Self-Magnetic Nanocomposite Monolithic Kit for Determining Bisphenol A in Bottled Mineral Water and Bottled Milk Samples. Anal. Bioanal. Chem. Res., 2019, 6, 137-156. https://doi.org/10.22036/ABCR.2018.143530.1235.
9. Pérez-Padilla, Y.; Medina Cetina, S.A.; Ávila-Ortega, A.; Barrón-Zambrano, J.A.; Vilchis-Néstor, A.R.; Carrera-Figueiras, C.; Muñoz-Rodríguez, D. J. Evaluation of Polydimethylsiloxane-Phenylsiloxane as a Coating for Stir Bar Sorptive Extraction. J. Mex. Chem. Soc., 2018, 62, 348-357. https://doi.org/10.29356/jmcs.v62i2.431
10. Fan, W.; Mao, X.; He, M.; Chen, B.; Hu, B. Development of novel sol–gel coatings by chemically bonded ionic liquids for stir bar sorptive extraction—application for the determination of NSAIDS in real samples. Anal. Bioanal. Chem., 2014, 406, 7261-7273. https://doi.org/10.1007/s00216-014-8141-9
11. Babarahimi, V.; Talebpour, Z.; Haghighi, F.; Adib, N.; Vahidi, H. Validated determination of losartan and valsartan in human plasma by stir bar sorptive extraction based on acrylate monolithic polymer, liquid chromatographic analysis and experimental design methodology. J. Pharm. Biomed. Anal., 2018, 153,204-213. https://doi.org/10.1016/j.jpba.2018.02.030.
12. Marques, L.A.; Nakahara, T.T.; Madeira, T.B.; Almeida, M.B.; Monteiro, A.M.; de Almeida Silva, M.; Carrilho, E.; Piccoli de Melo, L.G.; Nixdorf, S.L. Optimization and validation of an SBSE–HPLC–FD method using laboratory□made stir bars for fluoxetine determination in human plasma. Biomed. Chromatogr., 2019, 33, 4398. https://doi.org/10.1002/bmc.4398.
13. Ghani, M.; Ghoreishi, S.M.; Shahin, M.; Azamati, M. Zeolitic imidazole framework templated synthesis of nanoporous carbon as a coating for stir bar sorptive extraction of fluorouracil and phenobarbital in human body fluids. Microchem. J., 2019, 146, 798-806. https://doi.org/10.1016/j.microc.2019.02.007
14. Taghvimi, A.; Dastmalchi, S.; Javadzadeh, Y. Novel Ceramic Carbon-Coated Magnetic Nanoparticles as Stir Bar Sorptive Extraction Coating for Simultaneous Extraction of Amphetamines from Urine Samples. Arab J Sci Eng., 2019, 44, 6373-6380. https://doi.org/10.1007/s13369-019-03810-0
15. Neng, NR; Silva, A.R.M.; Nogueira, J.M.F. Adsorptive micro-extraction techniques—Novel analytical tools for trace levels of polar solutes in aqueous media. J. Chromatog. A, 2010, 1217, 7303-7310. https://doi.org/10.1016/j.chroma.2010.09.048
16. Ahmad, S.M.; Nogueira, J.M.F. High throughput bar adsorptive microextraction: A novel cost-effective tool for monitoring benzodiazepines in large number of biological samples. Talanta, 2019, 199, 195–202. https://doi.org/10.1016/j.talanta.2019.02.004
17. Liu, H.; Ousmane, D.; Gan, N.; Wu, D. Li. Novel Stir Bar Array Sorptive Extraction Coupled with Gas Chromatography–Mass Spectrometry for Simultaneous Determination of Three β2-Agonist Residues in Pork. Chromatographia, 2017, 80, 473-482. https://doi.org/10.1007/s10337-017-3242-1
18. Zhou, W.; Wang, C.; Wang, X.; Chen, Z. Etched poly(ether ether ketone) jacket stir bar with detachable dumbbell-shaped structure for stir bar sorptive extraction. J. Chromatogr. A, 2018, 1553, 43-50. http://doi.org/10.1016/j.chroma.2018.04.022.
19. Šrámková, I.H.; Horstkotte, B.; Erben, J.; Chvojka, J.; Švec, F.; Solich, P.; Šatínský, D. 3D-Printed Magnetic Stirring Cages for Semidispersive Extraction of Bisphenols from Water Using Polymer Micro- and Nanofibers. Anal. Chem. 2020, 92, 3964–3971. https://doi.org/10.1021/acs.analchem.9b05455.
20. Benedé, J.L.; Chisvert, A.; Giokas, D.L.; Salvador, A. Development of stir bar sorptive-dispersive microextraction mediated by magnetic nanoparticles and its analytical application to the determination of hydrophobic organic compounds in aqueous media. J. Chromatogr. A, 2014, 1362, 25–33. https://doi.org/10.1016/j.chroma.2014.08.024.
21. Hasan, C.K.; Ghiasvand, A.;Lewis, T.W.; Nesterenko, PN;Paull, B. Recent advances in stir-bar sorptive extraction: Coatings, technical improvements, and applications. Anal. Chim. Acta, 2020, 1139, 222-240. https://doi.org/10.1016/j.aca.2020.08.021
22. Invention patent Application No.HN/P/2022/001998.
23. Genina, N.; Holländer, J.; Jukarainen, H.; Mäkilä, E.; Salonen, J.; Sandler, N. Ethylene vinyl acetate (EVA) as a new drug carrier for 3D printed medical drug delivery devices. Eur. J. Pharm. Sci., 2016, 90, 53-63. https://doi.org/10.1016/j.ejps.2015.11.005
24. Madej, K.; Piekoszewski, W. Modern Approaches to Preparation of Body Fluids for Determination of Bioactive Compounds. Separations, 2019, 6, 53. https://doi.org/10.3390/separations6040053
25. Ascar, L.; Ahumada, I.; López, A.; Quintanilla, F.; Leiva, K. Nonsteroidal Anti-Inflammatory Drug Determination in Water Samples by HPLC-DAD under Isocratic Conditions. J. Braz. Chem. Soc., 2013, 24, 1160-1166. http://doi.org/10.5935/0103-5053.20130150.
26. Ramos Payán, M.; Bello López, MA; Fernández Torres, R.; Villar Navarro, M.; Callejón Mochón, M. Electromembrane extraction (EME) and HPLC determination of nonsteroidal anti-inflammatory drugs (NSAIDs) in wastewater samples. Talanta, 2011, 85, 394-399. http://doi.org/10.1016/j.talanta.2011.03.076.
27. Jain, B.; Jain, R.; Kabir, A.; Sharma, S. Rapid Determination of Nonsteroidal Anti-Inflammatory Drugs in Urine Samples after In-Matrix Derivatization and Fabric Phase Sorptive Extraction-Gas Chromatography-Mass Spectrometry Analysis. Molecules, 2022, 27, 7188. https://doi.org/10.3390/molecules27217188.

ARTICLE / INVESTIGACIÓN

Investigation of Crohn's Disease by Immunohistochemistry Technique in Iraqi Patients

Adnan Fayadh Sameer[1], Abed Hassan Barraj[1]*, Hayder Jamaal Mahmood[2]

DOI. 10.21931/RB/2023.08.02.2

[1,2] Department of Biology, College of Science, University of Baghdad, Baghdad, Iraq.

[3] Gastroenterologist and Hepatologist, Gastrointestinal of the hospital, City of Medicine Baghdad, Iraq.

Abstract: Crohn's disease (CD) is one of the most common IBD types. CD necessitates an erratic immune response. Previous research has shown that inflammation of the intestines is elevated or continues due to inappropriate immune responses that result from the relationships between environmental factors, intestinal microbiota, and genetic factors. Induces intense transmural inflammation. This study aimed to investigate (i) CD detection by Histopathology and Immunohistochemistry (IHC) Markers that are *Mycobacterium avium* subspecies *paratuberculosis* MAP antibody and TWEAK/Fn14 antibody and their association with CD. (ii) Prove or disprove the hypothesis of MAP as a potential cause of CD. Tissue biopsies of 30 cases with a recognized diagnosis of CD and 20 cases as control presented without disease symptoms were collected. They are 20 males and 10 females for patients, and 13 males and 7 females for control with ages ranging from 9-55(±34.78) years. From 2019 - 2020, Biopsies were collected from Medical City Hospitals in Baghdad. One tissue section has been stained by the Hematoxylin & Eosin (H&E) for histopathology examinations. IHC stained the other two sections to the markers mentioned earlier in the IHC technique. The results of IHC for MAP showed a highly significant relationship in the ileal tissues of patients with disease CD with varying degrees according to the intensity of the immune reaction, which represents the intensity of the color, which is distributed between weak, moderate and strong, according to the (Aperio image Scope) program. Where it was 10% weak, 43.33% medium, and 46.67% strong. The P-value for patients vs. control was 0.0052 and 0.0001, respectively (P-value 0 ≤ 0.01). The result of IHC proves the hypothesis of MAP as a potential cause of CD. The other effects of IHC staining for TWEAK/Fn14 marker showed a highly significant relationship in the ileal tissues of patients with Crohn's Disease with varying degrees according to the intensity of the immune reaction, according to the Aperio image Scope program. It was 10% weak, 36.67% medium, and 53.33% strong. P-value for patients vs control were 0.0003 and 0.0001, respectively (P-value 0 ≤ 0.01).

Key words: Inflammatory bowel disease, Crohn's disease, *Mycobacterium avium* subspecies *paratuberculosis*, tumor necrosis factor-like weak apoptosis inducer.

Introduction

CD can be defined as an inflammatory bowel disease (IBD) type that is quite common. The CD is a chronic, complicated condition primarily affecting the digestive system[1]. This disease necessitates an erratic immune response, which results in severe inflammation. It primarily affects intestinal walls, particularly the ileum and portions of the colon, where inflated tissues thicken and swell, the inside becomes swollen, and ulceration may form on the digestive system's inner surfaces[2]. CD usually appears between the ages of 10 and 20 but can occur at any age. Symptoms and signs reappear at various points in a person's life. The most typical symptoms of this disorder include persistent loss of appetite, diarrhea, stomachache, fever, and weight loss. As a result of inflamed bowel tissues, people with CD have blood in their stools; persistent bleeding can result in death. Sometimes, CD may as well cause inflammation in the eyes, ligaments and tendons, or skin[3,4]. Intestinal obstruction is one of the common complications of CD. Obstructions in the intestinal walls can be caused by thickening or scar tissue buildup. Infected people frequently have fistulas or irregular contacts between intestines and other tissues. Fistulas form when the ulcers tear through the intestinal wall, and passages are formed between loops of intestines or between the intestine and the surrounding structures (like bladder, genitals, or skin)[5]. Previous research has shown that inflammation of the intestines is elevated or persists due to associations between intestinal microbiota, external factors, and genetic factors, all contributing to IBD development.

Furthermore, the IBD prevalence and incidence vary from region to region and multiethnic[6,7]. The CD is most prevalent in northern Europe, North America, and New Zealand, all of which are part of the Western developing world; it manifests between the ages of 15 and 60 and is more visible in cities than in rural areas. In 1990, Germany had the highest reported happening of IBD in the developed world, with 322 CD patients 322/ 100,000 people[8,9]. And in North America, there are 319 / 100,000 people in the United States and Canada[9,10]. Similarly, Europe and North America have the highest rates of IBD, though these percentages are stable or steadily decreasing (23.82 and 15.4 /100000 person-year for Crohn's Disease in Canada and Italy, res-

Citation: Sameer A F, Barraj A H, Mahmood H J. Investigation of Crohn's Disease by Immunohistochemistry Technique in Iraqi Patients. Revis Bionatura 2023;8 (2) 2. http://dx.doi.org/10.21931/RB/2023.08.02.2

Received: 26 December 2022 / **Accepted:** 15 March 2023 / **Published:** 15 June 2023

Publisher's Note: Bionatura stays neutral with regard to jurisdictional claims in published maps and institutional affiliations.

pectively)[9]. However, in Asia, particularly the Middle East, frequencies have steadily increased, reaching percentages of 5 / 100000 individual-year for Crohn's Disease[11]. Northern Europeans and Jews of (Ashkenazi) origin have a high prevalence (3.2/1000), while South Americans, Africans, and Asians have a significantly unusual majority (10).

On the other hand, modern reports show a considerable increase in incidence in rapidly developing regions such as Australasia, Africa, and Asia[12]. According to well-known data, the prevalence of CD in Saudi Arabia has been steadily increasing. According to (13), the prevalence and incidence of CD in Kuwait are rising at around the same rate as in European societies[14,15], and the prevalence of IBD appears to be rising in Egypt[16]. Moreover, most CD in Iraq has increased over the last ten years[17]. The histopathological examination of the patient's lesion begins with an intestinal crypt invasion. This causes ulceration to form first in the surface level of mucosa and then spread to the deeper layers. If the infection persists, non-caseating granulomas will develop in all intestinal wall layers. It may create a classic cobblestone mucosal appearance and miss lesions along the intestinal sparing areas' length with normal mucosa. When a Crohn's flare subsides, scarring substitutes the inflammatory intestine areas[18]. Granuloma formation has been standard in CD; nonetheless, the absence of granuloma does not rule out the diagnosis. If the infection persists, non-caseating granulomas will develop in all intestinal wall layers. Continuous inflammation and scar tissue contribute to intestinal obstruction and fistula[19].

It is expected that new IBD-specific and responsive markers will be discovered. Such immunohistochemistry (IHC) markers could reduce utilizing the endoscopic and radiological assessments and encourage physicians to implement individualized strategies of treatment aimed at improving IBD patients' long-term prognosis[20]. Anti-MAP antibodies were used to diagnose MAP and to demonstrate MAP involvement in CD pathogenesis, antibody titers to MAP-specific proteins increased in CD patients' sera[21]. However, it is unknown whether MAP can invade humans[22]. The most commonly used treatment methods for CD are steroids and monoclonal tumor necrosis factor (TNF) antibodies[23,24]. TNF-like weak apoptosis inducer (TWEAK) is a TNF superfamily cytokine, promoting its impacts by binding to its specific receptor, fibroblast growth factor-inducible 14 (Fn-14)[25]. TWEAK has been found in various cell types, including leukocytes, astrocytes, neurons[26,27], and several tumor cell lines. Fn-14 has been found at low levels in normal tissues. Some growth factors, however, are found in injured and unhealthy tissues[28]. The intestines are one of the most commonly affected tissues by TWEAK/Fn14 during persistent inflammation[29]. Following the breakdown of the mucosal barrier, continued activation of Fn14 on intestinal epithelial cells may contribute to excessive intestinal immunogenicity to commensal flora. Consequences include delayed regeneration, dysregulated tissue regeneration, and fibrosis[30]. TWEAK/Fn14 activation aids tissue repair and regeneration, whereas extreme or persistent TWEAK/Fn-14 signals can result in severe chronic inflammation infiltration and tissue injury. In the current study, the Immunohistochemistry (IHC) technique is used to investigate both of the above immunological markers, which may increase the accuracy of the diagnosis and help doctors significantly track the stages of the disease. This study has aimed to (i) investigate CD using Histopathology and Immunohistochemistry (IHC) Markers such as (MAP) antibody and (TWEAK/Fn14) antibody and their association with CD. (ii) Support or refute the hypothesis of MAP as a possible cause of CD.

Materials and methods

The period from 2019 - 2020, t cases with proven diagnoses of CD based on typical clinical symptoms, endoscopic, imaging, and histopathological criteria. Patients who had resections and those taking biological treatments for CD and others were excluded from this study, and 20 cases as control presented without disease symptoms (apparently healthy individuals); biopsies were collected from Medical City Hospitals Gastro-Enterology and Hepatology Hospital in Baghdad. They are 20 male and 10 female patients and 13 males and 7 females for control with ages ranging from 9-55 (±34.87) years; one endoscopic tissue biopsy was collected. H&E stained one tissue section for histopathology examinations, and IHC stained the other two to (MAP) antibody and (TWEAK/Fn14) antibody.

Immunohistochemically labeling images that were analyzed with Aperio Image Scope Soft wear (Aperio version 12.3.3.5048 Scope software. This program measures the reaction intensity of the Anti- (MAP) marker and Anti TWEAKR/Fn14 antibody marker in terms of "positivity" for a quantitative amount of specific color in tissue section Fig.1. The default of this system was set to input parameter according to color intensity degree which ranged from brown color, orange color, and yellow color, blue or white color for strong positive, optimistic, weak positive and negative colors respectively, according to Leica BioSystems Imaging, instructions[31].

Images were opened in the Aperio Image Scope application by selecting the "Open Image" option. The areas of interest were chosen using the "Pen Tool" option. The specified area was then evaluated by selecting the "Analysis" option. By choosing the "Annotations" option, the number of strongly positive, positive, and weakly positive pixels was calculated.The positivity value has been estimated by dividing the total number of the positive pixels by the total number of the pixels (N Total - N n) / (N Total), where N Total represents the total number of the pixels, (N n) represents the total number of negative pixels, and (N Total - N n) represents the total number of positive pixels. In its analysis, Aperio Image Scope software used the positive pixel method.

Statistical analyses

Statistical Analysis System- SAS (2012) software has been utilized for the detection of the effects of the different factors in the parameters of the study. T-test has been utilized for significant comparison between the mean values. Chi (-square-square test has been used for multiple comparisons between the percentages (0.05 and 0.01 proba-

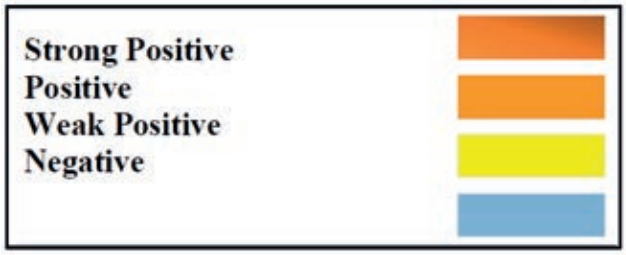

Figure 1. Reaction intensity of the Aperio Image Scope program.

bility in the present work. The allelic frequency and equilibrium of the studied genes were extracted according to the Hardy-Weinberg equation within the SAS.

Results and discussion

Histologically, the normal ileum structure is mucosa, lined by simple columnar epithelium and containing Peyer's patches, lamina propria and muscularis mucosae, submucosa, containing blood vessels, lymph nodes and the Meissner's plexus muscular consisting of an inner circular and outer longitudinal muscle layers and serosa, consisting of a simple squamous epithelium.

Pathologic principles in CD mucosal biopsies, even if superficial, can reveal characteristics suggestive of CD in the untreated situation. Mixed inflammatory infiltration and underlying lymphoid aggregation in sections of the ileum show moderate mononuclear cells infiltration with the proliferation of fibrous connective tissue between mucosal glands and neutrophils infiltration in the epithelial layer in the lumen of these glands that lead to destruct their epithelial layer Fig 2. In the damaged regions, architectural distortion is widespread, while nearby crypts might appear normal. In adults, granulomas are rare, but when they occur, they are usually badly formed, non-caseated, non-necrotizing, and linked with lymphocytic inflammations (Figs 3, 4 and 12). Sections in the ileum show marked mononuclear cell infiltration in the thickness lamina propria with hyperplasia and epithelial ulceration of epithelial Fig 5. Areas in the ileum show granuloma in the lamina propria with complete loss of epithelial layer Fig 6. The Section in the ileum shows severe mononuclear cells infiltration with the proliferation of fibrous connective tissue between mucosal glands and neutrophil infiltration in the lumen of these glands that lead to destruct their epithelial layer which helps differentiate CD from severe ulcerative colitis (UC).

In muscularis propria and submucosa with complete loss of villi Fig 7. At the same time, the Section in the ileum shows inflammatory reactions reaching the fatty tissues and crypts that are histologically normal Fig 8. The section in ileum shows marked mononuclear cells infiltration in the submucosa but do not present in the muscular mucosa Fig 9. In the submucosa of the ileum, a significant infiltration of neutrophils and peyer's patches is clearly present in Fig 10. In other cases, the Section in the ileum shows neutrophils and mononuclear cells infiltration between mucosal glands with cellular debris in the lumen of these glands Fig 11. Also, the Section in ileum shows non-caseated granuloma in the mucosa, in addition to neutrophils infiltration Fig 12. The Section in ileum shows hyperplasia of lymphoid tissue which as lymph nodes in the mucosal layer, and transmural inflammation areas, such as transmural lymphoid clusters with villi atrophy Fig 13. Inflammation can vary significantly in a single biopsy and across many biopsy fragments from one anatomic site. and occasionally with proliferation of fibrous connective tissue Fig 14. Additionally, Sections in ileum show severe neutrophils infiltration in the submucosa that forms micro abscess Fig 15. Other sections in ileum show granuloma that consists of the aggregation of the active macrophages and lymphocytes in sub epithelial layer Fig 16. Ulcers are frequently longitudinally orientated, separated with the histologically normal edematous mucosa. Sinuses, fistulas, fissures, and extensive inflammations, might be apparent. Transmural inflammations occur away from the deep ulcers Fig 17. And Section in ileum shows non-caseated granuloma in the lamina propria and proliferation of fibrous connective tissue between mucosal glands Fig 18.

The results of immunohistochemistry staining for (MAP), showed a highly significant relationship in ileal tissues of patients with CD with varying degrees according to the intensity of the immune reaction, which represents the intensity of the color, which is distributed between weak, moderate and strong, according to the (Aperio image Scope) program. Where it was 10% weak, 43.33% medium, and 46.67% strong. P-values (control vs. patients) were 0.0052 and 0.0001 (P-value 0 ≤ 0.01) Table (1) Figs. (19, 20, and 21).

The results of immunohistochemistry staining for (TWEAK/Fn14), showed a highly significant relationshipin the ileal tissues of patients who have CD with varying degrees according to the intensity of the immune reaction, which represents the intensity of the color, which are distributed between weak, moderate and strong, according to the (Aperio image Scope) program. Where it was 10% weak, 36.67% medium, and 53.33% strong. P-value (patients vs control) were 0.0003 and 0.0001 (P-value 0 ≤ 0.01) Table (3-5) Figs. (22, 23 and 24).

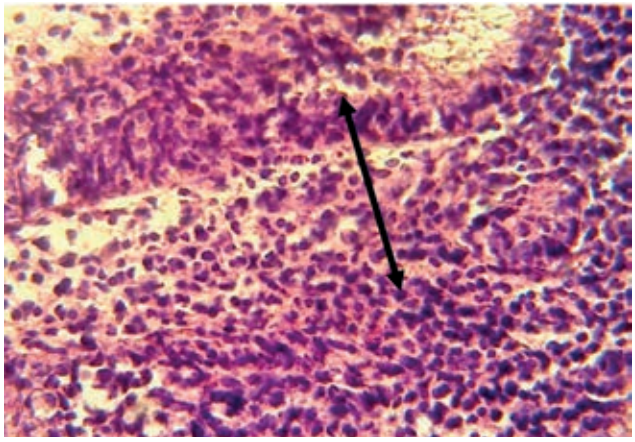

Figure 2. Section in ileum shows moderate mononuclear cell infiltration with proliferation of fibrous connective tissue between mucosal glands and neutrophils infiltration in the epithelial layer and in the lumen of these glands (H & E stain 40 x).

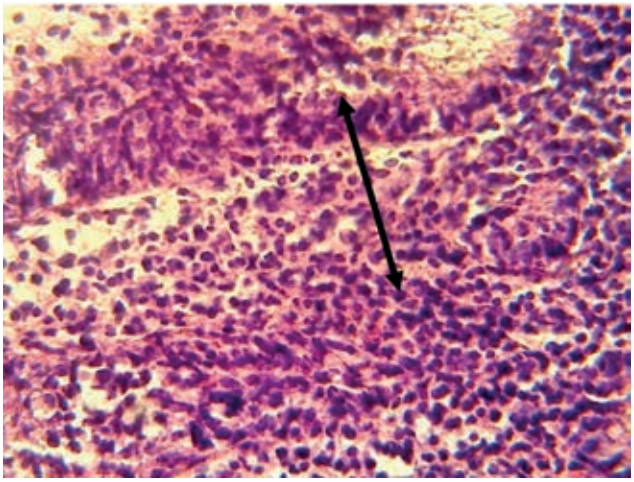

Figure 3. Sections in the ileum show granuloma in the lamina propria (H & E stains 40 x).

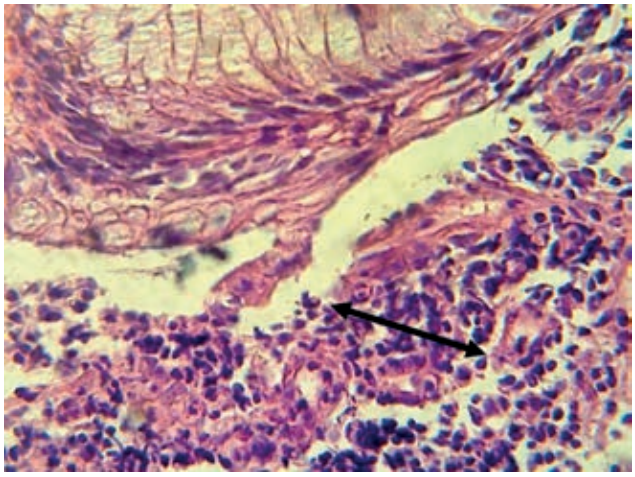

Figure 4. Section in ileum shows granuloma in the lamina propria in addition to neutrophils infiltration (H & E stains 40 x).

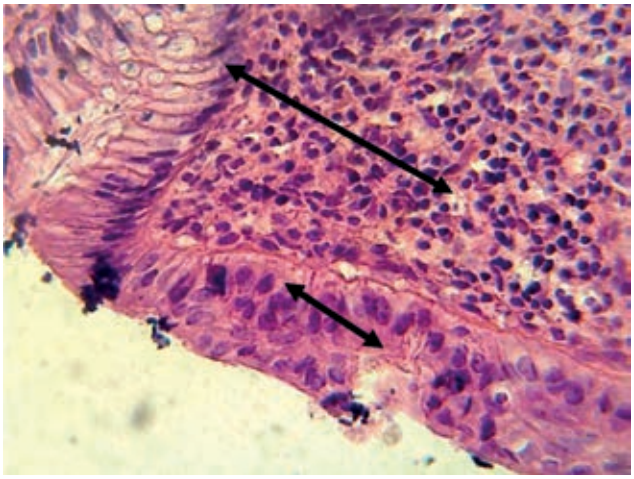

Figure 5. Section in ileum shows marked mononuclear cells infiltration in lamina propria with hyperplasia (H & E stains 40 x).

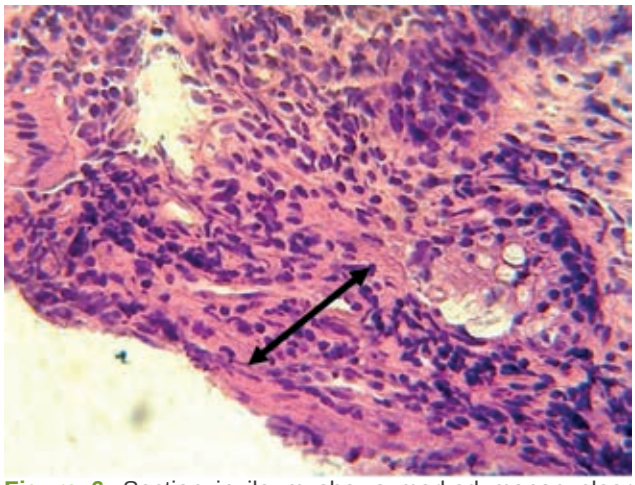

Figure 6. Section in ileum shows marked mononuclear cells infiltration in lamina propria with hyperplasia (H & E stains 40 x).

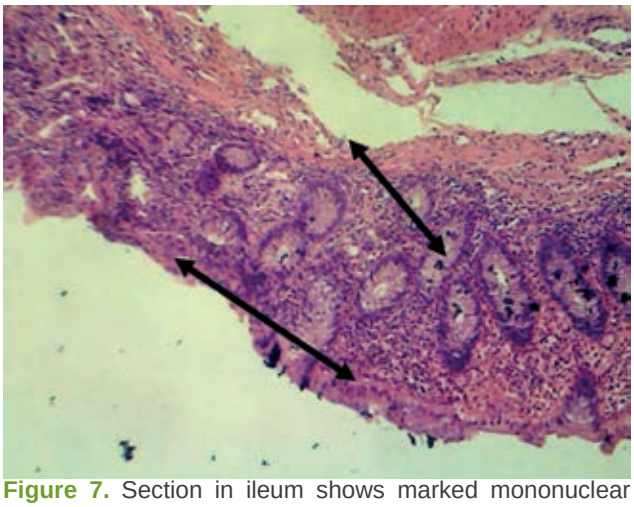

Figure 7. Section in ileum shows marked mononuclear cells infiltration in the mucosa with complete loss of villi (H & E stains 10 x).

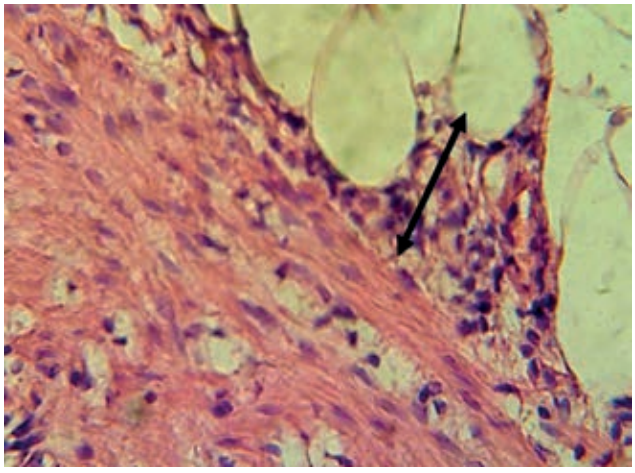

Figure 8. Section in ileum shows inflammatory reaction reach the adipose tissues (H & E stains 40 x).

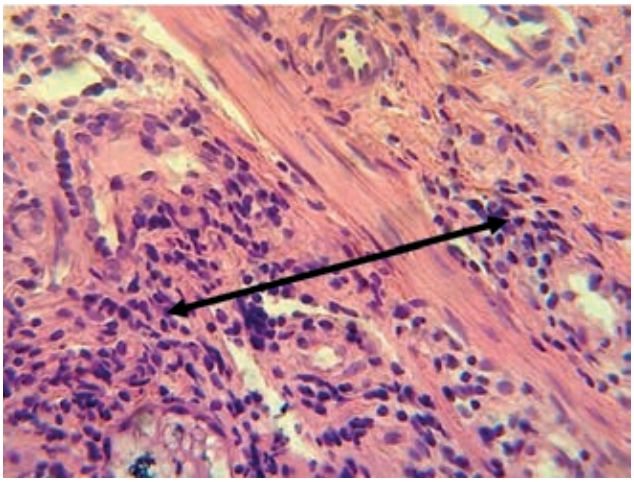

Figure 9. Section in ileum shows marked mononuclear cell infiltration in the submucosa (H & E stains 40 x).

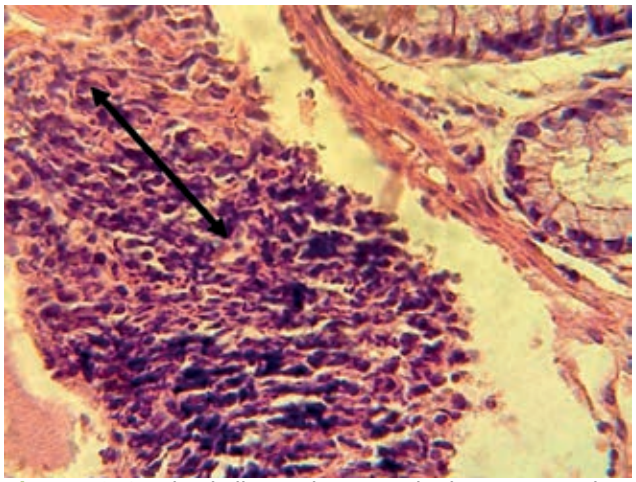

Figure 10. Section in ileum shows marked Payer's patches (H & E stains 40 x).

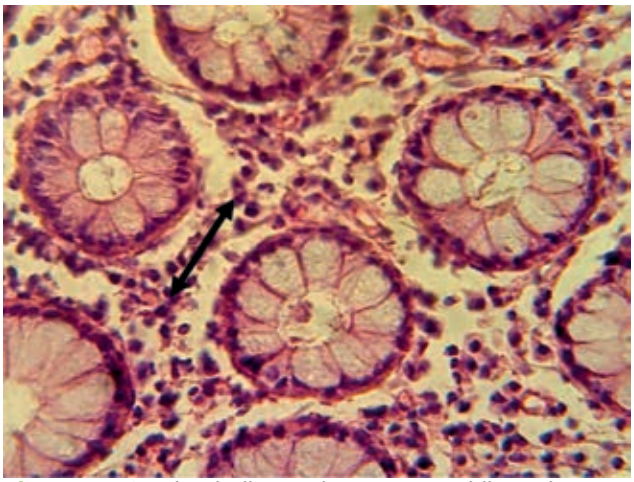

Figure 11. Section in ileum shows neutrophils and mononuclear cells infiltration between mucosal glands with cellular debris in the lumen of these glands (H & E stains 40 x).

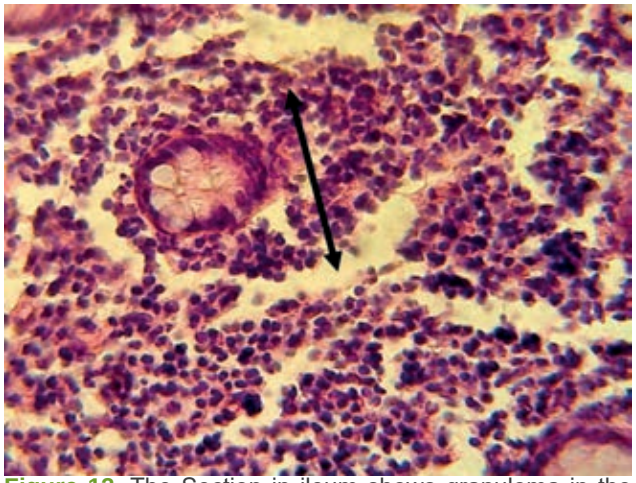

Figure 12. The Section in ileum shows granuloma in the mucosa and neutrophil infiltration (H & E stains 40 x).

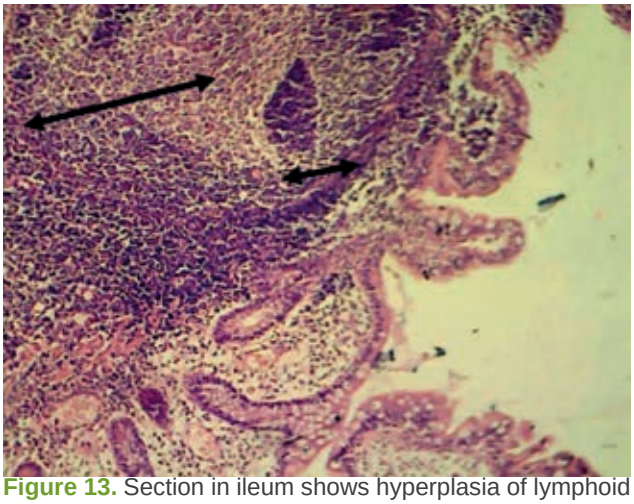

Figure 13. Section in ileum shows hyperplasia of lymphoid tissue in the mucosal layer and atrophy of villi (H & E stains 10 x).

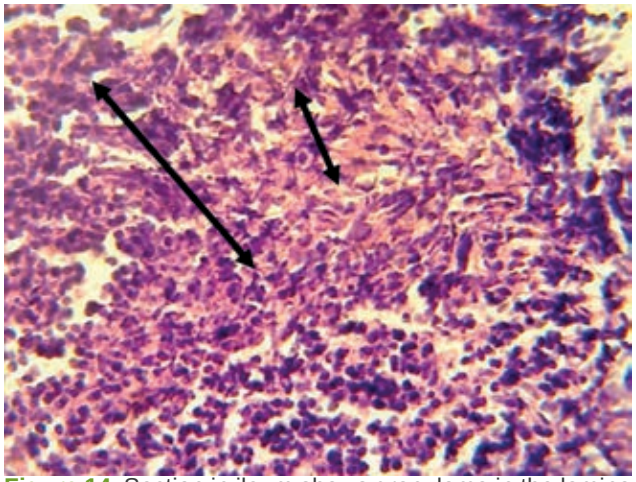

Figure 14. Section in ileum shows granuloma in the lamina propria in addition to neutrophils infiltration and proliferation of fibrous connective tissue (H & E stains 40 x).

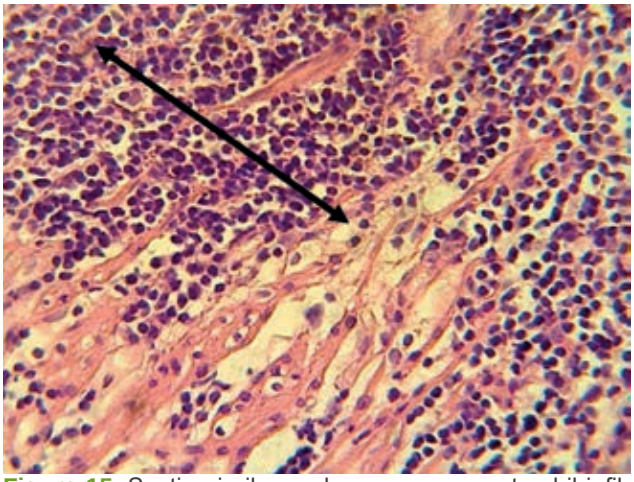

Figure 15. Section in ileum shows severe neutrophil infiltration in the submucosa, forming micro abscesses (H & E stains 40 x).

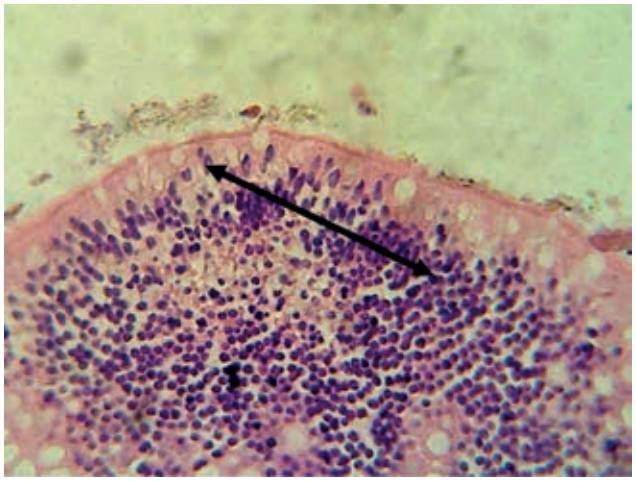

Figure 16. The Section in the ileum shows granuloma that consists of the aggregation of the active macrophages and lymphocytes in the subepithelial layer (H & E stains 40 x).

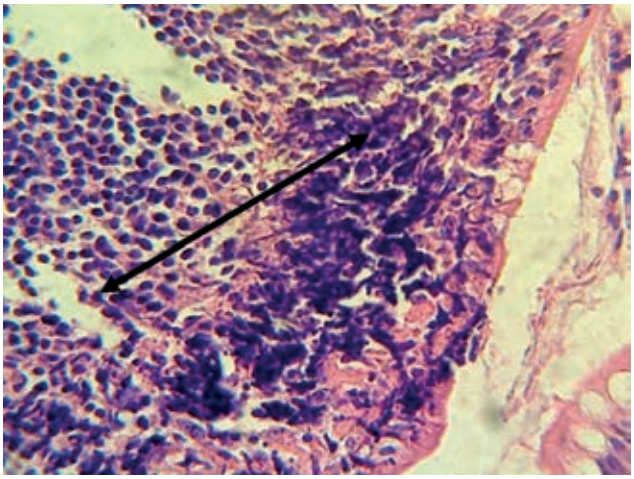

Figure 17. Section in ileum shows marked neutrophils and mononuclear cell infiltration in the lamina propria with ulceration of epithelial layer (H & E stains 40 x).

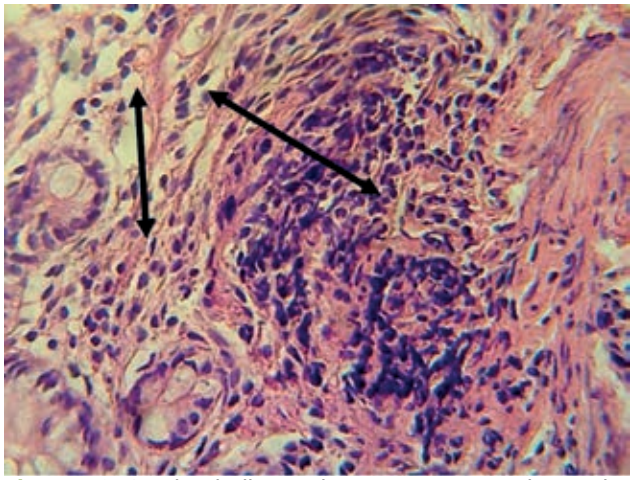

Figure 18. Section in ileum shows non-caseated granuloma in the lamina propria and proliferation of fibrous connective tissue between mucosal glands (H & E stains 40 x).

Inflammatory bowel disease IBD is histologically diagnosed by looking at four key characteristics, which are: (a) mucosal design, (b) submucosal cellularity and lamina propria, (c) neutrophil granulocyte infiltration, (d) epithelial irregularities[32]. Therefore, understanding the normal histology of the GI mucosa is essential for accurate analysis of biopsy results. I - Cryptographic architectural distortion refers to the morphologic aspects of mucosal architecture modifications. Normal crypts are straight and parallel, extending from the surface to just above muscularis mucosae. IBD crypt architectural distortions are well-defined by unevenly organized, dilated, branching, and/or truncated crypts. Which may be one of the symptoms of chronic inflammation or of renewal process[33]. The crypts in the normal rectum, on the other hand, can have slight irregularities suggesting architectural deformation[34]. II - Atypical lamina propria cellularity indicates a steadily increasing and diverse distribution of normally occurring types of cells. In the colorectal lamina propria, lymphocytes and plasma cells are typically observable. The proportion of inflammatory cells in normal colons ranges according to anatomical location. The cecum and right colon have been defined as the most cellular in overall, with a gradual decline in cellularity from right to left sides. Furthermore, there is a focally increased number of lymphoid cells near the lymphoid tissues of a typical gut-associated lymphoid tissue (GALT)[35]. In healthy individuals, eosinophil granulocytes vary significantly[34,35].

III - Neutrophil granulocyte infiltration characterizes the active disease. The neutrophils may be found in lamina propria or infect crypt surface epithelium and the lumen of the crypts, resulting in crypt abscesses. The neutrophils aren't commonly found in normal mucosa[36]. IV- Epithelial anomalies that are seen in the IBD include depletion of the Mucin, surface epithelial destruction and metaplastic alterations. The reduction of the number of goblet cells or a reduction in intra-cellular mucin amounts has characterized the depletion of the Mucin. The Pyloric gland metaplasia (which is one of the common indicators of chronicity in the ileal Crohn's Disease involvement) and Paneth's cell metaplasia have been defined as metaplastic alteration examples. Surface epithelial damage, like the flattening, localized cell loss, erosions, and ulcers, indicate the activity of the disease. None of those signs have been definitively disease-specific, and they may happen in the UC, Crohn's Disease, or other types of colitis[36].

The histological results for IBD differ according to the disease's clinical stages as well as levels of inflammatory activities. The IBD has been categorized into "Chronic inactive," "Chronic active," or "Active" (chronicity symptoms are absent)[34]. Histological features like crypt architectural deformations, widespread mixed lamina propria inflammation, crypt atrophy, basally located lymphoid clusters, basal plasmacytosis, and Paneth's cell metaplasia define chronicity (independent of "activity"). The presence of neutrophils confirms the presence of inflammatory activity. Neutrophilic cryptitis, bleeding, crypt abscesses, erosions, necrosis, and ulceration characterize active inflammation. The pathology report has to describe histological chronicity and activity aspects in detail and, if possible, grade the activity level as mild/moderate/severe. Grading has to begin with the most affected biopsy, and when possible, samples from different colon portions should be assigned a different grade. Because of the need for grading, many scoring systems or histology indices have been developed. There is no gold standard for activity grading, but the Nancy Index[37], which was endorsed by ECCO in 2020 as suitable for daily clinical grading of IBD, is one example[36]. The Nancy Index has 5 grades that range from 0 to 4. A normal biopsy with no (or very little) chronic inflammations and no active inflammations has been referred to as a grade zero biopsy. The presence of

MAP IHC marker	Patients No. (%)	Control No. (%)	P-value
Low: < 0.40	3 (10.00%)	20 (100%)	0.0001 **
Moderate: 0.4-0.6	13 (43.33%)	0 (0.00%)	0.0001 **
High: > 0.6	14 (46.67%)	0 (0.00%)	0.0001 **
P-value	0.0052 **	0.0001 **	---
** (P≤0.010). **High significant			

Table 1. Distribution of sample study according to MAP IHC marker in patients and control groups.

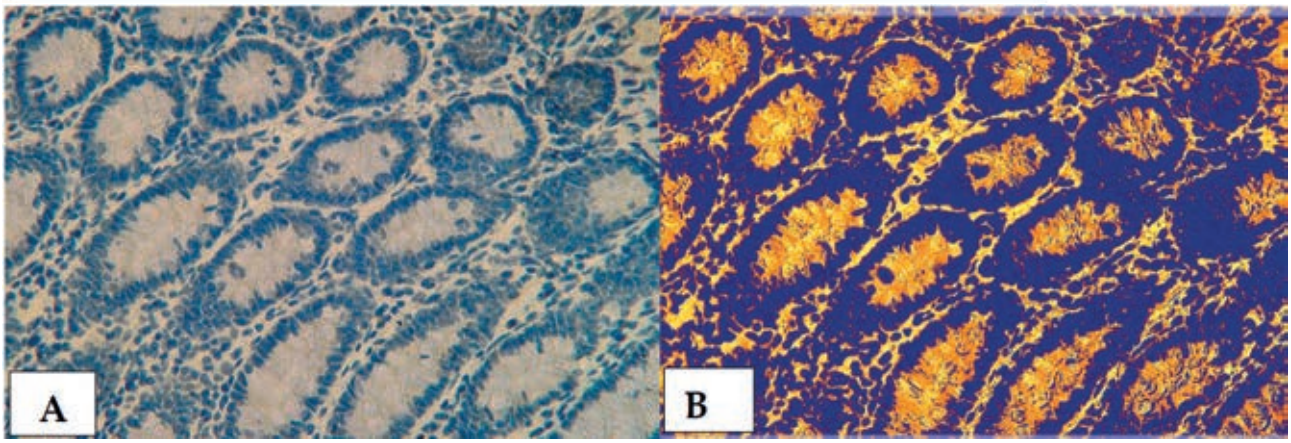

Figure 19. Cross section in ileum of CD patient with Anti-Mycobacterium tuberculosis antibody marker by IHC. Showing (A) Weak reaction 40X (B): Weak reaction analysis by Aperio Image Scope 40X

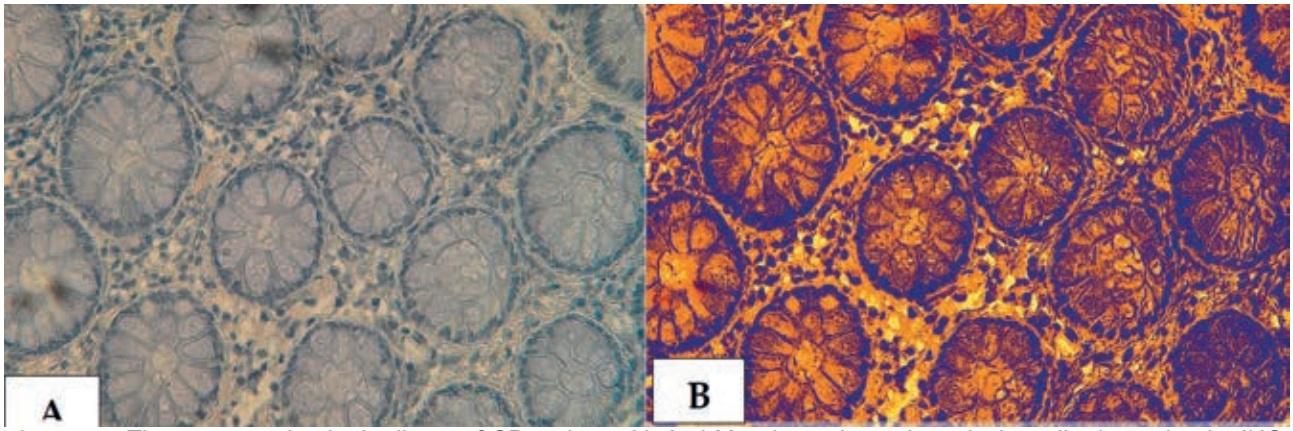

Figure 20. The cross section in the ileum of CD patient with Anti-Mycobacterium tuberculosis antibody marker by IHC. Showing (A) Moderate reaction 40X (B): Moderate reaction analysis by Aperio Image Scope 40X.

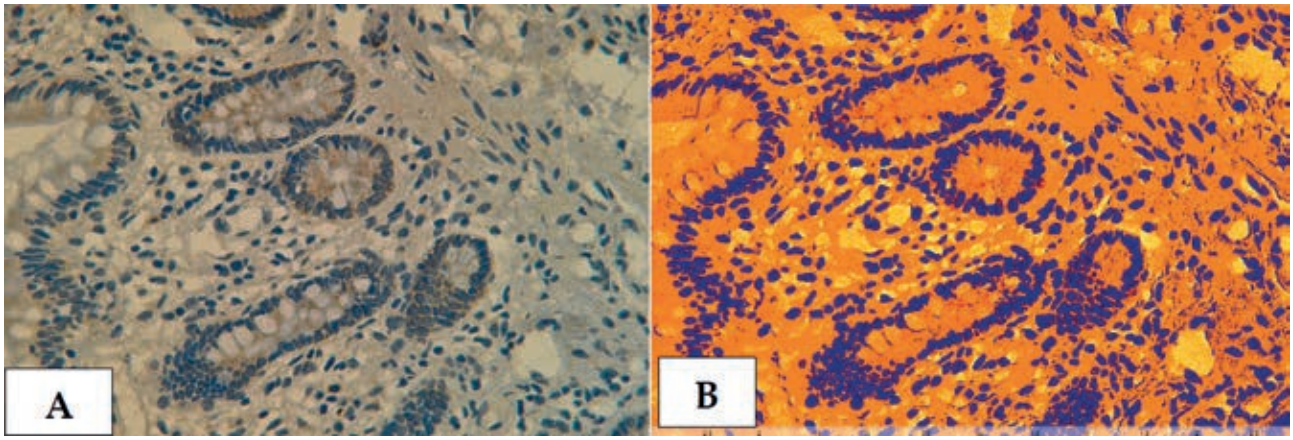

Figure 21. Cross section in ileum of CD patient with Anti-Mycobacterium tuberculosis antibody marker by IHC. Showing (A) Strong reaction 40X (B): Strong reaction analysis by Aperio Image Scope 40X.

TWEAK/Fn14 IHC	Patients No. (%)	Control No. (%)	P-value
Low: < 0.40	3 (10.00%)	20 (100%)	0.0001 **
Moderate: 0.4-0.6	11 (36.67%)	0 (0.00%)	0.0008 **
High: >0.6	16 (53.33%)	0 (0.00%)	0.0001 **
P-value	0.0003 **	0.0001 **	---
** (P≤0.010). **High significant			

Table 2. Distribution of sample study according to (TWEAK/Fn14) IHC. Marker in patients and control groups .

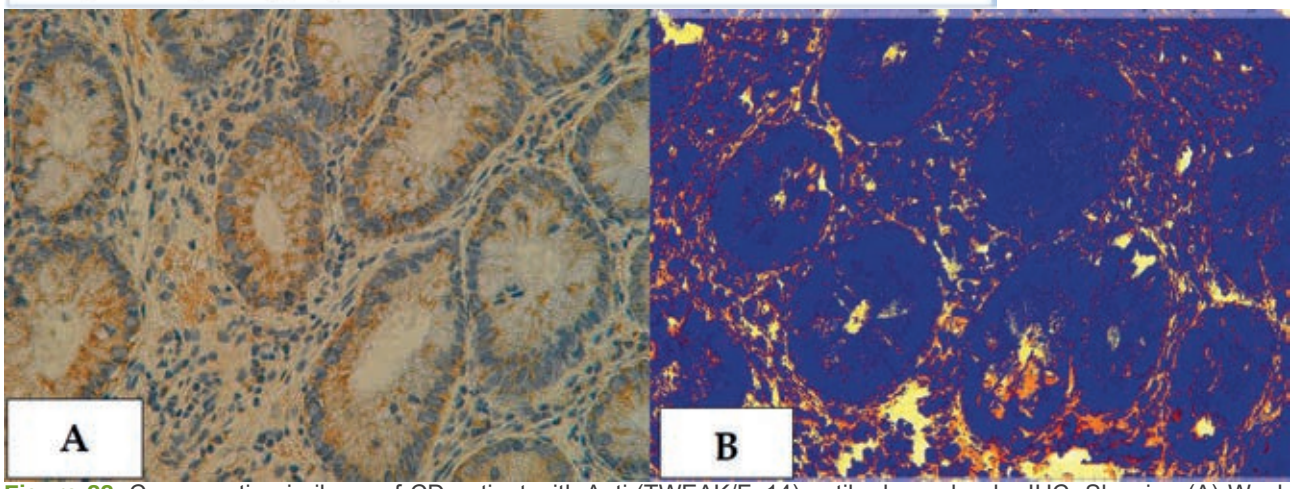

Figure 22. Cross section in ileum of CD patient with Anti-(TWEAK/Fn14) antibody marker by IHC. Showing (A) Weak reaction 40X (B): Weak reaction analysis by Aperio Image Scope 40X.

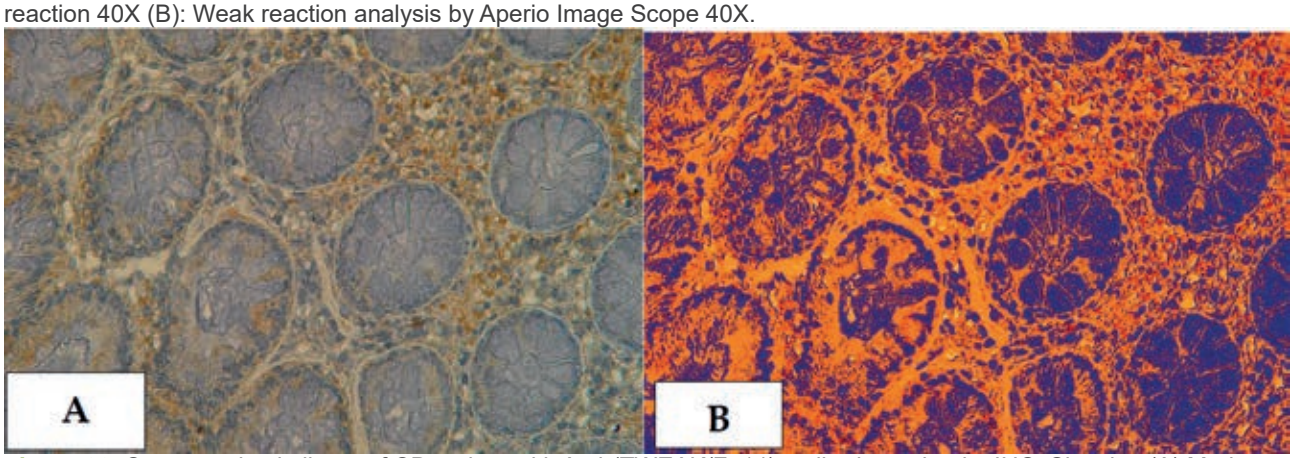

Figure 23. Cross section in ileum of CD patient with Anti-(TWEAK/Fn14) antibody marker by IHC. Showing (A) Moderate reaction 40X (B): Moderate reaction analysis by Aperio Image Scope 40X.

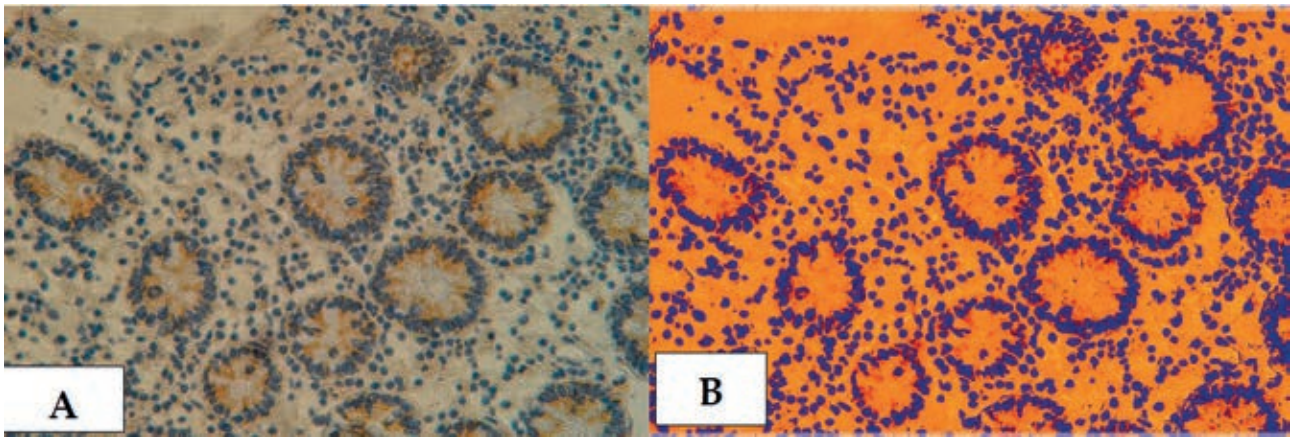

Figure 24. Cross section in ileum of CD patient with Anti-(TWEAK/Fn14) antibody marker by IHC. Showing (A) Strong reaction 40X (B): Strong reaction analysis by Aperio Image Scope 40X.

chronic inflammations but no active inflammations has been indicated by a grade one (chronic inflammation). Only a few neutrophils are visible in grade two ("mild activity"), and no ulceration exists. The term "ulceration" in grade four refers to superficial epithelial ulceration[37].

Due to the disease's patchy inflammatory patterns, endoscopic Crohn's Disease biopsies may exhibit varying inflammation degrees in one biopsy and between biopsies from one segment of the bowel. This is why the presence of focal microscopic alterations like chronic inflammations and focal crypt architectural distortion near normal crypts may be utilized for the diagnosis of Crohn's Disease. The inflammatory infiltrations in Crohn's Disease could be transmural. Deep fissures, fibrosis and ulcers have resulted from the transmural lymphoid aggregates and inflammatory cells infiltrating submucosa and even lamina muscularis. Transmural alterations may only be characterized in the resection due to the fact that the biopsies are more superficial. The existence of the non-caseating epithelioid granulomas results in promoting the diagnosis of Crohn's Disease; however, only in the case where they're characterized with no associations with the ruptured crypts, and identification of the granuloma isn't required strictly for the establishment of the diagnosis[34]. The epithelioid cell granuloma can be defined as epithelioid cell granuloma (i.e. the active histiocytes) with or with no multi-nucleated giant cells. Necrosis is not common in the granulomas of Crohn's Disease that are commonly ill-defined. In addition to that, the granulomas are more widespread in children compared to it in adults[38]. The uneven villous architecture in the terminal ileum biopsies is one of the Crohn's Disease symptoms; however, when it's continuous with the proximal colitis, it may as well be a backwash ileitis marker in the UC. Pyloric gland metaplasia can occur and is seen in up to 25% of ileal biopsies from CD patients (and quite more often in the ileal samples after the surgical resections); however, only seldom in the patients who have the UC[33].

Histopathological evaluation is also useful in detecting early signs of dysplasia and preventing cancer growth. The histopathological examination report must include the results that are suggestive of chronic colitis (such as basal lymphoid aggregates, basal plasmacytosis, crypt architectural/atrophic changes, metaplasia and mucin depletion) in addition to disease activity indication based upon neutrophil infiltration extent (in the lamia propria, crypt abscesses and cryptitis) and the epithelial damages for the symbol (i.e., the erosions). Even though histological remissions are not (yet) utilized as one of the treatment targets in routine clinical practices, it may be helpful for physicians in making decisions in the case of the establishment of a diagnosis and selection of the treatment. For the optimum implementations of histologic index and assessments of histological remissions in clinical settings, consensus agreement involving the clinicians/endoscopists and pathologists is necessary. If possible, a standardized endoscopic biopsy process has to be developed so that the samples for the histological evaluation are consistent across patients and medical facilities.

Furthermore, agreeing on a specific scoring criterion would make comparing facilities easier. Recent findings in CD ileocecal resection specimens suggested that it can be advantageous to routinely report on active inflammations, plexitis, and granulomas in the margins of resection for advising the clinical follow-up post-surgery[39]. The latest advancements in using the histologic indexes in clinical trials and their ability to assist as a predictive factor for guiding disease management even after diagnosis was established visibly prove that histopathology is still one of the significant factors in controlling the IBD[40].

The present statistical results of immunohistochemistry for the marker of *Mycobacterium avium paratuberculosis* (MAP), showed that there was a highly significant association with Crohn's patients according to the p-value that was 0.0052 and 0.0001(patients vs. control) (P-value 0 ≤ 0.01) table (1). And the results were distributed between weak, medium and strong, according to the program (Aperio image Scope). Where 10% were weak, 43.33% moderate, and 46.67% strong because of the severity of the infection, disease stage, taking antibiotics, immune-enhancing drugs and because of the severity of the infection as well as external environmental factors such as food, heat and sterilization conditions. This is consistent with the MAP Marker's relationship with CD[41]. As the twenty-first century arrived, a growing body of parallel studies had characterized 2 main bacteria groups as candidates for gross inflammatory disease pathogenesis of intestines in Crohn's Disease. This is a typical intestinal flora group[42]. An abnormal gut flora, like the adherent invasive *E. coli* (AIEC)[43]. Furthermore, given the global spread of Crohn's Disease and its serious implications for public safety in addition to the cumulative individual suffering, scientists and clinicians in the research area must recognize that accurate evidence that has been obtained from every one of the 3 evidence forms is convergent and that there aren't any conflicts between them. Based on experimental and clinical evidence, there isn't any reason to suspect that bacteria from normal gut microbes community can infect and inflame the gut wall, and this occurs in Crohn's Disease.

Nonetheless, without another distinct activating factor, the unexpected emergence and increase of Crohn's Disease in human societies worldwide due to an epidemic of normal intestinal flora appear highly suspicious. The gut bacteria serves as a nursery for horizontal gene transfer[44]. We've seen the pathological effects of this modification in common gut bacteria like *E. coli* that may be enterohaemorrhagic, enteropathogenic, enteroaggregative, enterotoxigenic, and, more lately, the entire adherent and infective AIEC[45]. Those changes are typically the result of some sort of external selection pressure. Recent studies reveal that typical gut flora, like *E. coli*, may be significant predictors[46]. MAP's status as a known multi-host inflammatory bowel pathogen identifies it from all other harmful microorganisms as the primary cause of Crohn's Disease. MAP has been shown in numerous animals, including primates, to have the unique capability for initiating and sustaining chronic inflammation of small bowel of various histological types. MAP infection causes both local and systemic immunological dysfunction in animals. In addition to that, it is neuropathogenic as well, particularly to the non-myelinated neurons, and small intestine disease has been linked to chronic enteric neuropathy[47]. Despite its widespread pathogenicity, MAP infection in animals can last for years without inevitably progressing into clinical illness.

When tried-and-true methods were used, the majority of the individuals who have Crohn's Disease have been found infected with MAP[48]. In layman's terms, most individuals with chronic inflammatory bowel disease (CD) have been infected with the Mycobacterium, one of the known IBD causes.

MAP infects the gut extensively in Crohn's Disease and can be found in the more normal-looking digestive tract as well as highly inflamed and infected parts of the intestine[49]. Immunological responses of CD-4 T cell lines derived from

patients' intestines appear to be dominated by MAP antigens[50]. Bacterial intracellular death is inhibited by mannans produced by MAP[51].

MAP infection results in causing primary microscopic inflammation, specific immunological dysregulation and enteric neuropathy[49]. Mucosal integrity, as well as other critical intestinal functions, are jeopardized. The visible components of gross chronic inflammation disease are caused by a dysregulated neuro-immune response to secondary gut flora penetration into the gut wall, including the normal intestinal bacteria and the ones that have undergone changes that lead to more invasive phenotypes, such as AIEC. Even though MAP has been discovered in human gut granulomas[47]. The occurrence or lack of those and other characteristics of the CD's variable histopathological image is determined primarily by big-scale responses to secondary co-pathogens like MAP, which is commonly recovered in the culture from the Crohn's Disease tissues[52]. As a result, the three current lines of research intersect in a two-tiered co-operative disease pathogenesis. The evidence for the link between MAP pathogens and CD is solid and effective and agrees with the previous investigation[41,53]. The present study utilized immunohistochemistry, which reflects true and specific immune reactions between anti-MAP and MAP using the Aprio imaging Scope program. In conjunction with other approved methods, this type of diagnosis can be one of the most dependable methodologies for specific diagnostic CD.

This immunohistochemistry investigation results show that the expression of TWEAK and its receptor Fn14 has been elevated in enteritis or (inflammatory bowel disease) tissue, particularly Crohn's disease. TWEAK protein expression was significantly higher in the Crohn's disease group than in the seemingly healthy group, as demonstrated by rigorous statistical analysis based on Aperio scope images, Where it was 10% weak, 36.67% medium, and 53.33% strong. P-value (patients vs control) were 0.0003 and 0.0001 (P-value 0 ≤ 0.01), and these differences in the proportions between patients may be due to the different stage of the disease and its severity, or Marker-inhibiting drugs, the person's immune status, and external factors. According to TWEAK and Fn-14, expression typically increases in response to stresses, tissue damage, or remodeling[54]. TWEAK has been expressed widely by monocytes, natural killer (NK) cells, and dendritic cells, with macrophages/monocytes being the main soluble TWEAK (sTWEAK) source in inflammatory body tissue[55]. In the current study, Fn14 expression has been found to be much higher in Enteritis patients than in seemingly healthy and healthy tissues; in comparison, Fn14 expression was relatively weak in the control. However, it can be strongly induced in injured and sick tissues by a range of different growth factors[28]. Fn14 can be found in many tissues, which include the colon, skin, small intestine, heart, brain, kidney, striated muscle, and pancreas[26,27]. TWEAK and Fn14 expression in healthy tissue is quite minimal. This is proven by the fact that the most frequently used CD treatments rely on steroids as well as the monoclonal antibodies against the TNF[24]. Overexpression of TWEAK During chronic inflammation, the digestive system is one of the tissue types most affected by the TWEAK/Fn-14[29]. Following mucosal barrier collapse continued Fn-14 stimulation on the intestinal epithelial cells may result in increased gut immune responses against the commensal flora. As a result, healing is slowing down, tissue repair is compromised, and fibrosis develops[56]. Although TWEAK/Fn-14 has been shown to have similar effects in models of enteritis caused by recurrent acute damage, the role of TWEAK/Fn14 in a more immunologically driven inflammation is unknown. The current study supports previous findings that showed increased expressions of TWEAK and Fn-14 in the Crohn's Disease tissue lesions compared to healthy controls[57]. Finally, to validate the current findings, we looked at the expressions of Fn-14 TWEAK in the ileal tissues of the IBD and non-IBD patients. TWEAK and Fn14 were significantly overexpressed during active inflammation in ileal biopsy specimens from CD patients compared to healthy humans. These findings support the theory that the TWEAK/Fn-14 signaling pathways have been activated as a defense mechanism during acute and chronic inflammation. However, over-activation in IBD could result in increased gut immune responses against intestinal flora. As a result, healing is slowed, tissue repair is compromised, and fibrosis develops[58,59]. Our findings differ from those of Kawashima and his team[55], TWEAK/Fn-14 levels have been higher in patients with active UC but not in CD patients or healthy controls for two reasons. First, only four CD patients have been included in the studies, compared to 30 in the current report. Second, the current studies primarily used small intestine tissue specimens, whereas previous studies only looked at colonic tissues. TWEAK/Fn-14 over-expression was discovered in tissue lesions obtained from patients with active CD, according to the current study[56]. To summarize, the current findings show significant TWEAK/Fn-14 overexpression in CD patients' small intestine tissue lesions, as well as a mechanistic role for Fn-14 signaling in CD pathogenesis. With the introduction of new TWEAK/Fn14-targeting medications[26].

Conclusions

The current findings support the notion that pharmacological inhibition of Fn-14 signaling can be one of the beneficial and feasible methods of preventing inflammatory responses in CD patients.

Funding

Self-Funding.

Conflicts of Interest

The authors declare no conflict of interest.

Bibliographic references

1. Lightner AL, McKenna NP, Alsughayer A, Loftus Jr EV, Raffals LE, Faubion WA, Moir C. Anti-TNF biologic therapy does not increase postoperative morbidity in pediatric Crohn's patients. Journal of pediatric surgery. 2019; 54(10):2162-2165.
2. Marazuela GP, López-Jurado A, Vicente BA. Acute abdominal pain in patients with Crohn's disease: what urgent imaging tests should be done? Radiologia. 2019;61(4):333–336.
3. Aksan A, Farrag K, Stein J. An update on the evaluation and management of iron deficiency anemia in inflammatory bowel disease. Expert Rev Gastroenterol Hepatol . 2019;13(2):95–97.
4. Hwang JH, Yu CS. Depression and resilience in ulcerative colitis and Crohn's disease patients with ostomy. Int Wound J. 2019; 16 (Suppl 1):62–70
5. Khan S, Rupniewska E, Neighbors M, Singer D, Chiarappa J, Obando C. Real-world evidence on adherence, persistence, switching and dose escalation with biologics in adult inflammatory bowel disease in the United States: A systematic review. J Clin Pharm Ther. 2019; 44(4):495–507.

6. Thia KT, Loftus EV Jr, Sandborn WJ, Yang S-K. An update on the epidemiology of inflammatory bowel disease in Asia. Am J Gastroenterol . 2008;103(12):3167–3182.
7. de Souza HSP, Fiocchi C. Immunopathogenesis of IBD: current state of the art. Nat Rev Gastroenterol Hepatol . 2016;13(1):13–27.
8. Hein R, Köster I, Bollschweiler E, Schubert I. Prevalence of inflammatory bowel disease: estimates for 2010 and trends in Germany from a large insurance-based regional cohort. Scand J Gastroenterol. 2014;49(11):1325–1335
9. Ng SC, Shi HY, Hamidi N, Underwood FE, Tang W, Benchimol EI, et al. Worldwide incidence and prevalence of inflammatory bowel disease in the 21st century: a systematic review of population-based studies. Lancet. 2017; 390(10114):2769–2778.
10. Coward S, Clement F, Benchimol EI, Bernstein CN, Avina-Zubieta JA, Bitton A, Carroll MW, Hazlewood G, Jacobson K, Jelinski S, Deardon R. Past and future burden of inflammatory bowel diseases based on modeling of population-based data. Gastroenterology.2019;156(5):1345-1353.e4.
11. Molodecky NA, Soon S, Rabi DM, Ghali WA, Ferris M, Chernoff G, Benchimol EI, Panaccione R, Ghosh S, Barkema HW, Kaplan GG. Increasing incidence and prevalence of the inflammatory bowel diseases with time, based on systematic review. Gastroenterology. 2012;142(1):46-54.
12. Ghersin I, Khteeb N, Katz LH, Daher S, Shamir R, Assa A. Trends in the epidemiology of inflammatory bowel disease among Jewish Israeli adolescents: a population-based study. Aliment Pharmacol Ther . 2019;49(5):556–563.
13. Al-Nooh BM, Alaslani MH, Almaghamsi A, Basehi M, Mufti F. Crohn's Disease Prevalence and Causes among Saudi Arabia Population. Int J Med Res Prof. 2018; 4(1):254–257.
14. Siddique I, Alazmi W, Al-Ali J, Al-Fadli A, Alateeqi N, Memon A, Hasan F. Clinical epidemiology of Crohn's disease in Arabs based on the Montreal Classification. Inflamm Bowel Dis. 2012;18(9):1689–1697.
15. Siddique I, Alazmi W, Al-Ali J, Longenecker JC, Al-Fadli A, Hasan F, Memon A. Demography and clinical course of ulcerative colitis in Arabs–a study based on the Montreal classification. Scandinavian Journal of Gastroenterology. 2014 ; 49(12):1432-1440.
16. Esmat S, El Nady M, Elfekki M, Elsherif Y, Naga M. Epidemiological and clinical characteristics of inflammatory bowel diseases in Cairo, Egypt. World J Gastroenterol .2014; 20(3):814–821.
17. Hamasur KS. Prevalence of Oral Manifestations of Inflammatory Bowel Disease in Patients Admitted to Sulaymaniyah teaching hospital – Iraq. Al-Kindy Col Med J . 2020;16(1):47–53.
18. Greuter T, Piller A, Fournier N, Safroneeva E, Straumann A, Biedermann L, Godat S, Nydegger A, Scharl M, Rogler G, Vavricka SR. Upper gastrointestinal tract involvement in Crohn's disease: frequency, risk factors, and disease course. Journal of Crohn's and Colitis. 2018 ;12(12):1399-1409.
19. Brennan GT, Melton SD, Spechler SJ, Feagins LA. Clinical implications of his- tologic abnormalities in ileocolonic biopsies of patients with Crohn's disease in remission. J Clin Gastroenterol. 2017;51(1):43-e48.
20. Mitsuyama K, Niwa M, Takedatsu H, Yamasaki H, Kuwaki K, Yoshioka S, Yamauchi R, Fukunaga S, Torimura T. Antibody markers in the diagnosis of inflammatory bowel disease. World J Gastroenterol [Internet]. 2016;22(3):1304–1310.
21. Nakase H, Nishio A, Tamaki H, Matsuura M, Asada M, Chiba T, Okazaki K. Specific antibodies against recombinant protein of insertion element 900 of Mycobacterium avium subspecies paratuberculosis in Japanese patients with Crohn's disease. Inflammatory bowel diseases. 2006 ;12(1):62-69.
22. Biet F, Gendt L, Anton E, Ballot E, Hugot J-P, Johanet C. Serum antibodies to Mycobacterium avium subspecies paratuberculosis combined with anti-Saccharomyces cerevisiae antibodies in Crohn's disease patients: prevalence and diagnostic role. Dig Dis Sci .2011; 56(6):1794–1800.
23. Feldman P, Wolfson, D. and Barkin, J. Medical management of Crohn's disease. Clin Colon Rectal Surg.2007; 20:269–281.
24. Lirhus SS, Hoivik ML, Moum B, Melberg HO. Regional differences in anti-TNF-alpha therapy and surgery in the treatment of inflammatory bowel disease patients: a Norwegian nationwide cohort study. Scand J Gastro- enterol. 2018; 53:952–957.
25. Burkly LC. TWEAK/Fn14 axis: the current paradigm of tissue injury-inducible function in the midst of complex- ities. Semin Immunol. 2014; 26:229–236.
26. Wajant H. The TWEAK-Fn14 system as a potential drug target: TWEAK/Fn14 targeting. Br J Pharmacol .2013; 170(4):748–764.
27. Chen J, Wei L, Xia Y. Roles of tumour necrosis factor-related weak inducer of apoptosis/fibroblast growth factor-inducible 14 pathway in lupus nephritis: A TWEAK/Fn14 pathway in lupus nephritis. Nephrology (Carlton). 2017; 22(2):101–106.
28. Burkly LC, Michaelson JS, Hahm K, Jakubowski A, Zheng TS. TWEAKing tissue remodeling by a multifunctional cytokine: role of TWEAK/Fn14 pathway in health and disease. Cytokine .2007;40(1):1–16.
29. Dohi T, Borodovsky A, Wu P, Shearstone JR, Kawashima R, Runkel L, Rajman L, Dong X, Scott ML, Michaelson JS, Jakubowski A. TWEAK/Fn14 pathway: a nonredundant role in intestinal damage in mice through a TWEAK/intestinal epithelial cell axis. Gastroenterology .2009;136(3):912–923.
30. Kawashima R, Kawamura YI, Oshio T, Son A, Yamazaki M, Hagiwara T, Okada T, Inagaki–Ohara K, Wu P, Szak S, Kawamura YJ.Interleukin-13 damages intestinal mucosa via TWEAK and Fn14 in mice-a pathway associated with ulcerative colitis. Gastroenterology .2011; 141(6):2119-2129.e8.
31. Firas, Riyadh & Muhammad, & Abdulammer, Hayder & Abdul-Ameer, Hayder. Immunohistochemical and morphometric study of early alveolar bone regeneration using Anti-Periostin antibody and xenograft in rabbit.2020.
32. Magro F, Langner C, Driessen A, Ensari AR, Geboes K, Mantzaris GJ, Villanacci V, Becheanu G, Nunes PB, Cathomas G, Fries W. European Society of Pathology (ESP), & European Crohn's and Colitis Organisation (ECCO) (2013). Journal of Crohn's & colitis. 7(10):827–851.
33. Langner C, Magro F, Driessen A, Ensari A, Mantzaris GJ, Villanacci V, Becheanu G, Borralho Nunes P, Cathomas G, Fries W, Jouret-Mourin A. The histopathological approach to inflammatory bowel disease: a practice guide. Virchows Archiv. 2014; 464:511-527.
34. Fenton TM, Jørgensen PB, Niss K, Rubin SJ, Mörbe UM, Riis LB, Da Silva C, Plumb A, Vandamme J, Jakobsen HL, Brunak S. Immune Profiling of Human Gut-Associated Lymphoid Tissue Identifies a Role for Isolated Lymphoid Follicles in Priming of Region-Specific Immunity. Immunity. 2020. 17(3):557-570.
35. Fenton TM, Jørgensen PB, Niss K, Rubin SJ, Mörbe UM, Riis LB, Da Silva C, Plumb A, Vandamme J, Jakobsen HL, Brunak S. Immune profiling of human gut-associated lymphoid tissue identifies a role for isolated lymphoid follicles in priming of region-specific immunity. Immunity. 2020 Mar 17;52(3):557-70.
36. Magro F, Doherty G, Peyrin-Biroulet L, Svrcek M, Borralho P, Walsh A, et al. ECCO position paper: Harmonization of the approach to ulcerative colitis histopathology. J Crohns Colitis. 2020; 14(11):1503–1511.
37. Marchal-Bressenot A, Scherl A, Salleron J, Peyrin-Biroulet L. A practical guide to assess the Nancy histological index for UC. Gut . 2016;65(11):1919.2-1920.
38. Hong SW, Yoon H, Shin CM, Park YS, Kim N, Lee DH, Kim JS. Clinical significance of granulomas in Crohn's disease: A systematic review and meta□analysis. Journal of Gastroenterology and Hepatology. 2020; 35(3):364-373.
39. Ananthakrishnan AN, Deshpande V. It is all in the fine print: A call for a histopathology checklist for IBD. Clin Gastroenterol Hepatol . 2021;19(3):446–447.
40. Kellermann L, Riis LB. A close view on histopathological changes in inflammatory bowel disease, a narrative review. Dig Med Res. 2021; 4:3–3.

41. Xia A, Stempak JM, Grist J, Bressler B, Silverberg MS, Bach H. Effect of inflammatory bowel disease therapies on immunogenicity of Mycobacterium paratuberculosis proteins. Scand J Gastroenterol .2014;49(2):157–163.
42. Martinez-Medina M, Aldeguer X, Lopez-Siles M, González-Huix F, López-Oliu C, Dahbi G, Blanco JE, Blanco J, Garcia-Gil JL, Darfeuille-Michaud A. Molecular diversity of Escherichia coli in the human gut: new ecological evidence supporting the role of adherent-invasive E. coli (AIEC) in Crohn's disease. Inflammatory bowel diseases. 2009 ;15(6):872-882.
43. Kurokawa K, Itoh T, Kuwahara T, Oshima K, Toh H, Toyoda A, Takami H, Morita H, Sharma VK, Srivastava TP, Taylor TD. Comparative metagenomics revealed commonly enriched gene sets in human gut microbiomes. Dna Research. 2007 ;14(4):169-181.
44. Darfeuille-Michaud A, Neut C, Barnich N, Lederman E, Di Martino P, Desreumaux P, Gambiez L, Joly B, Cortot A, Colombel JF. Presence of adherent Escherichia coli strains in ileal mucosa of patients with Crohn's disease. Gastroenterology. 1998 ;115(6):1405-1413.
45. Tagkopoulos I, Liu YC, Tavazoie S. Predictive behaviour within microbial genetic networks. Science. 2008;320:1313–137.
46. Zamani S, Zali MR, Aghdaei HA, Sechi LA, Niegowska M, Caggiu E, Keshavarz R, Mosavari N, Feizabadi MM. Mycobacterium avium subsp. paratuberculosis and associated risk factors for inflammatory bowel disease in Iranian patients. Gut pathogens. 2017 ;9:1-10.
47. Scanu AM, Bull TJ, Cannas S, Sanderson JD, Sechi LA, Dettori G, Zanetti S, Hermon-Taylor J. Mycobacterium avium subspecies paratuberculosis infection in cases of irritable bowel syndrome and comparison with Crohn's disease and Johne's disease: common neural and immune pathogenicities. Journal of clinical microbiology. 2007 ;45(12):3883-3890.
48. Olsen I, Lundin KE, Sollid LM. Increased frequency of intestinal CD4+ T cells reactive with mycobacteria in patients with Crohn's disease. Scandinavian journal of gastroenterology. 2013;48(11):1278-85.
49. Mpofu CM, Campbell BJ, Subramanian S, Marshall–Clarke S, Hart CA, Cross A, Roberts CL, McGoldrick A, Edwards SW, Rhodes JM. Microbial mannan inhibits bacterial killing by macrophages: a possible pathogenic mechanism for Crohn's disease. Gastroenterology. 2007;133(5):1487-1498.
50. Bull TJ, McMinn EJ, Sidi-Boumedine K, Skull A, Durkin D, Neild P, Rhodes G, Pickup R, Hermon-Taylor J. Detection and verification of Mycobacterium avium subsp. paratuberculosis in fresh ileocolonic mucosal biopsy specimens from individuals with and without Crohn's disease. Journal of clinical microbiology. 2003 ;41(7):2915-2923.
51. Shanahan F, O'Mahony J. The mycobacteria story in Crohn's disease. Am J Gastroenterol. 2005;100(7):1537–1538.
52. Cheng H, Xu M, Liu X, Zou X, Zhan N, Xia Y. TWEAK/Fn14 activation induces keratinocyte proliferation under psoriatic inflammation. Exp Dermatol. 2016; 25(1):32–37.
53. Liu Y, Peng L, Li L, Liu C, Hu X, Xiao S, et al. TWEAK/Fn14 activation contributes to the pathogenesis of bullous pemphigoid. J Invest Dermatol . 2017; 137(7):1512–1522.
54. Kawashima R, Kawamura YI, Oshio T, Son A, Yamazaki M, Hagiwara T, Okada T, Inagaki–Ohara K, Wu P, Szak S, Kawamura YJ. Interleukin-13 damages intestinal mucosa via TWEAK and Fn14 in mice—a pathway associated with ulcerative colitis. Gastroenterology. 2011; 141(6):2119-2129.
55. Di Martino L, Osme A, Kossak-Gupta S, Pizarro TT, Cominelli F. TWEAK/Fn14 is overexpressed in Crohn's disease and mediates experimental ileitis by regulating critical innate and adaptive immune pathways. Cellular and Molecular Gastroenterology and Hepatology. 2019;8(3):427-446.
56. Rieder F, Brenmoehl J, Leeb S, Schölmerich J, Rogler G. Wound healing and fibrosis in intestinal disease. Gut. 2007; 56(1):130–139.
57. Rogler G, Hausmann M. Factor's promoting development of fibrosis in Crohn's disease. Front Med (Lausanne) .2017; 4:96.

ARTICLE / INVESTIGACIÓN

Microencapsulación de licopeno extraido de los desechos agroindustriales del tomate de árbol (*Solanum Betaceum*)

Microencapsulation of lycopene extracted from the agroindustrial waste of the tree tomato (*Solanum Betaceum*)

Pilar Pazmiño Miranda[1]*, Danae Fernández[1], Diana Coello-Fiallos[1], Orestes Darío López[1] and Antonio Iraizoz[2]

DOI. 10.21931/RB/2022.08.02.3

[1] Universidad Técnica de Ambato, Ecuador.
[2] Universidad de la Habana, Cuba.
Corresponding author: od.lopez@uta.edu.ec

Resumen: Se realizó a escala industrial el proceso extracción y microencapsulación de licopenos a partir de los desechos agroindustriales del tomate de árbol (*Solanum betaceum*) mediante secado por aspersión. Se obtuvo el extracto a partir del secado y molido del material vegetal a la temperatura de 50 °C durante 55 horas hasta obtener un tamaño de partículas finas (≤ 250 µm), posteriormente se utilizó etanol al 96% en una relación material vegetal/volumen de disolvente 1:70. El microencapsulado fue obtenido a partir de una mezcla del 30 % de extracto, 35 % goma arábiga y 35 % de maltodextrina utilizando un secador por aspersión industrial de 100 kg/h de capacidad de evaporación de agua, empleando una temperatura de entrada de 120 °C y una temperatura de salida de 80 °C. Los extractos presentaron una eficiencia de extracción de: 48,90 mg/kg en el lote 1, 31,10 mg/kg en el lote 2 y de 27,08 mg/kg en el lote 3. Las concentraciones de licopenos alcanzaron valores de: 43,78 mg/g, 45,20 mg/g y 43,22 mg/g en los lotes 1, 2 y 3 respectivamente. La eficiencia de microencapsulación obtenida fue superior al 90% en los lotes producidos a escala industrial (lote 1: 93,61 %, lote 2: 90,44 % y lote 3: 96,78 %). Se evaluó la capacidad antioxidante *in vivo* de los microencapsulados, utilizando un cultivo de *Saccharomyces cerevisiae*, demostrando que tienen una actividad antioxidante similar a la de la vitamina C. Mediante el método del DPPH, se obtuvo un porcentaje de inhibición del 48,03 %, 35,07 % y 38,07 % en los 3 lotes respectivamente. En la morfología de las microcápsulas se observaron esferas con superficie lisa con tamaños de microcápsulas del orden de decenas de micrómetros (10 -70 µm) para su diámetro. Se demuestra que el proceso de microencapsulación de licopeno es efectivo por lo que puede para ser introducido a nivel industrial, siendo una tecnología que puede ser implementada en la industria para el aprovechamiento de los desechos agroindustriales de las cáscaras de tomate de árbol, brindando beneficios para la salud por sus características antioxidantes.

Palabras clave: Extracto, carotenoides, licopeno, secado por aspersión, microcápsulas.

Abstract: The extraction and microencapsulation of lycopene from tree tomatoes (*Solanum betaceum*) were done on an industrial scale by spray drying. The methodology used to obtain the extract was drying at 50 °C for 55 hours until a fine particle size (≤ 250 µm) was accepted, followed by dilution with 96% ethanol and, to obtain the microencapsulation, the extract was mixed with 85% gum arabic and 15% distilled water to pass through an industrial spray dryer of 100 kg/h of water evaporation capacity, using an inlet temperature of 120 °C and an outlet temperature of 80 °C. As a result, both the liquid extract and the microencapsulated extract were characterized, obtaining three batches with an extraction efficiency of batch 1: 48.90 mg/kg, batch 2: 31.10 mg/kg and batch 3: 27.08 mg/kg. A lycopene concentration of 43.78 mg/g, 45.20 mg/g and 43.22 mg/g and a microencapsulation efficiency of 93.61 %, 90.44 % and 96.78 %. The *in vivo* antioxidant capacity of the microencapsulates was evaluated in *Saccharomyces cerevisiae*, demonstrating that they have an antioxidant activity similar to that of vitamin C. And by the DPPH method found an inhibition percentage of 48.03 %, 35.07 % and 38.07 % in the 3 batches, respectively. In the morphology of the microcapsules, spheres with smoothness were observed with microcapsule sizes in the order of tens of micrometers (10 -70 µm) for their diameter. It is demonstrated that the lycopene microencapsulation process is effective so that it can be introduced at the industrial level. This technology can be implemented in the industry to use the agro-industrial waste of tree tomato peels, providing health benefits for its antioxidant characteristics.

Key words: Extract, carotenoids, lycopene, spray drying, microcapsules.

Citation: Pazmiño Miranda, P.; Fernández, D.; Coello-Fiallos, D.; López,D.; Airaizoz, A. Microencapsulación de licopeno extr . Revis Bionatura 2023;8 (2) 3. http://dx.doi.org/10.21931/RB/2023.08.02.3
Received: 26 December 2022 / **Accepted:** 15 March 2023 / **Published:** 15 June 2023

Introducción

La cáscara de tomate de árbol es un desecho que se produce industrialmente en las plantas procesadoras de alimentos, siendo un problema de carácter ambiental y económico para las empresas, al convertirse en un desecho sin aprovechamiento[1].

El ser humano, deja de aprovechar las propiedades beneficiosas de las cáscaras de las frutas, sin embargo científicamente se ha demostrado que contienen fibra y compuestos bioactivos[2]. Su uso representaría mayores fuentes de ingreso económico y alternativas para su aprovechamiento.

Una manera de aprovechar las cáscaras de tomate de árbol sería mediante procesos físico-químicos para extraer metabolitos secundarios, como son los carotenoides[3]. El licopeno, es un carotenoide responsable del color rojo del tomate de árbol[4], se ha demostrado que el licopeno es un carotenoide con actividad antioxidante[5] beneficioso para la salud humana, pues reduce el colesterol LDL, disminuye la cantidad de infartos, combate algunos tipos de cáncer y reduce el envejecimiento celular[6]. Siendo ésta una alternativa, para el aprovechamiento de los desechos agroindustriales provenientes del tomate de árbol.

El licopeno no es estable, debiendo su degradación a efectos de la temperatura, la luz u otros efectos de condiciones ambientales[7], razón por la que se debe buscar alternativas o métodos de conservación como es la microencapsulación mediante el secado por aspersión para proteger al licopeno de la oxidación[8].

Existen investigaciones previas de obtención de carotenoides a nivel laboratorio y nivel de banco[9-12], el objetivo de la presente investigación es evaluar industrialmente el proceso extracción y microencapsulación del licopeno a partir de los desechos del tomate de árbol (*Solanum betaceum*) mediante secado por aspersión.

Materiales y métodos

La obtención del extracto y microencapsulado de licopeno se realizó en la empresa Andes Kinkuna S.A. ubicada en Pujilí-Ecuador y los análisis físico-químicos, capacidad antioxidante se realizaron en la Universidad Técnica de Ambato, Facultad de Ciencia en Ingeniería en Alimentos y Biotecnología.

Obtención del extracto de Licopeno

Se trabajó a nivel industrial a partir de cáscaras del tomate de árbol (*Solanum betaceum*) que constituyen el residual de la fabricación de pulpa de tomate de árbol de una empresa procesadora de frutas.

Las cáscaras de tomate de árbol (*Solanum betaceum*), posteriormente se secaron a una temperatura de 50 °C durante 55 horas y fueron molinadas en un molino de cuchillas hasta obtener un tamaño de partículas finas (≤ 250 µm) de acuerdo a la metodología de Cardona *et.al*[13].

Para la obtención del extracto, se mezclaron en una relación de material vegetal/volumen de disolvente de 1:70, el disolvente orgánico que se empleó fue etanol industrial al 96 %, con un tiempo de extracción de 30 minutos a una temperatura de 50 °C[9]. Se produjeron 3 lotes consecutivos de extractos.

Obtención del microencapsulado

Una vez obtenido el extracto de licopeno, se realizó una mezcla con 85 % de goma arábiga y maltodextrina y 15 % de agua destilada , para luego pasar a una homogenización de 200 min^{-1} durante 10 minutos y microencapsular en un secador por aspersión industrial de 100 kg/h de capacidad de evaporación de agua, empleando una temperatura de entrada de 120 °C y una temperatura de salida de 80 °C[9].

Eficiencia de Extracción

Se determinó la eficiencia de extracción a través de la relación entre la masa de licopenos extraídos (mL) y la masa de material vegetal (MV) utilizado, expresado en la ecuación I[14].

Ecuación 1. Porcentaje de eficiencia de extracción

$$\%EE = \left(\frac{mL}{mv}\right) \times 100 \quad \text{(I)}$$

Donde:
mL=masa de licopenos extraídos
mv= masa del material vegetal

Concentración de Licopeno

Se utilizó el etanol como blanco, en donde se midió la absorbancia de cada extracto a una longitud de onda de 472 nm, el equipo que se utilizó fue el espectrofotómetro Fisher Scientific accuSkan GO. La ecuación II, se expresa en mgL^{-1} [15].

Ecuación II. Concentración de Licopeno

$$C = \frac{A \times 10^4}{E} \quad \text{(II)}$$

Donde:
A= absorbancia del extracto a 472nm
E= coeficiente de absortividad del etanol de 3450

Eficiencia de microencapsulación

Se realizó una dilución 1/10 de los lotes de microencapsulado tanto en agua como en etanol al 96 %, posteriormente estas soluciones se agitaron durante un tiempo de 15 minutos, se filtraron y se midió su absorbancia en el espectrofotómetro Fisher Scientific accuSkan GO a 515 nm[16].

Ecuación III. Eficiencia de microencapsulación

Donde:

$$E.M = \frac{CA\ agua - CE\ etanol}{CA\ agua} \times 100 \quad \text{(III)}$$

CA= concentración de licopeno en agua
CE= concentración de licopeno en etanol

Determinación de pH

Las muestras del extracto, se determinaron por triplicado con el pH-metro (Thermo Scientific ORION VERSASTAR).

Determinación de índice de refracción

Las muestras del extracto se determinaron por triplicado en el refractómetro Abbe Nar 2T a temperatura ambiente[17].

Determinación de viscosidad

Las muestras del extracto se determinaron por triplicado con el viscosímetro Quimis, las muestras fueron tomadas a temperatura ambiente.

Determinación de humedad

A las muestras del microencapsulado, se le determinó la humedad por triplicado empleando una balanza Citizen MB 50, colocando una muestra de 5 g en el plato. El resultado obtenido fue expresado en porcentaje.

Espectroscopía Infrarroja de la transformada de Fourier

Se comparó un lote del extracto sin microencapsular, con los tres lotes del microencapsulado en un intervalo desde 500 hasta 4000 cm^{-1}, el equipo que se usó fue FTIR espectrofotómetro Perkin Elmer Spectrum Two.

Morfología y aspecto de la superficie de las microcápsulas

Se estudió la morfología de las microcápsulas empleando un Microscopio Electrónico de Barrido (SEM) modelo Tescan Vega3 con aumento hasta 10000X. Las muestras de 3 lotes de licopeno microencapsulado se prepararon y fijaron sobre cinta de carbono de doble faz que se adhiere en un portamuestras de aluminio de 13mm; y al ser un material orgánico se recubrieron con una fina capa de oro utilizando un dispositivo de recubrimiento por pulverización catódica SPI-Module proceso necesario para que la muestra a ser analizada sea conductora de los electrones que emergen de la fuente de tungsteno del equipo. La obtención de las imágenes se realizó con una energía de 8 a 10 keV (HV High Voltage) en alto vacío (HV High Vacuum) con el detector de Electrones Secundarios (SE).

Actividad antioxidante *in vivo*

Se usó *Saccharomyces cerevisiae* ATCC 9763 como modelo de estudio, partiendo de una cepa de reserva de *Saccharomyces cerevisiae*, cultivada en el medio compuesto por extracto de levadura, peptona, dextrosa, (YPD) mediante siembra en estría durante 5 días a una temperatura de 28 °C.

Posteriormente se inoculó la cepa de *Saccharommyces cerevisiae* en 5 ml de caldo YPD incubándola a 28 °C durante 24 horas.

Al siguiente día se tomaron 5 □L de esa solución y se colocaron en 3 ml de caldo YPD, tomando esta solución como solución estándar para todos los tubos.

Se preparó una solución de peróxido de hidrógeno 0,5 mmol/L y de 5 mmol/L, además de soluciones de microencapsulados a una concentración de 25 mg/ml.

También se preparó una solución de vitamina C, con 25 mg/ml (control positivo)

En cada tubo se fue añadiendo 5 µL de la solución de levadura más 3 ml del caldo YPD y 1 ml de las soluciones preparadas, dejando un tubo únicamente con los 3 ml de caldo YPD y los 5 µL de la solución de levadura (denominado tubo control)

Estas soluciones fueron llevadas a incubación durante 18 horas a 28 °C.

Al siguiente día se centrifugaron a 2700 min^{-1} durante 10 min, luego se eliminó el líquido, quedando la levadura precipitada, la cual fue lavada con una solución búfer fosfato salino de pH 7,2, midiendo la absorbancia de cada tubo y ajustandola a 600 nm.

Posteriormente en cada tubo se añadieron las soluciones de peróxido de hidrógeno 0,5 mmol/l y 5 mmol/l, a excepción de en los tubos control, pues a estos tubos no se les añadió peróxido.

Nuevamente se centrifugó a 2700 min^{-1} durante 10 minutos, eliminando la parte acuosa y con el precipitado, que es *Saccharommyces cerevisiae*, se realizó un lavado con solución de búffer fosfato salino, luego se añadió en cada tubo 3 ml de caldo YPD.

Finalmente en la placa de 96 pocillos se tomaron 250 µL de cada una de las soluciones, se midieron en el espectrofotómetro Fisher Scientific accuSkan GO a 30 °C durante 18 horas, las mediciones se realizaron por triplicado, con las que se construyeron las curvas de crecimiento[18,19].

Actividad antioxidante *in vitro*

Se utilizó el método del 2,2-difenil-1-picrilhidrazilo conocido como (DPPH)[20].

El cual consistió en preparar una solución madre de 500 $\cdot 10^{-6}$ mol/l de trolox (0,0129 g de trolox en 50 ml de etanol al 96 % y 50 ml de agua destilada).

Posteriormente se realizaron varias diluciones a partir de la solución madre, obteniendo estándares de: 50 µmol/l, 100 µmol/l, 200 µmol/l, 300 µmol/l, 400 µmol/l y 500 µmol/l. También se preparó una solución de 150 $\cdot 10^{-6}$ mol/l de DPPH. Estas soluciones se protegieron de la luz y del calor.

Adicional se realizó una dilución de los tres lotes de microencapsulado en polvo 1/200 en una solución de agua-etanol 50:50.

Luego se realizó una dilución 1/200 de los tres lotes del concentrado del extracto en una solución de agua -etanol 50:50.

Posteriormente se colocó en la placa de 96 pocillos, 20 µl de cada una de las soluciones preparadas con 180 µl de la solución de 150 $\cdot 10^{-6}$ mol/l de DPPH. Denominándose Am (absorbancia de la muestra).

También se colocó en la misma placa de 96 pocillos 20µl de la solución agua-etanol 50:50 con 180µl de la solución de 150 $\cdot 10^{-6}$ mol/l de DPPH. Denominándose Ac (absorbancia control).

En la misma placa de 96 pocillos se colocaron 20µl de agua con 180µl de metanol. Denominándose Ab (absorbancia del blanco).

Se llevó la placa al espectrofotómetro Fisher Scientific accuSkan GO, incubándole durante 40 min a temperatura ambiente y leyendo su absorbancia de 515 nm.

Con los resultados obtenidos, se calculó el porcentaje de inhibición del DPPH, establecidos mediante la ecuación IV.

Ecuación IV. Porcentaje de inhibición del DPPH

$$\%Inhibición\ del\ DPPH = \left(1 - \left(\frac{Am-Ab}{Ac-Ab}\right)\right) x\ 100 \quad (IV)$$

Donde:
Am= absorbancia de la muestra
Ab= absorbancia del blanco
Ac= absorbancia control

Resultados y discusión

Caracterización del extracto líquido

Se obtuvieron tres lotes del extracto líquido, en la tabla 1 muestra la eficiencia de extracción, pH, índice de refracción y viscosidad del extracto líquido.

Los resultados de eficiencia de extracción (tabla 1) muestran un promedio de 35,69 mg/kg a partir de cáscara de tomate de árbol, estudios a nivel de banco indican que se obtiene una eficiencia de 34,34 mg/kg[9] lo que demues-

Lote	Eficiencia de Extracción (mg/kg)	pH	Índice de Refracción	Viscosidad (mPas)
1	48,90	5,37±0,01	1,44±0,001	112,40±0,361
2	31,10	5,65±,0,02	1,41±0,001	110,37±0,379
3	27,08	5,59±,0,07	1,41±0,002	114,50±0,346

Tabla 1. Caracterización de los extractos líquidos de licopeno.

tra que se obtienen similares resultados, cuando se emplea el mismo proceso de extracción con etanol al 96 %.

Otros estudios muestran una eficiencia de extracción de 559,9 mg de licopeno/kg de pulpa de tomate de árbol[13], este valor más alto se debe a la composición misma de la cáscara la cual contiene menor cantidad de licopeno en comparación con la pulpa de tomate de árbol. En otros trabajos se encontró una eficiencia de extracción de 12,2 mg/kg[11] en cáscaras de tomate de árbol obteniendo una menor eficiencia con respecto a los resultados obtenidos, lo cual indica que la eficiencia de extracción también está relacionada con la variedad de la fruta, época de cosecha y estado de madurez. El estado de madurez influye decisivamente en la composición de carotenoides, existen mayores niveles de carotenoides cuando han sido expuestos en mayor tiempo a la luz del sol y a elevadas temperaturas[13]. En lo que se refiere a condiciones de manejo influyen muchísimo el disolvente utilizado y las condiciones de temperatura a la que se realiza la extracción, obteniendo resultados favorables a 50 °C y con etanol al 96 %.

El valor de pH promedio del extracto líquido (tabla 1) obtenido fue de 5,54 a 20 °C, obteniendo un pH ácido, el cual fue influenciado por las características del disolvente, que en este caso fue el etanol. Estudios muestran un pH del extracto de licopeno de 4,68 usando como disolvente ácidos grasos[21]. Demostrando así que el pH del extracto tiene una relación directa con el tipo de disolvente que se utiliza en la extracción.

Comparando los resultados obtenidos a nivel industrial con los obtenidos a nivel de laboratorio se encuentran valores similares, obteniendo a nivel de laboratorio un pH desde 5,58 hasta 5,68[22].

El índice de refracción del extracto líquido (tabla 1) muestra un promedio de 1,42 a 15 °C, mientras que estudios a nivel de banco muestran para el extracto de licopeno un índice de refracción de 1,363[22]; variando un poco el resultado por la temperatura a la que se realizó la medición. El índice de refracción tiene una correlación con la concentración de sólidos y el disolvente, que en este caso fue etanol al 95 %, demostrando así las propiedades activas y la calidad del extracto obtenido[23].

Respecto a la viscosidad (tabla 1) se obtuvo un promedio de 112,42 mPas a 20 °C, estudios con extracto de semilla de mango muestran viscosidades de extractos desde 48 – 115 cP, que es equivalente a mPas[24] encontrándose el valor de viscosidad dentro de este intervalo.

Caracterización del microencapsulado

En la tabla 2 se muestra la concentración del licopeno, eficiencia y humedad del microencapsulado, para los lotes 1, 2 y 3 respectivamente.

En esta escala (tabla 2) se obtuvo un promedio de concentración de licopeno de 44,07 mg/kg, que comparando con estudios realizados a nivel de banco, en las mismas condiciones, se obtuvo una concentración de licopeno inferior, de 34,34 mg/kg[9].

En lo que se refiere a la eficiencia de microencapsulación (tabla 2), se obtuvo una eficiencia de microencapsulación superior al 90 %, por lo que se considera una eficiencia adecuada, estudios demuestran que la microencapsulación es buena cuando se alcanza una máxima cantidad del material a encapsular dentro de las partículas de polvo, una buena estabilidad de las microcápsulas y prevención de la pérdida de compuestos volátiles (González & Martínez, 2015). Estudios a nivel de laboratorio indican una eficiencia de microencapsulación del 84 %[10] demostrándose que el uso de los polímeros goma arábiga y maltodextrina son eficientes para la microencapsulación.

La humedad de los microencapsulados en polvo (tabla 2) fue aproximadamente de 6,15 %, al comparar con la normativa Ecuatoriana, normas INEN 616[25], se encuentra dentro del valor aceptable de humedad, pues la norma permite un porcentaje máximo de humedad del 14 % y en la farmacopea de los Estados Unidos un máximo del 10 %[26]. El valor de humedad tiene un alto impacto en la vida útil del producto, mientras menor es la humedad menor riesgo tiene de contaminación microbiana, la degradación de la pared de la microcápsula, evitando así degradaciones químicas y biológicas[27]. Lo que demuestra que el secado por aspersión es un método eficiente para reducir el contenido de agua de los microencapsulados.

Lote	Concentración de Licopeno (mg/kg)	Eficiencia de microencapsulación (%)	Humedad (%)
1	43,78	93,61	6,33±0,54
2	45,20	90,44	6,62±,0,36
3	43,22	97,78	5,89±,0,40

Tabla 2. Concentración de licopeno, eficiencia y humedad del microencapsulado.

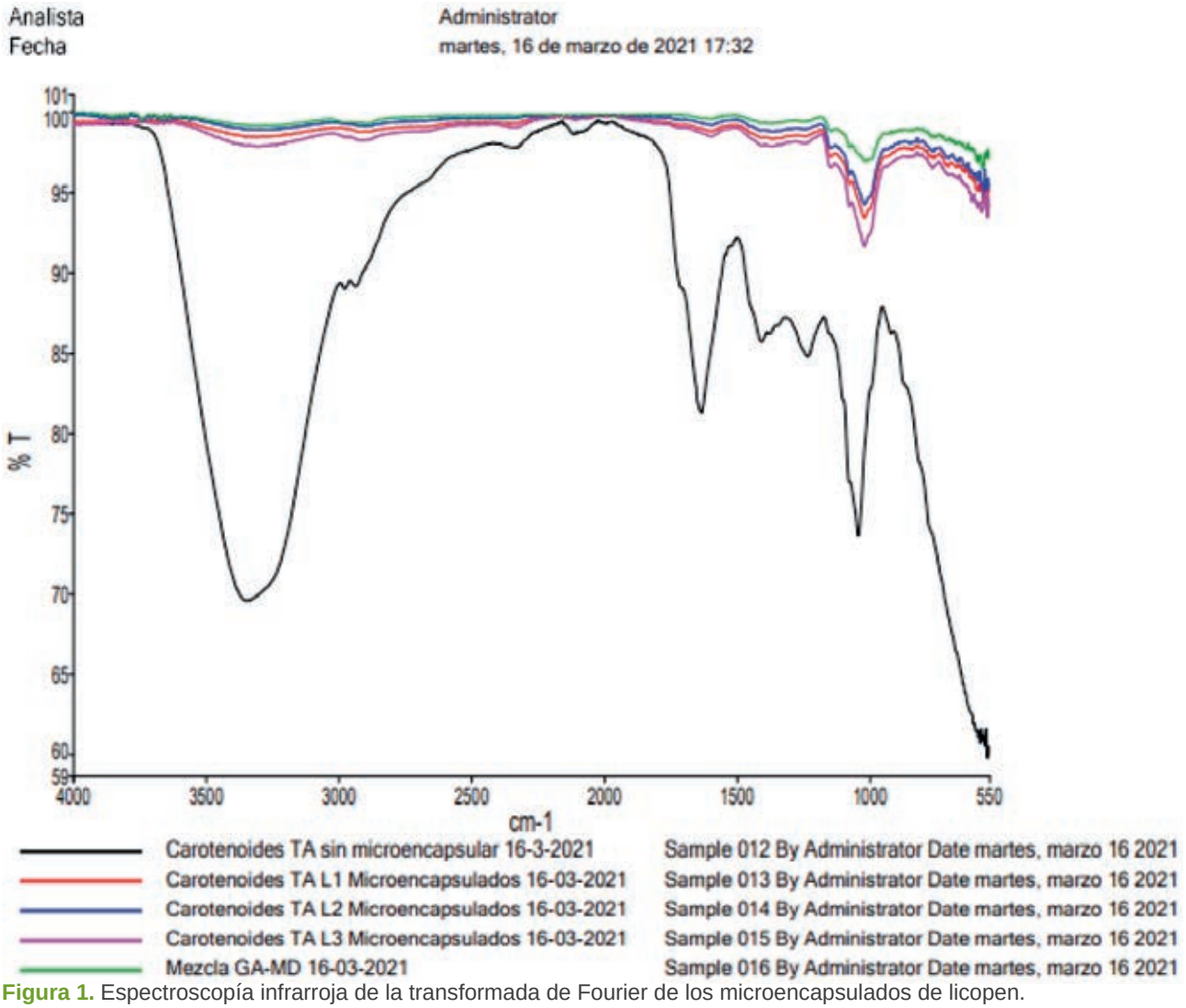

Figura 1. Espectroscopía infrarroja de la transformada de Fourier de los microencapsulados de licopen.

Espectroscopía infrarroja de la transformada de Fourier

En la figura 1 se muestra el resultado de la espectroscopia infrarroja de los microencapsulados en los lotes 1,2 y 3, además de un extracto líquido antes de realizar el proceso de microencapsulación.

En lo que respecta a la espectroscopia infrarroja de la transformada de Fourier (figura 1), la banda alrededor de 1000 cm^{-1} indica en los microencapsulados que el licopeno está enmascarado por la mezcla polimérica, lo que demuestra la efectividad del proceso de microencapsulación, estudios similares muestran la presencia de licopeno en bandas entre los 850 cm^{-1} y hasta los 1200 cm^{-1}, mientras mayor es la intensidad de la banda, mayor será el contenido de licopeno, siendo los espectros de la transformada de Fourier importantes características de absorción en la región de huellas dactilares con bandas de absorción debidas a vibraciones de deformación carbono-oxígeno[28]. Esta banda característica también demuestra que existe presencia de licopeno en el interior de las microcápsulas.

Morfología y aspecto de la superficie de las microcápsulas

En la figura 2 se muestran imágenes de microscopía de barrido electrónico de las microcápsulas de los tres lotes obtenidos.

Las microcápsulas formadas en los 3 lotes, tienen una morfología similar, siendo esféricas las partículas, presentan una superficie exterior redondeada con la formación de concavidades poco homogéneas. La aparición de irregularidades en la superficie, se atribuye a la rápida evaporación del agua durante el proceso de secado por aspersión y ha sido reportado también por otros autores[29,30]. También se puede observar la presencia de esferas con superficie lisa, los tamaños de las microcápsulas son del orden de decenas de micrómetros (10 -70 µm), lo que concuerda con el intervalo de tamaños que genera el tipo de atomizador empleado.

Como se aprecia, las superficies externas de las microcápsulas presentan paredes continuas sin fisuras o grietas (figura 3), lo que garantiza la retención del licopeno. En el lado superior izquierdo de la figura 3a se observa una microcápsula fragmentada, donde se evidencia la pared compacta y homogénea generada por el proceso de microencapsulación.

La figura 4 muestra el crecimiento de Saccharomyces cerevisiae durante 18 horas, al ser sometida a los diferentes microencapsulados (lote 1, lote 2 y lote 3), control positivo (vitamina C) y control negativo (solo Saccharomyces cerevisiae) y peróxido de hidrógeno con una concentración 0,5 mmol/L.

En la figura 4, se observa que en la curva control, el

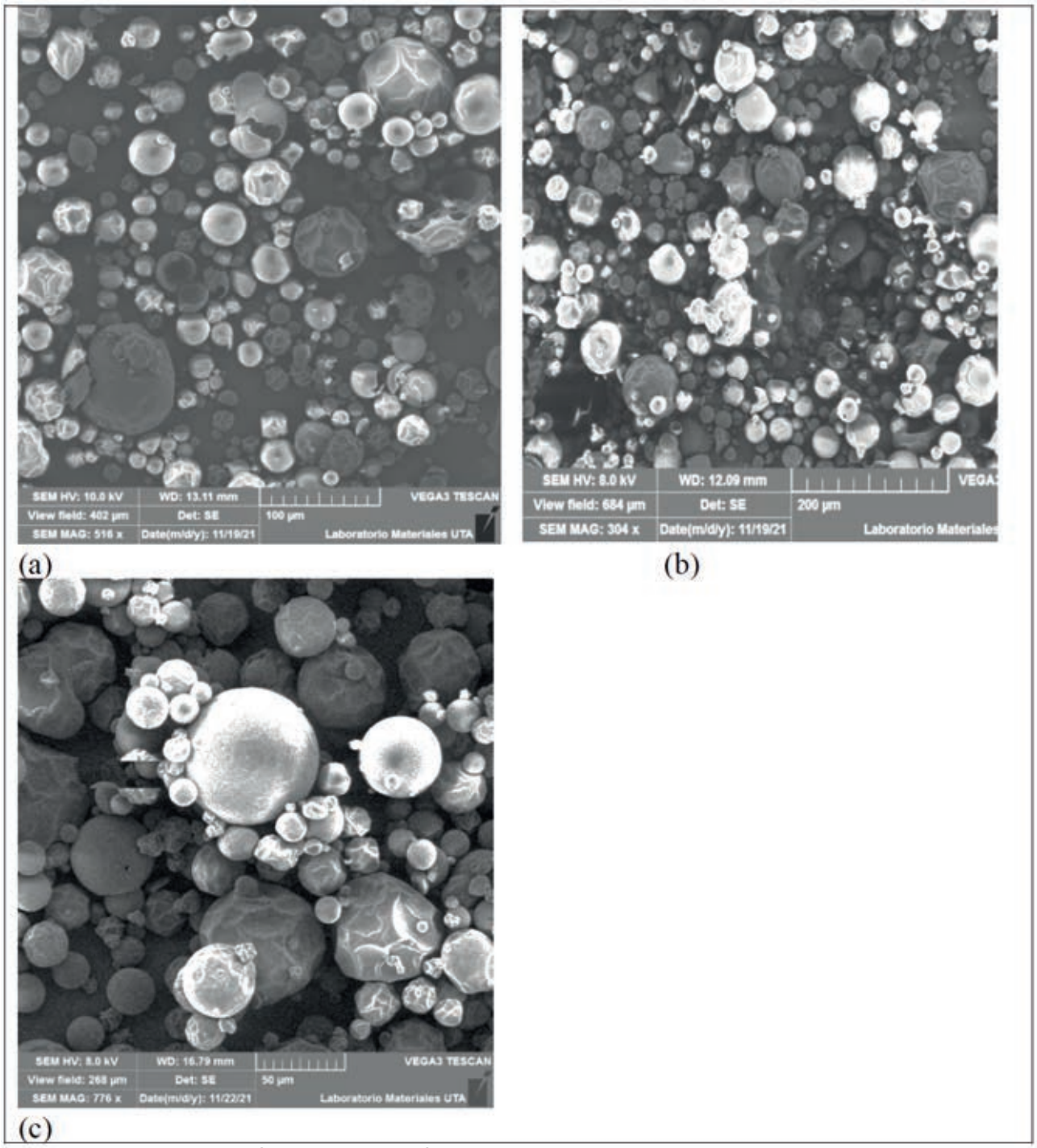

Figura 2. Fotos de Microscopía de barrido electrónico de los microencapsulados de licopeno (a) Lote 1 con aumento de 516X, (b) Lote 2 con un aumento de 304X y (c) Lote 3 con aumento de 776X.

microorganismo tuvo un crecimiento más rápido debido a que no estuvo sometido a ningún estrés.

La curva de peróxido, muestra el crecimiento de Saccharomyces cerevisiae sometida sólo al peróxido de hidrógeno teniendo como resultado el crecimiento más lento de la levadura, debido a que fue sometida al mayor estrés. Resultados similares se encontraron con peróxido de hidrógeno 0,3 mmol/l[31], investigaciones demuestran que el peróxido produce radicales libres de oxígeno, siendo tóxico para las levaduras, produciendo un estrés oxidativo[32].

Los tres lotes tuvieron un crecimiento similar y comparable al control de la vitamina C. Este crecimiento fue igual al de la curva control hasta los 160 min, luego el crecimiento de la levadura disminuyó y se demoró hasta alcanzar la fase estacionaria. La vitamina C es un eficaz antioxidante que favorece el metabolismo de la levadura[33]. Demostrando así que la vitamina C, al igual que los microencapsulados tienen propiedades antioxidantes sobre la levadura utilizada en este estudio.

La curva control alcanzó la fase estacionaria a los 440 min, mientras que las curvas con los tres lotes de microencapsulados de licopeno y vitamina C, alcanzaron la fase estacionaria a los 560 min y finalmente la curva que fue con peróxido de hidrógeno tardó más tiempo, alcanzando la fase estacionaria a los 660 min. Esto demuestra que los microencapsulados tienen capacidad antioxidante, corro-

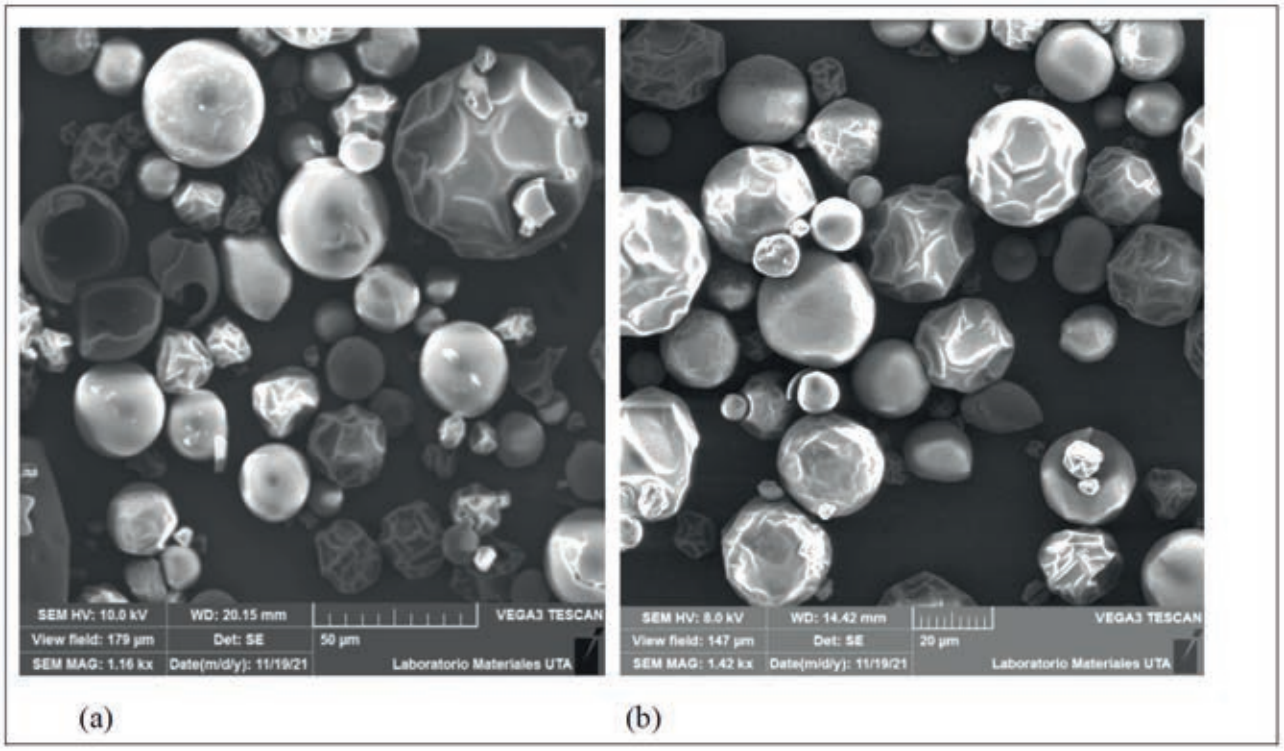

Figura 3. Imágenes de Microscopía de barrido electrónico de los microencapsulados de licopeno (a) Lote 1 con aumento de 516X, (b) Lote 2 con un aumento de 304X.

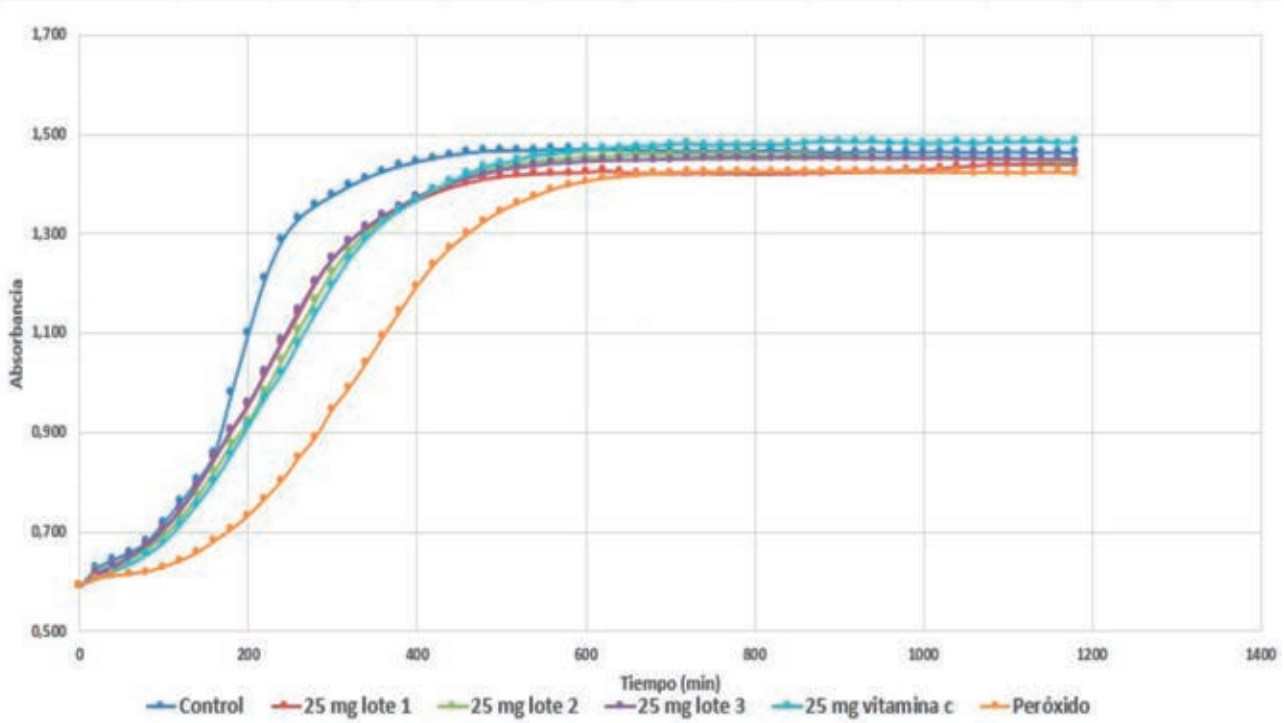

Figura 4. Curva de crecimiento de *Saccharomyces cerevisiae* frente al estrés oxidativo de H_2O_2 con una concentración 0,5 mmol/L.

borando éstos resultados en licopeno de tomate de árbol[34].

Referente a la fase de adaptación tanto los tratamientos que fueron microencapsulados, como control positivo y negativo tardaron 60 min, pero el tratamiento que fue sometido con peróxido tardó en adaptarse 100 min. La variación con respecto al peróxido de hidrógeno se debe, a que éste genera radicales hidroxilos, lo que produce un estrés oxidativo[35].

En la figura 5, se observa el crecimiento de Saccharomyces cerevisiae expuesta a una concentración de peróxido de hidrógeno 5 mmol/l, encontrando en la fase de adaptación de los tres lotes de microencapsulados y el control un tiempo de 60 minutos, existiendo variación con respecto al tiempo en la fase de adaptación en el tratamiento que fue sometido al peróxido de hidrógeno, donde la levadura tardó en adaptarse 100 min. Esta variación se debió a que el peróxido produjo un estrés en las mitocondrias de la levadura[36]. Con respecto a la fase de crecimiento, en el

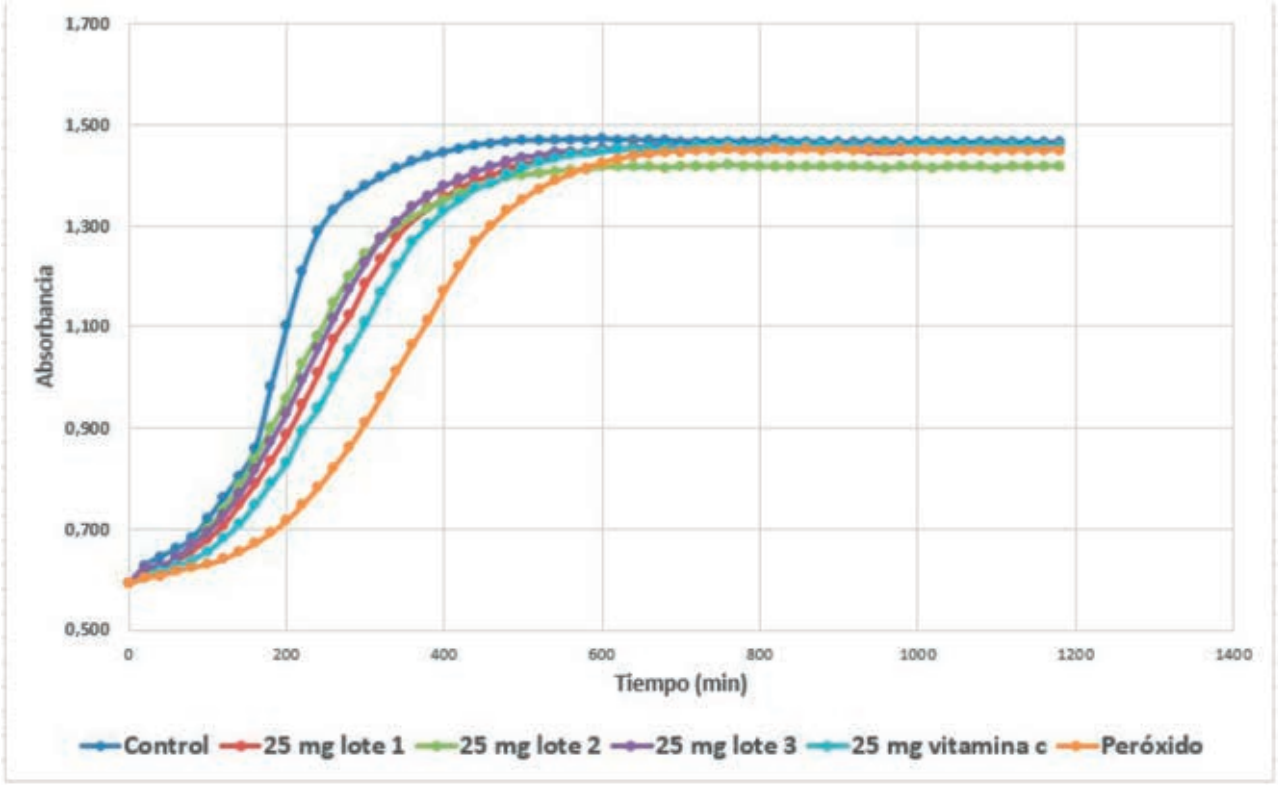

Figura 5. Curva de crecimiento de *Saccharomyces cerevisiae* frente al estrés oxidativo de H_2O_2 con una concentración 5 mmol/L.

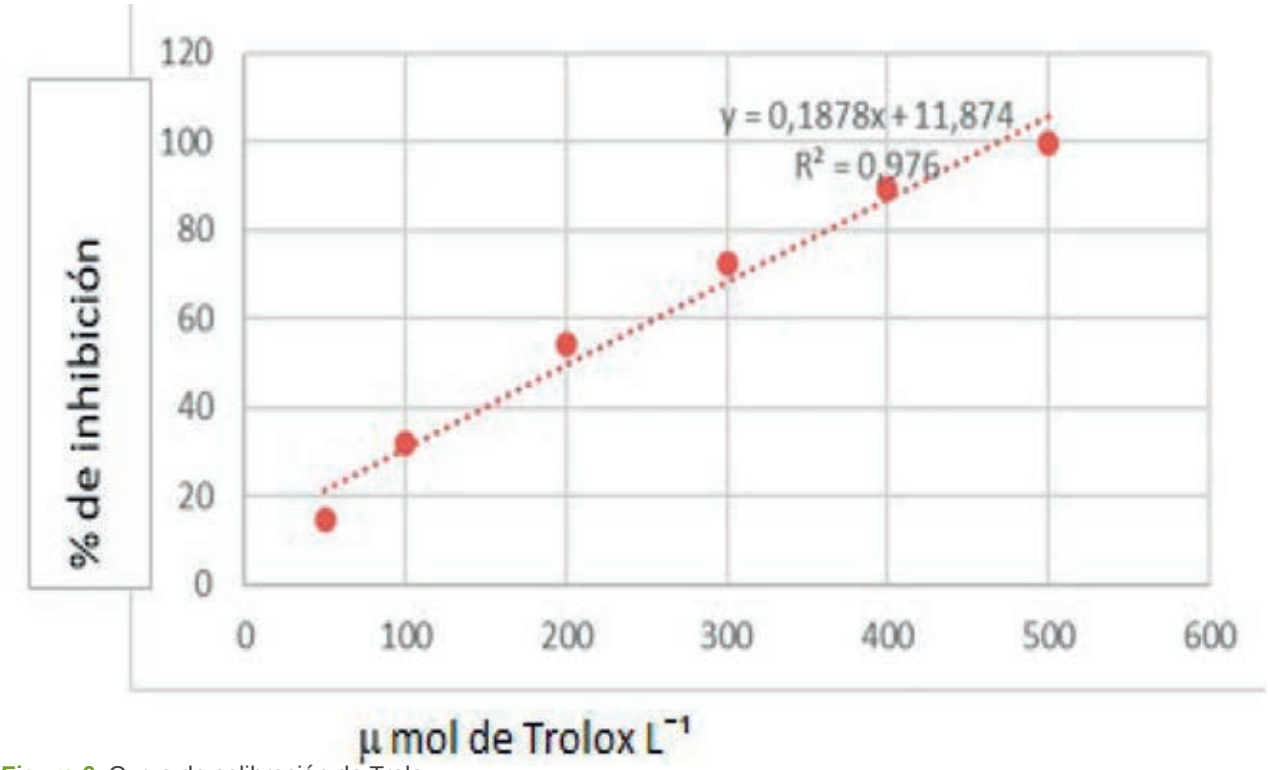

Figura 6. Curva de calibración de Trolox.

tratamiento control tarda 480 minutos en crecer, en cambio en los tres lotes de microencapsulados y vitamina C, tarda 560 min y con el peróxido de hidrógeno tarda 680 min en crecer. Demostrando así la actividad antioxidante que tienen los microencapsulados sobre la levadura.

Si se comparan los resultados obtenidos en la concentración de peróxido de hidrógeno 0,5 mmol/l con respecto a la gráfica obtenida con una concentración de peróxido de hidrógeno 5 mol/l se aprecia que una mayor concentración, influye en el crecimiento de la levadura, necesitando más tiempo para crecer.

Actividad antioxidante in vitro

En la figura 6, se muestra la curva de calibración de

Lote	% de inhibición	µmol equivalentes de Trolox L-1
1	48,03	192,50
2	35,07	123,52
3	38,07	139,50

Tabla 3. Resultados de inhibición por DPPH de los lotes de microencapsulado.

Trolox para la determinación de la actividad antioxidante in vitro del microencapsulado de licopeno, obteniendo un coeficiente de correlación lineal de 0,976, muy cercano a 1, lo que indica que existe una relación directa entre la concentración de trolox y el porcentaje de inhibición.

La tabla 3. muestra los resultados de inhibición de DPPH de los lotes microencapsulados. La técnica del DPPH (1,1 difenil-2picril-hidrazilo), se usa para evaluar la capacidad antioxidante de alimentos, este método se fundamenta en que el DPPH es un radical libre que al juntarse con el antioxidante produce una reacción redox de primer orden[37,38]. Consiguiendo similares resultados con el microencapsulado de licopeno, tanto a escala de banco con un equivalente a trolox de 142,72 µmoll^{-1} [9] como a nivel industrial, lo que demuestra que la tecnología usada para la microencapsulación de licopeno a partir de las cáscaras de tomate de árbol, es altamente efectiva.

Conclusiones

Se concluye que el método de microencapsulación empleado para el licopeno es efectivo para ser usada a nivel industrial, generando una elevada eficiencia de microencapsulación, siendo una tecnología que puede ser implementada en la industria para el aprovechamiento de los desechos agroindustriales de la cáscara de tomate de árbol, brindando beneficios para la salud de las personas por sus características antioxidantes.

Se caracterizó fisicoquímicamente el ingrediente bioactivo licopeno, encontrando en el extracto líquido un pH de 5,54 a 20 °C, obteniendo un pH ácido, el cual fue influenciado por las características del disolvente, que en este caso fue el etanol, un índice de refracción de aproximadamente 1,42 el cual tiene una relación directa con la concentración de sólidos, además del disolvente y una viscosidad de 112,42 mPas, en lo que se refiere al microencapsulado se obtuvo una humedad del 6,15 % siendo un valor que garantizará en el tiempo de la vida útil del producto, encontrándose acorde a la farmacopea de los Estados Unidos. Con respecto a la espectroscopía infrarroja de la transformada de Fourier, se evidencia que en los microencapsulados el licopeno está protegido por la mezcla polimérica, lo que demuestra la eficiencia del proceso de microencapsulación. Se obtuvieron microcápsulas con forma esfeérica, superficie lisa lo cual es de gran importancia también para la vida útil del producto.

Se demostró la capacidad antioxidante *in vivo* de los microencapsulados, en *Saccharomyces cerevisiae*, encontrándose que tienen una actividad antioxidante similar a la de la vitamina C. También se evaluó la capacidad antioxidante *in vitro* mediante el método del DPPH, encontrando un equivalente de trolox de 192,50 µmoll^{-1}, 123,53 µmoll^{-1} y 139,51 µmoll^{-1} en los tres lotes y respectivamente con un porcentaje de inhibición del 48,03 %, 35,07 % y 38,07 %.

Financiamiento

Este trabajo no recibió financiamiento externo.

Declaración de la Junta de Revisión Institucional

No aplicable.

Informed Consent Statement

No applicable

Declaración de disponibilidad de datos

Trabajo inédito

Agradecimientos

A la Agencia Española de Cooperación Internacional para el Desarrollo (AECID) y a la empresa Andes Kinkuna S.A.

Conflictos de Interés

Los autores declaran no tener conflicto de interés.

Referencias bibliográficas

1. Pataro, G., Carullo, D., Falcone, M. & Ferrari, G. Recovery of lycopene from industrially derived tomato processing by-products by pulsed electric fields-assisted extraction. Innov. Food Sci. Emerg. Technol. 63, 102369 (2020).
2. Martínez-Navarrete, N., del Mar Camacho Vidal, M. & José Martínez Lahuerta, J. Los compuestos bioactivos de las frutas y sus efectos en la salud. Act. Diet. 12, 64-68 (2008).
3. Reyna, M., Bojórquez, C., González, J. & Sánchez, P. Propiedades funcionales y beneficios para la salud del licopeno. Nutr. Hosp. 28, 6-15 (2013).
4. Salazar-lugo, R., Barahona, A., Ortiz, K., Chávez, C. & Freire, P. Efecto del consumo de jugo de tomate de árbol (Cyphomandra betacea) sobre el perfil lipídico y las concentraciones de glucosa en adultos con hiperlipidemia , Ecuador . Arch. Latinoam. nitrición 66, 121-127 (2016).
5. Tan, S. et al. Lycopene, polyphenols and antioxidant activities of three characteristic tomato cultivars subjectes to two drying methods. Food Chem. 338, (2020).
6. Lorenzo Fuentes, J. Las plantas como fuente de compuestos fotoprotectores frente al daño en el ADN producido por la radiación ultravioleta. Ciencias la Tierra 43, 550-562 (2019).
7. Periago, M. J., Martínez-valverde, I. & Ros, G. Propiedades biologicas y valor nutritivo del licopeno. Ant. Vet, 66, 51-66 (2001).
8. González, E. & Martínez, O. Microencapsulación mediante secado por aspersión de compuestos bioactivos. Rev. Iberoam. Tecnol. Postcosecha 162, 180-192 (2015).
9. Urbina, W., Fernández, D., López, O. & Iraizoz, A. Obtención de un extracto rico en carotenoides con capacidad antioxidante a escala de banco a partir de residuos agroindustriales de tomate de árbol (Solanum betaceum). Rev. Bionatura 5, 1356-1362 (2020).
10. Perez, C. & Fernandez, D. Extracción y microencapsulación de licopenos provenientes de residuos agroindustriales del tomate de árbol (Solanum betaceum). (Tesis de prefrado (Universidad Técnica de Ambato), 2019).

11. Candelas, M., Alanis, M. & Río, F. Lycopene measurement and other carotenoids in tomato and tomato powder . Rev. Mex. Agronegocios X, 1-13 (2006).
12. Shu, B., Yu, W., Zhao, Y. & Liu, X. Study on microencapsulation of lycopene by spray-drying. J. Food Eng. 76, 664-669 (2006).
13. Cardona, E. & Rios, L. Extraction of the carotenoid lycopene from chonto tomato (lycopersicum esculentum). Vitae 13, 44-53 (2006).
14. Strati, I. F. & Oreopoulou, V. Effect of extraction parameters on the carotenoid recovery from tomato waste. Int. J. Food Sci. Technol. 46, 23-29 (2011).
15. Strati, I. & Oreopoulou, V. Process optimisation for recovery of carotenoids from tomato waste. Food Chem. 129, 747-752 (2011).
16. Pérez, C. & Fernández, D. Extracción y microencapsulación de licopenos provenientes de residuos agroindustriales del tomate de árbol (Solanum betaceum). ((tesis de pregrado) Universidad Técnica de Ambato, 2019).
17. Cromer, A. H. & Fernández, J. Física en la ciencia y en la industria. (Reverté, 1998).
18. Peláez, P. & Montoya, P. Validación funcional de extractos polifenólicos de cacao mediante ensayos in vivo con organismos modelo. ((Tesis Doctoral) Universidad de Valencia, 2016).
19. Calle, D. & López, D. Extracción y microencapsulación de carotenoides de chonta (Bactris gasipaes). (Técnica de Ambato, 2020).
20. Bobo-García, G. et al. Intra-laboratory validation of microplate methods for total phenolic content and antioxidant activity on polyphenolic extracts, and comparison with conventional spectrophotometric methods. J. Sci. Food Agric. 95, 204-209 (2015).
21. Delgado, L. & Mallama, C. Evaluación del extracto de licopeno partiendo de residuos de diferentes frutas y hortalizas, aplicado en un producto cosmético. Fundación Universidad de América vol. 8 (2019).
22. Urbina, W. Obtención de un extracto rico en carotenoides con capacidad antioxidante a escala de banco a partir de residuos agroindustriales de tomate de árbol (Solanum betaceum). Universidad Técnica de Ambato (Universidad Técnica de Ambato, 2019).
23. Zhao, H. et al. The evaluation and selection of core materials for microencapsulation: A case study with fragrances. Flavour Fragr. J. 36, 652-661 (2021).
24. Maisuthisakul, P. & Gordon, M. H. Influence of polysaccharides and storage during processing on the properties of mango seed kernel extract (microencapsulation). Food Chem. 134, 1453-1460 (2012).
25. NTE. Instituto Ecuatoriano de Normalizacion. Instituto Ecuatoriano de Normalización 21 (2015).
26. Pharmacopoeia of United States USP, N. Reference Standards of Dietary Supplements and Herbal Medicines. https://store.usp.org/product/1370881#ads (2018).
27. Esquivel-González, B., Martínez-L, O. & Rutiaga-Quiñones, O. Microencapsulación mediante secado por aspersión de compuestos bioactivos. Rev. Iberoam. Tecnol. Postcosecha 16, 180-192 (2015).
28. Bunghez, I. R., Raduly, M., Doncea, S., Aksahin, I. & Ion, R. M. Lycopene determination in tomatoes by different spectral techniques (UV-VIS, FTIR and HPLC). Dig. J. Nanomater. Biostructures 6, 1349-1356 (2011).
29. Rosenberg, M., Talmon, Y., Kopelman, I. J. A scanning electron microscopy study of microencapsulation. Food Sci. 50, 139-144 (1985).
30. Buffo, R. A., Probst, K., Zehentbauer, G., Luo, Z. & Reineccius, G. A. Effects of agglomeration on the properties of spray-dried encapsulated flavours. Flavour Fragr. J. 17, 292-299 (2002).
31. Proaño, J. & Fernández Rivero, D. Extracción asistida por ultrasonido de licopenos provenientes de residuos agroindustriales de tomate de árbol (Solanum betaceum Cav.) con capacidad antioxidante. (Universidad Técnica de Ambato, 2021).
32. Folch-Mallol, L., Garay-Arroyo, J., Lledías, A. & Covarrubias Robles, F. La respuesta a estrés en la levadura Saccharomyces cerevisiae. Rev. Latinoam. Microbiol. 46, 24-45 (2004).
33. Saffi, J., Sonego, L., Varela, Q. D. & Salvador, M. Antioxidant activity of L-ascorbic acid in wild-type and superoxide dismutase deficient strains of Saccharomyces cerevisiae. Redox Rep. 11, 179-184 (2006).
34. Pazmiño, D. & Rivero Fernández, D. APROBACIÓN DEL TUTOR. (Universidad Técnica de Ambato, 2019).
35. Macedo-Marquez, A. Tip Revista Especializada en Ciencias. Tip Rev. Espec. en Ciencias Químico-Biológicas 15, 97-103 (2012).
36. Vargas, V. Avances en Química Universidad de los Andes. 2, 3-15 (2007).
37. Guija-Poma, E., Inocente-Camones, M., Ponce-Pardo, J. & Zarzosa-Norabuena, E. Evaluación de la técnica 2,2-Difenil-1-Picrilhidrazilo (DPPH) para determinar capacidad antioxidante. Horiz. Médico 15, 57-60 (2015).
38. Coba, P., Mayacu-Tivi, L. & Vidari, G. Importancia de la actividad antioxidante y evaluación de extractos en etanol del género Oryctanthus. La Granja. Rev. Ciencias la vida 11, 22-30 (2010).

ARTICLE / INVESTIGACIÓN

Molecular identification of a *Pseudomonas putida* strain isolated from Machángara river (Quito-Ecuador) tolerant to carbamazepine

Gabriela Méndez[1]*, Leslie Morales[2], Elena Coyago[3] and Valeria Garzón[2]

DOI. 10.21931/RB/2022.08.02.5

[1] Universidad Politécnica Salesiana; Grupo de investigación BIOARN, Ecuador.
[2] Universidad Politécnica Salesiana, Ecuador.
[3] Universidad Politécnica Salesiana; Grupo de investigación GIDCARB, Ecuador.
Corresponding author: gmendez@ups.edu.ec

Abstract: Carbamazepine is a molecule used to treat specific pathologies; however, it has become an emerging contaminant that is dangerous to the environment. In marine species and humans, it causes cytotoxicity, genotoxicity, reproductive disorders, and infertility. Thus, this pollutant has been subjected to conventional wastewater treatment, achieving low purification. In Ecuador, only some studies are related to emerging contaminants, and these show quantification but not treatment. Therefore, the implementation of biological techniques is necessary. In this sense, the research aimed to identify a bacteria in water samples from the Machangara River with carbamazepine tolerance. Morphological, biochemical, and molecular characteristics identified bacteria. The results indicated the presence of several microorganisms, including molecularly identified *Pseudomonas putida*. This was tolerant to carbamazepine concentrations of 15, 50, and 100 mg/L, with higher growth at the first concentration. This information can be valuable in wastewater treatment investigations.

Key words: Carbamazepine, degradation, Machangara river, *Pseudomonas putida*.

Introduction

Although water is an essential natural resource for life; however, it has been affected by natural and anthropogenic pollutants[1]. During the development of humanity, these resources have been affected, and in recent years contamination has increased. In this sense, the term emerging pollutant appears, which includes some chemicals in low concentrations that alter the beneficial conditions of water, becoming toxic to the environment. Thus, primary investigation in emerging pollutant and biological treatments was shown in Europe and Asia and very little in Latin American countries such as Ecuador[2-4]. In turn, one problem that makes the study of emerging contaminants difficult is that there are limited techniques to identify low concentrations (ng/L to ug/L). In this sense, liquid chromatography becomes an alternative[3-5].

On the other hand, carbamazepine is a drug used to treat epilepsy and trigeminal neuralgia. It is 72 % absorbed by the body and eliminated through the urinary and fecal tract[6]. In this regard, the highest concentrations of carbamazepine have been found in water discharge from healthcare systems, either by the human body's elimination or by the mishandling of drugs[7]. The contamination is also due to an inefficient elimination in wastewater treatment plants[8]. Carbamazepine in the environment is associated with producing adverse teratogenic and mutagenic effects, reproductive problems, infertility, masculinization of females, feminization of males in animals, and genetic issues in human beings[2,9]. Hence, it is crucial to develop technologies for its removal.

In this regard, Reichert *et al.*[3] and Peña-Guzman *et al.*[4] pointed out that the concentrations of emerging contaminants detected in Latin America are often higher than in other countries; for example, in Ecuador, the authors Voloshenko *et al.*[2] and Pacheco[10] identified a concentration between 1.5-830 µg/L of carbamazepine in Machangara, San Pedro, Guayllabamba, and Esmeralda rivers. Latin America does not have an established list of pollutants of concern or laws controlling their production or release to the environment[11]. Therefore, it is interesting to develop environment-friendly approaches to eliminate these contaminants; the first step is identifying microorganisms capable of tolerating them in high concentrations for future degradation tests.

Materials and methods

Reagents and standards

Chemical compounds studied in this article: Carbamazepine (≥ 99 % pure) was purchased from Sigma-Aldrich (Merck, Germany). Methanol and acetonitrile HPLC-grade were purchased from Dikma (DikmaTechnologies, USA).

Enrichment and isolation of bacteria potentially tolerant to carbamazepine

Isolation of carbamazepine-tolerant bacteria used the enrichment method. Thus, contaminated water was sampled, enriched with carbamazepine, and active bacteria that tolerated the contamination was isolated.

The contaminated water sample was obtained from the Machángara River in the Pichincha province in Quito-Ecuador (coordinates: 0°15'25.4"S 78°31'33.8"W) at 2644 masl. Thus, 250 mL of contaminated water was sampled in amber bottles, following the methodology of the sampling standard

Citation: Méndez G.; Coyago-Cruz, E.;Morales, L.; Garzón, V. Molecular identification of a Pseudomonas putida strain isolated from Machángara river (Qui-to-Ecuador) tolerant to carbamazepine. Revis Bionatura 2023;8 (2) 5. http://dx.doi.org/10.21931/RB/2023.08.02.5
Received: 26 December 2022 / **Accepted:** 15 March 2023 / **Published:** 15 June 2023

Publisher's Note: Bionatura stays neutral with regard to jurisdictional claims in published maps and institutional affiliations.

for microbiological analysis of the Ecuadorian Institute for Water Standardization (INEN)[12]. Sampling was performed in duplicate and at the same site.

Bacteria from the collected water samples were inoculated into a basal mineral medium (MBM). The medium used contains the following salts (g/L): K_2 HPO_4 3.5, KH_2PO_4 1.5, $(NH_4)2SO_4$ 0.5, NaCl 0.5, $MgSO_4 7H_2O$ 0.15, and 1mL of trace solutions. The trace elements contained: 2.0 g $NAHC_3$-$10H_2O$, 0.3g $MnSO_4$-$4H_2O$, 0.2g $ZnSO_4$-7H2O, 0.02g (NH4)Mo7 O24 - $4H_2O$, 0.1g $CuSO_4$ -$5H_2O$, 0.5g CoCl2-$6H_2O$, 0.05g $CaCI_2$ -$2H_2O$, 0.5g $FeSO_4$ - $7H_2O_6$. Next, 15mg/L of carbamazepine was added. The culture was incubated at 26 °C, 150 rpm for 15 days in darkness to develop a community of microorganisms capable of producing the enzymes responsible for consuming this recalcitrant compound[6]. The bacteria were isolated using MBM with carbamazepine in a solid medium, and subcultures were carried out until obtaining pure cultures.

Bacterias tolerant to carbamazepine were identified, cultivating these in 250 mL of MBM with carbamazepine (15 mg/L, 50mg/L, and 100mg/L) as the only carbon source[6], as it is shown in Figure 1. Samples were incubated at 150 rpm in the orbital shaker (Shanghai, China) at 30 °C in darkness for 33 days. The tests used a bacterial inoculum concentration of 2% v/v. In turn, to monitor bacterial growth and carbamazepine consumption, samples were taken from the culture at the beginning and end of the study. The experiment used a control with MBM and carbamazepine without bacteria. Plate count was performed in TSA medium at 30 °C and expressed in colony forming units (CFUs)[13-15]. All cultures were performed in triplicate.

Carbamazepine quantitation was performed by liquid chromatography using an HPLC Waters 1525 equipped with a diode-array detector and a binary pump, C_{18} column (Novapak® 4 x 300 mm). The HPLC conditions were as follows: a wavelength of 280 nm, a flow rate of 1 mL/min, an injection volume of 20 µl, and a retention time of 8.0 minutes. The mobile phase consisted of water: methanol: acetonitrile (50:25:25), pre-filtered by a 0.45 µm membrane and degassed[16]. A carbamazepine calibration curve was prepared with standards of 100 mg/L, 75 mg/L, 50 mg/L, 25 mg/L, 10 mg/L, and 5 mg/L. The chromatograms were monitored at 280 nm with the Empower™ 3 software (build 3471). The samples were analyzed in duplicate.

Morphological and biochemical characterization of the bacterial strain

The isolated bacteria strain was identified using morphological and biochemical techniques. Catalase and oxidase tests were used, and the Microgen TM GN-ID Identification Kit. The Microgen Identification Software (MID-60) was used to interpret the kit's results. Gram reactions were observed in cells cultivated for 24 h using an optical microscope[17].

Molecular identification of the bacterial strain

The bacterium was cultured in test tubes with Tryptone Soy Agar for 24 h at 26 °C, and the DNA extraction process was performed with the Purelink Genomic DNA kit by Thermo Fisher Scientific[18]. DNA integrity was evidenced by electrophoresis with the 1KB Ladder Express DNA (molecular weight marker). The purity and concentration of the resulting DNA preparation were determined spectrophotometrically at 260 nm using a Quibit® 2.0 Fluorometer.

PCR targeted the 16s ribosomal genes (16s rRNA). First, the 16S rRNA gene was amplified using a forward primer 27F (5`-AGTTTGATCCTGGCTCA-3`) and a reverse primer 1492R (5`-GGTTACTCTTGTTACGACTT-3`) under the following conditions: 95 °C for 5 minutes, 40 cycles, 95 °C for 30 seconds, 56 °C for 30 seconds, 72 °C for 1 minute and final extension at 72 °C for 10 minutes[19].

The success of amplification was checked in 1% agarose gel after amplification. The amplified fragment was sequenced by Molecular Research LP (MRDNA) in Texas-

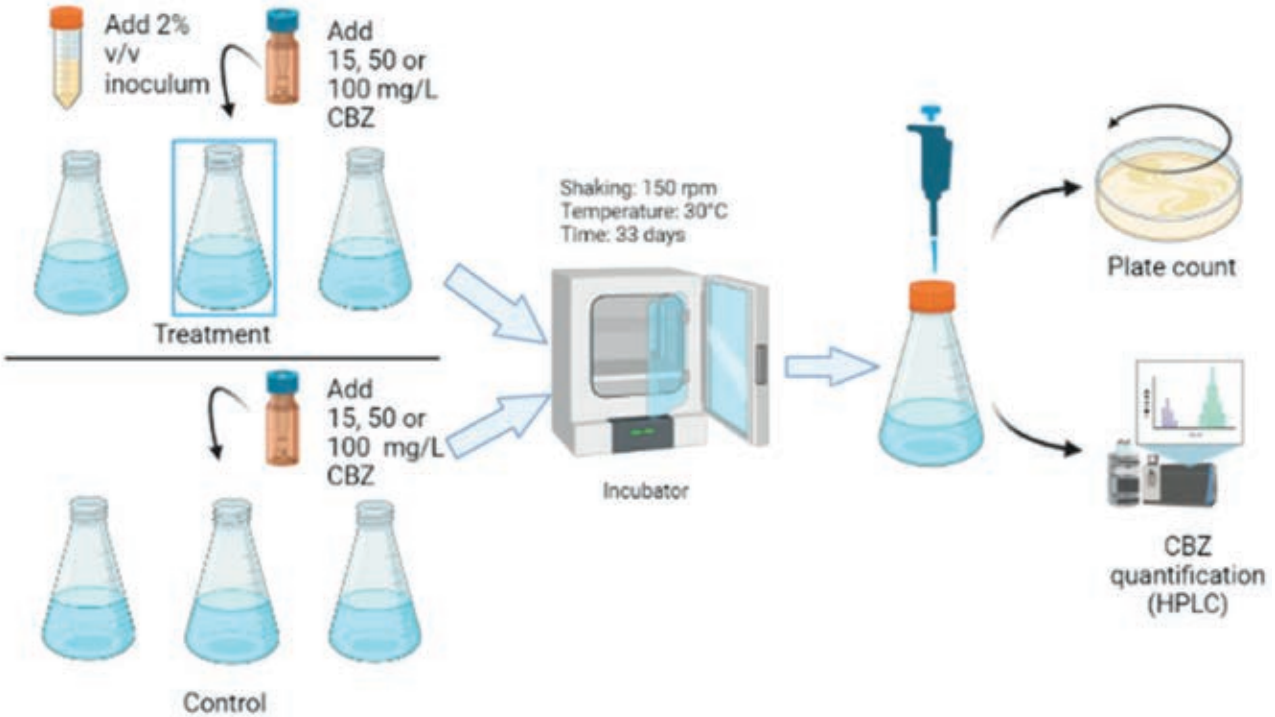

Figure 1. Tolerance essays include preparation of the inoculum, incubation, bacterial count, and quantification of carbamazepine (CBZ).

USA using an Illumina MiSeq platform following the manufacturer's guidelines (40 K average number of reads per assay). Sequence data were processed using the MR DNA analysis pipeline (MR DNA, Shallowater, TX, U.S.A.).

In summary, sequences <150 bp and ambiguous base calls were removed. Operational taxonomic units (OTUs) were generated, and chimeras were removed. OTUs were defined by 97% similarity. Final OTUs were taxonomically classified using BLASTn against the NCBI database. Sequencing reads from this study have been deposited in GeneBank with an accession number for the 16S rRNA gene (MW691110).

Results and discussion

Morphological and molecular characterization of the bacterial strain

Some bacteria were isolated from tolerance assays, and molecular identification was performed with one of them. The isolated bacterium showed a slightly yellow mucous colony with a smooth edge (Figure 2a). It was classified as a gram-negative bacillus (Figure 2b), oxidase and catalase positive[20-22], typical characteristics of *Pseudomonas*[23,24]. Microgen identification Software (MID-60) identified the bacteria isolated as *Pseudomonas pseudomallei* with a 94.38% identity.

On the other hand, molecular identification by electrophoresis reported the presence of DNA, with a region size of approximately 1500 bp (Figure 3). These results suggest that this is the size corresponding to the 16s rRNA region, as established by other studies[25]. Finally, sequencing was performed with the amplified samples at the Molecular Research LP (MRDNA lab) laboratory in Texas-USA, obtaining a 100% identity of *Pseudomonas putida* for the strain.

According to the literature, the bacteria identified as belonging to the *Pseudomonadaceae* family[26], are used in degradation tests by having a metabolism that makes it easier to adapt to different habitats, sources of carbon, and nitrogen, that can colonize several ecological niches[27]. Therefore, these microorganisms, isolated from a contaminant-containing medium, are presumed to tolerate toxic substances and may help degrade carbamazepine[28]. *Pseudomonas putida* is not associated with human disease[29], offering many advantages such as cost-effectiveness and utilization of native harmless microbial species[30].

Carbamazepine tolerance assays

Pseudomonas putida reached the highest biomass concentration at 15mg/L with a carbamazepine consumption of 49.56% (SD:5.6), which indicates that bacteria use the contaminant as a carbon source because there was no reduction of CBZ in controls. Bacterias showed poor growth at 50 and 100 mg/L (Figure 4), with 11.3% (SD:2) and 9.9% (SD:3.2) of degradation, respectively.

Figure 4 shows that bacterial growth and degradation were low at higher concentrations. Thus, the decrease in microorganisms could be because the bacteria finished the exponential phase, and the death phase began[31]. In addition, it should be considered that there are several kinetic models in biodegradation and that, in some instances, the concentration of organisms remains constant even when the substrate is degraded by inhibition. Therefore, it is associated with a decrease in specific growth rates. For example, in the study of Rathour *et al.*[32], it was shown that the specific growth rate was rapidly reduced due to the detrimental effects of benzo(a)pyrene on cell development and the subsequent inhibition of the substrate on culture growth. Likewise, some species of *Pseudomonas spp* use bioabsorption as a bioremediation mechanism that causes the accumulation of toxic compounds inside the cell, causing its death[33].

In the study conducted by (Li *et al.*[34], similar carbamazepine consumption percentages were observed, with values of 46.6%, where the drug was observed to decrease at day 6 (144 hours) with *Pseudomonas sp.* CBZ-4. In the

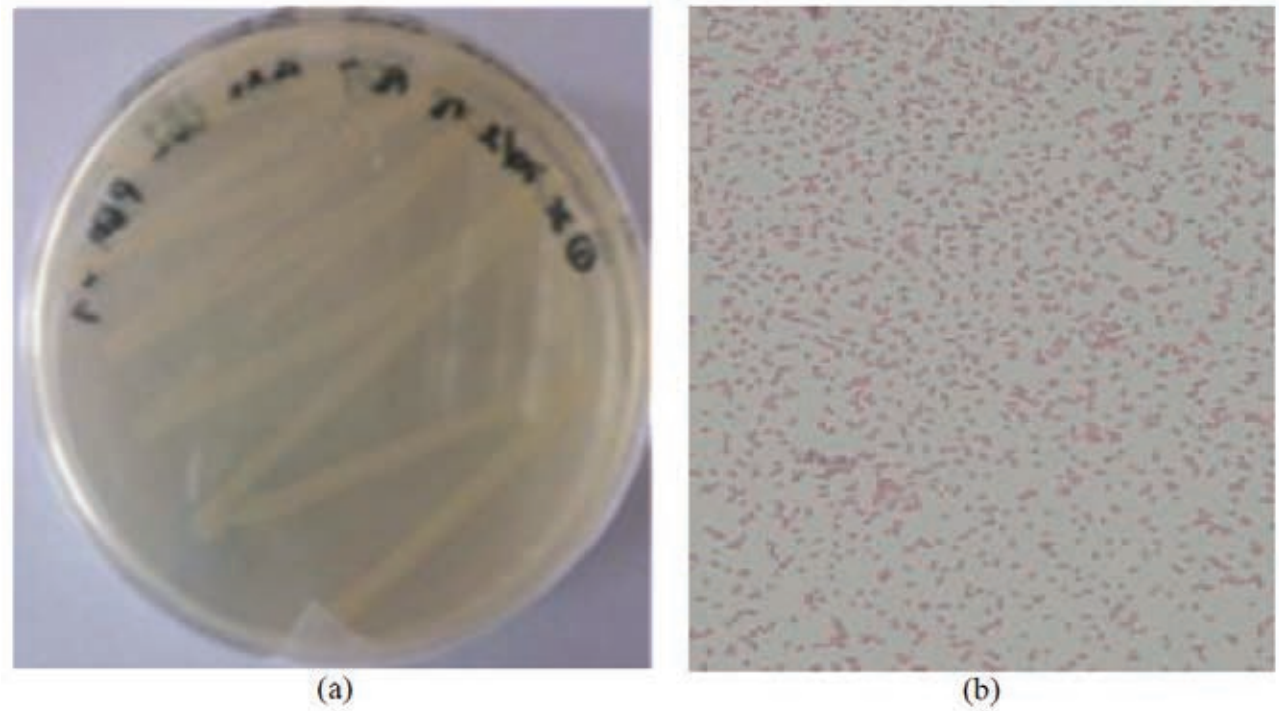

Figure 2. Bacterial identification. a) Isolated bacteria from Machángara river in TSA medium, b) Gram-negative *Bacillus*.

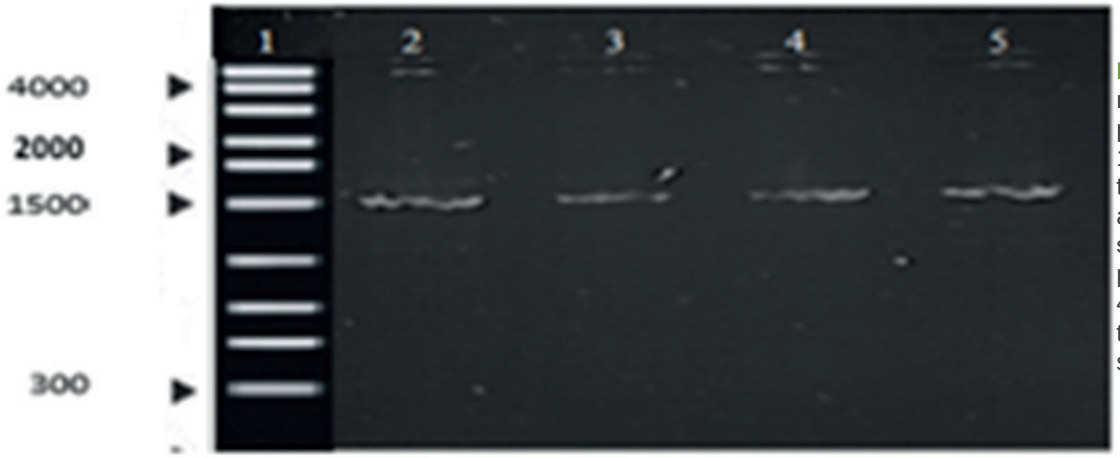

Figure 3. Agarose gel electrophoresis. Lane 1 represents the DNA ladder, and Lanes 2-5 show the PCR products from 4 samples of the strain in the study.

study by Ha, Mahanty, Yoon, & Kim[35], with mixed bacterial culture (*Pseudomonas, Bacillus*, and *Acinetobacter*), a 60% degradation was obtained in 12 days. It should also be noted that several studies have determined that microorganisms require a long period of prior adaptation to persistent chemical contaminants to degrade them effectively[36]. In this study, the strains evaluated were acclimated for 15 days to increase their tolerance.

Figure 4 shows that *Pseudomonas putida* has a better tolerance for low concentrations of carbamazepine, like the study of Gheorghe *et al.*[37], considering that pharmaceutical biodegradation could be affected by different factors such as temperature, pH, varying pharmaceutical concentrations, etc. For this reason, it is necessary to carry out future degradation tests with different culture conditions to determine the optimal ones to apply in wastewater treatment. According to the literature, carbamazepine, naproxen, and ibuprofen have harmful effects at 16.21 to 54.21 mg/L in bacteria, indicating that they influence the degradation route of the microorganism at higher concentrations, causing toxicity and inhibiting its metabolization. It is confirmed by Nogales *et al.*[38], who indicate that contaminants at high concentrations cause severe damage to the bacterial cell, causing death[38]. Similar results with emerging contaminants were mentioned by Ramos *et al.*[39] for Pseudomonas putida in degradation tests of aromatic hydrocarbons and short-chain alcohols; also, the degradation was reported of salicylic acid by *P. fluorescens* HK44 was inhibited at high concentrations of the substrate[40]. However, the concentration of carbamazepine in wastewater is usually found at concentrations below that evaluated in this study[2].

The capacity of *Pseudomonas putida* to tolerate carbamazepine could be due to the presence of central pathways to degrade these compounds, and a multifactorial response is generated to adapt to the environment when exposed to these, involving degradation routes and metabolism changes as a result of stress[38]. *Pseudomonas putida* produces oxidoreductases, hydrolases, and thiolases that help the microorganism overcome the damage caused by pollutants[39]. In addition, this bacterium finds new catabolic

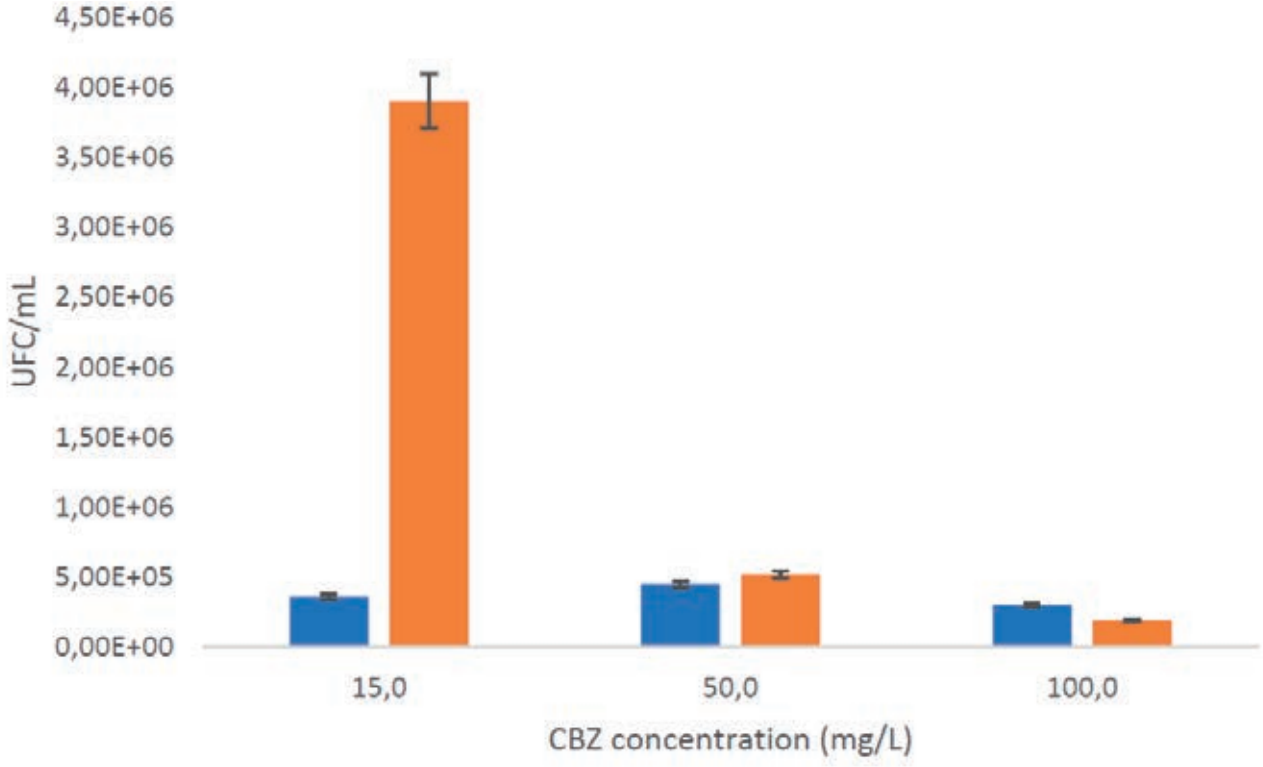

Figure 4. Plate count. The orange bar is the initial UFC/mL; the blue bar is the final UFC/mL

pathways to metabolize organic compounds[41] by presenting the catabolic TOL pWW0 plasmid, which, according to the literature, encodes specific metabolic activities so that the bacterium grows and uses it as the only source of carbon and energy, being closely related to biodegradation applications[42].

Conclusions

Carbamazepine is an emerging pollutant in the environment, resistant to conventional degradation processes, so microorganisms may be an option to biodegrade. *Pseudomonas* putida was molecularly identified from the wastewater from the Machángara River when exposed to 15, 50, and 100 mg/L of the contaminant carbamazepine at 30 °C temperature and evaluated over 33 days. *Pseudomonas putida* used carbamazepine as the sole carbon source during in-vitro tolerance assays, resulting in a reduction of 49.56 % at 15 mg/L of the contaminant quantified by HPLC. In conclusion, these microorganisms could be used in future degradation studies as a sustainable technology solution to be developed and applied for the recovery of contaminated environments, considering the ability of *P. putida* to increase in several hostile environments. In addition, bacteria isolated from a natural source exposed to this contaminant could be advantageous in bioremediation since biodegradation rates depend on different factors, such as previous adaptation of the microbial inoculum.

Author Contributions

Methodology, Méndez Gabriela, Morales Leslie, Garzón Valeria.; formal analysis, Méndez Gabriela, Morales Leslie, Coyago Elena.; investigation, Méndez Gabriela, Morales Leslie, Garzon Valeria, Coyago Elena.; resources, Méndez Gabriela.; writing—original draft preparation, Méndez Gabriela, Morales Leslie, Coyago Elena.; writing—review and editing, Méndez Gabriela, Morales Leslie, Garzon Valeria and Coyago Elena; project administration, Méndez Gabriela.; funding acquisition, Méndez Gabriela. All authors have read and agreed to the published version of the manuscript.

Data Availability Statement

Sequencing reads from this study have been deposited in GeneBank with accession numbers for 16S rRNA gene MW691110 (https://www.ncbi.nlm.nih.gov/nuccore/MW691110)

Conflicts of Interest

The authors declare no conflict of interest.

Bibliographic references

1. Franco, P. & Rodríguez, M. Formulación de líneas estratégicas para un proyecto participativo de conservación de un ojo de agua de la parroqui El Condado, barrio Colinas del norte, sector El manatial y sector Rancho bajo. Pontifica Universidad Católica del Ecuador (Pontificia Universidad Católica del Ecuador, 2016).
2. Voloshenko-Rossin, A. et al. Emerging pollutants in the Esmeraldas watershed in Ecuador: discharge and attenuation of emerging organic pollutants along the San Pedro–Guayllabamba–Esmeraldas rivers. Environ. Sci.: Processes Impacts 17, 41–53 (2015).
3. Reichert, G., Hilgert, S., Fuchs, S. & Azevedo, J. C. R. Emerging contaminants and antibiotic resistance in the different environmental matrices of Latin America. Environmental Pollution 255, (2019).
4. Peña-Guzmán, C. et al. Emerging pollutants in the urban water cycle in Latin America: A review of the current literature. J Environ Manage 237, 408–423 (2019).
5. Varo, P., López, C., Cases, V. & Ramírez, M. Presencia de contaminantes emergentes en aguas naturales. 33 Preprint at (2016).
6. Gauthier, H., Cooper, D. G. & Yargeau, V. Biodegradation of pharmaceuticals by common microorganisms. in WIT Transactions on Ecology and the Environment vol. 111 263–271 (2008).
7. Rojo, M. et al. Human pharmaceuticals in three major fish species from the Uruguay River (South America) with different feeding habits. Environmental Pollution 252, 146–154 (2019).
8. Viancelli, A. et al. A review on alternative bioprocesses for removal of emerging contaminants. Bioprocess Biosyst Eng 43, 2117–2129 (2020).
9. Robledo, Z. et al. Hidroquìmica y contaminantes emergentes en aguas residuales urbano industriales de Morelia, Michoacàn, México. Revista Internacional de Contaminacion Ambiental 33, 221–235 (2017).
10. Pacheco, A. Determinación de contaminantes emergentes carbamazepina y diclofenaco en el Río San Pedro y análisis de tratamiento con nanotecnología. (Universidad de las Fuerzas Armadas del Ecuador, 2021).
11. Zhang, Y., Geißen, S. U. & Gal, C. Carbamazepine and diclofenac: Removal in wastewater treatment plants and occurrence in water bodies. Chemosphere 73, 1151–1161 (2008).
12. INEN. Aguas. Muestreo para examen microbiològico. Norma Técnica Ecuatoriana (2012).
13. Camacho, A. et al. Cuenta en placa de bacterias. in (2009).
14. Sánchez, E. P., Núñez, D., Cruz, R. O., Torres, M. A. & Herrera, E. V. Simulación y Conteo de Unidades Formadoras de Colonias Simulation and Counting of Colony-Forming Units. vol. 28 (2016).
15. Matheus, P., Ramírez, E., Araque, J., Belandria, O. & Durán, J. Espectrofotometría de absorciòn molecular ultravioleta como una herramienta para estudiar el crecimiento de las cepas ATCC 25922 y ATCC 35218 de Escherichia coli. (2016).
16. Garzón, G. & Popayán, M. Estandarización de un método analítico por cromatografía líquida de alta eficiencia para la cuantificación de carbamazepina en tabletas. 130–137 (2008).
17. López-Jácome, L. E. et al. Las tinciones básicas en el laboratorio de microbiología. Investigación en Discapacidad 3, 10–18 (2014).
18. Life. PureLink ® Genomic DNA Kits For purification of genomic DNA.
19. Chen, Y. et al. Obtaining long 16S rDNA sequences using multiple primers and its application on dioxin- containing samples. 16, 1–11 (2015).
20. Pírez, M. & Mota, M. Morfología y estructura bacteriana. in 23–42 (2008).
21. Winn, W. C. & Koneman, E. W. Koneman diagnóstico microbiológico : texto y atlas en color. (Editorial Médica Panamericana, 2008).
22. Cuesta, C. & Pérez, J. Presencia de cepas de Staphylococcus spp. meticilino resistentes con resistencia inducible a la clindamicina de pacientes hospitalizados en el “Hospital Vicente Corral Moscoso (HVCM)”. (Universidad de Cuenca, 2016).
23. Bou, G., Fernández-Olmos, A., García, C., Sáez-Nieto, J. A. & Valdezate, S. Métodos de identificación bacteriana en el laboratorio de microbiología. Enfermedades Infecciosas y Microbiologia Clinica vol. 29 601–608 Preprint at https://doi.org/10.1016/j.eimc.2011.03.012 (2011).
24. Rojas-Triviño, A. Conceptos y prácticas de microbiologia general. (2011).
25. Ortíz, Á., Martínez, M. & Vargas, F. La secuencia completa del gen ARN ribosomal 16s, una promesa para mejorar laa presión en la asignación taxonómica microbiana. Microbiología Ambiental en México 22 (2017) doi:978-607-02-9617-8.
26. Molina, J. & Orozco, J. Detección de resistencia antimicrobiana en bacterias de interés clínico aisladas en el Río Chambo. Noviembre 2018 - enero 2019. (Universidad Nacional de Chimborazo, 2019).

27. Estupiñán, M. et al. Aislamiento e identificación de Pseudomonas sp. y Aeromonas sp. en aguas de piscinas públicas de Bogotá – Colombia. NOVA 25–29 (2017).
28. Ríos, S., Agudelo, R. & Gutiérrez, L. Patógenos e indicadores microbiológicos de calidad del agua para consumo humano. (2017) doi:10.17533/udea.rfnsp.v35n2a08.
29. Goverment of Canada. Pseudomonas putida - information sheet - Canada.ca. https://www.canada.ca/en/health-canada/services/chemical-substances/fact-sheets/chemicals-glance/pseudomonas-putida.html (2017).
30. Wang, S. N. et al. Biodegradation and detoxification of nicotine in tobacco solid waste by a Pseudomonas sp. Biotechnol Lett 26, 1493–1496 (2004).
31. Kareem, S., Kefas, H., Chior, T. & Latinwo, G. View of Kinetics of Fermentation by Enzymes: A Mathematical Approach. AU Journal of Technology 15, 109–114 (2011).
32. Rathour, R. K., Sharma, D., Sharma, N., Bhatt, A. K. & Singh, S. P. Chapter 14 - Engineered microorganisms for bioremediation. in Current Developments in Biotechnology and Bioengineering (eds. Joshi, S., Pandey, A., Sirohi, R. & Park, S. H.) 335–361 (Elsevier, 2022). doi:https://doi.org/10.1016/B978-0-323-88504-1.00002-9.
33. Vélez, J. M. B., Martínez, J. G., Ospina, J. T. & Agudelo, S. O. Bioremediation potential of Pseudomonas genus isolates from residual water, capable of tolerating lead through mechanisms of exopolysaccharide production and biosorption. Biotechnology Reports 32, e00685 (2021).
34. Li, A. et al. Characterization and biodegradation kinetics of a new cold-adapted carbamazepine-degrading bacterium, Pseudomonas sp. CBZ-4. Journal of Environmental Sciences 25, 2281–2290 (2013).
35. Ha, H., Mahanty, B., Yoon, S. & Kim, C.-G. Degradation of the long-resistant pharmaceutical compounds carbamazepine and diatrizoate using mixed microbial culture. Journal of Environmental Science and Health, Part A 51, 467–471 (2016).
36. Poursat, B. et al. Does long term exposure leads to biodegradation of carbamazepine ? (2016).
37. Gheorghe, S., Petre, J., Lucaciu, I., Stoica, C. & Nita, M. Risk screening of pharmaceutical compounds in Romanian aquatic environment. Environ Monit Assess (2016) doi:10.1007/s10661-016-5375-3.
38. Nogales, J., García, J. & Díaz, E. Degradation of Aromatic Compounds in Pseudomonas : A Systems Biology View. (2017) doi:10.1007/978-3-319-39782-5.
39. Ramos, J. L. et al. Mechanisms of solvent resistance mediated by interplay of cellular factors in Pseudomonas putida. FEMS Microbiol Rev 39, 555–566 (2015).
40. Silva, T. R., Valdman, E., Valdman, B. & Leite, S. G. F. Salicylic acid degradation from aqueus solutions using Pseudomonas fluorescens HK44: parameters studies and application tools. Brazilian Journal of Microbiology 38, 39–44 (2007).
41. Lacal, J. Caracterización bioquímica y moloecular del sistema de dos componentes TODS/TODT de Pseudomonas putida DOT-T1E. (Universidad de Granada, 2008). doi:9788433849175.
42. Nikel, P. & de Lorenzo, V. Pseudomonas putida as a functional chassis for industrial biocatalysis: From native biochemistry to trans-metabolism. Metab Eng 50, 142–155 (2018).

ARTICLE / INVESTIGACIÓN

Intervención educativa sobre *angiostrongiliasis* humana para mejorar conocimientos, percepciones y prácticas de médicos de atención primaria de salud, Ecuador 2018

Educational intervention on human *angiostrongyliasis* to improve primary health care physicians' knowledge, perceptions and practices, Ecuador 2018

Luis Solorzano[1], Carlos Chiluisa[2], Sunny Sánchez[3], Roberto Licuy[2], Hilda Hernández[4], Misladys Rodríguez[4], Jorge Sarracent[4], César Bedoya[1], Jose Pico[5], Francisco Sánchez[1], Patricio Vega-Luzuriaga[2]*, Lázara Rojas[4]

DOI. 10.21931/RB/2022.08.02.4

[1] Consejo Nacional de Investigaciones Científicas y Técnicas, Argentina.
[2] Laboratorio de Biotecnología Microbiana. Facultad de Ciencias Naturales y Ciencias de la Salud (Sede Trelew). Universidad Nacional de la Patagonia. Argentina.
Corresponding author: parada.ro91@gmail.com

Resumen: *Angiostrongylus cantonensis* fue identificado en Ecuador en el año 2008. Posteriormente, se notificaron brotes y casos aislados en varias zonas del pais. Un estudio realizado en Napo y Guayas mostró insuficiente conocimiento de los médicos de atención primaria sobre la angiostrongiliasis humana. Los objetivos de este estudio son realizar una intervención educativa y evaluar la eficacia de la misma para atenuar las deficiencias encontradas en el personal médico, con esta finalidad se realizaron un grupo de acciones, a modo de intervención educativa y se aplicó la encuesta sobre conocimientos, percepciones y prácticas (CPP) para evaluar la eficacia de esta intervención. La información obtenida se almacenó en una base de datos en Microsoft Access y se analizó mediante el software estadístico IBM, SPSS. Luego de la intervención educativa se constató mejoría en la mayoría de los aspectos evaluados, con un incremento en la media de las respuestas correctas de los participantes, lo que demuestra la eficacia de las acciones desarrolladas. Estos resultados contribuyen a la toma de decisiónes de los responsables de la educación médica del país, para mejorar el abordaje de esta temática en la atención primaria de salud, que representa el primer contacto con los pacientes.

Palabras clave: *Angiostrongylus cantonensis*, infección, conocimiento, atención primaria.

Abstract: *Angiostrongylus cantonensis* was identified in Ecuador in 2008. Subsequently, outbreaks and isolated cases were reported in several country areas. A study conducted in Napo and Guayas showed insufficient knowledge of primary care physicians about human angiostrongyliasis. This study aims to carry out an educational intervention and evaluate its effectiveness in mitigating the deficiencies found in medical personnel. To this end, a group of actions was carried out as an educational intervention and a survey on knowledge, perceptions and practices (KPP) was applied to evaluate the effectiveness of this intervention. The information obtained was stored in a database in Microsoft Access and analyzed using IBM SPSS statistical software. After the educational intervention, improvement was observed in most of the aspects evaluated, with an increase in the mean number of correct answers from the participants, demonstrating the effectiveness of the actions developed. These results contribute to the decision-making of those responsible for medical education in the country to improve the approach to this subject in primary health care, representing the first contact with patients.

Key words: *Angiostrongylus cantonensis*, infection, knowledge, primary care.

Introducción

Angiostrongylus cantonensis es la causa más frecuente de meningitis eosinofílica en el sur de Asia y en algunas islas del Pacífico y del Caribe[1]. Desde 1944, han sido notificados 2900 casos de meningoencefalitis eosinofílica por *A. cantonensis*[2]. En las Américas el primer informe de este parásito en humanos fue en Cuba en 1981[3], posteriormente, en Puerto Rico[4], Estados Unidos[5], Jamaica[6,7], Haití[8], Brasil[9] y Colombia[10].

El parásito tiene un ciclo de vida complejo. Las ratas son consideradas hospederos definitivos y diseminan la infección al medio circundante a través de las heces. El hombre, hospedero accidental, se infecta por la ingestión de larvas de tercer estadio (L3) que se encuentran en caracoles crudos o mal cocidos tales como, *Lissachatina spp*. y *Pomacea spp*. y también en babosas, que constituyen los hospederos intermediarios del parásito. Además, pueden ser vías de infección el agua dulce, ranas y peces previamente infectados[11].

Una vez que el hombre ingiere la L3 esta invade el tejido intestinal, causando una enteritis, antes de pasar por el

Citation: Solorzano L , Chiluisa C, Sánchez S, , Licuy R, Hernández H, Rodríguez M, Sarracent J, Bedoya C, Pico J , Sánchez F, Vega-Luzuriaga P, Rojas L. Intervención educativa sobre angiostrongiliasis humana para mejorar conocimientos, percepciones y prácticas de médicos de atención primaria de salud, Ecuador 2018. Revis Bionatura 2023;8 (2) 4. http://dx.doi.org/10.21931/RB/2023.08.02.4
Received: 26 December 2022 / **Accepted:** 15 March 2023 / **Published:** 15 June 2023
Publisher's Note: Bionatura stays neutral with regard to jurisdictional claims in published maps and institutional affiliations.

hígado. En su paso por los pulmones, el paciente desarrolla síntomas como tos, rinorrea, dolor de garganta, además de malestar general y fiebre. El parásito tiene un especial tropismo por el SNC[12].

La encefalitis/encefalomielitis causada por *A. cantonensis* es una enfermedad grave que se caracteriza por cambios en el estado mental que incluyen coma y signos neurológicos focales. Los pacientes con frecuencia desarrollan meningitis eosinofílica y/o un síndrome de dolor abdominal transitorio que evoluciona con trastornos sensoriales y motores de las piernas, con dolor, debilidad, ausencia de reflejos, disfunción intestinal/vesical, hipertensión lábil, coma y, en casos graves puede provocar la muerte[13].

La presentación clínica clásica de la infección es una meningitis/meningoencefalitis. Los pacientes con meningitis eosinofílica muestran al menos 10 eosinófilos por mm^3 de LCR o ≥10% de eosinófilos en el recuento total de leucocitos en LCR[14,15]. El período de incubación para el desarrollo de meningitis eosinofílica es de aproximadamente dos semanas, lo que coincide con el tiempo que tardan las L3 en migrar al tejido del SNC y desencadenar una reacción inflamatoria. Sin embargo, puede variar de un día a varios meses y eso depende del número de parásitos albergados[16,17].

La angiostrongiliasis es una enfermedad aguda que se resuelve espontáneamente en unas pocas semanas, rara vez conlleva secuelas y raramente es fatal. La duración media es de 20 días, pero puede variar de 6 a 34 días[16].

En Ecuador, en el año 2008 se evidenció por primera vez la presencia de *A. cantonensis* en humanos[18]. Desde entonces se han informado siete brotes en varias provincias del país, que afectaron a 19 adultos y 7 niños[19], se estiman en 50 los casos reportados[20] y un fallecido[21]. Si bien se emplea el inmunodiagnóstico y pruebas moleculares para su confrimacion, El diagnóstico en Ecuador es clinico y epedemiologico[18].

En un estudio de hospederos intermediarios de varias provincias en 2016 se encontró que Napo tenía la mayor tasa de infección de *A. cantonensis* (30,3%) (datos no publicados, Instituto Nacional de Investigación en Salud Publica); mientras que otra investigación publicada en 2019 muestra una tasa de infección de 27,2% en tanto que en Guayas tenia 9,1%22. Sobre la base de estos antecedentes se aplicó una encuesta sobre conocimientos, percepciones y prácticas (CPP) en relación a esta parasitosis a profesionales de atención primaria de las provincias de Napo y Guayas. En dicha encuesta se evidenció, el insuficiente conocimiento que tienen médicos de atencion primaria de estas provincias sobre un parte considerable de los temas abordados[13]. Para contribuir a la solución de estas deficiencias se ejecutaron un grupo de acciones que podrían incidir en el mejoramiento de los CPP sobre esta parasitosis en los médicos de atención primaria. Después de seis meses de terminada esta fase de intervención educativa, una segunda encuesta nos permitiría conocer si las acciones realizadas incidieron sobre los CPP de estos médicos. Como objetivo de la investigación nos propusimos realizar una intervención educativa y evaluar la eficacia de las acciones tomadas para atenuar las deficiencias encontradas en el personal de salud implicado en el estudio.

Materiales y métodos

Se realizó un estudio con diseño cuasiexperimental, tipo intervención educativa, con el propósito de mejorar el nivel de conocimientos sobre el diagnóstico, tratamiento y control de la angiostrongiliasis humana entre 2017-2018. El estudio constó de tres etapas: diagnóstica (primera encuesta línea base)[13], intervención educativa (conferencias y folleto) y ejecución de la segunda encuesta y evaluación, seis meses después.

Intervención para atenuar el problema

La intervención consistió en un grupo de acciones realizadas entre enero y febrero de 2018.

De los 163 médicos de atención primaria incluidos en

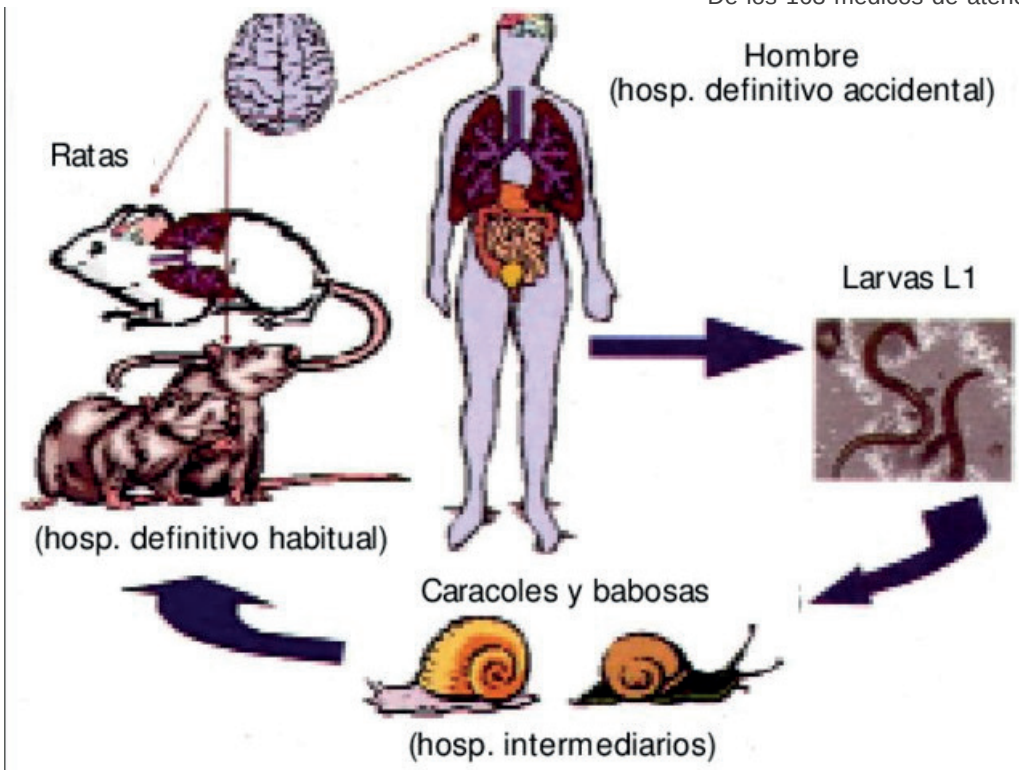

Figura 1. Ciclo de vida de la *Angiostrongylus cantonensis* es la causa más frecuente de meningitis eosinofílica.

la primera encuesta, 156 continuaron el estudio (95,70%). Estos fueron separados en dos grupos: el grupo con intervención integrado por 64 médicos de atención primaria de las catorces Unidades de Salud de los tres cantones de la provincia Napo y el grupo sin intervención conformado por 92 médicos de las siete parroquias del cantón Guayaquil de la provincia Guayas a los que no se les realizó intervención.

La fase de intervención consistió en un ciclo de cinco conferencias de actualización sobre generalidades del parásito, epidemiología, diagnóstico, tratamiento y medidas de prevención y control de la angiostrongiliasis, que incluyó discusiones de casos. Además, se preparó y distribuyó un folleto titulado "Angiostrongiliasis. Biología, clínica, diagnóstico y tratamiento a todos los médicos de forma gratuita.

La forma de organización de la enseñanza: consistió en conferencias (12 horas), clase práctica (4 horas) y estudio independiente (4 horas). La evaluación final 4 horas. A cada participante se le entregó una carpeta digital con artículos actualizados sobre el tema objeto de estudio.

Ejecución de la segunda encuesta

Seis meses después de finalizada la fase de intervención educativa se aplicó a los médicos de ambos grupos de estudio el cuestionario utilizado en la primera encuesta.

Análisis estadístico

Al finalizar la aplicación de la encuesta CPP se confeccionó la base de datos en Microsoft Access año 2016, con la información obtenida en la investigación. Se realizó el análisis estadístico con el software estadístico IBM, SPSS, versión 23[14]. Para el análisis de los cambios en el nivel de conocimientos, percepciones y práctica médica en relación a las variables seleccionadas antes y después de implementada la intervención educativa se utilizó la estadística inferencial. Se compararon las medias de respuestas correctas de los médicos incluidos en los siguientes grupos: grupo con intervención y sin intervención de la primera encuesta, grupo con intervención y sin intervención de la segunda encuesta, grupo con intervención primera y segunda encuesta y grupo sin intervención, primera y segunda encuesta. Para ello se aplicó el estadístico t-Student.

Se realizó prueba de comparación de proporciones de las respuestas correctas a cada pregunta antes y después de la intervención para lo cual se aplicó la prueba Chi-cuadrado de McNemar. Se consideró diferencias estadísticamente significativas para valores de P< 0,05.

Consideraciones éticas

El protocolo fue aprobado por la Comisión de Ética de Investigación en seres Humanos (CEISH) de la Clínica Kennedy de la Ciudad de Guayaquil, aprobado por el Ministerio de Salud de Ecuador, código único de aprobación DIS-CEISH-HCK-09-014. Los médicos estaban en total libertad de decidir participar en la investigación. Al finalizar la encuesta, firmaron y asentaron el número de su documento de identificación en la misma. Los investigadores declaran que no tienen conflicto de intereses.

Resultados

Con la aplicación de la encuesta CPP, previo a la realización de este estudio de intervención, no se encontró diferencia estadísticamente significativa en la media de respuestas correctas de los médicos del grupo con intervención y sin intervención, en cuanto a las preguntas relacionadas sobre aspectos cognoscitivos sobre angiostrongiliasis, (P = 0,115) (Tabla 1). Posterior a la intervención, la media de respuestas correctas a las 21 preguntas relacionadas con aspectos cognoscitivos mostró diferencias estadísticamente significativas (P = 0,004) al comparar la media de respuestas correctas de los médicos incluido en ambos grupos (15,89 en el grupo con intervención y 10,28 en el grupo sin intervención) (Tabla 1).

La media de las respuestas correctas de los médicos pertenecientes al grupo con intervención fue de 9,05, en la primera encuesta. Esta media, experimentó un aumento significativo a 15,89 después de la intervención educativa, que se evidenció con la aplicación de la segunda encuesta (Tabla 2) (P = 0,000). Sin embargo, en el grupo sin intervención, la media de respuestas correctas de los médicos, en la primera encuesta fue de 10,30 y de 10,28 en la segunda encuesta. Como puede observarse en la tabla 2, no se obtuvo diferencias estadísticamente significativas (P = 0,924) en la calidad de las respuestas de los médicos al comparar los resultados de las dos encuestas realizadas.

Respuesta sobre aspectos cognoscitivos

Generalidades

Una alta proporción de encuestados conocen que la angiostrongiliasis es una enfermedadde etiología parasitaria (61/66, 92,42%, antes vs 63/64, 98,44%, después P = 0,500). Después de la intervención, se incrementó en más

Tiempo	Grupos	N	Media de las respuestas correctas	Desviación estándar	P
Antes de la fase intervención	Con intervención	66	9,05	2,768	0,115
	Sin intervención	97	10,30	2,435	
Después de la fase intervención	Con intervención	64	15,89	3,908	0,004
	Sin intervención	92	10,28	3,014	

Fuente: Encuesta Anexo 1
N: número de médicos encuestados

Tabla 1. Media de respuestas correctas antes y después de la intervención educativa según grupo con intervención y en grupo sin intervención., Ecuador 2018.

Grupos	Tiempo	N	Media de las respuestas correctas	Desviación estándar	P
con intervención	Antes de la intervención	66	9,05	2,768	0,000
	Después de la intervención	64	15,89	3,908	
sin intervención	Antes de la intervención	97	10,30	2,435	0,924
	Sin intervención	92	10,28	3,014	

Fuente: Encuesta Anexo 1

Tabla 2. Comparación de las medias de las respuestas correctas de los médicos antes y después de la fase de intervención educativa, según grupo con intervención y grupo sin intervención, Ecuador 2018.

de la mitad los encuestados que consideraron correctamente que el parásito, con frecuencia, se localiza geográficamente en el sureste asiático (17/66, 25,76%, antes vs 38/64, 59,38%, después P = 0,000). Una mayor proporción de médicos consideraron adecuadamente que la vía de transmisión por la que se adquiere la enfermedad es por la ingestión de moluscos y caracoles crudos (47/66, 71,21%, antes vs 60/64, 93,75%, después P = 0,002).

Ciclo evolutivo

Con posterioridad a la puesta en marcha de las acciones, se incrementó el número de encuestados que opinan que los hospederos definitivos habituales son las ratas y otros roedores (22/66, 33,33%, antes vs 59/64, 92,19%, después P = 0,000). mientras que los hospederos intermediaros habituales son diferentes tipos de moluscos y caracoles (28/66, 42,42%, antes vs 57/64, 89,06%, después P = 0,000). Se incrementó considerablemente la proporción de encuestados que señalaron adecuadamente que la localización preferente del parásito en su forma adulta es en pulmones de ratas y otros roedores (12/66, 18,18%, antes vs 41/64, 64,06%, después P = 0,000). En casi cinco veces se incrementó el número de médicos que consideran que *A. cantonensis* en su forma larvaria se localiza preferentemente en el cerebro de humanos. (10/66, 15,15 %, antes vs 45/64, 70,31%, después P = 0,000). Se incrementó la proporción de médicos que identifican al hombre y otros mamíferos como hospederos accidentales. (38/66, 57,58%, antes vs 60/64, 93,75%, después P = 0,000). Una proporción de encuestados de 25/66, 37,88% (antes) vs 36/64, 56,25% (después) consideró correctamente que las larvas L3 es la forma infectante del parásito para el hombre (P = 0,117).

Clínica

Posterior a la intervención, casi 100 % de los participantes conocen que las manifestaciones clínicas más características son meningitis encefalitis y lesiones oculares con marcada eosinofilia. (38/66, 57,58%, antes vs 61/64, 95,31%, después P = 0,000). El comportamiento fue similar para aquellos que respondieron correctamente que el periodo de incubación de la enfermedad es de 1 a 3 semanas (32/66, 48,48%, antes vs 40/64, 62,50%, después P = 0,096. Una proporción mayor de encuestados consideran que la mayor parte de las infecciones producida por *A. cantonensis* se resuelven espontáneamente, sin tratamiento específico (33/66, 50,00%, antes vs 52/64, 81,25%, después P= 0,000). Posterior a la intervención, se incrementó, en tres veces, el número de médicos que señalan que la enfermedad usualmente tiene una duración de 2 a 8 semanas (10/66, 15,15%, antes vs 29/64, 45,31%, después P = 0,000).

Diagnóstico

Más de 85% de los encuestados antes y posterior a la intervención, conoce que el diagnóstico de la angiostrongiliasis en Ecuador se basa fundamentalmente en la sintomatología clínica y en los antecedentes epidemiológicos (57/66, 86,36% antes vs 63/64, 98,44%, después P = 0,070). La mayoría consideran que la eosinofilia de más de 10% en LCR, es el hallazgo de laboratorio más significativo en pacientes con angiostrongiliasis (55/66, 83,33%, antes vs 62/64, 96,88 %, después P = 0,039). Se duplicó la proporción de encuestados que opinan que los métodos inmunoenzimáticos (ELISA) e inmunotransferencia tienen una sensibilidad media y baja especificidad (25/66, 37,88%, antes vs 56/64, 87,50%, después P = 0,000). Se incrementó en casi tres veces la proporción de médicos que respondieron correctamente que solo en 1% de los casos es posible hallar larvas de A. cantonensis en LCR (12/66, 18,18%, antes vs 34/64, 53,13%, después P = 0,000).

Tratamiento

Una mayor número de encuestados opinan que la conducta más efectiva para el tratamiento de la angiostrongiliasis es el uso de corticosteroides como terapia única y/o albendazol o mebendazol. (9/66, 13,64%, antes vs 23/64, 35,94%, después P = 0,000). Casi la totalidad de los médicos después de la intervención conocen que la mejor opción de tratamiento en los pacientes que presenten daño ocular es la remoción quirúrgica del parásito intraocular ((36/66, 54,55%, antes vs 63/64, 98,44 %, después P = 0,000).

Prevención

Una mayor proporción de médicos consideran que la cocción adecuada de caracoles o moluscos antes de ser ingeridos es el aspecto de prevención que más debe considerarse (21/66, 31,82%, antes vs 45/64, 70,31%, después

P = 0,000). Casi la mitad de los encuestados respondieron correctamente que ninguna otra de las medidas profilácticas mencionadas, como uso de vacunas, uso de antihelmínticos, exámenes periódicos de heces y detección de anticuerpos en suero, podían prevenir la infección ((14/66, 21,21%, antes vs 30/64, 46,88%, después P = 0,000).

Respuesta a aspectos de percepción

La infección por *A. cantonensis* es una causa poco frecuente de enfermedad en Ecuador (35/66, 53,03%, antes vs 45/64, 70,31%, después, P = 0,870. La mitad de los médicos encuestados continúan pensando, después de la intervención, que los conocimientos recibidos sobre la enfermedad en las universidades fueron insuficientes 44/66, 66,66%, antes vs 40/64, 62,50%, después (P = 0,864).

Respuesta a los aspectos relacionados con la práctica

De igual forma, una alta proporción de encuestados antes (60/66, 90,91%) y después de la intervención (63/64, 98,44%) conocen que la conducta a seguir ante la presencia de signos y síntomas neurológicos y antecedentes de ingestión de caracoles es la búsqueda de atención hospitalaria lo más pronto posible (P = 0,250). Una mayor proporción de médicos respondió correctamente que la búsqueda del parásito y conteo de eosinófilos en el líquido cefalorraquídeo, además del conteo de eosinófilos en sangre son los exámenes de laboratorio idóneos para confirmar el diagnóstico (45/66, 68,18%, antes vs 59/64, 92,19%, después P = 0,04). Ver figura 3.

Discusión

Los resultados de la primera aplicación de la encuesta CPP en relación con la angiostrongiliasis a médicos de atención primaria tanto del grupo con intervención como del grupo sin intervención, mostraron insuficiencias cognoscitivas, percepciones inadecuadas y prácticas incorrectas con relación a esta enfermedad. El no encontrar diferencias significativas en las respuestas de los médicos que laboran en las diferentes provincias en que se aplicó la encuesta, Napo (grupo con intervención) y Guayas (grupo sin intervención), sugiere que el desconocimiento sobre la enfermedad podría estar presente en otras provincias del país. Para contribuir a la atenuación de las deficiencias encontradas se ejecutó, en las Unidades de Salud de la provincia Napo (grupo con intervención), un grupo de acciones que podría incidir sobre las deficiencias encontradas en relación con la angiostrongiliasis humana. Seis meses más tarde de aplicada la primera encuesta, se aplicó nuevamente la misma, a los dos grupos de estudio. Esto permitió constatar, un incremento estadísticamente significativo en el nivel de conocimiento en la mayoría de los temas evaluados en el grupo de médicos que recibieron intervención educativa, lo que se evidenció por el mayor número de médicos que respondían correctamente a las preguntas. Sin embargo, como era de esperar, esas diferencias no fueron encontradas en las respuestas de los médicos del grupo sin intervención, los cuales no recibieron la capacitación que les hubiera permitido incrementar sus conocimientos sobre la angiostrongiliasis. El estudio realizado en médicos de familia que prestan servicios en los municipios Playa y San Miguel del Padrón, La Habana, se demostró que en relación con el diagnóstico, tratamiento y control de las geohelmintosis existían insuficiencias cognoscitivas, percepciones inadecuadas y prácticas incorrectas por parte de los médicos encuestados, lo que puso de manifiesto la necesidad de intervenciones educativas para el control de las parasitosis[23].

En otro estudio realizado en la provincia de Guantánamo, Cuba, por Blanco y colaboradores sobre aspectos esenciales del diagnóstico, tratamiento y prevención de la helmintiasis por *Inermicapsifer madagascariensis*, se observó mejoría en el conocimiento de los temas analizados, luego de una intervención educativa[24].

En otras investigaciones similares las estrategias que incluyeron un grupo de acciones, a modo de intervención, ante insuficiencias cognoscitivas, percepciones inadecuadas y prácticas incorrectas en relación a la giardiasis permitieron atenuar estas deficiencias[25,26].

Por otra parte, Mena, Tudela y colaboradores, evaluaron la efectividad de la intervención educativa realizada en el programa de segundo año del Grado en Enfermería de la Universidad Jaime I (España) sobre los conocimientos, habilidades y actitudes del estudiantado hacia la práctica basada en la evidencia. Los resultados muestran que esta intervención educativa puede mejorar en general la competencia práctica, principalmente en los temas de conocimientos y actitudes[27].

Son varios los estudios en que se logra una mejoría significativa en las evaluaciones realizadas lo que demuestra la eficacia de la intervención. De ahí la necesidad de monitorear y actualizar con regularidad los programas de formación de médicos y especialistas en los aspectos relacionados con el diagnóstico, tratamiento y control de las enfermedades parasitarias[25], enfatizando la necesidad de programas educativos basados en conferencias, cursos, distribución de material científico actualizado, publicación de algún libro sobre el tema[20]. Sin embargo, se considera que estas acciones deben tener sostenibilidad y sistematicidad para alcanzar una mejoría continua de los CPP relacionadas con el diagnóstico y el tratamiento de las parasitosis[28].

Hay una necesidad creciente en los países occidentales de fortalecer la enseñanza de la misma y de formar parasitólogos que puedan enfrentar los desafíos de la aparición de las que alguna vez fueron consideradas enfermedades de la pobreza y que cada vez más están siendo reconocidas como importantes patógenos oportunistas[29].

Con la aplicación de una encuesta sobre CPP a médicos vinculados con el diagnóstico, tratamiento y control de la angiostrongiliasis, se demostró que existen insuficiencias en los temas mencionados. Estudios como este permiten la evaluación del impacto de programas educativos con el fin de fortalecer la vigilancia epidemiológica de las parasitosis. Los efectos de esta intervención educativa, evaluada a través de los CPP, fueron suficientes para evidenciar, diferencias estadísticamente significativas en la proporción derespuestas correctas de los médicos de ambos grupos de estudio.

Es importante señalar que en la literatura revisada, estudios similares relacionados con la angiostrongiliasis no fueron encontrados. Los resultados de este trabajo son un llamado de atención a los responsables de la educación médica del país, con el fin de tomar medidas para suplir las falencias encontradas. mediante programas de formación continua que permitan a los médicos considerar a la meningoencefalitis por *A. cantonensis* entre sus alternativas diagnósticas e instaurar oportunamente el tratamiento.

Conclusiones

Luego de las deficiencias encontradas, luego de la aplicación de la encuesta sobre angiostrongiliasis por primera vez, a los médicos de atención primaria, la intervención educativa realizada contribuyó a la mejora del conocimiento de esta parasitosis, lo que podría contribuir a su mejor manejo y control. Es la primera vez que se hace en el país un estudio de este tipo con relación a angiostrongiliasis. Por lo tanto es un estudio piloto que ha demostrado resultados objetivos por lo que podría ser aplicado a otras provincias.

Limitaciones del studio

El estudio esta limitado unicamente a dos provincias donde se han reportado hospederos intermediarios infectados, es importante ampliar el estudio a mas provincias.

Contribuciones de los autores

Contribuciones sustanciales a la concepción y el diseño, o adquisición de datos, o análisis e interpretación de datos: LS, CCH, SS, RL, HH, MR, JS, CB, JP, FS, LR, . 2) redacción del artículo o revisarlo críticamente en busca de contenido intelectual importante: LS, CCH, SS, HH, MR, JS, CB, FS, LR, RL 3) aprobación final de la versión a publicar: LS, HH, MR, JS, LR. 4) acuerdo para actuar como garante del trabajo: LS, CCH, SS, LR, HH, MR, JS, CB, JS, JP, FS, FV.

Todos los autores han leído y estan de acuerdo con la versión publicada del manuscr

Financiamiento

La presente revisión bibliográfica fue completamente financiada por los autores.

Disponibilidad de datos y materiales

Los datos se sustentan este manuscrito están disponibles bajo requisición al autor correspondiente.

Conflictos de Interés

Los autores no reportan conflicto de intereses Appendix A.

Referencias bibliográficas

1. Murphy GS, Johnson S. Clinical Aspects of Eosinophilic Meningitis and Meningoencephalitis caused by Angiostrongylus cantonensis, the Rat Lungworm. Hawaii J Med Public Health. junio de 2013;72(6 Suppl 2):35-40.
2. Cowie RH. Biology, Systematics, Life Cycle, and Distribution of Angiostrongylus cantonensis, the Cause of Rat Lungworm Disease. Hawaii J Med Public Health. junio de 2013;72(6 Suppl 2):6-9.
3. Aguiar PH, Morera P, Pascual J. First record of Angiostrongylus cantonensis in Cuba. Am J Trop Med Hyg. septiembre de 1981;30(5):963-5.
4. Andersen E, Gubler DJ, Sorensen K, Beddard J, Ash LR. First report of Angiostrongylus cantonensis in Puerto Rico. Am J Trop Med Hyg. marzo de 1986;35(2):319-22.
5. Campbell BG, Little MD. The finding of Angiostrongylus cantonensis in rats in new orleans. Am J Trop Med Hyg. mayo de 1988;38(3):568-73.
6. Lindo JF, Waugh C, Hall J, Cunningham-Myrie C, Ashley D, Eberhard ML, et al. Enzootic Angiostrongylus cantonensis in rats and snails after an outbreak of human eosinophilic meningitis, Jamaica. Emerg Infect Dis. marzo de 2002;8(3):324-326.
7. Lindo JF, Escoffery CT, Reid B, Codrington G, Cunningham-Myrie C, Eberhard ML. Fatal autochthonous eosinophilic meningitis in a Jamaican child caused by Angiostrongylus cantonensis. Am J Trop Med Hyg. abril de 2004;70(4):425-428.
8. Raccurt CP, Blaise J, Durette-Desset MC. [Presence of Angiostrongylus cantonensis in Haiti]. Trop Med Int Health TM IH. mayo de 2003;8(5):423-426.
9. Caldeira RL, Mendonça CL, Goveia CO, Lenzi HL, Graeff-Teixeira C, Lima WS, et al. First record of molluscs naturally infected with Angiostrongylus cantonensis (Chen, 1935) (Nematoda: Metastrongylidae) in Brazil. Mem Inst Oswaldo Cruz. noviembre de 2007;102(7):887-889.
10. Giraldo A, Garzón C, Castillo A, Córdoba-Rojas DF. Confirmation of the presence of Angiostrongylus cantonensis in lung tissue of the African giant snail (Lissachatina fulica) in Colombia. Infectio. 3 de febrero de 2019;23(2):129-132.
11. Botero D, Restrepo, M. Parasitosis humana. Angiostrongylus cantonensis. 6ta ed. Medellin, Colombia: CIB; 2019. 679–723. p.
12. Mathison BA, Pritt BS. A Systematic Overview of Zoonotic Helminth Infections in North America. Lab Med. 2018,49(4), e61–e93
13. Kuberski T. Eosinophils in cerebrospinal fluid: criteria for eosinophilic meningitis. Hawaii Med J. abril de 1981;40(4):97-98.
14. Lo Re V, Gluckman SJ. Eosinophilic meningitis. Am J Med. 15 de febrero de 2003;114(3):217-223.
15. Shah I, Barot S, Madvariya M. Eosinophilic meningitis: a case series and review of literature of Angiostrongylus cantonensis and Gnathostoma spinigerum. Indian J Med Microbiol. marzo de 2015;33(1):154-158.
16. Tsai HC, Liu YC, Kunin CM, Lee SS, Chen YS, Lin HH, et al. Eosinophilic meningitis caused by Angiostrongylus cantonensis: report of 17 cases. Am J Med. agosto de 2001;111(2):109-114.
17. Punyagupta S, Juttijudata P, Bunnag T. Eosinophilic meningitis in Thailand. Clinical studies of 484 typical cases probably caused by Angiostrongylus cantonensis. Am J Trop Med Hyg. noviembre de 1975;24(6 Pt 1):921-931.
18. Solorzano LF, Martini Robles L, Hernandez H, Sarracent J, Muzzio J, Rojas L. Angiostrongylus cantonensis: un parásito emergente en Ecuador. Rev Cuba Med Trop. 2014;66(1):23-33
19. Pincay T, García L, Narváez E, Decker O, Martini L, Moreira J. Angiostrongiliasis por Parastrongylus (Angiostrongylus) cantonensis en Ecuador. Primer informe en Sudamérica. Tropical Medical Int Health. 2009;14(2):S37.
20. Martini-Robles L, Muzzio J, Orlando A, Correoso M, Narvaez G. Distribucion y hospederos de Angiostrongylus cantonensis en Ecuador. En: Angiostrongylus cantonensis Emergencia en America. La Habana: Academia. Ministerio de Ciencia, Tecnología y Medio Ambiente 2016 p. 221-232.
21. Guerrero M, Vargas FM, Rosero AR, Nuques M de L, Bolaños ES, Briones MT, et al. Meningitis eosinofílica por angiostrongylus cantonensis. Reporte de caso de autopsia. Medicina (Mex). 30 de septiembre de 2008;13(4):312-218.
22. Solórzano L, Sánchez-Amador F, Valverde T. Angiostrongylus (Parastrongylus) cantonensis on intermediate and definitive hosts in Ecuador, 2014-2017. Biomed Rev Inst Nac Salud. 15 de 2019;39(2):370-384.
23. Moreira Perdomo Y, Fong González A, Domenech Cañete I, Hernández Barrios Y, Baldriche Álvarez J, Sollet Céspedes Y, et al. Conocimientos, percepciones y prácticas en relación con las geohelmintosis. Rev Cubana Med Trop. diciembre de 2017;69(3):1-15.
24. Blanco VC, Romero M del CS, Gómez YM del C, Boué LME, Torres FDG. Intervención educativa al personal médico y paramédico sobre Inermicapsifer madagascariensis. Rev Inf Científica. 2015;90(2):270-278.
25. Fonte Galindo L, Ali Almannoni S, MonzoteLópez A, Fonte Galindo O, Sánchez Valdés L. Intervención para mejorar conocimientos, percepciones y prácticas en relación con el diagnóstico, tratamiento y control de la giardiasis. Rev Cubana Med Trop. septiembre de 2013;65(3):297-308.

26. Fonte Galindo L, Almannoni SA, Monzote López A. Acerca de una intervención para atenuar insuficiencias cognoscitivas, percepciones incorrectas y prácticas inadecuadas en relación con giardiasis. Rev Cuba Med Gen Integral. marzo de 2010;26(1):0-0.
27. Mena-Tudela D, González-Chordá VM, Cervera-Gasch A, Maciá-Soler ML, Orts-Cortés MI, Mena-Tudela D, et al. Eficacia de una intervención educativa de Práctica Basada en la Evidencia en estudiantes de segundo año de enfermería. Rev Lat Am Enfermagem 2018;26:e3026
28. Rodriguez M,, López MEG, Cañete R, Triana DE. Resultados de una intervención educativa sobre parasitismo intestinal en personal médico. Rev Cub Med Mil 2016; 45(1): 40-52.
29. Acholonu ADW. Trends in teaching parasitology: the American situation. Trends Parasitol. enero de 2003;19(1):6-9.

ARTICLE / INVESTIGACIÓN

Evaluación del estilo de vida con el riesgo de diabetes mellitus tipo 2 en trabajadores universitarios ecuatorianos

Assessment of lifestyle and risk of type 2 diabetes mellitus in Ecuadorian university workers

Rosario Suárez[1], Patricia Diaz[1], Yoredy Sarmiento-Andrade[1], Marcela Cadena[1], Ludwig Alvarez[2]*, Evelyn Frias-Toral[2]

DOI. 10.21931/RB/2022.08.02.6

[1] Departamento de Ciencias de la Salud, Universidad Técnica Privada de Loja, San Cayetano, Loja 110104, Ecuador.
[2] Escuela de Medicina, Universidad Católica de Santiago de Guayaquil, Av. Pdte. Carlos Julio Arosemena Tola, Guayaquil 090615, Ecuador.
Corresponding author: ludwig.alvarez@cu.ucsg.edu.ec

Resumen: Algunos trabajadores mantienen estilos de vida no saludables que los hace propensos a tener un alto riesgo de diabetes tipo 2 (DT2). El presente estudio tuvo como objetivo evaluar el riesgo de DT2 (RDT2) en personal administrativo y docente de una universidad ecuatoriana y factores asociados. Estudio de corte transversal que evaluó el RDT2 según FINDRISC. Se consideró RDT2 alto si la puntuación ≥12 puntos. Se analizaron aspectos sociodemográficos, hábitos nocivos y saludables; se midieron el índice de masa corporal (IMC), el perímetro abdominal (PA) y la tensión arterial (TA). Se evaluaron las razones de prevalencia bruta (RPB) y ajustada (RPA) para identificar factores asociados con RDT2. De 311 participantes, edad media de 41,02 años (DE 10,1), 58,2% mujeres y 41,8% hombres. La prevalencia de RDT2 elevada fue mayor en mujeres respecto a varones (38,1% frente a 32,3%) y aumentó en mayores de 40 años [RPA 1.55 (1.11-2.15)], personas casadas [RPA 1.49 (1.07-2.05)], aquellos con actividad física moderada o menor [RPA 1.55 (1.11-2.15)], y en aquellos con PA elevado [RPA 2,41 (1,33 - 4,36)]. La edad, la baja actividad física y el PA, fueron factores asociados con una mayor prevalencia de RDT2. Se deben promover estilos de vida saludables, para incrementar la actividad física y disminuir el PA en trabajadores, para reducir el riesgo de DT2.

Palabras clave: Diabetes Mellitus tipo 2, Estilos de Vida, Factores de Riesgo, Salud Laboral.

Abstract: Some workers maintain unhealthy lifestyles that make them prone to have a high risk of type 2 diabetes (T2DM). This study aimed to evaluate the risk of type 2 diabetes (T2DM) in an Ecuadorian university's administrative and teaching staff and its associated factors. A cross-sectional study evaluated RDT2 according to FINDRISC. RDT2 was considered high if the score ≥12 points. Sociodemographic aspects, harmful and healthy habits were analyzed; body mass index (BMI), abdominal perimeter (AP) and blood pressure (BP) were measured. Crude (GBR) and adjusted prevalence ratios (APR) were evaluated to identify factors associated with RDT2. Of 311 participants, the mean age was 41.02 years (SD 10.1), 58.2% female and 41.8% male. The prevalence of elevated RDT2 was higher in women relative to men (38.1% vs. 32.3%) and increased in those older than 40 years [PAR 1.55 (1.11-2.15)], married persons [PAR 1.49 (1.07-2.05)], those with moderate or lower physical activity [PAR 1.55 (1.11-2.15)], and in those with elevated BP [PAR 2.41 (1.33 - 4.36)]. Age, low physical activity and BP were factors associated with a higher prevalence of RDT2. Healthy lifestyles should be promoted to increase physical activity and decrease BP in workers to reduce the risk of T2DM.

Key words: Diabetes Mellitus type 2, Lifestyles, Risk Factors, Occupational Health, Workplace Health.

Introducción

Según la Organización Panamericana de la Salud (OPS), se estima que en la región de las Américas, existen 62 millones de personas que viven con DT2. Esta región tiene la mayor prevalencia de sobrepeso/obesidad así como inactividad física en relación a las demás, estas cifras han estado incrementándose desde el año 2000[1]. Según la agenda 2030 de las Naciones Unidas, se pretende reducir en un tercio la mortalidad prematura por enfermedades no transmisibles (ENT) mediante la prevención y el tratamiento[2]. De acuerdo a los determinantes sociales de la salud publicados por la Organización Munidal de la Salud (OMS), se reconoció que las condiciones laborales sí promueven el desarrollo humano, pero también contribuyen a las desigualdades en salud[3]. En el Plan de Acción sobre la Salud de los Trabajadores 2015-2025, la OMS tiene como objetivo abordar los desafíos y cambios que imponen los entornos laborales y cuidar de manera integral la salud con el seguimiento de la exposición a los riesgos en el trabajo y los riesgos en la vida diaria. Por tanto, se requieren acciones coordinadas para brindar una atención integral de la salud y con el objetivo de mejorar los entornos laborales[4]. Sin embargo, en la práctica diaria, la salud de los empleados se centra con frecuencia en aspectos específicos del área de la medicina del trabajo, como las condiciones produci-

Citation: Suárez R; Diaz P; Sarmiento-Andrade Y; Cadena M; Alvarez L; Frias-Toral E. Evaluación del estilo de vida con el riesgo de diabetes mellitus tipo 2 en trabajadores universitarios ecuatorianos. Revis Bionatura 2023;8 (2) 6. http://dx.doi.org/10.21931/RB/2023.08.02.6

Received: 2 January 2023 / **Accepted:** 13 March 2023 / **Published:** 15 June 2023
Publisher's Note: Bionatura stays neutral with regard to jurisdictional claims in published maps and institutional affiliations.

das por la exposición a determinados agentes o factores, descuidando en ocasiones la prevención primaria de ENT como la DT2.

Las guías actuales de prevención de enfermedades crónicas, destacan la importancia de estimar el nivel de riesgo de DT2, y de los factores que limitan la adherencia de las personas a los cambios positivos de hábitos de vida saludable y adherencia al tratamiento farmacológico, para lograr que estas estrategias preventivas sean más efectivas[5,6]. En países considerados de ingresos medianos-altos existen guías de práctica clínica orientadas al manejo de la DT2. El Ecuador, mediante el Ministerio de Salud Pública (MSP) diseñó la Guía de Práctica Clínica para DT2, que recomienda utilizar el puntaje Findrisc para RDT2, para detectar personas en riesgo[7]. Actualmente, en la literatura no existen reportes relacionados con la medición de este nivel de riesgo y sus factores asociados en la población laboral ecuatoriana. Esto es preocupante porque en Ecuador, en 2020, la DT2 fue la segunda causa de muerte, luego de la covid-19[8]. Además, 62,8% de los ecuatorianos tienen riesgo de padecer sobrepeso u obesidad, así como Enfermedades cardiovasculares (ECV), y 27% de esta población tiene síndrome metabólico (SM)[9]. Por tanto, el objetivo de este estudio fue medir el RDT2 en empleados ecuatorianos y sus factores asociados para contribuir al diseño de programas de prevención de estas enfermedades adaptados a la población local.

Materiales y métodos

Diseño y entorno del estudio

Se realizó un estudio transversal, analítico con docentes y personal administrativo de la Universidad Técnica Privada de Loja (UTPL), Ecuador, quienes voluntariamente aceptaron participar. Se excluyeron mujeres embarazadas, personas con discapacidad, mayores de 65 años, personas que no tuvieran relación de dependencia con la institución, pacientes con diagnóstico de DT2.

Esta investigación obtuvo el respaldo del comité de ética de investigación en humanos de la UTPL (UTPL-CEI-SH-2019-12) y todos los participantes fueron notificados y los que accedieron a formar parte del mismo firmaron el consentimiento informado.

La convocatoria se la realizó a través del departamento de Recursos Humanos utilizando el correo electrónico institucional e información en los espacios autorizados del campus universitario. La invitación se la envió a 1.429 personas inscritas en nómina, de las cuales 314 personas aceptaron participar y 3 fueron excluídos por ser pacientes con diabetes. La muestra resultó conveniente en relación a la facilidad de acceso y disponibilidad de personas para participar en el estudio. La recolección de información se inició del 3 al 28 de febrero de 2020. Un cuestionario fue aplicado por estudiantes de medicina previamente capacitados, bajo la supervisión de los investigadores. El cuestionario incluyó preguntas sobre variables sociodemográficas: edad, sexo, estado civil, nivel de educación, salario; hábitos poco saludables: consumo de tabaco y alcohol; hábitos saludables: consumo de frutas y verduras, según la encuesta STEPS de la OMS[10]. La actividad física también se evaluó mediante el cuestionario IPAQ (Cuestionario Internacional de Actividad Física), versión corta[11]. El cálculo del riesgo de DT2 se realizó a través de la escala FINDRISC[12,13]. El RDT2 se consideró alto si era ≥ 12 puntos, según el punto de corte recomendado por la Guía de Práctica Clínica del MSP de Ecuador, para la toma de decisiones no farmacológicas[7].

Las variables antropométricas medidas fueron peso en Kg, talla en metros y centímetros y circunferencia abdominal en centímetros. Para peso y estatura se utilizó una báscula mecánica portátil Rise Lake® con tallímetro para adultos, la cual se colocó sobre un terreno estable y plano. Los participantes fueron pesados y medidos sin zapatos, y los valores se expresaron en kilogramos y metros. El índice de masa corporal (IMC) se calculó dividiendo el peso (kg) por la altura al cuadrado (m^2). Los valores se clasificaron según el estándar de referencia de la OMS como bajo peso con un IMC menor a 18,5kg/m^2, peso normal entre 18,5 a 24,9 kg/m^2, sobrepeso de 25 a 29,9 kg/m^2, obesidad grado I de 30 a 34,9kg/m^2, obesidad grado II 35 a 39,9kg/m^2, obesidad grado III de 40kg/m^2 o más[14].

La medición del PA se realizó a nivel de la línea axilar media, en el punto medio entre el borde costal y la cresta ilíaca, con una cinta métrica plástica indeformable. Se realizó con el paciente en bipedestación y al final de una espiración normal; se realizaron dos mediciones, las cuales se promediaron. Se realizó una medición con una precisión de 0,1 cm en la cinta[10]. Se consideraron valores alterados si eran mayores de 80 cm en mujeres y mayores de 90 cm en hombres, según la clasificación de la Federación Internacional de Diabetes (IDF)[7].

Se utilizó un tensiómetro digital de la marca OMRON® para medir la tensión arterial (TA). A cada participante se le realizaron tres mediciones con intervalos de tres minutos entre cada una, siguiendo las recomendaciones del método STEPwise, y para el análisis se utilizó la media de la segunda y tercera lecturas de TA.

La clasificación de la tensión arterial se realizó utilizando la Guía de Práctica Clínica 2019 para la hipertensión arterial del MSP de Ecuador, que define la hipertensión arterial como tensión arterial sistólica (TAS) ≥140 mmHg y / o tensión arterial diastólica (TAD) ≥90 mmHg(10).

Análisis estadístico

Para el análisis se utilizó el paquete estadístico SPSS versión 23. Se aplicaron las pruebas de normalidad de Kolmogorov-Smirnov. Para describir las variables cuantitativas se utilizaron medidas de tendencia central (media y mediana) y dispersión (desviación estándar y rango intercuartílico) y las variables cualitativas se expresaron en frecuencias y porcentajes. En el análisis bivariado, para comparar las características sociodemográficas y el riesgo de DT2, se estimó la prevalencia de RDT2 y se utilizó la chi cuadrado y la razón de prevalencia con el intervalo de confianza del 95%. Se utilizó la regresión de Poisson para el análisis multivariado.

Resultados

Análisis descriptivo

Participaron 311 trabajadores universitarios (50,2% profesores, 49,8% personal administrativo). La figura 1 muestra el diagrama de flujo de selección de participantes. La edad media poblacional fue de 41,02 años (DE 10,1), 42,25 años (DE 10,42) en hombres y 40,14 años (DE 9,8) en mujeres. La mayoría (58,2%) eran mujeres, el 67,2% había realizado estudios de posgrado, el 57,9% de la muestra

estaba casado, 37,9% recibía entre 3 y 4 salarios mínimos. Dentro de los hábitos tóxicos, 11,6% fumaron alguna vez, y de ellos 41,6% lo hacía diariamente. 64,6% reportó haber consumido alguna bebida alcohólica en los 30 días previos. En relación a los hábitos saludables, los participantes consumían frutas, en promedio 4,6 (DE 2,1) días a la semana y vegetales 4,49 (DE 2,1), con promedios de 1,77 (DE 1,36) porciones de frutas/día y 1,58 (DE 1,1) porciones de vegetales/día. Además, 41,5% realizaba actividad física al menos 30 minutos al día, sin embargo la mayoría (39,2%) con un nivel bajo de actividad física, según el cuestionario IPAQ.

Los valores de TAS fueron elevados en 11,9% de los participantes y la TAD en 11,3%. Asimismo, el 45,7% de los hombres y 81,4% de las mujeres, presentó PA por encima de los valores normales, considerados para este grupo de población. Además, 52,4% tenía sobrepeso y 12,9% tenía algún grado de obesidad.

Al estratificar a los participantes por riesgo alto (RA) (FINDRISC≥12 puntos) o riesgo bajo o moderado (RB/RM) (FINDRISC <12 puntos), se evidenció que en el grupo con RA, la edad media fue mayor, 46 años con desviación estándar de 10 vs 38 años con desviación estándar de 9 y que la prevalencia de RDT2 fue más alta en mujeres en relación a los hombres (38.1% vs 32.3%), en personas con nivel educativo inferior (75% en personas con nivel de educación primaria vs 39.2% en personas con postgrado), en personas con pareja (44.4% en casados vs 18% en solteros), en docentes en relación a los administrativos (40.4% vs 31%), en personas con menos ingresos mensuales (42% en personas con ingresos entre 1-2 salarios mínimos vs 32.4% en los que ganan más de 5 salarios mínimos), pero resulta menor en los que han consumido bebidas alcohólicas en los 30 días previos (40.2% vs 31.8% en los que si) y en los que han fumado alguna vez (30.6% vs 36.4%). Si bien la mayoría de los participantes tenía un nivel educativo alto, se destaca que las personas con niveles educativos más bajos (nivel primario) tienen una prevalencia muy alta de RDT2 (75%) (Tabla 1).

Las variables relacionadas con estilos de vida saludables como la actividad física y el consumo adecuado de frutas y verduras, junto con las variables antropométricas,

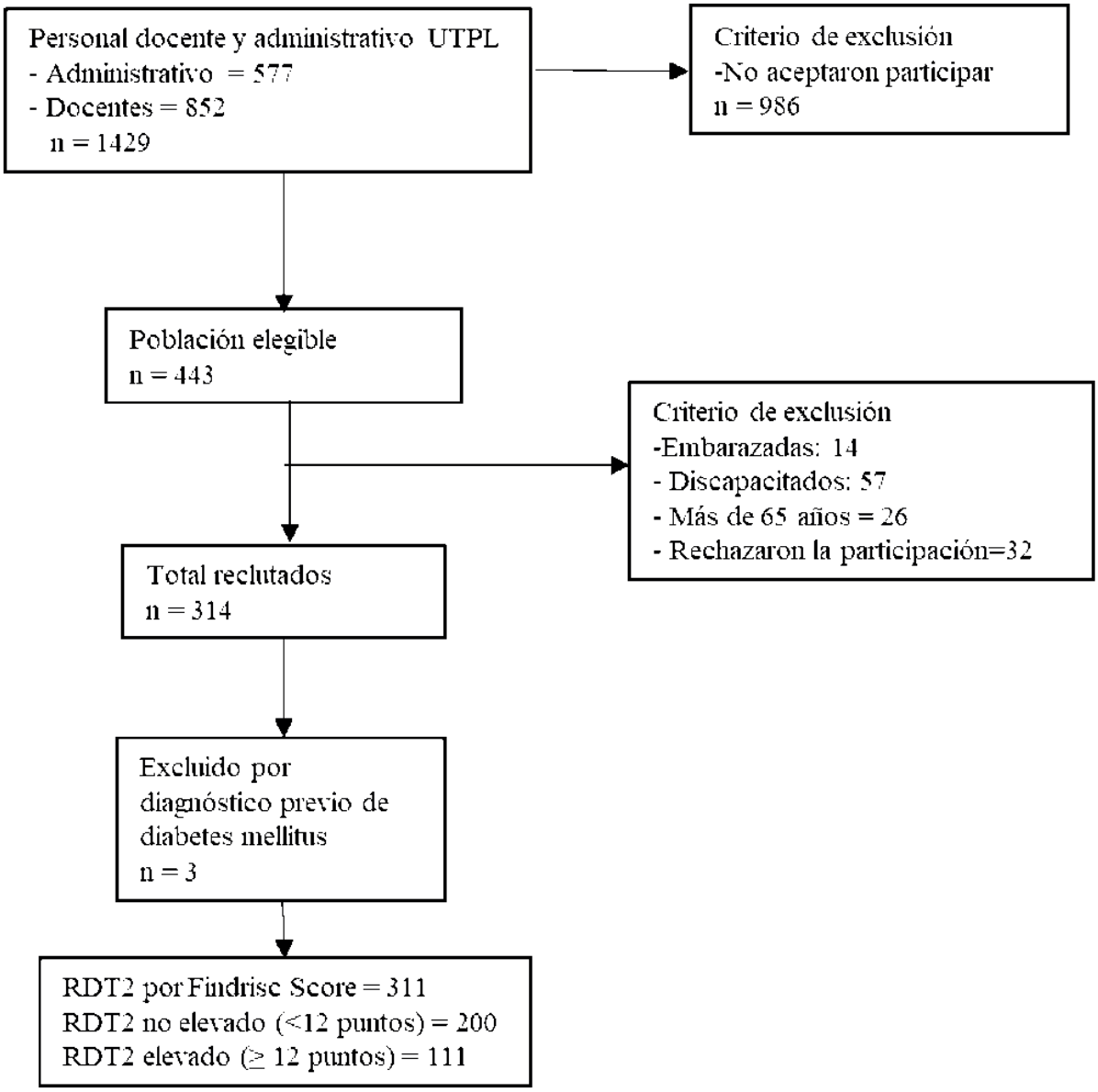

Figura 1. Diagrama de flujo de selección de participantes.

		RDT2	
		n = 311	
	Variables	**Riesgo bajo y moderado**	**Alto riesgo**
Sociodemográfico	**Edad, media (DE)**	38 (9)	46 (10)
	Género, n (%)		
	Masculino	88 (67,7)	42 (32,3)
	Femenino	112 (61,9)	69 (38,1)
	Nivel de educación, n (%)		
	Primario	1 (25)	3 (75)
	Secundario	7 (58,3)	5 (41,7)
	Universidad	65 (75,6)	21 (24,4)
	Posgrado	127 (60,8)	82 (39,2)
	Estado civil, n (%)		
	Soltero	73 (82)	16 (18)
	Casado	100 (55,6)	80 (44,4)
	Divorciado	18 (66,7)	9 (33,3)
	Union libre	7 (53,8)	6 (46,2)
	Viudo	2 (100)	0 (0)
	Actividad laboral, n (%)		
	Administrativo	107 (69)	48 (31)
	Docente	93 (59,6)	63 (40,4)
	Ingresos mensuales, n (%)		
	1-2 salarios mínimos	51 (58)	37 (42)
	3-4 salarios mínimos	78 (66,1)	40 (33,9)
	Más de 5 salarios mínimos	71 (67,6)	34 (32,4)

Tabla 1. Características sociodemográficas y hábitos no saludables asociados al riesgo de diabetes tipo 2, en trabajadores universitarios.

se presentan en la Tabla 2. Se evidencia mayor prevalencia de RDT2 elevado en personas que realizan un menor nivel de actividad física (45,9%) así como en los que consumen menos porciones al día de frutas y verduras y en obesos. Las medias de TA y PA fueron más altas en los participantes con mayor RDT2 (Tabla 2).

Análisis bivariado

El análisis bivariado evidenció en este estudio, que la prevalencia de RDT2 elevado, aumentó de acuerdo con la edad [RPB 1,94 (1,39 - 2,69)], estado civil casado [RPB 1,86 (1,32 - 2,62)], actividad física baja o moderada [RPB 1,64 (1,16 - 2,32)], IMC [RPB 2,20 (1,47-3,28)] y PA elevado [RPB 3,57 (2,07 - 6,18)]. El resto de los factores evaluados (sociodemográficos: sexo, nivel de educación, ingresos mensuales recibidos; hábitos tóxicos, consumo de tabaco o alcohol, hábitos saludables:consumo de frutas o vegetales; clínicos: nivel de TA) no se asociaron con RDT2 elevado (Tabla 3).

Análisis multivariado

En la Tabla 4 se muestra el análisis multivariado, con

Hábitos no saludables	**Tabaquismo, n (%)**		
	sí	25 (69,4)	11 (30,6)
	No	175 (63,6)	100 (36,4)
	¿Alguna vez ha consumido bebidas alcohólicas: cerveza, vino, aguardiente otros?, n (%)		
	sí	196 (65,1)	105 (34,9)
	No	4 (40)	6 (60)
	Consumo de bebidas alcohólicas en los últimos 30 días, n (%)		
	sí	137 (68,2)	64 (31,8)
	No	49 (59,8)	33 (40,2)
	Consumo excesivo de alcohol *		
	no	80 (64)	45 (36)
	sí	37 (80,4)	9 (19,6)

* 5 o más bebidas en hombres, 4 o más en mujeres.RDT2:riesgo de diabetes mellitus tipo 2

Tabla 1. Características sociodemográficas y hábitos no saludables asociados al riesgo de diabetes tipo 2, en trabajadores universitarios.

las razones de prevalencia ajustadas (RPA) por edad, sexo, nivel educativo, estado civil, tabaquismo, nivel de actividad física, TA, PA e IMC. En este caso, al hacer el ajuste se mantuvo la asociación con RDT2 elevado en los mayores de 40 años [RPA 1,55 (1,11-2,15)], en casados [RPA 1,49 (1,07-2,05)], en los que tienen actividad física baja o moderada [RPA 1,55 (1,11 - 2,15)], y en aquellos con PA elevado [RPA 2,41 (1,33 - 4,36)].

Discusión

Los resultados de esta investigación revelan que los factores de riesgo considerados como modificables, tales como la inactividad física y una PA alta, se asociaron con una mayor prevalencia de RDT2; aún luego del ajuste por otras variables sociodemográficas, clínicas y de hábitos tóxicos como el tabaquismo. Los factores de riesgo relacionados con presencia de DT2 fue aquellos con PA alterada, seguidos de los que realizaban actividad física baja o moderada y por último, los que eran casados. Al analizar los factores no modificables, una edad mayor (> 40 años) fue asociada a una mayor prevalencia de RDT2.

En relación a la edad como variable sociodemográfica asociada a mayor prevalencia de RDT2, un metaanálisis japonés determinó que éste es mayor a medida que progresa la misma, siendo mayor en personas que superan los 70; asimismo, este riesgo se mantiene en todos los grupos de edad a partir de los 40 años[15]. Por otra parte, a mayor tiempo de diagnóstico y progreso de la enfermedad, se incrementa el riesgo de padecer enfermedades cardiovasculares (ECV), como el del riesgo de muerte[16]. Un estudio realizado en Suecia mostró que la DT2 diagnosticada en ≤ 40 años, tenía un mayor riesgo de mortalidad total de 2,05 (IC 95% 1,81-2,33) y de ECV de 2,72 (IC 95% 2,13-3,48), con respecto a las poblaciones de control[17].

Asimismo, la OMS en América Latina en 2014 reportó una prevalencia de hiperglucemia de 9.3% en hombres y 8.1% en mujeres; siendo Guyana, Surinam, Chile y Argentina, los países con mayor prevalencia de DT2 en adultos ≥ 18 años[18]. La prevalencia de DTW, reportada por Encuesta Nacional de Salud y Nutrición 2011-2013 fue del 2,7% en el rango de 10-19 años, del 10,3% entre los 50 a 59 años, 5,4% en los que tenían 40 a 49 años y 1,9% para los de 30 a 39 años)[9]. Para 2016, según la OMS la prevalencia en Ecuador de DT2 fue de 7,3% y para 2018, 8%(19,20)[20]. Estos números muestran el aumento de casos de DT2 en Ecuador, así como la asociación del riesgo de presentar esta enfermedad con el aumento de las décadas de vida, lo que demuestra la importancia de implementar métodos de detección más eficientes y oportunos.

Analizando los factores sociodemográficos, no se encontró asociación con sexo, ni con el salario, pero si con el estado civil casado [RPA 1,49 (IC95%1,07-2,05), p=0,018]. Otros estudios informan resultados controvertidos, por ejemplo, uno de ellos encontró que estar casado tiene un menor RDT2 en un seguimiento de 5 años en ambos sexos[21]; sin embargo, otro estudio en mujeres encontró que, en comparación con el estado de casadas, el estado de viuda se asoció con un menor riesgo de DT2[22], mientras que en hombres la viudez se asoció con mayor riesgo[23]. En contraposición, un estudio realizado en población latina, no encontró relación entre ambos[24]. Un estudio realizado en España pone en evidencia el impacto del estado civil con el riesgo de presentar DT2 y sus complicaciones, determinando que el estado civil no casado podría relacionarse con su aparición, y que incluso podría modificar el efecto del nivel socioeconómico, esto considerando que los cuidados y el seguimiento terapéutico son fundamentales para disminuir el riesgo de aparición y complicaciones de DT2, tal vez debido a que las personas no casadas tendrían menor apoyo familiar y social, mayor tendencia a practicar hábitos

	RDT2	
	n = 311	
Variables	**Riesgo bajo y moderado**	**Alto riesgo**
Nivel de actividad física, n (%)		
Bajo	66 (54,1)	56 (45,9)
Moderado	48 (65,8)	25 (34,2)
Elevado	86 (74,1)	30 (25,9)
Realiza al menos 30 minutos de actividad física al día, n (%)		
No	95 (52,2)	87 (47,8)
Sí	105 (81,4)	24 (18,6)
Consumo de fruta, porciones por día, n (%)		
<5 porciones	179 (63,7)	102 (36,3)
> 5 porciones	8 (88,9)	1 (11,1)
Consumo de verduras, porciones por día, n (%)		
<5 porciones	182 (64,1)	102 (35,9)
> 5 porciones	7 (87,5)	1 (12,5)
Consumo diario de verduras, n (%)		
Todos los días	57 (72,2)	22 (27,8)
No todos los días	138 (63,3)	80 (36,7)
Consumo diario de frutas, n (%)		
Todos los días	48 (52,2)	44 (47,8)
No todos los días	148 (68,2)	66 (30,8)
IMC, media (DE)	25,8 (3,5)	28 (4)
Normal	86 (79,6)	22 (20,4)
Sobrepeso	97 (59,5)	66 (40,5)
Obesidad grado I	13 (40,6)	19 (59,4)
Obesidad grado II	2 (50)	2 (50)
Obesidad grado III	2 (50)	2 (50)
TAS, media (DE)	119 (16)	124 (16)
TAD, media (DE)	75 (10)	78 (10)
Perímetro abdominal*, media (DE)	86,6 (9,5)	93,3 (10,7)

Abreviaturas: RDT2: riesgo de diabetes mellitus tipo 2. IMC: Índice de masa corporal. TAS: tensión arterial sistólica. TAD: tensión arterial diastólica. * Perímetro abdominal elevado ≥90 cm en hombres, ≥80 cm en mujeres (según Federación Internacional de Diabetes para centro / sudamericanos).

Tabla 2. Estilo de vida, IMC, TA y PA asociados al riesgo de diabetes tipo 2, en trabajadores universitarios.

	RDT2			
Variables	**n (%)**	**Total**	**valor p[1]**	**RP bruta (IC del 95%)**
Edad <40 años	35 (24,1)	145		1
Edad> 40 años	79 (46,7)	169	<0,0001	1,94 (1,39 - 2,69)
Mujer	71 (38,8)	183		1
Masculino	43 (32,8)	131	0.333	0,85 (0,62 - 1,15)
Educación hasta la universidad	31 (29,8)			1
Nivel de educación (postgraduado)	83 (39,5)	203	0,076	1,37 (0,98 - 1,92)
Otro estado civil	32 (24,2)	132		1
Estado Civil: (Casado)	82 (45,1)	182	<0,001	1,86 (1,32 - 2,62)
Actividad laboral (administrativa)	50 (31,8)	157		1
Actividad laboral (docente)	64 (40,8)	157	0,127	1,28 (0,95 - 1,72)
Ingresos mensuales (> 5 salarios mínimos)	35 (33)	106		1
Ingresos mensuales (<5 salarios mínimos)	79 (38)	208	0,459	1,15 (0,83 - 1,59)
No fuma	103 (37,1)	278		1
Fuma	11 (30,6)	36	0.563	0,82 (0,49 - 1,38)
No ha consumido BA (%)	108 (35,5)	304		
Ha consumido BA.	6 (60)	10	0,137 *	1,69 (0,99 - 2,86)
Sin consumo de BA en los últimos 30 días (%)	34 (41)	83		1
Consumo de BA en los últimos 30 días (%)	65 (32,2)	202	0,201	0,79 (0,57 - 1,09)
Nivel de actividad física (alto) (%)	30 (27,9)	116		1
Nivel de actividad física (no alto) (%)	84 (42,4)	198	0,004	1,64 (1,16 - 2,32)
Consumo de fruta> 5 raciones diarias (sí)	1 (11,1)	9		1
Consumo de fruta <5 raciones diarias (sí)	105 (37)	284	0,119 *	3,33 (0,52 - 21,25)
Consumo de verduras> 5 raciones diarias (sí)	2 (22,2)	9		1
Consumo de verduras <5 raciones diarias (sí)	104 (36,4)	286	0,419 *	1,64 (0,48-5,61)
Consumo diario de verduras	23 (28,8)	80		1
Consumo de verduras no diario	82 (37,3)	220	0,171	1,30 (0,88-1,91)
Consumo diario de fruta	23 (28,7)	80		1
Consumo de fruta no diario	82 (37,3)	220	0,219	1,30 (0,88 - 1,91)
IMC normal	22 (20,4)	108		1
IMC (sobrepeso / obesidad)	92 (44,7)	206	<0,001	2,20 (1,47 - 3,28)
TAS normal	98 (35,5)	276		1
HTAS	16 (42,1)	38	0.539	1,19 (0,79 - 1,78)
TAD normal	97 (34,9)	278		1
HTAD	17 (47,2)	36	0,207	1,36 (0,92 - 1,98)
Perímetro abdominal normal *	12 (12,9)	93		1
Perímetro abdominal elevado *	102 (46,2)	221	<0,001	3,57 (2,07 - 6,18)

Abreviaturas: RDT2: riesgo de diabetes tipo 2. RP: razón de prevalencia. IMC: Índice de Masa Corporal. TAS: tensión arterial sistólica.TAD: tensión arterial diatólica. HTAS: hipertensión arterial sistólica. HTAD: hipertensión arterial diastólica. BA=bebidas alcohólicas. * Perímetro abdominal elevado ≥90 cm en hombres, ≥80 cm en mujeres (según Federación Internacional de Diabetes para centro / sudamericanos). 1Prueba de chi cuadrado.2Prueba exacta de Fisher

Tabla 3. Características sociodemográficas, clínicas, hábitos y factores asociados al riesgo de diabetes tipo 2 en trabajadores universitarios.

	RDT2	
Variables	**RP ajustada (IC del 95%)**	**valor p**
Edad> 40 años	1,55 (1,11 - 2,15)	0,010
Masculino	0,76 (0,57 - 1,02)	0,070
Nivel de educación (postgrado)	1,13 (0,82 - 1,56)	0,444
Estado civil casado	1,49 (1,07 - 2,05)	0,018
Fuma	1,07 (0,66 - 1,74)	0,786
Actividad física (no alta)	1,55 (1,11 - 2,15)	0,010
TAS	0,84 (0,51 - 1,39)	0,495
TAD	1,41 (0,84 - 2,37)	0,200
Perímetro abdominal	2,41 (1,33 - 4,36)	0,004
BMI (sobrepeso / obesidad)	1,40 (0,93 - 2,12)	0,105

Abreviaturas: RDT2: riesgo de diabetes tipo 2. RP: razón de prevalencia. TAS: tension arterial sistólica,TAD: tension arterial diastólica, IMC: indice de masa corporal

Tabla 4. Análisis multivariado. Factores asociados al riesgo de diabetes tipo 2 en trabajadores universitarios.

nocivos como el tabaquismo, el alcoholismo y sedentarismo y menor motivación para adherirse al plan terapéutico indicado[25].

En el presente estudio, el bajo nivel instruccional no fue un factor directamente relacionado con el RDT2. Un estudio ecuatoriano realizado en 2017, evidenció que las personas con menor nivel instruccional tenían peor control de DT2, sin embargo, no se encontró una relación clara del nivel educativo con el RDT2[26]. Otro estudio español demostró que un nivel socioeconómico bajo determinaba un perfil vascular desfavorable y la presencia de complicaciones que incluyeron amputación mayor de extremidades inferiores en pacientes varones, y encontró asociación significativa entre ese nivel socioeconómico bajo y la presencia de retinopatía diabética, pero no describió la asociación con RDT2[27]. Otras variables analizadas en este estudio, como hábitos poco saludables: consumo de tabaco y alcohol; y hábitos saludables: consumo de frutas y verduras, tampoco se asociaron con el RDT2.

En nuestro estudio, referente a las variables antropométricas no se encontró una mayor prevalencia de RDT2 con IMC elevado, ni TA alta; pero si con PA alterado. La obesidad, global (IMC) y visceral (PA), se relacionó con RDT2, pero no así la TA, al menos no una relación de causalidad. En Nigeria, se encontró asociación significativa entre hipertensión sistólica y el riesgo de desarrollar prediabetes como diabetes, en una muestra de 377 trabajadores de la salud[28]. Sin embargo, un estudio de cohorte investigó la relación bidireccional entre DT2 e hipertensión arterial (HTA), encontrando que puede haber causalidad desde DT2 a HTA, pero no hubo causalidad en sentido contrario[29].

En relación con la PA, se ha señalado la predisposición genética de la obesidad central asociado a un mayor riesgo de DT2 independientemente del IMC, los factores de riesgo dietéticos y de estilo de vida, con una razón de probabilidades (OR) de 1,04 (IC del 95%: 1,01-1,07)[30]. Por el contrario, un estudio en Irán, encontró que el poder predictivo del IMC y la circunferencia de la cintura (CC) eran similares para pronosticar riesgo de DT2 en ambos sexos. Los puntos de corte para predecir DT2 en hombres y mujeres fueron diferentes: en hombres, IMC de 26,2 kg /m2 y CC de 89,7 cm, y en mujeres, IMC de 28,6 kg / m2 y CC de 84,3 cm[31]. También se ha confirmado la relevancia de medir PA como indicador de obesidad abdominal dada su asociación con el aumento de la prevalencia de DT2[32-34]. Un metaanálisis encontró que PA ≥ 102/88 cm fue un mejor predictor que un IMC ≥ 30 para el desarrollo de DT2 (rRR = 0.81, 95% CI 0.68-0.96), pero no para hipertensión (rRR = 0.92, 95 CI% 0,80-1,06). Los análisis de subgrupos mostraron que PA ≥ 102/88 cm fue un mejor predictor de DT2 en mujeres que en hombres, y para edades de 60 años o más que otros grupos etários[35].

En 2019 se publicó un estudio en población latinoamericana que incluyó sujetos sin DT2 conocida. Se les aplicó el FINDRISC y posteriormente se les realizó una prueba de tolerancia oral a la glucosa, presentando un 21% de los participantes un trastorno del metabolismo de los carbohidratos. Además, el estudio informó que la edad (p = 0,0001), el IMC (p= 0,011) y la CC (p = 0,031) fueron significativamente más altos en los sujetos con alteración de la regulación de la glucosa en comparación con los que no la tenían[36].

En el presente estudio, el PA fue el factor más asociado con el RDT2 (RPA 2,41; IC 95%: 1,33-4,36). Por tratarse de un procedimiento sencillo para obtenerlo, podría utilizarse como medida de cribado, seguimiento o evaluación periódica de los trabajadores en relación con la prevención del riesgo de DT2. Aunque lo ideal sigue siendo el cribado de DT2 con mediciones de glucosa basal o con la prueba de tolerancia oral a la glucosa, con base en los resultados de este trabajo, la medición de PA y la escala FINDRISC pueden ser aplicados de forma rutinaria en la población laboral como método inicial de sospecha de DT2, y así optimizar recursos al realizar mediciones de glucosa en sangre solo en grupos de riesgo.

Los hábitos no saludables, en nuestro estudio demostró que la actividad física baja y moderada valorada por el IPAQ, se asoció con un RDT2 más alto [RPA 1,55 (IC 95% 1,11 - 2,15), p = 0,010]. Según la OMS, en Ecuador, la prevalencia de inactividad física para 2016 fue 24.5% (mujeres 29.9% vs hombres 18.9%) 2018[19,20]. Un estudio observacional de Taiwán informó que, si bien el aumento de la actividad física, una dieta saludable y la salud psicosocial tenían asociaciones no significativas con la DT2 analizadas individualmente; la combinación de los mismos (estilo de vida saludable, por sus siglas en inglés HLF) tuvo un efecto protector entre las personas de mediana y avanzada edad.

El grupo con HLF y un menor PA tuvo un riesgo relativo (RR) de DT2 de 0,54 (IC 95% 0,35-0,82) en comparación con el grupo sin HLF y con mayor PA. Mantener HLF y una PA normal podría posponer la incidencia de DT2, especialmente importante para los ancianos, y los efectos positivos se observan a partir de los 3 a 5 años de implementación de los mismos. La salud psicosocial es considerada también como un factor importante para prevenir la DT2[37]. En México, un estudio sobre el RDT2 no encontró mayor riesgo en personas con menos de 30 minutos diarios de actividad física; sin embargo, sí encontró un mayor riesgo de DT2 en aquellos con IMC alto, hipertensión, hipertrigliceridemia o síndrome metabólico[38]. Otro estudio ha encontrado un mayor riesgo de DT2 en personas con un menor nivel de actividad física, sin embargo, con escalas o puntajes distintos al IPAQ[39]. Varios autores informan que el nivel de sedentarismo, independiente de la actividad física, también aumenta el RDT2[40,41]. Por otro lado, una revisión sistemática analizó la información científica de diferentes protocolos de ejercicio y su asociación con la variabilidad glucémica a corto plazo en pacientes con DT2, y lo que se pudo observar es que el ejercicio agudo puede provocar modificaciones fisiológicas y bioquímicas que causen variaciones en los niveles de glucosa a corto plazo[42].

Otro de los factores que no se asoció a mayor prevalencia de RDT2 fue el tabaquismo, es posible que esté explicado por tratarse de una muestra pequeña. Un estudio prospectivo en hombres, realizado por la Asociación Americana de Diabetes, encontró que el tabaquismo se asoció con un aumento significativo del riesgo de DT2, incluso después del ajuste por edad, IMC y otros posibles factores de confusión. El beneficio de dejar de fumar sólo fue aparente después de 5 años de dejar de fumar, y el riesgo volvió al de quienes nunca habían fumado solo después de 20 años. Sin embargo, los hombres que dejaron de fumar durante los primeros 5 años de seguimiento mostraron un aumento de peso significativo y, posteriormente, un mayor riesgo de DT2 que los que continuaban fumando[43]. Otras publicaciones más recientes sí han encontrado mayor riesgo de DT2 en fumadores y exfumadores, que en no fumadores, además que este riesgo aumenta en relación con el mayor consumo de cigarrillos y disminuye luego de eliminar el consumo[44,45]. En el presente protocolo se evaluó sólo la relación entre fumar y el RDT2, por lo que la frecuencia del hábito, su suspensión o modificación pudiera ser objeto de investigaciones futuras.

Los hallazgos de nuestro estudio es brindar información sobre los factores de estilo de vida más asociados con una mayor prevalencia de RDT2 en trabajadores en Ecuador y enfatiza la necesidad de que desarrollen estrategias y programas educativos para disminuir el RDT2 en esta población.

Una limitación de esta investigación es la naturaleza de un estudio transversal que mide la prevalencia real en un momento dado pero no explica la causalidad. Sin embargo, este tipo de estudios permiten generar hipótesis, facilitando la elaboración de preguntas de investigación y orientando a los formuladores de políticas e investigadores en próximos proyectos. Por otro lado, el estudio fue realizado en una sola institución lo que podría afectar en cierto grado la generalización de los resultados.

Conclusiones

La edad es un factor asociado con un aumento en la prevalencia de RDT2 elevado. En relación a los factores modificables, el perímetro abdominal y la baja actividad física aumentan la probabilidad de RDT2. Por lo que es necesario incluir programas de intervención en la promoción de dietas saludables y actividad física adecuada a esta población.

Contribuciones de los autores

RS, MC, IC, PD, YS, contribuyeron al diseño y redacción del artículo. YS, RS, MC, LA y EFT escribieron y revisaron el artículo. RS, MC, IC, PD, YS, LA y EFT validaron la versión final del manuscrito.

Financiamiento

El nombre de la institución de financiación es Universidad Técnica Particular de Loja.

The name of FUNDER funded this research, grant number XXX" and "The APC was funded by XXX". Check carefully that the details given are accurate and use the standard spelling of funding agency names at https://search.crossref.org/funding. Any errors may affect your future funding.

Declaración Comité de Ética

El estudio fue conducido de acuerdo a los lineamientos de la Declaración de Helsinki y aprobado por Comité de ética de la UNIVERSIDAD TÉCNICA PARTICULAR DE LOJA (Código del protocolo UTPL-CEISH-2019-12, del 29 de noviembre de 2019).

Consentimiento informado

Consentimiento informado fue obtenido de todos los sujetos involucrados en el estudio.

Conflictos de Interés

Los autores declaran que no hay conflictos de interés.

Referencias bibliográficas

1. OPS OMS, OMS. Prevención de las enfermedades cardiovasculares. Directrices para la evaluación. Organización Panamericana de la Salud [Internet]. 2010;1–97. Available from: https://www.paho.org/hq/dmdocuments/2011/Directrices-para-evaluacion-y-manejo-del-riego-CV-de-OMS.pdf
2. United Nations. Sustainable Development Goals-Good Health and Well-Being [Internet]. [cited 2021 Nov 9]. Available from: https://www.un.org/sustainabledevelopment/es/health/
3. Commission on Social Determinants of Health.Subsanar las desigualdades en una generación : alcanzar la equidad sanitaria actuando sobre los determinantes sociales de la salud: informe final de la Comisión Sobre Determinantes Sociales de la Salud. Organización Mundial de la Salud [Internet]. 2009 [cited 2023 Mar 4]. Available from: https://apps.who.int/iris/handle/10665/44084.
4. Organización Panamericana de la Salud- Organización Mundial de la Salud. OPS/OMS. Plan de Acción para la Salud de los Trabajadores 2015-2025. 2015.
5. Arnett DK, Roger Blumenthal CCS, Michelle Albert CCA, Buroker AB, Goldberger ZD, Hahn EJ, et al. 2019 ACC/AHA Guideline on the Primary Prevention of Cardiovascular Disease. Circulation. 2019;140:596–646.

6. Cosentino F, Grant PJ, Aboyans V, Bailey CJ, Ceriello A, Delgado V, et al. 2019 ESC Guidelines on diabetes, pre-diabetes, and cardiovascular diseases developed in collaboration with the EASDThe Task Force for diabetes, pre-diabetes, and cardiovascular diseases of the European Society of Cardiology (ESC) and the European Association for the Study of Diabetes (EASD). Eur Heart J. 2020 Jan 7;41(2):255–323.
7. Ministerio de Salud Pública del Ecuador. Diabetes mellitus tipo 2. Guía de Práctica Clínica (GPC) [Internet]. Quito: Dirección Nacional de Normatización; 2017. Available from: https://www.salud.gob.ec/wp-content/uploads/2019/02/GPC_diabetes_mellitus_2017.pdf
8. Instituto Nacional de Estadísticas y Censos. Ecuador. Estadísticas Vitales. Registro Estadístico de Defunciones Generales de 2020 [Internet]. 2020 [cited 2021 Nov 10]. Available from: https://www.ecuadorencifras.gob.ec/documentos/web-inec/Poblacion_y_Demografia/Defunciones_Generales_2020/2021-06-10_Principales_resultados_EDG_2020_final.pdf
9. Freire WB, Ramirez MJ, Belmont P, Mendieta MJ, Silva MK, Romero N, et al. Encuesta Nacional de Salud y Nutrición del Ecuador. Quito, Ecuador: Ministerio de Salud Pública/Instituto Nacional de Estadísticas y Censos; 2013.
10. Organización Mundial de la Salud. Manual de vigilancia STEPS de la OMS. El método STEPwise de la OMS para la vigilancia de los factores de riesgo de las enfermedades crónicas [Internet]. Ginebra; 2006 [cited 2021 Nov 11]. Available from: https://apps.who.int/iris/bitstream/handle/10665/43580/9789244593838_spa.pdf?sequence=1&isAllowed=y
11. Mantilla Toloza SC, Gómez-Conesa A. El Cuestionario Internacional de Actividad Física. Un instrumento adecuado en el seguimiento de la actividad física poblacional. Revista Iberoamericana de Fisioterapia y Kinesiología [Internet]. 2007 Jan 1 [cited 2021 Nov 11];10(1):48–52. Available from: https://www.elsevier.es/es-revista-revista-iberoamericana-fisioterapia-kinesiologia-176-articulo-el-cuestionario-internacional-actividad-fisica--13107139
12. Saaristo T, Peltonen M, Lindström J, Saarikoski L, Sundvall J, Eriksson JG, et al. Cross-sectional evaluation of the Finnish Diabetes Risk Score: a tool to identify undetected type 2 diabetes, abnormal glucose tolerance and metabolic syndrome. Diab Vasc Dis Res. 2005 May 24;2(2):67–72.
13. Medina C, Barquera S, Janssen I. Validity and reliability of the International Physical Activity Ques-tionnaire among adults in Mexico. Rev Panam Salud Publica. 2013;34(1).
14. National Heart L and BI. Calculadora de BMI [Internet]. [cited 2021 Nov 14]. Available from: https://www.nhlbi.nih.gov/health/educational/lose_wt/BMI/bmicalc_sp.htm
15. Hirakawa Y, Ninomiya T, Kiyohara Y, Murakami Y, Saitoh S, Nakagawa H, et al. Age-specific impact of diabetes mellitus on the risk of cardiovascular mortality: An overview from the evidence for Cardiovascular Prevention from Observational Cohorts in the Japan Research Group (EPOCH-JAPAN). J Epidemiol. 2017 Mar 1;27(3):123–9.
16. Al-Saeed AH, Constantino MI, Molyneaux L, D'Souza M, Limacher-Gisler F, Luo C, et al. An Inverse Relationship Between Age of Type 2 Diabetes Onset and Complication Risk and Mortality: The Impact of Youth-Onset Type 2 Diabetes. Diabetes Care. 2016 May 1;39(5):823–9.
17. Sattar N, Rawshani A, Franzén S, Rawshani A, Svensson AM, Rosengren A, et al. Age at Diagnosis of Type 2 Diabetes Mellitus and Associations With Cardiovascular and Mortality Risks: Findings From the Swedish National Diabetes Registry. Circulation [Internet]. 2019 May 7 [cited 2021 Aug 26];139(19):2228–37. Available from: https://ndr.nu
18. Vargas-Uricoechea H, Casas-Figueroa LÁ. Epidemiología de la diabetes mellitus en Sudamérica: la experiencia de Colombia. Clínica e Investigación en Arteriosclerosis. 2016 Sep;28(5):245–56.
19. World Health Organization. Diabetes Country Profiles [Internet]. 2016 [cited 2022 Mar 25]. Available from: https://www.who.int/teams/noncommunicable-diseases/surveillance/data/diabetes-profiles
20. Pan American Health Organization-World Health Organization. Noncommunicable diseases country profiles 2018 - PAHO/WHO | Pan American Health Organization [Internet]. 2018 [cited 2022 Mar 25]. Available from: https://www.paho.org/en/node/64898
21. De Oliveira CMI, Tureck LV, Alvares D, Liu C, Horimoto ARVR, Balcells M, et al. Relationship between marital status and incidence of type 2 diabetes mellitus in a Brazilian rural population: The Baependi Heart Study. PLoS One. 2020 Aug 1;15(8 August):e0236869.
22. Ramezankhani A, Azizi F, Hadaegh F. Associations of marital status with diabetes, hypertension, cardiovascular disease and all-cause mortality: A long term follow-up study. PLoS One [Internet]. 2019 Apr 1 [cited 2021 Nov 22];14(4):e0215593. Available from: https://journals.plos.org/plosone/article?id=10.1371/journal.pone.0215593
23. Cornelis MC, Chiuve SE, Maria Glymour M, Chang SC, Tchetgen Tchetgen EJ, Liang L, et al. Bachelors, Divorcees, and Widowers: Does Marriage Protect Men from Type 2 Diabetes? PLoS One [Internet]. 2014 Sep 17 [cited 2021 Nov 22];9(9):e106720. Available from: https://journals.plos.org/plosone/article?id=10.1371/journal.pone.0106720
24. Garzón-Duque MO, Rodríguez-Ospina FL, Cardona D, Segura-Cardona ÁM, Borbón MC, Zuluaga-Giraldo AM, et al. Condiciones sociodemográficas, laborales, hábitos, estilos de vida y diabetes mellitus en trabajadores con empleos de subsistencia, Medellín-Colombia. Revista Brasileira de Medicina do Trabalho [Internet]. 2020 [cited 2021 Sep 1];18(3):280–92. Available from: http://rbmt.org.br/details/1546/en-US/socio-demographic--labor-conditions--habits--lifestyles-and-diabetes-mellitus-in-workers-with-subsistence-jobs--medellin--colombia
25. Escolar-Pujolar A, Córdoba Doña JA, Goicolea Julían I, Rodríguez GJ, Santos Sánchez V, Mayoral Sánchez E, et al. El efecto del estado civil sobre las desigualdades sociales y de género en la mortalidad por diabetes mellitus en Andalucía. Endocrinol Diabetes Nutr [Internet]. 2018 Jan 1 [cited 2022 Mar 24];65(1):21–9. Available from: https://www.elsevier.es/es-revista-endocrinologia-diabetes-nutricion-13-articulo-el-efecto-del-estado-civil-S2530016417302501
26. Fernández Freire M, Fernández F A. Relación del nivel de instrucción educativa con el control glicémico de diabetes mellitus tipo 2 en pacientes del Hospital Alberto Correa Cornejo de enero a diciembre de 2017. Práctica Familiar Rural. 2018 Nov 28;3(3).
27. Gutiérrez Fernández M, Carrasco de Andrés D, Salmerón Febres LM, González Herrera L, Jiménez Brobeil S. Impact of socioeconomic status on the clinical profile of patients with non-traumatic lower-limb amputation. Cir Esp [Internet]. 2021 Jan 1 [cited 2022 Mar 24];99(1):55–61. Available from: https://pubmed.ncbi.nlm.nih.gov/32061379/
28. Onyemelukwe OU, Mamza AA, Suleiman YK, Iyanda MA, Bello-Ovosi B, Bansi KI, et al. Prevalence of Pre-Diabetes, Diabetes and Associated Cardiovascular Risk Amongst Healthcare Workers in Ahmadu Bello University Teaching Hospital (ABUTH), Zaria using Glycated Haemoglobin. West Afr J Med [Internet]. 2020 Apr [cited 2021 Nov 23];37(2):91–9. Available from: https://pubmed.ncbi.nlm.nih.gov/32150625/
29. Sun D, Zhou T, Heianza Y, Li X, Fan M, Fonseca VA, et al. Type 2 Diabetes and Hypertension. Circ Res [Internet]. 2019 Mar 15 [cited 2021 Nov 23];124(6):930–7. Available from: https://pubmed.ncbi.nlm.nih.gov/30646822/
30. Huang T, Qi Q, Zheng Y, Ley SH, Manson JAE, Hu FB, et al. Genetic predisposition to central obesity and risk of type 2 diabetes: Two independent cohort studies. Diabetes Care [Internet]. 2015 Jul 1 [cited 2021 Aug 26];38(7):1306–11. Available from: https://care.diabetesjournals.org/content/38/7/1306

31. Haghighatdoost F, Amini M, Feizi A, Iraj B. Are body mass index and waist circumference significant predictors of diabetes and prediabetes risk: Results from a population based cohort study. World J Diabetes [Internet]. 2017 [cited 2021 Nov 18];8(7):365. Available from: https://pubmed.ncbi.nlm.nih.gov/28751960/
32. Caspard H, Jabbour S, Hammar N, Fenici P, Sheehan JJ, Kosiborod M. Recent trends in the prevalence of type 2 diabetes and the association with abdominal obesity lead to growing health disparities in the USA: An analysis of the NHANES surveys from 1999 to 2014. Diabetes Obes Metab [Internet]. 2018 Mar 1 [cited 2021 Aug 26];20(3):667–71. Available from: https://dom-pubs.onlinelibrary.wiley.com/doi/full/10.1111/dom.13143
33. Ross R, Neeland IJ, Yamashita S, Shai I, Seidell J, Magni P, et al. Waist circumference as a vital sign in clinical practice: a Consensus Statement from the IAS and ICCR Working Group on Visceral Obesity. Nat Rev Endocrinol [Internet]. 2020 Feb 4 [cited 2021 Aug 26];16(3):177–89. Available from: https://www.nature.com/articles/s41574-019-0310-7
34. Chen CC, Liu K, Hsu CC, Chang HY, Chung HC, Liu JS, et al. Healthy lifestyle and normal waist circumference are associated with a lower 5-year risk of type 2 diabetes in middle-aged and elderly individuals: Results from the healthy aging longitudinal study in Taiwan (HALST). Medicine (United States) [Internet]. 2017 [cited 2021 Aug 26];96(6). Available from: https://journals.lww.com/md-journal/Fulltext/2017/02100/Healthy_lifestyle_and_normal_waist_circumference.24.aspx
35. Seo DCC, Choe S, Torabi MR. Is waist circumference ≥ 102/88 cm better than body mass index ≥ 30 to predict hypertension and diabetes development regardless of gender, age group, and race/ethnicity? Meta-analysis. Preventive Medicine Academic Press; Apr 1, 2017 p. 100–8.
36. Muñoz-González MC, Lima-Martínez MM, Nava A, Trerotola G, Paoli M, Cabrera-Rego JO, et al. FINDRISC Modified for Latin America as a Screening Tool for Persons with Impaired Glucose Metabolism in Ciudad Bolívar, Venezuela. Medical Principles and Practice [Internet]. 2019 Jul 1 [cited 2021 Aug 26];28(4):324–32. Available from: https://www.karger.com/Article/FullText/499468
37. Chen CC, Liu K, Hsu CC, Chang HY, Chung HC, Liu JS, et al. Healthy lifestyle and normal waist circumference are associated with a lower 5-year risk of type 2 diabetes in middle-aged and elderly individuals: Results from the healthy aging longitudinal study in Taiwan (HALST). Medicine [Internet]. 2017 [cited 2022 Mar 25];96(6). Available from: https://pubmed.ncbi.nlm.nih.gov/28178143/
38. Flores YN, Toth S, Crespi CM, Ramírez-Palacios P, McCarthy WJ, Briseño-Pérez A, et al. Risk of developing pre-diabetes or diabetes over time in a cohort of Mexican health workers. PLoS One [Internet]. 2020 [cited 2021 Aug 26];15(3):e0229403. Available from: https://journals.plos.org/plosone/article?id=10.1371/journal.pone.0229403
39. Indrahadi D, Wardana A, Pierewan AC. The prevalence of diabetes mellitus and relationship with socioeconomic status in the Indonesian population. Jurnal Gizi Klinik Indonesia [Internet]. 2021 Jan 7 [cited 2021 Aug 26];17(3):103. Available from: https://jurnal.ugm.ac.id/jgki/article/view/55003
40. Leiva AM, Martínez MA, Cristi-Montero C, Salas C, Ramírez-Campillo R, Martínez XD, et al. El sedentarismo se asocia a un incremento de factores de riesgo cardiovascular y metabólicos independiente de los niveles de actividad física. Rev Med Chil [Internet]. 2017 Apr 1 [cited 2021 Aug 26];145(4):458–67. Available from: http://www.scielo.cl/scielo.php?script=sci_arttext&pid=S0034-98872017000400006&lng=en&nrm=iso&tlng=en
41. Rodríguez; LM. Mendoza; CM. Sirtori; AM., Rodríguez Leyton M, Mendoza Charris M, Sirtori Campo AM, Caballero Torres I, Suárez Muñoz M, et al. Riesgo de Diabetes Mellitus tipo 2, Sobrepeso y Obesidad en adultos del Distrito de Barranquilla. RESPYN Revista de Salud Pública y Nutrición. 2018;17(4):1–10.
42. von Oetinger G A, Trujillo G LM, Soto I N. Impacto de la actividad física en la variabilidad glucémica en personas con diabetes mellitus tipo 2. Rehabilitacion (Madr) [Internet]. 2021 Apr 14 [cited 2021 Aug 26]; Available from: https://linkinghub.elsevier.com/retrieve/pii/S004871202030133X
43. Goya Wannamethee S, Gerald Shaper A, Perry IJ. Smoking as a Modifiable Risk Factor for Type 2 Diabetes in Middle-Aged Men. Diabetes Care. 2001 Sep 1;24(9):1590–5.
44. Akter S, Goto A, Mizoue T. Smoking and the risk of type 2 diabetes in Japan: A systematic review and meta-analysis. J Epidemiol. 2017 Dec 1;27(12):553–61.
45. Yuan S, Larsson SC. A causal relationship between cigarette smoking and type 2 diabetes mellitus: A Mendelian randomization study. Scientific Reports 2019 9:1 [Internet]. 2019 Dec 18 [cited 2021 Nov 22];9(1):1–4. Available from: https://www.nature.com/articles/s41598-019-56014-9

REVIEW / ARTÍCULO DE REVISIÓN

Antifungal activity of metabolites from *Trichoderma spp.* against *Fusarium oxysporum*

González M.F[1,2,3]*, Galarza L[1,2], Valdez L.L[3], Quizhpe G.M[3]

DOI. 10.21931/RB/2022.08.02.7

[1] Escuela Superior Politécnica del Litoral, ESPOL, Biotechnology Research Center (CIBE), Campus Gustavo Galindo, Guayaquil, Ecuador.
[2] Escuela Superior Politécnica del Litoral, ESPOL, Faculty of Life Sciences, Campus Gustavo Galindo, Guayaquil, Ecuador.
[3] Universidad de Guayaquil, Facultad de Ingeniería Química, Facultad de Ciencias Química Cdla, Guayaquil, Ecuador.
Corresponding author: marfgonz@espol.edu.ec

Abstract: The *Trichoderma* genus is well known as one of the most valuable biological control agents against several phytopathogens used in different plant species. Managing phytopathogenic fungi using the Trichoderma genus through various associated antifungal mechanisms is a sustainable and eco-friendly strategy that reduces the harmful presence of pathogens in soil, roots and aerial parts of plants. However, using biocontrol agents combined with chemical pesticides has evidenced further potential to reduce pathogen growth and benefit plant development. A better characterization of active metabolites secreted by *Trichoderma* and their mechanisms of action is necessary to improve its use as a biocontrol agent. This review summarizes current evidence on *Trichoderma spp.*, used as a biocontrol against *Fusarium oxysporum*, the active secondary metabolites secreted by the former fungi, and the effect of three widely used agrochemicals to control the latter, namely Mancozeb, Chlorothalonil, and Propiconazole. A total of 155 studies were selected and used to extract information that was analyzed, resulting in more than 590 identified secondary metabolites. Fifty-four percent of these have at least one biological function. Results highlight the potential of *T. harzianum* and *T. reesei* as biological control agents to control *Fusarium oxysporum*. The antifungal activity of *T. Espirale* is associated with enzymatic reactions. Additional findings show that management of diseases caused by *F. oxysporum* can be combined by using Trichoderma as biological control and agrochemicals to reach: (1) higher access to the different plant tissues; (2) higher degradation of the cell wall; and (3) and activation of oxidative metabolism of Trichoderma.

Key words: *Trichoderma*, secondary metabolites, fungicide, mycoparasitism, biocontrol, *Fusarium oxysporum*.

Introduction

Fusarium oxysporum is one the most economically important phytopathogens when referring to agriculturally important crops such as bananas and other crops[1]. The fungus infects the host plant through the roots or stems, causing wilt, blight, rot, and cancer of many plant species leading to significant yield loss in economically important crops such as banana[2], onion[3], tomato[4], chili[5], watermelon[6], cabbage[7], ginger[8], chickpea[9], soybean[10,11], eggplant plants[12], as well as ornamental plants like *Chrysanthemum spp.*, *Dianthus spp.*, *Gerbera spp.*, *Gladiolus spp.* and *Lilium spp.*[1]. No curative control method is currently available against this pathogen[1]. Current approaches to control *F. oxysporum* infestation are based on prophylactic measures and cultural practices[1] like keeping tools, soils and substrates in good sanitary conditions, planting resistant or tolerant genotypes, paying particular attention to crop monitoring, appropriate management of irrigation and crop rotation[1].

Chemical fungicides have also been essential in managing *Fusarium oxysporum* wilt for decades. However, these chemical control agents often become ineffective since pathogens may develop resistance, and the chemicals may adversely affect soil fertility and accumulate in the crop[13]. Since chemical pesticides are not selective, they can influence many beneficial non-target biotas and potentially harm the farmer's health[14-16]. Due to the harmful effects of these products, different policies that limit pesticide use have been implemented in several nations in the world[1,17].

Alternatively, biocontrol agents aim to regulate the growth of the pathogen with less harm to the plant and farmers. In this line, mycopesticides are exciting products because they use several mechanisms of action that reduce plant disease caused by phytopathogenic fungi[1,13,18]. Biopesticides are often less toxic than chemical products and decompose quickly. This can avoid pollution problems, resistance and residue concerns. Biopesticides generally affect only the target pest and closely related organisms, thereby protecting other organisms living in the same environment. The commercial evolution of the biopesticide market is promising to be a potential tool for pathogen control with a current annual growth rate of 14.1%[13].

Trichoderma spp. comprises more than 200 validly described species distributed in soils worldwide and across various habitats and are considered a valuable resource for structurally novel natural products with diverse bioactivities, including biological control of phytopathogens[19]. In the interest of obtaining more effective methods of pathogen control, plant growth-promoting rhizosphere microorganisms have been used as a consortium or in combination with chemical pesticides by our group and other authors[20-23]. Bioassays have revealed great potential to improve current methods of managing antifungal treatments to plant culti-

Citation: Gonzalez MF; Galarza L; Valdez L, Quizpe G . A systematic review of antifungal activity of metabolites from trichoderma spp., and fungicides against Fusarium oxysporum. Revis Bionatura 2023;8 (2) 7. http://dx.doi.org/10.21931/RB/2023.08.02.7
Received: 2 January 2023 / **Accepted:** 13 March 2023 / **Published:** 15 June 2023

Publisher's Note: Bionatura stays neutral with regard to jurisdictional claims in published maps and institutional affiliations.

vars. Yet, summarized evidence about active metabolites and the mechanism of actions of both biocontrol agents and chemical pesticides is needed to better use this possibility.

In this work, we reviewed the use of *Trichoderma spp*. as a biocontrol agent and the secondary metabolites and enzymes that have been characterized as active molecules. As additional findings, we also summarized the antifungal activity of commercial fungicides Mancozeb, Chlorothalonil, and Propiconazole, which are often used to control plant diseases caused by F. oxysporum.

Narrative Findings on *Trichoderma spp*

Trichoderma is a genus that belongs to the family *Hypocreaceae* and comprises many different fungi strains found in most diverse ecosystems[19]. *Trichoderma* strains proliferate and have a characteristic morphology, white and cottons at the beginning, then developing into yellowish green to deep green compact tufts. *Trichoderma* strains are characteristically branched[24]. The distinctive species categorized in the genus of *Trichoderma* are hard to differentiate morphologically. Based on morphology, *Trichoderma* strains have been classified into five sections: *Saturnisporum, Pachybasium, Longibrahiatum, Trichoderma* and *Hypocreanum*[25]. New genetic tools and physiological activity are used to determine the different functional groups within *Trichoderma spp*. Thus, current identification methods of *Trichoderma* strains include morphological and molecular characterization.

Many *Trichoderma* fungi act as biocontrol agents of phytopathogens and plant growth promoters[26]. They can also stimulate plant defense mechanisms against insect pests and be efficient soil bioremediation agents[27]. *Trichoderma spp*. can also be used in waste/organic materials decomposition and polluted area detoxification[28]. Some examples have emerged as human pathogens, for example *T. longibrachiatum*. Consequently, while the studies on effective biocontrol fungal are ongoing, further research to avoid the risk for humans, plants, and other organisms contributed by *Trichoderma spp.* also need to be accomplished.

The Mechanisms of biological control by *Trichoderma spp*

Biological control by *Trichoderma spp.* is based on the activation of indirect and direct mechanisms. Direct and indirect mechanisms can act synergistically and depending on species and strain[29]. The indirect mechanisms are competition for space and nutrients, growth promotion, and systemic resistance induction. The mechanisms by which *Trichoderma* induces systemic resistance in plants vary depending on plant species, *Trichoderma* species, pathogen species, abiotic stress conditions, and culture methods. It has been shown that *Trichoderma* colonization of plant rhizosphere may simultaneously activate both systemic acquired resistance and induced systemic resistance mechanisms of the plant. *Trichoderma* is also known to induce the resistance of plants towards diseases by root architecture alteration during the interaction with pathogens[30].

Direct mechanisms are mycoparasitism and the production of active metabolites and lytic enzymes[3,31]. Mycoparasitism, the ability to parasitize on fungi, is a unique characteristic of *Trichoderma* since they can parasitize even taxonomically close species[19]. The antifungal activity of *Trichoderma* against phytopathogenic fungi is attributed to the combined action of secondary metabolites (SMs) and hydrolytic enzymes i.e., cellulases, proteases, chitinases, and xylanases[3,32,33]. About 500,000 secondary metabolites have been described; of these, 15.600 (47 %) are of fungal origin.

Characterization of genes involved in fungal–fungal interactions has indicated that are mainly those involved in signal transduction, fungal cell wall degradation, and production of secondary antifungal metabolites (SMs)[19].

Secondary metabolites and enzimes produced by *Trichoderma spp*

SMs are not essential for normal growth but are synthetized for specific environmental conditions. SMs can be either volatile or non-volatile organic compounds. Volatile SMs diffuse over a distance through systems in the soil affecting the physiology of competitor organisms[34-36]. Non-volatile SMs exert their activity through direct interactions between *Trichoderma* species and their antagonists[35].

Our search for current evidence on SMs secreted by *Trichoderma spp*. Or enzymes resulted in annotating 590 unique compounds listed in the sup[A5] plementary Table S1. It includes many structural classes like pyrones, butenolides, steroids, peptaibols and terpenoids[19]. Fifty-four percent of all SMs or enzymes retrieved in our search have at least one biological effect associated, described in Table S1. Even though this list of biological activities should not be considered exhaustive, it allows appreciation of the incredibly broad range of biological activities of *Trichoderma* SMs i.e, antifungal, antibacterial, antitumor, DPPH-radical-scavenging, positive effect on plant growth and development, among others (Table S1). Further investigation is required using isolated compounds to obtain a comprehensive understanding of all effects at different for the different combinations.

The list of SMs shown in supplementary Table S1 is consistent with previous papers that emphasize that the quality and the number of volatile compounds produced are variable for each strain of *Trichoderma*. As example of the diversity in SMs produced by different *Trichoderma* species. A total of 115 SMs were reported for *T. reesei, T. harzianum* and *T. spirale* (Table S1). SM or enzymes identified for *T. reesei, T. harzianum* and *T. spirale* are indicated in Table 1, 2 and 3, respectively, which could be potentially used to control *Fusarium oxysporum*, due to their antifungal activity.

This result should not be understood as only *T. harzianum* secretes all these compounds. Genes encoding for proteins responsible for synthesizing these SMs are usually not expressed constitutively but due to interactions with the pathogen in the plant rhizosphere[4,45]. For example, the SM trichosetin, presumably secreted by *T. harzianum*, has only been identified in dual culture of *T. harzianum* and calli of *Catharathus roseus* but not in single cultures[31]. However, the vast diversity of SMs isolated and characterized from *T. harzianum* indicates the great potential value of this fungus as a biocontrol agent against phytopathogenic fungi.

In vitro and *in vivo* assays have shown *T. harzianum* isolates with higher inhibitory activity against *F. oxysporum* (F3) than other *Trichoderma* species[46]. Biocontrol potential of *T. harzianum* against *Fusarium Oxysporum* has been demonstrated *in vitro* e *in vivo* against *F. oxysporum* in Poplar[47], ginger[8], cucumber[29,48], lettuce[49], white yam[50], chili[51], tomato and cucumber[52]. Nonetheless, *T. reesei* is one of the top fungal species used in industrial biotechnology and is used safely for decades in enzyme production. In contrast to *T. harzianum*, *T. reesei* is considered to have a limited production of mycotoxins[53]. Table 2 lists all SMS associated with antifungal activity.

Despite the literature did not specifically listed the SMs

Reference	Secondary Metabolite (SMs)
37	1,8-dihydroxy-3-methylanthraquinone
	1-hydroxy-3-methylanthraquinone
	1-hydroxy-3-methylanthraquinone
	6-methyl-1,3,8-trihydroxyanthraquinone
	6-methyl-1,3,8-trihydroxyanthraquinone
38	6-pentyl-α-pyrone
37	8-dihydroxy-3-methylanthraquinone
38	Farzianopyridone
39	Glutaryl-CoA
31–33,37,40–43	Harzianic acid
31–33,37	Harzianolide
37	Hydroxylphenylethanol
39	N-Undecanoylglycine
13	Pachybasin
39	Psoromic acid
32,38	Stigmasterol
31,32,37	T39butenolide
43	Trichocaranes A – D
44	Trichodermaol
37	Trichodermin
37	Trichokindin II*

Table 1. SMs of *Trichoderma harzianum* with antigungal activity.

Reference	Secondary Metabolite (SMs) or Enzime *
37	Harzialactone A
54	Ilicicolin H
37,55	Oxosorbicillinol
56	Trichodermin
57	*Xylanase
58	α-aminobutyric acid
59,60	α-aminoisobutyric acid

Table 2. SMs or enzymes of *Trichoderma reesei* with antifungal activity.

of *T. spirale* associated with the antifungal activity, it was worth to list the asociated enzimes *Trichoderma spirale* (Table 3). This list is short but shows the potential use of *T. spirale* [A9] in the control of pathogenic fungi.

In this work, we reviewed the use of *Trichoderma spp.* as biocontrol agents, the secondary metabolites characterized as active molecules and the enzymes found in this bibliographic review which present antifungal characteristics that act directly on the phytopathogenic fungi. The following graph highlights the following strains of *Trichoderma spp.*, *T. reesei, T. harzianum* and *T. spirale* with the most critical metabolites and enzymes.

Additional findings on the use of *Trichoderma spp.* and 3 synthetic pesticides[A10]

The low input cost and higher crop productivity of applying biological control agents (or biopesticides) are the economic benefits observed when compared to synthetic pesticides[63]. Thus, the use of *Trichoderma* is regarded as a sustainable approach not only ecologically but also from an economic perspective.

However, using microbial-based products as biocontrols or biostimulants has some disadvantages compared to their chemical counterparts. Microbial products have a limited shelf life and require special conditions for conser-

Reference	Enzymes associated with antifungal activity on *Trichoderma Spirale*
61	Chitinase
62	Endochitinase
37	Trichodemic acid
61	β-1,3-Glucanase

Table 3. Enzymes associated with antifungal activity of *Trichoderma spirale*.

vation to maintain viability and efficacy[44]. Also, they have constraints due to dependency on the crop, geographical, and meteorological regimes and pathogens[3,63].

One interesting approach that has emerged to cope with the advantages and limitations of the different methods to control crop infestation with *F. oxysporum* is the simultaneous application of *Trichoderma* as biological control with chemical pesticides and other biological control agents. For example, a combined treatment with *T. polysporum* LCB50 and irrigation with liquid compost applied resulted in a strong synergistic effect in controlling melon wilt and a 100% increase in the productivity of commercial fruit[64].

Recent results from our group have shown a synergistic effect using *T. reesei* and Mancozeb, inhibiting the mycelial growth of *F. oxysporum* (F1)20. Also, a synergic activity was obtained in vitro assays using *T. ressei* combined with Chlorothalonil or Propiconazole (unpublished data). However, the molecular basis of these agents' biological activity that results in an increased capacity to inhibit *F. oxysporum* infection is unknown.

Chlorothalonil (tetrachloroisophthalonitrile) and Mancozeb (manganese ethylene bis (dithiocarbamate) (polymeric) complex with zinc salt) are multisite enzyme inhibitors that act as protective broad spectrum fungicides[65]. Both are non-systemic, preventive fungicides that form a protectant barrier at the surface of the plant against the germination of spores and inhibit pathogen development[65,66]. Propiconazole (((2RS 4RS;2RS,4SR)-1-[2-(2,4-dichlorophenyl)-4-propyl-1,3-dioxolan-2-ylmethyl]-1H-1,2,4-triazole)) belongs to a group of systemic fungicides that destabilize the cell membrane integrity and affects ergosterol biosynthesis through the inhibition of C14-demethylation[65]. Systemic fungicides are adsorbed into the leafs and translocated via the xylem, thus protecting the plant and controlling the circulating pathogens[65].

The co-inoculation strategy is possible as long as the fungus used as biopesticide tolerates the minimum concentration of the chemical fungicide required. This latter does not interfere with its development but contributes to increased control over the phytopathogenic specie. In this scenario, as proposed by Pelàez-Alvarez *et al.*(2016)[23], the presence of the chemical pesticide retards the growth of the phytopathogen, providing an advantage in the competition for space and nutrients in favor of the biopesticide. Chemical sensing of the competing fungus would induce the secretion of an arsenal of SMs that may act in both senses, facilitating the activity of the chemical fungicide and stimulating the plant's defense system[29,67]. Hence, the movement of chemical fungicides takes place from the upper parts of the plant and, in the case of those of systemic activity, disseminates to lower parts.

F. oxysporum fungus enters through the roots and disseminates throughout the plant using the vascular system. In contrast to chemical fungicides, *Trichoderma* fungi are part of the rhizosphere and generally grow on plant root surfaces and therefore control root diseases in particular[68]. Consequently, using *Trichoderma* as a biological control agent will provide an effective first barrier at the site of infection that will be complemented by the activity from top to bottom of chemical pesticides.

Previous work on *Trichoderma spp.* used as biocontrol agents have shown that cell wall degrading enzyme secreted by fungi i.e chitinase, cellulase, protease, and β-(1-3) glucanase and peptaibols are produced concurrently during biocontrol and interact synergistically as antifungal agents[69]. The proposed mechanism for such an effect is based on the fact that enzymes degrade the cell wall of host fungal pathogens. This activity directly inhibits the growth of the pathogen, at the same time, facilitates the access of peptaibols to the cellular membrane. Peptaibols. are small peptides of 15-20 residues characterized by non-standard amino acids in their sequences, with a special propensity for aminoisobutyric acid. The antimicrobial activity of peptaibols is related to their capacity to form pores in lipid membranes[70].

The same synergistic effect has been described for the activity of cell wall degrading enzymes and other SMs targeting specific target molecules in inhibiting *F. oxysporum* by *T. asperellum*[29]. Table 4 summarizes SMs identified as present in extracts with potent antifungal activity against *F. oxysporum*; or assayed from purified preparations and with proven inhibitory activity against this phytopathogen. Yet, important differences have been reported in the activity of cell wall degrading enzymes for *T. asperellum* and *T. harzianum*[29]. Thus, this mechanism could not be similarly effective for all *Trichoderma species*.

A similar synergistic activity could explain the outcome observed by co-inoculating *Trichoderma* species with biocontrol capacity against *F. oxysporum* and Mancozeb, Chlorothalonil and Propiconazole 20. It is reasonable to expect a similar effect on facilitating the penetration of these chemical fungicides.

Systemic effects resulting from *Trichoderma* interaction with the plant would also contribute to the observed synergistic effect when used with chemical pesticides. Reactive oxygen species scavenging enzymes have been found significantly increased in plants treated with *Trichoderma T-soybean, T. longibrachiatum* and *T. harzianum*, thus improving plant resistance to oxidative stress[3,11,72]. Exposure of plants to pesticides has evidenced that most of these chemicals lead to the development of oxidative stress[17]. Also, root colonization by *Trichoderma* has been found to result in intensified levels of defense-related, including β-peroxidases

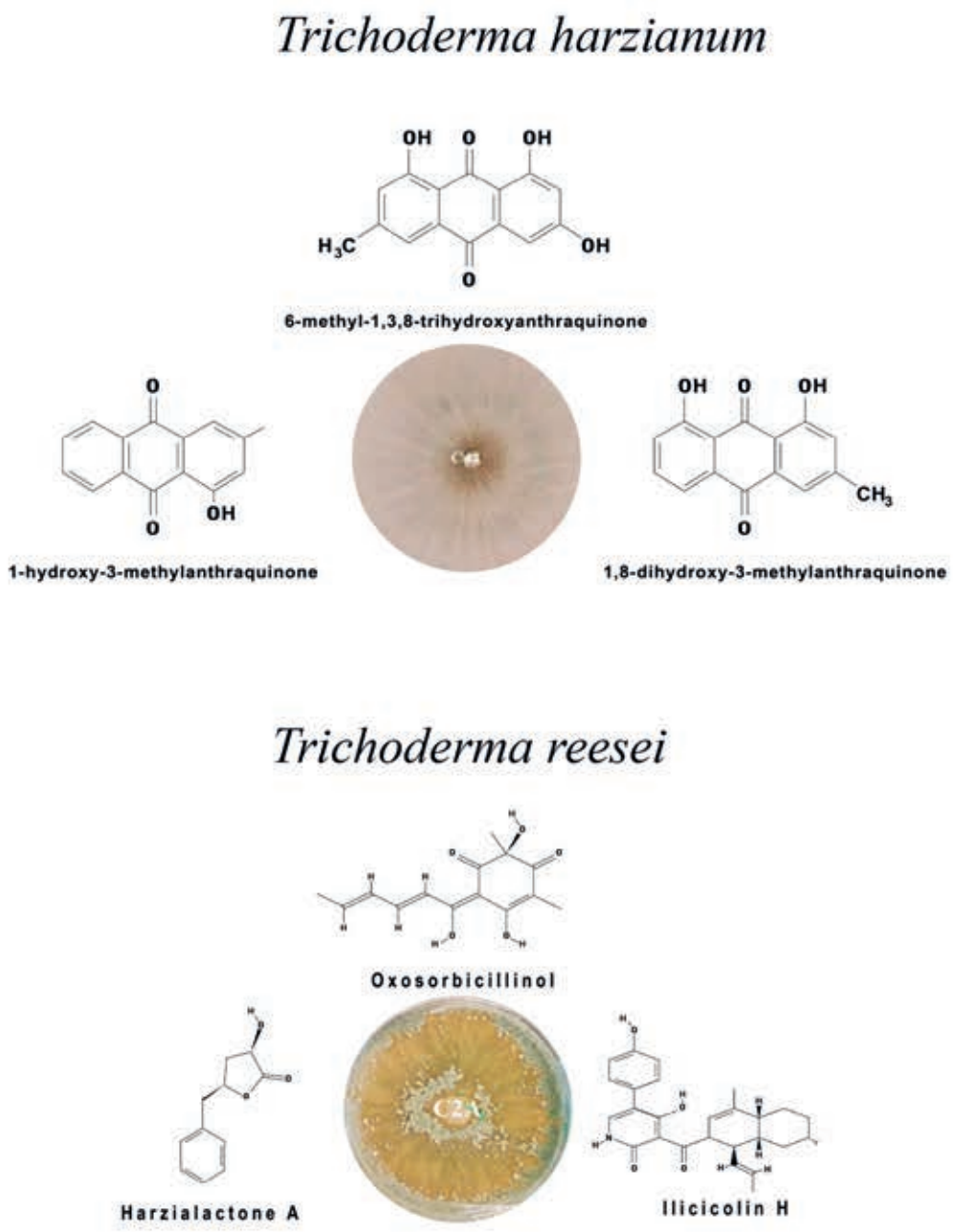

Figure 1. Secondary metabolites and enzymes associated with antifungal activity that stand out in *T. reesei, T. harzianum* and *T. spirale* strains identified in the literature review on using *Trichoderma spp.* as biocontrol agents against *Fusarium Oxysporum.*

Metabolite	Trichoderma isolate	Experiment	Reference
N-â-(tert-Butoxycarbonyl)-L-Valine*	*T. asperellum* CCTCC-RW14	*In vitro* and *in vivo* (greenhouse)	29
6-Dimethylamino-4-keto hexanoic acid*			
1,3-Dioxolane,2-(3-bromo-5,5,5-trichloro-2,2-dimethylpentyl)*			
1-Aminocyclopentanecarboxylic acid, N-ethoxycarbonyl-, heptyl ester*			
2-[2-[2-Methoxyethoxy]ethoxy-1,3-dioxalane*			
1,6-diphenylhexane-1,3,4,6-tetrone*			
2-Octenoic acid*			
Methylmalonic acid*			
Milbemycin B*			
5-demethoxy-5-one-6,28-anhydro-25-ethyl-4-methyl-13-chloro-oxime*			
Koninginin G	*T. aureoviride*		71,38
Cremenolide	*T. cremeum*	*In vitro*	71,38
6-pentyl-α-pyrone	*T. Harzianum, T. koningii and*		71,38
trichodermin	*T. Harzianum*	*In vitro*	71
farzianopyridone		*In vitro* and *in vivo*	38
8-dihydroxy-3-methylanthraquinone			
1,8-dihydroxy-3-methylanthraquinone			
1-hydroxy-3-methylanthraquinone			
6-methyl-1,3,8-trihydroxyanthraquinone			
1-hydroxy-3-methylanthraquinone			
6-methyl-1,3,8-trihydroxyanthraquinone			
Stigmasterol			
Koninginin E	*T. koningii*	*In vitro*	71,38
trichokonin VI		*In vitro*	38
trichokoninVII			
trichokonin VIII			
Koninginin A	*T. koningiopsis*	*In vitro*	38
Koninginin B			
Koninginin D	*T. koningiopsis, T.harzianum, T. koningii, T. aureoviride*	*In vitro*	71,38,67,31
Koninginin F	*T. koningii, koningiopsis*	*In vitro*	71,38

*, denote compounds identified in extracts with antifungal activity.
CCTCC-RW14 is represented

Table 4. Metabolites identified in extracts, or purified, with antifungal activity against *Fusarium oxysporum*.

and hydroxide lyase of lipoxygenase-pathway of the plant[73]. Moreover, it has been evidenced that *T. harzianum* alleviates oxidative stress by minimizing reactive oxygen species accumulation during *F. oxysporum* infection[52]. Thus, the contribution to activating a systemic response to oxidative stress in plants could be another level of cooperative action between chemical and biological control agents to control the attack of this phytopathogenic fungus.

Conclusions

Deleterious effects caused by *F. oxysporum* on plant species cause significant economic losses in agriculture at domestic and industrial levels. This review presents an organized narrative of information starting with the antifungal mechanism of *Trichoderma*, listing the SMs and enzymes involved in these mechanisms and finally the potential synergy of 3 synthetic pesticides for a better control of *F. oxysporum*. Our findings suggest that there is a need to develop more effective and ecologically friendly methods of controlling *F. oxysporum*, compared to the current control methods. Both chemical and biological control agents have individually played important roles protecting crops for millenniums. Also, both have advantages and disadvantages in their use. Thus, recent approaches have proposed the simultaneous use of chemical and biological pesticides and obtained promising results evidencing a synergistic activity controlling *F. oxysporum* infestation at *in vitro* and *in vivo* experiments. A better understanding of modes of action and cooperative effects of these two types of fungicide agents should let make better use of them in co-inoculation programs. The review of current knowledge on modes of action of *Trichoderma* in the control of *F. oxysporum* infection

as well as the chemical fungicides Mancozeb, Chlorothalonil and Propiconazole confirms that their inhibitory activities may be compensatory and may lead to synergistic effects.

Supplementary Materials

Supplementary Table 1 (S1) is available under request.

Author Contributions

GMF, GL, VL and QG made substantial contributions conception and design, or acquisition of data, or analysis and interpretation of data. GMF and GL contributed drafting the article or revising it critically for important intellectual content. GMF and GL revised the final version of the manuscript before publication. GMF and GL ensures that any part of the work was appropriately investigated and resolved.

Funding

This study did not receive any funding.

Institutional Review Board Statement

Ethical review and approval were waived for this study because it does not involve humans or animals.

Data Availability Statement

Data is available fully in open access.

Acknowledgments

Thanks to the scientific advisors who guided the initial design of this review.

Conflicts of Interest

The authors declare no conflict of interest.

Bibliographic references

1. Lecomte C, Alabouvette C, Edel-Hermann V, Robert F, Steinberg C. Biological control of ornamental plant diseases caused by Fusarium oxysporum: A review. Biol Control. 2016;101:17-30. doi:10.1016/j.biocontrol.2016.06.004
2. Damodaran T, Rajan S, Manoharan M, Gopal R. Biological Management of Banana Fusarium Wilt Caused by Fusarium oxysporum f . sp . cubense Tropical Race 4 Using Antagonistic Fungal Isolate CSR-T-3 (Trichoderma reesei). 2020;11(December):1-19. doi:10.3389/fmicb.2020.595845
3. Abdelrahman M, Abdel-Motaal F, El-Sayed M, et al. Dissection of Trichoderma longibrachiatum-induced defense in onion (Allium cepa L.) against Fusarium oxysporum f. sp. cepa by target metabolite profiling. Plant Sci. 2016;246:128-138. doi:10.1016/j.plantsci.2016.02.008
4. Cucu MA, Gilardi G, Pugliese M, Lodovica M, Garibaldi A. AGROINNOVA - Centre of Competence for the Innovation in the Agro-Environmental Sector , Department of Agricultural , Forest and Food Sciences (DISAFA), Turin University , Largo P . Biol Control. Published online 2019:104158. doi:10.1016/j.biocontrol.2019.104158
5. Utami U, Nisa C, Putri AY, Rahmawati E. The potency of secondary metabolites endophytic fungi Trichoderma sp as biocontrol of Colletotrichum sp and Fusarium oxysporum causing disease in chili The Potency of Secondary Metabolites Endophytic Fungi Trichoderma sp as Biocontrol of Colletotrichum sp. 2019;080020.
6. Petkar A, Harris-Shultz K, Wang H, Brewer MT, Sumabat L, Ji P. Genetic and phenotypic diversity of Fusarium oxysporum f. Sp. Niveum populations from watermelon in the southeastern United States. PLoS One. 2019;14(7). doi:10.1371/journal.pone.0219821
7. Palyzová A, Sokolová L. Metabolic profiling of Fusarium oxysporum f . sp . conglutinans race 2 in dual cultures with biocontrol agents Bacillus amyloliquefaciens , Pseudomonas aeruginosa , and Trichoderma harzianum. Published online 2019:779-787.
8. Das MM, Haridas M, Sabu A. Biological control of black pepper and ginger pathogens, Fusarium oxysporum, Rhizoctonia solani and Phytophthora capsici, using Trichoderma spp. Biocatal Agric Biotechnol. 2018;3. doi:10.1016/j.bcab.2018.11.021
9. Faisal M, Tiwari S, Tiwari U. Variation in antagonistic effects of Trichoderma species on Fusarium oxysporum f. sp. ciceri. ~ 1828 ~ J Pharmacogn Phytochem. 2019;8(5):1828-1832. http://www.phytojournal.com
10. Cruz DR, Ellis ML, S. GPM, L. F. S. Leandro. Isolate × Cultivar Interactions, In-Vitro Growth and Fungicide Sensitivity of Fusarium oxysporum Isolates Causing Seedling Disease on Soybean. Plant Dis. Published online 2018:1-38.
11. Zhang F, Chen C, Zhang F, et al. Trichoderma harzianum containing 1-aminocyclopropane-1-carboxylate deaminase and chitinase improved growth and diminished adverse effect caused by Fusarium oxysporum in soybean. J Plant Physiol. 2017;210:84-94. doi:10.1016/j.jplph.2016.10.012
12. Melongenae OFS, Kareem HJ, Al-araji AM. Evaluation of Trichoderma Harzianum Biological Control Against Fusarium Fusarium ضد الفطر Trichoderma harzianum المقاومة الحيوية للفطر oxysporum f . sp . Melongenae. 2017;58(4):2051-2060. تشقي
13. Zhang S, Sun F, Liu L, et al. Dragonfly-Associated Trichoderma harzianum QTYC77 Is Not only a Potential Biological Control Agent of Fusarium oxysporum f. sp. cucumerinum but Also a Source of New Antibacterial Agents. J Agric Food Chem. 2020;68(48):14161-14167. doi:10.1021/acs.jafc.0c05760
14. Michel C, Baran N, André L, Charron M, Joulian C. Side Effects of Pesticides and Metabolites in Groundwater: Impact on Denitrification. Front Microbiol. 2021;12. doi:10.3389/fmicb.2021.662727
15. Reyna PB, Albá ML, Rodríguez FA, et al. What does the freshwater clam, Corbicula largillierti, have to tell us about chlorothalonil effects? Ecotoxicol Environ Saf. 2021;208. doi:10.1016/j.ecoenv.2020.111603
16. Haas J, Zaworra M, Glaubitz J, et al. A toxicogenomics approach reveals characteristics supporting the honey bee (Apis mellifera L.) safety profile of the butenolide insecticide flupyradifurone. Ecotoxicol Environ Saf. 2021;217. doi:10.1016/j.ecoenv.2021.112247
17. Systemic Effects of the Pesticide Mancozeb – A Literature Review.
18. SIAMAK SB, ZHENG S. Banana Fusarium Wilt (Fusarium oxysporum f. sp. cubense) Control and Resistance, in the Context of Developing Wilt-resistant Bananas Within Sustainable Production Systems. Hortic Plant J. 2018;4(5):208-218. doi:10.1016/j.hpj.2018.08.001
19. Röhrich CR, Jaklitsch WM, Voglmayr H, et al. Front line defenders of the ecological niche! Screening the structural diversity of peptaibiotics from saprotrophic and fungicolous Trichoderma/Hypocrea species. Fungal Divers. 2014;69(1):117-146. doi:10.1007/s13225-013-0276-z
20. Gonzalez MF, Magdama F, Galarza L, Sosa D, Romero C. Evaluation of the sensitivity and synergistic effect of Trichoderma reesei and Mancozeb to inhibit under in vitro conditions the growth of Fusarium oxysporum. Commun Integr Biol. 2020;13(1):160-169. doi:10.1080/19420889.2020.1829267
21. Shang J, Liu B. Application of a microbial consortium improves the growth of Camellia sinensis and influences the indigenous rhizosphere bacterial communities. J Appl Microbiol. 2021;130(6):2029-2040. doi:10.1111/jam.14927
22. Jones JG, Korir RC, Walter TL, Everts KL. Reducing chlorothalonil use in fungicide spray programs for powdery mildew, anthracnose, and gummy stem blight in melons. Plant Dis. 2020;104(12):3213-3220. doi:10.1094/PDIS-04-20-0712-RE
23. Peláez-álvarez A, Santos-villalobos SDL, Yépez EA, Isela F, Reyna P cota. Synergistic effect of Trichoderma asperelleum T8A and captan 50® against Colletotrichum gloeosporioides (Penz.) Abigail. Rev Mex Ciencias Agrícolas. 2016;7(6):1401-1412.

24. Zin NA, Badaluddin NA. Biological functions of Trichoderma spp. for agriculture applications. Ann Agric Sci. 2020;65(2):168-178. doi:10.1016/j.aoas.2020.09.003
25. Suebrasri T, Somteds A, Harada H, et al. Novel endophytic fungi with fungicidal metabolites suppress sclerotium disease. Rhizosphere. 2020;16. doi:10.1016/j.rhisph.2020.100250
26. Indriyanti D, Rahmawati R, Widiatningrum T, Purwantoyo E. Effect of Trichoderma sp . secondary metabolite on the increase in leaf number of coconut plant Effect of Trichoderma sp . secondary metabolite on the increase in leaf number of coconut plant. J Phys. 2020;1567:7-11. doi:10.1088/1742-6596/1567/3/032040
27. Tian Y, Yu D, Liu N, Tang Y, Yan Z, Wu A. Confrontation assays and mycotoxin treatment reveal antagonistic activities of Trichoderma and the fate of Fusarium mycotoxins in microbial interaction. Environ Pollut. 2020;267. doi:10.1016/j.envpol.2020.115559
28. Hadibarata T, Syafiuddin A, Al-Dhabaan FA, Elshikh MS, Rubiyatno. Biodegradation of Mordant orange-1 using newly isolated strain Trichoderma harzianum RY44 and its metabolite appraisal. Bioprocess Biosyst Eng. 2018;41(5):621-632. doi:10.1007/s00449-018-1897-0
29. Saravanakumar K, Yu C, Dou K, Wang M, Li Y, Chen J. Synergistic effect of Trichoderma-derived antifungal metabolites and cell wall degrading enzymes on enhanced biocontrol of Fusarium oxysporum f. sp. cucumerinum. Biol Control. 2016;94:37-46. doi:10.1016/j.biocontrol.2015.12.001
30. Kumar T, Veena S, Karthikeyan S. Compatibility of Trichoderma asperellum with Fungicides, Insecticides, Inorganic fertilizers and Bio-pesticides Mushroom View project Production of tube rcrops View project. ResearchGate. Published online 2017. https://www.researchgate.net/publication/331519611
31. Vinale F, Sivasithamparam K, Ghisalberti EL, et al. Trichoderma Secondary Metabolites Active on Plants and Fungal Pathogens. Published online 2014:127-139.
32. Khan RAA, Najeeb S, Hussain S, Xie B, Li Y. Bioactive secondary metabolites from Trichoderma spp. Against phytopathogenic fungi. Microorganisms. 2020;8(6). doi:10.3390/microorganisms8060817
33. Tchameni SN, Cotârleț M, Ghinea IO, et al. Involvement of lytic enzymes and secondary metabolites produced by Trichoderma spp. in the biological control of Pythium myriotylum. Int Microbiol. 2020;23(2):179-188. doi:10.1007/s10123-019-00089-x
34. Napitupulullyas M, Kanti A, Im S. In vitro evaluation of Trichoderma harzianum strains for the control of Fusarium oxysporum f . sp . cubense. 2019;9(January):152-159. doi:10.5943/ppq/9/1/13
35. Stracquadanio C, Quiles JM, Meca G, Cacciola SO. Antifungal Activity of Bioactive Metabolites Produced by Trichodermaasperellum and Trichodermaatroviride in Liquid Medium. J fungi (Basel, Switzerland). 2020;6(4):1-18. doi:10.3390/jof6040263
36. Li N, Alfiky A, Wang W, Nourollahi K. Volatile Compound-Mediated Recognition and Inhibition Between Trichoderma Biocontrol Agents and Fusarium oxysporum. 2018;9(October):1-16. doi:10.3389/fmicb.2018.02614
37. Li MF, Li GH, Zhang KQ. Non-volatile metabolites from Trichoderma spp. Metabolites. 2019;9(3). doi:10.3390/metabo9030058
38. Rahman Khan M, Shahid S, Mohidin FA, Mustafa U. Interaction of Fusarium oxysporum f. sp. gladioli and Meloidogyne incognita on gladiolus cultivars and its management through corm treatment with biopesticides and pesticides. Biol Control. 2017;115:95-104. doi:10.1016/j.biocontrol.2017.09.010
39. Hu D, Yu S, Yu D, et al. Biogenic Trichoderma harzianum-derived selenium nanoparticles with control functionalities originating from diverse recognition metabolites against phytopathogens and mycotoxins. Food Control. 2019;106. doi:10.1016/j.foodcont.2019.106748
40. Manganiello G, Sacco A, Ercolano MR, et al. Modulation of tomato response to rhizoctonia solani by Trichoderma harzianum and its secondary metabolite harzianic acid. Front Microbiol. 2018;9(AUG). doi:10.3389/fmicb.2018.01966
41. Dini I, Marra R, Cavallo P, et al. Trichoderma strains and metabolites selectively increase the production of volatile organic compounds (Vocs) in olive trees. Metabolites. 2021;11(4). doi:10.3390/metabo11040213
42. Lombardi N, Salzano AM, Troise AD, et al. Effect of Trichoderma Bioactive Metabolite Treatments on the Production, Quality, and Protein Profile of Strawberry Fruits. J Agric Food Chem. 2020;68(27):7246-7258. doi:10.1021/acs.jafc.0c01438
43. Contreras-Cornejo HA, Macías-Rodríguez L, Del-Val E, Larsen J. Full Title: Ecological Functions of Trichoderma Spp. and Their Secondary Metabolites in the Rhizosphere: Interactions with Plants Downloaded From.; 2016. http://femsec.oxfordjournals.org/
44. Kumari N, Srividhya S. Secondary metabolites and lytic tool box of trichoderma and their role in plant health. In: Molecular Aspects of Plant Beneficial Microbes in Agriculture. Elsevier; 2020:305-320. doi:10.1016/b978-0-12-818469-1.00025-0
45. Damodaran T, Rajan S, Muthukumar M, et al. Biological Management of Banana Fusarium Wilt Caused by Fusarium oxysporum f. sp. cubense Tropical Race 4 Using Antagonistic Fungal Isolate CSR-T-3 (Trichoderma reesei). Front Microbiol. 2020;11. doi:10.3389/fmicb.2020.595845
46. Álvarez-García S, Mayo-Prieto S, Gutiérrez S, Casquero PA. Self-inhibitory activity of trichoderma soluble metabolites and their antifungal effects on fusarium oxysporum. J Fungi. 2020;6(3):1-11. doi:10.3390/jof6030176
47. Zhu F, Zhao X, Li J, Guo L, Bai L, Qi X. A new compound Trichomicin exerts antitumor activity through STAT3 signaling inhibition. Biomed Pharmacother. 2020;121. doi:10.1016/j.biopha.2019.109608
48. Redda ET, Mei J, Li M, Wu B, Jiang X. Biological Control of Soilborne Pathogens (Fusarium oxysporum F. Sp. Cucumerinum) of Cucumber (Cucumis sativus) by Trichoderma sp. 2018;12:1-12. doi:10.17265/1934-7391/2018.01.001
49. Alamri SAM, Hashem M, Moustafa YS, Nafady NA, Abo-elyousr KAM. Biological control of root rot in lettuce caused by Exserohilum rostratum and Fusarium oxysporum via induction of the defense mechanism. Biol Control. 2018;7:1-3. doi:10.1016/j.biocontrol.2018.09.014
50. Ao N, Vi G. Evaluation of Antagonistic Effect of Trichoderma Harzianum against Fusarium oxysporum causal Agent of White Yam (Dioscorearotundata poir) Evaluation of Antagonistic Effect of Trichoderma Harzianum against Fusarium oxysporum causal Agent of White Yam (D. 2018;(May). doi:10.19080/TTSR.2018.01.555554
51. Sinha A, Singh R, Verma A. Bioefficacy of Trichoderma harzianum and Trichoderma viride against Fusarium oxysporum f. sp. capsici causing wilt disease in chilli. ~ 965 ~ J Pharmacogn Phytochem. 2018;7(5). http://agriculture.gov.in
52. Chen S chen, Ren J jing, Zhao H jiao, et al. Trichoderma harzianum Improves Defense Against Fusarium oxysporum by Regulating ROS and RNS Metabolism , Redox Balance , and Energy Flow in Cucumber Roots. Phytopathology. 2019;109(6):972-982. doi:10.1094/PHYTO-09-18-0342-R
53. Frisvad JC. Safety of the fungal workhorses of industrial biotechnology : update on the mycotoxin and secondary metabolite potential of Aspergillus niger , Aspergillus oryzae , and Trichoderma reesei. Published online 2018:9481-9515.
54. Shenouda ML, Ambilika M, Cox RJ. Trichoderma reesei contains a biosynthetic gene cluster that encodes the Antifungal Agent Ilicicolin H. J Fungi. 2021;7(12):1034.
55. Yang Z, Qiao Y, Li J, Wu FG, Lin F. A Novel Water-Soluble Photosensitizer for Photodynamic Inactivation of Gram-Positive Bacteria. doi:10.1101/2020.05.29.124768
56. Watts R, Dahiya J, Chaudhary K, Tauro P. Isolation and characterization of a new antifungal metabolite of Trichoderma reesei. Plant Soil. 1988;107(1):81-84.
57. Pachauri S, Sherkhane PD, Mukherjee PK. Secondary Metabolism in Trichoderma: Chemo- and Geno-Diversity BT - Microbial Diversity in Ecosystem Sustainability and Biotechnological Applications: Volume 2. Soil & Agroecosystems. In: Satyanarayana T, Das SK, Johri BN, eds. Springer Singapore; 2019:441-456. doi:10.1007/978-981-13-8487-5_17

58. Speckbacher V. Secondary Metabolites of Mycoparasitic Fungi. In: Raja SZERVESSS, ed. IntechOpen; 2018:Ch. 3. doi:10.5772/intechopen.75133
59. Mukherjee PK, Horwitz BA, Kenerley CM. Secondary metabolism in Trichoderma–a genomic perspective. Microbiology. 2012;158(1):35-45.
60. Marik T, Tyagi C, Balázs D, et al. Structural Diversity and Bioactivities of Peptaibol Compounds From the Longibrachiatum Clade of the Filamentous Fungal Genus Trichoderma . Front Microbiol . 2019;10. https://www.frontiersin.org/articles/10.3389/fmicb.2019.01434
61. Baiyee B, Pornsuriya C, Ito S ichi, Sunpapao A. Trichoderma spirale T76-1 displays biocontrol activity against leaf spot on lettuce (Lactuca sativa L.) caused by Corynespora cassiicola or Curvularia aeria. Biol Control. 2019;129:195-200. doi:https://doi.org/10.1016/j.biocontrol.2018.10.018
62. Abdel-Monaim MF, Abdel-Gaid MA, Zayan SA, Nassef DMT. Enhancement of Growth Parameters and Yield Components in Eggplant using Antagonism of Trichoderma spp. Against Fusarium Wilt Disease. Int J Phytopathol Vol 3, No 1 Int J Phytopathol. Published online 2014. doi:10.33687/phytopath.003.01.0510
63. Lombardi N, Salzano AM, Troise AD, et al. E ff ect of Trichoderma Bioactive Metabolite Treatments on the Production, Quality, and Protein Pro fi le of Strawberry Fruits. Published online 2020. doi:10.1021/acs.jafc.0c01438
64. Gava CAT, Pinto JM. Biocontrol of melon wilt caused by Fusarium oxysporum Schlect f. sp. melonis using seed treatment with Trichoderma spp. and liquid compost. Biol Control. 2016;97:13-20. doi:10.1016/j.biocontrol.2016.02.010
65. Yang C, Hamel C, Vujanovic V, Gan Y. Fungicide: Modes of Action and Possible Impact on Non-target Microorganisms. ISRN Ecol. 2011;2011:1-8. doi:10.5402/2011/130289
66. Gisi U, Sierotzki H. Fungicide modes of action and resistance in downy mildews. In: European Journal of Plant Pathology. Vol 122. ; 2008:157-167. doi:10.1007/s10658-008-9290-5
67. Contreras-Cornejo HA, Macías-Rodríguez L, Del-Val1 E, Larsen J. Ecological functions of Trichoderma spp . and their secondary metabolites in the rhizosphere : interactions with plants. FEMS. 2016;(February):1-17. doi:10.1093/femsec/fiw036
68. Macías-Rodríguez L, Contreras-cornejo HA, Adame-garnica SG, Larsen J. The interactions of Trichoderma at multiple trophic levels: inter- kingdom communication. Microbiol Res. Published online 2020. doi:10.1016/j.micres.2020.126552
69. Woo S, Fogliano V, Scala F, Lorito M. Synergism between fungal enzymes and bacterial antibiotics may enhance biocontrol. Published online 2002:353-356.
70. Whitmore L, Wallace BA. The Peptaibol Database: A database for sequences and structures of naturally occurring peptaibols. Nucleic Acids Res. 2004;32(DATABASE ISS.):593-594. doi:10.1093/nar/gkh077
71. Meng-Fei L, LGuo-Hong L, Ke-Qin Z. Non-Volatile Metabolites from Trichoderma spp. Metabolites. 2019;9(58). doi:10.3390/metabo9030058
72. Chen S chen, Zhao H jiao, Wang Z hong, Zheng C xia. Trichoderma harzianum -induced resistance against Fusarium oxysporum involves regulation of nuclear DNA content , cell viability and cell cycle-related genes expression in cucumber roots. Eur J Plant Pathol. Published online 2017:43-53. doi:10.1007/s10658-016-0978-7
73. Kumari I, Sharma S, Ahmed M. Tripartite Interactions between Plants, Trichoderma and the Pathogenic Fungi. INC; 2020. doi:10.1016/B978-0-12-818469-1.00032-8

CLINICAL REPORT / REPORTE DE CASO

Miocardiopatía no compactada diagnosticada por Resonancia Magnética Cardíaca. Reporte de caso

Noncompaction cardiomyopathy diagnosed by cardiac magnetic resonance imaging. Case report

Laura Cevallos Ch*, Alvaro Gudiño G
Hospital General San Vicente de Paúl Ibarra Ecuador.
Corresponding author: laura.cevallos@hsvp.gob.ec

DOI. 10.21931/RB/2023.08.02.8

Resumen: La Miocardiopatía no compactada es una entidad rara, con una prevalencia no bien definida, caracterizada por un desarrollo anormal de la morfología miocárdica. Puede ocurrir en todos los grupos etarios, y su presentación clínica es variada, llegando a estar asociada a condiciones clínicas potencialmente mortales. El diagnóstico en la actualidad sigue siendo un reto, ya que no existe uniformidad de criterios y estos varían dependiendo de la técnica de imagen utilizada. A continuación, se expone el caso de una paciente femenina de 45 años de edad, con clínica de insuficiencia cardíaca, palpitaciones y eventos de presíncope. El estudio electrocardiográfico demostró una importante inestabilidad eléctrica y la resonancia magnética cardiaca hallazgos compatibles con miocardio no compactado.

Palabras clave: Arritmias, cardiomiopatía, imagen por resonancia magnética, insuficiencia cardiaca.

Abstract: Non-compaction cardiomyopathy is a rare entity, with a not well-defined prevalence, characterized by abnormal development of myocardial morphology. It can occur in all age groups, and its clinical presentation is varied, even being associated with life-threatening clinical conditions. Diagnosis remains a challenge at present since there is no uniformity of criteria and these vary depending on the imaging technique used. The following is the case of a 45-year-old female patient with clinical symptoms of heart failure, palpitations, and presyncope events. The electrocardiographic study showed significant electrical instability and cardiac magnetic resonance imaging findings compatible with non-compacted myocardium.

Key words: Arrhythmias, cardiomyopathy, magnetic resonance imaging, heart failure, heart failure

Introducción

La Miocardiopatía No Compactada es un trastorno del miocardio, producido por una alteración en la compactación del ventrículo izquierdo durante la embriogénesis[1].

Morfológicamente, se caracteriza por presentar una pared ventricular con una capa epicárdica de aspecto denso y uniforme, y una capa endocárdica gruesa, de aspecto esponjoso, con prominentes trabeculaciones y profundos recesos intertrabeculares que se comunican con la cavidad ventricular[2].

Fue descrita por primera vez hace más de 80 años y hasta la actualidad existe discrepancia entre las diferentes sociedades científicas, respecto a su clasificación y criterios diagnósticos[1].

Con base a estos antecedentes, se presenta a continuación el caso de una paciente adulta joven, referida a nuestra unidad, con clínica de insuficiencia cardiaca y arritmias de 3 meses de evolución.

Caso clínico

Paciente femenina de 45 años, de nacionalidad venezolana, sin antecedentes cardiovasculares personales ni familiares. Acude a nuestra unidad por presentar desde hace 3 meses disnea progresiva (al momento la valoración en clase funcional IV), palpitaciones y eventos de presíncope.

Al examen físico se evidenció ingurgitación yugular de 3 cm, edema de miembros inferiores y estertores crepitantes basales bilaterales. Al examen cardiaco, el ápex estuvo desplazado más allá del quinto espacio intercostal izquierdo y a la auscultación se evidenció extrasístoles frecuentes y un soplo sistólico regurgitativo en foco mitral grado III/VI

En los exámenes de laboratorio se evidenció anemia leve, normocítica, normocrómica (Hemoglobina: 10.7g/l, Hematocrito: 32.4%), alteración de la función renal (Creatinina 1.57mg/dl), y elevación de los valores de troponina (169ng/l) y del NT-proBNP (propéptido natriurético cerebral N- terminal) (10101pg/ml). Adicionalmente, por los antecedentes demográficos de la paciente, se realizó serología para enfermedad de Chagas, la cual fue negativa.

El estudio de monitorización electrocardiográfica de 24 horas demostró extrasístoles ventriculares frecuentes y eventos de taquicardia ventricular monomorfa no sostenida (figura 1).

El ecocardiograma evidenció aumento del volumen ventricular izquierdo, crecimiento auricular izquierdo, con disfunción sistólica severa (Fracción de Eyección de 26%

Citation: Cevallos Ch L, Alvaro Gudiño G. Miocardiopatía no compactada diagnosticada por Resonancia Magnética Cardíaca. Reporte de caso. Revis Bionatura 2023;8 (2) 8. http://dx.doi.org/10.21931/RB/2023.08.02.8
Received: 2 January 2023 / **Accepted:** 13 March 2023 / **Published:** 15 June 2023

Publisher's Note: Bionatura stays neutral with regard to jurisdictional claims in published maps and institutional affiliations.

por método de Simpson) y presencia de trombo intracavitario en ventrículo izquierdo. Sin evidencia de alteraciones valvulares.

Con estos antecedentes, se solicitó un estudio por Resonancia Magnética Cardiaca que demostró hipocinesia biventricular difusa, con disfunción biventricular grave, y un patrón de realce tardío de tipo no coronario a nivel mesocárdico en los segmentos infero-septal y medial. Adicionalmente, se demostró un aumento de las trabeculaciones en las porciones medio y apical de las paredes anterior y lateral del ventrículo izquierdo, con una relación miocardio no compacto/ miocardio compacto > 3.68 (valor normal hasta 2.3) (figura 2).

Discusión

La Miocardiopatía No Compactada es una entidad no muy bien definida, cuyo diagnóstico requiere de un alto grado de presunción tanto clínica como imagenológica[1].

La prevalencia de esta patología no está bien definida y varía considerablemente entre las diferentes series. Se estima que podría estar presente entre un 0,05% a 0,25% en la población general[3].

Fisiopatológicamente, la no compactación del ventrículo izquierdo se produce durante el período embrionario al haber una detención del proceso normal de trabeculación y compactación ventricular a partir de la octava semana de gestación[4].

Esta condición puede presentarse de manera hereditaria (transmisión autosómica dominante o ligada al cromosoma X), de forma aislada o formando parte de otras entidades como anomalías congénitas o trastornos neuromusculares[1].

La base genética aún no ha sido bien dilucidada, sin embargo, varias mutaciones de genes asociados a la codificación de las proteínas sarcoméricas del citoesqueleto, mitocondriales o de la membrana nuclear tales como la tafacina, betaDTNA, *LDB3*, laminaA/C, *SCN5A*, *MYH7* o *MYBPC3* podrían estar involucrados en la génesis de este trastorno[2].

Clínicamente, puede manifestar síntomas atribuibles a la insuficiencia cardíaca, eventos tromboembólicos y arritmias[3].

En nuestro caso en particular, la paciente presentó clínica de insuficiencia cardiaca progresiva y palpitaciones asociadas a eventos arrítmicos tal como fue demostrado en el monitoreo electrocardiográfico de 24 horas.

En lo referente a los hallazgos laboratoriales, estos pueden ser normales o evidenciar alteraciones de los biomarcadores de necrosis miocárdica o de disfunción miocárdica, situación que fue corroborada en nuestro caso con valores elevados de troponina y de NT-proBNP.

El diagnóstico inicial se basa en los hallazgos ecocardiográficos el cual podría ser considerado como técnica de primera elección por su accesibilidad y bajo costo. Sin embargo, el diagnostico final se basará en los hallazgos de la resonancia magnética cardiaca la cual permitirá, por su mejor resolución espacial, definir la distribución anatómica de los recesos intertrabeculares y la relación entre el miocardio compactado versus no compactado[1].

En nuestro caso, el estudio por Resonancia Magnética Cardiaca, demostró con base a los criterios de Petersen el al. una relación entre miocardio compactado versus no compactado mayor a 2,3 y el aumento de las trabeculaciones miocárdicas[1].

Respecto al tratamiento, la evidencia es limitada y las principales estrategias terapéuticas están orientadas al manejo de las complicaciones provocadas por la disfunción miocárdica, las arritmias y el tromboembolismo sistémico[1].

Finalmente, cabe señalar que el pronóstico vital de esta patología no está claramente definido, sin embargo, hay que considerarla como una enfermedad grave, con una alta tasa de morbi-mortalidad y ligada a múltiples complicaciones[1].

Conclusiones

La miocardiopatía no compactada es una entidad poco conocida y en muchos casos subdiagnosticada, con una

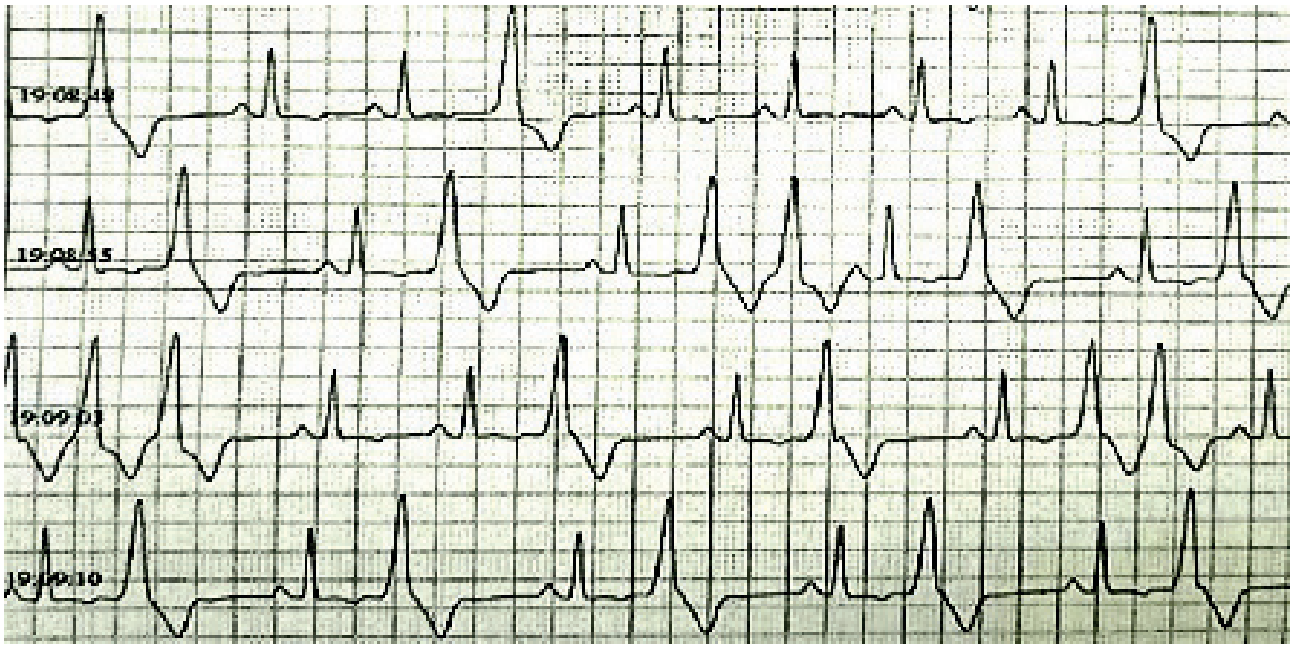

Figura 1. Estudio de monitorización electrocardiográfica de 24 horas con varios eventos de extrasístoles ventriculares monomorfas, bigeminismo, trigeminismo ventricular y taquicardia ventricular monomorfa no sostenida.

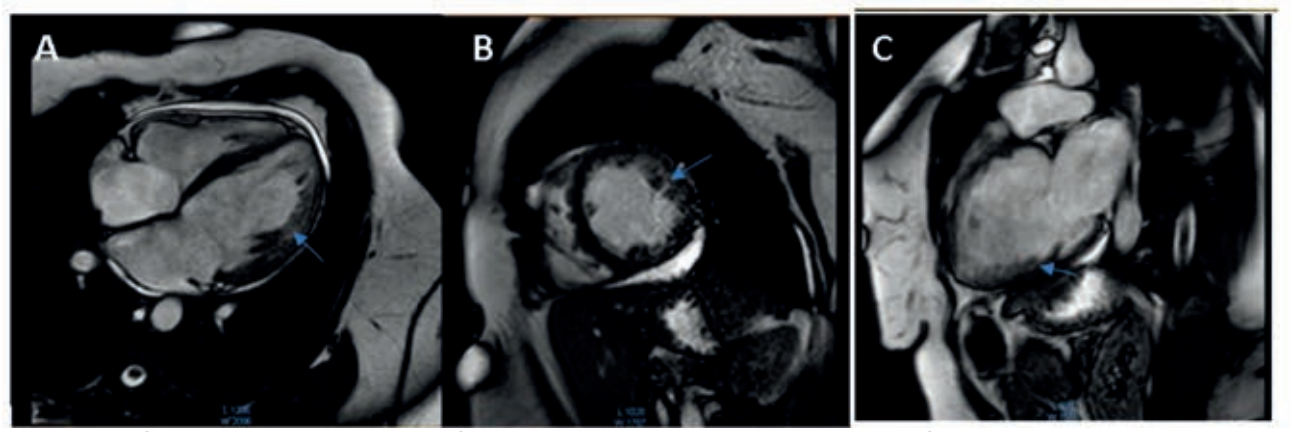

Figura 2. Imágenes de Resonancia magnética de secuencia cine en A: plano cuatro cámaras, B: eje corto y C: eje largo, que demuestran aumento del espesor de la capa de miocardio no compactado en relación con el miocardio compacto (flecha azul).

importante implicación pronóstica para los pacientes.La falta de uniformidad en los criterios diagnósticos hace que su prevalencia sea desconocida, lo que limita su detección y posterior aplicación de medidas terapéuticas encaminadas a la prevención de sus complicaciones. La presencia de miocardiopatía no compactada debe ser investigada en todo paciente joven con clínica de insuficiencia cardiaca sin una etiología clara que justifique su aparición. A diferencia de otros casos citados en la literatura, nuestro diagnóstico se basó exclusivamente en el uso de resonancia magnética cardiaca, dado que los criterios diagnósticos por esta técnica de imagen pueden ser detectados de manera más sensible y específica.

Contribuciones de los autores

Todos los autores contribuyeron activamente en la elaboración y redacción del artículo

Financiamiento

La elaboración de este artículo se realizón con los recursos de los autores.

Institutional Review Board Statement

Este artículo fue realizado en concordancia a la declaración de Helsisnki y aprovado por el comite de ética institucional.

Informed Consent Statement

Se adjunta el consentimiento informado.

Conflictos de Interés

Los autores declaran no tener conflictos de intereses.

Referencias bibliográficas

1. Almeida AG, Pinto FJ. Non-compaction cardiomyopathy. Heart. 2013 ;99(20):1535-42. doi: 10.1136/heartjnl-2012-302048. PMID: 23503402.
2. Serrano D, Gonzáles F. Miocardiopatía no compactada. Revista Uruguaya de Cardiología. 2019 ;34(1):114–21.
3. Engberding R, Stöllberger C, Ong P, Yelbuz TM, Gerecke BJ, Breithardt G. Isolated non-compaction cardiomyopathy. Dtsch Arztebl Int. 2010;107(12):206-213. doi:10.3238/arztebl.2010.0206.
4. Petersen SE, Selvanayagam JB, Wiesmann F, Robson MD, Francis JM, Anderson RH, Watkins H, Neubauer S. Left ventricular non-compaction: insights from cardiovascular magnetic resonance imaging. J Am Coll Cardiol. 2005; 46:101-5. doi: 10.1016/j.jacc.2005.03.045. PMID: 15992642.

REVIEW / ARTÍCULO DE REVISIÓN

The problem associated with tuberculosis in cattle and how this is being addressed

Roxana Zuniga Sanchez, Oliberto Sanchez Ramos, Frank Camacho*

DOI. 10.21931/RB/2023.08.02.9

[1] Center of Agrobiotechnological Development and Innovation – CEDAIT, Universidad de Antioquia,Colombia.
[2] Biology Institute, Universidad de Antioquia, Colombia.
Corresponding author: amaria.henao@udea.edu.co

Abstract: Bovine tuberculosis (bTB) is a zoonotic disease caused by Mycobacterium bovis that primarily infects cattle but has a wide range of hosts. It represents a global health problem affecting the livestock industry tremendously, with economic losses of about 3 billion annually. Dairy cattle produce a decline of 10% in terms of liters of milk produced and 5% in the meat industry because of live weight loss and seized carcasses in abattoirs. The core of the current control measures implemented in most countries against bTB is based on the diagnosis with tuberculin skin test (TST) and culling of infected animals. Unfortunately, control programs have failed to eradicate the disease since no vaccine protects cattle from infection. Moreover, the strain of M. bovis Bacillus Calmette Guerin, BCG used as a vaccine for human tuberculosis, interferes with surveillance tools. Nowadays, most researchers have been working on improving the efficacy of BCG through a prime-boost strategy that involves a first immunization with BCG and a booster with different types of vaccines. A less explored approach by experts has been the development of a new vaccine that only includes some protective antigens of M. bovis that should be absent ot in low representation in TST. On the other hand, because TST precludes implementation of Bacille Calmette-Guérin (BCG) vaccine–based control programs, several investigations have been carried out to replace the TST with a DIVA test that allows to differentiation infected from vaccinated animals. In this review, most of the studies cited agree that without an effective vaccine and a compatible diagnosis, no program for eradication would be successful against tuberculosis in cattle.

Key words: Bovine tuberculosis, bTB, *Mycobacterium bovis*, diagnosis, tuberculin skin test, TST, bPPD, vaccines, DIVA.

Introduction

Bovine tuberculosis (bTB) is a chronic zoonotic pathology caused by Mycobacterium bovis that belongs to the reportable diseases of the World Organization for Animal Health WOAH (OIE). *Mycobacterium bovis* may mostly affect cattle, humans, and other domestic and wildlife animals[1-3]. It belongs to the phylum Actinobacteria, family Mycobacteriaceae and genus *Mycobacterium*[4,5]. In the *Mycobacterium* genus has been identified more than 120 different species, and some of them belong to the *Mycobacterium tuberculosis complex* (MTC). The most common members of the MTC are *M. bovis, M. tuberculosis, M. canettii* (oldest strain), *M. africanum* (responsible for human tuberculosis in Africa), *M. pinnipedi* (infect seals), *M. microti* (rodents), and *M. caprae* (goats and other mammals). *M. bovis* and *M. tuberculosis* have 99.95% of genomic homology in their shared genes[6].

Bovine tuberculosis has a worldwide prevalence of about 13% and can be found in 82 countries around the world[7]. The biggest challenge in those countries is the control of *M. bovis* in wildlife animals as they act as a reservoir of the pathogen[8]. In all these countries, the disease is associated to tremendous economic losses for the livestock industry, which according to a study performed in USA were estimated in 3 billion dollars per year[9]. Research have shown that bTB generates a fertility loss in females and a decrease in milk production per lactation of 10%. On the other side, the disease also generates losses of 5% in the meat industry since carcasses are seized in slaughterhouses, and there is a live weight loss of animals[10]. It has also been observed that close to 1% of positive bTB cows can develop mastitis[11]. On the other hand, the disease produces high costs in terms of international cattle trading restrictions and dairy and meat by-products to OTF countries[12]. Other costs associated with bTB are control and eradication programs that have as central measures the diagnosis through TST and culling of infected animals to avoid spreading the disease in the herd.

Furthermore, control and eradication programs require removing and replacing infected animals from the pen. Therefore, it causes economic losses not only to farmers but also to the government in terms of indemnity expenses and replacement cost of cattle which can vary from around $500 to 900 USD[13]. The measures included in the control and eradication programs implemented by governments in the countries where bovine tuberculosis is present have shown to be non-enough to prevent infection and eliminate the disease. The need for an effective vaccine that can be applied in cattle and would be authorized by the OIE is still a challenge. Moreover, it is imperative to have a diagnostic tool that can be used with an effective vaccine to support the surveillance strategies. An effective vaccine that strengthens and complements those programs is pivotal in contro-

Citation: Zuniga Sanchez R, Sanchez Ramos O , Camacho F.The problem associated with tuberculosis in cattle and how this is being addressed. Revis Bionatura 2023;8 (2) 9. http://dx.doi.org/10.21931/RB/2023.08.02.9
Received: 2 January 2023 / **Accepted:** 13 March 2023 / **Published:** 15 June 2023

Publisher's Note: Bionatura stays neutral with regard to jurisdictional claims in published maps and institutional affiliations.

lling the pathology. Indeed, it has been demonstrated that a strong immunity triggered by a vaccine may defeat *M. bovis*. The vaccine BCG (Bacillus Calmette-Guérin) used against human tuberculosis but made of Mycobacterium bovis has been trialed before in cattle; however, it has demonstrated a variable range of protection[14]. Currently, most studies are led to improve the effectiveness of BCG in cattle, and in this context, it has been carrying out assays in cows and other animal models. The primary strategy implemented in those studies is based on the prime boost with BCG as a prime and a boost with different types of vaccines, such as subunit recombinant and adenovirus vaccines. Another less explored approach is the development of a new protective vaccine that could include only some immunogenic proteins of *M. bovis*. These proteins must be included in a low proportion of bPPD of tuberculin so they may not interfere with the TST. On the other side, researchers have also been working on differentiating infected and vaccinated animals and DIVA tests to replace TST because it is incompatible with BCG. The diagnosis of cattle with TST does not allow to discrimination between infected and vaccinated animals since it causes a cross-reaction with the BCG vaccine.

In this article, we seek to review and discuss different studies related to the global problem caused by tuberculosis in cattle. Here it has not only been described the current strategies used in the control of the disease and their drawbacks, but most importantly, we propose an approach that has not been deeply explored as an alternative in developing a new protective vaccine. This could be the study of the most immunogenic proteins of *M. bovis* that are less representative in bPPD to be included in producing a new vaccine that should not cross-react with the tuberculin skin test.

The Disease In Cattle

In natural conditions, airways are the most frequent route of infection of *M. bovis*. Using inhalation of the pathogen that is suspended in aerosols, bovines may get infected. Nevertheless, the oral route is the second most common infection in bovines, and they can ingest the bacterium from contaminated water and food[15]. When the microorganism comes from the upper airways, it moves to the pulmonary alveoli. In the alveoli, molecular patterns associated with pathogens are recognized by receptors of innate immune cells, such as macrophages[16]. These cells engulf *M. bovis* and release chemokines that attract neutrophils and other cells to the infection site, leading to edema with the accumulation of fibrin (inflammatory exudate). Macrophages display the antigen to lymphocytes which then are activated, and as a result, more cells from the immune system reach the site of infection[17]. When immune cells migrate to the site of infection, they accumulate and form tuberculous, which are granulomatous lesions pathognomonic of the disease. In some animals, the immune system can restrain the initial infection by eliminating the bacterium or inhibiting its multiplication into the tissue[18]. Thus, the microorganism can get into a latency phase in which *M. bovis* decreases its metabolism to basal levels and remain in a non-replicative state to survive. Nevertheless, the bacterium can reactivate, and the disease will progress, causing a transformation of the granuloma structural organization that in chronic cases, have a necrotic center surrounded by a thick fibrotic tissue layer[19]. The microorganism contained in the granuloma of the lower airways can be transported by phagocytic cells through the lymphatic system until a regional lymph node where a second infection occurs. The primary infection in the lungs, plus the new in the lymph node, integrates the "primary complex" of the disease. When the immune system cannot hold the infection in the primary complex, the pathogen disseminates through the blood (bacteremia) toward other tissues and organs, triggering the generalization of the bTb[20]. Owing to bTB being a chronic disease with slow progress, most infected animals do not manifest clinical signs in the short term but in months or years after infection. Most animals show unspecific symptoms at the onset of the disease, for example, fluctuating fever, cough, diarrhea, anorexia, weakness, and lymph node inflammation. While acute presentation of bTb is not frequent, it has been observed that the pathology evolves very fast in non-immunocompetent animals, causing death. On the other hand, in animals that overcome the initial infection, the pathology becomes chronic. Some of the clinical signs that infected animals exhibit in advanced stages of the disease are dyspnea, pneumonia, weight loss and emaciation, granulomatous lesions in different organs, and finally ending with the, death[21]. Granulomas can be encountered most frequently in lungs and lymph nodes if *M. bovis* has come in throughout the respiratory system. Otherwise, granulomas may be in the stomach, spleen, liver or mesenteric lymph nodes if the pathogen penetrates an oral or digestive route. In the inspection, post-mortem is very frequent to find granulomatous lesions in retropharyngeal, mediastinal, and tracheobronchial lymph nodes. Those lesions also commonly affect the lungs (mainly apex zone), stomach, liver, spleen, kidneys, and mammary gland[21]. In severe cases, there is an extrapulmonary presentation of the disease because of the dissemination of *M. bovis* to the rest of the organism.

Control and prevention of bovine tuberculosis

Despite several countries from European Union, North America, Asia, and Oceania being OTF, the disease has not been fully eradicated. In these countries, bTB is remitted to certain areas, and control and eradication programs against the pathogen's spread are still in force. These programs require huge economic investment because of animal screening and indemnity for culling infected individuals besides other measures such as restrictions in animal movement and surveillance strategies in farms and slaughterhouses.

Detection of *M. bovis*-infected cattle.

One of the central control measures achieved in the programs against bTB is the identification of infected cattle in the field through the tuberculin skin test TST[22]. The single intradermal tuberculin SIT consists of injecting 0.1 mL of 3000 IU of a bPPD (bovine purified protein derivative), eliciting delayed hypersensitivity response (type IV) mediated by cells when the animal has been previously exposed to the pathogen[23]. This cell immune response is triggered by chemokines and cytokines recruited in the PPD injection site due to previous contact with the microorganism. It has been reported that TST sensitivity range from 57 to 95%, whereas its specificity ranges from 55 to 100%[24]. There are three types of SIT: i) the single caudal fold test (SCFT) which a bPPD is administrated in the tail base, ii) the single intradermal cervical tuberculin (SICT) which a bPPD is injected in the middle of the neck of the animal, iii) the intradermal comparative cervical tuberculin (SICCT) which a bPPD and aPPD (avian purified protein derivative) are applied in two central points of the neck of cattle[25]. In this last, both PPDs are administrated since they allow to discriminate between infections produced by *M. bovis* and other environmental

mycobacteria such as *Mycobacterium avium spp* paratuberculosis. The tuberculin test results are read 72 hours post-administration and are interpreted according to the skin fold thickness of the inflammatory lesion generated at the injection site. Following the interpretation of the TST, it can be obtained two results: i) negative animals, when was neither observed nor touched any thickness changed at the inoculated site ii) reactor animals, when can be observed and touched a type of edema that maybe go along with blush, warm, and pain at the inoculated site. The intradermal test cannot be performed in animals with an interval of fewer than two months between each application to avoid false positive cases because of the previous sensitization with the PPD[26].

All suspected or responder animals to the tuberculin test are confirmed through laboratory techniques such as interferon-gamma release assay (IGRAs) and enzyme-linked immunosorbent assay (ELISA).

The IGRA is an in vitro technique that measures a cell-mediated immunity stimulated in response to *M. bovis* infection. The cytokine IFNγ produced by T lymphocytes of an infected animal is detected in blood samples stimulated with PPD throughout an ELISA plate which is coated with a monoclonal antibody anti- IFNγ. With this assay, infected animals can be identified as soon as two weeks since they were in contact with the pathogen[27].

On the other side, the ELISA test kit IDDEX is frequently employed in diagnosing infected herds with tuberculosis. However, unlike IGRA, the ELISA is a serological technique that measures antibody immune response against two specific antigens of *M. bovis*, MPB70 and MPB83, which are immobilized in the plate. Antibodies in sera samples are detected using a secondary conjugated anti-bovine antibody[28].

Cattle culling and surveillance in slaughterhouses

When a cow is reactive to the tuberculin skin test or confirmed as positive through a laboratory diagnosis, the animal is first isolated and eventually removed from the pen and slaughtered, limiting the risk of continuing to transmit the disease toward the rest of the animals[29]. Culling is one of the control measures mostly used in programs against bovine tuberculosis worldwide. Veterinarians kill the animal in an official abattoir, where the individuals are subjected to an inspection for granulomatous lesions findings[30]. This procedure involves the inspection and incision of lymph nodes in the head (retropharyngeal and tracheobronchial), chest cavity (mediastinal), and organs such as lungs and liver[31]. Samples from these lymph nodes are then sent to an official accredited laboratory for further analysis, such as culture, PCR, and histopathology, to confirm the cases. Once reactive and suspect animal cases are confirmed as positive after organs and carcass inspection, they are included in an official register by the respective government organization[3]. Consequently, in infected farms is performed a sanitation process which provides for quarantine, restriction on animal movement, and the disinfection of premises to remove the disease. After the removal of infected animals and sanitization of the farms, whole herds must periodically be re-evaluated through a tuberculin skin test until the entire herd in negative. These tests should be applied in animals with at least 2 months between and complemented with laboratory analysis[33,34]. Besides the sanitation and removal strategies, in several countries, the governments provide financial compensation per culled animal to farmers[30]. In England, for example, per animal slaughtered, it is paid about €1500, and in the USA, between $500-2500 US[35]. Because test-and-slaughter approaches are unfeasible, there is an imperative need to develop a new effective vaccine that can support control and eradication programs. Vaccines provide immunity that may protect individuals from pathogens; in reality, they are nearly the most cost-effective solution for controlling infectious diseases.

The vaccine against bTB must meet two main criteria: first, do not interfere with the intradermal tuberculin skin test performed in vivo on animals, and second provide full protection against the *Mycobacterium bovis*, which is responsible for causing the pathology.

Challenges of vaccination in cattle

Currently, no vaccine is approved by the OIE to be used in cattle against bTB. In the case of human tuberculosis (hTB) produced by *Mycobacterium tuberculosis*, the strain of *M. bovis Bacillus* Calmette-Guerin (BCG) is authorized by the World Health Organization (OMS) to be employed as an attenuated vaccine. Despite, both pathologies are closely related in terms of high homology between the microorganisms and similarity in the clinical manifestation of the disease, the use of BCG in cattle for immunization is not allowed[36]. There are two key reasons for this: firstly, BCG is a live attenuated vaccine that includes the whole pathogen; therefore, it shares several antigens with bovine PPD used in the tuberculin skin test or TST[37]. This means that TST failed to distinguish BCG-vaccinated cattle from infected ones with a live virulent strain of *M. bovis*. The interference between BCG and bPPD generates a cellular immune cross-response mediated by memory T cells. These cells generate a recall response when they have been previously exposed to the pathogen, and then animals become positive in TST[38]. Second, BCG has been successfully tested in cattle; however, it has been demonstrated to induce varying levels of protection against *M. bovis*[39]. The lack of an efficient vaccine against bovine tuberculosis during all these years has provoked the problem caused by the disease has increased due to it still spreading between the species. Hence, it is crucial to have a protective vaccine that complements control and eradication programs executed in most countries where the disease is present. Based on this, in the last 15 years have resurged the interest on the development of a vaccine against bTB that must fulfill all the criteria required to be used in the immunization of cattle.

Requirements must meet a suitable vaccine against bTB

First, an ideal vaccine to bTB must prevent the infection's transmission and establishment, offering whole protection in cattle. Secondly, it must not interfere with the disease's diagnosis and must be cost-effective[39].

Two main parameters support the effectiveness of a vaccine against bovine tuberculosis. Firstly, the level of lessons in pathognomonic organs and tissues directly relates to bacterial load after a challenge with a virulent strain of *M. bovis*. In the second place, the immune response triggered by the vaccine is determined by different subsets of T cells and antibodies[40].

It has been necessary to establish a set of immunological markers, predictors and correlatives of a protective response toward *M. bovis*. Thanks to different studies performed on human and bovine tuberculosis, it has been discovered essential attributes are involved in protective response against virulent strains of the pathogen[41]. A protective

vaccine must lead to a robust innate response, the first line of protection. Specialized antigen-presenting cells (APCs) like dendritic cells (CDs), macrophages, natural killer (NK) cells and gamma delta T (γδ T) cells play a crucial role then for stimulating proper adaptive immunity[42].

If the vaccine can induce a solid initial innate response, it can later trigger an early and potent adaptive immunity mediated by T CD4+ and CD8+ lymphocytes. The adaptive response through T CD4+ lymphocytes it should be Th1 type, characterized by the expression of proinflammatory cytokines such as IFNγ, TNFα, IL12 e IL2[43]. The vaccine must induce high levels of IFNγ produced by memory and effector T cells. In several studies, IFNγ has been associated with a protective immune response against *M. bovis* and its role in activating effector T lymphocytes and macrophages responsible for killing the mycobacteria. On the other side, it has also been described that IFNγ stimulates cytotoxic cells capable of destroying infected cells. An ideal vaccine must also induce a proper memory cell response that can answer faster and competently in reinfection cases[44].

Furthermore, the vaccine should stimulate polyfunctional cells that express the surface markers CD44hi, CD45RO+, and CD62Lo, and have the capacity of simultaneously secrete IFNγ, TNFα, and IL2[45]. On the other hand, it has been demonstrated that cell immune response type Th17 also plays a crucial role in protection against *M. bovis* during the initial establishment of the infection. This Th17 response is specific toward some antigens of the microorganism, and it is mediated by the cytokines IL17, IL21, e IL22. The action of Th17 cells and the respective cytokines have been negatively correlated with the development of the pathology and positively with protection against the disease in cattle[46]. The level of security a vaccine against tuberculosis provides is measured according to bacterial loading associated with the number of colony-forming units (CFU).

Consequently, in vaccinated groups of animals, an ideal vaccine must avoid or reduce the colonization of the microorganism in the different organs. This last means that the vaccine must inhibit the establishment of the infection in comparison with animal control groups that have not been received vaccinated. Figure 1 briefly displayed the main cell type, signaling pathways activated and cytokines pattern that is expected to be involved in the innate and adaptive immune response after vaccination of cattle with a protective vaccine.

The second requirement that a bTB-suitable vaccine candidate must meet is not to sensitize animals to react with the TST, which is used as the main tool for cattle diagnosis. This cross-reactivity is in response to immunogenic proteins of *Mycobacterium bovis*, which are components of bovine PPD (bPPD) of tuberculin skin test. Therefore, when an animal is immunized with a vaccine that shares the same antigens as the TST, as is the case of the live attenuated BCG when TST is performed, the animal will develop a local cellular response in the site of injection. This, hinder differentiating vaccinated from infected animals with a pathogenic strain[47]. One approximation for this problem may consider the development of new protective vaccines that only include some antigens from *M. bovis* that would be absent or in low proportion in the bPPD of the tuberculin. This list is based on the theory that as bPPD is a cocktail of numerous proteins, the immune response of the antigens that are in low amounts can be waned by the others that are in high doses. According to this, different studies have described the composition of the bPPD; however, none provide full knowledge of the protein conformation. A well-defined understanding of bPPD composition can contribute to identifying and selecting suitable candidate proteins for developing a new vaccine. It is important to note that has been observed some discrepancies in terms of protein components of different PPD preparations. Currently, there are different research that has studied the PPD composition. Among them stand out, a study performed by Rberto *et al.* 2017 compared the composition of four other preparations of bPPD from the AN5 strain. One of the bPPD was from Spain, two from Italy and the last one from the Netherlands. Proteins from each bPPD were precipitated by TCA and analyzed through bottom-up proteomics and then by mass spectrometry. In this work, 356 proteins were identified; 85% were found to be shared among the four bPPD preparations. From the total, 198 proteins were detected for the first time; 19 proteins were concordant with previously analyzed bPPD proteomes from the United Kingdom and Brazil, and 78 with bPPD from Korea. In addition, 78 proteins were found in common with the United Kingdom, Brazilian and Korean bPPDs. According to the same research, the most abundant proteins in all bPPD preparations are ten: 1) ESAT-6-like protein EsxB, 2) 6 kDa early secretory antigenic target, 3) Immunogenic protein MPB70, 4) ESAT-6-like protein EsxN, 5) 14 kDa antigen, 6) Meromycolate extension acyl carrier protein, 7)10 kDa chaperonin, 8) GroES protein, 9) Immunogenic protein MPB63, and 10) 50S ribosomal protein L7/L12.

Another research carried out by Borsuk *et al.*, 2009, compared two bovine and two avium PPD preparation from Brazil and UK. This study used the microcolumn reversed-phase liquid chromatography-electrospray ionization tandem mass spectrometry (LC/MS/MS). This method allows the separation of proteins through HPLC and their detection by a mass spectrometer. In total, 171 proteins were discovered among the four bPPD. Among the Brazilian and UK bovine PPD was found 37 common proteins, 11 were unique in Brazilian bPPD and 52 to UK bPPD. On the other hand, 21 proteins were present exclusively in the bovine PPDs but were not identified in the avium PPDs. According to this work, in the Brazilian bPPD it was observed that the most abundant proteins were elongation factor EF-Tu – Rv0685 and Rv0865 (probable molyb- dopterin biosynthesis Mog protein), whereas in the UK bPPDs the most abundant proteins were EsxB protein (ESAT-6 like protein EsxB – Rv3874) and the 10 kDa chaperone protein (Rv3418c).

A second approach to the problem of the cross-reaction between bTB vaccine and TST is the development of differentiating infected from vaccinated animals (DIVA) tests. These assays may replace the tuberculin skin test, and heterologous prime boost strategies with BCG can be used as effective immunization. In order to develop a DIVA test to diagnose bovine tuberculosis in animals, it is necessary first to identify potential protein candidates. The two antigens well-characterized from *M. tuberculosis* and *M. bovis* ESAT-6 and CFP-10 have been tested as putative DIVA candidates. Both proteins are encoded in the RD1 region of the genome of the Mycobacterium, which is absent in BCG strains because of its attenuation process. As the RD1 locus is not in the genome of no BCG, neither ESAT-6 nor CFP-10 would be expressed in the strain. Thus, these antigens should not elicit a cross reactivity when animals are vaccinated with BCG. In fact, in a study, ESTA-6 and CFP-10 have been used as diagnostic proteins that can differentiate infected from vaccinated animals.

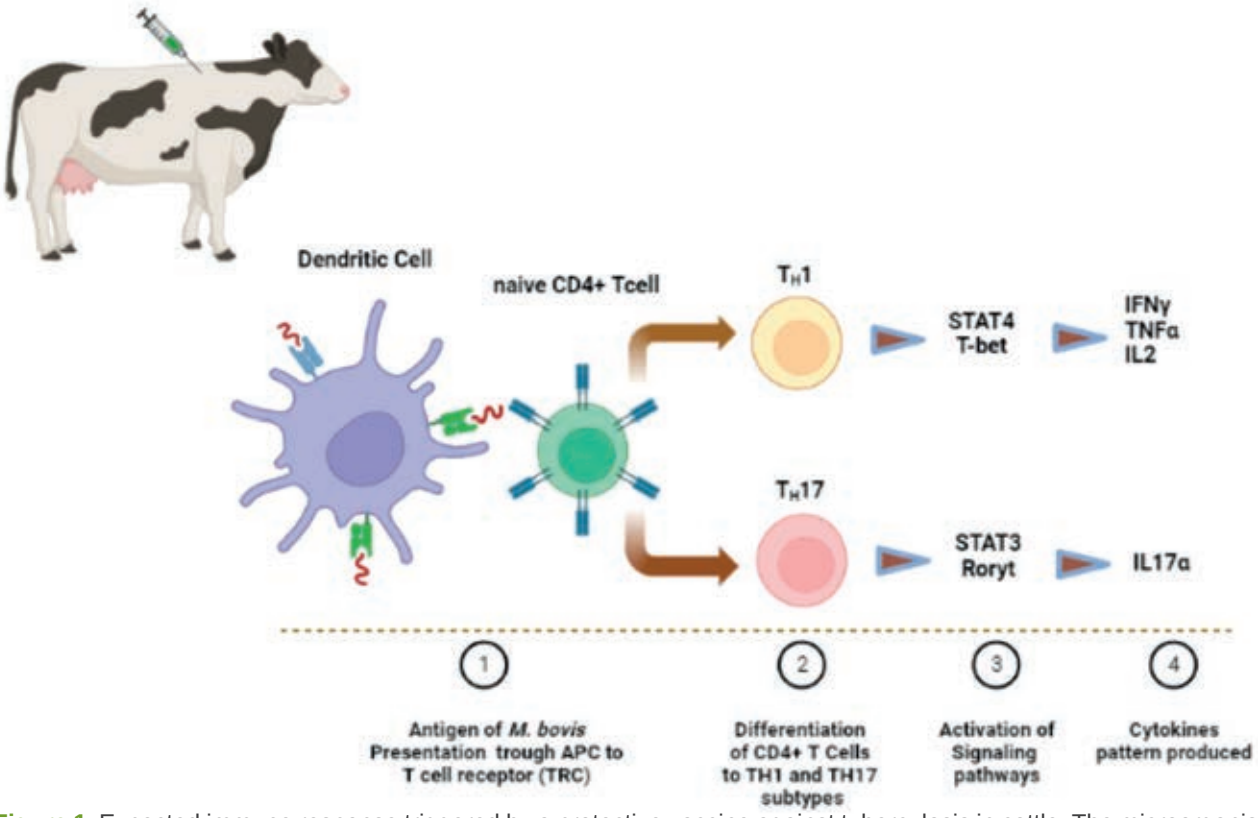

Figure 1. Expected immune response triggered by a protective vaccine against tuberculosis in cattle. The microorganism or antigens of *M. bovis* inoculated through a vaccine are first recognized by phagocytic cells that ingest the pathogen. This is processed inside of specialized vesicles containing different types of enzymes. Then, the antigens are exposed through histocompatibility molecules (MHC) located on the surface of antigen-presenting cells (APC) to naïve lymphocytes. A protective vaccine against *Mycobacterium bovis* should mainly activate CD4+ T cells and prompt its differentiation into T helper Th1 and Th17 subsets. Specific signaling pathways must be activated in both responses, the STAT4 and the STAT3, for the expression of the transcription factor T-bet and Roryt since they are responsible for the proinflammatory cytokines profile related to protective responses that involve INFγ, TNFα, IL2 e IL17, respectively.

On the other hand, the bPPD applied in animals during the same study showed that over 70% of BCG-vaccinated cattle reacted to the TST 50. In another work performed in Chile, researchers from University of Chile implemented and validated an ELISA DIVA assay using the proteins ESAT-6, CFP-10 and Rv3615. Based on this study, it was found that the test was effective in detecting infected animals with M. bovis, yet it is inefficient to test many samples because it is costly and slow[51]. More studies are required to discover new DIVA antigens that can be used in diagnosing bTB. Figure 2 summarizes two potential approaches mentioned in this article to develop a strategy that could allow the use of a compatible vaccine with a diagnosis in bovine tuberculosis.

New strategies of vaccination

Thus far, there is not an approved vaccine by the OIE against bovine tuberculosis. On the contrary, for human tuberculosis caused by *Mycobacterium tuberculosis*, the Bacillus Calmette-Guérin, BCG is allowed, which is a live attenuated vaccine produced from *M. bovis*. BCG is administrated in infants all around the world as an immunization routine for *M. tuberculosis*[52]. Although *M. tuberculosis* and *M. bovis* are closely related regarding genomic homology and disease presentation, BCG can not be used to prevent bTB since it has low effectiveness and interferes with the major surveillance tool, the tuberculin skin test[53].

Because bTB tremendously impacts the livestock industry and public health, in the last decades have emerged high interest in developing new effective vaccines against the disease. Researchers have been studying different type of vaccines in animal models to assess their ability to protect against a challenge with *M. tuberculosis* and *M. bovis*. The approaches in the development of human tuberculosis vaccines could also be applied for bovine tuberculosis as *M. bovis* and *M. tuberculosis* share high genomic homology, and thus, the mechanism of both pathogens in causing the disease is very alike. Therefore, it is important to consider human tuberculosis advances in terms of studying how to face the problem of tuberculosis in cattle caused by *M. bovis*.

Nowadays, the efforts are mostly focused on vaccination strategies that increase BCG efficacy. These involve a heterologous prime boost with BCG as a prime and recombinant BCG (rBCG)[54,55], subunit proteins[56], DNA vaccines[57], or viral vector vaccines[55] as a boost. Next, we described some of these vaccines and those currently under clinical trials (Table 1).

Recombinant BCG includes strains producing Th1 cytokines to augment the efficacy of wild-type BCG. One type of this rBCG is rBCG::IL-2, that shown to enhance the T-cell and antibody immune response in mice after immunization, proving its greater immunomodulatory effects compared with regular BCG[58]. There are rBCG strains producing non-bacterial immunomodulatory proteins, such as rBCG::-Flt3L. The Fms-like tyrosine kinase 3 ligand (Ftl3L) promoted APCs and was over-produced in an rBCG strain. Mice

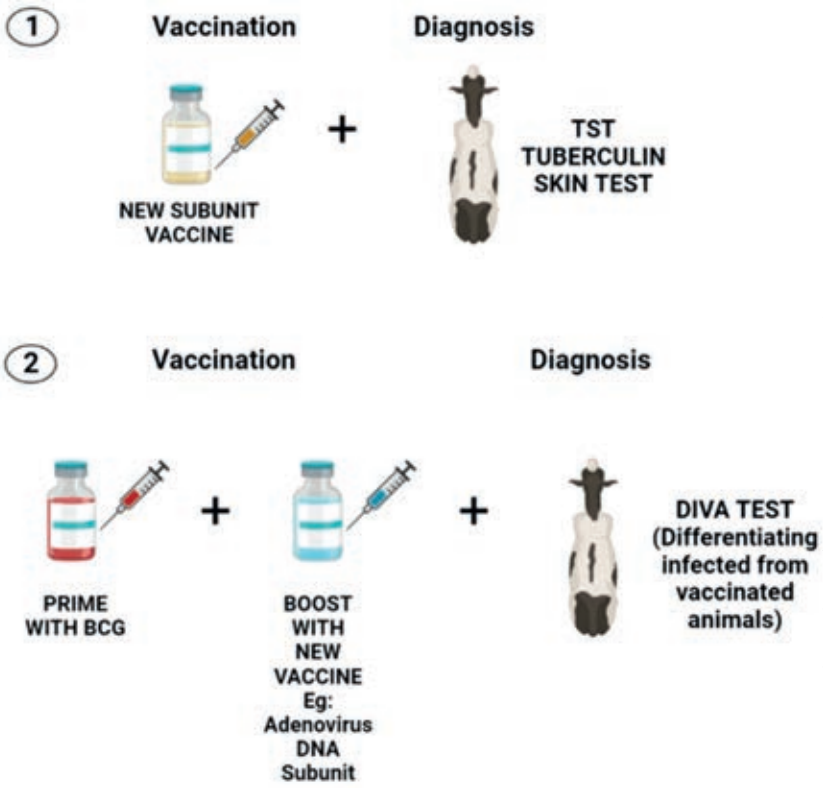

Figure 2. Two potential approaches for consistent vaccination and diagnosis in bovine tuberculosis. The first approach (1) involves the development of a new subunit vaccine that should include the most immunogenic proteins of *M. bovis*. Those proteins must be absent or in a lower proportion in bPPD to diminished cross-reactivity with TST. This first approach seems to be less studied because only a few reports describe the protein composition of bPPD. In addition, it entails the development of a new vaccine that must demonstrate to elicit a better immune response than BCG. The second approach (2) requires a heterologous prime boost using BCG and a new vaccine that must improve the immunity offered by BCG. Furthermore, this vaccination strategy needs the development of a DIVA diagnosis that only includes antigens that are missing in BCG to avoid cross-reactivity with the vaccine.

vaccinated with rBCG::Flt3L exhibited more robust IFN-γ responses in the spleen and draining lymph nodes contrasted to wild-type BCG. The recombinant strain was also safer than the parental strain in immune-deficient mice[59]. Other rBCG are strained, over-producing high immunogenic *M. bovis* proteins like Ag85b. Vaccination with rBCG::Ag85b has shown in mice a lessing of the lessons in lungs compared to immunized groups with the wild-type BCG[54]. Another example of recombinant BCG is the one that lacks of zmp-1gene, associated with hindering phagolysosome fusion in infected macrophages. It was reported that this vaccine induce a more robust T-cell response characterized by a rise in the secretion of IFNγ compared with the wild-type BCG[60].

Several protein subunit vaccines have been tested alone or co-administrated with BCG in animals under experimental conditions. These vaccines have demonstrated its capacity to induce a protective response by itself or boost BCG immunity against virulent *M. bovis* and *M. tuberculosis* challenge. In a study, culture filtrate proteins or CFP from M. bovis in combination with bovine IL-2 were used to immunize calves of 6 months old to assesses the effectiveness of the vaccine for stimulating a protective immune response against an intratracheal challenge. The results showed that the vaccine prompted a strong cellular and antibody response significantly reducing the degree of lung lesions in comparison with the control group[61].

In another investigation, a protein subunit vaccine known as H107 that included antigens from *M. tuberculosis* (PPE68, ESAT-6, EspI, EspC, and EspA, MPT64, MPT70, and MPT83) was tried. The analysis performed with the vaccine in a murine model disclosed that all chosen antigens induced substantial protection except for MPT64. Protein ESAT-6 was the most protective antigen in mice, followed by EspI, EspA, and EspC. Furthermore, it was found that combining BCG with H107 increases the immunity triggered by BCG alone, characterized by an expansion of the CD4 T cells and a Th17 cell response[62]. Recently, a group of researchers have been developing a new subunit vaccine based on highly antigenic fusion proteins from *M. bovis* and *M. tuberculosis*. This is H65, composed of six ESX-secreted antigens EsxD, EsxC, ExsG, EsxH, ExsW and EsxV formulated in CAF01 liposomal adjuvant. According to this, it was shown that in the *M. bovis* mouse model of infection the administration of BCG plus H65 was much more protective than H65 alone[63]. In addition to protein subunit vaccines, DNA vaccines have been developed that encode specific antigens of M. bovis. An example is a DNA-E6 that encodes the protein ESAT-6, which is absent in BCG strains. Researchers immunized groups of BALB/c mice with DNA-E6 alone and co-administrated with BCG, and afterward, the animals were challenged with low-dose virulent M*. tuberculosis* H37Rv. This study found that the administration of DNA-E6 and BCG induced more secretion of IFNγ and less pathological changes in lung and spleen than the DNA-E6 alone[64]. In another study, a DNA vaccine that encodes for three mycobacterial antigens Rv3407, Ag85A, and HspX was tested in a murine model. The vaccine triggered an antigen-specific cellular and humoral immune response as well as conferred protection against a challenge performed with *M. Tuberculosis* aerosol[65].

Moreover, adenoviruses vaccines boosting BCG have been tried. Among these is MVA85A, which corresponds to a modified vaccine from a recombinant attenuated Ankara virus engineered to express Ag85A from *M. tuberculosis*. Individuals immunized with a prime-boost BCG- MVA85A showed high antigen 85A-specific CD8+ T cells after being boosted with MVA85A[66]. Another adenovirus vaccine used to boost BCG is Ad85A, an attenuated recombinant vaccine based on the human adenovirus type 5 (AdHu5), which was also developed to express Ag85A. It was found that Ad85A stimulates polyfunctional CD4+ and CD8+ T cell immunity in previously BCG-vaccinated individuals[67].

Viral Vector	Subunit Recombinant	Whole Cell/Extract	Attenuated/Live Recombinant
MVA85A **Composition:** Vaccinia Virus Ankara (MVA) expressing antigen 85A (MVA85A). **Use:** Preventive **Clinical Trial phase:** I **Sponsoring:** University of Oxford.	H56:IC31 **Composition:** Fusion protein antigens Ag85B, ESAT-6 and Rv2660c formulated in IC31. **Use:** Preventive **Clinical Trial phase:** IIb **Sponsoring:** Aeras.	Vaccae™ **Composition:** Whole cell from *M. vaccae*. **Use:** Therapeutic **Clinical Trial phase:** III **Sponsoring:** AnHui Longcom.	MTBVAC **Composition:** Live attenuated *M. tuberculosis* from a human isolate MT103. **Use:** Preventive **Clinical Trial phase:** IIa **Sponsoring:** Biofabri,SL; University of Saragoza; Centre Hospitalier Universitaire Vaudois; TuBerculosis Vaccine Initiative.
Ad5Ag85A **Composition:** Adenovirus serotype 5 vaccine vector expressing antigen 85A. **Use:** Preventive **Clinical Trial phase:** I **Sponsoring:** McMaster University, CanSino.	H4:IC31 **Composition:** Fusion protein antigens Ag85B and TB10.4 formulated in IC31. **Use:** Preventive **Clinical Trial phase:** IIa **Sponsoring:** HIV Vaccines Trials Network; Sanofi Pasteur; Statens Serum Institute.	RUTI® **Composition:** Whole cell extract from *M. tuberculosis* delivered in liposomes. **Use:** Therapeutic **Clinical Trial phase:** III **Sponsoring:** Archivel Farma, SL.	VPM1002 **Composition:** Live recombinant BCG that uses the Lysteriolysin O (LLO)- encoding gene from *Listeria. monocytogenes* (Hly) to replace the urease C encoding gene (UreC). **Use:** Preventive **Clinical Trial phase:** III **Sponsoring:** University Health Network, Toronto; Serum Institute of India Pvt. Ltd; Max Planck Institute for Infection Biology; Verity Pharmaceutycals.
TB/FLU-04L **Composition:** Influenza virus mucosal vector expressing antigens Ag85A and ESAT-6 **Use:** Preventive **Clinical Trial phase:** IIa **Sponsoring:** Research Institute for Biological Safety Problems.	M72+AS01E **Composition:** Fusion protein antigens MTB32A and MTB39A formulated in AS01E. **Use:** Preventive **Clinical Trial phase:** IIb **Sponsoring:** GlaxoSmithKline; Aeras.	DAR-901 **Composition:** Whole-cell, heated-killed NTM vaccine. **Use:** Preventive **Clinical Trial phase:** IIb **Sponsoring:** Darmouth University; Aeras.	
	ID93+GLA-SE **Composition:** Fusion protein antigens Rv2608, Rv3619, Rv3620 and Rv1813 formulated in GLA-SE. **Use:** Preventive **Clinical Trial Phase:** IIa **Sponsoring:** Quratis Inc; IDRI.		

Table 1. Shows several vaccine candidates currently under clinical trials and were classified according to its composition. The information for all these vaccines was retrieved from the following website https://clinicaltrials.gov/.

Conclusions

This article briefly describes the enormous damage caused by *Mycobacterium bovis* in the livestock industry and gives an approach to its possible solutions. According to the studies reviewed, all of them agree that without an effective vaccine and a compatible diagnosis, no program for eradication would be victorious against tuberculosis in cattle. In these terms, based on the scientific information gathered, two approaches could offer a true solution for bovine tuberculosis. The first one is the development of a new protective vaccine that precludes in the near future the use of BCG in animals, so it may be used with TST. This vaccine should comprise some of the most immunogenic proteins from M. bovis to protect against de pathogens.

Moreover, those selected proteins should be less representative in bPPD of tuberculin, hence may not cause a cross-reaction with the diagnosis. However, we noticed that only few studies describe the protein composition of bPPD. For this purpose, it is essential a deep knowledge of all protein components of bPPD. The second one is the replacement of TST with a DIVA test which also involves a strategy of vaccination that allows to the improvement of the effectiveness of BCG. Then finally, BCG would be used in cattle. The DIVA tests consider *M. bovis* proteins that are not expressed in BCG (e.g.: ESAT6/CFP10), so unlikely could occur a cross-reaction between the vaccine and the surveillance tool.

On the other hand, BCG enhancement consists of a prime-boost where the immune system is first primed with a dose of BCG, and later it is boosted with a subunit vaccine. This last approach seems to be more explored than the first one because more studies about it are available, and it was easier to incorporate them in our review. In brief, even though there is a lot of evidence in the literature that prime-boost with BCG and other types of vaccines gives better results in terms of protection than administrating BCG by itself, it needs to be compatible with an efficient diagnosis of the disease. Therefore, a definitive solution for tuberculosis in cattle would not be accomplished in the short term.

Conflicts of Interest

The authors declare no conflict of interest.

Bibliographic references

1. O'reilly LM, Daborn CJ. The epidemiology of Mycobacterium bovis infections in animals and man: a review. Vol. 1, Tubercle and Lung Disease. 1995.
2. de La Rua-Domenech R. Human Mycobacterium bovis infection in the United Kingdom: Incidence, risks, control measures and review of the zoonotic aspects of bovine tuberculosis. Vol. 86, Tuberculosis. 2006. p. 77–109.
3. Walker TM, Ip CLC, Harrell RH, Evans JT, Kapatai G, Dedicoat MJ, et al. Whole-genome sequencing to delineate Mycobacterium tuberculosis outbreaks: A retrospective observational study. Lancet Infect Dis. 2013 Feb;13(2):137–46.
4. Tibesso G. Review on epidemiological features of Mycobaterium bovis at the human, cattle and wildlife interface in Ethiopia. Biom Biostat Int J. 2018 Sep 28;7(5).
5. Integrated Taxonomic Information System - Report (ITIS). 2022.

6. Forrellad MA, Klepp LI, Gioffré A, García JS, Morbidoni HR, de la Paz Santangelo M, et al. Virulence factors of the mycobacterium tuberculosis complex. Vol. 4, Virulence. Taylor and Francis Inc.; 2013. p. 3–66.
7. World Organization for Animal Health (WHOA). Bovine Tuberculosis [Internet]. 2022 [cited 2023 Feb 26]. Available from: https://www.woah.org/en/disease/bovine-tuberculosis/
8. The European Union One Health 2019 Zoonoses Report. EFSA Journal. 2021 Feb 1;19(2).
9. Olmstead AL, Rhode PW. An impossible undertaking: The eradication of bovine tuberculosis in the United States. Journal of Economic History. 2004;64(3):734–72.
10. Tschopp R, Zinsstag J, Conlan A, Gemechu G, Wood J. Productivity loss and cost of bovine tuberculosis for the dairy livestock sector in Ethiopia. Prev Vet Med. 2022 May 1;202.
11. Bolaños CAD, de Paula CL, Guerra ST, Franco MMJ, Ribeiro MG. Diagnosis of mycobacteria in bovine milk: An overview. Vol. 59, Revista do Instituto de Medicina Tropical de Sao Paulo. Instituto de Medicina Tropical de Sao Paulo; 2017.
12. Phoenix JH. Trading with risk: associating bovine tuberculosis to cattle commodities in risk-based trading. J Cult Econ. 2021;14(3):293–305.
13. Smith RL, Tauer LW, Sanderson MW, Gröhn YT. Minimum cost to control bovine tuberculosis in cow-calf herds. Prev Vet Med. 2014 Jul 1;115(1–2):18–28.
14. Ábalos P, Valdivieso N, de Val BP, Vordermeier M, Benavides MB, Alegría-Morán R, et al. Vaccination of Calves with the Mycobacterium bovis BCG Strain Induces Protection against Bovine Tuberculosis in Dairy Herds under a Natural Transmission Setting. Animals. 2022 May 1;12(9).
15. Cassidy JP. The pathogenesis and pathology of bovine tuberculosis with insights from studies of tuberculosis in humans and laboratory animal models. In: Veterinary Microbiology. 2006. p. 151–61.
16. Domingo M, Vidal E, Marco A. Pathology of bovine tuberculosis. Res Vet Sci. 2014;97(S):S20–9.
17. Neill SD, Pollock JM, Bryson DB, Hanna J. Pathogenesis of Mycobacterium bovis infection in cattle. Vol. 40, Veterinary Microbiology. 1994.
18. Sakamoto K. The Pathology of Mycobacterium tuberculosis Infection. Vol. 49, Veterinary Pathology. 2012. p. 423–39.
19. Gengenbacher M, Kaufmann SHE. Mycobacterium tuberculosis: Success through dormancy. Vol. 36, FEMS Microbiology Reviews. 2012. p. 514–32.
20. Heemskerk D, Caws M, Marais B, et al. Clinical Manifestations. In: Tuberculosis in adults and children. London: Springer; 2015.
21. Ayele WY, Neill SD, Zinsstag J, Weiss MG, Pavlik I. Bovine tuberculosis: an old disease but a new threat to Africa. Vol. 8, INT J TUBERC LUNG DIS. 2004.
22. Awah-Ndukum J, Temwa J, Ngwa VN, Mouiche MM, Iyawa D, Zoli PA. Interpretation criteria for comparative intradermal tuberculin test for diagnosis of bovine tuberculosis in cattle in Maroua Area of Cameroon. Vet Med Int. 2016;2016.
23. Bayissa B, Sirak A, Zewude A, Worku A, Gumi B, Berg S, et al. Field evaluation of specific mycobacterial protein-based skin test for the differentiation of Mycobacterium bovis-infected and Bacillus Calmette Guerin-vaccinated crossbred cattle in Ethiopia. Transbound Emerg Dis. 2022 Jul 1;69(4):e1–9.
24. Doan TN, Eisen DP, Rose MT, Slack A, Stearnes G, McBryde ES. Interferon-gamma release assay for the diagnosis of latent tuberculosis infection: A latent-class analysis. PLoS One. 2017 Nov 1;12(11).
25. Good M, Clegg TA, Costello E, More SJ. The comparative performance of the single intradermal test and the single intradermal comparative tuberculin test in Irish cattle, using tuberculin PPD combinations of differing potencies. Veterinary Journal. 2011 Nov;190(2).
26. Monaghan A' ML, Doherty ML, Collins JD, Kazda JF, Quinn PJ. The tuberculin test. Vol. 40, Veterinary Microbiology. 1994.
27. Sadatsafavi M, Shahidi N, Marra F, FitzGerald MJ, Elwood KR, Guo N, et al. A statistical method was used for the meta-analysis of tests for latent TB in the absence of a gold standard, combining random-effect and latent-class methods to estimate test accuracy. J Clin Epidemiol. 2010 Mar;63(3):257–69.
28. Filho PMS, Ramalho AK, Silva AM, Issa MA, Mota PMPC, Silva CHO, et al. Diagnostic performance of a commercial ELISA used as a complementary test for bovine tuberculosis in two bovine herds with different disease status. Arq Bras Med Vet Zootec. 2020 Jan 1;72(1):1–8.
29. Donnelly CA, Woodroffe R, Cox DR, Bourne FJ, Cheeseman CL, Clifton-Hadley RS, et al. Positive and negative effects of widespread badger culling on tuberculosis in cattle. Nature. 2006 Feb 16;439(7078):843–6.
30. Arnot LF, Michel A. Challenges for controlling bovine tuberculosis in south africa. Vol. 87, Onderstepoort Journal of Veterinary Research. AOSIS (pty) Ltd; 2020.
31. Woldemariyam FT, Markos T, Shegu D, Abdi KD, Paeshuyse J. Evaluation of postmortem inspection procedures to diagnose bovine tuberculosis at debre birhan municipal abattoir. Animals. 2021 Sep 1;11(9).
32. Asseged B, Woldesenbet Z, Yimer E, Lemma E. Evaluation of Abattoir Inspection for the Diagnosis of Mycobacterium bovis Infection in Cattle at Addis Ababa Abattoir. 2004.
33. Smith RL, Tauer LW, Schukken YH, Lu Z, Grohn YT. Minimization of bovine tuberculosis control costs in US dairy herds. Prev Vet Med. 2013 Nov 1;112(3–4):266–75.
34. Che-Amat A, Risalde MÁ, González-Barrio D, Ortíz JA, Gortázar C. Effects of repeated comparative intradermal tuberculin testing on test results: A longitudinal study in TB-free red deer. BMC Vet Res. 2016 Sep 5;12(1).
35. Smith RL, Tauer LW, Schukken YH, Lu Z, Grohn YT. Minimization of bovine tuberculosis control costs in US dairy herds. Prev Vet Med. 2013 Nov 1;112(3–4):266–75.
36. Milián-Suazo F, González-Ruiz S, Contreras-Magallanes YG, Sosa-Gallegos SL, Bárcenas-Reyes I, Cantó-Alarcón GJ, et al. Vaccination Strategies in a Potential Use of the Vaccine against Bovine Tuberculosis in Infected Herds. Vol. 12, Animals. MDPI; 2022.
37. Chandran A, Williams K, Mendum T, Stewart G, Clark S, Zadi S, et al. Development of a diagnostic compatible BCG vaccine against Bovine tuberculosis. Sci Rep. 2019 Dec 1;9(1).
38. Chambers MA, Carter SP, Wilson GJ, Jones G, Brown E, Hewinson RG, et al. Vaccination against tuberculosis in badgers and cattle: An overview of the challenges, developments and current research priorities in Great Britain. Vol. 175, Veterinary Record. British Veterinary Association; 2014. p. 90–6.
39. Balseiro A, Thomas J, Gortázar C, Risalde MA. Development and challenges in animal tuberculosis vaccination. Vol. 9, Pathogens. MDPI AG; 2020. p. 1–31.
40. Garrido JM, Sevilla IA, Beltrán-Beck B, Minguijón E, Ballesteros C, Galindo RC, et al. Protection against tuberculosis in eurasian wild boar vaccinated with heat-inactivated mycobacterium bovis. PLoS One. 2011 Sep 14;6(9).
41. Thomas J, Risalde MÁ, Serrano M, Sevilla I, Geijo M, Ortíz JA, et al. The response of red deer to oral administration of heat-inactivated Mycobacterium bovis and challenge with a field strain. Vet Microbiol. 2017 Sep 1;208:195–202.
42. Blanco FC, Gravisaco MJ, Bigi MM, García EA, Marquez C, McNeil M, et al. Identifying Bacterial and Host Factors Involved in the Interaction of Mycobacterium bovis with the Bovine Innate Immune Cells. Front Immunol. 2021 Jul 15;12.
43. Flesch IEA, Kaufmann SHE. Role of Cytokines in Tuberculosis. Immunobiology. 1993;189(3–4):316–39.
44. Rhodes SG, Palmer N, Graham SP, Bianco AE, Hewinson RG, Vordermeier HM. Distinct Response Kinetics of Gamma Interferon and Interleukin-4 in Bovine Tuberculosis. Vol. 68, INFECTION AND IMMUNITY. 2000.
45. Lewinsohn DA, Lewinsohn DM, Scriba TJ. Polyfunctional CD4+ T cells as targets for tuberculosis vaccination. Vol. 8, Frontiers in Immunology. Frontiers Media SA; 2017.

46. Lyadova I v., Panteleev A v. Th1 and Th17 Cells in Tuberculosis: Protection, Pathology, and Biomarkers. Mediators Inflamm. 2015;2015.
47. Buddle BM, Vordermeier HM, Chambers MA, de Klerk-Lorist LM. Efficacy and safety of BCG vaccine for control of tuberculosis in domestic livestock and wildlife. Vol. 5, Frontiers in Veterinary Science. Frontiers Media SA; 2018.
48. Roperto S, Varano M, Russo V, Lucà R, Cagiola M, Gaspari M, et al. Proteomic analysis of protein purified derivative of Mycobacterium bovis. J Transl Med. 2017 Apr 3;15(1).
49. Borsuk S, Newcombe J, Mendum TA, Dellagostin OA, McFadden J. Identification of proteins from tuberculin purified protein derivative (PPD) by LC-MS/MS. Tuberculosis. 2009 Nov;89(6):423–30.
50. Vordermeier HM, Whelan A, Cockle PJ, Farrant L, Palmer N, Hewinson RG. Use of synthetic peptides derived from the antigens ESAT-6 and CFP-10 for differential diagnosis of bovine tuberculosis in cattle. Clin Diagn Lab Immunol. 2001;8(3):571–8.
51. VASQUES ILLANES MN. IMPLEMENTACIÓN Y VALIDACIÓN DE UNA PRUEBA SANGUÍNEA DIVA CON ANTÍGENOS ESAT-6, CFP-10 Y Rv3615c PARA EL DIAGNÓSTICO DE TUBERCULOSIS BOVINA EN CHILE. [SANTIAGO]: UNIVERSIDAD DE CHILE; 2018.
52. World Organization for animal health. Bovine Tuberculosis. 2022.
53. Whelan AO, Coad M, Upadhyay BL, Clifford DJ, Hewinson RG, Vordermeier HM. Lack of correlation between bcg-induced tuberculin skin test sensitisation and protective immunity in cattle. Vaccine. 2011 Jul 26;29(33):5453–8.
54. Yuan X, Teng X, Jing Y, Ma J, Tian M, Yu Q, et al. A live attenuated BCG vaccine overexpressing multistage antigens Ag85B and HspX provides superior protection against Mycobacterium tuberculosis infection. Appl Microbiol Biotechnol. 2015 Dec 1;99(24):10587–95.
55. Khan A, Sayedahmed EE, Singh VK, Mishra A, Dorta-Estremera S, Nookala S, et al. A recombinant bovine adenoviral mucosal vaccine expressing mycobacterial antigen-85B generates robust protection against tuberculosis in mice. Cell Rep Med. 2021 Aug 17;2(8).
56. Santema W, Hensen S, Rutten V, Koets A. Heat shock protein 70 subunit vaccination against bovine paratuberculosis does not interfere with current immunodiagnostic assays for bovine tuberculosis. Vaccine. 2009 Apr 14;27(17):2312–9.
57. Skinner MA, Buddle BM, Wedlock DN, Keen D, De Lisle GW, Tascon RE, et al. A DNA prime-Mycobacterium bovis BCG boost vaccination strategy for cattle induces protection against bovine tuberculosis? Infect Immun. 2003 Sep 1;71(9):4901–7.
58. Young S, O'Donnell M, Lockhart E, Buddle B, Slobbe L, Luo Y, et al. Manipulation of immune responses to Mycobacterium bovis by vaccination with IL-2- and IL-18-secreting recombinant bacillus Calmette Guerin. Immunol Cell Biol. 2002;80(3):209–15.
59. Triccas JA, Shklovskaya E, Spratt J, Ryan AA, Palendira U, Barbara BF, et al. Effects of DNA- and Mycobacterium bovis BCG-based delivery of the Flt3 Ligand on protective immunity to Mycobacterium tuberculosis. Infect Immun. 2007 Nov;75(11):5368–75.
60. Johansen P, Fettelschoss A, Amstutz B, Selchow P, Waeckerle-Men Y, Keller P, et al. Relief from Zmp1-mediated arrest of phagosome maturation is associated with facilitated presentation and enhanced immunogenicity of mycobacterial antigens. Clinical and Vaccine Immunology. 2011 Jun;18(6):907–13.
61. Wedlock DN, Vesosky B, Skinner MA, De Lisle GW, Orme IM, Buddle BM. Vaccination of Cattle with Mycobacterium bovis Culture Filtrate Proteins and Interleukin-2 for Protection against Bovine Tuberculosis. Vol. 68, INFECTION AND IMMUNITY. 2000.
62. Woodworth JS, Clemmensen HS, Battey H, Dijkman K, Lindenstrøm T, Laureano RS, et al. A Mycobacterium tuberculosis-specific subunit vaccine that provides synergistic immunity upon co-administration with Bacillus Calmette-Guérin. Nat Commun. 2021 Dec 1;12(1).
63. Blanco FC, García EA, Aagaard C, Bigi F. The subunit vaccine H65 + CAF01 increased the BCG- protection against Mycobacterium bovis infection in a mouse model of bovine tuberculosis. Res Vet Sci. 2021 May 1;136:595–7.
64. Fan X, Gao Q, Fu R. DNA vaccine encoding ESAT-6 enhances the protective efficacy of BCG against Mycobacterium tuberculosis infection in mice. Scand J Immunol. 2007 Nov;66(5):523–8.
65. Mir FA, Kaufmann SHE, Eddine AN. A multicistronic DNA vaccine induces significant protection against tuberculosis in mice and offers flexibility in the expressed antigen repertoire. Clinical and Vaccine Immunology. 2009 Oct;16(10):1467–75.
66. Whelan KT, Pathan AA, Sander CR, Fletcher HA, Poulton I, Alder NC, et al. Safety and immunogenicity of boosting BCG vaccinated subjects with BCG: Comparison with boosting with a new TB vaccine, MVA85A. PLoS One. 2009 Jun 16;4(6).
67. Smaill F, Jeyanathan M, Smieja M, Medina MF, Thanthrige-Don N, Zganiacz A, et al. A Human Type 5 Adenovirus-Based Tuberculosis Vaccine Induces Robust T Cell Responses in Humans Despite Preexisting Anti-Adenovirus Immunity [Internet]. 2013. Available from: www.ScienceTranslationalMedicine.org

ARTICLE / INVESTIGACIÓN

Prognostic index of hypertensive cardiopathy evolutionary changes: from mild diastolic dysfunction to depressed systolic function

Alexis Álvarez-Aliaga*, Liannys Lidia Naranjo Flores, Alexis Suárez-Quesada, David Salvador del Llano-Sosa, Andrés José Quesada Vázquez, Adonis Frómeta Guerra

DOI. 10.21931/RB/2023.08.02.10

Carlos Manuel de Céspedes General University Hospital of Bayamo, Granma Province, Cuba.
Corresponding author: alexis.grm@infomed.sld.cu

Abstract: Hypertensive cardiopathy is a variable and complex group of effects that can provoke a chronic elevation of arterial pressure in the heart. Its morbidity and mortality are increasing. To evaluate the capacity of an index based on prognostic factors to predict the evolution of hypertensive cardiopathy with mild diastolic dysfunction to depressed systolic function. We carried out a prospective cohort study in patients with hypertensive cardiopathy, followed at the specialized arterial hypertension physician's office of the Specialty Policlinic attached to "Carlos Manuel de Céspedes" General University Hospital, Bayamo Municipality, Granma Province, Cuba. The period evaluated was from Jan 1, 2008, to Dec 31, 2021. The patients followed had at least four appointments per year. Index internal validity. The mean values of the proposed index were twice as high in patients with hypertensive heart disease with depressed systolic function (mean: 11.05; p= 0.000) than in those who did not develop it. The optimal cutpoint was seven (sensitivity: 92.2 {IC: 88.94 to 95.42}; specificity: 86.7 {IC: 81.67 to 87.17}; validity index 86.7 {IC: 84.55 to 88.85}). External validity. The index showed excellent discriminative ability (area under the ROC curve of 0.954), and the calibration was adequate (Hosmer and Lemeshow: X2= 3.485; p= 0.900). The index obtained for the prognosis of hypertensive cardiopathy evolutionary changes from normal ejection fraction to cardiac insufficiency with reduced ejection fraction has an adequate predictive capacity and calibration, as well as accuracy and reliability.

Key words: Hypertension, hypertensive cardiopathy, prognostic factors, prognostic index.

Introduction

In 2002 was demonstrated that the relationship between arterial blood pressure and cardiovascular and renal complications is continuous. This fact suggests that the distinction between arterial normotension and hypertension based on arterial blood pressure cut values is somewhat arbitrary[1-3].

Nevertheless, these arterial blood pressure cut values are helpful in clinical practice for several reasons, among which stand out the necessity of simplifying the diagnosis and decision-making about treatment.

Within this range of target organ damage caused by HT, hypertensive heart disease stands out, defined as a complex and variable set of effects that cause in the heart the chronic elevation of blood pressure and is characterized by anatomical or biochemical signs, or even both of left ventricular hypertrophy or diastolic or systolic ventricular dysfunction, of myocardial ischemia and heart rhythm disturbances[4,5].

It is essential to point out that arterial hypertension seldom appears alone since it is frequently associated with a group of cardiovascular risk factors. This aspect increases the probability of cardiovascular complications. Identifying these factors makes possible the stratification of risk of people who suffer from this condition[6-8].

Despite the new diagnostic and therapeutic developments in hypertensive cardiopathy and the increasing number of studies about the prognosis of this condition, it is necessary to continue researching the topic due to its high prevalence and an increase in the mortality and impairment of patients.

Likewise, it is not known whether an index based on prognostic factors can estimate the evolution of hypertensive cardiopathy with mild diastolic dysfunction to depressed systolic function.

In the present study, we hypothesized that an index based on factors specific to HT, comorbidity and biological markers could predict the evolution of hypertensive heart disease with mild diastolic dysfunction to depressed systolic function.

In answer to the stated hypothesis, the research aimed to evaluate the ability of an index based on prognostic factors to predict the progression of hypertensive heart disease with mild diastolic dysfunction to depressed systolic function.

Materials and methods

Methodological Design

We carried out a prospective cohort study in patients with hypertensive cardiopathy, followed at the specialized arterial hypertension physician's office of the Specialty Po-

Citation: Álvarez-Aliaga A, Naranjo Flores L L, Suárez-Quesada A, del Llano-Sosa D S, Quesada Vázquez A J, Frómeta Guerra A. Prognostic index of hypertensive cardiopathy evolutionary changes: from mild diastolic dysfunction to depressed systolic function. Revis Bionatura 2023;8 (2) 10. http://dx.doi.org/10.21931/RB/2023.08.02.10
Received: 2 January 2023 / **Accepted:** 13 March 2023 / **Published:** 15 June 2023
Publisher's Note: Bionatura stays neutral with regard to jurisdictional claims in published maps and institutional affiliations.

liclinic attached to "Carlos Manuel de Céspedes" General University Hospital, Bayamo Municipality, Granma Province, Cuba. The period evaluated was from Jan 1, 2008, to Dec 31, 2021. The patients followed had at least four appointments per year.

Inclusion and exclusion criteria

Patients over 20 years diagnosed with essential hypertension and grade I hypertensive cardiopathy (diastolic dysfunction without left ventricular hypertrophy diagnosed by echocardiogram) was included. The diagnosis and classification of arterial hypertension were based on the Seventh Report of High Blood Pressure[1].

Patients with ischemic cardiopathy were excluded from the research. Despite its high frequency in hypertensive patients and is one of the main causes of cardiac insufficiency, the present study aimed to evaluate the isolated effects of arterial hypertension; therefore, including patients with con ischemic cardiopathy could bias the results. For the same reason, patients with interventricular and auriculoventricular conduction disorders were excluded.

Likewise, it was decided to exclude patients with systemic diseases who, due to their natural evolution or the use of different drugs in their treatment, might cause structural cardiopathies such as thyroid diseases, chronic bowel inflammatory disease, collagen disease, cancer or any other disease that for their characteristics could cause cardiopathy. Patients who had received or were being treated with cytostatic agents were also excluded from the study because these drugs can cause cardiopathy by structural lesions of the myocardium.

Typical background of patients

The patients included in the cohort were selected from the specialized arterial hypertension physician's office of the Specialty Policlinic attached to "Carlos Manuel de Céspedes" General University Hospital, followed up for several years before the beginning of the study. The evaluation of the cohort started on Jan 1, 2008.

Each patient was submitted to an initial interview and a thorough physical exam to obtain the necessary information. Clinical evaluations were carried out every six months. They included the analysis of clinical data, whereas echocardiograms and electrocardiograms were done annually, except when the patient's situation required such studies done at any other time.

During the study, all subjects received an initial uniform medical treatment based on a therapeutic protocol accepted by the Research Ethics Commission of the hospital, taking into consideration the latest scientific evidence about arterial hypertension[1]. The protocol was updated as new recommendations appeared[6,7,9].

Characteristics of the sample

Several years before the beginning of the cohort evaluation, 5019 patients were seen at the doctor's office. Out of them, 3517 (70. 07%) came from urban areas and 1502 (29. 93%) from rural areas; most of them came from Granma Province (Bayamo, it's the capital city). Considering the criteria previously mentioned, 2707 patients were included in the study.

During the patients' follow-up (14 years) by the arterial hypertension doctor's office, there were 207 deaths by causes other than hypertensive cardiopathy (standing out infections and other cardiovascular conditions including ictus) and 306 dropouts (did not attend appointments anymore, the onset of excludible diseases).

Jan 1, 2008, was defined as zero hours or the beginning of the cohort. Once the cohort was started, it was decided not to include any more patients (closed cohort). Each individual evaluation concluded when the patient developed grade IV hypertensive cardiopathy or at the end of the fourteen-year study period in patients who did not produce the condition.

To create and validate a prognostic index, the sample was divided into two parts; the first part was the developing simple with 1194 patients to choose the items to be included in the index, and it's weighing out (results already published[8]). The second part was the validation sample that included 1000 patients. This process was carried out using the algorithm included in the Windows SPSS software (version 25.0).

In the validation sample prevailed, the male sex (50.8%), 60.7% of the patients had salt in their diet, and only 3.7% were alcoholic.

Dependent variable

Two categories were included: developing or not grade IV hypertensive cardiopathy (left ventricular hypertrophy with depressed systolic function). For the diagnosis were considered all the hypertensive patients who met the following criteria[9-11]:

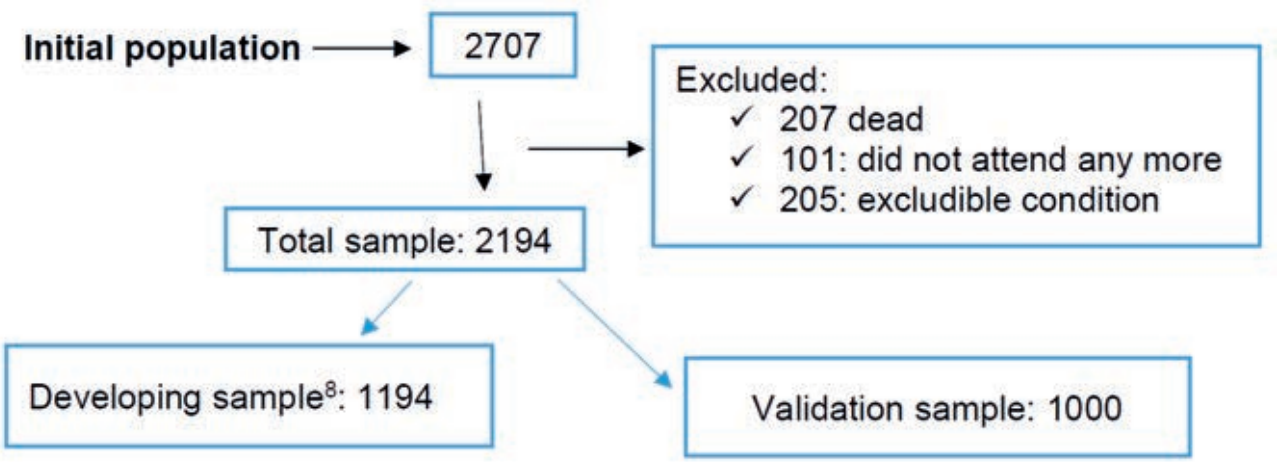

Figure 1. Sample selection.

Grade IV hypertensive cardiopathy: all patients with left ventricular hypertrophy and left ventricle with an ejection fraction under 35% (LVEF: percentage of blood expelled from the ventricle with each heartbeat).

Two cardiologists with 25 years of experience in echocardiography performed the echocardiogram. They were using ASAOTE Caris PLUS equipment based on the guidelines of the American Association of Echocardiography[10].

Independent variables

Those factors Cox's proportional regression[8] showed to be associated with the development of grade IV hypertensive cardiopathy. They are described below.

Age was quantified in years. Patients over 60 years were considered exposed.

The smoking habit was grouped into two categories: smokers (exposed) if they smoked daily or nearly daily cigarettes, cigars or pipes, no matter the number smoked, and ex-smokers for less than a year. Nonsmokers were those who were not in the habit or had quit it for over a year.

Obesity was established by calculating the body mass index (BMI: weight in kilograms divided by size in square meters). Every subject with a muscular mass index greater or equal to 30 or with a waist circumference greater or equal to 102 centimeters for men and 88 centimeters for women was considered exposed.

The biological markers selected were cholesterol, glycemia, C-reactive protein, microalbuminuria and the cholesterol/HDL quotient. The blood samples for each laboratory test were obtained in a fasting state (8 to 12 hours), and were centrifuged at room temperature at 2000 rpm for 10 minutes. Enzymatic methods did all the study determinations.

The cutpoints for the dichotomization of each laboratory variable used in the statistic analysis were established according to a method used to find optimum cutpoints proposed in the literature. The most extreme values on both ends of the variable (under percentile 5 and above percentile 95) were not considered to determine the possible cutpoints.

Likewise, due to the increased probability of type I error when using several hypothesis tests, the following formula was used to correct it: $p = -3.13\ pmin\ (1 + 1.65\ Ln\ (pmin))$, where pmin is the minimum probability value obtained and p is the corrected value.

The C value was chosen as the optimal cutpoint since it had the highest chi-square result (that is, it was the one with the lowest p-value) for all the values of the dichotomized variables[8]. In this way, it was selected as a cutpoint for each variable the value that best differentiated patients who developed grade IV hypertensive cardiopathy from those who did not.

In this way, the cutpoints were established, which defined the "exposed" cases at the following values: serum cholesterol more significant than 4.8 mmol/l, cholesterol/HDL quotient greater than 4 mmol/l, fasting glycemia greater than 5 mmol/l. C-reactive protein was determined using the quantitative turbidimetric determination method. Patients with values over 4 mg/l were considered exposed.

Patients with microalbuminuria were considered exposed when their figures ranged from 0. 02 to 0. 2 g/l in 24 hours[12], and it was quantified using the Microalb-Latex technique (consisting in the measurement of this substance in the morning first urine void.

During the first year of patient follow-up, they attended three appointments to obtain the quantitative variables' values (mean of the three results).

Control of HT. Controlled patients were those with blood pressure readings below 140 and 90 mmHg (systolic and diastolic, respectively) in 100% of the HT determinations during each year of follow-up (at least four resolutions per year), complying with optimal medical treatment according to the protocol. Those who did not meet the above criteria were considered not controlled[12].

Other blood pressure determinations during other contacts with the health system for whatever reason out of the hospital doctor's office were also taken into consideration (for this purpose, the patients were instructed to bring in writing their blood pressure values); to guarantee the authenticity of this variable each patient was given a form demanding the following information: date, time, blood pressure values, and doctor's signature and seal. This document should be presented to the hypertension specialist on the day of the follow-up appointment.

The time of evolution and the hypertension stage were also considered. Concerning the time of evolution, the patients were grouped into two categories: patients with a time of evolution between 5 and 14 years (non-exposed), and patients with a time of evolution equal to or greater than 15 years (exposed). The hypertension stage was classified according to the HTN 7th report proposal, considering the measures proposed for the correct classification and blood pressure determination[1].

For the blood pressure determinations, aneroid and mercury sphygmomanometers were previously calibrated by the Territorial Quality and Normalization Office, accredited in Cuba.

Chronic renal disease was also considered (patients in the terminal stage were excluded) as a kidney structural or functional lesion, shown by damage markers (urine, blood or images), independent of the cause that provoked it, for a period equal to or greater than three months[14].

To diagnose diabetes mellitus, independent of its type, up-to-date diagnostic criteria were considered[15].

The data were obtained in the different appointments using interviews conducted by the authors with the patient's previous knowledge and consent.

Bias control

To increase the precision and accuracy of the necessary data for the study the following biases were considered:

Selection biases: the out-patient clinical history was used to minimize memory use. Two authors interviewed each patient separately, and their results were compared later. Structured questionnaires were applied to make the interviews more homogeneous.

Information biases: control of these biases was achieved using validated measurement instruments and standardized criteria for sample collection.

Accuracy biases: the data were processed by the authors, and an extrinsic biostatistician and the results obtained coincided.

Adequate data processing was guaranteed with quality control.

Statístic analysis

The statistic analysis started with sample characterization (validation) and the description of all the variables. The means and standard deviations for the quantitative variables were described, as well as the minimum and maximum

values for each distribution.

For the comparison of the samples of developing processes[8] and validation, Pearson's chi-square was calculated for the qualitative variables and the Student's t test for was calculated for the quantitative variables provided that there was a normal distribution (evaluated by the determination of Kolmogorov-Smirnovy normality test, Levene's variance homogeneity test) Mann Whitney's U for those quantitative variables whose distribution was different to normal. The analysis made it possible to evaluate whether there were significant differences between the two samples.

Index construction

It was considered that the index should contain items that could be integrated into a global index that would take the form of a linear combination between the items: I= W1X1+W2X2+……+ WKXK.

Xi is the i-esimal variable to constitute a risk factor in each statistic analysis, and Wi is the "weight" chosen for that variable. Thus, selecting the items that would make up the indicator was considered for the construction stage.

The index was derived from a Cox's proportional regression analysis of a cohort carried out previously in the same population where the sample was obtained (for ten years)[8] taking the cutpoints which would make the greater contribution to the model and that, at the same time, was clinically significant. Each variable ascribed to the model was assigned a score based on the hazard rate (HR) value and approximated to whole numbers. Later, the hazard was classified on an ordinal scale by dividing the index distribution into four zones delimited by the percentiles 10, 50 and 90. In this way, a risk index was proposed. It can be described as an ordinal variable with four categories from minor to significant risk (category I {low}: 0 to 3 points; category II {moderate}: 4 to 6 topics; category III {high}: 7 to 9 points; category IV {very high}: 10 to 19 points).

Index internal validation

Once the index had been constructed, the predictive capacity was calculated: sensitivity, specificity, false positive rate (1- Specificity), positive predictive value, negative predictive value, the positive and negative likelihood ratio and the overall accuracy of the test. We also determined the Youden index to evaluate the optimal cut-off point (it allowed us to classify its performance: sensitivity + specificity - 1).

Index external validation

Its content, presentation, construction and criterion validity were evaluated.

Content and presentation validity:

Expert consultancy. Out of 35 possible experts examined 10 of them were selected, using the preference qualymetric method, based on the determination of the expert's competence and their willingness to cooperate with this study. Based on the K coefficient, the expert's self-evaluation of the study was used to obtain scores between 0.7 and 1.

Calculation of K coefficient: K= ½ (Kc + ka) for 35 possible experts.

Where Kc is the expert's knowledge or information coefficient about risk factors for hypertensive cardiopathy, calculated based on the expert's awareness in a scale from 0 (total unawareness) to 10 (maximum awareness) and then it is multiplied by 0.1.

And Ka is the argumentation or elaboration coefficient of the criteria determined as a result of the addition of the points obtained in a table.

Calculations were made for each case to obtain each expert's argumentation coefficient, and the 10 experts with the highest competence were chosen. All of them ranged from 0.8 to 1 point, which suggested that their competence levels ranged from medium to high. The remaining 25 candidates whose competence level was lower than 0.8 were excluded. Each expert was consulted individually and anonymously using a guide created for this purpose.

Out of the 10 experts used: five of them were first and second-degree specialists in Internal Medicine. The test was performed by doctors of medical sciences and full professors and researchers with 15 to 25 years of experience in health care, teaching and research.

The experts have consulted anonymously based on their knowledge and experience in HTN. The experts expressed their opinions about the degree of accomplishment of the five basic properties that should be met by indexes[16]. Each expert was given an information gathering form to be filled in accompanied by a written explanation of the meaning of the aspects they were expected to evaluate.

The experts stated their opinions about the degree accomplishment of each element according to 3 possibilities: nothing, moderately or very much. The aspects of being evaluated were: understanding of the different items to be assessed concerning the phenomenon to be measured, whether an index can be derived that distinguishes the different prognostic categories if the presence of each item in the instrument is justified[16].

Construction validity: to evaluate this indicator, it was taken into account that the greatest morbidity corresponded to patients classified in the highest risk categories. The association between the ordinal index and the risk of developing grade IV hypertensive cardiopathy was evaluated based on calculating the coefficient of association for ordinal and nominal variables, Eta. The comparison of the average index values among patients with grade IV hypertensive cardiopathy and without it was determined using the Student's t-test for independent samples.

Index discrimination capacity and calibration

Data analysis permitted to obtain of the data for the construction of the ROC (*Receiver Operating Characteristics*) curve and to determine the index discriminative capacity. A value under the area of the ROC curve greater or equal to 0.7 indicates good discrimination capacity[17,18].

Calibration was also estimated employing the Hosmer and Lemeshow test, with a contrast of 10 cutpoints among the observed and expected results. A test value greater than 0.05 means a good calibration.

Accuracy and exhaustiveness determination

Accuracy was calculated to estimate if the positive predictions obtained with the index were correct; also, exhaustiveness was determined to identify whether any bias was present in positive or negative values. High values in both measurements guarantee that the model does not introduce any bias toward positive or negative classes, respectively.

The Gine index was used as a complement to determine the index score differences between the patients with a bad prognosis (evolution to hypertensive cardiopathy with depressed systolic function) and those with favorable evolution.

The Kolmogorov-Smirnov test was used to contrast

whether the observations would reasonably result from the specified distribution.

Internal reliability and consistency

It was obtained by determining the Agreement among ten doctors who acted as "judges" and applied the instrument separately to the forms used for the validation sample. The low correlation coefficients for all the possible pairs of judges were obtained. The association between the index categories and the probability of developing hypertensive heart disease was determined by the Kappa coefficient by more than two judges and the Kappa coefficients for each level. Statistical significance was calculated by categories for global Kappa and for each individual Kappa.

The reliability coefficients R and R^2 were also determined to know how much of the total variation was due to the patients. Finally, the general Cronbach's alpha coefficient and the standardized alpha were used to evaluate internal consistency.

Ethical considerations

In the present study, the fundamental ethical principles of clinical and epidemiological research processes for observational studies were met. The Board of Directors and the Ethics Committee of the hospital gave their approval for the study. Potentially eligible patients were informed about the study, and their written consent was obtained. They were also guaranteed that their personal identity and data would not be disclosed. The patients also received appropriate treatment for their condition during the time that the study lasted. None of the patients declined to participate in the study.

Statistical processing was done using the Windows SPSS (version 25.0) computer software.,

Results

The index was validated in 1000 patients from a 14-year follow-up cohort. Its baseline characteristics are shown in Table 1.

Table 2 shows the comparison between both samples (development[8] and validation) and no significant differences were found.

The index was constructed through a variable selection process and their punctuation, based on the results obtained from Cox's proportional regression (data published in the Mewade Journal)8. For this purpose, the HR values approximated to whole numbers were used (Table 3).

Table 4 shows the index with each of the items and their weighing-out. It also presents the four risk categories, showing high morbidity in categories III and IV. This fact should be highlighted since it indicates that the index permits a good classification of the patients with the worst prognosis¸ so much so that out of the patients classified in category IV, 86.66% developed hypertensive cardiopathy with depressed systolic function.

The average values of the proposed index were significantly higher (p= 0.000) in patients who developed hypertensive cardiopathy with depressed systolic function (mean: 11.05) than those who did not (mean: 4. 61).

The internal index validation is represented in Table 5. The optimal cutpoint was seven (sensitivity: 92.2 {CI: 88.94 to 95.42}; specificity: 86.7 {CI: 81.67 to 87.17}; validity index de 86.7 {CI: 84.55 to 88.85}). However, cutpoint 10 was the one that showed the best positive plausibility rate, which means that the probability of a patient classified as high risk to develop hypertensive cardiopathy with depressed systolic function is 30 times greater than in patients classified with lower risk. The Youden index shows that the test output is adequate, where the optimal cutpoint was 7 (Youden index: 0.77; CI: 0.73 to 0.81).

External validation

The index components were submitted to the specialists' consideration for the analysis of presentation and content validity. It stands out that 90% stated that the content was derivative from the obtainable data and that the components had been clearly defined. 80% of them agreed that the index items were utterly justifiable.

The construction validity (Table 6) was demonstrated by the Eta coefficient value (0.720). 96.58% of the patients with hypertensive cardiopathy with depressed systolic function were classified in categories III and IV.

Figure 2 shows that the index discriminating capacity was excellent, with an area under the ROC curve of 0.954.

Table 7 shows that the index has an adequate calibration (Hosmer and Lemeshow: X^2= 3.485; p= 0.900) where there was a matching relationship between observed and expected cases in all risk levels.

The index accuracy was evaluated in Figure 3; for cutpoint 7, accuracy was 0.711 and an exhaustivity of 0.922. The Gini index was 0.908, showing the index score differences (high) between the patients with bad prognosis (evolution to cardiopathy with depressed systolic function) and those with favorable development. The Kolmogorov-Smirnov test (0.766) demonstrated that the observations could reasonably come from the specified distribution.

The reliability coefficient (R) value showed that the major part of the index variation was significantly due to the patients (R= 0.903; p=0.000). Correlation coefficients for all pairs of observers were 0.949 or higher and statistically significant (p: 0.000). Agreement was demonstrated in the 10 pairs of "judges" for all the categories (all of them over 0), the global kappa coefficient was 0.979 (p: 0.001).

The Cronbach's alpha coefficient to evaluate internal consistency was adequate (0.811). None of the items had values under 0.35, which shows that the index items measure what is intended to be reckoned with them.

Finally, the determination coefficients (R^2) were also calculated as part of this process. As seen in Table 8, there was an excellent correlation between each item and the rest.

Discussion

Hypertensive cardiopathy is one of the lesions to target organs caused by arterial hypertension with high morbidity and mortality; hence, a correct stratification of its prognosis is significant but, at the same time, a complex task.

As a matter of fact, in the natural evolution of hypertensive cardiopathy, some changes range from a standard or lightly depressed ejection fraction to a cardiac insufficiency with reduced ejection fraction, and it is precisely this evolutionary change the that renders the worst prognosis in comparison with patients who remain stable[19].

In the same way, it is a fact that the population aging, the increase of life expectancy and the increment in the prevalence of comorbidities will boost the number of hospitali-

Qualitative variables	Categories	Number	Percent
No control of HTN	Yes	409	40.9
	No	591	59.1
Stage 2 HTN	Yes	410	41.0
	No	590	59.0
Diabetes mellitus	Yes	44	4.4
	No	956	95.6
Chronic renal disease	Yes	218	21.8
	No	782	78.2
Microalbuminuria	Yes	637	63.7
	No	363	36.3
Smoking habit	Yes	424	42.4
	No	576	57.6
Obesity	Yes	627	62.7
	No	373	37.3
Quantitative variables	**Mean**		**Standard deviation**
Time of evolution of HTN ≥ 15 years	17,49		7.92
C-reactive protein > 4mg/L	4,16		1.88
Glycemia > 5 mmol/L	4,70		1.02
Cholesterol/HDL > 4 mmol/L	4,07		3.35
Cholesterol > 4.8 mmol/L	4,74		1.15
Age over 60 years	58,05		12.05
Pulse pressure >60mmHg	43,77		15.84

Table 1. Sample characterization. Baseline values.

zations by cardiac insufficiency in the future, perhaps up to 50% in the next 25 years[19-21].

For that reason, it is necessary to have tools available that permit to estimate the prognosis of patients with this frequent condition in an objective manner; so with this purpose in mind, the present authors designed an index taking as a point of departure the results previously obtained in a model derived from a Cox's proportional regression[8], which contains 14 items that fitted the context where the studied was done and responded to a probabilistic need of morbidity in vulnerable populations.

The index items and their weighing out are entirely justified from the physiopathological, clinical and practical points of view, as it is evidenced by different studies[6-9,19,21-25].

An index based on a cohort has never been used to predict the evolutionary changes of hypertensive cardiopathy from diastolic dysfunction to cardiac insufficiency with a reduced fraction ejection.

In this sense, it should be emphasized that although there are tools available to estimate the risk of dying for patients with acute or chronic cardiac insufficiency[24-27], it does not seem advisable to use them to predict the evolution of hypertensive cardiopathy; because even though it shares several prognostic factors, in the present study were evaluated the effects *per se* of HTN and associated factors which are partially responsible for the structural and functional changes of the myocardium present in the hypertensive patient[4,8].

Qualitative variables	Development		Validation		p
	Number	%	Number	%	
No control of HTN	479	53.9	409	46.1	0.710
Stage 2 HTN	475	53.7	410	46.3	0.563
Diabetes mellitus	48	52.7	44	47.3	0.569
Chronic renal disease	245	52.9	218	47.1	0.299
Microalbuminuria	421	53.7	363	46.3	0.613
Smoking habit	510	54.6	424	45.4	0.882
Obesity	444	54.3	373	45.7	0.956
Quantitative variables	**Mean**	**SD**	**Mean**	**SD**	**p**
Time of evolution of HTN ≥ 15 years	17.07	7.80	17.49	7.92	0.215
C-reactive protein > 4mg/L	4.13	1.86	4.16	1.88	0.706
Glycemia > 5 mmol/L	4.69	1.01	4.70	1.02	0.834
Cholesterol/HDL > 4 mmol/L	3.97	3.18	4.07	3.35	0.491
Cholesterol > 4.8 mmol/L	4.72	1.16	4.74	1.15	0.675
Age over 60 years	57.85	12.08	58.05	12.05	0.693
Pulse pressure >60mmHg	48.22	17.86	43.77	15.84	0.000

Table 2. Comparison of developing samples and index validation.

The construction stage showed that the proposed could adequately predict the evolutionary changes of hypertensive cardiopathy; the worst index's major punctuation will be the prognosis. This aspect is entirely justified by the physiopathologic importance of each item in greater risk[8,19,21-26].

The construction stage showed that the proposed index's high negative predictive values in each cutpoint indicate that the index ice is unlikely to be classified as low-risk individuals with the worst prognosis. The present study suggests that patients must be classified as high risk from the seven points obtained in the index since the evolution to grade IV hypertensive cardiopathy is very likely. Therefore in these patients, it is paramount to act timely to control or minimize the effects of the factors of the dire prognosis.

For the presentation and content validity, an extensive literature review was carried out, and it was corroborated that the factors considered in the present study are used to predict the evolution of cardiovascular diseases and others are considered important markers of risk of dying1,7-11,13-15 nowadays.

This process may be challenging to evaluate, but clearly defined variables were selected for the index, and experienced professionals in the field were used. It was taken into account that an expert in the topic may point out a relationship between what the study mastery represents for him and the items contained in the indicator[16]. The result of this study was considered adequate.

In addition, there is a strong relationship between the worst prognosis and the categories of the proposed index, as demonstrated by the values of the Eta coefficient (worst prognosis in the patients classified in categories III and IV); although they do not reflect the exact value of the prognosis, they are considered acceptable, easy to use and reproduce; in addition, the variables and their selected values are reasonable and are based on the pathogenic importance of each of the factors quoted in the literature[2-4,7-9,19-24].

The index discriminative capacity and its calibration show that a tool could identify patients with the worst prognosis better than chance. Undoubtedly, the index can assign the correct result to a couple of subjects selected at random; that is, it permits the classification of the issues in the context of appraisal criterion with binary prediction. In this sense, it should be emphasized that the results mentioned above have a pathogenic base centered on the factors that point to the worst prognosis[8,19,22-25].

The proposed index also disclosed adequate accuracy and exhaustivity since it was shown that the patients with the worst prognosis always had higher scores. The results of this study have discarded the existence of a significant error in the classification of patients that would suggest avoiding its use in medical practice.

The correlation coefficients obtained with the Agreement between judges and the kappa coefficient were adequate according to the literature[28-30]. They reveal that after

Variables	B	Standard error	P value	HR	Confidence interval 95%	
					Inferior	Superior
No control of HTN	0.737	0.109	0.000	2.090	1.688	2.588
Stage 2 HTN	0.686	0.115	0.000	1.987	1.584	2.491
Diabetes mellitus	0.562	0.194	0.004	1.755	1.201	2.565
Chronic renal disease	0.520	0.112	0.000	1.682	1.350	2.096
Microalbuminuria	0.485	0.105	0.000	1.623	1.321	1.996
Time of evolution of HTN ≥ 15 years	0.399	0.104	0.000	1.491	1.216	1.827
C-reactive protein > 4mg/L	0.285	0.104	0.006	1.330	1.084	1.632
Pulse pressure >60mmHg	0.278	0.106	0.008	1.321	1.074	1.625
Smoking habit	0.238	0.029	0.000	1.268	1.199	1.342
Glycemia> 5 mmol/L	0.128	0.047	0.007	1.136	1.035	1.246
Cholesterol/HDL > 4 mmol/L	0.123	0.040	0.002	1.131	1.046	1.222
Cholesterol> 4.8 mmol/L	0.065	0.014	0.000	1.067	1.039	1.096
Age over 60 years	0.057	0.006	0.000	1.059	1.047	1.071
Obesity	0.012	0.005	0.026	1.012	1.001	1.022

β: model estimated coefficient, which expresses the probability of acquiring the condition.
HR: hazard rate. HTN: arterial hypertension. mmHg: millimeters of mercury. mg/L: milligram per liter. mmol/L: millimol per liter.
***Source**: Álvarez-Aliaga A, Frómeta-Guerra A, Suárez-Quesada A, del Llano-Sosa D, Berdú-Saumell J, Lago-Santiesteban YA. A prognostic model of the adaptive changes from hypertensive cardiopathy: from mild diastolic dysfunction to depressed systolic function. Medwave2020;20(3):e7873.*

Table 3. Results of the application of Cox's proportional multivariate model.

a short training period, the doctors assisting patients with hypertensive cardiopathy can use the index to predict the evolutionary changes of hypertensive cardiopathy with minimum error. It is essential to point out that these coefficients are very high for categories III and IV, which is very relevant because these patients are precisely the ones who need a better classification.

The internal consistency of the index was shown with the value reached by Cronbach's Alpha coefficient (according to different studies[31-33]). Each of the items used in the index measures what is really intended to be measured by them; that is, they can be used to predict the evolutionary changes of hypertensive cardiopathy with mild diastolic dysfunction to depressed systolic function.

The elements of statistical reference of the proposed index have proved to have a high predictive capacity based on their good discrimination and calibration, as well as their internal consistency, showing feasibility and safety for its use in medical practice.

The proposed index uses variables that are available in doctors' offices, and this makes possible its application in the management of hypertensive patients. In addition, it can be used quickly and economically and provides risk categories with an acceptable performance that can impact decision-making and the patient's final clinical result.

It should be insisted that the estimation of the prognosis of hypertensive cardiopathy is complex. Despite the new treatments, many patients end up with terminal cardiopathy. Therefore, we must use tools like the one we are proposing to objectively evaluate the medical care provided to hypertensive patients in general and hypertensive cardiopathy patients in particular.

Conclusions

In short, with the present study, we propose an index to predict the evolutionary changes of hypertensive cardio-

Items	Weighing out	
	Present	Absent
No control of HTN	2	0
Stage 2 HTN	2	0
Diabetes mellitus	2	0
Chronic renal disease	2	0
Microalbuminuria	2	0
Time of evolution of HTN ≥ 15 years	1	0
C-reactive protein > 4mg/L	1	0
Pulse pressure>60mmHg	1	0
Smoking habit	1	0
Glycemia> 5 mmol/L	1	0
Cholesterol/HDL > 4 mmol/L	1	0
Cholesterol> 4.8 mmol/L	1	0
Age over 60 years	1	0
Obesity	1	0
Total	19	0
Risk categories	Patients	Morbidity
Category I: low risk (0- 3 points)	273	0
Category II: moderate risk (4-6 points)	278	3.59%
Category III: high risk (7-9 points)	209	36.36%
Category IV: very high risk (10 -19 points)	240	86.66%
Total of patients	1000	29.4%

Table 4. Prognostic index of hypertensive cardiopathy evolutionary changes: diastolic dysfunction to depressed systolic function.

Cutpoints	Se	S	VI	PPV	NPV	PVR	NPR	HR	CI at 95%	p
7	92.2	84.4	86.7	71.1	96.3	5.9	0.1	19.1	12.7-28.7	0.000
8	84.3	90.9	89.0	79.4	93.3	9.3	0.2	11.8	8.9-15.8	0.000
9	70.7	95.5	88.2	86.7	88.7	15.6	0.3	7.6	6.2-9.4	0.000
10	56.8	98.2	86.0	92.8	84.5	30.8	0.4	5.9	5.1-7.1	0.000

Se: sensitivity; S: specificity; VI: validity index; PPV: Positive Predictive Value; NPV: Negative Predictive Value; PVR: Positive Plausibility Rate; NPR: Negative Plausibility Rate

Table 5. Cutpoints of the prognostic index of hypertensive cardiopathy evolutionary changes: diastolic dysfunction to depressed systolic function. Internal validity.

pathy with mild diastolic dysfunction to cardiac insufficiency with reduced ejection fraction Based on previous research[8]. The adequate predictive capacity, calibration, accuracy and reliability suggest that the index can be used as a clinical and epidemiological surveillance instrument by identifying the subjects with the worst prognosis.

Novelty and limitations

The novelty resides in the fact that the proposed index is unique. It does not improve or perfect any existing index on cardiac insufficiency. It personalizes the patient's evaluation and involves only one cardiovascular event (hypertensive cardiopathy). It is not one more general model than the different ones previously published.

Its limitation, however, is that its application in managing hypertensive patients will depend on the doctors' skills to make good use of it.

Interest conflict statement

The authors deny any conflict of interest.

Funding

The authors claim that there were no external funding sources

Index Categories		Hypertensive Cardiopathy				Total
		Sí	%	No	%	
I	Low risk (0-3)	0	0	273	100	273
II	Moderate risk (4-6)	10	3.6	268	96.4	278
III	High risk (7-9)	76	36.4	133	63.6	209
IV	Very high risk (10-19)	208	86.7	32	13.3	240
Total		294	29.4	706	70.6	1000
Eta: 0.720						

Table 6. Relationship between the index categories and the risk of hypertensive cardiopathy and depressed systolic function.

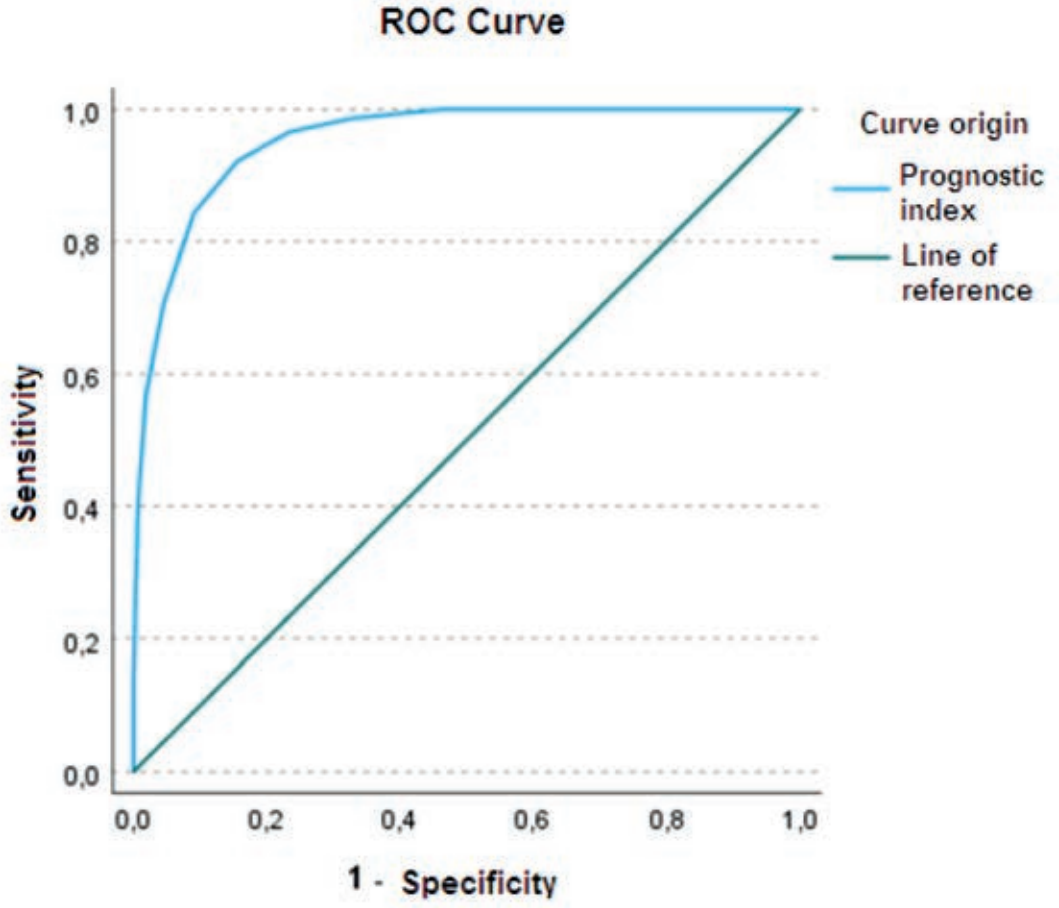

Area under the ROC curve

Area	Dev. Error	p	95% asymptotic confidence interval	
			Inferior limit	Superior limit
0.954	0.006	0.000	0.942	0.966

Figure 2. Prognostic index of hypertensive cardiopathy evolutionary changes: diastolic dysfunction to depressed systolic function. Evaluation of the index discriminative capacity.

Steps	With hypertensive cardiopathy		Without hypertensive cardiopathy		Total
	Observed	Expected	Observed	Expected	
1	0	0.29	158	157.70	158
2	0	0.71	115	114.28	115
3	0	1.55	107	105.44	107
4	4	3.31	94	94.68	98
5	6	5.59	67	67.40	73
6	13	11.17	55	56.82	68
7	23	21.94	46	47.05	69
8	81	81.23	51	50.77	132
9	89	89.58	11	10.41	100
10	78	78.58	2	1.41	80

Table 7. Prognostic index of hypertensive cardiopathy evolutionary changes: diastolic dysfunction to depressed systolic function. Calibration.

Dependent variables	R	R^2	R^2 Adjusted	F	p
No control of HTN	0.335	0.112	0.102	11.454	0.000
Stage 2 HTN	0.330	0.109	0.099	11.079	0.000
Diabetes mellitus	0.204	0.042	0.031	3.961	0.000
Chronic renal disease	0.314	0.099	0.089	9.919	0.000
Microalbuminuria	0.274	0.075	0.065	7.392	0.000
Time of evolution of HTN ≥ 15 years	0.261	0.068	0.058	6.658	0.000
C-reactive protein > 4mg/L	0.427	0.182	0.173	20.208	0.000
Pulse pressure>60mmHg	0.211	0.045	0.034	4.231	0.000
Smoking habit	0.261	0.068	0.058	6.657	0.000
Glycemia > 5 mmol/L	0.324	0.105	0.095	10.673	0.000
Cholesterol/HDL > 4 mmol/L	0.388	0.151	0.141	16.125	0.000
Cholesterol > 4.8 mmol/L	0.400	0.160	0.151	17.317	0.000
Age over 60 years	0.207	0.043	0.032	4.066	0.000
Obesity	0.258	0.469	0.056	6.485	0.000

Table 8. Elements of internal consistency for the simple index through correlation and determination coefficients.

Acknowledgments

The authors acknowledge the invaluable contributions of the Clinical Laboratory and the Imaging and Cardiology Departments.

Claimer

The authors state the availability of data delivery upon request of the editorial committee.

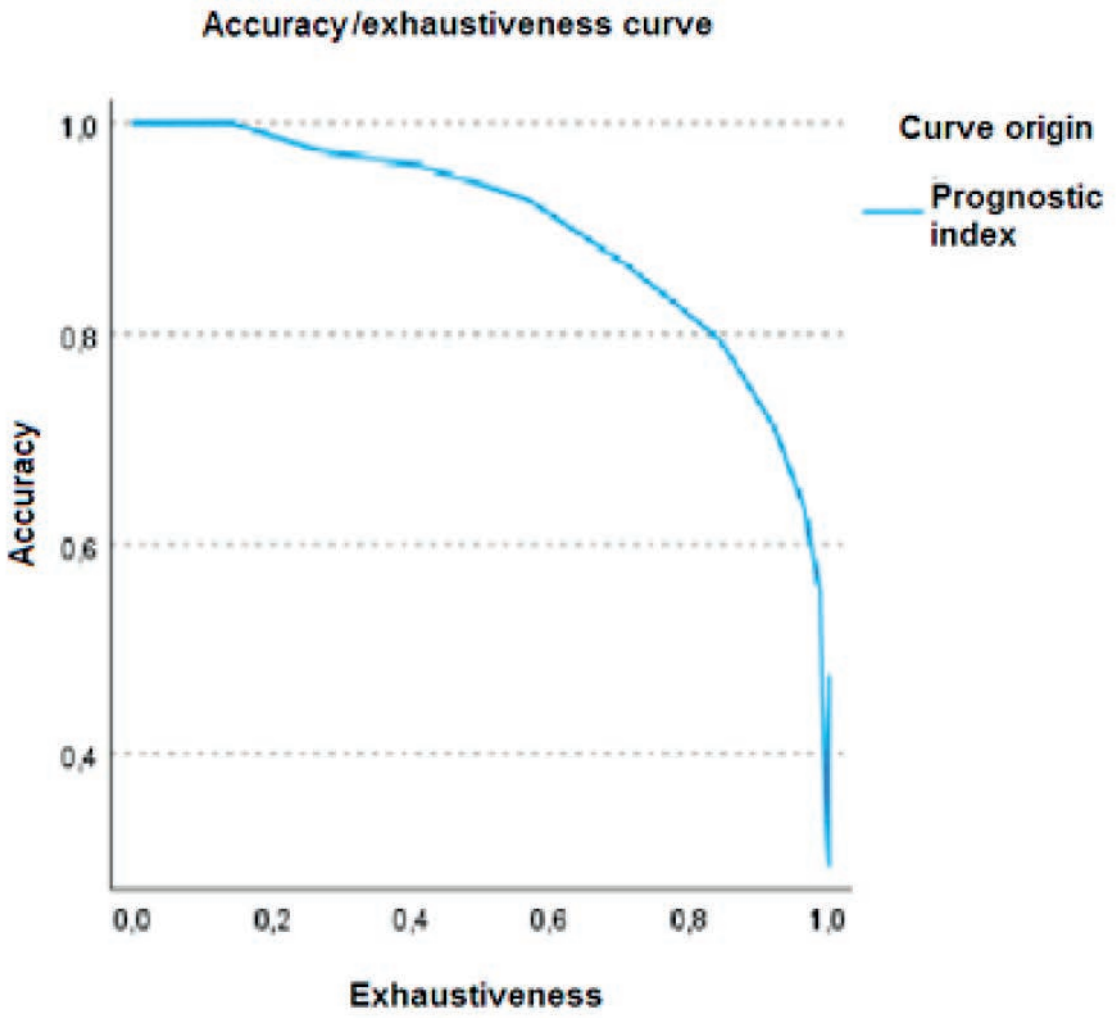

Classifier evaluation metrics		
Gini Index	K-S statistics	
	Max K-S[a]	Cut
0.908	0.766	7.000
a. Maximum.Kolmogorov-Smirnov (K-S) metric		

Figure 3. Prognostic index of hypertensive cardiopathy evolutionary changes: diastolic dysfunction to depressed systolic function. Evaluation of the index accuracy.

Bibliographic references

1. Chobanian AV, Bakris GL, Black HR, Cushman WC, Green LA, Izzo JL Jr, et al; Joint National Committee on Prevention, Detection, Evaluation, and Treatment of High Blood Pressure. National Heart, Lung, and Blood Institute; National High Blood Pressure Education Program Coordinating Committee. Seventh report of the Joint National Committee on Prevention, Detection, Evaluation, and Treatment of High Blood Pressure. Hypertension. 2003 Dec;42(6):1206-52. doi: 10.1161/01.HYP.0000107251.49515.c2. Epub 2003 Dec 1. PMID: 14656957.
2. Lewington S, Clarke R, Qizilbash N, Peto R, Collins R; Prospective Studies Collaboration. Age-specific relevance of usual blood pressure to vascular mortality: a meta-analysis of individual data for one million adults in 61 prospective studies. Lancet. 2002 Dec 14;360(9349):1903-13. doi: 10.1016/s0140-6736(02)11911-8.
3. Ettehad D, Emdin CA, Kiran A, Anderson SG, Callender T, Emberson J, Chalmers J, Rodgers A, Rahimi K. Blood pressure lowering for prevention of cardiovascular disease and death: a systematic review and meta-analysis. Lancet. 2016 Mar 5;387(10022):957-967. doi: 10.1016/S0140-6736(15)01225-8. Epub 2015 Dec 24. PMID: 26724178.

4. Díez J, Frohlich ED. A translational approach to hypertensive heart disease. Hypertension. 2010 Jan;55(1):1-8. doi: 10.1161/HYPERTENSIONAHA.109.141887. Epub 2009 Nov 23. PMID: 19933923.
5. Álvarez-Aliaga A, Quesada-Vázquez AJ, Suárez-Quesada A, del Llano Sosa D. Design and validation of an Index to predict the development of Hypertensive cardiopathy. J Cardiol Cardiovasc Med. 2018; 3:008-022. https://doi.org/10.29328/journal.jccm.1001022.
6. Heidenreich PA, Bozkurt B, Aguilar D, Allen LA, Byun JJ, Colvin MM, et al. 2022 AHA/ACC/HFSA Guideline for the Management of Heart Failure: A Report of the American College of Cardiology/American Heart Association Joint Committee on Clinical Practice Guidelines. J Am Coll Cardiol. 2022 May 3;79(17):e263-e421. doi: 10.1016/j.jacc.2021.12.012. Epub 2022 Apr 1. PMID: 35379503.
7. Visseren FL, Mach F, Smulders YM, Carballo D, Koskinas KC, Bäck M, et al. Guía ESC 2021 sobre la prevención de la enfermedad cardiovascular en la práctica clínica: Con la contribución especial de la European Association of Preventive Cardiology (EAPC). Rev Esp de Cardiología. 2022; 75(5):429.e1-429.e104. https://doi.org/10.1016/j.recesp.2021.10.016
8. Álvarez-Aliaga A, Frómeta-Guerra A, Suárez-Quesada A, del Llano-Sosa D, Berdú-Saumell J, Lago-Santiesteban YA. Prognostic model of the adaptive changes from hypertensive cardiopathy: from mild diastolic dysfunction to depressed systolic function. Medwave2020;20(3):e7873. Doi 10.5867/medwave.2020.03.7873.
9. Williams B, Mancia G, Spiering W, Agabiti Rosei E, Azizi M, Burnier M, et al; ESC Scientific Document Group. 2018 ESC/ESH Guidelines for the management of arterial hypertension. Eur Heart J. 2018 Sep 1;39(33):3021-3104. doi: 10.1093/eurheartj/ehy339.
10. Lang RM, Bierig M, Devereux RB, Flachskampf FA, Foster E, Pellikka PA, Picard MH, Roman MJ, Seward J, Shanewise JS, Solomon SD, Spencer KT, Sutton MS, Stewart WJ; Chamber Quantification Writing Group; American Society of Echocardiography's Guidelines and Standards Committee; European Association of Echocardiography. Recommendations for chamber quantification: a report from the American Society of Echocardiography's Guidelines and Standards Committee and the Chamber Quantification Writing Group, developed in conjunction with the European Association of Echocardiography, a branch of the European Society of Cardiology. J Am Soc Echocardiogr. 2005 Dec;18(12):1440-63. doi: 10.1016/j.echo.2005.10.005. PMID: 16376782.
11. Lang RM, Bierig M, Devereux RB, Flachskampf FA, Foster E, Pellikka PA, Picard MH, Roman MJ, Seward J, Shanewise J, Solomon S, Spencer KT, St John Sutton M, Stewart W; American Society of Echocardiography's Nomenclature and Standards Committee; Task Force on Chamber Quantification; American College of Cardiology Echocardiography Committee; American Heart Association; European Association of Echocardiography, European Society of Cardiology. Recommendations for chamber quantification. Eur J Echocardiogr. 2006 Mar;7(2):79-108. doi: 10.1016/j.euje.2005.12.014. Epub 2006 Feb 2. PMID: 16458610.
12. Pérez Caballero MD, Dueñas Herrera A, Alfonso Guerra JP, Vázquez Vigoa A, Navarro Despaigne D, Hernández Cueto M, et al. Hipertensión arterial. Guía para la prevención, diagnóstico y tratamiento. Comisión Nacional Técnica Asesora del Programa de Hipertensión Arterial. La Habana: Editorial Ciencias Médicas; 2008.
13. Zhao W, Hasegawa K, Chen J. The use of food-frequency questionnaires for various purposes in China. Public Health Nutr. 2002 Dec;5(6A):829-33. doi: 10.1079/phn2002374. PMID: 12638592.
14. Levey AS, Eckardt KU, Tsukamoto Y, Levin A, Coresh J, Rossert J, De Zeeuw D, Hostetter TH, Lameire N, Eknoyan G. Definition and classification of chronic kidney disease: a position statement from Kidney Disease: Improving Global Outcomes (KDIGO). Kidney Int. 2005 Jun;67(6):2089-100. doi: 10.1111/j.1523-1755.2005.00365.x. PMID: 15882252.
15. Genuth S, Alberti KG, Bennett P, Buse J, Defronzo R, Kahn R, et al; Expert Committee on the Diagnosis and Classification of Diabetes Mellitus. Follow-up report on the diagnosis of diabetes mellitus. Diabetes Care. 2003 Nov;26(11):3160-7. doi: 10.2337/diacare.26.11.3160. PMID: 14578255.
16. Moriyama IM. Problems in the measurement of health status. En: Sheldon EB, Moore W. eds. Indicators of social change: concepts and measurements. New York: Rusell Sage fundation. 1968: 573-99.
17. Harrell FE Jr, Lee KL, Mark DB. Multivariable prognostic models: issues in developing models, evaluating assumptions and adequacy, and measuring and reducing errors. Stat Med. 1996 Feb 28;15(4):361-87. doi: 10.1002/(SICI)1097-0258(19960229)15:4<361::AID-SIM168>3.0.CO;2-4. PMID: 8668867.
18. Steyerberg EW. Clinical prediction models: a practical approach to development, validation, and updating. Springer; 2009:255-79. https://doi.org/10.1111/j.1751-5823.2009.00085_22.x
19. McDonagh TA, Metra M, Adamo M, Gardner RS, Baumbach A, Böhm M, et al. Guía ESC 2021 sobre el diagnóstico y tratamiento de la insuficiencia cardiaca aguda y crónica. Rev Esp Cardiol. 2022;75(6):523.e1–523.e114. https://doi.org/10.1016/j.recesp.2021.11.027.
20. Savarese G, Lund LH. Global Public Health Burden of Heart Failure. Card Fail Rev. 2017 Apr;3(1):7-11. doi: 10.15420/cfr.2016:25:2. PMID: 28785469; PMCID: PMC5494150.
21. Al-Mohammad A, Mant J, Laramee P, Swain S; Chronic Heart Failure Guideline Development Group. Diagnosis and management of adults with chronic heart failure: summary of updated NICE guidance. BMJ. 2010 Aug 25;341:c4130. doi: 10.1136/bmj.c4130. Erratum in: BMJ. 2018 Sep 26;362:k4080. PMID: 20739363.
22. Gorostidi M, Gijón-Conde T, de la Sierra A, Rodilla E, Rubio E, Vinyoles E, et al. Guía práctica sobre el diagnóstico y tratamiento de la hipertensión arterial en España, 2022. Sociedad Española de Hipertensión - Liga Española para la Lucha contra la Hipertensión Arterial (SEH-LELHA) [2022 Practice guidelines for the management of arterial hypertension of the Spanish Society of Hypertension]. Hipertens Riesgo Vasc. 2022 Oct-Dec;39(4):174-194. Spanish. doi: 10.1016/j.hipert.2022.09.002. Epub 2022 Sep 22. PMID: 36153303.
23. Schulz R, Heusch G. C-reactive protein: just a biomarker of inflammation or a pathophysiological player in myocardial function and morphology? Hypertension. 2011 Feb;57(2):151-3. doi: 10.1161/HYPERTENSIONAHA.110.165837. Epub 2011 Jan 10. PMID: 21220709.
24. Huang Y, Wang HY, Jian W, Yang ZJ, Gui C. Development and validation of a nomogram to predict the risk of death within 1 year in patients with non-ischemic dilated cardiomyopathy: a retrospective cohort study. Sci Rep. 2022 May 20;12(1):8513. doi: 10.1038/s41598-022-12249-7. PMID: 35595787; PMCID: PMC9123170.
25. Selvaraj S, Claggett B, Pozzi A, McMurray JJV, Jhund PS, Packer M, et al. Prognostic Implications of Congestion on Physical Examination Among Contemporary Patients With Heart Failure and Reduced Ejection Fraction: PARADIGM-HF. Circulation. 2019;140(17):1369-1379. doi: 10.1161/CIRCULATIONAHA.119.039920.
26. Simpson J, Jhund PS, Lund LH, Padmanabhan S, Claggett BL, Shen L, et al. Prognostic Models Derived in PARADIGM-HF and Validated in ATMOSPHERE and the Swedish Heart Failure Registry to Predict Mortality and Morbidity in Chronic Heart Failure. JAMA Cardiol. 2020 Apr 1;5(4):432-441. doi: 10.1001/jamacardio.2019.5850.
27. Voors AA, Ouwerkerk W, Zannad F, van Veldhuisen DJ, Samani NJ, Ponikowski P, et al. Development and validation of multivariable models to predict mortality and hospitalization in patients with heart failure. Eur J Heart Fail. 2017;19(5):627-634. doi: 10.1002/ejhf.785.
28. Feinstein AR, Cicchetti DV. High Agreement but low Kappa: I. The problems of two paradoxes. J Clin Epidemiol. 1990;43(6):543-9. doi: 10.1016/0895-4356(90)90158-l. PMID: 2348207.

29. Streiner DL, Norman GR. 'Measuring change', Health Measurement Scales: A practical guide to their development and use , 4th edn (Oxford,2008;online edn,Oxford Academic , Sept 1 2009), https://doi.org/10.1093/acprof:oso/9780199231881.003.0011.
30. Jiménez RE, Vázquez J, Fariñas H. Construcción y validación de un índice de gravedad de la enfermedad para pacientes hospitalizados en áreas clínicas. Gac Sanit [Internet]. 1997 [citado 24 Feb 2009]; 11:122-30. Available at: http://www.elsevier.es/es/revistas/gaceta-sanitaria-138/construccion-validacion-un-indice-gravedad-pacientes-hospitalizados-13141136-articulo-1997.
31. García Cadena CH. La medición en las ciencias sociales y la psicología, en estadística con SPSS y metodología de la investigación de René Landeros Hernández y Mónica T González Ramírez. México, Trillas (comp). 2006.
32. Soler Cárdenas Silvio F. Coeficientes de confiabilidad de instrumentos escritos en el marco de la teoría clásica de los tests. Educ Med Super [Internet]. 2008 Jun [citado 2022 Dic 10] ; 22(2). Available at: http://scielo.sld.cu/scielo.php?script=sci_arttext&pid=S0864-21412008000200006&lng=es.
33. García-Vargas MLE., Martínez Ayala L, Cerón-Reyes MG, Molina-RuizHD. Validez y confiabilidad de un instrumento que permite detectar una revista depredadora. TEPEXI Boletín Científico De La Escuela Superior Tepeji Del Río. 2022;9(18):9-14. https://doi.org/10.29057/estr.v9i18.8744.

ARTICLE / INVESTIGACIÓN

Caracterización de protocolos de ensayos clínicos de productos farmacéuticos radicados para evaluación regulatoria en Colombia: consideraciones bioéticas y metodológicas

Characterization of clinical trial protocols of pharmaceutical products filed for regulatory evaluation in Colombia: bioethical and methodological considerations

Carlos J. Bello-Gándara[1,3]*, Erika Vergara-Cano[2], David Osorio-Gallardo[2], Juanita M. Recalde-Miranda[3]

DOI. 10.21931/RB/2023.08.02.12

[1] Centro de Biociencias SURA, Medellín, Colombia.
[2] Programa de Química Farmacéutica, Universidad Icesi, Cali, Colombia.
[3] Departamento de Ciencias Farmacéuticas, Universidad Icesi, Cali, Colombia.
Corresponding author: carlos.bello@u.icesi.edu.co

Resumen: Los ensayos clínicos son esenciales para la evaluación de la seguridad y eficacia de productos farmacéuticos. Regiones emergentes como Latinoamérica han tenido un aumento en la ejecución de este tipo de estudios, tradicionalmente concentrados en países desarrollados. El propósito de este trabajo fue identificar las principales características con relevancia metodológica y bioética de los protocolos de ensayos clínicos de medicamentos presentados en Colombia ante la agencia regulatoria nacional. Se realizó un estudio observacional descriptivo, con base en el consolidado de los protocolos radicados al INVIMA y la información de EudraCT. Se incluyeron 597 protocolos, en los que se destaca el diseño aleatorizado (83,1%) doble ciego (66,7%), controlados por placebo (57,1%) y grupos paralelos (64,5%). Las enfermedades en investigación más frecuentes fueron neoplasias (22,8%). Se observó una baja representación de poblaciones vulnerables específicas como mujeres embarazadas (0,7%) o sujetos en situación de emergencia (2,4%) y escasas formulaciones especiales para población pediátrica (3,0%). La caracterización evidencia similitudes respecto al contexto regional y sugiere factores relevantes para evaluar y planificar protocolos en centros de investigación clínica.

Palabras clave: Características del estudio, Desarrollo de medicamentos, Investigación farmacéutica, Ensayos clínicos como tema, Protocolos de ensayos clínicos como tema.

Abstract: Clinical trials are essential for the evaluation of safety and efficacy of pharmaceutical products. Emerging regions such as Latin America have had an increase in the execution of this type of study, traditionally concentrated in developed countries. The purpose of this work was to identify the main characteristics with methodological and bioethical relevance of drug clinical trial protocols submitted in Colombia to the national regulatory agency. A descriptive observational study was carried out, based on the consolidation of protocols filed with INVIMA and the information from EudraCT. 597 protocols were included, in which the randomized (83,1%), double-blind (66,7%), placebo-controlled (57,1%), and parallel group (64,5%) design stands out. The most frequent diseases under investigation were neoplasms (22,8%). A low representation of specific vulnerable populations was evidenced, such as pregnant women (0.7%) or subjects in an emergency situation (2.4%) and few special formulations for pediatric population (3.0%). The characterization shows similarities concerning the regional context and suggests relevant factors for evaluating and planning protocols in clinical research centers.

Key words: Study characteristics, Drug development, Pharmaceutical research, Clinical trials as topic, Clinical trial protocols as topic.

Introducción

Los ensayos clínicos constituyen el diseño metodológico fundamental para la evaluación de diversas intervenciones en salud en seres humanos, destinadas principalmente al diagnóstico, profilaxis y tratamiento de diversas patologías[1]. En el desarrollo de nuevos productos farmacéuticos, los ensayos clínicos son esenciales para generar la evidencia requerida acerca de su seguridad y eficacia para sustentar la autorización de comercialización por parte de agencias sanitarias, lo cual conlleva la implementación de protocolos de investigación con diferentes propósitos y atributos[2].

De acuerdo con los lineamientos internacionales, como la guía para las Buenas Prácticas Clínicas de la Conferencia Internacional de Armonización (ICH, por sus siglas en inglés) y la pautas de la Declaración SPIRIT 2013, el protocolo es un elemento que tiene una función clave en la planificación y conducción de los ensayos, por lo que deben contar con unas características estándar que contribuyan a

Citation: Bello-Gándara C J, Vergara-Cano E, Osorio-Gallardo D, Recalde-Miranda J M. Caracterización de protocolos de ensayos clínicos de productos farmacéuticos radicados para evaluación regulatoria en Colombia: consideraciones bioéticas y metodológicas. Revis Bionatura 2023;8 (2) 12. http://dx.doi.org/10.21931/RB/2023.08.02.12
Received: 2 January 2023 / **Accepted:** 19 April 2023 / **Published:** 15 June 2023
Publisher's Note: Bionatura stays neutral with regard to jurisdictional claims in published maps and institutional affiliations.

garantizar la sistematicidad en la ejecución de actividades, la integridad de los datos y la protección de los participantes en la investigación[3,4].

Esta estricta regulación en investigación de medicamentos ha aportado a la calidad de los ensayos clínicos a nivel global, los cuales históricamente se han concentrado principalmente en regiones de altos ingresos como Norteamérica o Europa, dada su capacidad instalada y la ubicación de las principales empresas farmacéuticas[5]. Sin embargo, en las últimas décadas la investigación clínica se ha extendido a otras regiones emergentes como Asia, África y Latinoamérica, debido a condiciones más favorables para el reclutamiento de sujetos y la reducción de costos[6]. Específicamente en Latinoamérica han aumentado progresivamente el número de estudios en países como Chile, Argentina, Perú y Colombia[7-10].

No obstante, debido a los distintos entornos regulatorios, es posible que los ensayos clínicos realizados fuera de los países de altos ingresos presenten diferencias en diseño y realización[5]. Adicionalmente, el acceso a la información sobre las características de los protocolos presenta limitaciones en ciertas regiones, ya que algunos países como Colombia no poseen registros primarios nacionales de ensayos clínicos con los lineamientos internacionales para tal fin, que faciliten la disponibilidad pública a información respecto a sus propiedades principales y conducción[11]. En este aspecto cabe resaltar el desarrollo de la Agencia Europea de Medicamentos (EMA, por sus siglas en inglés), que desde 2004 posee un registro detallado de ensayos clínicos que cumple los estándares estipulados por la Organización Mundial de la Salud (OMS) y se articula con la Plataforma de Registros Internacionales de Ensayos Clínicos[12].

Teniendo en cuenta lo anterior, el presente estudio tuvo como objetivo identificar las principales características metodológicas e implicaciones bioéticas de los ensayos clínicos de medicamentos radicados en Colombia ante la agencia sanitaria nacional INVIMA (Instituto Nacional de Vigilancia de Medicamentos y Alimentos) para su evaluación regulatoria, a través de los datos disponibles por parte de la EMA de estos protocolos.

Materiales y métodos

Se realizó un estudio observacional descriptivo, para lo cual se consultó el listado consolidado de los protocolos de investigación de medicamentos y productos biológicos radicados para evaluación de la autoridad regulatoria sanitaria INVIMA desde el año 2014 hasta enero 2022 (disponible en https://www.invima.gov.co/). La información detallada de las características específicas de los estudios clínicos fue buscada y extraída de la Base de Datos de Ensayos Clínicos de las Autoridades Reguladoras de Medicamentos de la Unión Europea (EudraCT) de la EMA, la cual registra todos los ensayos clínicos de intervención con medicamentos en la Unión Europea a partir del 1 de mayo de 2004 (disponible en https://eudract.ema.europa.eu).

Los ensayos clínicos elegibles para análisis debían contar con número de radicado en el consolidado colombiano y con número EudraCT asignado en el registro europeo. Se excluyeron estudios cuya codificación no permitiera su búsqueda efectiva en EudraCT para consultar su información correspondiente.

Se recolectaron datos agrupados en los siguientes dominios: identificación del estudio, estado regulatorio, características del medicamento en investigación, clasificación sistema órgano (SOC, por sus siglas en inglés) de la enfermedad según la terminología MedDRA de la ICH, características de la metodología experimental y características de la población elegible. Para el análisis descriptivo de las variables cuantitativas se calculó la mediana y rango intercuartílico (RIC) dada su distribución no normal, mientras que las variables cualitativas se abordaron a través de frecuencias absolutas y porcentaje. Los análisis estadísticos se efectuaron en el programa Stata 15 (StataCorp LLC; College Station, Texas, Estados Unidos).

Los datos empleados en este estudio se encuentran disponibles públicamente por parte de las agencias regulatorias. No se utilizaron datos de sujetos ni se identificaron individualmente los protocolos o patrocinadores. Por lo tanto, el estudio estuvo exento de revisión por comité de ética en investigación.

Resultados

Se extrajeron 726 estudios clínicos a partir del consolidado de protocolos de investigación con medicamentos y productos biológicos radicados para evaluación regulatoria. Se excluyeron 129 estudios clínicos, de los cuales 121 no se tenían registro EudraCT y 8 presentaban un número de registro EudraCT no rastreable. En total, se incluyeron para análisis 597 ensayos clínicos conformados por 528 aprobados (88,4%), 15 requeridos (2,5%), 30 en desistimiento (5,0%), 7 en evaluación (1,2%), 11 negados (1,8%) y 6 en declaración de abandono (1,0%).

Respecto a la clasificación de las enfermedades en investigación, las más frecuentes fueron las neoplasias benignas, malignas y no especificadas (n=136, 22,8%) seguido de los trastornos musculoesqueléticos y del tejido conjuntivo (n=80, 13,4%) y las infecciones e infestaciones (n=77, 12,9%), Además, se observó que 14,9% (n=89) corresponden a enfermedades raras (Tabla 1).

Así mismo, se encontró que entre las formas farmacéuticas de los medicamentos en investigación predominan las soluciones para inyección/infusión (n=210, 35,2%), seguido de las tabletas (n=181, 30,3%) y las cápsulas (n=58, 9,7%). Por otra parte, se observó una alta proporción de ingredientes farmacéuticos activos (IFA) de síntesis química (n= 326, 54,6%) seguido de IFA de origen biológico/biotecnológico (n= 269, 45,1%). Se resalta que 9,1% son catalogados como medicamentos huérfanos y 3,0% son formulaciones pediátricas (Tabla 2).

Respecto al diseño de los protocolos de investigación (Tabla 3), la etapa de desarrollo clínico con mayor proporción es la fase III (79,6%). La mayoría de los estudios se caracterizan por ser aleatorizados (83,1%) doble ciego (66,7%), controlados por placebo (57,1%) y de grupos paralelos (64,5%). Un 67,0% incluye dentro de su alcance aspectos de farmacocinética y 25,3% contempla farmacogenética. Es importante enfatizar que 12,4% de los protocolos pertenecen a un plan de investigación pediátrico y 41% tiene resultados publicados en la base de datos. Adicionalmente, se estableció que la mediana del número de brazos de tratamiento en los estudios es 2 (RIC: 2-3) y tienen de 3 años (RIC: 2-5) de duración total, buscando reclutar una mediana de 580 sujetos (RIC: 252-1022) para la muestra total por protocolo, con variaciones de acuerdo con el grupo etario.

En las características de la población elegible, se evi-

Clasificación sistema órgano (SOC) MedDRA	n (%)
Exploraciones complementarias	1 (0,2)
Infecciones e infestaciones	77 (12,9)
Neoplasias benignas, malignas y no especificadas (incl. quistes y pólipos)	136 (22,8)
Procedimientos médicos y quirúrgicos	12 (2,0)
Trastornos cardiacos	18 (3,0)
Trastornos congénitos, familiares y genéticos	31 (5,2)
Trastornos de la piel y del tejido subcutáneo	11 (1,8)
Trastornos de la sangre y del sistema linfático	4 (0,7)
Trastornos del metabolismo y la nutrición	26 (4,4)
Trastornos del sistema inmunológico	4 (0,7)
Trastornos del sistema nervioso	26 (4,4)
Trastornos endocrinos	3 (0,5)
Trastornos gastrointestinales	38 (6,4)
Trastornos generales y alteraciones en el lugar de administración	1 (0,2)
Trastornos hepatobiliares	3 (0,5)
Trastornos musculoesqueléticos y del tejido conjuntivo	80 (13,4)
Trastornos oculares	15 (2,5)
Trastornos psiquiátricos	20 (3,4)
Trastornos renales y urinarios	31 (5,2)
Trastornos respiratorios, torácicos y mediastínicos	50 (8,4)
Trastornos vasculares	10 (1,7)

SOC: *System Organ Class*, por sus siglas en inglés

Tabla 1. Clasificación de las enfermedades en investigación.

denció que 84,8% de los protocolos incluyen participantes de edad adulta, mientras que 25,0% incluyen menores de 18 años. También se observa escasa presencia de las poblaciones vulnerables específicas que se evaluaron, entre las cuales la principal proporción se presenta en sujetos incapaces de dar su consentimiento personalmente (n= 103, 17,3%) (Tabla 4).

Discusión

El presente estudio buscó identificar los principales atributos de los protocolos de ensayos clínicos de medicamentos que se radican ante la agencia sanitaria para su ejecución en Colombia. En primer lugar, se evidencia que las áreas de enfoque para desarrollo de los nuevos esfuerzos terapéuticos presentan estrecha similitud con las tendencias de investigación clínica a nivel regional. Aproximadamente, uno de cada cuatro estudios está relacionado con neoplasias y dicha categoría representa el área con mayor cantidad de estudios, lo cual ratifica el comportamiento reportado previamente para este grupo de patologías[13].

Así mismo, se destacan también las investigaciones en infectología y trastornos musculoesqueléticos, estos últimos principalmente representados por condiciones reumatológicas. Por lo tanto, a nivel general los hallazgos están en línea con lo publicado previamente por otros autores en el contexto latinoamericano para países como Perú, Chile y Argentina[7-9]. Sin embargo, es notable la baja proporción de trastornos endocrinos, respiratorios y cardíacos observada en la muestra de protocolos, lo cual podría indicar una disminución de propensión hacia estas categorías frente a los resultados de Carreño y de Molina et al., en los cuales dichas áreas terapéuticas eran preponderantes en los ensayos clínicos en Colombia[13,14].

Por otra parte, el estudio brinda un acercamiento a las características farmacéuticas de los productos involucrados en los ensayos clínicos. Se observa una amplia diversidad de formas farmacéuticas en las propuestas de investigación, con la principal proporción enfocada en soluciones parenterales y sólidos orales. En este ámbito, los productos parenterales ameritan especial atención por cuanto pueden implicar mayores requerimientos técnicos y logísticos por parte de los actores del proceso de investigación para garantizar el manejo integral del medicamento y la seguridad de los participantes[15].

El estudio también denota el bajo porcentaje en formulaciones específicas para pacientes pediátricos. Esto constituye un indicio del limitado desarrollo de nuevas alternativas desde la fase de investigación para las necesidades especiales de los menores en aspectos como dosificación, administración y biodisponibilidad, implicando que en ciertos contextos de la práctica clínica se empleen formulaciones sin suficiente evidencia de uso en niños o se deba optar por preparaciones extemporáneas para pacientes

Variable	n (%)
Forma farmacéutica	
Aerosol nasal	2 (0,3)
Cápsula	58 (9,7)
Concentrado para solución inyectable	41 (6,9)
Emulsión para inyección	1 (0,2)
Gas medicinal	1 (0,2)
Gel	1 (0,2)
Gotas oftálmicas	3 (0,5)
Implante	3 (0,5)
Jarabe	3 (0,5)
Liofilizado para solución inyectable	8 (1,3)
No disponible	1 (0,2)
Polvo para inhalación	8 (1,3)
Polvo para solución inyectable	42 (7,0)
Polvo para solución oral	1 (0,2)
Polvo para suspensión inyectable	4 (0,7)
Polvo para suspensión oral	2 (0,3)
Sistema de liberación vaginal	1 (0,2)
Solución de nebulización	2 (0,3)
Solución oral	3 (0,5)
Solución para inhalación	3 (0,5)
Solución para inyección/infusión	210 (35,2)
Suspensión oral	1 (0,2)
Suspensión para inhalación	2 (0,3)
Suspensión para inyección	14 (2,3)
Suspensión para nebulizador	1 (0,2)
Tableta	181 (30,3)
Tipo de IFA	
Síntesis química	326 (54,6)
Biológico/biotecnológico	269 (45,1)
Terapia avanzada	2 (0,3)
Vacuna	73 (12,2)
Medicamento huérfano	54 (9,1)
Formulación pediátrica específica	18 (3,0)

IFA: ingrediente farmacéutico activo

Tabla 2. Características de los medicamentos en investigación.

Característica	n (%)
Alcance	
Farmacocinética	400 (67,0)
Farmacodinámica	226 (37,9)
Dosis respuesta	89 (14,8)
Farmacogenética	151 (25,3)
Farmacoeconomía	56 (9,4)
Fase de desarrollo	
I	10 (1,7)
II	123 (20,6)
III	475 (79,6)
IV	30 (5,0)
Control	
Activo	160 (26,9)
Placebo	341 (57,1)
Otro	67 (11,2)
Aleatorización	496 (83,1)
Enmascaramiento	
Abierto	175 (29,3)
Simple ciego	2 (0,3)
Doble ciego	398 (66,7)
Tipo	
Grupos paralelos	385 (64,5)
Grupos cruzados	8 (1,3)
Otro	77 (12,9)
Plan de investigación pediátrico	74 (12,4)
Ensayo contiene un subestudio	140 (23,5)
Comité de monitoreo de datos	461 (77,2)
Resultados publicados	245 (41,0)
Número de brazos de tratamiento [a]	2 (2-3)
Duración total estimada inicial (años) [a]	3 (2-5)
Número total estimado de sujetos [a]	580 (252-1022)
Número estimado de sujetos por edad [a]	
Menores de 18 años	113 (30-274)
Adultos (18-64 años)	411 (190-800)
Ancianos (≥65 años)	151 (50-405)

[a] Mediana (rango intercuartílico)

Tabla 3. Características del diseño de los protocolos de investigación.

Característica	n (%)
Edad	
Menores de 18 años	149 (25,0)
Adultos (18-64 años)	506 (84,8)
Ancianos (≥ 65 años)	477 (79,9)
Sexo	
Masculino	575 (96,3)
Femenino	580 (97,2)
Poblaciones vulnerables específicas	
Mujeres en edad fértil que no utilizan métodos anticonceptivos	16 (2,7)
Mujeres embarazadas	4 (0,7)
Mujeres lactantes	4 (0,7)
Situación de emergencia	14 (2,4)
Sujetos incapaces de dar su consentimiento personalmente	103 (17,3)

Tabla 4. Características de la población elegible en los ensayos clínicos.

individuales[16,17]. Además, la poca presencia de protocolos de terapias avanzadas señala otro campo de investigación con escasa incursión en el país con amplio potencial de crecimiento, lo cual incluye una variedad de abordajes novedosos de medicamentos que involucran terapia celular, terapia génica o ingeniería de tejidos.

Frente al origen del principio activo, se observa una paridad entre estudios con compuestos de síntesis química y aquellos con moléculas complejas de origen biológico o biotecnológico. Lo anterior puede explicarse por el fuerte enfoque global de la industria farmacéutica en éstos últimos, ya que representan un importante enfoque de investigación y desarrollo por sus diversas ventajas y aplicaciones terapéuticas en diferentes patologías[18].

Al indagar las características del diseño metodológico de los ensayos clínicos, es posible evidenciar que en Colombia predominan ampliamente los protocolos de fase III aleatorizados, de dos grupos paralelos, doble ciego y controlados con placebo, lo cual es propio de los estudios pivotales que sustentan las solicitudes de autorización de nuevos medicamentos ante agencias regulatorias. Esto coincide con los hallazgos previos en Colombia y otros países latinoamericanos, donde dicho perfil era el más común para los estudios[7-10]. Así mismo, el número global de sujetos a enrolar en dichos protocolos es alto, lo que da cuenta que principalmente se radican estudios de confirmación terapéutica por encima de aquellos de fases exploratorias o de prueba de concepto que implican un menor tamaño de muestra.

Adicionalmente, en línea con las tendencias farmacotécnicas mencionadas, son escasos los protocolos que pertenecen formalmente a un plan de investigación pediátrico y se observa que solo un cuarto del total de protocolos contempla la inclusión de menores de 18 años. En dicho grupo etario, la mediana de la meta de enrolamiento fue sustancialmente menor que para otras edades, aspecto ligado a las consideraciones éticas especiales que influyen en el reclutamiento y retención de estos participantes.

Respecto a la población elegible, es destacable la reducida cantidad de estudios que incluyen alguna de poblaciones vulnerables que fueron evaluadas, especialmente aquellos relacionados con mujeres en estado de embarazo y lactantes. Esto refuerza la reflexión planteada por el Foro Global de Bioética en Investigación respecto a las limitaciones para incluir este grupo específico, lo que genera como consecuencia la dificultad que afrontan los profesionales de la salud para encontrar evidencia sobre la eficacia y seguridad de los medicamentos en dicha población[19]. Por lo tanto, resulta necesario promover la investigación farmacéutica que incluya mujeres embarazadas y otras poblaciones sistemáticamente excluidas de los estudios, garantizando las medidas especiales de protección y minimización de riesgos, además de actualizar de manera oportuna los paradigmas éticos y la normatividad asociada[20].

Conclusiones

La perspectiva obtenida a través del registro EudraCT acerca de las características metodológicas de los protocolos de ensayos clínicos de medicamentos en Colombia da cuenta de similitudes respecto a las tendencias del contexto regional latinoamericano, permitiendo identificar que predomina la investigación en neoplasias y estudios de confirmación terapéutica en fase 3 doble ciego controlados con placebo, presentando una gran diversidad de formas farmacéuticas y tipos de IFA respecto a los produc-

tos en investigación. Así mismo, desde el ámbito bioético es pertinente resaltar la escasa inclusión de poblaciones vulnerables específicas en los protocolos junto a la poca investigación de formulaciones pediátricas y medicamentos huérfanos como factores sustanciales que deben optimizarse para mejorar la generación de evidencia clínica de productos farmacéuticos.

Contribuciones de los autores

CJBG y JMRM realizaron la conceptualización, diseño del estudio y gestión de la investigación. CJBG, DOG, EVC fueron responsables de la recolección de datos. CJBG, DOG, EVC y JMRM desarrollaron el análisis e interpretación de datos, así como en la redacción, revisión y aprobación de la versión final del artículo. Todos los autores asumen la responsabilidad por el artículo.

Financiamiento

El estudio fue autofinanciado.

Conflictos de Interés

Los autores declaran no tener conflictos de interés.

Referencias bibliográficas

1. Umscheid CA, Margolis DJ, Grossman CE. Key concepts of clinical trials: A narrative review. Postgrad Med. 2011;123(5):194–204. doi: 10.3810/pgm.2011.09.2475.
2. Fruhner K, Hartmann G, Sudhop T. Analysis of integrated clinical trial protocols in early phases of medicinal product development. Eur J Clin Pharmacol. 2017;73(12):1565–77. doi: 10.1007/s00228-017-2335-y.
3. Chan AW, Tetzlaff JM, Altman DG, Laupacis A, Gøtzsche PC, Krleža-Jeric K, et al. Declaración SPIRIT 2013: definición de los elementos estándares del protocolo de un ensayo clínico. Revista Panamericana de Salud Pública. 2015;38(6):506–14.
4. International Council for Harmonisation of Technical Requirements for Pharmaceuticals for Human Use (ICH). ICH Harmonised Guideline Integrated Addendum to ICH E6(R1): Guideline for Good Clinical Practice E6(R2) [Internet]. 2016 [citado el 26 de mayo de 2022]. Disponible en: https://database.ich.org/sites/default/files/E6_R2_Addendum.pdf
5. Murthy S, Mandl KD, Bourgeois FT. Industry-sponsored clinical research outside high-income countries: An empirical analysis of registered clinical trials from 2006 to 2013. Health Res Policy Syst. 2015;13:28. doi: 10.1186/s12961-015-0019-6.
6. Jeong S, Sohn M, Kim JH, Ko M, Seo H won, Song YK, et al. Current globalization of drug interventional clinical trials: Characteristics and associated factors, 2011-2013. Trials. 2017;18:288. doi: 10.1186/s13063-017-2025-1.
7. Traversi L, Bolaños R. Analysis of clinical drug trials in children compared to clinical drug trials in adults, in Argentina. Arch Argent Pediatr. 2019;117(1):34–40. doi: 0.5546/aap.2019.eng.34.
8. Aguilera B. Trends in clinical trials performed in Chile. Rev Med Chil. 2021;149:110–8. doi: 10.4067/S0034-98872021000100110
9. Minaya G, Fuentes D, Obregón C, Ayala-Quintanilla B, Yagui M. Características de los ensayos clínicos autorizados en el Perú, 1995-2012. Rev Peru Med Exp Salud Publica. 2012;29(4):431–6. doi: 10.17843/rpmesp.2012.294.385.
10. Molina de Salazar DI, Álvarez-Mejía M. Estado de la investigación clínica en Colombia. Acta Médica Colombiana. 2018;43(4):179–82. doi: 10.36104/amc.2018.1374.
11. Lemmens T, Herrera Vacaflor C. Transparencia sobre los ensayos clínicos en la Región de las Américas: necesidad de coordinar las esferas regulatorias. Revista Panamericana de Salud Pública. 2019;43:1–7. doi: 10.26633/rpsp.2019.303.
12. Venugopal N, Saberwal G. A comparative analysis of important public clinical trial registries, and a proposal for an interim ideal one. PLoS One. 2021;16(5):e0251191 doi: 10.1371/journal.pone.0251191.
13. Carreño Dueñas A. Situación de los ensayos clínicos en Colombia. Medicina. 2013;35(2):123–9.
14. Molina de Salazar DI, Botero SM, Giraldo GC. Investigación clínica y ensayos clínicos ¿En qué vamos? Acta Médica Colombiana. 2016;41(3S):43–50.
15. de Camargo Silva AEB, Moreira Reis AM, Inocenti Miasso A, Oliveira Santos J, de Bortoli Cassiani SH. Eventos adversos causados por medicamentos en un hospital centinela del Estado de Goiás, Brasil. Rev Lat Am Enfermagem. 2011;19(2):1–9. doi: 10.1590/S0104-11692011000200021.
16. Sánchez-González E. ¿Qué sabe ud. acerca de formulaciones pediátricas? Revista Mexicana de Ciencias Farmacéuticas. 2015;46(2):68–70.
17. González C. Farmacología del paciente pediátrico. Revista Médica Clínica Las Condes. 2016;27(5):652–9. doi: 10.1016/j.rmclc.2016.09.010.
18. Barrera LA. Desarrollo de medicamentos biotecnológicos. Del laboratorio al paciente. Medicina. 2018;40(1):44–55.
19. Saenz C, Alger J, Beca JP, Belizán JM, Cafferata ML, Arturo J, et al. Un llamado ético a la inclusión de mujeres embarazadas en investigación: Reflexiones del Foro Global de Bioética en Investigación. Revista Panamericana de Salud Pública. 2017;41:e13. doi: 10.26633/RPSP.2017.13.
20. Carracedo S, Palmero A, Neil M, Hasan-Granier A, Saenz C, Reveiz L. El panorama de los ensayos clínicos sobre COVID-19 en América Latina y el Caribe: evaluación y desafíos. Revista Panamericana de Salud Pública. 2021;45:e33. doi: 10.26633/RPSP.2021.33.

REVIEW / ARTÍCULO DE REVISIÓN

An overview of vaccine production against shrimp White Spot Syndrome Virus, effects and the possible impact of this technology in Ecuador

E. D. Proaño[1], L.M Rivera[3] and L. E. Trujillo[1,2]*

DOI. 10.21931/RB/2023.08.02.11

[1] Life Sciences and Agriculture Department, DCVA, Multidisciplinary Laboratory, Universidad de las Fuerzas Armadas – ESPE, Sangolquí, Ecuador.
[2] Industrial Biotechnology and Bioproducts Research Group, Center for Nanoscience and Nanotechnology - CENCINAT, Universidad de las Fuerzas Armadas ESPE, Sangolquí, Ecuador.
[3] Universidad Técnica de Machala, UTEMACH, Machala. Ecuador.
Corresponding author: amaria.henao@udea.edu.co

Abstract: Although aquaculture in Ecuador has a high economic and socio-cultural importance, pathogenic microorganisms affect the development and vitality of crustaceans, fish, and mollusks, reducing their production yields. Among these pathogens, White Spot Syndrome Virus (WSSV) is an invertebrate virus that induces high mortality, generating severe economic losses due to its wide geographical distribution and high infection rate finding the most significant devastation worldwide in the shrimp sector. Although several strategies are described to fight against WSSV, this study points to an updated overview of vaccines used against this virus, including types, effects and large-scale production ways. Thus, this research supplies an analysis of possible treatments based on vaccination to combat the WSSV caused-disease that significantly impacts the aquaculture economy and could be helpful to those working in this field.

Key words: *Whispovirus*, White Spot Syndrome Virus, Shrimp, virus, vaccine, production, Ecuador.

Introduction

In the last 50 years aquaculture industry in Ecuador has become one of the most critical sectors for the domestic economy since more than 40% of Ecuadorian exports are related to this income source[1]. During 2021-2022, shrimp production reached in the country 848,000 MT with a profit of 5323.30 million dollars[2], making the country one of the largest shrimp exporters worldwide. The European Union (EU), Russia, the United States and China are currently the four main destinations for Ecuadorian shrimp exports[3]. However, diverse types of diseases caused by DNA and RNA viruses significantly affect shrimp production. Three types of viruses have been identified that drastically affect farmed shrimps in the country: Infectious Hypodermal and Haematopoietic Necrosis Virus (IHHNV), Taura Syndrome Virus (TSV) and White Spot Syndrome Virus (WSSV)[4,5]. All these three viruses in Ecuador caused significant economic and social losses. The primary example is the appearance of WSSV in 1999, which caused a 50% decrease in production and exports during the first years of the incidence, with the subsequent jobs lost in multiple families[4,6,7].

WSSV can infect many aquatic crustaceans, especially decapods, such as marine brackish and freshwater shrimps, sea crabs, crayfish and lobsters[6]. However, neither does it cause problems for human health or food safety nor affects human shrimp consumption while causing a detrimental effect on shrimp farmers' production[8].

World Organisation for Animal Health (WOAH) included White Spot Syndrome Virus in a list of infectious diseases that are considered to be of national socioeconomic and/or public health significance and whose effects on international trade in animals and animal products are not negligible[6,7].

Several approaches have been used to combat the incidence of infectious diseases, including antivirals, prebiotics, plant extracts-based drugs and antibiotics[9-12]. Although several strategies exist to combat WSSV[13-15], this study provides an up-to-date overview of production, effects and types of vaccines against WSSV in shrimp.

Thus, this research supplies an analysis of potential possible treatments and new tools to fight against this disease that significantly impacts the aquaculture economy, not only in our country.

Shrimp immune system and response to vaccines

The innate immune system is pronounced in shrimps to protect them from external agents and pathogenic microorganisms[16]. Crustaceans are generally known not to have a specific immune system[17], which precludes the use of conventional vaccines to treat pathogens. According to Afsharnasab (2014), crustaceans' immune system comprises three defense mechanisms, all needed to defend themselves, as depicted in Figure 1.

The first is the cuticle and skin's physical and chemical defense system encompassing secretions[18-20]. This system is inefficient in protecting the organism from all pathogens because most crustaceans have an open circulatory system. The second line of defense is the cellular one. In the crustacean's world, these cells are called hemocytes and are composed of hyaline, granular and semi-granular cells. Each of them has a significant role in disease prevention. The last one to mention is the humoral defense[21].

Innate immunity is triggered when pathogens are detected by host proteins, such as antimicrobial, coagulation and pattern recognition proteins, which, in turn, activate humoral or cellular effector mechanisms to destroy invading pathogens[22].

Citation: Proaño E. D., Rivera L.M and Trujillo L. E. An overview of vaccine production against shrimp White Spot Syndrome Virus, effects and the possible impact of this technology in Ecuador. Revis Bionatura 2023;8 (2) 11. http://dx.doi.org/10.21931/RB/2023.08.02.11
Received: 2 January 2023 / **Accepted:** 13 March 2023 / **Published:** 15 June 2023

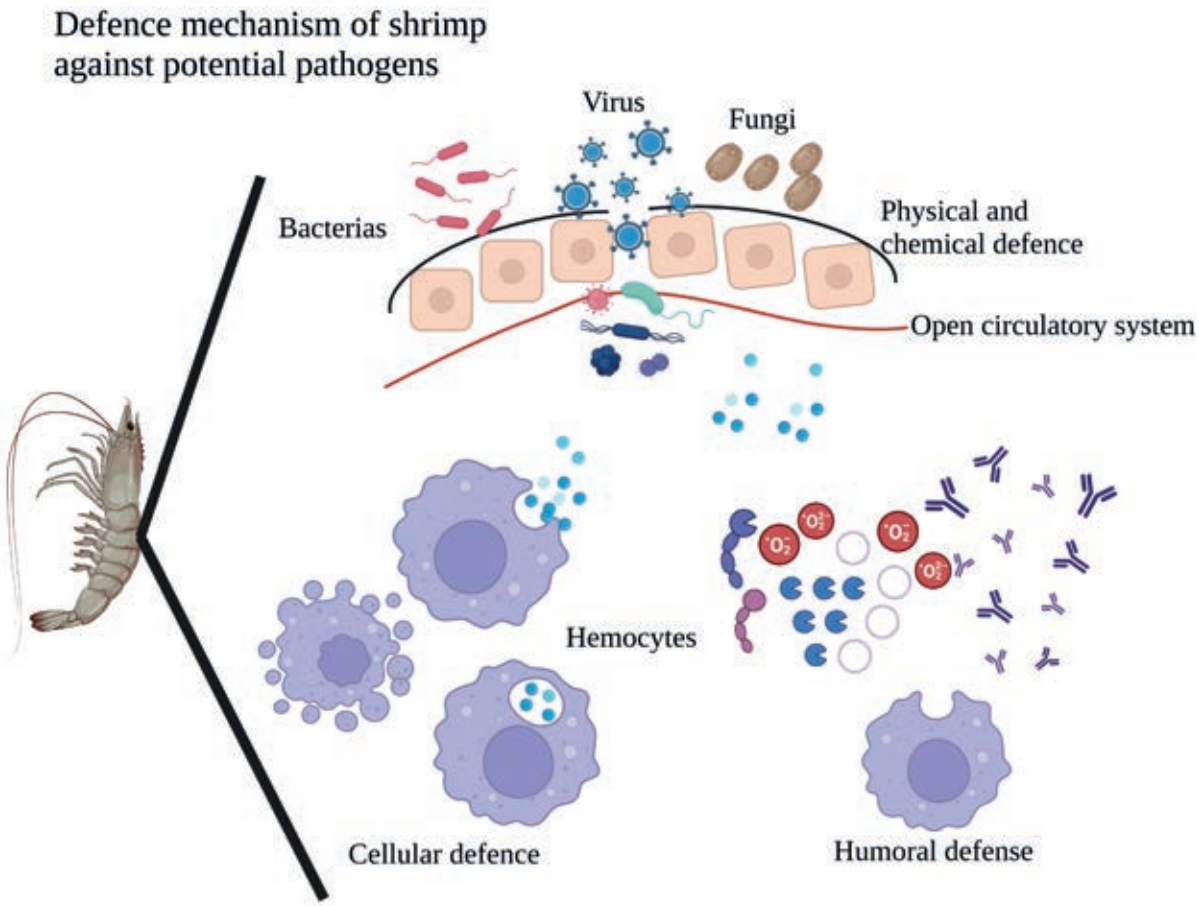

Figure 1. Shrimp defense mechanisms against potential pathogens. The first defense mechanism is the cuticle, and the second consists of cellular defense, including cytotoxicity, coagulation, encapsulation, phagocytosis, melanization, apoptosis and modulation. The third humoral defense mechanism is based in the action of hydrolytic enzymes, agglutinins, coagulation proteins, antimicrobial peptides, oxygen and nitrogen free radicals, and effectors. All three mechanisms act together to eliminate foreign agents[13,17,23,24].

Figure 2 shows the 3D structure of Beta 1,3-Glucan Binding Protein (BGBP) found in plasma, which serves as a protein recognizer in the arthropod immune system[17]. This is in conjunction with the transglutaminase enzyme which is released by hemocytes in the presence of pathogens through receptors[25]. Lectin protein is also represented in the immune system with an antiviral function recognizing WSSV proteins[25,26]. In addition, antimicrobial peptides like Stilicin have antibacterial activity when interacting with the LPS endotoxin of gram-negative and show vigorous activity against filamentous fungi[27].

On the other hand, Alpha 2 macroglobulin, a high molecular mass proteinase, generates opsonization activities against invading pathogens by mediating endocytosis[28]. Penisidins, other essential proteins, are active against Gram-positive bacteria by binding them, causing agglutination, and additionally, in high concentrations, have a good effect against fungi[29]. These are some of the main proteins responsible for humoral immunity[31].

Studies show an alternative memory immune response; however, there are no T cells, B cells or major histocompatibility complex (MHC) molecules[30] in shrimps. Recent experimental data from shrimp and other arthropods have shown that invertebrates own an alternative memory type of immune response. This memory-like peculiarity is called resistant priming[22,31]. With this mechanism, shrimps could improve their defenses after initial pathogenic exposure and then generate better protection after subsequent infections with the same or a different pathogen.

Laboratory tests have shown that vaccinated shrimp and crayfish have improved survival rates following exposure to WSSV[32]. *Penaeus japonicus*, which survived natural and experimental WSSV infections, initially resisted subsequent WSSV exposure. However, these results were not replicated under different conditions - such as temperature, country or type of shrimp[33]. But it is not a treatment that can be applied overnight, mainly because of the unique adaptive immunity of shrimps[34-36].

White spot syndrome virus

Several virus families affect invertebrates; some include DNA viruses[37] such as N*imaviridae, Parvoviridae, Baculoviridae* and *Iridoviridae*[38,39], which has the most significant impact on shrimp farming.

This article focuses on vaccines against the White Spot Syndrome Virus (WSSV), one of the most lethal arthropods viruses worldwide, with a mortality and infectivity rate in shrimp of up to 100%, significantly affecting the larval stage generating large economic losses[4,40].

WSSV is a double-stranded DNA virus with an approximate genome size of 290 to 300 kb, which makes it one of the most complex viruses infecting shrimp[4,40]. Most of its putative translated gene products have no homology with other virus proteins or host cells. Because of this peculiar

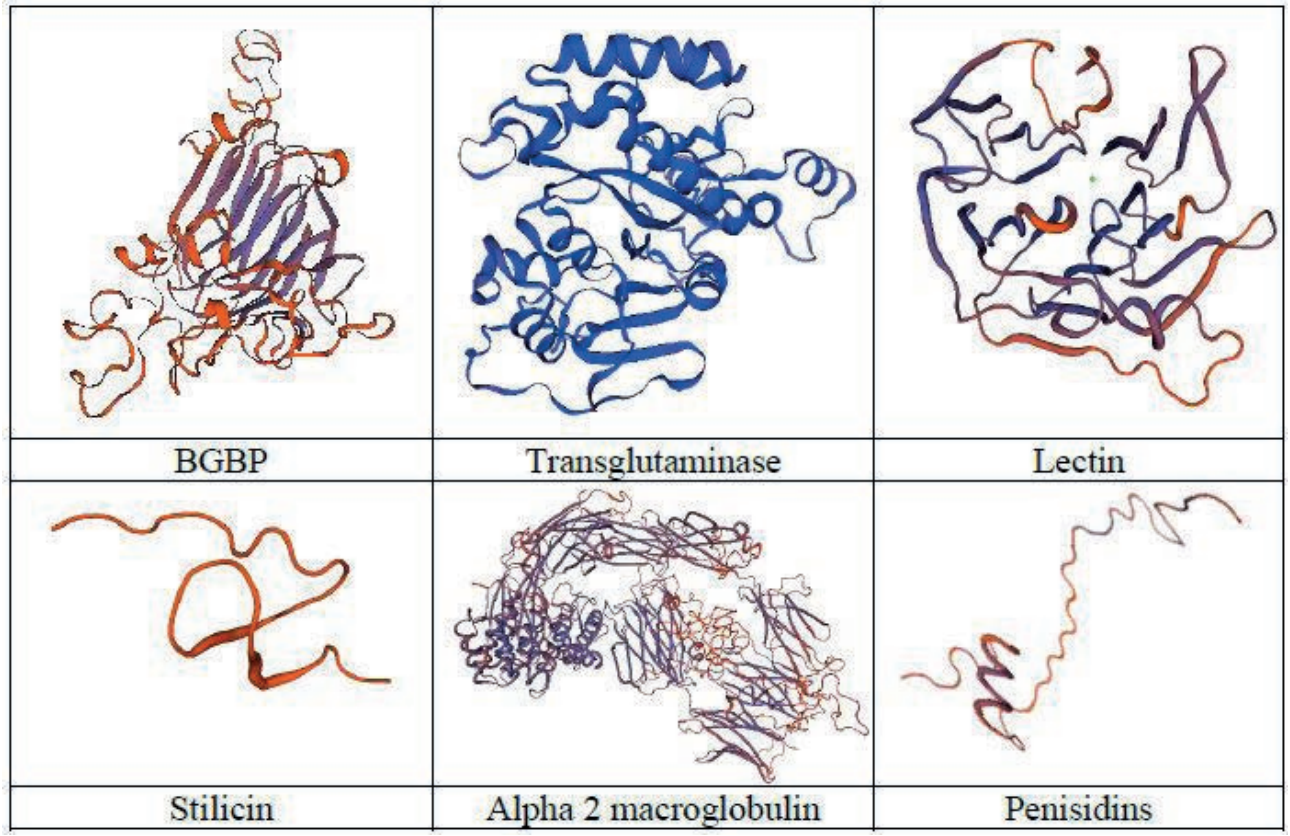

Figure 2. 3D structures of the main proteins involved in pathogen recognition as a humoral defense.

feature, the International Committee on Taxonomy of Viruses (ICTV) classified WSSV in its own family: *Nimaviridae*, within a unique genus *Whispovirus*[40,41].

Impact of WSSV virus on Ecuador's Economy

It is believed that WSSV entered Ecuador by importing contaminated larvae from Panama, spreading to the natural environment and later contaminating all farms. The virus was established between 1999 and 2000[42], causing great economic losses for the producer and the country itself. The National Institute of Fisheries (NIF), attached to the Ministry of Agriculture, Livestock, Aquaculture and Fisheries (MALAF), carries out annual tests[43] in several shrimp farms to determine the presence of different diseases using molecular tests.

There is evidence from the early 1990s that exports generated revenues for the country of around 3.5% of gross domestic product (GDP) on average, rising to almost 4.5% of GDP in 1997, 1998 and 1999[1]. After these years, the White Spot Syndrome epidemic broke out all over the world, and shrimp exports dropped to 2% in 2000 and to less than 1.5% in 2001. The shrimp industry and the Ecuadorian economy suffered significant damage until 2010, when a new increase in the export earnings of this product began reaching higher levels than before due to the control of the shrimp farms before the disease, as seen in Figure 3. Currently, the government conducts annual monitoring that allows the early detection of diseases. It is necessary to point out, that there is no protocol to deal with this virus in case it emerges again[1,44,45].

In August/September 2019, shrimp exports from Ecuador to China significantly dropped due to the presence of WSSV in the shipments; China is the leading importer of Ecuadorian shrimp worldwide. Therefore this problem generated a significant loss in annual profit, affected subsequent trades and caused the suspension of shrimp exports to China from various Ecuadorian companies[48].

As a result of the last infectious trade between Ecuador and China in 2019 a, better product management, constant monitoring and an adequate prevention protocol allowed to control the virus outbreak and thus not generate problems as such, increasing exports to that country[49].

Major vaccines designed to combat infectious diseases in shrimp

Disease-fighting protocol development in shrimp involves the characterization of immune system effectors and understanding defense reactions to potentially lethal pathogens, considering that pathogen-host interactions are constantly changing[49].

Vaccination is a defense mechanism used to enhance the shrimp immune system, which has been studied since the 1990s[9,50,51]. WSSV is one of the most serious pathogens affecting shrimp farming worldwide, so vaccine supplies constitute a significant protective benefit for the shrimp host.

Different vaccines have also been developed to combat the WSSV based on both the capsid and the core proteins, but also virus fragments or even completely inactivated viruses have been used[52,53]. The technologies currently employed are nanoparticles as vectors and gene silencing to prevent virus proteins from binding to shrimp cells generating an efficient immune response[53].

In aquaculture, 3 types of vaccines are commonly used. Live Attenuated Vaccines include a suspension of a live attenuated pathogen that generates a response that does not allow excessive replication despite the ability to multiply in the host[54]. Live vaccines cause an asymptomatic, self-limiting infection. Therefore, the host immune system resem-

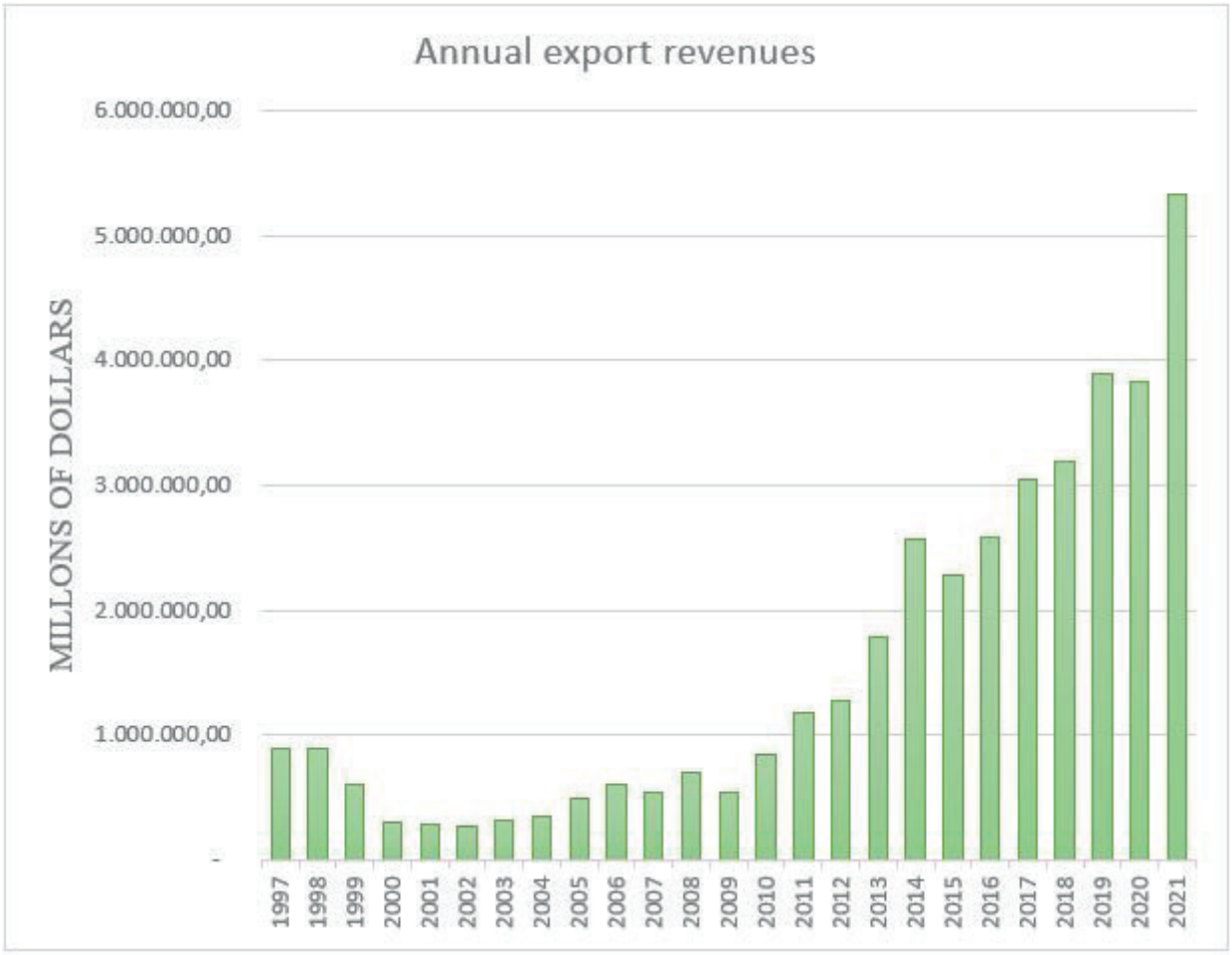

Figure 3. Annual shrimp exports from Ecuador between 1997 - 2021[2,44-47].

bles natural infections in a controlled system[55].

The second type of vaccine is recombinant vaccines which refer to immunogenic proteins or purified epitopes obtained from the pathogens or carriers. These can also be composed of the virus's DNA or dsRNA, as in the Recombinant Infectious Haematopoietic Tissue Necrosis Vaccines[56]. This type of vaccine has been one of the busiest in the last decade, primarily to molecular advances and studies of recombinant virus subunits[57]. More than 40 WSSV structural proteins have been identified[22] and used to manufacture efficient recombinant vaccines. Among these proteins are VP19, VP24, VP26, VP28, Vp36, VP36B, Vp37, VP39. Proteins VP19, VP24, Vp36B and VP39 are found on the WSSV envelope[22,58]. VP15, VP26 and VP36 are proteins found in nucleocapsid[22,59]. Because the structural proteins are the first to act with the host[60], those are considered the basis for neutralization strategies or the most likely candidates for vaccine development.

Particular studies have also shown that shrimp vaccinated with recombinant plasmids or microorganisms carrying a gene for the most studied WSSV coat protein (vp28) could efficiently protect shrimp against WSSV infection[57,61-64].

The third type is the inactivated virus vaccine, prepared from the suspension of completely killed cells of bacteria, viruses, or fungi. This type of vaccine has been successful against different disease-caused agents, such as *Vibrio anguillarum, Vibrio salmonsida*, also used in white shrimp, with good results. These vaccines are produced using chemical and physical (heat and radiation) inactivation methods. The most critical step in the production of such vaccines is inactivation[54].

Lastly, there is another type of vaccine that is not widely used in aquaculture but is commonly used in the veterinary and human area., that is the case of synthetic vaccines manufactured from polypeptides that simulate the primary sequence of antigenic amino acids. Its function is very similar to that which occurs with inactivated viruses[54]. Table 1 shows the type of vaccine, composition, how the active ingredient was obtained and the survival rate for each study.

According to the gathered data, the vaccines with the highest incidence were the envelope protein vaccines VP28[54-56,65]. This protein plays a role in interacting with the host cell surface[64], which has been the most studied since the virus first appeared in 1992[62,63]. VP28 is one of the most critical targets for vaccine manufacture, as it is one of the main WSSV coat proteins and acts as a binding protein, allowing the virus to combine with the shrimp cells and letting it join the cytoplasm[57].

The combination of this protein and others, such as Vp37, an envelope protein that facilitates infection, does not reduce the infection rate. Still, it does allow an improvement in the time of resistance to WSSV. Another of the mixtures is with VP24, as it is the only infection protein that has been shown to interact with the host polymeric immunoglobulin receptor protein (MjpIgR), which can mediate WSSV infection, generating good resistance results[57,66].

Designed specific vaccines against WSSV used in shrimp production

The primary purpose of vaccines is to stimulate the

TYPE OF VACCINE	COMPOSITION OF THE VACCINE	METHOD OF OBTAINING THE ACTIVE SUBSTANCE	METHOD OF ADMINISTRATION	PERCENTAGE OF SURVIVAL SOURCE	SOURCE
Inactivated virus	Gamma-inactivated virus	Gamma-irradiated WSSV virus produced in crab	Immersion	85	54,67–71
				86,66	
			Intramuscular	62	
				57	
				76	
		Gamma-irradiated WSSV produced in shrimp		73	
	Formalin-inactivated virus	Formalin-inactivated virus replicated in shrimp	Immersion	71,2 ± 3,13	31,72,73
			Oral	50	
			Intramuscular	60	
Subunit, recombinant, polysaccharide, and combination vaccines	Recombinant Vp28 and vp37 proteins	Protein cloning in *E. coli* of MrNv-VLP, amplification of VP28 and 37 dsRNA T7 RiboMAX™ Express large-scale RNA production system.	Intramuscular	45	64
	Recombinant VP28 and VP24 Proteins	Protein cloning in *E. coli* with amplification of VP28 and 24	Oral	100	57
	Recombinant VP15 protein	Protein cloning in *E. coli* with VP15 amplification	Intramuscular (2 doses)	80	74,75
				60	
	Recombinant VP28 protein	Protein cloning in *E. coli* with amplification of recombinant VP28	oral	87,10	52,62,63,76–79
				70	
				60	
				50	
			Intramuscular (2 doses)	81	
			Intramuscular	44,99	
				67	
		Use of recombinant *B. subtilis* CotB-VP28 expressing the VP28 protein of WSSV	Oral	70	80,81
				65	
		Use of recombinant filamentous cyanobacteria expressing the VP28 protein of WSSV		28,68	82
	Recombinant VP19 + VP28 proteins	Protein cloning in *E. coli* with recombinant VP19 + VP28 amplification	Oral	71,1	61,83
		Protein cloning in lentiviruses with amplification of VP19 + recombinant VP28	Immersion	86	
	dsRNA	Amplified protease fragments and cloning in *E. coli*	Intramuscular	70	84–87
		The double-stranded RNA corresponding to the vp28 protein-coding gene of WSSV		73	
		The double-stranded RNA corresponds to the genes coding for rr1 and vp28 of WSSV.		93,3 entre 90	
		A partial fragment of C-type lectin cDNA associated with *M. japonicus* stomach virus was amplified by PCR.		75	
	lcppae2	Amplification of the gene encoding WSV056 was amplified from the DNA of the WSSV genome.	Intramuscular	85	88
	CQD with RNA	Total RNA was isolated using TRIzo reagent	Oral	20	89
	Recombinant DNA	Genomic DNA isolated from pleopod tissue in microsatellites	Intramuscular	88,1	90
		Design of two primer pairs using the viral VP24 gene for nested PCR	Oral	50	21
	Recombinant *baculovirus*	Recombinant *baculovirus* viral DNA isolated from recombinant *baculovirusas* containing VP28, VP19 and FL2 using a NucleoS RNA Virus kit	Oral	89,5	91
		Establishment of recombinant vectors harboring VP28 and gene encoding dsRNA specific for rr2 and egfp		64	92
	CotC: Vp26 fusion protein	Recombinant spores (RS) of *B. subtilis*, showing CotC: Vp26 fusion protein (FP)	Oral	100	93
	Recombinant vp39 and vp28 proteins	Protein cloning in *E. coli* with amplification of VP28 and 24	Intramuscular and oral	60 y 50	94
	Recombinant VP28 and VP36B proteins	Protein cloning in *E. coli* with amplification of VP28 and VP36B	Intramuscular (2 doses)	100	58
	Antiviral vp28-siRNA	Sequencing vp28-siRNA randomly organised and mutated at one nucleotide.	Intramuscular	60	95
	Recombinant rVP26 and rVP28 proteins	WSSV DNA from WSSV-infected shrimp tissue by RNase-PEG precipitation method	Oral, immersion, intramuscular	100, 71 y 61	96
	Recombinant VP24 protein	Protein cloning in *E. coli* with amplification of recombinant VP24	Oral	64	97,98
				43	
	Recombinant Wsv477 protein	Protein cloning in *E. coli* with recombinant wsv477 amplification	Intramuscular y oral	40 y 30	99
Synthetic vaccine	Protein pmrab7	Protein cloning in *Agrobacterium tumefaciens* with amplification of pmrab7	Intramuscular	87	100
	Phagocytosis Activating Protein recombinant plasmid (phMGFP-PAP)	Protein cloning in *E. coli* with phMGFP-PAP amplification	Oral	62	68
	Anti-sense constructions	Specific primers to amplify the H3 promoter of *P. monodon* and selected portions of the viral ORFs (structural proteins)	Intramuscular	90	70

Table 1. Efficiency and composition of different vaccine preparations according to the 46 consulted papers.

shrimp's immune system and generate a defense response against WSSV to prevent virus scape and thus reduce its replication and spread[101]. These cell responses against WSSV are given in different ways. Two of them stimulate the cell response by: 1-the presence of biomolecules belonging to the virus and 2-molecules that interfere with the receptors where the virus assembles to the host cell. On the other hand, genetic modifications that provide a protective response by not generating interactions in the cells with the virus[102] also result in good practice.

Among the revised papers, 34 deal with recombinant vaccines, the most used ones based on recombinant proteins from the structural parts of WSSV. The combination of 2 or more structural recombinant proteins[5] generates a higher protection rate against this virus[61,83]. The revised reports also determined that the main type of vaccine is composed of the subunit-recombinant, polysaccharide, and combined subunit vaccines. According to Figure 4, the vaccines mentioned above showed a protection percentage of 73.91%, while other treatments related to both; synthetic or inactivated virus vaccines reached lower protection percentages of only 6.52% and 19.57%, respectively. In this figure is also noticed that the most frequent active principle is the recombinant vp28 protein, reaching 21.74% of incidence.

Experimental conditions are very important in reaching a good performance of any vaccine treatment against WSSV since protection results could change from one experiment to another according to the experimental conditions. Some parameters to take under consideration in this experiment are a) the type of shrimp, b) the form of virus replication referring specifically to the animal used, c) the region in which the study was carried out where the environmental parameters varied and d) the variation of virus infection that can reach mortality levels up to 100%[103,104]. Interestingly, in some research reports, there was no total mortality, mainly due to the resistance some arthropods can generate against WSSV[105].

Also, administration methods at the production level deal with the efficiency in the vaccination methods[99,100]. It is worth noting that the most common method of vaccine administration is intramuscular administration, with a frequency of 48%, followed by oral administration at 42% and finally by immersion at 10%. However, oral vaccine administration is the best and most studied method at the industrial level.

The effect on the immune system produced by the vaccine in shrimp is calculated by the efficiency of the treatment against WSSV, demonstrated by the number of vaccinated animals that survived exposure to the virus; the treatment with the highest efficiency and best protective effect was the intramuscular administration. The treatment with the highest efficiency and best protective effect was the intramuscular route, with 18% of treatments having a survival rate of more than 75%; the oral way had an efficiency of 10% for medicines with a survival rate of more than 75%, and the immersion route had a frequency of 6% for treatments with a survival rate of more than 75% (Figure 5).

It was determined that, in general, the efficiency of the vaccine is between 50% and 75% of shrimp survival rate

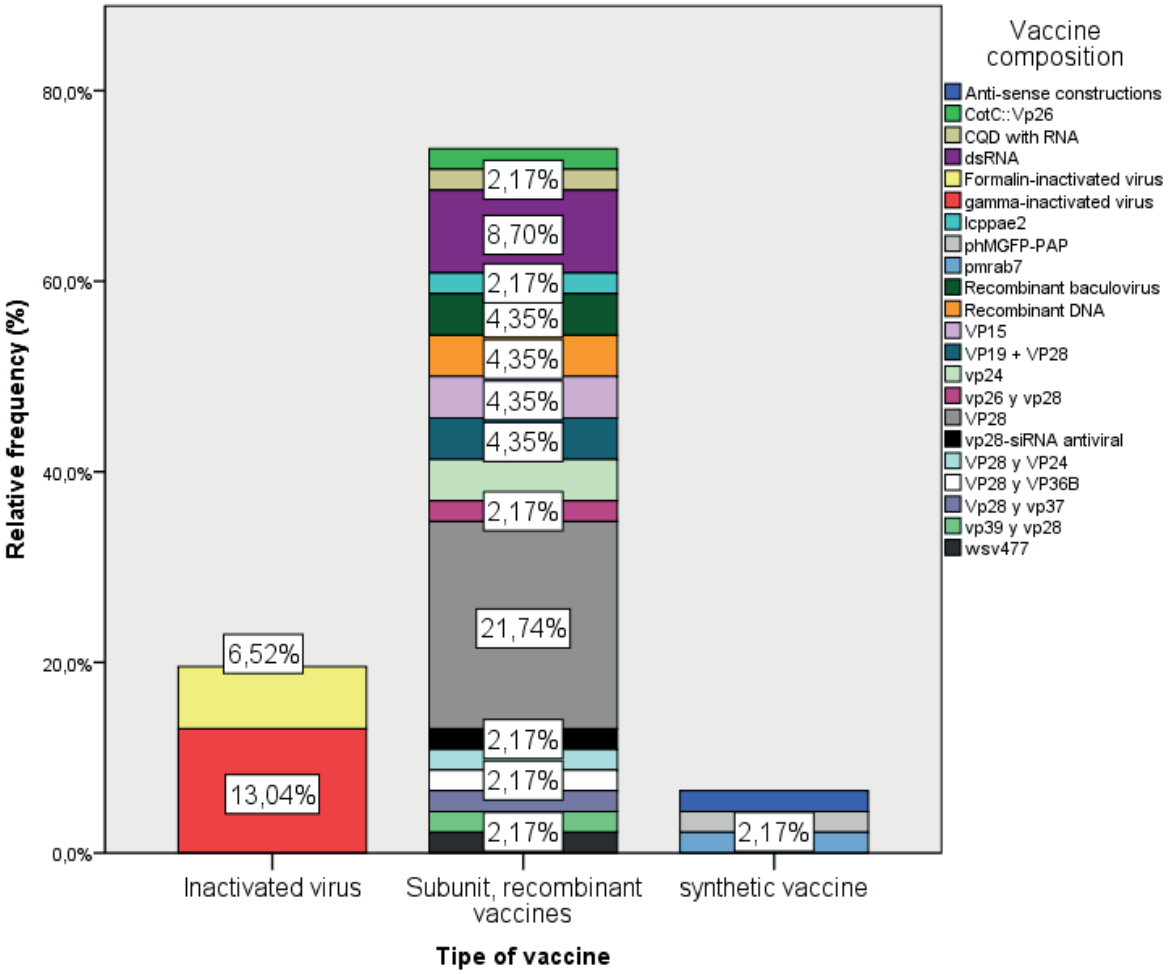

Figure 4. Types and composition of WSSV vaccines in shrimp.

reaching 52% of frequency in the studied articles, followed by others that reached an effectiveness of more than 75% having 34% of frequency, allowing to assert that vaccination is an effective treatment against the virus.

Detailing the efficiency depending on the vaccine composition, it was determined that gamma-inactivated virus is the most effective, reaching a 6% frequency in treatments with a survival rate of 75%, followed by vaccines made with recombinant VP28 protein, which reached a 4% frequency. However, vaccines with recombinant VP28 had the highest frequency of 12% among all treatments, with a survival rate between 50% and 75%.

WSSV vaccine production for *Litopenaeus spp*.

Penaeidae is a crustaceans family of great commercial value[106,107]. Among its different genera, *Litopenaeus* stands out as one of the most important shrimp species in the world industry[108-110]. *Litopenaeus vannamei* is among the principal species of this genus, commonly known as Pacific white shrimp111, the main farming species on the Ecuadorian coast[48]. However, this genus is prone to devastating diseases such as WSSV, which generate significant economic losses, and no commercial cure can eradicate the disease. Table 2 shows recent reports on conditions affecting the Litopenaeus genus, showing some updated general approaches to fighting them.

According to the research reviewed, vaccine manufacturing has been carried out *ex-situ*. Therefore, this technology is still limited to the laboratory level. Further studies on production scale-up should be carried out to reduce costs, maintain product quality and develop *in situ* trials, allowing more accurate data to be generated during shrimp treatment.

Whispovirus vaccines aren't currently being commercialized at large-scale in the industry because of the high degree of variation in response to laboratory-tested vaccines and the high economic value of vaccine development[9,115]. Nevertheless, interest in controlling the devastating effects of the virus on *Litopenaeus vannamei* farms has led to increased interest in producing a vaccine that is efficient and affordable for field application.

The most efficient way to immunize *Litopenaeus spp*. with vaccines is by oral or infusion as it is not productive at the industrial level to apply it intramuscularly as this implies the application of the vaccine organism by the organism.

The vaccine industry and production is a complex activity with risks, which takes place in a harsh environment. Protocols for potential occupational hazards are necessary concerning contamination issues such as, product contamination, cross-contamination, amplification of contaminants, infection of workers and contamination of the environment[116].

The animal vaccines currently available worldwide are developed by the veterinary pharmaceutical industry. Developing a vaccine requires an economic effort that takes years to perfect and guarantees its safety.

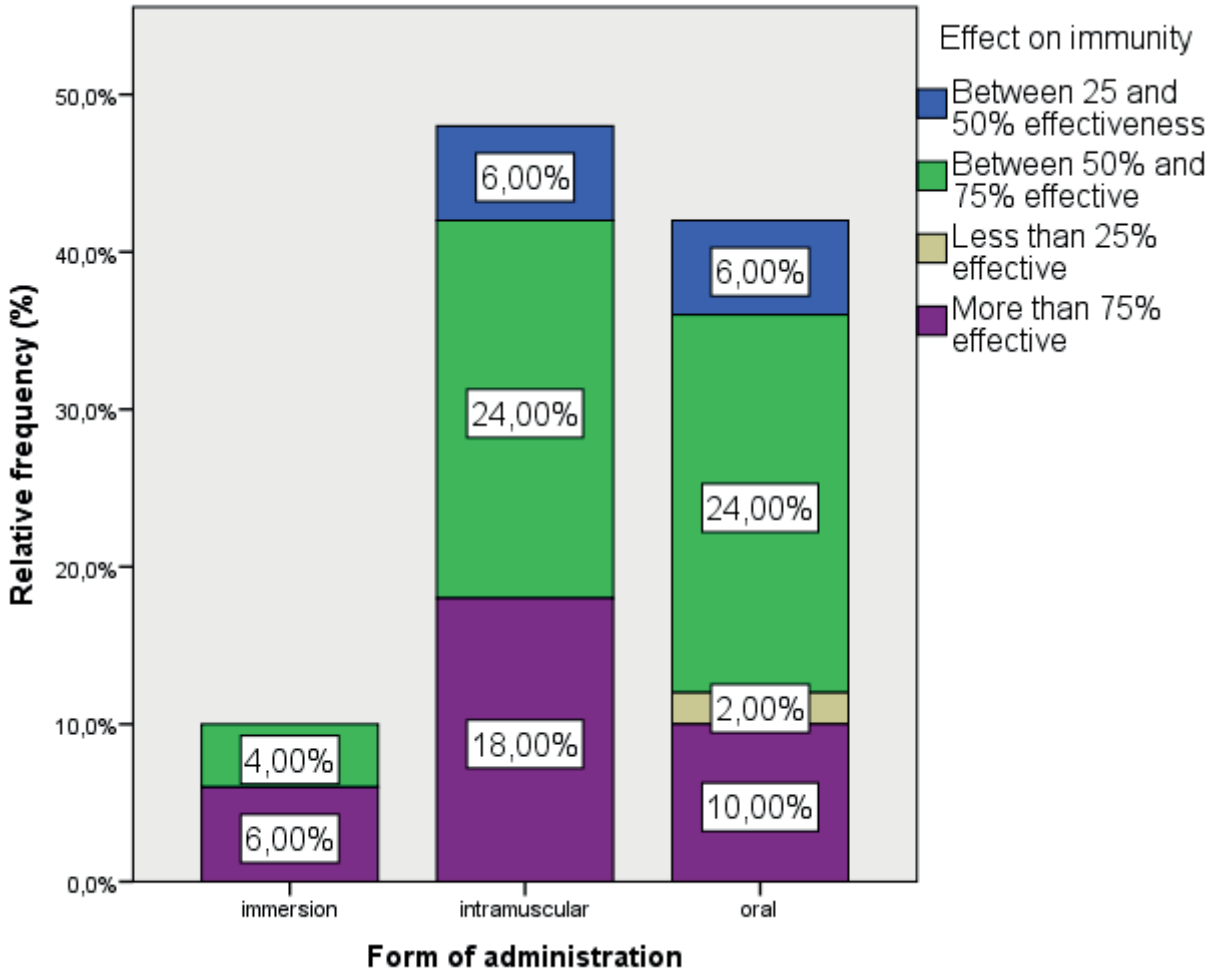

Figure 5. Routes of vaccine administration and effect on the immune system of shrimp.

TITLE	DESCRIPTION	YEAR OF PUBLICATION	REFERENCE
RNA Nanovaccine Protects against White Spot Syndrome Virus in Shrimp	A double-stranded RNA-based nanovaccine was developed as a shrimp disease control with emphasis on the Pacific white shrimp *L. vannamei*.	2022	108
Characterization of *Litopenaeus vannamei* secreted protein acidic and rich in cysteine -like in WSSV infection	Cloned the full-length cDNA sequence of an acidic, cysteine-rich secreted protein from the shrimp *Litopenaeus vannamei* (LvSPARC-L) that encodes 333 amino acids and promotes haemocyte expression.	2021	112
The Active Microbiota of the Eggs and the Nauplii of the Pacific Blue Shrimp *Litopenaeus stylirostris* Partially Shaped by a Potential Vertical Transmission	Analysed the active microbiota associated with *L. stylirostris* eggs and nauplii, using HiSeq sequencing of the V4 region of the 16S rRNA gene, demonstrating that the microbiota is transmitted vertically at different growth stages.	2022	113
Deciphering the virulent Vibrio *harveyi* causing spoilage in muscle of aquatic crustacean *Litopenaeus vannamei*	The research showed that proven not only viral diseases destroy muscle tissue in crustaceans but also bacterial agents are capable of causing this reaction by changing the microbial composition and that crustaceans could be used as a sensitive broad-spectrum bio detector to indicate the degree of microbial contamination.	2022	114

Table 2. Recent research on WSSV affecting *Litopenaeus spp.* and used fighting strategies.

Industrial development usually starts after laboratory testing that is based on solid academic research. A vaccine can only be made available to the veterinary community once the authorities have granted marketing approval, verifying its effects and potential harm[117].

Industrial development must be seen in an economic context, which is not always the case in academic research so the use of reagents has large economic differences.

Farm Animals' vaccines are produced in large quantities at low cost, while vaccines for companion animals are produced in smaller quantities and sold at higher prices. It should also be taken into account that for-profit companies will generate the development of vaccines for higher incidence diseases or vaccines for high population species[118]. In the case of shrimp, being a species of large-scale production generates interest in aquaculturists, and although *Whispovirus* is sporadic, it generates losses that affect shrimp production during these periods of appearance[42].

Figure 6 shows a production scheme for recombinant protein vaccines that could be used for further implementation in the industry. There is a small amount of commercialization of shrimp vaccines against WVVS. Yet, it is guessed that by having an efficient and replicable treatment in any environment, an industrial process could be implemented for its elaboration and oral administration.

According to figures 4 and 5 of the results obtained from the extracted articles, the production of vaccines with 2 genes has had a higher effectiveness rate. It confers more excellent protection to shrimps, being a process that can be used at the industrial level[61,83].

The bacteria most commonly involved in the replication of recombinant proteins are *Escherichia coli* and *Bacillus subtilis* because of their more efficient replication, procurement and easy genetic manipulation[119-121].

Conclusions

Antibiotics use on shrimp production cause: 1-potential adverse effect on human health[9,122],2-appearance of antibiotic-resistant strains[123,124] and 3-affections on shrimp larvae[125]. Contrarily, vaccine administration to control or lessen the incidence of vibriosis is an attractive choice nowadays.

Vaccination strategies against WSSV, such as inactivated viruses, subunit antigens, and DNA-based vaccines, have shown promise on a laboratory scale. However, drawbacks such as variable efficacy, high manufacturing cost, and limited field applicability need further investigation[126].

A recent study describes a new attractive strategy based on RNAi technologies and polyanhydride nanoparticle-based delivery to develop a nanovaccine[108]. In aquaculture systems, the concept of RNAi-based vaccines has been advocated for several reasons: (a) RNAi functions as an antiviral immune response in shrimp; (b) it is pathogen-specific; and (c) it generates a long-term protective immune response.

On the other hand, another new technology combining vaccines with prebiotics has been shown to maximize the protective efficacy127–129 (Table 1). β-glucans, for example, is a joint prebiotic used in aquaculture and has long been used as an additive in the fish diet to improve the immune response enhancing the innate immune response127,130,131,132.

Despite all these new alternatives to vaccine production and applications, more and more research, mainly on field trials, needs to be carried out to validate further and enhance the vaccine application effectiveness in shrimp.

Funding

This research received no external funding.

Institutional Review Board Statement

Not applicable.

Informed Consent Statement

Not applicable.

Acknowledgments

Authors thanks to Ing. Janyna Calderón Martinez and Ing. Christian Ortega for the critical reading of this manuscript. Their suggestions improved its content. Also, thanks to Ivan Andres Proaño and Björn Ludwig for their help in improving the manuscript's English graphics.

Conflicts of Interest

The authors declare no conflict of interest.

Bibliographic references

1. García, F. Analisis del sector camaronero. Apunt. Econ. 29, 1–60 (2003).
2. Camara Nacional de Acuacultura de Camarón – Reporte de Exportaciones Ecuatorianas Totales. https://www.cna-ecuador.com/estadisticas/ (2022).
3. Gonzabay, C., Ámbar, N., Cevallos, V. & Harry, A. Analysis of shrimp production in Ecuador for export to the European Union in the 2015-2020 period. Polo del Conoc. 6, 1040–1058 (2021).
4. Montero, W. Principales enfermedades virales que afectan la producción de caamrón blanco del pacífico Litopenaeus vannamei. 1–24 (2017).

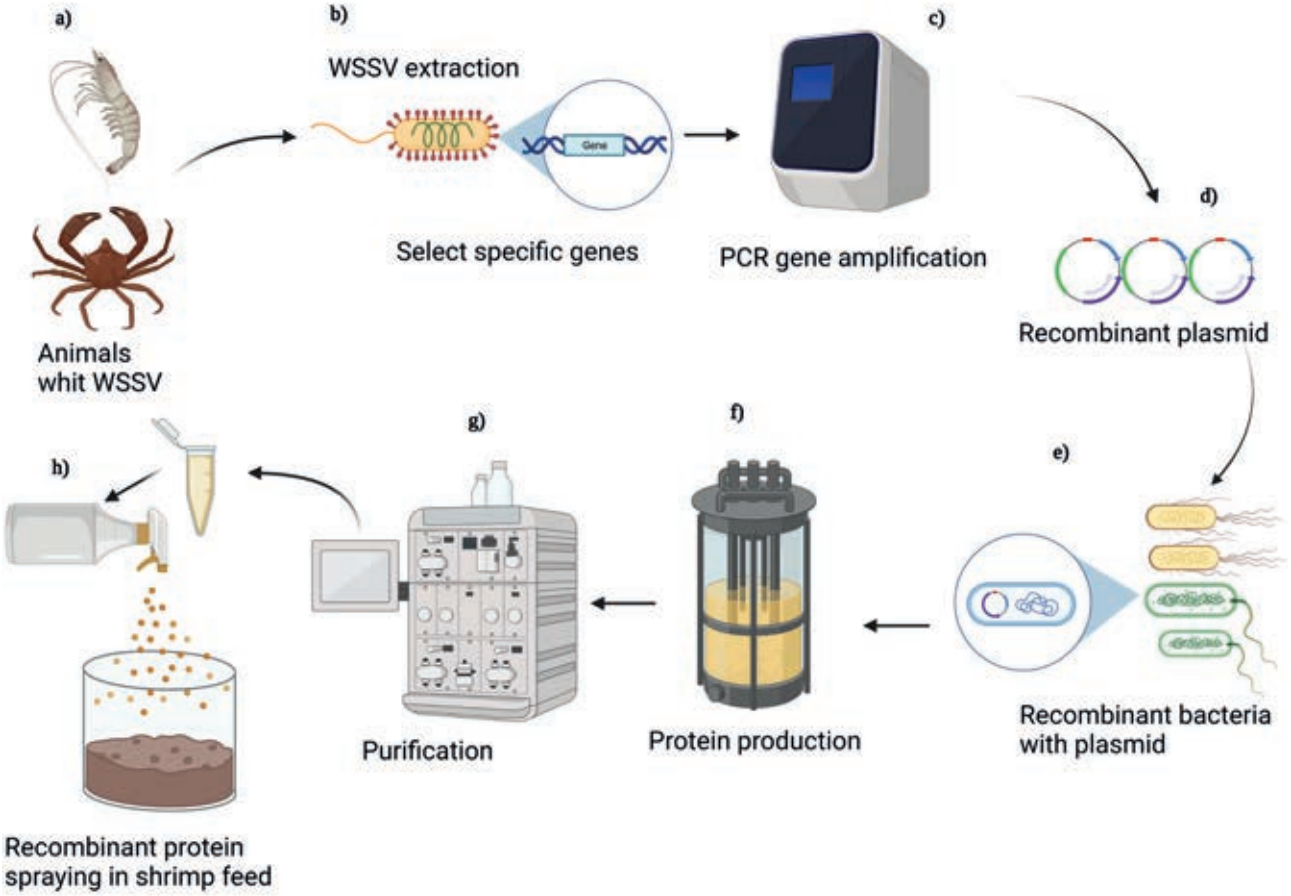

Figure 6. The production process of the oral vaccine in shrimp to combat WSSV. a) The first step is extracting the virus from animal sources such as crabs and shrimps. b) Selection of specific genes for each protein and isolation. c) Amplification. d) Generation of recombinant plasmids. (e) cloning of recombinant bacteria (f) large-scale production and replication in bioreactors of proteins from the recombinant bacteria (g) purification of the medium and extraction of proteins by affinity chromatography (h) combination of purified recombinant proteins with commercial shrimp feed.

5. Soo, T. C. C. & Bhassu, S. Signature selection forces and evolutionary divergence of immune-survival genes compared between two important shrimp species. PLoS One 18, 1–17 (2023).
6. OMSA - Organización Mundial de Sanidad. Infeccion por el virus de la mancha blanca. 1, 2.2.8 (2021).
7. OMSA - Organización Mundial de Sanidad. Lista B, enfermedades de animales. https://www.woah.org/fr/ce-que-nous-faisons/sante-et-bien-etre-animale/maladies-animales/ancienne-classification-des-maladies-notifiables-a-loie-liste-b/ (2021).
8. Leu, J. H., Tsai, J. M. & Lo, C. F. White Spot Syndrome Virus. Encycl. Virol. 450–459 (2008) doi:10.1016/B978-012374410-4.00776-7.
9. Amatul-Samahah, M. A. et al. Vaccination trials against vibriosis in shrimp: A review. Aquac. Reports 18, 100471 (2020).
10. Chakraborty, S., Ghosh, U., Balasubramanian, T. & Das, P. Screening, isolation and optimization of anti-white spot syndrome virus drug derived from marine plants. Asian Pac. J. Trop. Biomed. 4, S107–S117 (2014).
11. Chaudhari, A., Pathakota, G. B. & Annam, P. K. Design and construction of shrimp antiviral DNA vaccines expressing long and short hairpins for protection by RNA interference. Methods Mol. Biol. 1404, 225–240 (2016).
12. Korea institute of science and Technology Information. □□□□ □□ □□□□□(2□). 23, (2014). URL: https://repository.kisti.re.kr/bitstream/10580/2639/1/2014□ □□□□□□ □□□□□(2□).pdf
13. Syed Musthaq, S. K. & Kwang, J. Evolution of specific immunity in shrimp - A vaccination perspective against white spot syndrome virus. Dev. Comp. Immunol. 46, 279–290 (2014).
14. Feng, S., Wang, C., Hu, S., Wu, Q. & Li, A. Recent progress in the development of white spot syndrome virus vaccines for protecting shrimp against viral infection. Arch. Virol. 162, 2923–2936 (2017).
15. Mekata, T. Strategy for understanding the biological defense mechanism involved in immune priming in kuruma shrimp. Dev. Comp. Immunol. 125, 104228 (2021).
16. Campa-Córdova, A. I., Luna-González, A., Flores-Miranda, M. del C., Pacheco-Marges, M. del R. & Ascencio-Valle, F. Respuesta Inmune en Camarón Blanco, Litopenaeus vannamei, Expuesto a Infecciones Bacterianas y Virales. Av. en Nutr. Acuicola 0, 317–344 (2011).
17. Rendón, L. & Balcázar, J. L. Inmunología de camarones : Conceptos básicos y recientes avances Introducción Sistema inmune Hemocitos. Rev. Aquat. 1, 30 (2003).
18. Tanekhy, M. & Fall, J. Expression of innate immunity genes in kuruma shrimp Marsupenaeus japonicus after in vivo stimulation with garlic extract (allicin). Vet. Med. (Praha). 60, 39–47 (2015).
19. Wang, F., Li, S. & Li, F. Different immune responses of the lymphoid organ in shrimp at early challenge stage of vibrio parahaemolyticus and wssv. Animals 11, 1–15 (2021).
20. Bachere, E. Shrimp immunity and disease control. Aquaculture 191, 3–11 (2000).
21. Afsharnasab, M., Kakoolaki, S. & Afzali, F. The Status of white spot syndrome virus (WSSV) in Islamic Republic of Iran. Iran. J. Fish. Sci. 13, 1021–1055 (2014).
22. Tuan, V. Van. Antibacterial and antiviral activity of different haemocyte subpopulations of Litopenaeus vannamei. 156 (2016).

23. Gutiérrez-Dagnino, A. et al. Efecto de la inulina y del ácido fúlvico en la supervivencia, crecimiento, sistema inmune y prevalencia de WSSV en Litopenaeus vannamei. Lat. Am. J. Aquat. Res. 43, 912–921 (2015).
24. Kulkarni, A. et al. Immune responses and immunoprotection in crustaceans with special reference to shrimp. Rev. Aquac. 13, 431–459 (2021).
25. Davier, L., Ríos, M., López, G. E. & Farnés, O. C. The Immune System of Penaeid Shrimp : A review. 34, (2022).
26. Sánchez-Salgado, J. L. et al. Participation of lectins in crustacean immune system. Aquac. Res. 48, 4001–4011 (2017).
27. Smith, V. J., Fernandes, J. M. O., Kemp, G. D. & Hauton, C. Crustins: Enigmatic WAP domain-containing antibacterial proteins from crustaceans. Dev. Comp. Immunol. 32, 758–772 (2008).
28. Yedery, R. D. & Reddy, K. V. R. Identification, cloning, characterization and recombinant expression of an anti-lipopolysaccharide factor from the hemocytes of Indian mud crab, Scylla serrata. Fish Shellfish Immunol. 27, 275–284 (2009).
29. Cuthbertson, B. J. et al. Diversity in penaeidin antimicrobial peptide form and function. Dev. Comp. Immunol. 32, 167–181 (2008).
30. Little, T. J., Hultmark, D. & Read, A. F. Invertebrate immunity and the limits of mechanistic immunology. Nat. Immunol. 6, 651–654 (2005).
31. Amar, E. C., Faisan, J. P. & Gapasin, R. S. J. Field efficacy evaluation of a formalin-inactivated white spot syndrome virus (WSSV) vaccine for the preventive management of WSSV infection in shrimp grow-out ponds. Aquaculture 531, 735907 (2021).
32. Feng, S. Y. et al. Meta-analysis of antiviral protection of white spot syndrome virus vaccine to the shrimp. Fish Shellfish Immunol. 81, 260–265 (2018).
33. Verbruggen, B. et al. Molecular mechanisms of white spot syndrome virus infection and perspectives on treatments. Viruses 8, 1–29 (2016).
34. Kurtz, J. & Franz, K. Evidence for memory in invertebrate immunity. Nature 425, 37–38 (2003).
35. Chou, P. H. et al. The putative invertebrate adaptive immune protein Litopenaeus vannamei Dscam (LvDscam) is the first reported Dscam to lack a transmembrane domain and cytoplasmic tail. Dev. Comp. Immunol. 33, 1258–1267 (2009).
36. Watson, F. L. et al. Immunology: Extensive diversity of Ig-superfamily proteins in the immune system of insects. Science (80-.). 309, 1874–1878 (2005).
37. Williams, T., Bergoin, M. & van Oers, M. M. Diversity of large DNA viruses of invertebrates. J. Invertebr. Pathol. 147, 4–22 (2017).
38. Biomin.net. Enfermedades de los camarones. (2019).
39. Godínez-Siordia Daniel Enrique González-Ochoa Oscar et al. Major Shrimp Pathogenic Virus in America and Their Relationship With Low Salinity Environments. Ra Ximhai 8, 61–69 (2012).
40. Thammasorn, T. et al. Large-scale production and antiviral efficacy of multi-target double-stranded RNA for the prevention of white spot syndrome virus (WSSV) in shrimp. BMC Biotechnol. 15, 5–8 (2015).
41. Mayo, M. A. A summary of taxonomic changes recently approved by ICTV. 8, 1–2 (2002).
42. Marcillo, F. Crisis por la mancha Blanca y su recuperación actual. Dsp. Repos. 4 (2003).
43. Ministerio de Agricultura y Ganaderia del Ecuador. Ecuador refuerza medidas para evitar enfermedad que afecta al camarón – Ministerio de Agricultura y Ganadería. https://www.agricultura.gob.ec/ecuador-refuerza-medidas-para-evitar-enfermedad-que-afecta-al-camaron/ (2019).
44. Notarianni, E. Ecuador despues de la Mancha Blanca. 20–21 (2006).
45. Montoya Barrionuevo, J. A. Análisis De La Exportación Del Camarón Y Su Efecto En la balanza comercial en el Ecuador. (2021).
46. Sánchez Méndez, D. C. Enfermedades que afectaron la producción de camarón y análisis de las exportaciónes de camarón en el ecuador. Univ. ESTATAL PENÍNSULA St. ELENA 2003–2005 (2022).
47. Food Agriculture Organization. El estado mundial de la pesca y acuicultura. Marine Pollution Bulletin vol. 3 (2020).
48. Barzola, M. D. E. & Pesántez Quezada, G. D. Análisis de la afectación de la mancha blanca en las exportaciones de camarón hacia china del periodo 2017 – 2019. Fac. CIENCIAS Adm. CARRERA Ing. EN Comer. Exter. 1–172 (2020).
49. Parraga, L. Estudio de supervivencia entre líneas de postlarvas silvestres y domesticadas de Pennaeus vannamei desafiadas per os con el virus de la mancha blanca (WSSV). Univ. GUAYAQUIL Fac. CIENCIAS Nat. Maest. EN CIENCIAS MANEJO SUSTENTABLE BIORRECURSOS Y MEDIO Ambient. 62 (2017).
50. Adams, A. Response of penaeid shrimp to exposure to Vibrio species. Fish Shellfish Immunol. 1, 59–70 (1991).
51. SUNG, H. H., SONG, Y. L. & Kou, G. H. Potential uses of bacterin to prevent shrimp vibriosis. Fish Shellfish Immunol. 311–312 (1991).
52. Taengchaiyaphum, S. et al. Vaccination with multimeric recombinant VP28 induces high protection against white spot syndrome virus in shrimp. Dev. Comp. Immunol. 76, 56–64 (2017).
53. Johnson, K. N., van Hulten, M. C. W. & Barnes, A. C. 'Vaccination' of shrimp against viral pathogens: Phenomenology and underlying mechanisms. Vaccine 26, 4885–4892 (2008).
54. Ghaednia, Babak; Mirbakhsh, M.; Zendehbouy, A.A.; Keshtkar, I.; Nazary, M.A.; Sabohi, M.; Rajabifar, S.; Shafaee, K.; Raeesali, Gh.; Zarin, E.; Gorjifar, R.; Heidary, M.; Afsharnasab, M.; Kakoolaki, S.; Motamedi, F.; Gharibi, G. & Iranian. Study on health and Immunity index of vaccinated Litopenaeus vannamei against white spot virus disease. (2022).
55. PENAGOS, G. SISTEMA INMUNE Y VACUNACIÓN DE PECES. Acta Biológica Colombiana vol. 14 3–24 https://revistas.unal.edu.co/index.php/actabiol/article/view/9766 (2009).
56. Alonso M., F., Estepa, A. & Coll, J. M. Vacunas DNA en Acuicultura. (1998).
57. Lei, H., Li, S., Lu, X. & Ren, Y. Oral administration of Saccharomyces cerevisiae displaying VP28-VP24 confers protection against white spot syndrome virus in shrimp. Virus Res. 302, 198467 (2021).
58. Yang, J. Y. et al. Viral resistance and immune responses of the shrimp Litopenaeus vannamei vaccinated by two WSSV structural proteins. Immunol. Lett. 148, 41–48 (2012).
59. Bustillo-Ruiz, M. I., Escobedo-Bonilla, C. M. & Sotelo-Mundo, R. R. Revisión de patogénesis y estrategias moleculares contra el virus del síndrome de la mancha blanca en camarones peneidos. Rev. Biol. Mar. Oceanogr. 44, 1–11 (2009).
60. Solis, M. Bioselección de Péptidos y Fragmentos de Anticuerpos Desplegados en Fagos que se Unen al Virus del Síndrome de la Mancha Blanca. 1–42 (2011).
61. Zhu, C., Shi, D., Liao, S., He, P. & Jia, R. Effects of Synechococcus sp. PCC 7942 harboring vp19, vp28, and vp (19 + 28) on the survival and immune response of Litopenaeus vannamei infected WSSV. Fish Shellfish Immunol. 99, 1–8 (2020).
62. Lanh, P. T. et al. Generation of microalga Chlamydomonas reinhardtii expressing VP28 protein as oral vaccine candidate for shrimps against White Spot Syndrome Virus (WSSV) infection. Aquaculture 540, 736737 (2021).
63. Le Linh, H. et al. Yeast cell surface displaying VP28 antigen and its potential application for shrimp farming. Appl. Microbiol. Biotechnol. 105, 6345–6354 (2021).
64. Weerachatyanukul, W., Chotwiwatthanakun, C. & Jariyapong, P. Dual VP28 and VP37 dsRNA encapsulation in IHHNV virus-like particles enhances shrimp protection against white spot syndrome virus. Fish Shellfish Immunol. 113, 89–95 (2021).
65. Moreno, F., Salas, G. & Gutiérrez, R. Sistema inmune de los camarones Introducción Materiales y métodos. Aquatic 68–84 (2013).

66. Niu, G. J. et al. The polymeric immunoglobulin receptor-like protein from Marsupenaeus japonicus is a receptor for white spot syndrome virus infection. PLoS Pathog. 15, 1–28 (2019).
67. Motamedi-Sedeh, F., Afsharnasab, M. & Heidarieh, M. Immunization of Litopenaeus vannamei shrimp against white spot syndrome virus (WSSV) by gamma-irradiated WSSV plus Vibrio paraheomolyticus. Vaccine Res. 2, 107–112 (2015).
68. Ilham, S. Prevention of White Spot Syndrome Viral of White Shrimp (Litopenaeus vannamei) by RPS3a Protein and PAP DNA. (2012).
69. Afsharnasab, M., Kakoolaki, S. & Mohammadidost, M. Immunity enhancement with administration of Gracilaria corticata and Saccharomyces cerevisiae compared to gamma irradiation in expose to WSSV in shrimp, in juvenile Litopenaeus vannamei: A comparative study. Fish Shellfish Immunol. 56, 21–33 (2016).
70. Afsharnasab, M.; Motalebi, A.A.; Sharifpor, M.; Pazir, M.Kh.; Ghaednia, B.; Kakoolaki, S. & Iranian. Feasibility study of white spot syndrome virus vaccine with gamma radiation. (2022).
71. Heidarieh, M., Sedeh, F. M., Soltani, M. & ... Immunization of Shrimp by Irradiated Vibrio Paraheamolyticus Against White Spot Syndrome Virus. J. Nucl. … 72–79 (2016).
72. Sudheer, N. S. et al. Expression profile of bio-defense genes in Penaeus monodon gills in response to formalin inactivated white spot syndrome virus vaccine. Antiviral Res. 117, 60–68 (2015).
73. Ahanger, S. et al. Protection of Shrimp Penaeus monodon from WSSV Infection Using Antisense Constructs. Mar. Biotechnol. 16, 63–73 (2014).
74. Boonyakida, J. et al. Identification of antigenic domains and peptides from VP15 of white spot syndrome virus and their antiviral effects in Marsupenaeus japonicus. Sci. Rep. 11, 1–12 (2021).
75. Boonyakida, J. et al. Antigenic properties of VP15 from white spot syndrome virus in kuruma shrimp Marsupenaeus japonicus. Fish Shellfish Immunol. 101, 152–158 (2020).
76. Ma, Y. et al. An attenuated Vibrio harveyi surface display of envelope protein VP28 to be protective against WSSV and vibriosis as an immunoactivator for Litopenaeus vannamei. Fish Shellfish Immunol. 95, 195–202 (2019).
77. Solís-Lucero, G., Manoutcharian, K., Hernández-López, J. & Ascencio, F. Injected phage-displayed-VP28 vaccine reduces shrimp Litopenaeus vannamei mortality by white spot syndrome virus infection. Fish Shellfish Immunol. 55, 401–406 (2016).
78. Sun, Y., Li, F., Chi, Y. & Xiang, J. Enhanced resistance of marine shrimp Exopalamon carincauda Holthuis to WSSV by injecting live VP28-recombinant bacteria. Acta Oceanol. Sin. 32, 52–58 (2013).
79. Qiu, Z. guang, Liu, Q. hui & Huang, J. Efficiency of two fragments of VP28 against White Spot Syndrome Virus in Litopenaeus vannamei. Aquaculture 338–341, 2–12 (2012).
80. Yogeeswaran, A. et al. Protection of Penaeus monodon against white spot syndrome virus by inactivated vaccine with herbal immunostimulants. Fish Shellfish Immunol. 32, 1058–1067 (2012).
81. Nguyen, A. T. V. et al. Bacillus subtilis spores expressing the VP28 antigen: A potential oral treatment to protect Litopenaeus vannamei against white spot syndrome. FEMS Microbiol. Lett. 358, 202–208 (2014).
82. Jia, X. H. et al. Oral administration of Anabaena-expressed VP28 for both drug and food against white spot syndrome virus in shrimp. J. Appl. Phycol. 28, 1001–1009 (2016).
83. Chen, X., Chen, Y., Shen, X., Zuo, J. & Guo, H. The Improvement and Application of Lentivirus-Mediated Gene Transfer and Expression System in Penaeid Shrimp Cells. Mar. Biotechnol. 21, 9–18 (2019).
84. Chaimongkon, D., Assavalapsakul, W., Panyim, S. & Attasart, P. A multi-target dsRNA for simultaneous inhibition of yellow head virus and white spot syndrome virus in shrimp. J. Biotechnol. 321, 48–56 (2020).
85. Wang, X.-W., Xu, Y.-H., Xu, J.-D., Zhao, X.-F. & Wang, J.-X. Collaboration between a Soluble C-Type Lectin and Calreticulin Facilitates White Spot Syndrome Virus Infection in Shrimp. J. Immunol. 193, 2106–2117 (2014).
86. Sanjuktha, M. et al. Comparative efficacy of double-stranded RNAs targeting WSSV structural and nonstructural genes in controlling viral multiplication in Penaeus monodon. Arch. Virol. 157, 993–998 (2012).
87. Guertler, C. Defesa antiviral em Litopenaeus vannamei contra o vírus da síndrome da mancha branca (WSSV), induzida via RNA de interferência, e sua influência na expressão de alguns genes imunológicos. (2012).
88. Wang, W. et al. LvPPAE2 induced by WSV056 confers host defense against WSSV in Litopenaeus vannamei. Fish Shellfish Immunol. 96, 319–329 (2020).
89. Huang, H. T. et al. Synthesis and evaluation of polyamine carbon quantum dots (CQDs) in Litopenaeus vannamei as a therapeutic agent against WSSV. Sci. Rep. 10, 1–11 (2020).
90. Mondal, D., Dutta, S., Chakrabarty, U., Mallik, A. & Mandal, N. Development and characterization of white spot disease linked microsatellite DNA markers in Penaeus monodon, and their application to determine the population diversity, cluster and structure. J. Invertebr. Pathol. 168, 107275 (2019).
91. Park, N. H. et al. Fusion of flagellin 2 with bivalent white spot syndrome virus vaccine increases survival in freshwater shrimp. J. Invertebr. Pathol. 144, 97–105 (2017).
92. Rattanarojpong, T., Khankaew, S., Khunrae, P., Vanichviriyakit, R. & Poomputsa, K. Recombinant baculovirus mediates dsRNA specific to rr2 delivery and its protective efficacy against WSSV infection. Journal of Biotechnology vol. 229 (Elsevier BV, 2016).
93. Valdez, A., Yepiz-Plascencia, G., Ricca, E. & Olmos, J. First Litopenaeus vannamei WSSV 100% oral vaccination protection using CotC::Vp26 fusion protein displayed on Bacillus subtilis spores surface. J. Appl. Microbiol. 117, 347–357 (2014).
94. Dharnappa S, A. et al. Protection of Litopenaeus vannamei against White Spot Syndrome Virus (WSSV) Using Bacterially Expressed Recombinant Envelope Proteins VP39 and VP28. (2014).
95. Zhu, F. & Zhang, X. Protection of Shrimp against White Spot Syndrome Virus (WSSV) with β-1,3-d-glucan-encapsulated vp28-siRNA Particles. Mar. Biotechnol. 14, 63–68 (2012).
96. Satoh, J. Studies on prevention measure of white spot disease of kuruma shrimp Marsupenaeus japonicus. 57–110 (2012).
97. Thomas, A. et al. Immunogenicity and protective efficacy of a major White Spot Syndrome Virus (WSSV) envelope protein VP24 expressed in Escherichia coli against WSSV. J. Invertebr. Pathol. 123, 17–24 (2014).
98. Huang, P. Y., Huang, Y. H., Leu, J. H. & Chen, L. L. Feasibility study on the use of fly maggots (Musca domestica) as carriers to inhibit shrimp white spot syndrome. Life 11, (2021).
99. Puneeth, T. G. et al. Protective efficacy of recombinant wsv477 protein against white spot syndrome virus infection in the tiger shrimp Penaeus monodon. Indian J. Fish. 68, 76–81 (2021).
100. Thagun, C., Srisala, J., Sritunyalucksana, K., Narangajavana, J. & Sojikul, P. Arabidopsis-derived shrimp viral-binding protein, PmRab7 can protect white spot syndrome virus infection in shrimp. J. Biotechnol. 161, 60–67 (2012).
101. Pantoja, M. J. A. A. M. A. B. J. C.-A. D. V. L. E. S. M. A. M. L. P. M. S. M. C. C., Coze, L. M. P. R. D. R. A. S. & Gesteira, T. C. V. Patología e Inmunología de Camarones Penaeidos. (2008).
102. Robinson, N. A. et al. QTL for white spot syndrome virus resistance and the sex-determining locus in the Indian black tiger shrimp (Penaeus monodon). BMC Genomics 15, 1–21 (2014).
103. Mu, Y. et al. A vector that expresses VP28 of WSSV can protect red swamp crayfish from white spot disease. Dev. Comp. Immunol. 36, 442–449 (2012).
104. Wang, W., Pan, C., Huang, Z., Yuan, H. & Chen, J. WSV181 inhibits JAK / STAT signaling and promotes viral replication in Drosophila. Dev. Comp. Immunol. (2018) doi:10.1016/j.dci.2018.11.003.

105. Kulkarni, A. D., Viswanath, K., Rombouta, J. H. W. M. & Brinchmanna, M. F. Protein profiling in the gut of Penaeus monodon gavaged with oral WSSV-vaccines and live white spot syndrome virus Authors: Amod D. Kulkarni. 1–48 (2014) doi:10.1002/pmic.201300405.This.
106. Moraes, A. B. D., DE Moraes, D. C. S., Alencar, C. E. R. D. & Freire, F. A. M. Native and non-native species of Litopenaeus Pérez-Farfante, 1969 (Crustacea: Penaeidae) from the East Atlantic: Geometric morphometrics as a tool for taxonomic discrimination. An. Acad. Bras. Cienc. 93, e20200107 (2021).
107. Cuéllar-Anjel, J. et al. Enfermedades virales de los camarones. Guía técnica -Patología e inmunología de camarones penaeidos (2014).
108. Phanse, Y. et al. RNA Nanovaccine Protects against White Spot Syndrome Virus in Shrimp. Vaccines 10, (2022).
109. Arancibia Cano, E. I. & Cáceres Balmaceda, D. Comparación del ritmo de crecimiento del Litopenaeus vannamei y las fluctuaciones de los parámetros físicos, químicos y biológicos, de los estanques 1 y 2 de la granja camaronera Playa Hermosa, en el periodo comprendido de Abril a Junio del 2017. Univ. Nac. Autónoma Nicar. 1, 1–22 (2018).
110. Fischer, W. et al. Guía FAO para la identificación de especies para los fines de pesca. Guía FAO para la Identificacion de Especies para los Fines de la Pesca. Pacífico Centro-Oriental. Vol. 1. Plantas e Invertebrados (1995).
111. Ruales, A. Evaluación del rendimiento del camarón (Litopenaeus vannamei) en cautiverio a través de un sistema de producción tradicional y un sistema de producción con aireadores de paletas. 1–112 (2012).
112. Zou, R. F., Ren, X. C. & Liu, Q. H. Characterization of Litopenaeus vannamei secreted protein acidic and rich in cysteine -like in WSSV infection. J. Invertebr. Pathol. 183, 107593 (2021).
113. Giraud, C. et al. The Active Microbiota of the Eggs and the Nauplii of the Pacific Blue Shrimp Litopenaeus stylirostris Partially Shaped by a Potential Vertical Transmission. Front. Microbiol. 13, (2022).
114. Gan, L. et al. Deciphering the virulent Vibrio harveyi causing spoilage in muscle of aquatic crustacean Litopenaeus vannamei. Sci. Rep. 12, 1–9 (2022).
115. Molla, M. H. R. & Aljahdali, M. O. Identification of phytochemical compounds to inhibit the matrix-like linker protein VP26 to block the assembles of White Spot syndrome Virus (WSSV) envelope and nucleocapsid protein of Marine Shrimp: In silico Approach. J. King Saud Univ. - Sci. 34, 102346 (2022).
116. Soulebot, J. P., Palya, V. J., Rweyemamu, M. & Sylla, D. Qualitiy assurance and good manofacturin practice. 130 (1992).
117. Heldens, J. G. M. et al. Veterinary vaccine development from an industrial perspective. Vet. J. 178, 7–20 (2008).
118. Schetters, T. Vaccine development from a commercial point of view. Vet. Parasitol. 57, 267–275 (1995).
119. Lara, A. R. Recombinant protein production in escherichia coli. Rev. Mex. Ing. Quim. 10, 209–223 (2011).
120. Vargas Pabón, L., Montoya Castaño, D. & Aristizábal Gutiérrez, F. Clonación y expresión en Escherichia coli de genes de celulasas de Clostridium IBUN 22A. Rev. Colomb. Biotecnol. 4, 29–35 (2002).
121. García, J. et al. Estrategias de obtención de proteínas recombinantes en escherichia coli. Vaccimonitor 22, 30–39 (2013).
122. Walker, P. J. & Mohan, C. V. Viral disease emergence in shrimp aquaculture: origins, impact and the effectiveness of health management strategies. Rev. Aquac. 1, 125–154 (2009).
123. Suzuki, S. et al. Science of the Total Environment Occurrence of sul and tet (M) genes in bacterial community in Japanese marine aquaculture environment throughout the year : Pro fi le compari- son with Taiwanese and Finnish aquaculture waters. Sci. Total Environ. 669, 649–656 (2019).
124. Zago, V., Veschetti, L., Patuzzo, C., Malerba, G. & Lleo, M. M. Shewanella algae and Vibrio spp . strains isolated in Italian aquaculture farms are reservoirs of antibiotic resistant genes that might constitute a risk for human health. Mar. Pollut. Bull. 154, 111057 (2020).
125. Zhu, Z. M., Dong, C. F., Weng, S. P. & He, J. G. The high prevalence of pathogenic Vibrio harveyi with multiple antibiotic resistance in scale drop and muscle necrosis disease of the hybrid grouper , Epinephelus fuscoguttatus (♀) 3 E . lanceolatus (♂), in China. 589–601 (2017) doi:10.1111/jfd.12758.
126. Iwasaki, A. & Medzhitov, R. Control of adaptive immunity by the innate immune system. Nat. Immunol. 16, 343–353 (2015).
127. Traifalgar, R. F. M., Corre, V. L. & Serrano, A. E. Efficacy of dietary immunostimulants to enhance the immunological responses and vibriosis resistance of juvenile Penaeus monodon. (2013) doi:10.3923/jfas.2013.340.354.
128. Vinay, T. et al. Vibrio harveyi biofilm as immunostimulant candidate for high-health pacific white shrimp, Penaeus vannamei farming. Fish Shellfish Immunol. (2019) doi:10.1016/j.fsi.2019.11.004.
129. Karunasagar, I., Pai, R., Malathi, G. R. & Karunasagar, I. Mass mortality of Penaeus monodon larvae due to antibiotic-resistant Vibrio harveyi infection. 128, 203–209 (1994).
130. Pilarski, F. et al. Different β-glucans improve the growth performance and bacterial resistance in Nile tilapia. Fish Shellfish Immunol. (2017) doi:10.1016/j.fsi.2017.06.059.
131. Ringø, E., Erik, R. & Ingvill, O. Application of vaccines and dietary supplements in aquaculture : possibilities and challenges. (2014) doi:10.1007/s11160-014-9361-y.
132. Saucedo-Vázquez, J.P.; Gushque, F.; Vispo, N.S.; Rodriguez, J.; Gudiño-Gomezjurado, M.E.; Albericio, F.; Tellkamp, M.P.; Alexis, F. Marine Arthropods as a Source of Antimicrobial Peptides. Mar. Drugs 2022, 20, 501. https://doi.org/10.3390/md20080501

REVIEW / ARTÍCULO DE REVISIÓN

Production of nanobodies in Andean camelids and their most common applications: A general review in the medical field

C. P. Ortega[1], L. M. Rivera[3], L. E. Trujillo[1,2]

DOI. 10.21931/RB/2023.08.02.13

[1] Departamento de Ciencias de la Vida y la Agricultura, Laboratorio Multidisciplinario, Universidad de las Fuerzas Armadas – ESPE, Sangolquí, Ecuador.
[2] Centro de Nanociencia y Nanotecnología – CENCINAT, Universidad de las Fuerzas Armadas ESPE, Sangolquí, Ecuador
[3] Universidad Técnica de Machala, Machala, Ecuador
Corresponding author: letrujillo3@espe.edu.ec

Abstract: The heavy chain fraction present in Camelidae antibodies is so-called nanobodies. They have different characteristics when compared to immunoglobulin G, like more diminutive size, higher affinity, shorter half-life in serum, etc. These proteins are codified by B lymphocytes cDNAs and can be produced in different hosts like *Escherichia Coli, Pichia Pastoris*, plant cells and even insect cells. Andean camelids have been mainly used in the Andean region of South America as transport means and source of raw materials like fibers and meat, then being of great economic importance. However, in Ecuador, the potential of these animals as a source of biomedical products has not been investigated or exploited yet. Due to the scarce information related to these molecules and their industrial production in the country, this review aims to remark on the most common medical application of nanobodies produced from Andean camelids; also, industrial applications are described.

Key words: Cancer, Coronavirus, VHH, production, treatment, diagnosis.

Introduction

Camelid produces antibodies composed of heavy chain constant domains and a single variable domain; this variable domain is known as nanobody (Nb). It possesses a single antigen-binding domain called VHH[1,2]. Antibodies with a single variable chain, known as vNARs, have also been reported in the fish subclass Elasmobranchii to which sharks and rays belong[3-5]. Phylogenetic studies have shown that antibodies from Camelidae and Elasmobranchii evolved independently[6,7]. In recent years, Nb has been used as therapeutic agents, in diagnostic tests and as research tools[8-10]. Camelidae and Elasmobranchii possess different kinds of antibodies[6], but only the antibodies that lack the light chains are of interest in this review.

Camelidae is a family that includes the old-world camelids: -*Camelus dromedarius* (dromedaries), and *C. bactrianus* (camels)- and the new-world *camelids*[11-13]. There are four species of new-world *camelids* in South America[14,15]: *Lama glama* (llamas), *L. guanicoe* (guanacos), *Vicugna vicugna* (vicuñas) and *V. pacos* (alpacas). All of them represent a genetic resource of great importance, not only from a scientific point of view[16-18], since they could represent an opportunity for economic, social and technological development in Ecuador.

Nbs were first discovered and described by the Hamers-Casterman team[19] at the Free University of Brussels while analyzing *C. dromedarius* serum. The potential use of Nbs in the medical field is focused on the prevention, diagnosis and disease treatments[20,21]. Additionally, several preclinical and clinical studies regarding their use in phases 1 and 2[22,23]. The development of a drug at the laboratory scale until its sanitary registration takes about 10 years[24-26]. In fact, in 2019, the Food and Drug Administration (FDA) approved for the first time the therapeutic use of a humanized Nb[27]. Due to the great potential of Nbs, Steeland *et al.*[28] concluded that these molecules could be positioned as pharmaceuticals in a short period for daily use.

The main objective of this review is to describe the most common medical application of nanobodies produced from *Andean camelids* to demonstrate the potential of these molecules as a medical product. In addition, a little overview of its recombinant production in different biotechnological hosts and other industrial fields is described.

Immunoglobulin G VS Nanobodies

Structurally, immunoglobulins G possess 2 light and 4 heavy chains. Heavy chains contain 3 constant domains and 1 variable domain (VH), while the light chains contain 1 constant and 1 variable domain (VL)[29,30]. However, Camelidae antibodies lack the light chain[31], and their 3 chains are composed of 2 constant domains and 1 variable domain (Nb)[32,33]. In addition, *Camelidae*-like shark antibodies (which lack a light chain and possess 7 chains) are called New Antigen Receptors (NAR) antibodies[34]. They comprise 5 constant domains and 1 variable domain (vNAR)[6,35]. Figure 1 shows the structural comparison between mammalian IgG and the IgG-like antibodies from Elasmobranchii and Camelidae. Figure 2 shows the alignment of Elasmobranchii vNAR, Camelidae Nb and a *Mus musculus* heavy chain antibody sequences.

The figure shows the amino acid variation between vNAR, VHH and mAb heavy chains. In parenthesis protein name according to DATA bank information.

Despite the biotechnological importance of immunoglo-

Citation: HOrtega C P, Rivera L M, Trujillo L E. Production of nanobodies in Andean camelids and their most common applications: A general review in the medical field. Revis Bionatura 2023;8 (2) 13. http://dx.doi.org/10.21931/RB/2023.08.02.13
Received: 2 January 2023 / **Accepted:** 13 March 2023 / **Published:** 15 June 2023

Publisher's Note: Bionatura stays neutral with regard to jurisdictional claims in published maps and institutional affiliations.

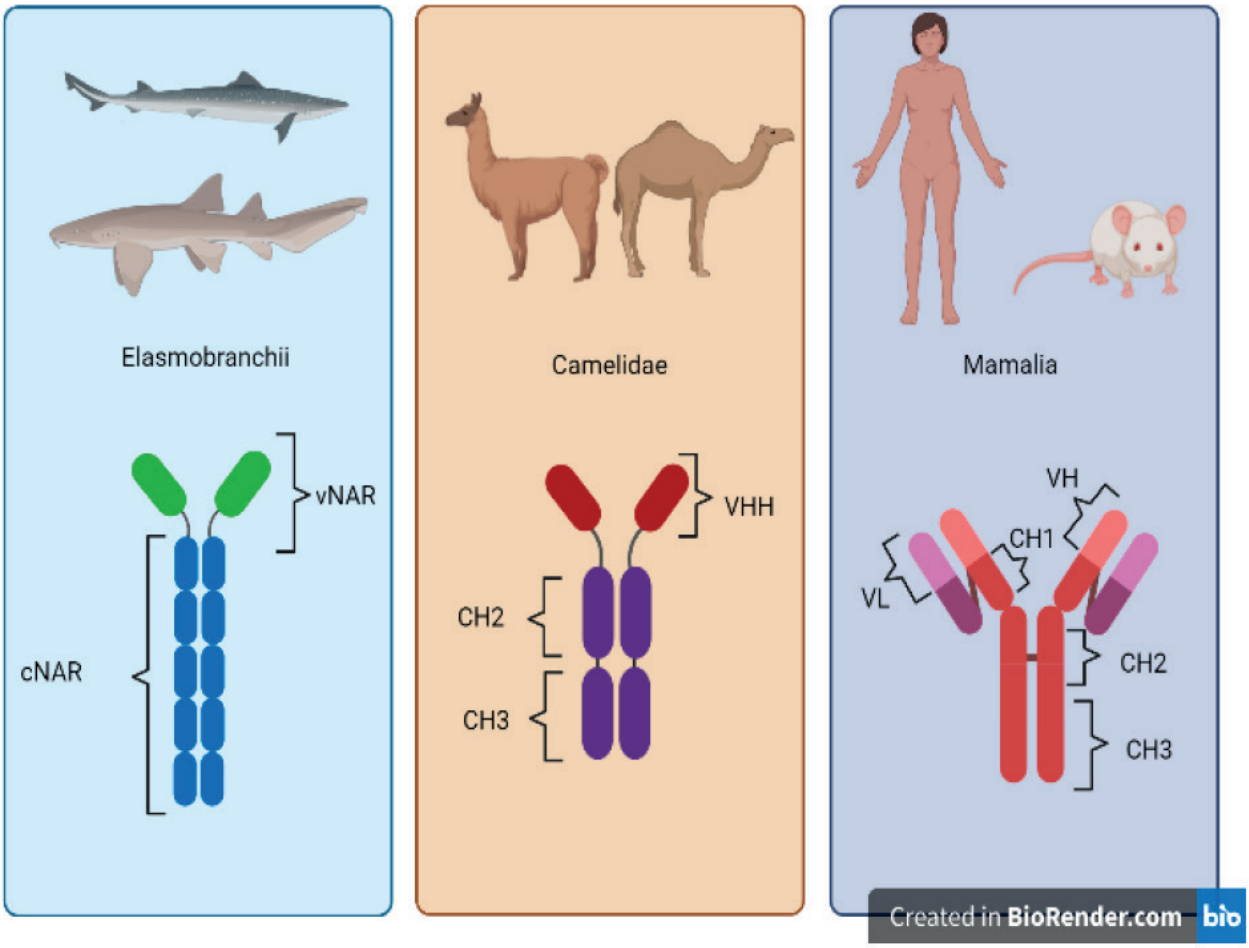

Figure 1. Structural comparison between IgG-like Elasmobranchii, Camelidae and Mammalian antibodies. *Elasmobranchii* antibodies possess a variable region called vNAR and a constant region composed of five constant domains (cNAR). *Camelidae antibodies* are conformed by one variable heavy chain domain (VHH) and 2 constant heavy chain domains (CH2 and CH3). Mammalian antibodies are composed of one variable heavy chain domain (VH), three constant heavy chain domains (CH1, CH2, CH3) and a constant light chain domain (VL).

bulin G, Nbs have certain differences over IgG, which are summarized in Table 1.

The main Nbs disadvantage is their low half-life in human blood serum because they are filtered by the kidney in 26 to 60 minutes[46-48]. However, they have low toxicity and can be eliminated from the human body by filtration by the kidneys[49]. Nbs have a low immunogenicity risk profile, which drives their use to develop potential clinical applications[50]. Using Nbs conjugated with small molecules like drugs, toxins, enzymes and imaging agents allows an approach to target sites with low systemic toxicity[51]. In addition, Nbs do not present the solubility and aggregation problems typical of conventional antibodies due to their hydrophilicity[36,52].

The size of a camelid antibody is around 95 kDA[53-55] due to the absence of the light chain; Elasmobranchii antibodies size is about 175 kDA[56] while the variable antigen-binding domains (Nbs and vNAR) measure between 12 and 15 kDA[46,56,57]. There is a vast difference between the IgG medical development and the research performed on Nbs and vNAR molecules[58]. Nevertheless, Nb and vNAR have similar advantages to the IgG (more specificity, smaller capacity to bind crypto antigens, more stability)[59,60]. Figure 3 represents the 3D structure of a Nb, a vNAR and a Mus musculus monoclonal antibody (mAb). This figure shows that the Nb and vNAR structures are smaller and more straightforward than the *M. musculus* mAb, facilitating their production[58].

How are Nanobodies produced?

The development of Nb libraries can be achieved from a naive or synthetic source or by immunization. All of them are great ways to get the appropriate Nb that best meets the final research goal. For this reason, Nbs are expressed and produced at a large scale in the chosen host[64]. Libraries obtained by immunization are the most widely used and consist in injecting the animal with the correct antigen[65]. Native libraries are developed from non-immunized camelids blood[66], and synthetic libraries are developed from a determined sequence framework[67,68] or the target antigen[69], from which randomization of oligonucleotides in the hypervariable regions is performed[70].nThe yields in the production of Nbs from immune libraries and synthetic libraries can vary significantly[71].

Figure 1 shows a general diagram for Nb production by immunization. This process starts with the inoculation of a young-adult camelid with 50 to 200 µg of the chosen antigen[72]. After the first immunization, the animal must be injected from 4 to 8 times during 2 months[64]. Once the immunization process is completed, the camelid's blood must be extracted and B lymphocytes purified. Further, B lymphocyte mRNA is isolated, purified and recovered to finally get the total complementary cDNA using polymerase chain reaction (PCR) techniques[73,74].

Then, a Nb library is generated from the above-obtai-

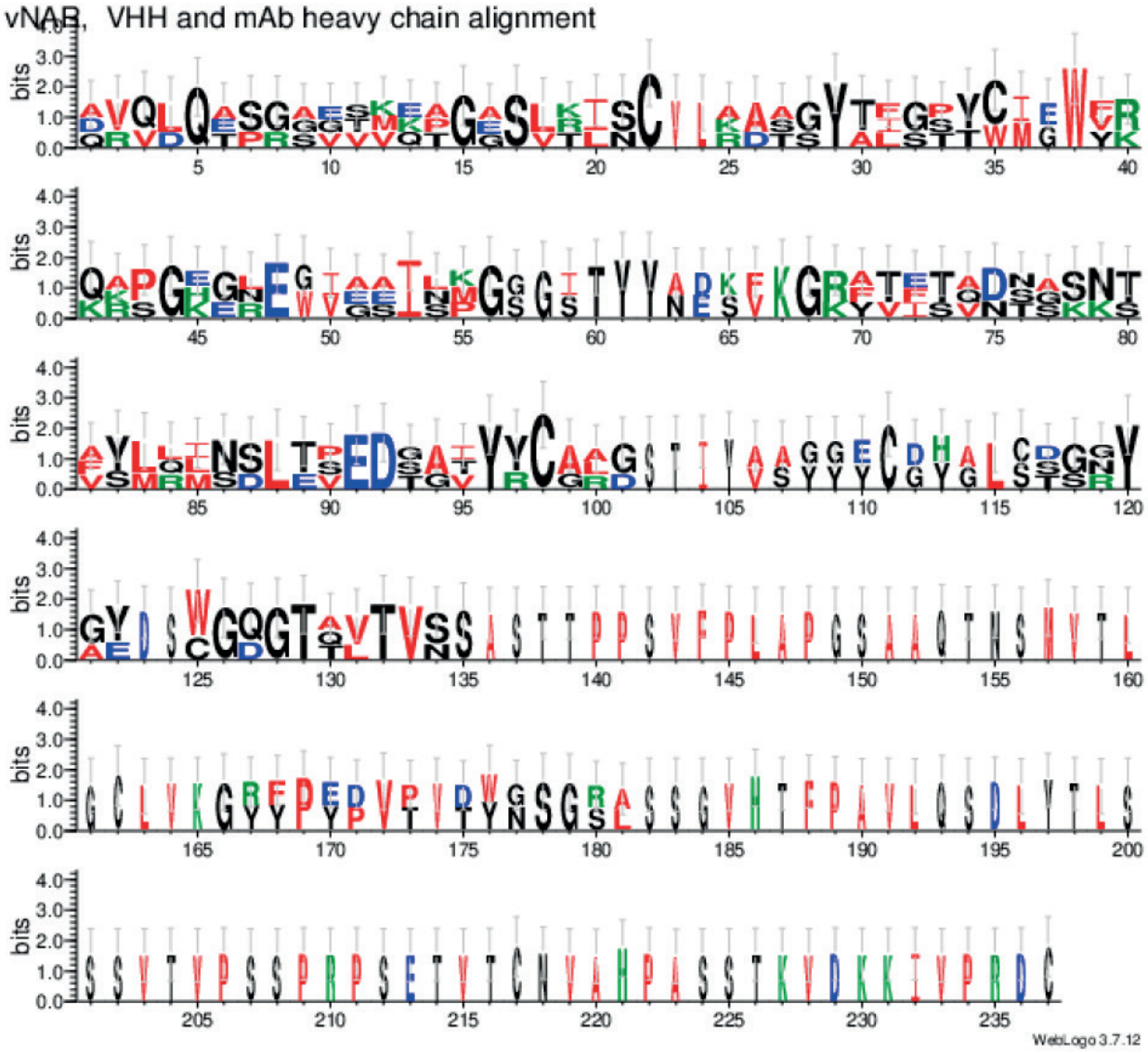

Figure 2. Sequence logo plot of the alignment of vNAR (1T6V), VHH (1MEL) and monoclonal *Mus musculus* heavy chain (1MLC).

ned cDNA, for which the VHH regions are amplified using specific primers[73,75]. Muyldermans (2021) research suggests that the amplification of the VHH regions should be performed using mainly the nested PCR technique[64].

From the PCR products, a gene library is generated[67]; then the fragments must be chosen by a display technique; the most common technique is the phage display[64]. The phage display library consists of bacteriophages with the antigenic molecule (Nb) in their coat; then, all the library is exposed to the specific antigen[76]. Finally, the selected fragments are screened and then chosen those that produce specific Nbs for the particular antigen[64,73,75,77].

The selected VHH sequences are cloned at the industrial level in appropriate hosts like bacteria such as *Escherichia coli*[64,78,79] or yeasts such as *Pichia pastoris*[75]. Mammalian cells[73], insects or plants[71] are also excellent options as industrial production hosts[80]. Table 2 exposes the kind of expression and yields of the different host cells. Finally, the proteins are extracted and purified, generally using the ammonium sulfate precipitation method in conjunction with other types of chromatography[73] as shown in Figure 1.

Applications of camelid nanobodies in Human Health

The small Nb size, joined with their high stability, solubility and a great capacity to recognize crypto-antigens place them as excellent alternatives for the prevention[86], diagnosis[87,88] and human diseases treatment[46,89,90].

Disease diagnosis using Nbs points to:1- the generation of images from tissues and organs[57,91]; and 2- the performance of immunoassays to detect pathogen antigens[89,92,93]. Meanwhile, nanobodies as a therapeutic agents seek to attack an antigen, mainly to block virus replication[94,95] or bacteria growth[96].

Another novel application is their use in antiphonic serums as neutralizers and blockers of toxins present in different types of poisons[97-99].

Finally, a search was made for medical applications of nanobodies developed in Andean camelids. About 518 articles were found using the "Publish or perish" program where Andean camelids were used. The reported applications belonged mainly to the health branch and articles published in the last 5 years including 50 scientific publications that were not review articles.

Using descriptive statistics and frequency histograms, it

Immunoglobulin G	Nanobodies
It has two variable domains: VH and VL. The latter provides stability and antigen-binding specificity.	The only variable domain it possesses is the VHHs; they have high stability despite lacking VLs.
They have a large size (150 kDa).	They are one-tenth the size of traditional antibodies (15 KDa), increasing the permeability of the molecule.
Low tissue permeability.	It can be entered into different types of tissues.
They may have flat surfaces, making them difficult to attach to specific antigen sites.	Its configuration allows it to bind to crypto antigens like protein cleavages and enzyme active sites.
It has low resistance to proteolysis and thermal denaturation.	They have a high resistance to proteolysis and thermal denaturation.

Information is taken from [36–45]. VH=Variable Heavy domine, VL= Variable Light domine.

Table 1. Comparison between conventional antibodies and nanobodies.

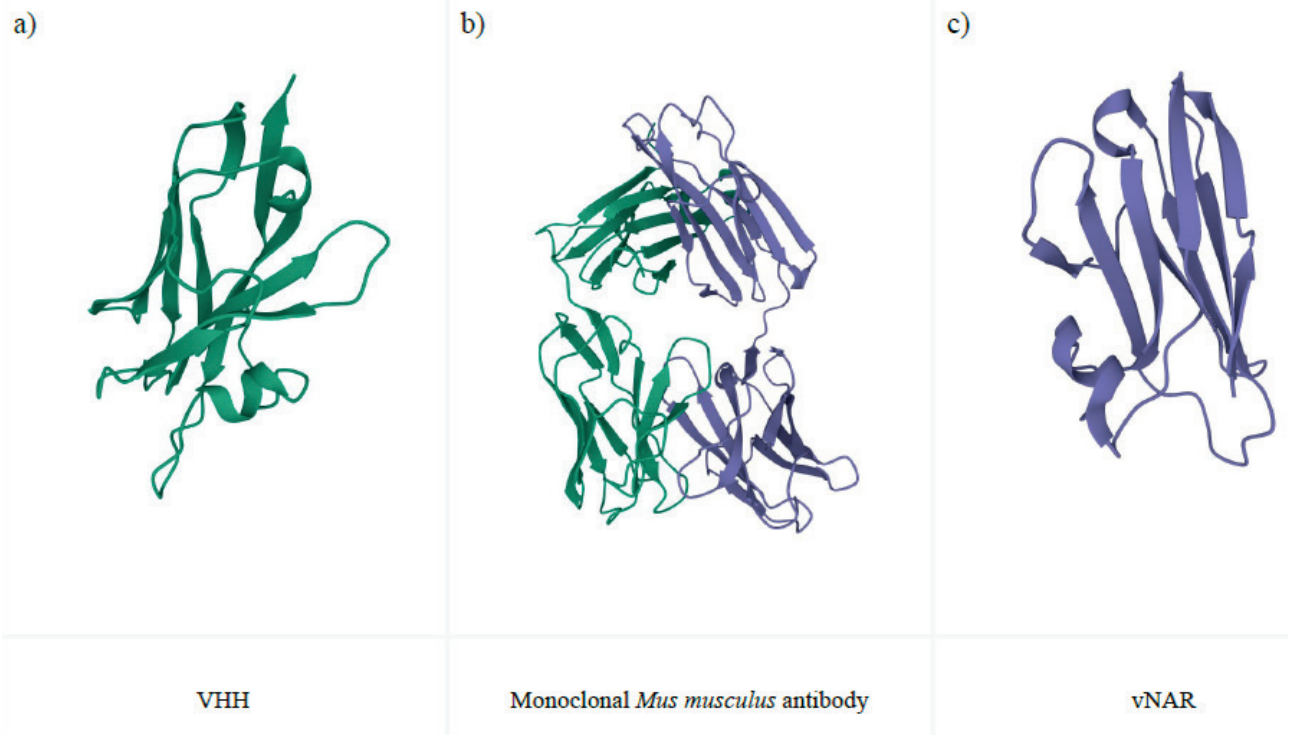

Figure 3. 3D structure of antibody domains. a) VHH (1MEL). b) mAb of *Mus musculus* (1MLC). c) cNAR (1T6V). Information and images are taken from[61-63].

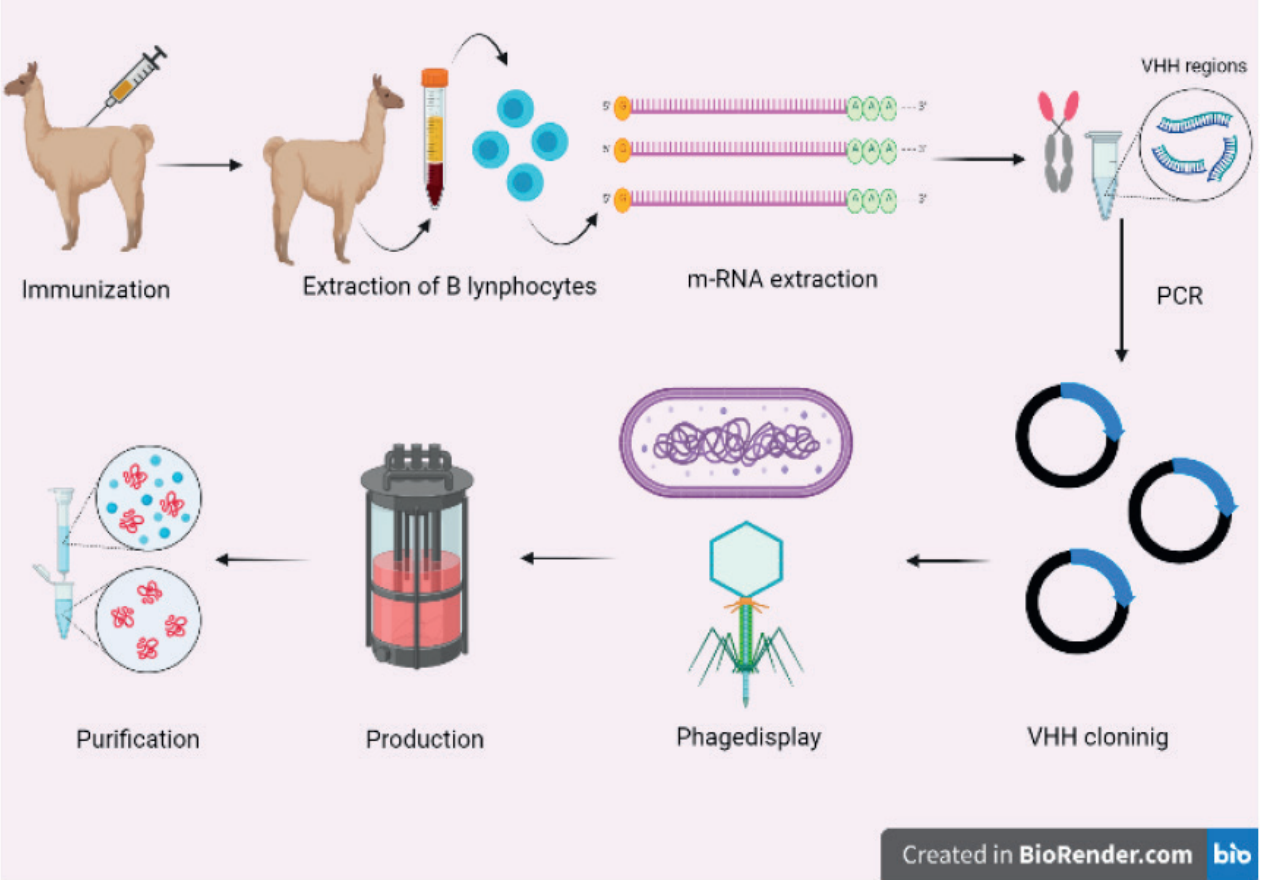

Figure 4. Production process of recombinant nanobodies. The first step is to immunize the camelide. Then, the B lymphocytes must be extracted and purified to extract m-RNA. The VHH sequences are obtained by PCR. Thereafter, the nanobody sequences are selected by phage display (or any display method). Finally, the chosen nanobodies are produced recombinantly and purified.

Author	Host	Kind of Expression	Yield
T. Iwaki, *et al* (2020)	*E. coli*	Extracellular	1.67-13.3 mg/L
Ruano-Gallegos, *et al* (2019)	*E. coli*	Extracellular	0.3–1.3 mg/L
Chen, *et al* (2018)	*P. pastoris*	Extracellular	46.68-51.71 mg/L
Sheikholeslami, *et al* (2010)	*P. pastoris*	Extracellular	0.3–0.5 mg/L
Shokrollahi, et al (2021)	insect cells	Intracellular	equal as bacterial systems
Wang *et al,* (2021)	Plant cells	Intracellular	1.7%of total soluble proteins 30% f total leaf protein

Information is taken from [37,81–85]

Table 2. Comparison between conventional antibodies and nanobodies.

was determined that the most common application of Nbs is the treatment and diagnosis of infectious diseases (Figure 3). However, the condition for which the largest number of Nbs have been developed was cancer (Figure 4).

The 2020 pandemic greatly spurred the development of Nbs and other pharmaceuticals for the treatment and/or diagnosis of COVID-19[100,101]. However, Nbs development focused on diagnosis, as shown in table 3; cancer treatment has been developed since before 2020.

Cancer is a disease in which uncontrolled cell multiplication can spread to other parts of the body[102]. Alternatives for cancer prevention have existed since the 1700s[103], and their treatments include surgeries, chemotherapies, radiotherapies, immunotherapies and hormone therapies[104]. Nbs have a good synergy with these treatments[105], so they could be used together, although the full range of Nbs applications in cancer has not yet been explored thoroughly[106,107].

On the other hand, COVID-19 caused by SARS-CoV-2 generates affections on the respiratory system[108]. On March 11 of 2020, the World Health Organization (WHO) declared a world pandemic for this infection[109]. There is still no defined treatment for this disease, although monoclonal antibodies[100,110] and nanobodies seem to be the best option to fight the virus[111-113]. The future evolution of the virus must be awaited as it could generate less infectious and virulent variants or more aggressive strains resistant to the current preventive treatments[114].

Applications of camelid nanobodies in different branches of industry

The main focuses of Nbs in plants are to protect crops by providing immunity against pathogens[72,85] and rapid

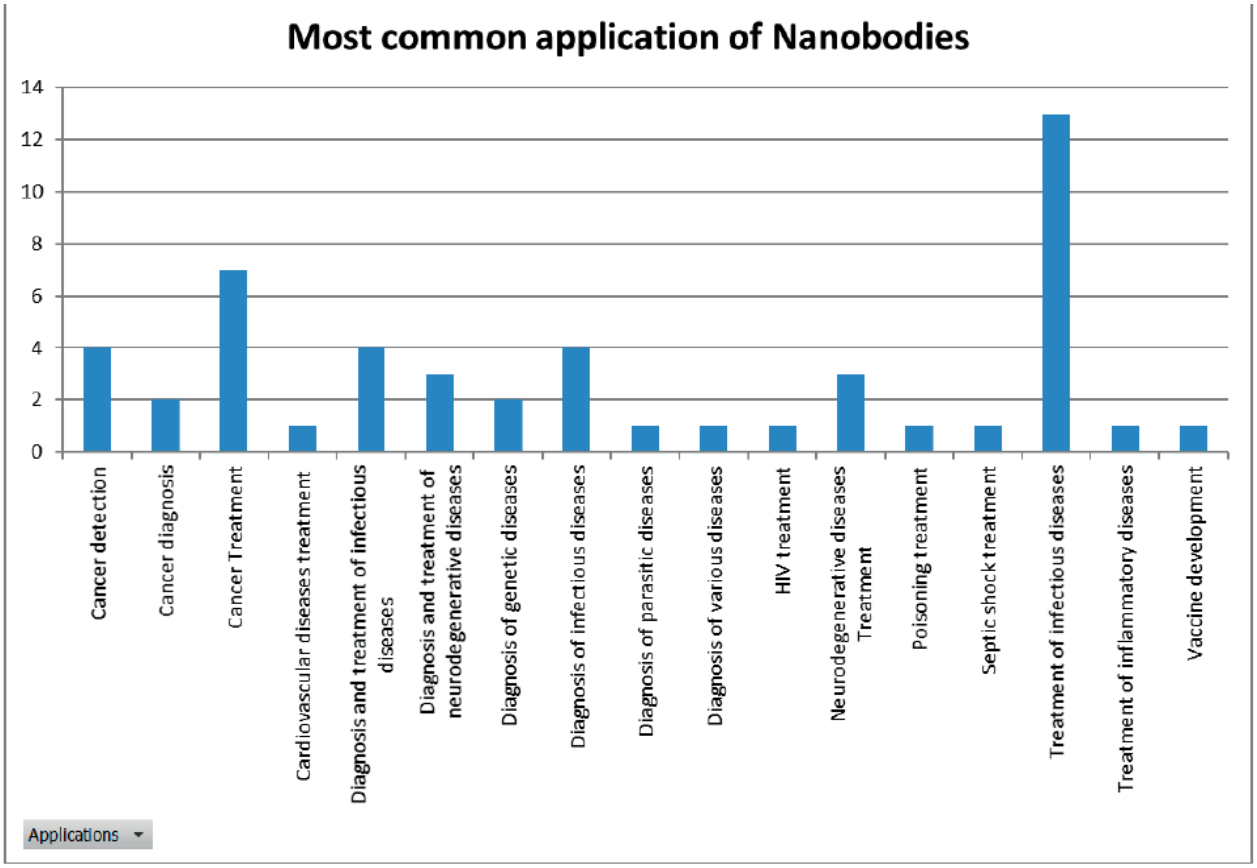

Figure 5. Most common applications of nanobodies.

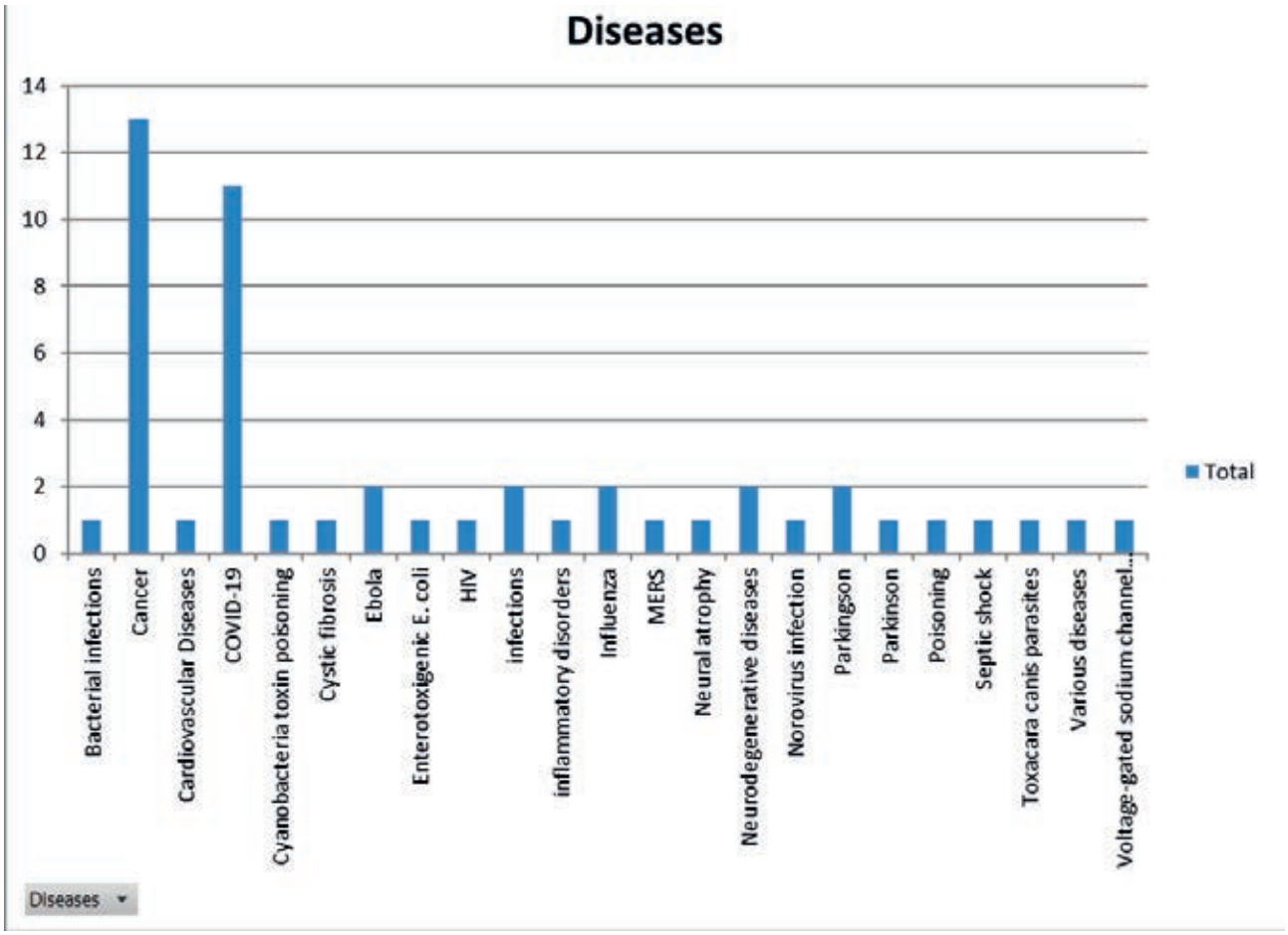

Figure 6. Diseases for which nanobodies were developed.

		Year of nanobodies development.					
Published papers on the development of nanobodies in Andean camelids	**Disease**	**2018**	**2019**	**2020**	**2021**	**2022**	**Total**
	Cancer	5	2	4	1	1	13
	COVID-19	0	0	2	8	1	11

Table 3. Comparison between published papers reporting the development of Nanobodies in Andean camelids for cancer and COVID-19.

detection of toxins that may affect food safety[115]. Passive immunity is the use of external antibodies to protect a patient[116-118]; this concept can be extrapolated to plants, where antibodies would protect them against pathogens[85,119,120]. On the other hand, Nbs can identify toxins in absorbance, fluorescence or Enzyme-Linked ImmunoSorbent Assay (ELISA) tests, depending on the toxin to be tested[121-123].

In the livestock sector, the main Nbs application is on early disease detection[124,125] to avoid zoonoses[3,126,127]. Nbs can also provide passive immunity in animals, especially those sensitive to diseases after weaning, such as piglets[128]. This is very important to avoid using antibiotics that could generate resistant bacterial strains[89,129].

Nanobodies used in water and soil allow the quick and accurate identification and detection of toxins and contaminants to the nanogram levels so, becoming a handy tool for these purposes[130-132].

The ability of nanobodies to bind to specific compounds makes them good alternatives in high-affinity chromatography[133,134]. They can also help to determine the protein structure[135] with dynamic properties in case of proteins with various conformations and shapes which are difficult to solubilize[64,136]. Another application is identifying protein functions and protein-protein interactions by mass spectrometry that could replace conventional antibodies by Nbs[137].

The use of intrabodies that consist of nucleic acid sequences with the genetic coding information of an antibody or Nb[138,139] that can be expressed inside a cell to modify cellular activity[140,141]. This biological application could be used to alter cellular functions[142], blocking or reducing the activity of endogenous proteins[143].

Future Perspectives and Conclusions

This mini-review presented applications of nanobodies that could promote the use of Andean camelids in Ecuador as new sources of products of high social, economic and public health interest.

The SARS-CoV-2 virus generated a global health crisis. Therefore, several methods for the diagnosis of COVID-19 were rapidly developed[144]. Nonetheless, there is still no defined treatment[100,110]. Becker's study in 2020[145] e mentions that a great deal of research is being carried out, mainly focused on blocking the replication and translation of the virus RNA; moreover, some treatments seek to block the binding of the virus and its ACE2 receptors[146-148] so, Nbs could be used as therapeutic molecules against COVID-19.

Ecuador has the greatest number of reptile species per unit area; one of the groups of greatest interest are snakes. Among them, about 35 species are reported to be venomous and are distributed along the Ecuadorian coast and Amazon[149]. On the other hand, scorpions, of which 40 species are known to be venomous, have been little studied[150]. In the past, serums to treat poisonings were produced by the "Instituto Nacional de Investigación en Salud Pública" INSPI, but production was suspended in 2014 so only antivenoms were imported[151]. In 2022, INSPI produced a batch of 300 experimental antivenom sera[152]. The Nbs could be used to act as high-affinity antivenom.

The incidence of cancer in Ecuador is 61% in women while 41% in men[153]; the types of cancer most reported in male patients are prostate, lymphoma and stomach[154], while for female patients, they are breast cancer, cervix and lymphoid leukemia[153]. Nanobodies could be an interesting alternative for treating these types of cancer in Ecuador. However, the fact that they are rapidly filtered by the kidney makes them less attractive as a therapeutic alternative[58].

In conclusion, the most common application of Nbs after analyzing more than 50 articles was the treatment and diagnosis of infectious diseases in cancer, so the future development of nanobodies should be linked to the treatment and diagnosis of these diseases. It is suggested that Nbs that achieve a balance between tissue permeability and a longer half-life in serum be developed for treating diseases such as cancer. However, other exciting applications in other fields are also not ruled out for the use of nanobodies.

Bibliographic references

1. ALLELE-Biotechnology. Nanoantibodies [Internet]. Nanobodies. 2020. Disponible en: https://www.allelebiotech.com/nanoantibodies
2. Mir MA, Mehraj U, Sheikh BA, Hamdani SS. Nanobodies: The "Magic Bullets" in therapeutics, drug delivery and diagnostics. Hum Antibodies. 13 de febrero de 2020;28(1):29-51.
3. Alvez R. Obtención de Nanobodies específicos contra ROR-1 y AgB de Echinococcus Granulosus [Internet]. Universidad de la República I; 2018. Disponible en: https://www.colibri.udelar.edu.uy/jspui/bitstream/20.500.12008/19174/1/uy24-19055.pdf
4. Mitch L. Mini-antibodies discovered in sharks and camels could lead to drugs for cancer and other diseases [Internet]. Science. 2018. Disponible en: https://www.sciencemag.org/news/2018/05/mini-antibodies-discovered-sharks-and-camels-could-lead-drugs-cancer-and-other-diseases
5. Stanfield RL, Dooley H, Flajnik MF, Wilson IA. Crystal Structure of a Shark Single-Domain Antibody V Region in Complex with Lysozyme. Science. 17 de septiembre de 2004;305(5691):1770-3.

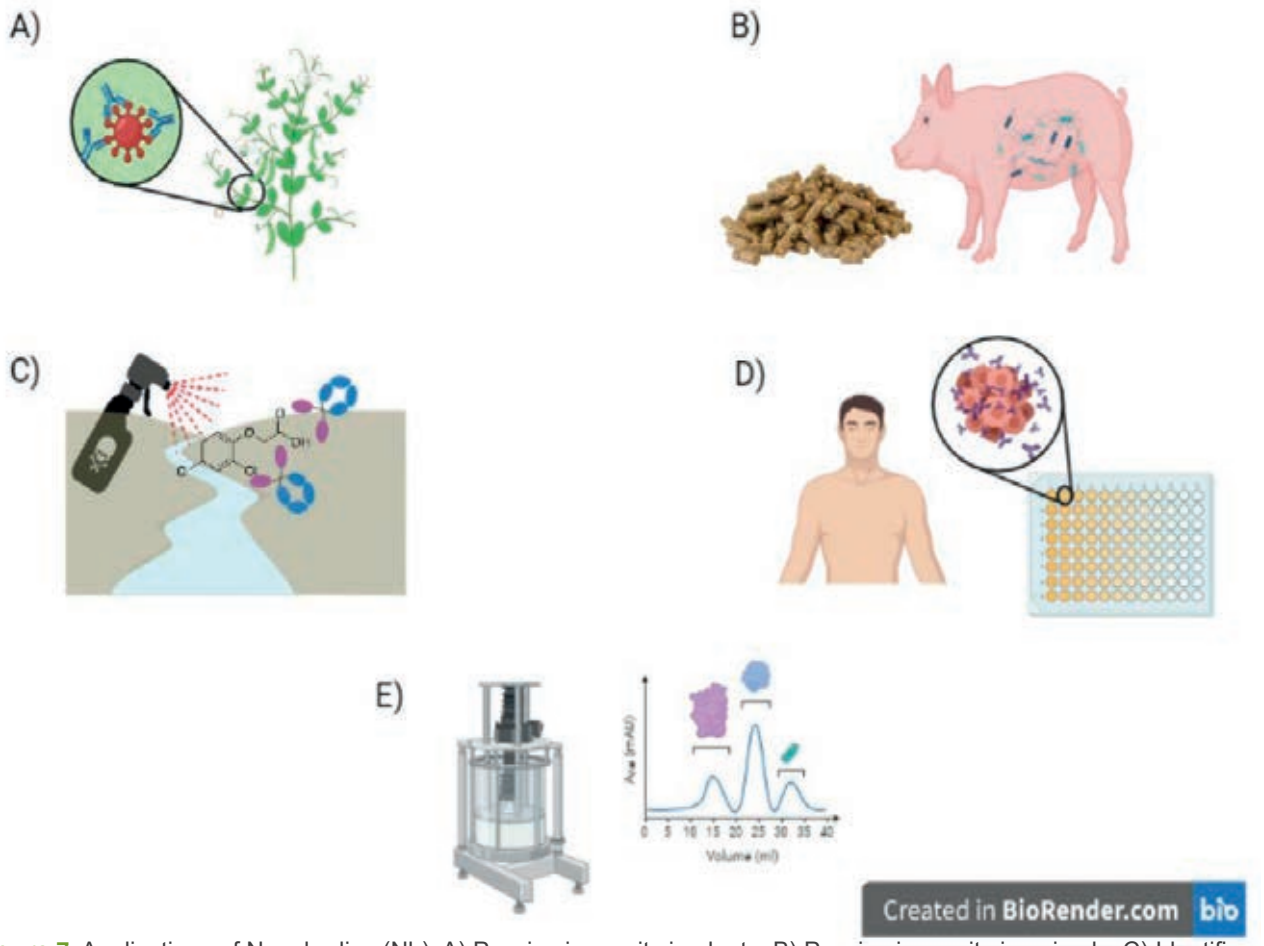

Figure 7. Applications of Nanobodies (Nb). A) Passive immunity in plants. B) Passive immunity in animals. C) Identification of contaminants in soil and water, D) Identification of human diseases. E) Nbs as a solid phase in chromatography.

6. Matamoros, Alcivar E Ivanova,, González, Avilés M Selena,. Study review of camelid and shark antibodies for biomedical and biotechnological applications. Bionatura. 15 de noviembre de 2021;6(4):2331-40.
7. Flajnik M, Deschacht N, Muyldermans S. A Case Of Convergence: Why Did a Simple Alternative toCanonical Antibodies Arise in Sharks and Camels. PLOS Biol [Internet]. 2011;9. Disponible en: https://journals.plos.org/plosbiology/article/citation?id=10.1371/journal.pbio.1001120
8. Hersh L. Nanobodies®: The «hot» new research tool. [Internet]. Nanobodies®: The «hot» new research tool. 2021. Disponible en: https://cobre.med.uky.edu/cobre-nanobody#:~:text=The%20nanobodies%20to%20your%20protein,as%20its%20sequence%20as%20deliverables.&text=In%20many%20cases%20our%20core,mammalian%20cells%20and%20purifying%20it.
9. Scarrone M, González-Techera A, Alvez-Rosado R, Delfin-Riela T, Modernell Á, González-Sapienza G, et al. Development of anti-human IgM nanobodies as universal reagents for general immunodiagnostics. New Biotechnol. septiembre de 2021;64:9-16.
10. Xu J, Kim AR, Cheloha RW, Fischer FA, Li JSS, Feng Y, et al. Protein visualization and manipulation in Drosophila through the use of epitope tags recognized by nanobodies. eLife. 25 de enero de 2022;11:e74326.
11. Cui P, Ji R, Ding F, Qi D, Gao H, Meng H, et al. A complete mitochondrial genome sequence of the wild two-humped camel (Camelus bactrianus ferus): an evolutionary history of camelidae. BMC Genomics. diciembre de 2007;8(1):241.
12. gnew D. Chapter 7 - Camelidae. 2018;22.
13. López P. EL PLEISTOCENO DE LA CUENCA DE CALAMA. 2018;1. Disponible en: https://www.researchgate.net/publication/323845017_Camelidae
14. Fundación Heifer Ecuador. CAMELIDOS SUDAMERICANOS [Internet]. Escuala Nacional de agro ecología; 2018. Disponible en: http://www.heifer-ecuador.org/wp-content/uploads/2018/03/22.-Camelidos-sudamericanos.pdf
15. Marín JC, Zapata B, González BA, Bonacic C, Wheeler JC, Casey C, et al. Sistemática, taxonomía y domesticación de alpacas y llamas: nueva evidencia cromosómica y molecular. Rev Chil Hist Nat [Internet]. junio de 2007 [citado 4 de agosto de 2022];80(2). Disponible en: http://www.scielo.cl/scielo.php?script=sci_arttext&pid=S0716-078X2007000200001&lng=en&nrm=iso&tlng=en
16. Durand MDC, Paytán A. La milenaria familia camelidae y el Nevado Huaytapallana. Universidad Continental, editor. Nat Soc [Internet]. 30 de junio de 2018 [citado 30 de mayo de 2022];01(01). Disponible en: http://journals.continental.edu.pe/index.php/naturalezaysociedad/article/view/425
17. FAO. 3.5. CAMÉLIDOS [Internet]. CAMÉLIDOS. 1989. Disponible en: https://www.fao.org/3/v8300s/v8300s18.htm
18. Avilés D, Montero M, Barros-Rodriguez. LOS CAMÉLIDOS SUDAMERICANOS: PRODUCTOS Y SUBPRODUCTOS USADOS EN LA REGIÓN ANDINA SOUTH AMERICAN CAMELIDS: PRODUCTS AND SUB-PRODUCTS USED IN THE ANDEAN REGION. Actas Iberoam En Conserv Anim. mayo de 2018;(11):30-8.
19. Hamers-Casterman C, Atarhouch T, Muyldermans S, Robinson G, Hamers C, Bajyana E, et al. Naturally occurring antibodies devid of ligth chains. Nature. 1993;363.
20. Khodabakhsh F, Behdani M, Rami A, Kazemi-Lomedasht F. Single-Domain Antibodies or Nanobodies: A Class of Next-Generation Antibodies. Int Rev Immunol. 3 de diciembre de 2018;37(6):316-22.

21. Muyldermans S. Applications of Nanobodies. Annu Rev Anim Biosci. 16 de febrero de 2021;9(1):401-21.
22. Chames P, Rothbauer U. Special Issue: Nanobody. Antibodies. 6 de marzo de 2020;9:4.
23. Boulenouar H, .Amar Y, Bouchoutrouch N, Faouzi MEA, Cherrah Y, Sefrioui H. Research Article Nanobodies and their medical applications. Genet Mol Res [Internet]. 2020 [citado 27 de junio de 2022];19(1). Disponible en: http://www.funpecrp.com.br/gmr/articles/year2020/vol19-1/pdf/gmr18452_-_nanobodies-and-their-medical-applications.pdf
24. World Healt Organization. Handbook : good laboratory practice (GLP)/ UNDP/World Bank/WHO Special Programme for Research and Training in Tropical Diseases [Internet]. 2001. Disponible en: https://apps.who.int/iris/bitstream/handle/10665/66894/TDR_PRD_GLP_01.2.pdf?sequence=1&isAllowed=y
25. Elsevier Connect. Fases de desarrollo de un nuevo fármaco [Internet]. Fases de desarrollo de un nuevo fármaco. 2020. Disponible en: https://www.elsevier.com/es-es/connect/medicina/edu-fases-de-desarrollo-de-un-nuevo-farmaco
26. Guerrero GAM. Las fases en el desarrollo de nuevos medicamentos. Medigraphic. 2009;5.
27. Morrison C. Nanobody approval gives domain antibodies a boost. Nat Rev Drug Discov. julio de 2019;18(7):485-7.
28. Steeland S, Vandenbroucke RE, Libert C. Nanobodies as therapeutics: big opportunities for small antibodies. Drug Discov Today. julio de 2016;21(7):1076-113.
29. Janeway C, Travers P, Walport M. Immunobiology: The Immune System in Health and Disease. 5th edition. [Internet]. Grand Science; 2001. Disponible en: https://www.ncbi.nlm.nih.gov/books/NBK27144/#:~:text=The%20IgG%20antibody%20molecule%20is,a%20flexible%20Y%2Dshaped%20structure
30. Gosnell W, Kramer K, Yamaga K. Immunology: Antibody Basics [Internet]. John A. Burns School of Medicine; 2008. Disponible en: https://jabsom.hawaii.edu/docs/Antibodies_Instructional_Module.pdf
31. Mitchell LS, Colwell LJ. Comparative analysis of nanobody sequence and structure data. Proteins Struct Funct Bioinforma. julio de 2018;86(7):697-706.
32. Schumacher D, Helma J, Schneider AFL, Leonhardt H, Hackenberger CPR. Nanobodies: Chemical Functionalization Strategies and Intracellular Applications. Angew Chem Int Ed. 23 de febrero de 2018;57(9):2314-33.
33. Kunz P, Zinner K, Mücke N, Bartoschik T, Muyldermans S, Hoheisel JD. The structural basis of nanobody unfolding reversibility and thermoresistance. Sci Rep. diciembre de 2018;8(1):7934.
34. Gauhar A, Privezentzev CV, Demydchuk M, Gerlza T, Rieger J, Kungl AJ, et al. Single domain shark VNAR antibodies neutralize SARS□CoV□2 infection in vitro. FASEB J [Internet]. noviembre de 2021 [citado 19 de agosto de 2022];35(11). Disponible en: https://onlinelibrary.wiley.com/doi/10.1096/fj.202100986RR
35. Cheong WS, Leow CY, Abdul Majeed AB, Leow CH. Diagnostic and therapeutic potential of shark variable new antigen receptor (VNAR) single domain antibody. Int J Biol Macromol. marzo de 2020;147:369-75.
36. Ryding S. VHH Antibodies (Nanobodies) Advantages and Limitations [Internet]. AZO Life Science. 2021. Disponible en: https://www.azolifesciences.com/article/VHH-Antibodies-(Nanobodies)-Advantages-and-Limitations.aspx
37. Ruano-Gallego D, Fraile S, Gutierrez C, Fernández LÁ. Screening and purification of nanobodies from E. coli culture supernatants using the hemolysin secretion system. Microb Cell Factories [Internet]. 11 de marzo de 2019 [citado 15 de mayo de 2021];18. Disponible en: https://www.ncbi.nlm.nih.gov/pmc/articles/PMC6410518/
38. Sandin S, Öfverstedt LG, Wikström AC, Wrange Ö, Skoglund U. Structure and Flexibility of Individual Immunoglobulin G Molecules in Solution. Structure. marzo de 2004;12(3):409-15.
39. Gettemans J, De Dobbelaer B. Transforming nanobodies into high-precision tools for protein function analysis. Am J Physiol-Cell Physiol. 1 de febrero de 2021;320(2):C195-215.
40. Tang Q, Owens RJ, Naismith JH. Structural Biology of Nanobodies against the Spike Protein of SARS-CoV-2. Viruses. 3 de noviembre de 2021;13(11):2214.
41. Cohen S. Antibody structure. J Clin Pathol. 1 de enero de 1975;s1-6(1):1-7.
42. Kunz P, Flock T, Soler N, Zaiss M, Vincke C, Sterckx Y, et al. Exploiting sequence and stability information for directing nanobody stability engineering. Biochim Biophys Acta BBA - Gen Subj. septiembre de 2017;1861(9):2196-205.
43. vinayagam M. Antibody Structure & Function [Internet]. Thiruvalluvar University; 2002. Disponible en: https://www.academia.edu/4978816/Antibody_Structure_and_Function
44. Kanmert D. Structure and interactions of human IgG-Fc. [Link??ping]: Department of Physics, Chemistry and Biology, Link??ping University; 2011.
45. Feige MJ, Hendershot LM, Buchner J. How antibodies fold. Trends Biochem Sci. abril de 2010;35(4):189-98.
46. Jovčevska I, Muyldermans S. The Therapeutic Potential of Nanobodies. Biodrugs. 2019;11-26.
47. Shen Z, Xiang Y, Vergara S, Chen A, Xiao Z, Santiago U, et al. A resource of high-quality and versatile nanobodies for drug delivery. iScience. septiembre de 2021;24(9):103014.
48. Shen Z, Xiang Y, Vegara S, Chen A, Xiao Z, Santiago U, et al. A robust and versatile nanobody platform for drug delivery [Internet]. Bioengineering; 2020 ago [citado 4 de agosto de 2022]. Disponible en: http://biorxiv.org/lookup/doi/10.1101/2020.08.19.257725
49. Schoonooghe S, Laoui D, Van Ginderachter JA, Devoogdt N, Lahoutte T, De Baetselier P, et al. Novel applications of nanobodies for in vivo bio-imaging of inflamed tissues in inflammatory diseases and cancer. Immunobiology. diciembre de 2012;217(12):1266-72.
50. Ackaert C, Smiejkowska N, Xavier C, Sterckx YGJ, Denies S, Stijlemans B, et al. Immunogenicity Risk Profile of Nanobodies. Front Immunol. 9 de marzo de 2021;12:632687.
51. Kang W, Ding C, Zheng D, Ma X, Yi L, Tong X, et al. Nanobody Conjugates for Targeted Cancer Therapy and Imaging. Technol Cancer Res Treat. 1 de enero de 2021;20:153303382110101.
52. Bannas P, Hambach J, Koch-Nolte F. Nanobodies and Nanobody-Based Human Heavy Chain Antibodies As Antitumor Therapeutics. Front Immunol. 22 de noviembre de 2017;8:1603.
53. Arbabi-Ghahroudi M. Camelid Single-Domain Antibodies: Historical Perspective and Future Outlook. Front Immunol. 20 de noviembre de 2017;8:1589.
54. Sathyajith D. What are Camelid Antibodies? News Med Life-Science. 23 de enero de 2022;3.
55. Fernandes CFC, Pereira S dos S, Luiz MB, Zuliani JP, Furtado GP, Stabeli RG. Camelid Single-Domain Antibodies As an Alternative to Overcome Challenges Related to the Prevention, Detection, and Control of Neglected Tropical Diseases. Front Immunol. 9 de junio de 2017;8:653.
56. Absolute Antibody. Antibody Fragments [Internet]. Antibody Enginnering. 2022. Disponible en: https://absoluteantibody.com/antibody-resources/antibody-engineering/antibody-fragments/
57. Bao G, Tang M, Zhao J, Zhu X. Nanobody: a promising toolkit for molecular imaging and disease therapy. EJNMMI Res. diciembre de 2021;11(1):6.
58. Asaadi Y, Jouneghani FF, Janani S, Rahbarizadeh F. A comprehensive comparison between camelid nanobodies and single chain variable fragments. Biomark Res. diciembre de 2021;9(1):87.
59. Payandeh Z, Kofeiti A, Sefid F. Nanobody structure analysis and determination of the functional conserve amino acid with bioinformatic tools. 2015;8.
60. Zielonka S, Empting M, Grzeschik J, Könning D, Barelle CJ, Kolmar H. Structural insights and biomedical potential of IgNAR scaffolds from sharks. mAbs. 2 de enero de 2015;7(1):15-25.
61. Protein Data Bank. 1MEL [Internet]. CRYSTAL STRUCTURE OF A CAMEL SINGLE-DOMAIN VH ANTIBODY FRAGMENT IN COMPLEX WITH LYSOZYME. 1997. Disponible en: https://www.rcsb.org/structure/1mel

62. Protein Data Bank. 1MLC [Internet]. MONOCLONAL ANTIBODY FAB D44.1 RAISED AGAINST CHICKEN EGG-WHITE LYSOZYME COMPLEXED WITH LYSOZYME. 1995. Disponible en: https://www.rcsb.org/structure/1mlc
63. Protein Data Bank. 1T6V [Internet]. Crystal structure analysis of the nurse shark new antigen receptor (NAR) variable domain in complex with lysozyme. 2004. Disponible en: https://www.rcsb.org/structure/1T6V
64. Muyldermans S. A guide to generation and design of nanobodies. FEBS J. 2021;288:2084-102.
65. Olichon A, de Marco A. Preparation of a Naïve Library of Camelid Single Domain Antibodies. En: Saerens D, Muyldermans S, editores. Single Domain Antibodies [Internet]. Totowa, NJ: Humana Press; 2012 [citado 4 de agosto de 2022]. p. 65-78. (Methods in Molecular Biology; vol. 911). Disponible en: http://link.springer.com/10.1007/978-1-61779-968-6_5
66. Yan J, Wang P, Zhu M, Li G, Romão E, Xiong S, et al. Characterization and applications of Nanobodies against human procalcitonin selected from a novel naïve Nanobody phage display library. J Nanobiotechnology. diciembre de 2015;13(1):33.
67. Yan J, Li G, Hu Y, Ou W, Wan Y. Construction of a synthetic phage-displayed Nanobody library with CDR3 regions randomized by trinucleotide cassettes for diagnostic applications. J Transl Med. diciembre de 2014;12(1):343.
68. Liu B, Yang D. Easily Established and Multifunctional Synthetic Nanobody Libraries as Research Tools. Int J Mol Sci. 27 de enero de 2022;23(3):1482.
69. Xiang Y, Sang Z, Bitton L, Xu J, Liu Y, Schneidman-Duhovny D, et al. Integrative proteomics identifies thousands of distinct, multi-epitope, and high-affinity nanobodies. Cell Syst. marzo de 2021;12(3):220-234.e9.
70. Zupancic JM, Desai AA, Tessier PM. Facile isolation of high-affinity nanobodies from synthetic libraries using CDR-swapping mutagenesis. STAR Protoc. marzo de 2022;3(1):101101.
71. de Marco A. Recombinant expression of nanobodies and nanobody-derived immunoreagents. Protein Expr Purif. agosto de 2020;172:105645.
72. Njeru FN, Kusolwa PM. Nanobodies: their potential for applications in biotechnology, diagnosis and antiviral properties in Africa; focus on application in agriculture. Biotechnol Biotechnol Equip. 1 de enero de 2021;35(1):1331-42.
73. Fang Z, Cao D, Qiu J. Development and production of nanobodies specifically against green fluorescence protein. Appl Microbiol Biotechnol. junio de 2020;104(11):4837-48.
74. Pardon E, Laeremans T, Triest S, Rasmussen SGF, Wohlkönig A, Ruf A, et al. A general protocol for the generation of Nanobodies for structural biology. Nat Protoc. marzo de 2014;9(3):674-93.
75. Pourasadi S, Gargari SLM, Rajabibazl M, Nazarian S. Efficient production of nanobodies against urease activity of Helicobacter pylori in Pichia pastoris. Turk J Med Sci. 2017;7.
76. Clackson T, Hoogenboom H, Griffiths A, Winter G. Making antibody fragments using phage display libraries. Lett Nat. 1991;624-8.
77. Deffar K, Shi H, Li L, Wang X, Zhu X. Nanobodies - the new concept in antibody engineering. 2009;8.
78. Yu J, Guo Y, Gu Y, Fan X, Li F, Song H, et al. A novel silk fibroin protein–based fusion system for enhancing the expression of nanobodies in Escherichia coli. Appl Microbiol Biotechnol. marzo de 2022;106(5-6):1967-77.
79. Kariuki CK, Magez S. Improving the yield of recalcitrant Nanobodies® by simple modifications to the standard protocol. Protein Expr Purif. septiembre de 2021;185:105906.
80. Li D, Huang H. Heterologous Expression of Nanobodies:a Recent Progress. China Biotechnol [Internet]. 25 de agosto de 2017; Disponible en: https://manu60.magtech.com.cn/biotech/EN/10.13523/j.cb.20170813
81. Iwaki T, Hara K, Umemura K. Nanobody production can be simplified by direct secretion from Escherichia coli. Protein Expr Purif. junio de 2020;170:105607.
82. Chen Q, Zhou Y, Yu J, Liu W, Li F, Xian M, et al. An efficient constitutive expression system for Anti-CEACAM5 nanobody production in the yeast Pichia pastoris. Protein Expr Purif. marzo de 2019;155:43-7.
83. Sheikholeslami F, Rasaee MJ, Shokrgozar MA, Dizaji MM, Rahbarizadeh F, Ahmadvande D. Isolation of a Novel Nanobody Against HER-2/ neu Using Phage Displays Technology. Lab Med. febrero de 2010;41(2):69-76.
84. Shokrollahi N, Habibi Anbouhi M, Jahanian-Najafabadi A, AliRahimi E, Behdani M. Expressing of Recombinant VEGFR2-specific Nanobody in Baculovirus Expression System. Iran J Biotechnol [Internet]. marzo de 2021 [citado 19 de agosto de 2022];19(1). Disponible en: https://doi.org/10.30498/IJB.2021.2783
85. Wang W, Yuan J, Jiang C. Applications of nanobodies in plant science and biotechnology. Plant Mol Biol. 10 de octubre de 2020;1-11.
86. Ortega-Monge C, Arce-Rodríguez N, Santamaría-Muñoz M, Chavarría-Rojas M, Rojas Salas MF, Baltodano Viales E, et al. Aplicaciones de los nanoanticuerpos en la medicina. Ars Pharm Internet. 21 de marzo de 2022;63(2):189-203.
87. Van Audenhove I, Gettemans J. Nanobodies as Versatile Tools to Understand, Diagnose, Visualize and Treat Cancer. EBioMedicine. junio de 2016;8:40-8.
88. Hosseindokht M, Bakherad H, Zare H. Nanobodies: a tool to open new horizons in diagnosis and treatment of prostate cancer. Cancer Cell Int. diciembre de 2021;21(1):580.
89. Sanaei M, Setayesh N, Sepehrizadeh Z, Mahdavi M, Yazdi MH. Nanobodies in Human Infections: Prevention, Detection, and Treatment. Immunol Invest. 16 de noviembre de 2020;49(8):875-96.
90. Hassanzadeh-Ghassabeh G, Devoogdt N, De Pauw P, Vincke C, Muyldermans S. Nanobodies and their potential applications. Nanomed. junio de 2013;8(6):1013-26.
91. De Vlaminck K, Romão E, Puttemans J, Pombo Antunes AR, Kancheva D, Scheyltjens I, et al. Imaging of Glioblastoma Tumor-Associated Myeloid Cells Using Nanobodies Targeting Signal Regulatory Protein Alpha. Front Immunol. 30 de noviembre de 2021;12:777524.
92. Gu K, Song Z, Zhou C, Ma P, Li C, Lu Q, et al. Development of nanobody-horseradish peroxidase-based sandwich ELISA to detect Salmonella Enteritidis in milk and in vivo colonization in chicken. J Nanobiotechnology. diciembre de 2022;20(1):167.
93. Girt GC, Lakshminarayanan A, Huo J, Dormon J, Norman C, Afrough B, et al. The use of nanobodies in a sensitive ELISA test for SARS-CoV-2 Spike 1 protein. R Soc Open Sci. septiembre de 2021;8(9):211016.
94. Keown JR, Zhu Z, Carrique L, Fan H, Walker AP, Serna Martin I, et al. Mapping inhibitory sites on the RNA polymerase of the 1918 pandemic influenza virus using nanobodies. Nat Commun. diciembre de 2022;13(1):251.
95. DeMarco S. Snakebite antivenoms step into the future. 10 de septiembre de 2022;14.
96. Garaicoechea L, Aguilar A, Parra GI, Bok M, Sosnovtsev SV, Canziani G, et al. Llama Nanoantibodies with Therapeutic Potential against Human Norovirus Diarrhea. Sestak K, editor. PLOS ONE. 12 de agosto de 2015;10(8):e0133665.
97. Laustsen A, Gutiérrez J, Knudsen C, Johansen K, Bermúdez-Méndez E, Cerni F, et al. Pros and cons of different therapeutic antibody formats for recombinant antivenom development. Toxicon [Internet]. 2018; Disponible en: https://www.sciencedirect.com/science/article/pii/S0041010118301144#bib101
98. Bailon H, Yaniro V, Cáceres O, Colque E, Leiva W, Padilla C, et al. Development of Nanobodies Against Hemorrhagic and Myotoxic Components of Bothrops atrox Snake Venom. Front Immunol. 7 de mayo de 2020;11:1-12.
99. Hmila I, Saerens D, Abderrazek RB, Vincke C, Abidi N, Benlasfar Z, et al. A bispecific nanobody to provide full protection against lethal scorpion envenoming. FASEB J. septiembre de 2010;24(9):3479-89.

100. Yavuz SŞ, ÇeliKyurt İK. An update of anti-viral treatment of COVID-19. Turk J Med Sci. 2021;19.
101. Aria H, Mahmoodi F, Ghaheh HS, Faranak mavandadnejad, Zare H, Heiat M, et al. Outlook of therapeutic and diagnostic competency of nanobodies against SARS-CoV-2: A systematic review. Anal Biochem. marzo de 2022;640:114546.
102. NIH Instituto Nacional del Cancer. ¿Qué es el cáncer? [Internet]. 2021. Disponible en: https://www.cancer.gov/espanol/cancer/naturaleza/que-es
103. Lippman SM, Hawk ET. Cancer Prevention: From 1727 to Milestones of the Past 100 Years. Cancer Res. 1 de julio de 2009;69(13):5269-84.
104. NIH National Cancer INstitute. Cancer Treatment [Internet]. 2021. Disponible en: https://www.cancer.gov/about-cancer/treatment#:~:text=Some%20people%20with%20cancer%20will,targeted%20therapy%2C%20or%20hormone%20therapy
105. Yang EY, Shah K. Nanobodies: Next Generation of Cancer Diagnostics and Therapeutics. Front Oncol. 23 de julio de 2020;10:1182.
106. Verhaar ER, Woodham AW, Ploegh HL. Nanobodies in cancer. Semin Immunol. febrero de 2021;52:101425.
107. Wang J, Kang G, Yuan H, Cao X, Huang H, de Marco A. Research Progress and Applications of Multivalent, Multispecific and Modified Nanobodies for Disease Treatment. Front Immunol. 18 de enero de 2022;12:838082.
108. World Healt Organization. Coronavirus [Internet]. 2020. Disponible en: https://www.who.int/es/health-topics/coronavirus#tab=tab_1
109. World Healt Organization. WHO Director-General's opening remarks at the media briefing on COVID-19 - March 11 2020 [Internet]. 2021. Disponible en: https://www.who.int/director-general/speeches/detail/who-director-general-s-opening-remarks-at-the-media-briefing-on-covid-19---11-march-2020
110. Rodriguez-Guerra M, Jadhav P, Vittorio TJ. Current treatment in COVID-19 disease: a rapid review. Drugs Context. 29 de enero de 2021;10:1-8.
111. Hanke L, Sheward DJ, Pankow A, Vidakovics LP, Karl V, Kim C, et al. Multivariate mining of an alpaca immune repertoire identifies potent cross-neutralizing SARS-CoV-2 nanobodies. Sci Adv. 25 de marzo de 2022;8(12):eabm0220.
112. Verkhivker G. Structural and Computational Studies of the SARS-CoV-2 Spike Protein Binding Mechanisms with Nanobodies: From Structure and Dynamics to Avidity-Driven Nanobody Engineering. Int J Mol Sci. 8 de marzo de 2022;23(6):2928.
113. Saied AA, Metwally AA, Alobo M, Shah J, Sharun K, Dhama K. Bovine-derived antibodies and camelid-derived nanobodies as biotherapeutic weapons against SARS-CoV-2 and its variants: A review article. Int J Surg. febrero de 2022;98:106233.
114. United Nations. Three possible evolutions for the coronavirus causing COVID-19 [Internet]. 2022. Disponible en: https://news.un.org/es/story/2022/03/1506482
115. Ceretta M, Ramos B. Desarrollo de una estrategia para la obtención de nanobodies contra las toxinas botulínicas A y B de Clostridium botulinum [Internet]. Universidad ORT Uruguay; 2018. Disponible en: https://dspace.ort.edu.uy/bitstream/handle/20.500.11968/3919/Material%20completo.pdf?sequence=-1&isAllowed=y
116. Abbas A, Lichtman A, Pillai S. Celular and Molecular Immunology. novena. Philadelphia: Elsevier; 2017.
117. NIH. Glossary of HIV/AIDS-Related Terms. 2021;202.
118. Allmen D von, Shochat S. PRINCIPLES OF ADJUVANT THERAPY IN CHILDHOOD CANCER. En: Ashcraft's Pediatric Surgery [Internet]. Elsevier; 2010 [citado 4 de agosto de 2022]. p. 837-52. Disponible en: https://linkinghub.elsevier.com/retrieve/pii/B9781416061274000665
119. Adel M Z, Abdullah A AD, Markus S, Ahmed A A, Emad M S, Basem S A, et al. Cloning and characterisation of nanobodies against the coat protein of Zucchini yellow mosaic virus. Plant Prot Sci. 25 de agosto de 2018;54(No. 4):215-21.
120. Hemmer C, Djennane S, Ackerer L, Hleibieh K, Marmonier A, Gersch S, et al. Nanobody□mediated resistance to Grapevine fanleaf virus in plants. Plant Biotechnol J [Internet]. 2017;16. Disponible en: https://onlinelibrary.wiley.com/doi/full/10.1111/pbi.12819
121. He J, Tian J, Xu J, Wang K, Li J, Gee SJ, et al. Strong and Oriented Conjugation of Nanobodies onto Magnetosomes for the Development of a Rapid Immunomagnetic Assay for the Environmental Detection of Tetrabromobisphenol-A. Anal Bioanal Chem. octubre de 2018;410(25):6633-42.
122. Peltomaa R, Benito-Peña E, Moreno-Bondi MC. Bioinspired recognition elements for mycotoxin sensors. Anal Bioanal Chem. enero de 2018;410(3):747-71.
123. Wang Y, Fan Z, Shao L, Kong X, Hou X, Tian D, et al. Nanobody-derived nanobiotechnology tool kits for diverse biomedical and biotechnology applications. Int J Nanomedicine. julio de 2016;Volume 11:3287-303.
124. Janke BH. Influenza A virus infections in swine: pathogenesis and diagnosis. Vet Pathol. marzo de 2014;51(2):410-26.
125. Pinto Torres JE, Goossens J, Ding J, Li Z, Lu S, Vertommen D, et al. Development of a Nanobody-based lateral flow assay to detect active Trypanosoma congolense infections. Sci Rep [Internet]. 13 de junio de 2018 [citado 22 de mayo de 2021];8. Disponible en: https://www.ncbi.nlm.nih.gov/pmc/articles/PMC5998082/
126. Rexroad C, Vallet J, Matukumalli LK, Reecy J, Bickhart D, Blackburn H, et al. Genome to Phenome: Improving Animal Health, Production, and Well-Being – A New USDA Blueprint for Animal Genome Research 2018–2027. Front Genet [Internet]. 2019 [citado 16 de mayo de 2021];10. Disponible en: https://www.frontiersin.org/articles/10.3389/fgene.2019.00327/full?report=reader
127. Deckers N, Saerens D, Kanobana K, Conrath K, Victor B, Wernery U, et al. Nanobodies, a promising tool for species-specific diagnosis of Taenia solium cysticercosis. Int J Parasitol. abril de 2009;39(5):625-33.
128. Virdi V, Coddens A, De Buck S, Millet S, Goddeeris BM, Cox E, et al. Orally fed seeds producing designer IgAs protect weaned piglets against enterotoxigenic Escherichia coli infection. Proc Natl Acad Sci U S A. 16 de julio de 2013;110(29):11809-14.
129. Tang KL, Caffrey NP, Nóbrega DB, Cork SC, Ronksley PE, Barkema HW, et al. Restricting the use of antibiotics in food-producing animals and its associations with antibiotic resistance in food-producing animals and human beings: a systematic review and meta-analysis. Lancet Planet Health. 1 de noviembre de 2017;1(8):e316-27.
130. Yang J, Si R, Wu G, Wang Y, Fang R, Liu F, et al. Preparation of Specific Nanobodies and Their Application in the Rapid Detection of Nodularin-R in Water Samples. Foods. 10 de noviembre de 2021;10(11):2758.
131. Otero J. Los anticuerpos y su papel como herramientas analíticas en los ensayos inmunoenzimáticos. Rev Cubana Med Trop. agosto de 2010;62(2):85-92.
132. Nykiel-Szymańska J, Stolarek P, Bernat P. Elimination and detoxification of 2,4-D by Umbelopsis isabellina with the involvement of cytochrome P450. Environ Sci Pollut Res Int. 2018;25(3):2738-43.
133. Huang L, Muyldermans S, Saerens D. Nanobodies ®: proficient tools in diagnostics. Expert Rev Mol Diagn. septiembre de 2010;10(6):777-85.
134. Steyaert J, Pardon E, Wohlkönig A, Zögg, Kalichuk V, De Keyser P, et al. NANOBODY EXCHANGE CHROMATOGRAPHY [Internet]. p. 146. Disponible en: https://patentimages.storage.googleapis.com/63/2c/94/15a6e50d9a4a9f/WO2021123360A1.pdf
135. McMahon C, Baier AS, Pascolutti R, Wegrecki M, Zheng S, Ong JX, et al. Yeast surface display platform for rapid discovery of conformationally selective nanobodies. Nat Struct Mol Biol. marzo de 2018;25(3):289-96.

136. Uchanski T, Pardon E, Steyaert J. Nanobodies to study protein conformational states. Curr Opin Struct Biol. 2020;60.
137. Beghein E, Gettemans J. Nanobody Technology: A Versatile Toolkit for Microscopic Imaging, Protein–Protein Interaction Analysis, and Protein Function Exploration. Front Immunol. 4 de julio de 2017;8:771.
138. Marschall ALJ, Dübel S. Antibodies inside of a cell can change its outside: Can intrabodies provide a new therapeutic paradigm? Comput Struct Biotechnol J. 2016;14:304-8.
139. Dong JX, Lee Y, Kirmiz M, Palacio S, Dumitras C, Moreno CM, et al. A toolbox of nanobodies developed and validated for use as intrabodies and nanoscale immunolabels in mammalian brain neurons. eLife. 30 de septiembre de 2019;8:e48750.
140. Trimmer JS. Genetically encoded intrabodies as high-precision tools to visualize and manipulate neuronal function. Semin Cell Dev Biol. junio de 2022;126:117-24.
141. Lo ASY, Zhu Q, Marasco WA. Intracellular Antibodies (Intrabodies) and Their Therapeutic Potential. En: Chernajovsky Y, Nissim A, editores. Therapeutic Antibodies [Internet]. Berlin, Heidelberg: Springer Berlin Heidelberg; 2008 [citado 4 de agosto de 2022]. p. 343-73. (Starke K. Handbook of Experimental Pharmacology; vol. 181). Disponible en: http://link.springer.com/10.1007/978-3-540-73259-4_15
142. Lecerf JM, Shirley TL, Zhu Q, Kazantsev A, Amersdorfer P, Housman DE, et al. Human single-chain Fv intrabodies counteract in situ huntingtin aggregation in cellular models of Huntington's disease. Proc Natl Acad Sci. 10 de abril de 2001;98(8):4764-9.
143. Marzilli AM, McMahan JB, Ngo JT. Precision control of intrabodies in live cells. Nat Methods. marzo de 2020;17(3):259-60.
144. NIH. Coronavirus Disease 2019 (COVID-19) Treatment Guidelines [Internet]. 2022. Disponible en: https://www.ncbi.nlm.nih.gov/books/NBK570371/pdf/Bookshelf_NBK570371.pdf
145. Becker RC. Covid-19 treatment update: follow the scientific evidence. J Thromb Thrombolysis. julio de 2020;50(1):43-53.
146. Yu B, Li S, Tabata T, Wang N, Kumar R, Liu J, et al. Accelerating PERx Reaction Enables Covalent Nanobodies for Potent Neutralization of SARS-Cov-2 and Variants. BioRxiv Prepr [Internet]. 2022;1. Disponible en: https://www.ncbi.nlm.nih.gov/pmc/articles/PMC8936105/
147. Shi Z, Li X, Wang L, Sun Z, Zhang H, Chen X, et al. Structural basis of nanobodies neutralizing SARS-CoV-2 variants. Structure. mayo de 2022;30(5):707-720.e5.
148. Wagner T, Schnepf D, Beer J, Ruetalo N, Klingel K, Kaiser P, et al. Biparatopic nanobodies protect mice from lethal-challenge with SARS-CoV-2variants of concern. EMBO Rep. 20 de diciembre de 2021;4(23):12.
149. Torres O. REPTILES DEL ECUADOR [Internet]. Bioweb. 2021. Disponible en: https://bioweb.bio/faunaweb/reptiliaweb/
150. Ministerio de Salud Pública del Ecuador. Manejo clínico del envenenamiento por mordeduras de serpientes venenosas y picaduras de escorpiones [Internet]. Puyo: Gobierno de la república del ecuador; 2017. Disponible en: http://hgp.gob.ec/index.html/images/Protocolo%20serpientes%202017.pdf
151. Fan HW, Natal Vigilato MA, Augusto Pompei JC, Gutiérrez JM, en representación de la Red de Laboratorios Públicos Productores de Antivenenos de América Latina (RELAPA). (Los autores de la RELAPA y sus afiliaciones se mencionan al final del manuscrito.). Situación de los laboratorios públicos productores de antivenenos en América Latina. Rev Panam Salud Pública. 19 de noviembre de 2019;43:1.
152. Ministerio del Ambiente Ecuador. NORMA DE CALIDAD AMBIENTAL Y DE DESCARGA DE EFLUENTES : RECURSO AGUA. 2015.
153. Jaramillo-Feijoo L, Real-Cotto J, Tanca-Campozano J, Puga-Peña G, Quinto-Briones R. Incidencia y mortalidad del cáncer, en Hospital Solca - Guayaquil. :6.
154. National Tumor Registry (RNT). Cancer epidemiology in Quito 2011-2015 [Internet]. 2019. Disponible en: https://issuu.com/solcaquito/docs/epidemiolog_a_del_c_ncer_en_quito_2011-2015

ARTICLE / INVESTIGACIÓN

Synthesis, Structural Characterisation and Biological Activity; New Metal Complexes Derived from Semicarbazone Ligand

Baraa Kasim Mohammed[1]* and Enaam Ismail Yousif[2]

DOI. 10.21931/RB/2023.08.02.14

1Department of Chemistry, College of Education for Pure Science (Ibn Al-Haitham), Iraq

enaamismail@yahoo.com; anaam.i.y@ihcoedu.uobaghdad.edu.iq

2 Department of Chemistry, College of Education for Pure Science (Ibn Al-Haitham), University of Baghdad, Adhamiyah, Baghdad, Iraq

*Corresponding authors: Email: dr.baraakasim3@gmail.com,

Abstract: The results of synthesizing a novel tridentate Schiff-base ligand and its metal complexes have been given. The ligand itself is described as being tridentate. The synthesis of the ligand has the following chemical formula: (E)-2-((2S)-4-(tert-butyl) -2-((S)-(phenylamino) (p-tolyl) methyl) cyclohexylidene) hydrazine -1-carboxamide was produced as a byproduct of the reaction between benzoic acid and benzoic acid between (((4-(tert-butyl)-2-((S)-(phenylamino)(p-to and (HL). The ligand was reacted with 1:1 (L:M) mole ratios of ions containing Mn(II), Co(II), Ni(II), Cu(II), Zn(II), and Cd(II), which resulted in the production of title complexes. In cases where it was necessary, physicochemical techniques were utilized to characterize both the ligand and the complexes. Examples include magnetic susceptibility and conductance measurements, microanalysis of elements, nuclear magnetic resonance (1H, 13C), mass spectrometry, Fourier transform infrared (FT-IR), electronic spectra, and more. The results of these studies demonstrated that the ions Mn (II), Co (II), Cu(II), Ni(II), Zn(II), and Cd(II) can be partitioned into four-coordinate and six-coordinate complexes, respectively. In addition, the TGA was used to investigate whether or not the ligand and specific complexes were thermally stable. Several different bacterial and fungus strains were utilized to examine the ligand and its complexes for potential antibacterial activity. According to the findings, the complexes are far more effective than the free ligand in combating a wider variety of species.

Key words: Structural study, Metal complexes, Mannich -β-amino carbonyl, Thermal stability, *Staphylococcus aureus* (G+).

Introduction

It is common knowledge that chemical molecules with an azomethine group, collectively called Schiff bases, are known to have biological action[1]. It is one of the most important bonds representing many coordination complexes by linking metal elements and specializing in transition metal[2]. It is the elemental imine compound prepared by a German scientist named Hugo in 1864. It synthesizes a condensation reaction between a ketone or an aldehyde with primary amines[1]. It is one of the most important bonds representing many coordination complexes by linking metal elements and specializing with transition metal[3]. Because of their great variety of pharmacological and biological properties, Schiff complexes of important metals constitute a significant basic research topic for creating safe and effective therapeutic materials for treating bacterial infections and cancers. For example, the fact that transition metal complexes of Schiff base ligands with "O" and "N" donor atoms have antibacterial, antifungal, and anti-inflammatory characteristics makes them particularly significant[4], an anticonvulsant[5,6], an analgesic[7], an anthelmintic[8], an antitubercular[9], and an antioxidant[10]. Not very long ago, we attended the installation of the base Schiff and its complexes[11-13]. The ligand was synthesized from the reaction of the Mannich precursor ((((4)(tributyl)-2-(((S))-(phenylamino)(p-tolyl)methyl) cyclohexane-1-one)) with Semicarbazone, then the prepared compounds were tested, because of its effectiveness against bacteria and fungal organisms. In this study, we used two types of mushrooms and four distinct types of bacteria (Escherichia coli, Pseudomonas aeruginosa, Staphylococcus aureus, and Bacillus subtitles) (Candida albicans, and Rhizosporium). These species are responsible for most fungal infections found in humans. It is a common component of the flora that lives on human skin, vaginal membranes, and in the intestines of individuals living in healthy communities. In immunocompromised persons, fungal overgrowth and severe cutaneous or systemic infections caused by Clostridium albicans and other Candida species can cause morbidity and mortality. These infections can occur on the skin or elsewhere in the body[14].

Materials and methods

Reactor design

After obtaining the reagents from a commercial organization, you should use them precisely in the same manner you did to get the best results. To provide a reference, 1H- and 13C-NMR spectra were acquired for the linker in DMSO-d6 using a Brucker instrument at a frequency of 300 MHz for 1H-NMR and 75 MHz for 13C-NMR. KBr discs were used in an FT-IR spectrometer of the FTIR-600 type to gather data in the 4000-400 cm^{-1} to acquire FT-IR spectra. Electrospray (+) mass spectrometry has been worked on with the Sciex Esi mass analyzer. When taking the melting

Citation: Mohammed B K, Ismail Yousif E. Synthesis, Structural Characterisation and Biological Activity; New Metal Complexes Derived from Semicarbazone Ligand. Revis Bionatura 2023;8 (2) 14. http://dx.doi.org/10.21931/RB/2023.08.02.14

Received: 2 January 2023 / **Accepted:** 19 April 2023 / **Published:** 15 June 2023

Publisher's Note: Bionatura stays neutral with regard to jurisdictional claims in published maps and institutional affiliations.

point measurements, the researcher utilized a Stewart thermoelectric instrument of type SMP40. Electronic spectra were collected in the 1000–200 nm range on a Shimadzu UV-160 by using a 1.0 cm quartz cell at a concentration of 10^{-3} mol L^{-1} of samples in DMSO solutions. The spectra were taken in the region of 1000–200 nm. The measurements were obtained from a specific place referred to as the range. Using a Eutech Instruments Cyber scan, the temperature was maintained at room temperature. 510 digital conductivity meter calculation was made to establish the molar conductance of the complexes. The measurements were carried out on solutions of the chemicals in DMSO that ranged from 10^{-3}-10^{-5} M in concentration. For the element analysis (CHNS), we used the analyzer (Eager 300 for EA1112), and for the assessment of the metal content, we used the atomic absorption spectrophotometer manufactured by Shimadzu (A A-680G). To determine the amount of chloride present in the complexes, we carried out a potentiometric titration using a 686-Titro Processor-665 Dosim A-Metrohm/Swiss instrument. We utilized an STA PT-1000 manufactured by the Linseis Company in Germany for the thermogravimetric analysis, including TGA and DSC measurements. A magnetic susceptibility balance was used on Johnson Matthey to determine magnetic moments at a temperature of 306 kelvin. The ligand and its metal complexes were tested for their biological efficacy using an agar-well diffusion method against four different types of bacteria (*Escherichia coli, Pseudomonas aeruginosa, Staphylococcus aureus*, and *Bacillus subtitles*), as well as two different types of fungi. The results showed that the ligand and its metal complexes effectively inhibited the growth of the bacteria (*Candida albicans* and *Rhizosporium*). A spotless metallic borer was utilized to make wells in the medium at regular intervals of at least 6 mm in depth. The test samples were dispensed into the wells at the appropriate concentration of 1 mg/mL in DMSO (100µ L). After the plates had been prepared, they were kept in an incubator at 37 °C for twenty-four hours. Measurements of the inhibition zone's diameter are used to figure out the amount of activity (mm). To determine whether or not chemicals are effective against pathogenic bacteria, the well diffusion method was performed in an aerobic setting. On Mueller-Hinton agar, all potentially dangerous bacteria were tested for their capacity to inhibit growth.

Synthesis

Preparation of precursor

The preparation of (((4-(tert-butyl)-2-((S)-(phenylamino) (p-tolyl) methyl)cyclohexan-1-one)) was achieved adopting metod reported in[15,16].

Synthesis of Schiff-base ligand (HL)

With Respect to a Compound of (4-(tert-butyl)-2-((S)-(phenylamino)(p-tolyl)methyl)cyclohexan-1-one) During the addition of hot EtOH (0.5g, 1.4mmol), which was done so while stirring, a solution of semicarbazide (0.159g, 1.4mmol) in 15ml of EtOH with 3 drops of glacial acetic acid was created. The reaction mixture was refluxed for a total of six hours, during which time a white crystal formed. This crystal was filtered out, washed with five milliliters of cold ethanol, and then air-dried. The quantity produced was 0.3g (51%), and the melting point was 226-228°C.

Methodology for Complex Synthesis in General

Combined 0.4 millimoles of semicarbazone ligand with 10 milliliters of ethyl alcohol in a solution and added it while stirring to reduce the pH to approximately 9. After that, ten milliliters of ethanol that had been combined with a salt mixture of metal chloride were progressively added while the mixture was stirred. After that, the mixture was allowed to stand for ten minutes. This procedure was carried out on multiple occasions. After stirring the reaction mixture for four hours, a colorful precipitate had already begun forming in the mixture. As shown in Scheme 1, after creating a solid, it was filtered, then washed in 15 ml of cold 100% ethanol, and then finally air-dried (1). The yields, colors, and melting points of the complexes, as well as information regarding the quantities of metal salts, are included in the provided material (Table 1).

Results and discussion

After the reaction of (4-(tert-butyl)-2-((S)-(phenylamino) (p-tolyl)methyl)cyclohexan-1-one with semicarbazide in a 1:1 molar ratio at reflux, Scheme), the ligand ((E)-2-((2S)-4-(tert-butyl) -2-((S)-(phenylamino) (p-tolyl)methyl) (1). The ligand reacted with metal chloride salts of Mn(II), Co(II), Ni(II), Cu(II), and Cd(II) at a mole ratio of 1:1 (L: M), which resulted in the formation of six and four coordinate monomeric complexes, respectively. The monomeric chemicals that are produced as a result exist as solids at room temperature and are soluble in both DMSO and DMF. We have concluded that the complexes are extremely complicated and engage in highly coordinated activity based on the physical and chemical characteristics of the complexes. The results of Table 2 demonstrate that the data agree with the model that has been proposed. The results obtained by conducting the complexes in DMSO solutions containing these substances have demonstrated that there are both neutral and non-neutral, bringing the total number of complexes to (16).

Metal ion	Weight of metal salt(g)	Weight of complex(g)	Yield (%)	Colour	m.p.°C
[Mn(HL)Cl_2.H_2O]	0.079	0.17	41.87	pale pink	>300*
[Co(HL)Cl_2.H_2O]	0.096	0.19	46.45	Pink	280
[Ni(HL) Cl_2.H_2O]	0.095	0.20	48.89	Pale green crystals	268
[Cu(HL)Cl_2H_2O]	0.068	0.21	50.98	green	>300*
[Zn(HL)Cl]Cl	0.054	0.25	58.68	Deep-brown	275
[Cd(HL)Cl]Cl	0.080	0.26	56.39	Deep-brown	290

Table 1. Calculating HL complicated metal salt concentrations, products' hues, and temperatures of melting.

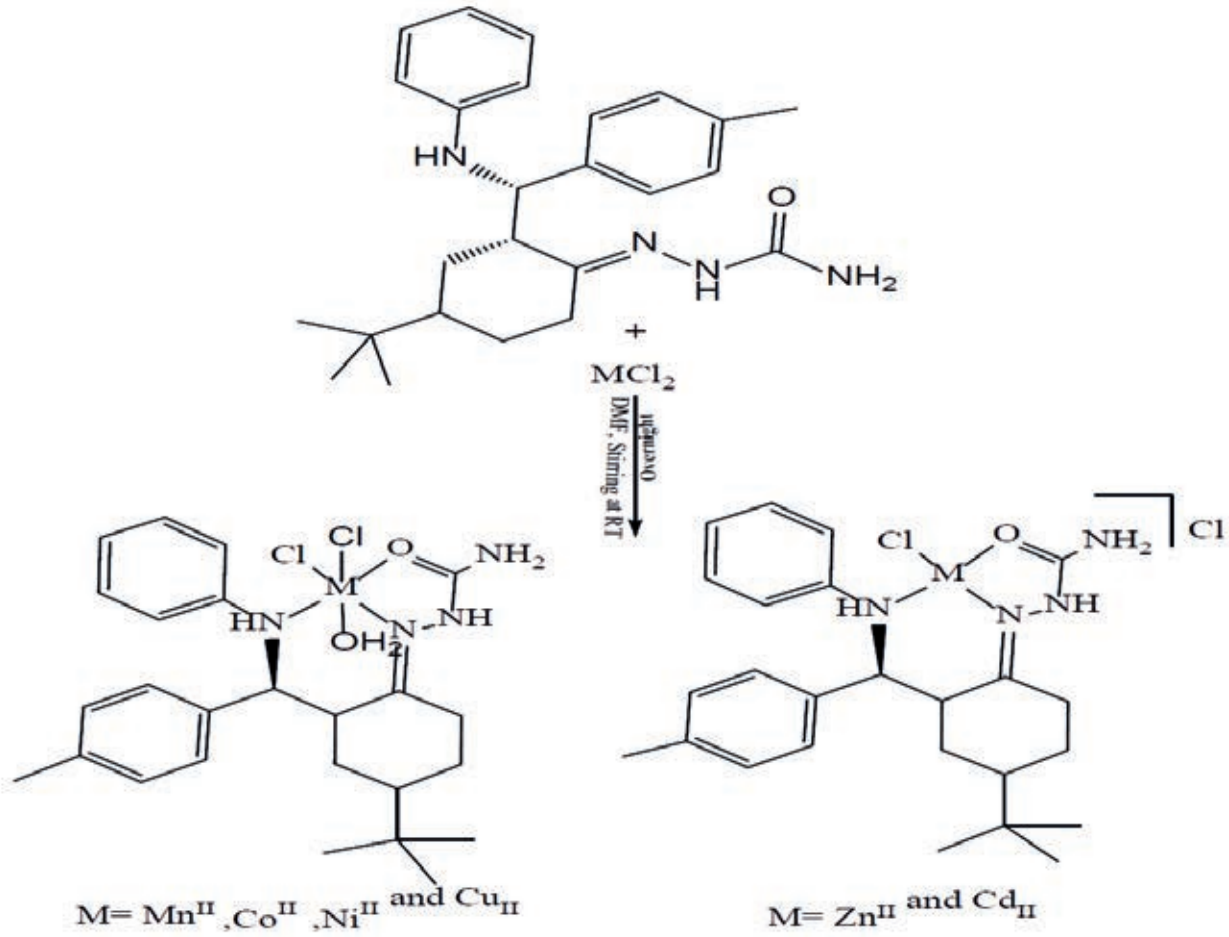

Figure 1. Synthesis route of HL complexes.

FT-IR Spectra

The FT-IR spectrum of the free semicarbazone ligand (HL) shows characteristic bands at 3460, 3282, 3194;3167,1693,1666and1600cm^{-1} that are attributed to v(NH)),v(NH)$_{am}$, v(NH$_2$)$_{sy,asy}$, v(C=O)$_{ket}$,v(C=N) imine and v(-C=C) aromatic, respectively[17,18]. The assigned complexes and their corresponding infrared data have been assembled in (Table 3). The creation of complexes was confirmed by analyzing their FT-IR spectra, which revealed altered ligand bands. The imine band, first detected at 1666 cm^{-1} in the free ligand (HL), was shown to have migrated to a lower frequency and be present at around 1600-1658 cm^{-1} in complexes[19]. This change demonstrated the iminic group's nitrogen atom was playing a role in the coordination process with the metal center[20,21]. This shift may indicate that the ligand is coordinated to the metal ions via the O atom when compared to the shift in the v(C-O) group in the spectra of complexes, which happened in comparison to the shift in the free ligand. Novel bands, identified as v (M-O), can be seen in the FT-IR spectra of the complexes between 609 and 694 cm^{-1} and 401-497 cm^{-1}, respectively (M-N). 22,23 Additionally, bands were seen in the 227-299 cm^{-1} range that was attributed to (M-Cl)[22].

NMR Spectra

NMR spectra of HL in dimethylsulfoxide-d6 displayed characteristic peaks at δH;(400MHz, DMSO-d6): 7.39-7.37 ($C_{14,14}$`)-H (1H, d, J = 17Hz). 7.23-7.22 ($C_{13,13}$`)-H (1H, t, J = 3Hz). 7.20-7.18 , 7.15 ($C_{15,15}$`)-H (1H, d, J = 12Hz) , ($C_{10,10}$`)-H (1H, d, J = 18Hz). 2.32-2.31 ($C_{9,9}$-)-H (1H, t, J =8Hz). 6.44 NHc (1H, N-H, d, J = 4Hz). 2.64-2.62 (C7-H) (1H, d). 2.46-2.44 (C_2)-H (1H, m, J=4Hz). 2.26:2.24 (C_6)-H (2H, t). 2.18 CH_3 C_{17}-H (3H, s,–(Me)). (C_5)-H (2H, m). 1.23. 1.06;1.04 C_3-H (2H, t). 1.00;0.99 C_4-H (1H, m). 0.71-0.57, 3(CH_3) C_{18}-H (9H, s).10.19-10.16 (NH_b). 8.19 NHa ,Fig.1. The 13C-NMR spectrum of the HL in dimethylsulfoxide-d6 showed peaks at;(100MHz, dimethylsulfoxide-d6): 147.6 ,137.5,135.6 (C_{12}), (C_8) and (C_{11}).($C_{14,14}$-), ($C_{10,10}$-),($C_{9,9}$-), (C_{15}), and ($C_{13,13}$-) were detected at 129.5,128.8, 126.5,120.8 and 113.5. 60.0, 41.6, 40.8,32.5, 32.81 ,32.17 (C_7) (C_4),(C_2) (C_{16}) (C_6) (C_5) . (C_{18}) (C_3), (C_{17}) 27.6,22.7 , 21.3. C=O δ = 179.0. (-C=N-) 166.60. 38.52-39 ppm, Fig.2.

Mass spectrum

The electrospray (+) mass spectrum of HL showed a band of at m/z = 405.60 amu (3%) (M-H)$^+$ calculated for $C_{25}H_{33}N_4O^+$ requires = 406.57. Peaks detected at m/z = 329.47(5 %), 272.35 (22 %), 218.28 (13 %), 117.17 (40 %), and 77.11 (29 %), related to [(M-H)-($C_2H_8N_2O$)], [(M-H)-($C_2H_8N_2O$) + (C_4H_9+)], [(M-H)-($C_2H_8N_2O$) + (C_4H_9+) + (C_3H_4N+)], [(M-H) ($C_2H_8N_2O$) + (C_4H_9+) + (C_3H_4N+) + (C_7H_3N.+)] and [(M-H)-($C_2H_8N_2O$)+(C_4H_9+) + (C_3H_4N+) + (C_7H_3N.+) +(C_3H_3.)], respectively, Fig.3.

Electronic Spectra and Magnetic Moment Measurements

Strong absorption peak may be seen in the UV-Vis spectrum of HL, (228nm =43859cm^{-1}, εmax= 458molar^{-1} cm^{-1}), (284nm =35211cm^{-1}, εmax= 807 molar^{-1}cm^{-1}) and (347nm =28818cm^{-1}, εmax= 515 molar^{-1}cm^{-1}) which are assigned to

Complex	Molecular formula	M.Wt	Micro analysis found, calculated (%)				
			C	H	N	M	Cl
[Mn(HL)Cl$_2$H$_2$O]	$C_{25}H_{36}MnN_4O_2Cl_2$	550.6	54.10 (54.40)	5.32 (6.53)	9.15 (10.17)	8.78 (9.97)	11.71 (12.89)
[Co(HL) Cl$_2$H$_2$O]	$C_{25}H_{36}CoN_4O_2Cl_2$	554.6	53.11 (54.09)	6.21 (6.49)	9.11 (10.09)	10.24 (10.62)	11.02 (12.80)
[Ni(HL) Cl$_2$ H$_2$O]	$C_{25}H_{36}NiN_4O_2Cl_2$	554.36	53.21 (54.11)	5.40 (6.49)	9.44 (10.10)	9.34 (10.58)	11.33 (12.80)
[Cu(HL) Cl$_2$H$_2$O]	$C_{25}H_{36}CuN_4O_2Cl_2$	559.21	52.55 (53.64)	5.35 (6.43)	9.56 (10.01)	10.22 (11.36)	11.53 (12.69)
[Zn(HL) Cl]Cl	$C_{25}H_{34}ZnN_4OCl_2$	542.95	54.21 (55.25)	5.67 (6.26)	9.03 (10.31)	11.05 (12.04)	12.11 (13.07)
[Cd(HL) Cl]Cl	$C_{25}H_{34}CdN_4OCl_2$	589.98	49.44 (50.84)	4.35 (5.76)	8.55 (9.49)	18.21 (19.05)	11.11 (12.03)

Table 2. Characterization of HL and its compounds on a microscopic scale, together with their physical properties.

Compounds	ν(NH)	ν(NH) am	ν(NH2)sy,asy	ν(H2O)	ν(C=O)	ν(C=N)	δ(N-H)	ν(C=C)	ν(M-O)	ν(M-N)	ν(M-Cl)
HL	3460	3282	3194, 3167	-	1693	1666	1600	1504	-	-	-
[Mn(HL)Cl2H2O]	3431	3404	3342	3157	1668	1627	1595	1564	671,622	480,426	291,260
[Co(HL)Cl2H2O]	3440	3421	3301, 3240	3197	1678	1658	1593	1540	694,621	455,405	299,254
[Ni(HL) Cl2H2O]	3436	3394	3342, 3139	3114	1652	1631	1575	1527	632	457,422	283,266
[Cu(HL)Cl2H2O]	3525	3421	3363, 3255	3163	1678	1658	1593	1527	667,624	497,424	287,243
[Zn(HL)Cl] Cl	3437	3360	3278, 3197	-	1680	1600	1562	1504	624	447,401	281
[Cd(HL)Cl] Cl	3450	3286	3190, 3167	-	1681	1647	1597	1508	609	482,451	227

Table 3. Analysis of HL and its compounds using FT-IR spectroscopy (cm^{-1}).

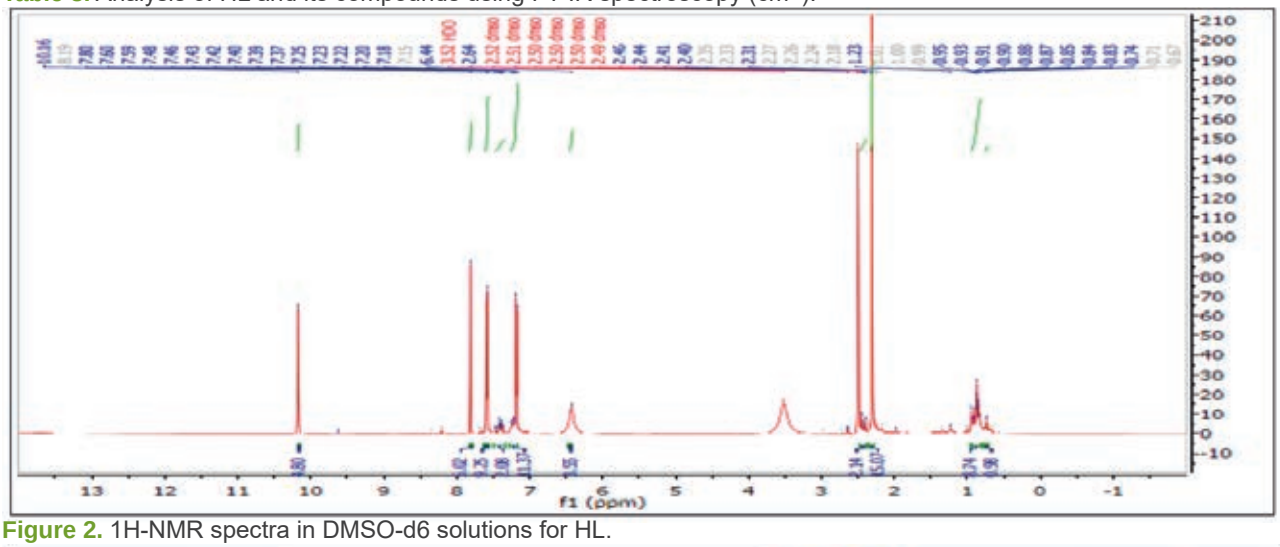

Figure 2. 1H-NMR spectra in DMSO-d6 solutions for HL.

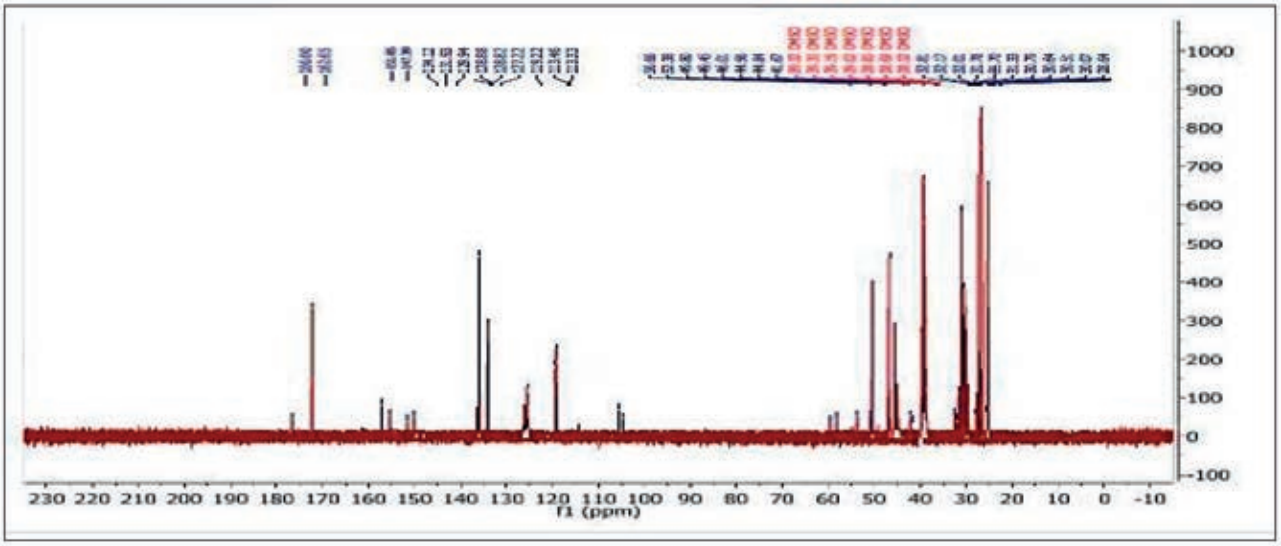

Figure 3. ^{13}C-NMR spectra in DMSO-d6 solutions for HL.

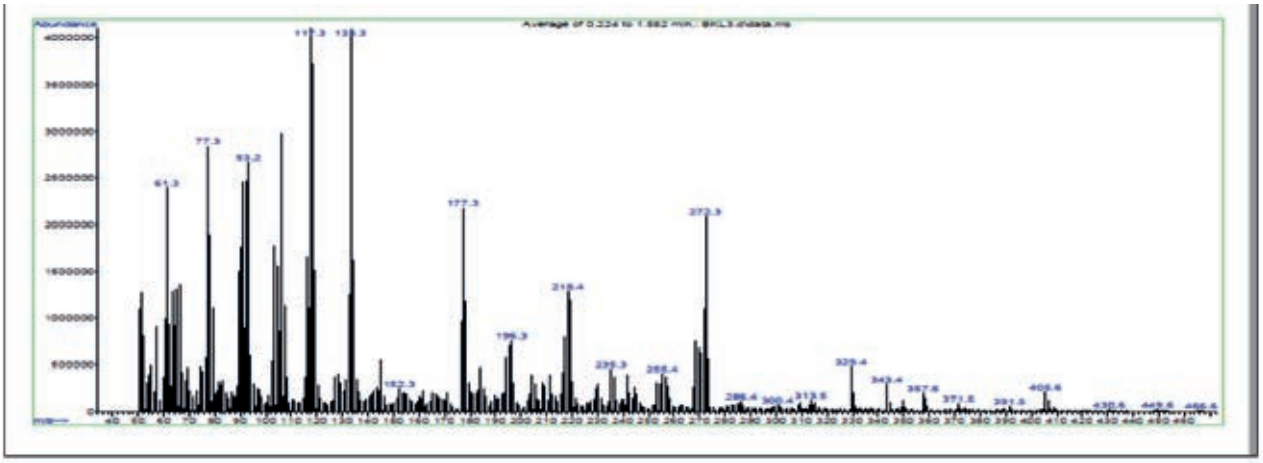

Figure 4. The electrospray (+) mass spectrum of HL.

π→π*, π→π*and n→π* transitions, respectively[23]. Electronic spectra and magnetic moment data for HL and its compounds are compiled in (Table 4). The electronic spectra of the complexes exhibit several peaks in the vicinity of 214-269 and 301-310 nm. These peaks can be attributed to π→π*, n→π* and charge transfer, respectively[24]. Peaks in the d-d region are observed at 841 nm in the electronic spectra of the Mn(I) complex, and these peaks are associated to $6A_1g \rightarrow 4T_1g(4G)$ transitions[23]. Because the Co(II) combination formed a distorted octahedral structure[23], the electronic spectrum of the compound conforms to its magnetic values. The electronic spectra of the Ni(II) complex displayed a peak in the d-d region at 794. This peak was caused by the type transition $3A_2g(F) \rightarrow 3T_2g(F)$, and it indicated that the geometry of Ni atom[24] was octahedral. In the d-d region, the Cu(II) complex produced one peak at 941 that was attributed to the $2Eg \rightarrow 2T_2g$ transition. This confirmed a distorted octahedral structure about the Cu atom[25]. This spectrum agrees with the eff value that was given for the geometry that was shown. In which the spectra of the Zn(II) and Cd(II) complexes had distinct bands for the → π* and n → π associative domain transitions, respectively. It has been suggested that the tetrahedral geometric structure of the center of Zn(II) and Cd(II) is present[26].

Thermal Analysis

The thermal decomposition of solid ligands (HL) was investigated in an atmosphere composed of nitrogen. After reaching 800 degrees Celsius, the sample experienced a weight drop that was measured. The results of the TGA analysis showed quite clearly that the breakdown of the ligand occurs in four distinct stages (Fig. 4). The weight loss at the 1st peak, as indicated by the TGA curve at 97-215 °C, many attributes to the loss of ($2NH_3$) segments and one acetylene molecule (obs. = 0.1701 mg, 8.418 % ; calc.= 0.1701 mg, 8.418 %). The second step happened from 215 to 359 °C stated the elimination of (C_5H_4+C-$(CH_3)_3$+NH_3+-CO+$N(CH_3)_2$+C_6H_6) fragments; (obs. = 1.439 mg, 71.19 % ; calc. = 1.439 mg, 71.19 %). The third step recorded at 359-532 °C may indicate the loss of the ($2CH_4$+$3H_2$) segment (obs. = 0.1913 mg, 9.466 %; calc. = 0.1913 mg, 9.466 %). The final step at 532-800 °C is attached to the (CH_3+$4H_2$) segment (obs. = 0.1211 mg, 5.991 %; calc. = 0.1211 mg, 5.991 %). The thermogram $[Co(HL)_2Cl_2H_2O]$ complex proceeds in four steps, Fig 5. The loss of one molecule of the H_2O segments may be responsible for the appearance of the first peak, which was observed between 49 and 132 degrees Celsius (obs. =0.083 mg, 3.271%; calc. =0.082 mg, 3.52%). The second step occurred at 132-194°C, indicating the loss of ($4H_2$+ CH_4) fragment; (obs.=0.2078mg, 5.033%;calc.=0.200mg, 5.011%). The third step recorded at 194-370°C indicated the loss of ($2NH_3$) fragment, (obs.=0.253mg,6.133%;calc.=0.230mg,6.1%). The ford step recorded at 370-800°C indicated the loss of (CO + Cl_2 + $2H_2$ + N_2H_4) fragment, (obs.=1.006mg, 24.38%; calc.=0.998mg, 24.30%). The final residue of the ($2CH_4$ + CH_3 + C_2H_6 + C_3H_6 + $2C_6H_6$ + $3H_2$ + Co) calc.= 340.69mg, 61.37%. The thermogram of $[Cu(HL)_2Cl_2H_2O]$ is depicted in, Fig 6. The first peak detected at 52-172°C may attribute to the loss of a molecule of the (H_2O + CH_3) segment; (obs.=0.1974mg, 6.058%; calc.= 0.1954mg, 6.016). The second step occurred at 172-235°C indicated the loss of (CO + Cl_2 + CH_4 + $2NH_3$) fragment; (obs.=0.87mg,26.70%; calc.=0.85mg,26.53%). The third peak detected at 235-642°C may attribute to the loss of a molecule of the (Cu + $2H_2$) segment; (obs.=0.391mg, 12.02%; calc.= 0.380mg, 11.86). The four peak detected at 642-800°C may attribute to the loss of a molecule of the (N_2H_4 + $4H_2$) segment; (obs.=0.2374mg, 7.285%; calc.= 0.2300mg, 7.186). The final residue of the ($C_{13}H_{19}$ + $2NH_3$ + Cu) calc.= 304.35mg, 48.31%. The burning of the organic ligand in an environment composed mostly of nitrogen.

Biological Activity

Tests were conducted on the semicarbazone (HL) ligand as well as its analogs against four distinct types of bacteria, including two Gram-negative bacteria and two Gram-positive bacteria (*Staphylococcus aureus, Bacillus stubtilis, Escherichia coli* and *Pseudomonas aeruginosa*). The Mueller-Hinton agar technique is utilized to analyze all 27 of the chemicals. The DMSO solvent did not affect whatsoever the compounds that were investigated. DMSO in a concentration of 100 ppm is used in the solution. Table 5 shows that the ligand (HL) had no effect whatsoever on any of the tested bacteria types. When it came to eliminating bacteria of every variety, the HL complexes proved to be more effective than the free ligand (HL). The formation of complexes results in an enhancement of the antibacterial effect. This phenomenon and the chelation hypothesis of why complexes become more active might be related to one another in some way. Therefore, chelation reduces the polarity of the metal atom, which results in some of the atom's positive charge being shared with the donor group and possibly in the delocalization of electrons across the entirety of

Complex	λ_{nm}	Wave number $\bar{\upsilon}$ (cm^{-1})	Molar extinction coefficient ε_{max} ($dm^3\ mol^{-1}\ cm^{-1}$)	Assignment	Suggested geometry	μeff
[Mn (HL)Cl_2 H_2O]	298 385 841	33557 25974 11890	2296 1323 66	Intra-ligand π → π*,n→π* CT $^6A_1g \rightarrow {}^4T_1g(^4G)$	Distorted octahedral	6.06
[Co(HL) Cl_2 H_2O]	267 301 681 934	37453 33222 14684 10706	1400 1320 87 7	Intra-ligand π → π*,n→π* CT $^4T_1g^{(F)} \rightarrow {}^4A_2g^{(F)}$ $^4T_1g^{(F)} \rightarrow {}^4T_2g^{(p)}$	Distorted octahedral	5.19
[Ni(HL) Cl_2 H_2O]	285 350 421 794	26954 28571 23753 12594	2323 392 45 18	Intra-ligand π → π*,n→π* CT $^3A_2g^{(F)} \rightarrow {}^3T_1g^{(P)}$ $^3A_2g^{(F)} \rightarrow {}^3T_2g^{(F)}$	Distorted octahedral	3.10
[Cu(HL)Cl_2H_2O]	293 348 941	34129 28735 10626	2186 2498 42	Intra-ligand π → π*,n→π* CT $^2Eg \rightarrow {}^2T_2g$	Distorted octahedral	1.89
[Zn(HL) Cl]Cl	270 298	27037 33557	1768 1884	Intra-ligand π → π*,n→π* CT	Tetrahedral	Diamagnetic
[Cd(HL)Cl]Cl	268 301	37313 33222	1554 1384	Intra-ligand π → π*,n→π* CT	Tetrahedral	Diamagnetic

Table 4. Data on electronic spectra in solutions of DMSO, as well as magnetic moments of HL complexes.

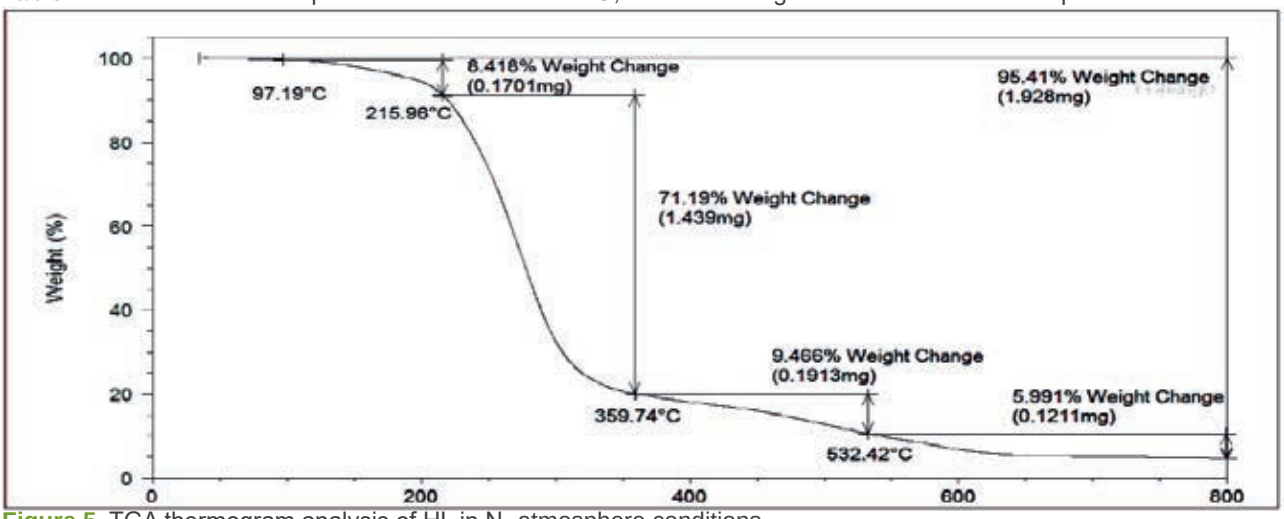

Figure 5. TGA thermogram analysis of HL in N_2 atmosphere conditions.

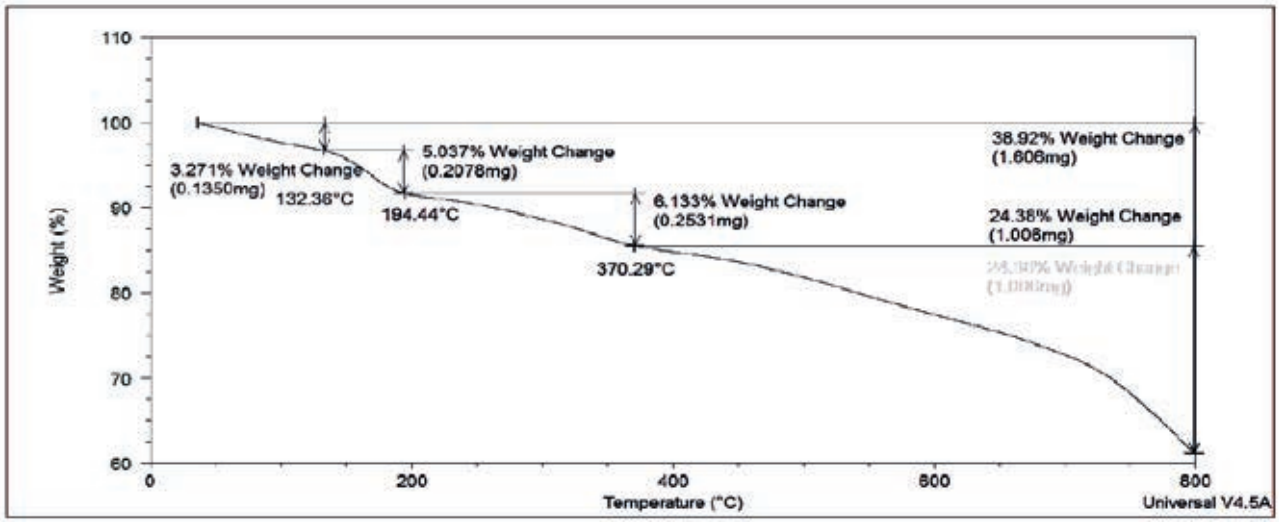

Figure 6. TGA of [Co(HL)Cl_2 H_2O] analyses in N_2 atmosphere conditions.

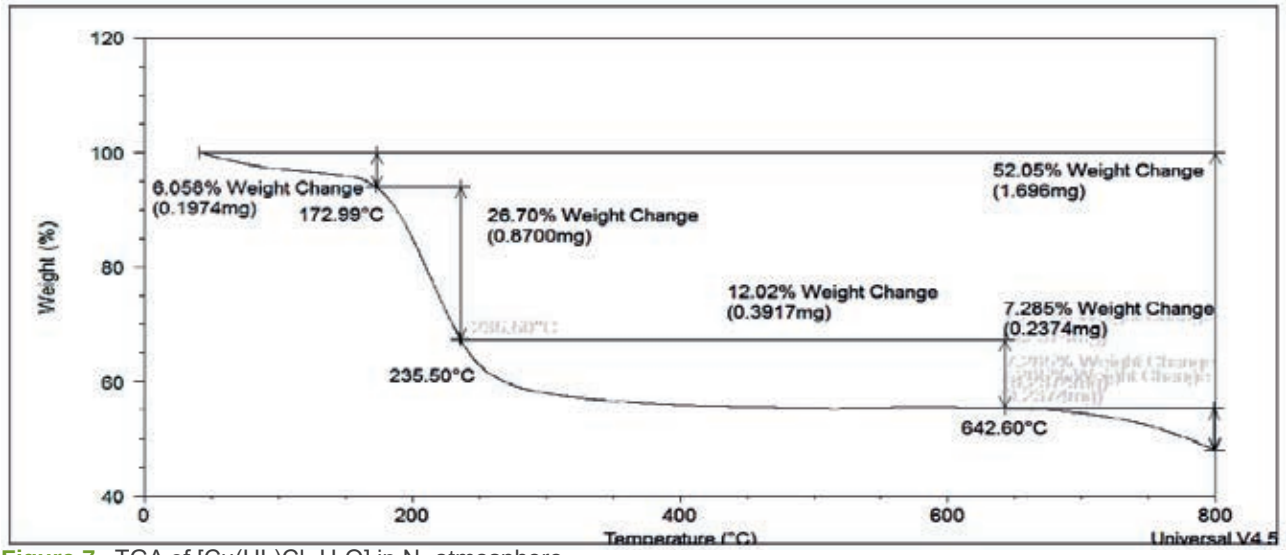

Figure 7. TGA of $[Cu(HL)Cl_2 H_2O]$ in N_2 atmosphere.

the ring. Zn(II)-complex almost had the highest antibacterial activity compared to other compounds. This is because, in comparison to those of other metal complexes, both their molecular weight and electronic configuration (using the d10 system) are on the lighter side. Compared to the free bonds and the other complexes, the cadmium (II) complex demonstrated significantly higher activity levels against all of the bacterial strains. As a result, we are now in a position to discuss the activity of the complexes in light of the chelation theory and the Overton model[28]. It describes the capacity of the metal component to penetrate the bacterial cell layer. The positive charge on the metal core will then be reduced due to this process, ultimately leading to coordinated bonding between the N and O atoms. Because of this, the lipophilic nature of the metal chelate system will increase, facilitating its movement across the lipid layer in the cell membranes of microorganisms. The research on the antifungal properties of semicarbazone ligand (HL) and its derivatives was conducted using two distinct kinds of fungi as test subjects (Candida and Rhizosporium), Table No. 5, which shows that the association found evidence of activity against both types of fungi. Compared to free ligands, HL complexes demonstrated much higher levels of antibacterial activity against all species of bacteria (HL). It was discovered that the molecule with the formula Cd(II) is more potent against (Candida and Rhizosporium). Because of the research that has been presented up until this point, new tridentate Schiff-base ligands have been tested to determine whether they are effective against a wide variety of pathogenic bacteria, viruses, and parasites. As mentioned earlier, the analysis was carried out to determine the effectiveness of these ligands. Some of these bacteria include *Clostridium perfringens*[29], *Brucella melitensis*[30], *Proteus vulgaris*[31,32], *Staphylococcus aureus*[33], *Pseudomonas aeruginosa*[34], and *Toxoplasma spp*[35,36], SARS-Cov-2[37]

Conclusions

The present study synthesized and described a carbazone half-ligand (HL) and its metal complexes. In monomer isolation, this is formed when the ligand combines with Mn(II), Co(II), Ni(II), Cu(II), Zn(II), and Cd(II) metal ions in a 1:1 (L: M) mol ratio. Physical, chemical, and spectroscopic investigations illuminated complex structures and linkages. These results yield compounds with quaternary or hexagonal coordination. The effectiveness of the ligand and its derivatives against bacteria and fungus was investigated. Free ligands were more bactericidal than semicarbazone complexes.

Funding

Self-Funding.

Conflicts of Interest

The authors declare no conflict of interest.

Compounds	*Escherichia coli* (G−)	*Pseudomonas aeruginosa*(G−)	*Bacillus stubtilis* (G+)	*Staphylococcus aureus* (G+)	*Candida*	*Rhizopus porium*
HL	13	14	13	12	17	15
$[Mn(HL)_2Cl_2]$	18	12	15	20	21	20
$[Co(HL)_2Cl_2].H_2O$	20	20	20	21	22	25
$[Ni (HL)_2 Cl_2]$.	16	15	17	16	20	16
$[Cu(HL)_2Cl_2].H_2O$	19	17	16	13	20	15
$[Zn (HL)_2].Cl_2$	16	15	17	16	19	16
$[Cd (HL)_2].Cl_2$	22	26	22	21	23	30

Table 5. The inhibition zones (mm) of antibacterial activity and antifungal activity for ligand and their complexes.

Bibliographic references

1. Cotton FA, Wilkinson G, Murillo CA, Bochmann M. Advanced inorganic chemistry. John Wiley and Sons, Inc.; 1999.
2. Hadi Kadhim S, Abd-Alla Q. I, Jawad Hashim T. Synthesis and Characteristic Study of Co (II), Ni (II) And Cu (II) Complexes of New Schiff Base Derived from 4-Amino Antipyrine. Int J Chem Sci. 2017; 15(1):107.
3. Hathaway BJ, Wilkinson G, Gillard RD, McCleverty JA. Comprehensive coordination chemistry. The synthesis, reactions, properties and applications of coordination compounds. 1987; 5 (1):533-774.
4. Sathe BS, Jayachandran E, Jagtap VA, Sreenivasa GM. Synthesis and antibacterial, antifungal activity of novel analogs of fluoro benzothiazole Schiff's base. Journal of Chemical and Pharmaceutical Sciences. 2010; 3(4):216-217.
5. Sondhi SM, Singh N, Kumar A, Lozach O, Meijer L. Synthesis, anti-inflammatory, analgesic and kinase (CDK-1, CDK-5 and GSK-3) inhibition activity evaluation of benzimidazole/benzoxazole derivatives and some Schiff's bases. Bioorganic & medicinal chemistry. 2006;14(11):3758-3765.
6. Sondhi SM., Singh N, Kumar A, Lozach O, Meijer L. Synthesis, anti-inflammatory, analgesic and kinase (CDK-1, CDK-5 and GSK-3) inhibition activity evaluation of benzimidazole/benzoxazole derivatives and some Schiff's bases. Bioorganic & medicinal chemistry, 2006; 14(11):3758-3765.
7. Chaubey AK, Pandeya SN. Synthesis & anticonvulsant activity (Chemo Shock) of Schiff and Mannich bases of Isatin derivatives with 2-Amino pyridine (mechanism of action). International Journal of PharmTech Research. 2012;4(4):590-598.
8. Aboul-Fadl T, Mohammed FA, Hassan EA. Synthesis, antitubercular activity and pharmacokinetic studies of some Schiff bases derived from 1-alkylisatin and isonicotinic acid hydrazide (INH). Archives of pharmacal research. 2003;26(10):778-784.
9. Wei D, Li N, Lu G, Yao K. Synthesis, catalytic and biological activity of novel dinuclear copper complex with Schiff base. Science in China Series B. 2006;49(3):225-229.
10. Avaji PG, Kumar CV, Patil SA, Shivananda KN, Nagaraju C. Synthesis, spectral characterization, in-vitro microbiological evaluation and cytotoxic activities of novel macrocyclic bis hydrazone. European Journal of medicinal chemistry. 2009;44(9):3552-3559.
11. Samraa Ali Hussein and Enaam Ismail Yousif. Metal complexes of semicarbazone ligand derived from Mannich-β-aminocarbonyl : Synthesis, structural characterisation, thermal properties and biological activity. Biochem. Cell. Arch. 2021; 21(2): 4855-4863. DocID: https://connectjournals.com/03896.2021.21.4855.
12. Yousif EI, Hussien AK, Hasan HA.COII, NIII and CDII complexes derived from mixed Azo-linked schift base ligands: Formation, characterization, thermal analysis and biological study. Plant Archives, 2020; 20(1):2405-2411.
13. Ahmed AI, Yousif EI. New Metal Complexes with AZO ligand; Synthesis, Spectral Characterisation and Biological Evaluation. Pakistan Journal of Medical & Health Sciences. 2022; 16(07):550-554.
14. Gow NA, Van De Veerdonk FL, Brown AJ, Netea MG. Candida albicans morphogenesis and host defence: discriminating invasion from colonization. Nature reviews microbiology. 2012; 10(2):112-122.
15. Hussain SA, Al-Jeboori MJ. New metal complexes derived from Mannich-base ligand; Synthesis, spectral characterisation and biological activity. J. Global Pharma Tech. 2019; 11(2):548-560.
16. Nakamoto, K. Infrared Spectra of Inorganic and Coordination Compounds. John Wiley and Sons, New York, 1996. 4th Edn.
17. Volkert WA, Hoffman TJ. Therapeutic radiopharmaceuticals. Chemical reviews. 1999;99(9):2269-2292.
18. Bal S, Bal SS. Cobalt (II) and Manganese (II) complexes of novel Schiff bases, synthesis, charcterization and thermal, antimicrobial, electronic, and catalytic features. Adv. Chem. 2014;2014:1-2.
19. Castonguay LA, Treasurywala AM, Caulfield TJ, Jaeger EP, Kellar KE. Prediction of q-values and conformations of gadolinium chelates for magnetic resonance imaging. Bioconjugate chemistry. 1999; 10(6):958-964.
20. Hasan HA, Yousif EI, Al-Jeboori MJ. Metal-assisted assembly of dinuclear metal (II) dithiocarbamate Schiff-base macrocyclic complexes: Synthesis and biological studies. Global J. Inorg. Chem. 2012; 3(10):1-7.
21. Abass RU, Yousif EI. New Metal Complexes Derived from Schiff-Base Ligand: Synthesis Structural Characterisation, Thermal Properties and Biological Evaluation. HIV Nursing. 2022; 22(2):3561-3571.
22. Ramachandran E, Gandin V, Bertani R, Sgarbossa P, Natarajan K, Bhuvanesh NS, Venzo A, Zoleo A, Glisenti A, Dolmella A, Albinati A. Synthesis, characterization and cytotoxic activity of novel copper (II) complexes with aroylhydrazone derivatives of 2-Oxo-1, 2-dihydrobenzo [h] quinoline-3-carbaldehyde. Journal of Inorganic Biochemistry. 2018; 182:18-28.
23. Dong XY, Kang QP, Li XY, Ma JC, Dong WK. structurally characterized solvent-induced homotrinuclear cobalt (II) N2O2-donor bisoxime-type complexes. Crystals. 2018; 8(3):139-141.
24. Hassaan AM, Khalifa MA, Shehata AK. COMPLEXES OF SOME METAL IONS WITH A SCHIFF BASE LIGAND DERIVED FROM ISATIN AND O□AMINOPHENOL. Bulletin des Sociétés Chimiques Belges. 1995; 104(3):121-124.
25. Souza P, Mendiola MA, Matesanz AI, Fernández V, Arquero A. Synthetic and physicochemical studies of divalent metal complexes with cyclic hydrazone and semicarbazone ligands. Transition Metal Chemistry. 1995; 20(2):157-161.
26. Lever, A. B. P. Inorganic Electronic Spectroscopy, Elsevier Publishing House, Amsterdam-London-New York. 1984.
27. Choudhary MI, Thomsen WJ. Bioassay techniques for drug development. CRC Press; 2001.
28. Singh RV, Dwivedi R, Joshi SC. Synthetic, magnetic, spectral, antimicrobial and antifertility studies of dioxomolybdenum (VI) unsymmetrical imine complexes having a No N donor system. Transition Metal Chemistry. 2004;29(1):70-74.
29. Hashim ST, Fakhry SS, Rasoul LM, Saleh TH, Alrubaii BA. Genotyping toxins of Clostridium perfringens strains of rabbit and other animal origins. Tropical Journal of Natural Product Researchthis link is disabled. 2021;5(4):613-616.
30. abdulkaliq Awadh H, Hammed ZN, Hamzah SS, Saleh TH, AL-Rubaii BA. Molecular identification of intracellular survival related Brucella melitensis virulence factors. Biomedicine. 2022;42(4):761-765.
31. Abdul-Gani MN, Laftaah BA. Purification and characterization of chondroitinase ABC from Proteus vulgaris, an Iraqi clinically isolate. Current Science. 2017:2134-2140.
32. kadhim AL-Imam MJ, AL-Rubaii BA. The influence of some amino acids, vitamins and anti-inflammatory drugs on activity of chondroitinase produced by Proteus vulgaris caused urinary tract infection. Iraqi Journal of Science. 2016:2412-2421.
33. Sabah Fakhry S, Noori Hammed Z, Abdul-elah Bakir W, Abdullah Laftaah ALRubaii B. Identification of methicillin-resistant strains of Staphylococcus aureus isolated from humans and food sources by Use of mecA 1 and mecA 2 genes in Pulsed-field gel electrophoresis (PFGE (technique. Revis Bionatura 2022; 7 (2) 44. http://dx.doi.org/10.21931/RB/2022.07.02.44.
34. Shehab ZH, AL-Rubaii BA. Effect of D-mannose on gene expression of neuraminidase produced from different clinical isolates of Pseudomonas aeruginosa. Baghdad Science Journal. 2019;16(2):291–298.
35. Abdulla L, Ismael MK, Salih TA, Malik SN, Al-Rubaii BA. Genotyping and evaluation of interleukin-10 and soluble HLA-G in abortion due to toxoplasmosis and HSV-2 infections. Annals of parasitology. 2022;68(2):385-390.
36. Jiad AL, Ismael MK, Muhsin SS, Al-Rubaii BA. ND2 Gene Sequencing of Sub fertile Patients Recovered from COVID-19 in Association with Toxoplasmosis. Bionatura. 2022;7(3):45. http://dx.doi.org/10.21931/RB/2022.07.03.45.
37. Rasoul LM, Nsaif MM, Al-Tameemi MT, Al-Rubaii BA. Estimation of primer efficiency in multiplex PCR for detecting SARS-Cov-2 variants. Bionatura, 2022, 7(3), 48. http://dx.doi.org/10.21931/RB/2022.07.03.49.

ARTICLE / INVESTIGACIÓN

New dimeric complexes with semicarbazone mannich-based ligand; formation, structural investigation and biological activity

Hadeel J. Abaas and Mohamad J. Al-Jeboori*

DOI. 10.21931/RB/2023.08.02.15

Department of Chemistry, College of Education for Pure Science (Ibn Al-Haitham), University of Baghdad, Adhamiyah, Baghdad, Iraq.
Corresponding author: mohamad.al-jeboori@ihcoedu.uobaghdad.edu.iq

Abstract: The formation of a new semicarbazone Schiff-base ligand (E)-2-(2-(phenyl(2-phenylhydrazinyl)- methyl) cyclohexylidene)hydrazine-1-carboxamide (HL) and its complexes are reported. The new ligand was prepared from the condensation of the Mannich-base 2-(phenyl(2-phenylhydrazinyl)methyl)cyclohexan-1-one (M) with the semicarbazide. A series of metal complexes were prepared by the reaction of the ligand with the metal chlorides of Cr(III), Mn(II), Co(II), Ni(II), Cu(II)), Zn(II) and Cd(II). The structure of the ligand and its complexes were elucidated through analytical and spectroscopic techniques. The analyses indicated the ligand behaves as a monobasic tridentate species and the isolation of dimeric complexes with the general formula; $[Cr(L)(Cl)_2(H_2O)]_2$, $[M(L)Cl]_2$ (where M= Mn(II), Co(II), Ni(II), Cu(II)), Zn(II) and Cd(II)). These studies revealed a distorted octahedral geometry for Cr(III), a distorted square planar for Cu(II) and a tetrahedral arrangement for Mn(II), Co(II), Ni(II), Zn(II) and Cd(II). The biological activity of the prepared compounds against *Escherichia coli*, *Pseudomonas auroginosa, Staphylococcus aureus* and *Bacillus subtilis* compared with Cefotaxime (as a standard antibiotic) was also explored. Some of the examined compounds indicated a similar antibacterial activity to Cefotaxime. Furthermore, antifungal activity against *Candida albicans* and *Rhizopus sporium* was investigated, which showed that the ligand and its complexes exhibited good antifungal activity.

Key words: Schiff-base ligand, Structural characterization, Dimeric semicarbazone complexes, Biological activity.

Introduction

Mannich bases are one of the necessary reagents that play an essential role in developing synthetic organic chemistry. Mannich approach is a one-pot multicomponent reaction. This type of reaction represents a feasible procedure for highly reactive intermediates that can be quickly transformed into various new compounds[1]. These include their role as precursors for synthesizing a range of natural product compounds and forming heterocyclic phenanthridine derivatives[2,3]. Further, a variety of exciting ligands and, subsequently, their metal complexes have been derived from Mannich compounds[4]. Mannich base ligands and their complexes are of great interest as they have a range of applications, including their uses in medicine[5] and as potential pharmaceutical agents[6]. Further, they exhibit applications in polymer and surfactant chemistry, as detergent additives, and as antioxidants[7]. Upon using ligands derived from Mannich bases as complexation agents, the biological activities of these complexes are enhanced[8]. Schiff bases are important species that are used as complexation agents for metal ions. This is because they can form stable compounds with almost all metal ions. These compounds have applications in medicine, as a mimic of bioactive molecules, in catalysis, in analytical and environmental chemistry and as a scavenger for removing heavy metal ions[9]. Their bioavailability makes these materials excellent antiviral, antiinflammatory, antiapoptotic and antibacterial agents[10,11]. Semicarbazones are a Schiff base compound bearing N, O-chelating site for complexation[12]. They can bind transition and non-transition ions and have a range of exciting applications, including their pharmaceutical and biological activities[12,13]. Semicarbazone Schiff base compounds have a range of applications, including their ability to bind with DNA and act as antibacterial, antifungal, anticancer, antiinflammatory, antioxidant, antiviral, analgesic, and anticonvulsant agents[14-16]. In the present work, we report the synthesis, structural characterization and biological behavior (antibacterial and antifungal influence) of a new semicarbazone ligand and its dimeric complexes. The ligand is designed to incorporate phenylhydrazine within the framework of the Mannich base that is used as a precursor for the preparation of the ligand. The aim of using phenylhydrazine in the formation of the ligand is (i) to explore the impact of this segment on the structural and coordination mode upon the reaction of the ligand with metal ions and (ii) to observe the influence of the phenylhydrazine on the biological activity of the prepared compounds against microbiological species.

Materials and methods

All reagents used in this work were commercially available and used as received. The mass spectrum for the ligand was measured using the electrospray technique (positive mode) on the Agilent mass spectrometer Sciex ESI mass analysis. The ^{1}H-NMR for the ligand was recorded in DMSO-d_6 using a Brucker 400 MHZ with a tetramethylsilane (TMS) as an internal reference. A Shimadzu Fourier Transform Infrared Spectrometer (FTIR-600) was used to record the spectra of compounds using KBr and CsI discs from 4000–250 cm^{-1}. Electronic spectra were measured

Citation: Abaas H J, Al-Jeboori M J. New dimeric complexes with semicarbazone mannish-based ligand; formation, structural investigation and biological activity. Revis Bionatura 2023;8 (2) 15. http://dx.doi.org/10.21931/RB/2023.08.02.15
Received: 2 January 2023 / **Accepted:** 19 April 2023 / **Published:** 15 June 2023

Publisher's Note: Bionatura stays neutral with regard to jurisdictional claims in published maps and institutional affiliations.

from 200–1100 nm for 10^{-3} M solutions in DMSO at room temperature with a Shimadzu 160 spectrophotometer. Melting points were determined using an electrothermal Stuart apparatus, model SMP_{40}. Elements analysis (CHN) for ligand and their metal complexes were performed on an Eager 300 for EA1112. Metal and chloride percentages for compounds were conducted using a Shimadzu (AA) 680G atomic absorption spectrophotometer and potentiometric titration method on a 686-nitro processor-665 Dosimat-Metrom Swiss. A Eutech Instruments Cyberscan con 510 digital conductivity meter recorded molar conductance for complexes. Magnetic moments measurements were performed at 298.6 K using Sherwood Scientific Devised. The biological activities of compounds against bacterial and fungi species were examined at the Iraqi Ministry of Science and Technology's Central Service Laboratory.

Synthesis

Preparation of 2-(phenyl(2-phenylhydrazinyl)methyl) cyclohexan-1-one (M)

The synthesis of Mannich-base precursor 2-(phenyl(2-phenylhydrazinyl)- methyl)cyclohexan-1-one was achieved by adopting the reported method in (17-19) and as follows; In to 100ml round-bottomed flask charged with a solution of $CaCl_2$ (1.1g, 10mmol) in ethanol (10ml) and three drops of HCl (37%) were added benzaldehyde (1.06ml, 10mmol), phenylhydrazine (1.00ml, 10mmol) and cyclohexanone (1.03ml, 10mmol) consecutively. The reaction mixture was allowed to stir at room temperature for 12h, during which time an off-white solid was generated. This was removed by filtration, washed with distilled water (30ml) and ethanol (30ml), then dried in air. Yield: 1.8g (61%); m.p =158-160°C ; M.wt=294 amu. FT-IR (KBr) cm^{-1}; 3471 $\nu(O\text{-}H)_{enol}$, 3414 and 3313 ν(N-H) stretching of the secondary amine, 1620 $\nu(C{=}C)w\ cm^{-1}$.

Synthesis of (E)-2-(2-(phenyl(2-phenylhydrazinyl) methyl)cyclohexylidene)hydrazine-1-carboxamide (HL)

A mixture of M (0.18g, 0.62 mmol) in 10 ml of EtOH was added with stirring semicarbazide hydrochloride (0.07g, 0.62 mmol) in 10 ml of EtOH. The reaction mixture was heated at reflux for 6h and then allowed to slow evaporation at RT. Upon standing, light-brown crystals were formed, which were collected by filtration, washed with cold ethanol (5ml) and diethyl ether (10ml) then dried in air. Yield: 0.12g (52%), m.p =179-180°C.; M.wt=351 amu. FT-IR (KBr) cm^{-1}; 3460 $\nu(N_4\text{-}H)$, 3309 $\nu(N_5\text{-}H)$, 3286 $\nu(N_2\text{-}H)$, 3194 and 3163 $\nu(N_1\text{-}H)$, 1685 $\nu(C{=}O)$ 1647 cm^{-1} $\nu(C{=}N)_{imine}$. The ^{1}HNMR (400 MH_Z, DMSO-d_6) ppm; δH= 10.26 (1H, s, N_2-H), 7.84, 7.72-7.70 ppm (2H, dd, J= 1.2, 1.7 Hz), 7.08 (N_4-H), 4.63 (N_4-H), 3.05 (N_1-H) and (C-H) of the cyclohexyl segment, 2.08 (C-H) ppm that is next to the (N_4-H). EI–MS= m/z (%) = 305.10 observed for $[M\text{-}(NH_2CHO)]+$ (100%), 278.0 $[M\text{-}(NHCHO{+}N_2)]^+$ (5%), 208.1 $[M\text{-}(NHCHO{+}N_2{+}(CH_2)3N_2)]^+$ (101%), 178.0 $[M\text{-}(NHCHO{+}N_2{+}(CH_2)3N_2{+}C2H_4)]^+$ (72%), 134.1 $[M\text{-}(NHCHO{+}N_2{+}(CH_2)3N_2{+}C_6H_2)]^+$ (25%), 121.0 $[M\text{-}(NHCHO{+}N_2{+}(CH)11N)]^+$ (90%), 93.1 $[M\text{-}(NHCHO{+}N_2{+}(CH)11N{+}C_2H_6)]^+$ (45%), 77.1$[M\text{-}(NHCHO{+}N_2{+}(CH)11N{+}C_2H_6{+}NH_2)]^+$ (48%), 63.1$[M\text{-}(NHCHO{+}N_2{+}(CH)11N{+}C_3H_6{+}NH_2)]^+$ (28%) and 44.1 $[M\text{-}(NHCHO{+}N_2{+}(CH)11N{+}C_5H_{12}{+}NH_2)]+$ (33%) .

General Synthetic Procedure for Complexes

A solution of the semicarbazone ligand (0.1g, 0.28mmol) in ethanol (15ml) was allowed to stir then an ethanolic solution of potassium hydroxide was added dropwise to adjust the pH of the mixture to ca. 9. After stirring for 15 min an equivalent amount of the title metal chloride in 5ml of EtOH was added slowly. The mixture was heated at reflux with stirring for 3h. The resultant colored solid products formed were collected by filtration, washed with diethyl ether (5ml), and dried in air. Elemental analysis data, colors, and yields for the complexes are given in Table 1. The FT-IR and electronic data are listed in Tables 2 and 3, respectively.

Biological Evaluation

The semicarbazone ligand (HL) and its transition metal complexes were screened for their antibacterial activity against *Escherichia coli, Pseudomonas auroginosa, Staphylococcus aureus* and *Bacillus subtilis* strains. The activity was performed using the agar well diffusion method, in which wells were dug in the media using a sterile metallic borer with a center diameter of at least 6 mm[17,18]. The activity of tested compounds was compared with Cefotaxime as an antibiotic standard. The tested compounds were dissolved in DMSO and incubated at 37°C for 24h. The role of DMSO against the tested species was also performed, which showed it has no effect. The concentrations of tested compounds and antibiotic standard were; 50mg/ml. The obtained data is included in Table 4. The antifungal activity of compounds was studied against two fungal strains *Candida albicans* and *Rhizopus sporium* species and data are placed in Table 4.

Results and discussion

Chemistry

The formation of the Mannich-base precursor 2-(phenyl(2-phenylhydrazinyl)- methyl)cyclohexan-1-one (M) was accomplished through a one-pot three-component approach using calcium chloride as a catalyst.

The reaction of benzaldehyde, phenylhydrazine, cyclohexanone and CaCl2 in a 1:1:1:1 mole ratio, using EtOH as a medium, gave the title compound (Scheme 1). The condensation reaction of the precursor with the semicarbazide in a 1:1 mole ratio in EtOH medium resulted in the formation of the title ligand (E)-2-(2-(phenyl(2-phenylhydrazinyl)methyl)cyclohexylidene)hydrazine-1-carboxamide (HL), Scheme 1. The reaction of the ligand with metal chlorides of Cr(III), Mn (II), Co(II), Ni(II), Cu(II), Zn(II), and Cd(II) in a 2:1 (L:M) mole ratio (using KOH as a base and EtOH as a medium) resulted in no pure complexes and subsequently, it was difficult to confirm the entity of the products. Therefore, the reaction proceeded in a 1:1 (L:M) mole ratio (using KOH as a base and EtOH as a medium), isolating six-coordinate and four-coordinate dimeric complexes, Scheme 2. KOH was essential to deprotonate the ligand and generate the monobasic species, and no reaction proceeded without adjusting the pH of the reaction to ca. 9. A range of physicochemical techniques characterized the prepared compounds (ligand and complexes). These include; 1H-NMR and mass spectroscopy (for ligand), micro-elemental analyses and metal and chloride ratio (Table 1), FT-IR (Table 2), and UV-Vis spectroscopy (Table 3). Conductance measurement was implemented to confirm metal complexes' electrolytic and non-electrolytic nature and to understand the number of counter ions out site the coordination sphere.

The molar conductance of complexes in DMSO solutions indicated nonelectrolyte complexes' isolation. Further, the electronic data suggested the isolation of a six-coordinate dimeric Cr(III)-complex in which two water molecules require to give this structure. The FTIR data and the elemental microanalyses supported this. Based on the above data, dimeric complexes of the general formula $[Cr(L)(Cl_2)(H_2O)]2$ and $[M(L)Cl]_2$ (where; M= Mn(II), Co(II), Ni(II), Cu(II), Zn(II) and Cd(II)) were isolated.

FT-IR datas

FT-IR of precursor

The spectrum of M shows no band around 1700 cm^{-1} may relate to the carbonyl of the cyclohexanone (Figure 1). This could be attributed to a tautomerism phenomenon, the enol and keto-form[17-20]. Therefore, the species in the solid state exists in the enol form. This was supported by the appearance of a band at 3471 cm^{-1} related to $v(O-H)_{enol}$, which was formed due to tautomerism within the cyclohexyl moiety, Scheme 3. This was backed up by a weak band at ca. 1620 cm^{-1} assigned to v(C=C) of the cyclohexyl segment. The two bands at 3414 and 3313 cm^{-1} attributed to v(N-H) stretching of the secondary amine. Peaks at 3055, 3024 and 1593 cm^{-1} in the M spectrum are attributed to the v(C-H)aromatic, v(C-H)aliphatic and v(C=C)aromatic stretching[17-19,21], respectively.

NMR, FT-IR and mass spectrum of semicarbazone ligand

The ^{1}H-NMR of HL, Figure 2, which was recorded in DMSO-d_6 indicated two sets of peaks in the aliphatic and aromatic regions. The singlet peak at 10.26 ppm (1H, s) corresponds to (N_2-H). The signal observed at chemical shift 7.84 with a two proton integral and the doublet of doublet peak at 7.72-7.70 ppm (2H, dd, J= 1.2, 1.7 Hz) equivalent to two protons is correlated to the aromatic protons. A chemical shift that was recorded as a broad peak at 7.08 ppm correlated to (N_5-H). The multiple signals appeared between 7.39-7.09 ppm, with integration corresponding to four protons assigned to the aromatic protons. Further, a peak at 6.46 ppm that is equivalent to two protons has related to the aromatic protons. The chemical shift observed at 4.63 ppm is assigned to (N_4-H). A peak recorded at 3.05 ppm, which is equivalent to three protons is due to 2 protons of (N_1-H) and one proton of the (C-H) of the cyclohexyl segment. A peak detected at 2.08 ppm equivalent to one proton was related to the (C-H) that is next to the (N_4-H). Other peaks detected between 2.26 and 0.82 ppm correlated to the aliphatic protons of the remaining protons of the cyclohexyl segments.

The FT-IR of HL, Figure 5, showed bands at 3460 and 3309 cm^{-1} attributed to v(N4-H) and v(N5-H) of the hydrazine group, respectively. A band at 3286 cm^{-1} can be assigned to the $v(N_2-H)$ stretching vibration. Peaks recorded at 3194 and 3163 cm^{-1} are attributed to the asymmetric and symmetric bands of v(N1-H). The spectrum showed new bands at 1685 and 1647 cm^{-1}, which correlated to the $v(C=O)_{amide}$ group of semicarbazone and $v(C=N)_{imine}$[18], respectively.

The electrospray (+) mass spectrum of HL is placed in Figure, and the fragmentation pathway is in Scheme 4. The spectrum showed no peak at m/z = 351 amu may attribute to the molecular ion of the parent compound (M)+. Peaks detected at m/z=305.10 (100%), 278.0 (4.54%), 208.1 (10.61%), 178.0 (72.72%), 134.1 (25.75%), 121.0 (90.90%), 93.1 (45.62%), 77.1 (48.52%), 63.1 (28.55%) and 44.1 (33.33%) related to $[M-(NH_2CHO)]^+$, $[M-(NHCHO+N_2)]^+$, $[M-(NHCHO+N_2+(CH_2)3N_2)]^+$, $[M-(NHCHO+N_2+(CH_2)3N_2+C_2H_4)]^+$, $[M-(NHCHO+N_2+(CH_2)3N_2+C_6H_2)]^+$, $[M-(NHCHO+N_2+(CH)_{11}N)]^+$, $[M-(NHCHO+N_2+(CH)_{11}N+C_2H_6)]^+$, $[M-(NHCHO+N_2+(CH)_{11}N+C_2H_6+NH_2)]^+$, $[M-(NHCHO+N_2+(CH)_{11}N+C_3H_6+NH_2)]^+$ and $[M-(NHCHO+N_2+(CH)_{11}N+C_5H_{12}+NH_2)]^+$, respectively.

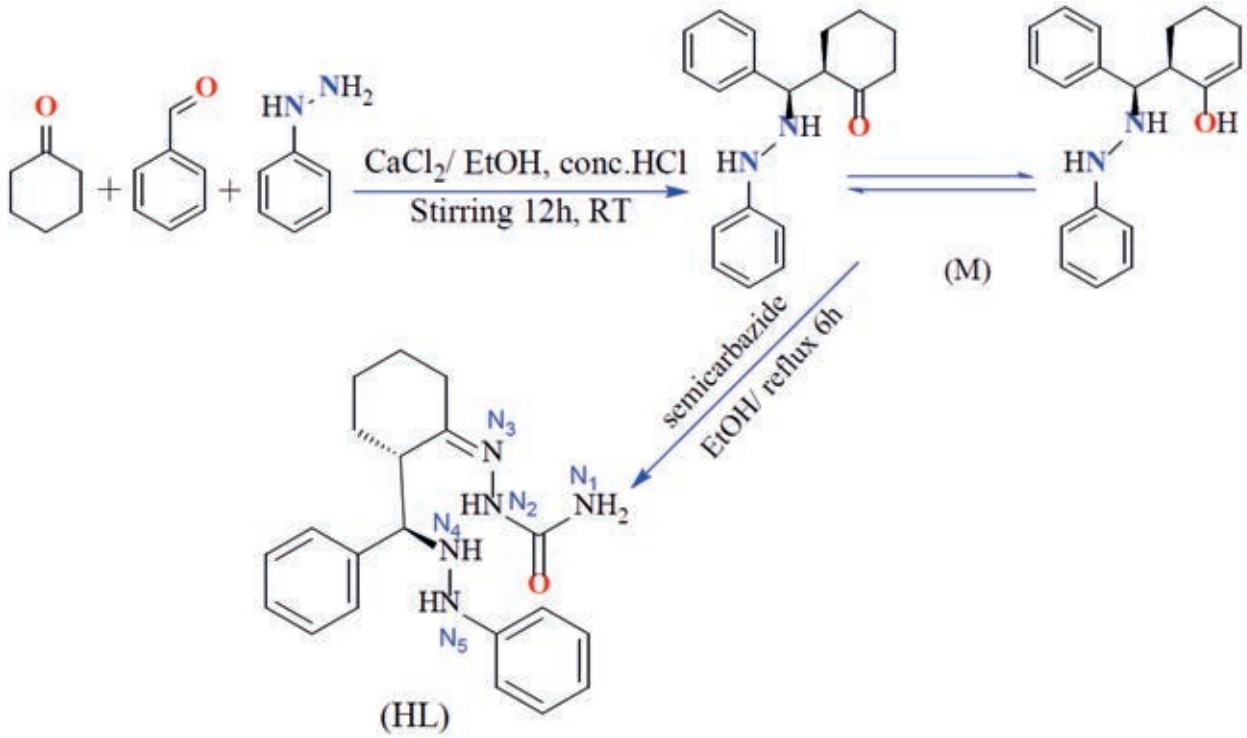

Figure 1. Synthesis route of the precursor and ligand.

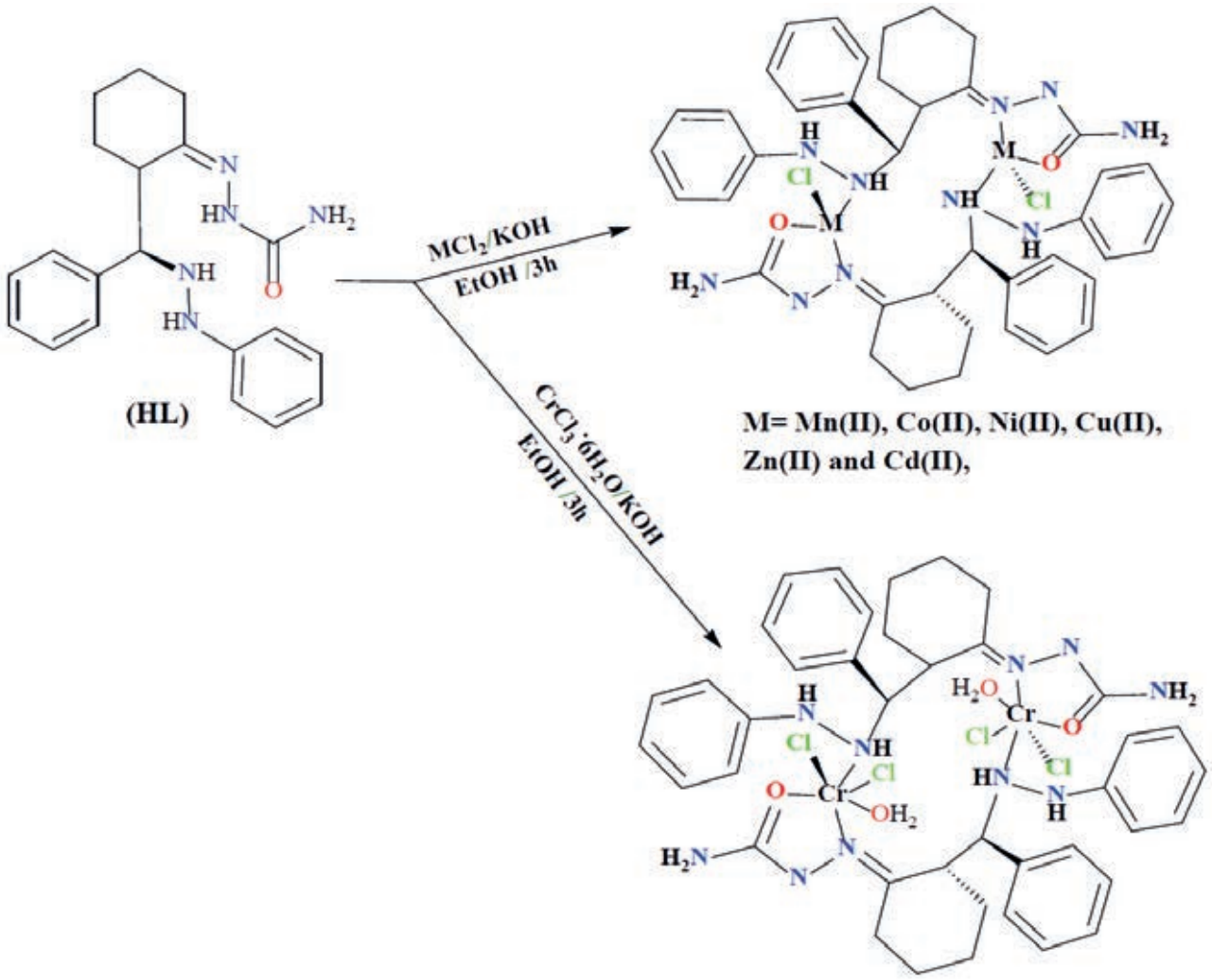

Figure 2. Synthesis route of dimeric complexes.

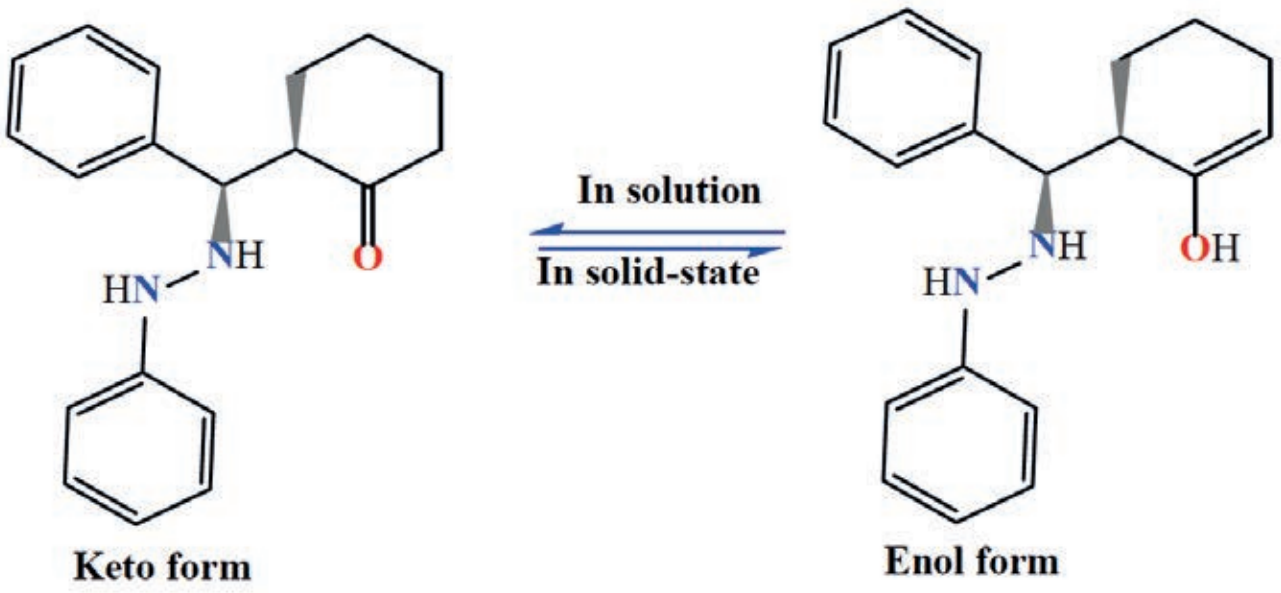

Figure 3. A tautomerism phenomenon within the cyclohexyl moiety.

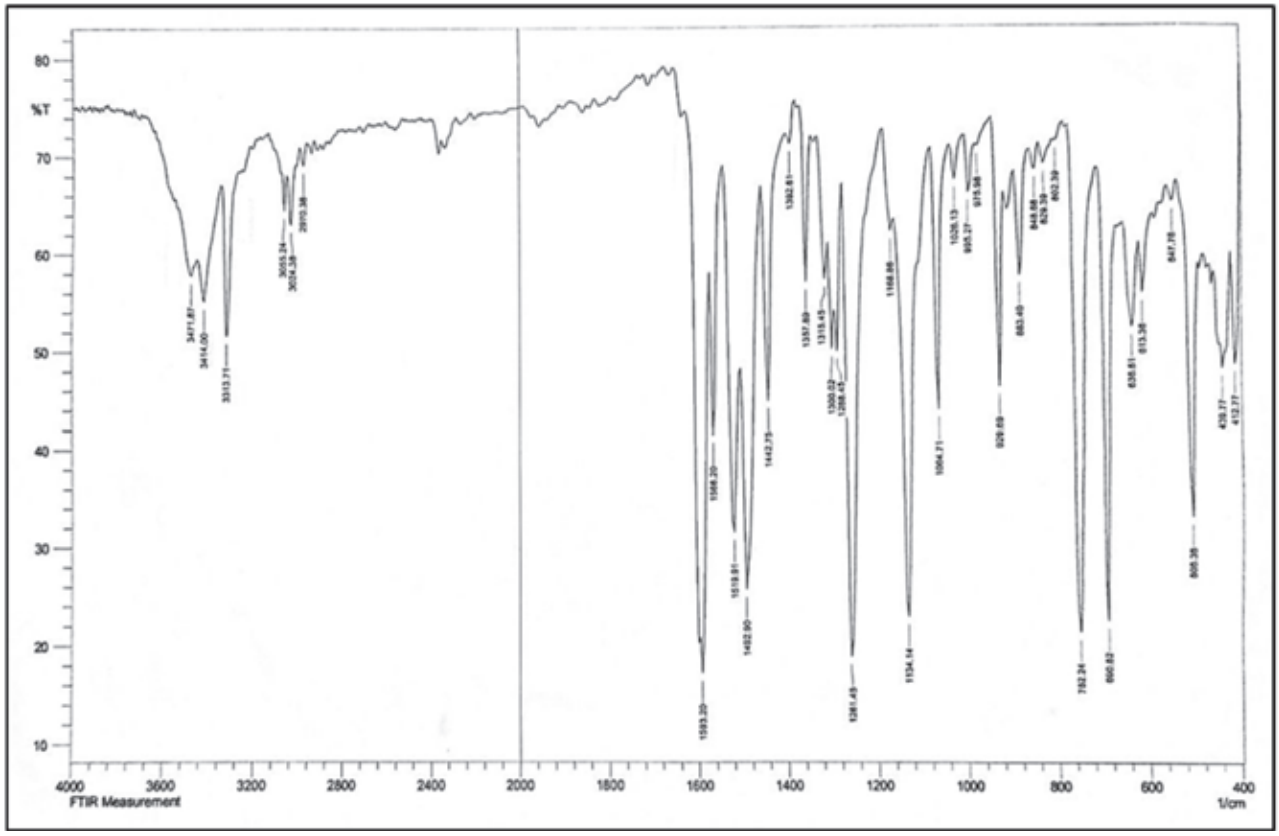

Figure 4. FT-IR spectrum of M.

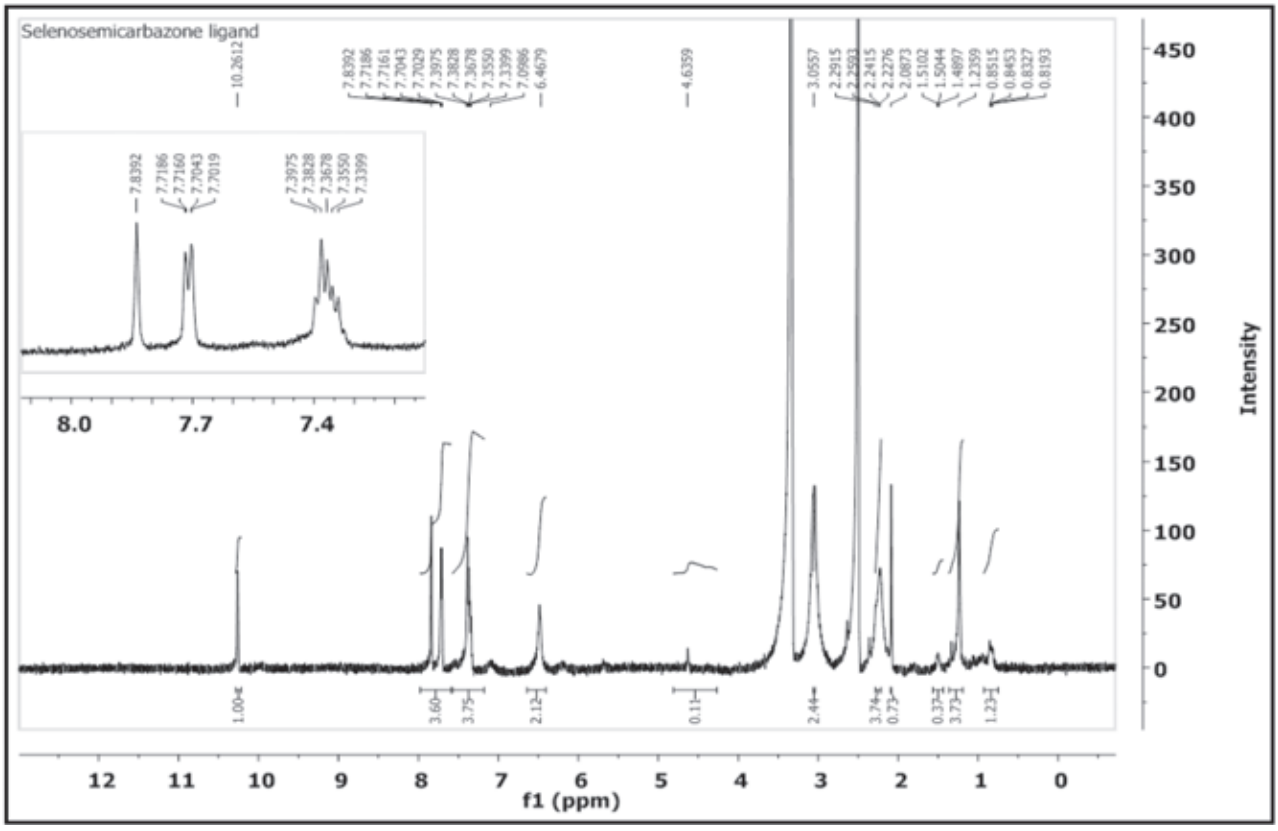

Figure 5. ^{1}H-NMR spectrum of HL in DMSO-d_6 solution.

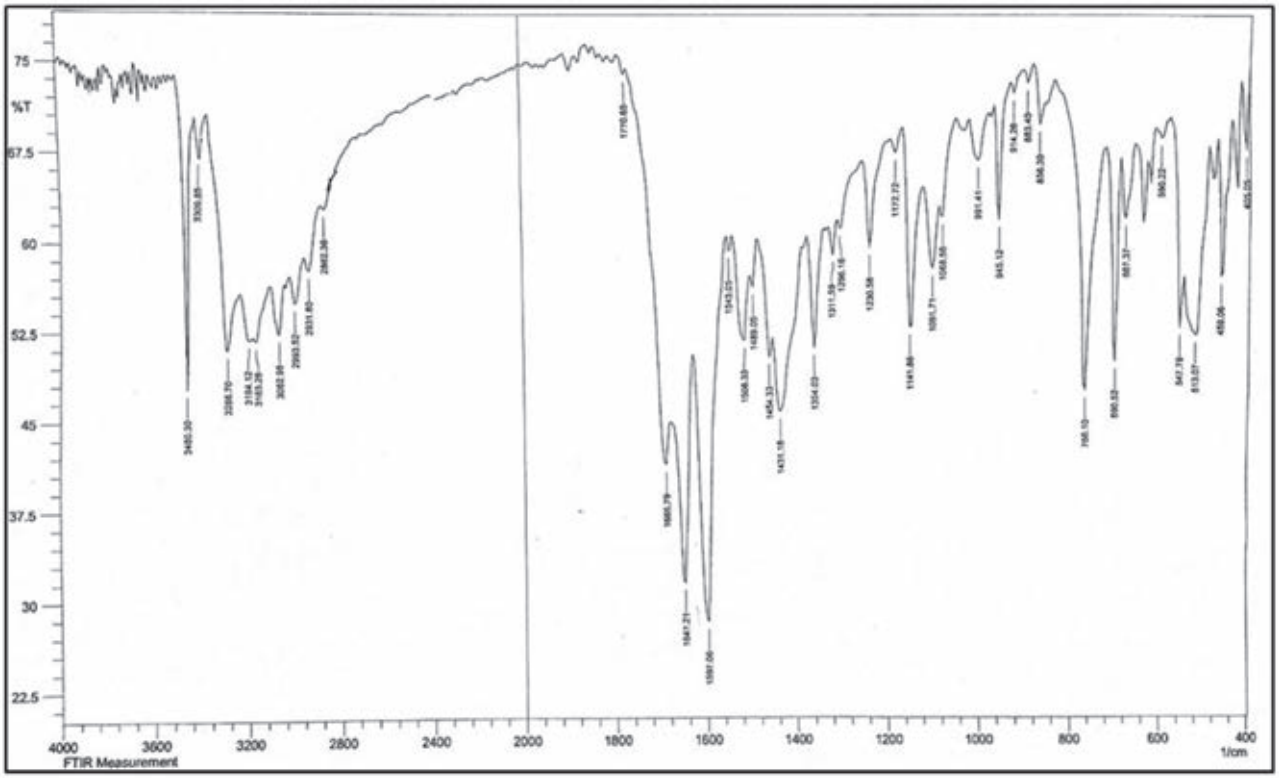

Figure 6. FT-IR spectrum of HL.

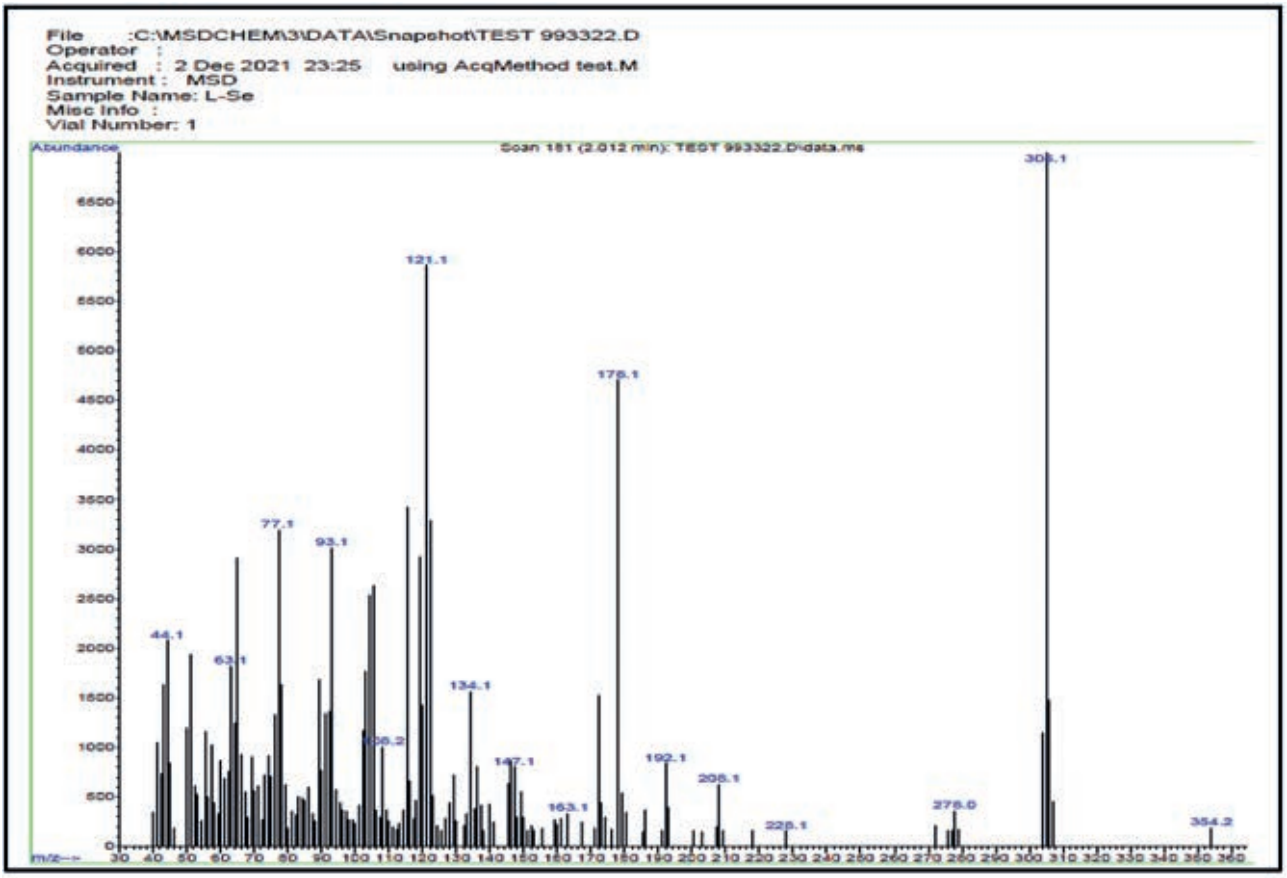

Figure 7. The electrospray (+) mass spectrum of HL.

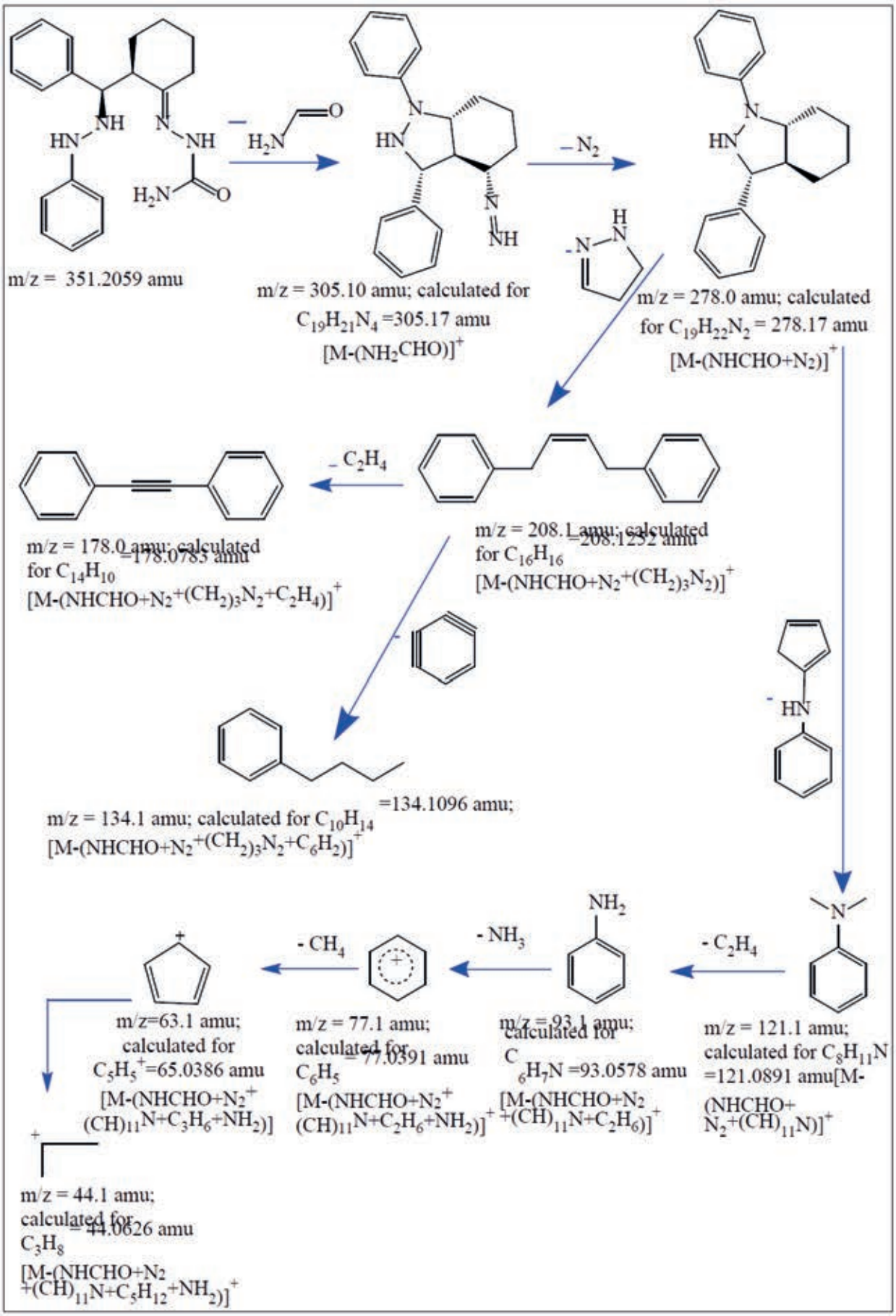

Figure 8. Fragmentation pathway of HL.

FT- IR spectra for complexes

The spectra of complexes showed no stretching band that may assign to v(N2-H), indicating the deprotonation of the ligand upon complexation. The spectra revealed a shift in the imine stretching band, v(C=N), by 4-20 cm^{-1} (compared with that at 1647 cm^{-1} in the free ligand) and appeared at 1631, 1631, 1627, 1639, 1643, 1635 and 1635 cm^{-1} in Cr(III), Mn(II), Co(II), Ni(II), Cu(II)), Zn(II) and Cd(II). respectively. The shifting of this band is due to the coordination of the nitrogen atom of the -C=N group of the imine to the metal center. The band at 1685 cm^{-1}, which is due to v(C=O)amide in the free ligand, is shifted by 11-39 cm^{-1} to lower frequency and appeared at 1666, 1664, 1672, 1668 and 1669 cm^{-1} in Cr(III), Ni(II), Cu(II)), Zn(II) and Cd(II) complexes, respectively. However, this band was shifted to a higher wavenumber (compared with the spectrum of the ligand) by 4 and 12 cm^{-1} and appeared at 1689 and 1697 cm^{-1} for complexes Mn(II)and Co(II), complexes respectively. This shifting is a piece of evidence for the coordination of the oxygen atom of the semicarbazone to the metal center[19]. The spectrum of the free ligand revealed a peak at 3460 related to v(N_4-H) stretching of the hydrazine group. This peak suffered a shift, compared with the spectrum of the ligand, and appeared at 3433, 3402, 3440, 3444, 3375,3379 and 3394 for Cr(III), Mn(II), Co(II), Ni(II), Cu(II)), Zn(II) and Cd(II) complexes, respectively. The shift in the v(N-H) confirmed the involvement of the nitrogen atom in the coordination with the metal ions[17]. Bands displayed in the range 3302-3340 attributed to v(N_5-H). More, bands at 3199; 3159, 3190; 3159, 3175; 3109, 3159;3124, 3175; 3109, 3199;3170 and 3155; 3109 cm^{-1} assigned to v(N1-H) in Cr(III), Mn(II), Co(II), Ni(II), Cu(II)), Zn(II) and Cd(II) complexes, respectively. The spectra indicated the appearance of new bands at 551, 567, 562, 536, 505, 543 and 543 cm^{-1} referred to v(M-O) of Cr(III), Mn(II), Co(II), Ni(II), Cu(II), Zn(II) and Cd(II) complexes, respectively[19,23]. Bands related to v(M-N) were observed at 455, 451, 450, 420,462, 443 and 445 cm^{-1} for Cr(III), Mn(II), Co(II), Ni(II), Cu(II), Zn(II) and Cd(II), respectively[17,18,22-24]. Finally, The FT-IR spectra recorded bands related to v(Cr_Cl) at 231;237 cm^{-1}, v(Mn_Cl) at 244 cm^{-1}, v(Co_Cl) at 243 cm^{-1}, v(Ni_Cl) at 247 cm^{-1}, v(Cu_Cl) at 239 cm^{-1}, v(Zn_Cl) at 246 cm^{-1}, v(Cd_Cl) at 248 cm^{-1} [23-25]. These bands confirmed the coordination of the chlorido moiety to the metal centre. Further, the appearance of two peaks in the spectrum of the Cr(III)-complex indicated the two coordinated chlorido moieties adopt the cis configuration. The spectrum of $[Cr(L^1)Cl_2H_2O]_2$.indicated peaks at 3525 and 694 cm^{-1} related to v(OH) and v(M-OH_2), respectively[26].

Electronic spectra and magnetic moment measurements

The UV-Vis spectrum of HL exhibits peaks at 288, 343 and 363 nm due to π→π*, n→π* and charge transfer transitions[25-28], respectively. The electronic spectrum of the Cr(III)-complex indicated peaks at 462, 554 and 644 nm assigned to $^4A_2g(F)\rightarrow{}^4T_2g(F)$, $^4A_2g(F)\rightarrow{}^4T_1g(F)$ and $^4A_2g(F)\rightarrow{}^4T_1g(P)$, respectively suggesting an octahedral geometry about the Cr atom[24,28]. The spectrum of the Mn(II)-complex displayed peaks in the visible region at 664 and 730 nm attributed $^6A_1\rightarrow{}^4T_2$ (G) and $^6A_1\rightarrow{}^4A_1$ (G),4E(G), respectively. This data suggest the coordination sphere of the Mn atom is tetrahedral[29]. The Co(II)-complex revealed peaks in the visible region at 503 and 620 nm correlated to $^4T_1(F)\rightarrow{}^4T_1(p)$ and $^4T_1(F)\rightarrow{}^4A_2(F)$ transitions, respectively and indicating tetrahedral structure around the Co atom[25]. The spectrum of the Ni(II)-complex exhibited absorption peaks at 635, 797 and 840 nm attributed to $^3T_1(F)\rightarrow{}^3T_1(P)$, $^3T_1(F)\rightarrow{}^3A_2$ (F) and $^3T_1(F)\rightarrow{}^3T_2(F)$, respectively confirming tetrahedral arrangement about the Ni atom[29]. Peaks recorded at 675 and 756 nm in the Cu(II)-complex spectrum were assigned to $^2B_1g\rightarrow{}^2B_2g$ and $^2B_1g\rightarrow{}^2A_2g$, respectively, suggesting a distorted square planar geometry about the Cu(II). The spectra of the Zn(II) and Cd(II) complexes showed peaks around 281 nm assigned to the ligand field. Further, a peak at ca. 358 nm may attribute to charge transfer transition type M→L. As the two metal ions are d^{10} configuration, the spectra showed no bands in the d-d region[24,25,28,30]. Therefore, the suggested tetrahedral geometry of the metal centre of the d^{10} configuration was based on the other characterisation tools. The magnetic susceptibility data for the HL complexes are presented in Table 3. The lowering of such magnetic moments may relate to the anti-ferromagnetic that occurred due to the formation of a dimeric species. The value for the Cr(III) complex is 3.87 BM, which indicates an octahedral geometry about the Cr atom. The magnetic moment measurements values of Mn(II), Co(II) and Ni(II) complexes are 2.46, 2.23 and 3.28 BM, respectively. These values are lower than the total spin-only values, indicating a tetrahedral geometry around the metal centre[31]. The measured magnetic data of the Cu(II) complex 1.40 BM, may indicate a distorted square planer geometry about the Cu atom[31].

Biological activity

The synthesised ligand and its metal complexes were tested for their microbiological activity against bacterial species: G-positive (*Staphylococcus aurius, Bacillus subtilis*) and G-negative (*Escherichia coli, Pseudomonas auroginosa*). The selected bacteria are considered to be the most harmful and deadly kind of bacteria. These bacteria are widely detected in the surgery operation rooms of hospitals. Further, two types of fungi were explored that have an impact on human beings (*Candida albicans* and *Rhizopus sporium* species). The commercial antibiotic Ceftriaxone was implemented as a reference drug for bacteria species[32]. In general, all the prepared compounds showed excellent activity against bacterial strains, compared with the activity of Cefotaxime. Further, the Cu(II) and Ni(II)-complexes showed the highest activity against the two types of fungi, compared with the free ligand. The enhanced activity of the complexes against the examined microbial species may be attributed to the chelating theory[17-19,32]. Further, the involvement of phenylhydrazine in the formation of the Mannich-base and subsequently in the structure of the ligand and complexes, could be another factor in enhancing the biological activity of compounds. Figures 5 and 6 and Table 4 display the biological activity data.

Conclusions

This work is based on the synthesis of a new semicarbazone Schiff-base ligand (E)-2-(phenyl(2-enylhydrazinyl) methyl)cyclohexylidene)hydrazine-1-carboxamide, and its dimeric complexes with Cr(III), Mn(II), Co(II), Ni(II), Cu(II), Zn(II), and Cd(II). The formation of the ligand was derived from the reaction of the prepared Mannich-based precursor with the semicarbazide. The ligand is designed to include a phenylhydrazine segment within the structure of the Mannich base precursor, which is then used in the formation of the ligand. The objective of using phenylhydrazine in the formation of the ligand is to study the structural influence, coordination mode and biological effects that occurred on

Comp.	Molecular Formula	Colour	m.p	Y. (%)	Microanalysis; calculated found (%)				Λ_m S.cm^2. mole^{-1}
					C	H	N	Cl	
HL	$C_{20}H_{25}N_5O$	Light-brown	179-180	52	(68.35) 67.87	(7.17) 6.79	(19.93) 19.65	-	-
$[Cr(L)(Cl)_2(H_2O)]_2$	$C_{40}H_{50}Cl_4Cr_2N_{10}O_4$	Light-green	228-230	63	(48.99) 48.90	(5.14) 5.20	(14.28) 14.25	(14.46) 14.40	13.32
$[Mn(L)Cl]_2$	$C_{40}H_{46}Cl_2Mn_2N_{10}O_2$	Deep Brown	231-233	60	(54.62) 54.56	(5.27) 5.22	(15.92) 15.88	(8.06) 8.11	16.05
$[Co(L)Cl]_2$	$C_{40}H_{46}Cl_2Co_2N_{10}O_2$	Red brown	235-237	71	(54.13) 54.25	(5.22) 5.28	(15.78) 15.74	(7.99) 7.92	15.36
$[Ni(L)Cl]_2$	$C_{40}H_{46}Cl_2Ni_2N_{10}O_2$	Brown	246-248	68	(54.15) 54.19	(5.23) 5.28	(15.79) 15.70	(7.99) 7.90	12.74
$[Cu(L)Cl]_2$	$C_{40}H_{46}Cl_2Cu_2N_{10}O_2$	Dark blue	228-230	62	(53.57) 53.53	(5.17) 5.22	(15.62) 15.68	(7.91) 7.97	11.42
$[Zn(L)Cl]_2$	$C_{40}H_{46}Cl_2Zn_2N_{10}O_2$	Light brown	238-240	64	(53.35) 53.31	(5.15) 5.11	(15.55) 15.58	(7.87) 7.81	14.02
$[Cd(L)Cl]_2$	$C_{40}H_{46}Cl_2Cd_2N_{10}O_2$	Light brown	221-223	70	(48.30) 48.36	(4.66) 4.60	(14.08) 14.14	(7.13) 7.11	16.44

Table 1. Microanalysis and physical properties of HL and its complexes.

Comp.	$\nu(N_4\text{-}H)$ $\nu(N_5\text{-}H)$	$\nu(N_1\text{-}H)$	$\nu(C{=}O)$	$\nu(C{=}N)$ $\nu(C{=}C)$	$\delta(NH)$	$\nu(M\text{-}O)$	$\nu(M\text{-}N)$	$\nu(M\text{-}Cl)$
HL*	3460, 3309	3194, 3163	1685	1647 1597	1508	-	-	-
$[Cr(L)(Cl)_2(H_2O)]_2$*	3433, 3302	3199, 3159	1666	1631 1620	1523	551	455	231,237
$[Mn(L)Cl]_2$	3402, 3302	3190, 3159	1689	1631 1598	1554	567	451	244
$[Co(L)Cl]_2$	3440, 3333	3175, 3109	1697	1627 1600	1512	562	450	243
$[Ni(L)Cl]_2$	3444, 3340	3159, 3124	1664	1639 1589	1512	536	420	247
$[Cu(L)Cl]_2$	3375, 3323	3175, 3109	1672	1643 1620	1531	505	462	239
$[Zn(L)Cl]_2$	3379, 3313	3199, 3170	1668	1635 1593	1512	543	443	246
$[Cd(L)Cl]_2$	3394, 3332	3155, 3109	1669	1635 1600	1535	543	445	248

*HL; $\nu(N_2\text{-}H)$ = 3286 cm^{-1}; peaks at 3525 and 694 cm^{-1} related to $\nu(OH)$ and $\nu(M\text{-}OH_2)$, respectively in $[Cr(L)Cl_2H_2O]_2$.

Table 2. FT-IR data (cm^{-1}) of HL and its complexes.

Comp.	λ_{nm}	$\bar{\upsilon}(cm^{-1})$	ε_{max} ($dm^3.mol^{-1}.cm^{-1}$)	Assignment	Suggested Geometry	μ_B BM
HL	288	34722	2029	$n \rightarrow \pi^*$	--------	-
	343	29154	1088	$\pi \rightarrow \pi^*$		
	363	27548	1165	C.T*		
$[Cr(L)(Cl)_2(H_2O)]_2$	284	35211	2420	LF*	Distorted octahedral	3.78
	360	27777	860	CT		
	460	21739	90	$^4A_2g_{(F)} \rightarrow {}^4T_1g_{(P)}$		
	554	18050	76	$^4A_2g_{(F)} \rightarrow {}^4T_1g_{(F)}$		
	644	15527	74	$^4A_2g_{(F)} \rightarrow {}^4T_2g_{(F)}$		
$[Mn(L)Cl]_2$	281	35587	2442	LF	Distorted Tetrahedral	2.46
	348	28735	713	CT		
	664	15060	30	$^6A_{1(G)} \rightarrow {}^4T_{2(G)}$		
	730	13698	19	$^6A_{1(G)} \rightarrow {}^4A_{1(G)}, {}^4E_{(G)}$		
$[Co(L)Cl]_2$	283	35335	2443	LF	Distorted Tetrahedral	2.23
	360	27777	250	CT		
	503	19880	38	$^4T_{1(F)} \rightarrow {}^4T_{1(P)}$		
	620	16129	22	$^4T_{1(F)} \rightarrow {}^4A_{2(F)}$		
$[Ni(L)Cl]_2$	262	38167	270	LF	Distorted Tetrahedral	3.28
	340	29411	160	CT		
	635	15748	40	$^3T_{1(F)} \rightarrow {}^3T_{1(P)}$		
	797	12547	58	$^3T_{1(F)} \rightarrow {}^3A_{2(F)}$		
	840	11904	10	$^3T_{1(F)} \rightarrow {}^3T_{2(P)}$		
$[Cu(L)Cl]_2$	263	38022	522	LF	Distorted square planar	1.40
	349	28653	225	CT		
	675	14814	45	$^2B_1g \rightarrow {}^2B_2g$		
	756	13227	30	$^2B_1g \rightarrow {}^2A_2g$		
$[Zn(L)Cl]_2$	281	35587	1823	LF	Distorted Tetrahedral	-
	359	27855	972	CT		
$[Cd(L)Cl]_2$	282	35460	1558	LF	Distorted Tetrahedral	-
	358	27932	757	CT		

*L.F=ligand field, C.T=charge transfer

Table 3. UV-Vis, suggested structures and magnetic moment data of HL and its complexes.

the ligand and its metal complexes. The entity of the prepared compounds was established using several analytical and spectroscopic techniques. These analyses indicated the Schiff base ligand behaves as a monobasic tridentate species and coordinated through the nitrogen atoms of the imine and hydrazine group and the oxygen carbonyl atom. Further, the isolation of a dimeric six-coordinate for the Cr(III)-complex and a dimeric four-coordinate for the Mn(II), Co(II), Ni(II), Cu(II), Zn(II), and Cd(II) complexes was supported by the physicochemical investigation. Due to the formation of a dimeric species, these complexes' low magnetic moment values may account for their anti-ferromagnetic behavior. The biological activities of the prepared compounds against four types of bacteria and two types of fungi were investigated. It was found that compounds showed good anti-microbiological activity.

Author Contributions

Hadeel H. Abaas: Performed All Experiments, Data Curation, and manuscript Writing. Mohamad J. Al-Jeboori: Supervision, Methodology, Project Administration, Conceived the Experimental Plan, Analysed the Data, Writing- Original draft, Writing- Reviewing and Editing.

Acknowledgments

The authors thank the University of Baghdad, College of Education for Pure Science (Ibn Al-Haitham) and Department of Chemistry for providing Ms. HHA with the facilities for the MSc studentship and labs.

Conflicts of Interest

The authors declare there is no conflict of interest.

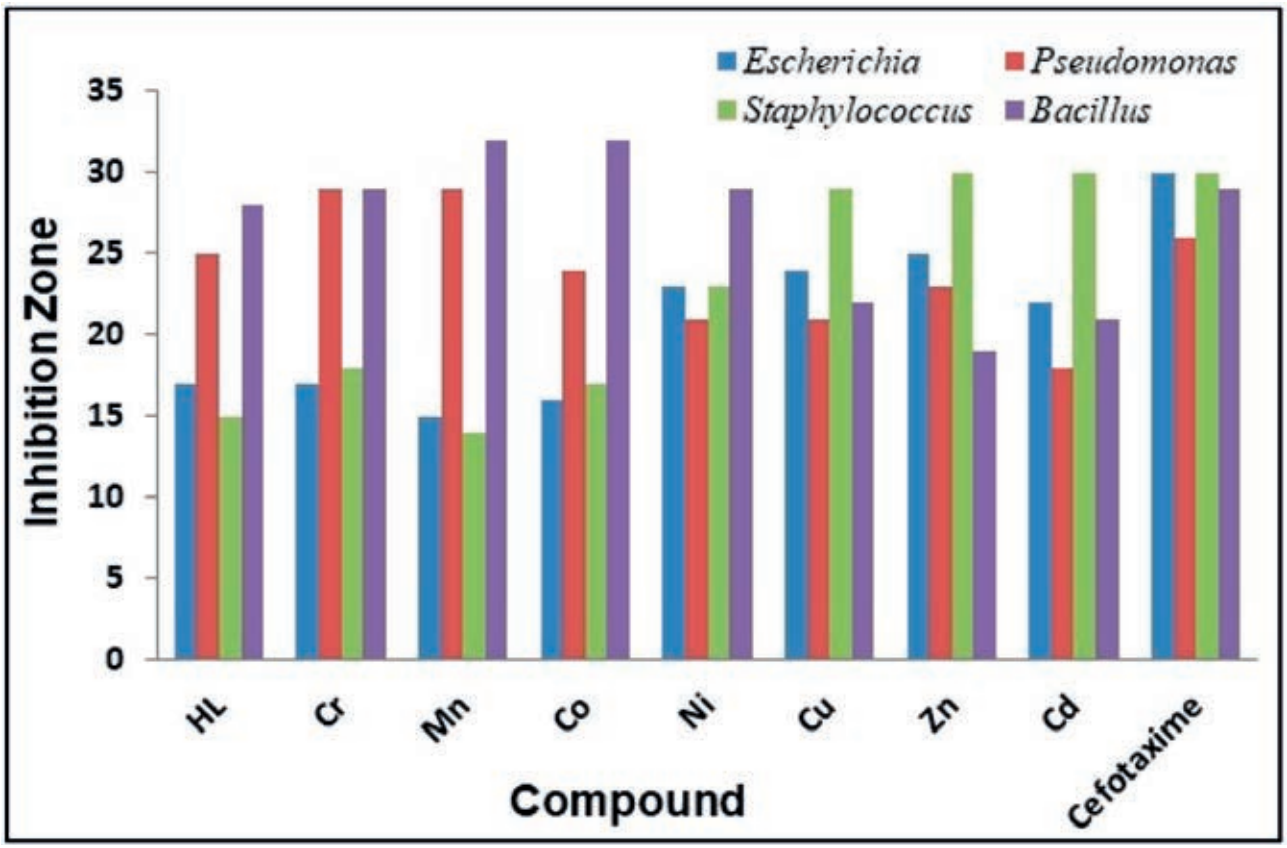

Figure 9. The inhibition zone diameter (mm) against bacterial species for HL ligand and its complexes.

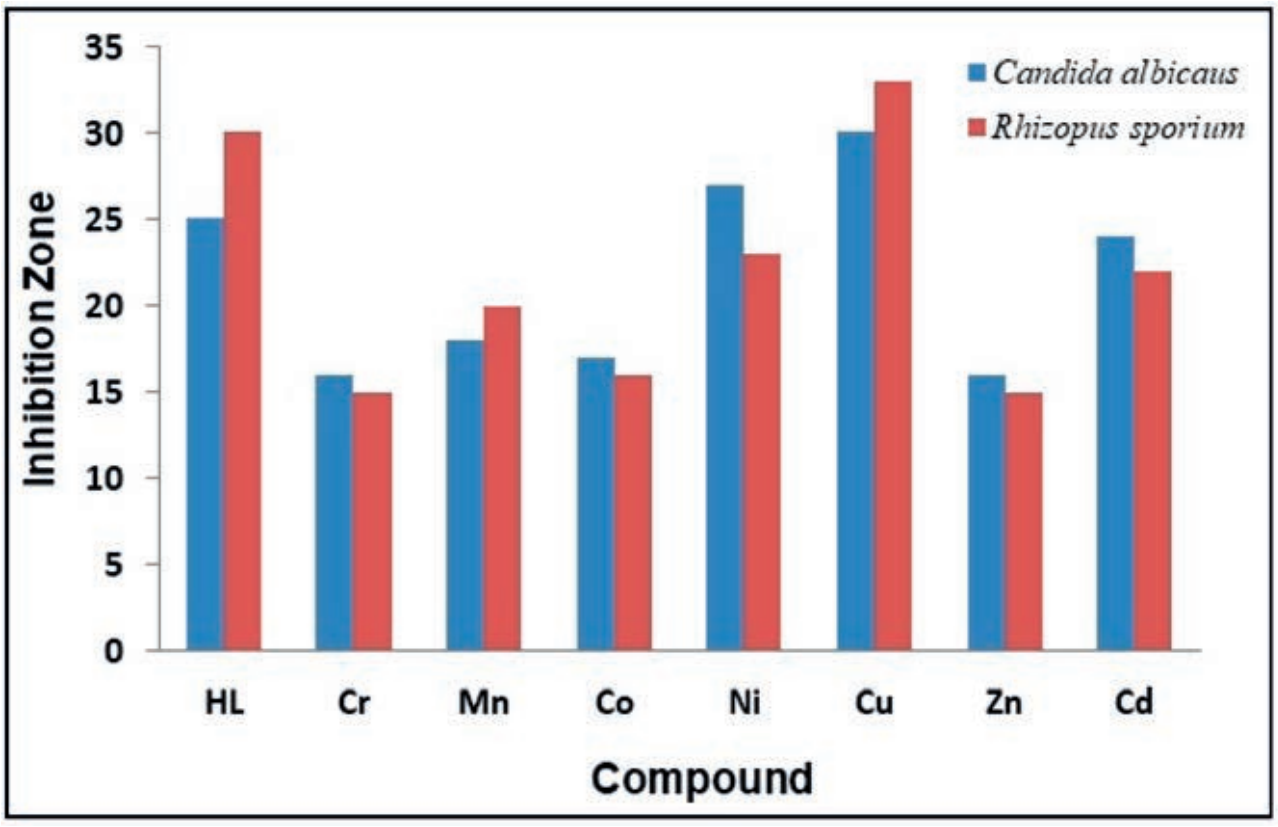

Figure 10. The inhibition zone diameter (mm) against fungi for HL ligand and its complexes.

Compound	Bacteria				Fungi	
	Gram-negative		Gram-positive			
	E. Coli	*Pseudomonas auroginosa*	*Staphylococcus aurius*	*Bacillus subtilis*	*Candida albicaus*	*Rhizopus sporium*
DMSO	---	19	21	---	---	---
Cefotaxime	18	16	23	15	-	-
M	9	21	20	16	10	17
$[Cr(M)(Cl)_2(H_2O)_2]Cl$	29	24	25	20	9	20
$[Fe(M)(Cl)_2].H_2O$	33	25	27	22	13	17
$[Co(M)(Cl)_2].H_2O$	33	24	30	19	10	20
$[Ni(M)]Cl_2.H_2O$	25	20	26	20	13	20
$[Cu(M)(Cl)_2].H_2O$	31	27	24	20	9	16

Table 4. The biological evaluation screening data (zone of inhibition in mm) of semicarbazone ligand and its complexes.

Bibliographic references

1. Al-Rubaye, B. K.; Al-Jeboori, M. J.; Potgieter, H. Metal Complexes of Multidentate N2S2 Heterocyclic Schiff-base Ligands; Formation, Structural Characterisation and Biological Activity. Journal of Physics: Conference Series, 2021, 1879(22074), 3-20.
2. Al-Rubaye, B. K.; Brink, A.; Miller, G. J.; Potgieter, H.; Al-Jeboori, M. J. Crystal structure of (E)-4-benzylidene-6-phenyl-1,2,3,4,7,8,9,10-octahydrophenanthridine. Acta Crystallographica Section E: Crystallographic Communications, 2017, 73(7), 1092-1096.
3. Al-Rubaye, B. K.; Potgieter, H.; and Al-Jeboori, M. J. An Efficient One-Pot Approach for the Formation of Phenanthridine Derivative; Synthesis and Spectral Characterisation. Der Chemica Sinica, 2017, 8(3), 365-370.
4. Al-Jeboori, M. J.; Al-Jebouri, F. A.; and Al-Azzawi, M. A. Metal complexes of a new class of polydentate Mannich bases: Synthesis and spectroscopic characterisation. Inorganica Chimica Acta, 2017, 379(1), 163-170.
5. Liu, X.; Manzur, C.; Novoa, N.; Celedón, S.; Carrillo, D.; Hamon, J. R. Multidentate unsymmetrically-substituted Schiff bases and their metal complexes: Synthesis, functional materials properties, and applications to catalysis. Coordination Chemistry Reviews, 2018, 357, 144-172.
6. Naeimi, H.; Nazifi, Z. S.; Amininezhad, S. M.; Amouheidari, M. Synthesis, characterization and in vitro antimicrobial activity of some new Schiff bases and their complexes. The Journal of Antibiotics, 2013, 66(11), 687-689.
7. Mukherjee, T.; Pessoa, J. C.; Kumar, A.; Sarkar, A. R. Synthesis, structure, magnetic properties and biological activity of supramolecular copper (II) and nickel (II) complexes with a Schiff base ligand derived from vitamin B6. Dalton Transactions, 2013, 42(7), 2594-2607.
8. Fetoh, A.; Asla, K. A.; El-Sherif, A. A.; El-Didamony, H.; El-Reash, G. M. A. Synthesis, structural characterization, thermogravimetric, molecular modelling and biological studies of Co (II) and Ni (II) Schiff bases complexes. Journal of Molecular Structure, 2019, 1178, 524-537.
9. Al-Jeboori, M. J., Al-Dujaili, A. H., and Al-Janabi, A. E. Coordination of carbonyl oxygen in the complexes of polymeric N-crotonyl-2-hydroxyphenylazomethine. Transition Metal Chemistry, 2019, 34(1), 109-113.
10. Enyedy, É. A.; Bognár, G. M.; Nagy, N. V.; Jakusch, T.; Kiss, T.; Gambino, D. Solution speciation of potential anticancer metal complexes of salicylaldehyde semicarbazone and its bromo derivative. Polyhedron, 2014, 67, 242-252.
11. Li, L.; Zhang, Y. Z.; Liu, E.; Yang, C.; Golen, J. A.; Rheingold, A. L.; Zhang, G. Synthesis and structural characterization of zinc (II) and cobalt (II) complexes based on multidentate hydrazone ligands. Journal of Molecular Structure, 2016, 1110, 180-184.
12. Al-Rubaye, B. K.; Hussien, N. J.; Abul Rahman, A. A.; Yousif, E. I.; Al-Jeboori, M. J. "New organotin (IV) complexes derived from 3,4-dihydroxybenzaldehydeN(4)-ethyl-3-semicarbazone ligand; synthesis, characterisation and biological activity". Biochemical and Cellular Archives, 2020, 20(2), 6571-6579.
13. Hosseini-Yazdi, S. A.,; Samadzadeh-Aghdam, P.; Mirzaahmadi, A.; Khandar, A. A.; Mahmoudi, G.; Ruck, M.; Doert, T.; Balula, S. S.; Cunha-Silva, L. Synthesis, crystal structures, spectroscopic and electrochemical studies on Cu (II) and Ni (II) complexes with compartmental nitrogen–oxygen mixed donor ligands. Polyhedron, 2014, 80, 41-46.
14. Crook, A. J.; Lisic, E. C.; and Ensor, D. D. Thiosemicarbazone and semicarbazone chelating resins and their potential use in environmental applications. Separation Science and Technology, 2012, 47(14-15), 2225-2229.
15. Asghari, A.; Ghazaghi, M.; Rajabi, M.; Behzad, M.; Ghaedi, M. Ionic liquid-based dispersive liquid-liquid microextraction combined with high-performance liquid chromatography-UV detection for simultaneous preconcentration and determination of Ni, Co, Cu and Zn in water samples. Journal of the Serbian Chemical Society, 2014, 79(1), 63-76.
16. Liaqat, M.; Mahmud, T.; Ashraf, M.; Muddassar, M.; Imran, M.; Ahmad, T.; Mitu, L. Synthesis, Characterization and Biological Activities of a Novel Mannich Base 2-[(3,4-dimethoxyphenyl) (pyrrolidinyl)methyl] cyclohexanone and its Complexes with Cu (II), Ni (II), Co (II) and Fe (II) Ions. Revista De Chimie, 2017, 68(12), 2845-2849.

17. Al-Qazzaz, A. H.; Al-Jeboori, M. J. New metal complexes derived from Mannich ligands; synthesis, spectral investigation and biological activity. Biochemical and Cellular Archives, 2020, 20, Supplement 2, 4207-4216.
18. Hussain, S. A.; Al-Jeboori, M. J. New Metal Complexes Derived from Mannich-Base Ligand; Synthesis, Spectral Characterisation and Biological Activity. Journal of Global Pharma Technology, 2019, 11(2), 548-560.
19. Saleh, H. A.; Al-Khatib, A. S.; and Al-Jeboori, M. J. Synthesis, structural characterisation and biological evaluation of new semicarbazone metal complexes derived from Mannich-base. Biochem. Cell. Arch., 2021, 21(1), 159-168.
20. Moradi, R.; Jameh-Bozorghi, S.; Kadivar, R.; Mahdiani, A.; Soleymanabadi, H. Study of mechanism keto-enol tautomerism (isomeric reaction) structure cyclohexanone by using Ab initio molecular orbital and density functional theory (DFT) method with NBO Analysis. APCBEE Procedia, 2012, 3, 70-74.
21. Al-Jeboori, M. J.; Al-Fahdawi, M. S.; and Sameh, A. A. New homoleptic metal complexes of Schiff bases derived from 2,4-di-p-tolyl-3-azabicyclo [3.3.1] nonan-9-one. Journal of Coordination Chemistry, 2009, 62(23), 3853-3863.
22. Al-Jeboori, M. J.; Ameer, A. A.; Aboud, N. A. (2016). Novel Pentadentate Ligand of N3S2 Donor Atoms and It's Complexes With (NiII, CoII, CuII, FeII, HgII, AgI and ReV. Journal of Ibn Al-Haitham for Pure and Applied Sciences, 2004, 17(3),80-89
23. Al-Jeboori, F. H. A.; Hammud, K. K.; Al-Jeboori, M. J. Synthesis and characterization of new acyclic octadentate ligand and its complexes. Iranian Journal for Science & Technology, 2014, 38A (4): 489-497.
24. Al-Jeboori, M. J.; Abdul-Ghani, A. J.; Al-Karawi, A. J. Synthesis and structural studies of new Mannich base ligands and their metal complexes. Transition Metal Chemistry, 2008, 33(7), 925-930.
25. Ahmed, R. M.; Yousif, E. I.; Al-Jeboori, M. J. Co(II) and Cd(II) complexes derived from heterocyclic Schiff-bases: synthesis, structural characterisation, and biological activity. The Scientific World Journal, 2013, 2013, 1-6.
26. Al-Jeboori, M. J.; Hasan, H. A.; Al-Sa'idy, W. A. J. Formation of polymeric chain assemblies of transition metal complexes with a multidentate Schiff-base. Transition Metal Chemistry, 2009, 34(6), 593-598.
27. Mawat, T. H.; Al-Jeboori, M. J. Novel Metal Complexes Derived from Selenosemicarbazone Ligand; Synthesis, Spectral Investigation and Biological Activity. J. Global Pharma Tech, 2019, 11(09), 126-138.
28. Abdul-Ghani, A. J.; Al-Jeboori M. J.; Al-Karawi, A. M. Synthesis and characterisation of new N2S2 and N2O2 Mannich base ligands derived from phosphinic acid and their metal complexes. Journal of Coordination Chemistry, 2009, 62(16), 2736-2744.
29. Shaker, S. A.; Khaledi, H.; Cheah, S. C.; and Ali, H. M. New Mn (II), Ni (II), Cd (II), Pb (II) complexes with 2-methylbenzimidazole and other ligands. Synthesis, spectroscopic characterization, crystal structure, magnetic susceptibility and biological activity studies. Arabian Journal of Chemistry, 2016, 9, S1943-S1950.
30. Mawat, T. H.; Al-Jeboori, M. J. Synthesis, characterisation, thermal properties and biological activity of coordination compounds of novel selenosemicarbazone ligands. Journal of Molecular Structure, 2020, 1208, 127867.
31. Ahmed, R. M.; Hamdan, T. A.; Numan, A. T.; Al-Jeboori, M. J.; Potgieter, H. Formation of polymeric assemblies of six-coordinate metal complexes with mixed bridges of dicarboxylato-azido moieties. Complex Metals: An Open Access Journal, 2014, 1(1), 38-45.
32. Etheb, A. M.; Al-Jeboori, M. J. Synthesis, Structural Characterisation and Biological Activity of New Mannich Compounds Derived from Cyclohexanone Moiety, HIV Nursing, 2022, 22 (2), 3659-3666.

SHORT ARTICLES / INVESTIGACIÓN

Realizando una encuesta poblacional en tiempos de pandemia: Experiencias de campo desde Ecuador

Conducting a Population Survey in Times of Pandemic: Field Experiences from Ecuador

Ikram Benazizi[1], Andrés Peralta[2]*, Elisa Chilet[1], Ana Lucía Torres[2], Juan Vásconez[3], Jessica Pinto[2], María Hernández[2], María Gabriela Galarza[2], Abigail Álvarez[2], Tania Ron[2], Lucy Parker[1,4]

DOI. 10.21931/RB/2023.08.02.16

[1] Departamento de Salud Pública, Universidad Miguel Hernández de Elche.
[2] Instituto de Salud Pública, Pontificia Universidad Católica del Ecuador.
[3] Facultad de Enfermería. Pontificia Universidad Católica del Ecuador.
[4] CIBER, Epidemiología y Salud Pública. Ecuador.
Corresponding author: aperalta@puce.edu.ec

Resumen: El Proyecto Contextualización de la Evidencia para la Acción en Diabetes en entornos con bajos recursos tiene como objetivo explorar los procesos por los cuales las recomendaciones en salud pública pueden ser traducidas a acciones informadas por la evidencia y adaptadas al contexto específico. Una de sus primeras fases es establecer una línea base sobre factores de riesgo de enfermedades crónicas no transmisibles y prevalencia de diabetes en los territorios en los que trabaja, usando el Método paso a paso de la Organización Mundial de la Salud para la vigilancia de factores de riesgo para las enfermedades crónicas no trasmisibles. La realización de esta encuesta poblacional se vió afectada por el contexto de pandemia en Ecuador. Entre noviembre y diciembre del 2020, se realizó un piloto para poder adaptar la encuesta y sus procedimientos a la situación epidemiológica que se vivió en la ciudad de Quito. El piloto permitió identificar las principales barreras y dificultades y proponer soluciones y medidas de mejora.

Palabras clave: Encuesta poblacional, diabetes, enfermedades crónicas no transmisibles, COVID-19, Ecuador.

Abstract: The Contextualizing project Evidence for Action on Diabetes in low-resource Settings: a Mixed-methods case study in Quito and Esmeraldas, Ecuador, aims to analyze the social process by which global recommendations for the prevention of diabetes can translate into evidence-based actions tailored to low-resource settings. One of its first phases is establishing a baseline on risk factors for chronic noncommunicable diseases and the prevalence of diabetes in the territories in which it works, using the WHO STEPSwise approach to noncommunicable conditions risk factor surveillance. The conduct of this population survey was affected by the pandemic context in Ecuador. Between November and December 2020, a pilot was carried out to adapt the study and its procedures to the epidemiological situation in the city of Quito. The pilot allowed us to identify the main barriers and difficulties related to COVID-19 and propose solutions and improvements for the best performance of the project.

Key words: Nopulation survey, diabetes, chronic noncommunicable diseases, COVID-19, Ecuador.

Introducción

La diabetes mellitus (DM) es una emergencia sanitaria mundial que afecta a todos los grupos de edad en todos los países del mundo, siendo especialmente frecuente en países de ingresos bajos y medianos, como es el caso de Ecuador. La Federación Internacional de Diabetes estima que el 5,5% (3,5–8,5) de la población de Ecuador entre 20 y 79 años padece DM, de la cual el 40% no está diagnosticada. En 2019, la DM fue la segunda causa de mortalidad general, segunda para las mujeres y tercera para los hombres[1,2].

El proyecto "Contextualización de la Evidencia para la Acción en Diabetes en entornos con bajos recursos: Un estudio utilizando métodos mixtos en Quito y Esmeraldas, Ecuador" es un proyecto de ciencia de implementación cuyo objetivo es explorar los procesos por los cuales las recomendaciones en salud pública pueden ser traducidas a acciones informadas por la evidencia y adaptadas al contexto específico[3,4].

La primera fase del proyecto incluye la realización de la encuesta poblacional STEPS, con el fin de analizar la prevalencia de diabetes y los factores de riesgo de ECNT, considerando las desigualdades sociales. En una primera fase, se realiza una encuesta que recoge información demográfica y socioeconómica, comportamientos, prácticas y estilos de vida (consumo de tabaco o alcohol, dieta, actividad física, condiciones de trabajo y ocio), antecedentes médicos (presión sanguínea, colesterol o triglicéridos elevados, enfermedades cardiovasculares, diabetes), y posibles recomendaciones sanitarias que puede haber recibido el / la participante. En una segunda fase, se realizan pruebas de laboratorio (nivel de glucosa en sangre, prueba de sobrecarga oral de glucosa, niveles de colesterol y triglicé-

Citation: Benazizi I, Peralta A, Chilet E , Torres A L , Vásconez J , Pinto J , Hernández M , Galarza M G , Álvarez A, Ron T, Parker L. Realizando una encuesta poblacional en tiempos de pandemia: Experiencias de campo desde Ecuador. Revis Bionatura 2023;8 (2) 16. http://dx.doi.org/10.21931/RB/2023.08.02.16
Received: 2 January 2023 / **Accepted:** 19 April 2023 / **Published:** 15 June 2023
Publisher's Note: Bionatura stays neutral with regard to jurisdictional claims in published maps and institutional affiliations.

ridos) y medidas antropométricas (estatura, peso, perímetro abdominal y presión arterial). Se realizó un muestreo multietápico en el que las primeras unidades de muestreo fueron secciones censales; las segundas, lotes residenciales (parcelas de terreno) dentro de cada sección censal; la tercera hogares dentro de cada lote y la final personas mayores de 18 años dentro de cada hogar. La muestra final estimada fue de 720 personas[3].

Sin embargo, la realización de la encuesta poblacional presentaba una serie de retos desprendidos del contexto de la pandemia en la ciudad de Quito. Ecuador ha sido uno de los países más afectados por la pandemia en el continente[5]. Hacia el mes de diciembre del 2020, Quito era el territorio con más contagios a nivel nacional; y persistían restricciones de movilidad en la ciudad. Si bien las medidas más restrictivas a nivel nacional acabaron en el mes de septiembre, se volvieron a plantear otras similares hacia finales de diciembre.

El objetivo de este trabajo es adaptar el trabajo de campo de la encuesta poblacional a la situación contextual y epidemiológica de Quito, Ecuador.

Materiales y métodos

Entre el 27/11/2020 y el 22/12/2020 se realizó un piloto de la encuesta con los siguientes objetivos: 1) analizar si era posible realizar la encuesta dada la situación pandémica y las restricciones de movilidad en Quito; 2) adaptar los manuales y procedimientos de la encuesta a la situación epidemiológica; y 3) revisar los mecanismos para realizar las tomas de muestra de laboratorio en los hogares de las personas participantes; tomando en cuenta el contexto.

Ante la situación producida por la pandemia por COVID-19, se realizaron ajustes iniciales al piloto planificado (tabla 1). En primer lugar, se adaptó el protocolo de encuesta para incluir medidas básicas de bioseguridad: uso de mascarilla, distanciamiento físico, uso de alcohol gel para manos y alcohol 70% para desinfección de superficies y equipos. Además, se adaptaron los procedimientos de acorde a las realidades y necesidades cambiantes. Finalmente, se incluyeron preguntas sobre el impacto de la pandemia en la situación económica, salud física y emocional, relaciones familiares/sociales, y comportamientos relacionados a la salud.

Resultados y discusión

En total durante el piloto, realizado entre noviembre y diciembre 2021, se visitaron 89 lotes seleccionados y se llegó a realizar 49 encuestas completas, incluyendo medidas antropométricas y toma de muestras de laboratorio. Las principales razones por las que no se llegó a realizar la encuesta fueron: 1) 17 personas (19% de los puntos de muestreo) no dan su consentimiento para participar; 2) 8 personas quedan con visitas pendientes ya que solicitan que se realice la entrevista en otro momento; 3) 6 personas seleccionadas se encuentran ausentes en más de 3 visitas al hogar; 4) En tres lotes no viven personas (local comercial, casa vacía); 5) 2 encuestas no se realizaron porque personas seleccionadas presentaban síntomas respiratorios al momento. Cabe destacar que durante el período de ejecución del piloto, no hubo ninguna sospecha de contagio por COVID-19 en el equipo de trabajo.

De las 49 personas encuestadas, 31 (63%) fueron mujeres. La edad mediana fue de 54.41 años (min 20.48, max 82.54 años). Un 87.75% de las personas participantes se identifican como mestizas, mientras que solamente un 8.16% se identificaron étnicamente con grupos históricamente excluidos (indígena, afroecuatoriano). Un 32.64% de las personas participantes tienen estudios primarios o menos, un 40.82% estudios secundarios y un 26.53% estudios superiores. La mediana de ingresos mensuales del hogar fue de 400 dólares de los EEUU (min 100, max 4000 USD). Un 73.47% de las personas encuestadas valora que su situación económica había empeorado en comparación con su situación antes de la pandemia (77.78% en hombres, 70.97% en mujeres).

Si revisamos los cambios en comportamientos relacionados con la salud con la pandemia podemos resaltar que: 1) 12.24% de las personas encuestadas refiere que su consumo de azúcar (dulces y bebidas azucaradas) ha aumentado (12.90% en mujeres, 11.11% en hombres); y 2) 44.88% de las personas encuestadas disminuyeron su actividad física (48.39% en mujeres, 38.89% en hombres) y 18.37% la suspendieron (19.35% en mujeres, 16.67% en hombres).

En lo que respecta a la salud: 1) 34.69% de las personas participantes percibieron que su estado de salud física se ha deteriorado en comparación con su situación antes de la pandemia (38.89% en hombres, 32.26% en mujeres); 2) 44.90% de las personas refieren que su estado de ánimo se ha deteriorado (33.33% en hombres, 56.61% en mujeres); 3) 28.57% refieren que sus relaciones sociales o familiares se han deteriorado (27.78% en hombres, 29.03% en mujeres).

Implicaciones para la práctica

A pesar de la preparación previa y de las adaptaciones realizadas en el trabajo de campo, se encontraron algunas dificultades (no relacionadas a la situación epidemiológica) que dificultaron el trabajo y que vale la pena mencionar (tabla 2).

Las recomendaciones presentadas en la Tabla 2 fueron generadas mediante un proceso participativo entre encuestadoras y el resto de personas investigadoras en el proyecto. Los manuales se adaptaron siguiendo estas recomendaciones para su uso en la encuesta.

En primer lugar, hubo mayor participación de mujeres (el 63% de las encuestas completadas), los hombres negaban dar su consentimiento en mayor grado que las mujeres, éstas últimas mostraron mayor apertura a participar y a hablar de su salud. Un posible factor que podría explicar esto es el género, dado que los hombres suelen ser menos dispuestos a hablar abiertamente de su salud en comparación con las mujeres. También el hecho de que los hombres presentan mayor afiliación a la seguridad social, con mayor acceso a los servicios de salud, y por lo tanto, perciben menor beneficio de su participación en el estudio. Como propuesta de mejora, destacar la importancia de estratificar la muestra por sexo para asegurar que sea equitativa entre hombres y mujeres, y mejorar la comunicación para resaltar los beneficios colectivos y llegar mejor a la población masculina.

En segundo lugar, la cartografía estaba poco actualizada y para la aleatorización se usó información catastral y de usos de suelo del Municipio de Quito. En algunos casos, la zonificación residencial en el mapa no coincidía con la realidad (ej. locales comerciales) o lotes seleccionados estaban vacíos o abandonados. Esto se debe a los cambios urbanos rápidos en algunos sectores de la ciudad y a la falta de actualización d ellos datos municipales. Y como

propuesta de mejora realizar visita previa a las secciones censales elegidas para determinar si la cartografía está actualizada. De esta manera se puede identificar de forma más fácil lotes que no corresponden a uso residencial (comercial, industrial etc.).

En tercer lugar, hubo poca señal en algunas áreas, lo que dificultaba la visualización de mapas y la identificación de lotes seleccionados en el muestreo. Lo que se debe a una distribución desigual de la señal móvil en la ciudad y a la heterogeneidad en señal entre empresas. Esto se solucionó mediante la pre-carga de mapas en los teléfonos móviles de los encuestadores antes de iniciar la jornada.

En cuarto lugar, se presentaron dificultades para realizar la antropometría debido a las características de ciertas viviendas (pisos irregulares, paredes en mal estado, techos muy bajos), y a la necesidad de mantener distanciamiento físico, lo que se explica por la privación socioeconómica y las condiciones inadecuadas de muchas viviendas en el territorio de estudio. Para ello, buscamos espacios para la antropometría desde el primer contacto con participantes, y en los casos necesarios se usaron espacios exteriores.

Por último, también hubo dificultades para referir a personas con resultados anormales de laboratorio, tensión arterial o antropometría. Dos personas tuvieron glucosa en ayunas elevada; una persona tuvo intolerancia a la glucosa y otra recibió un posible diagnóstico de diabetes. Se encontraron valores elevados de tensión arterial en 9 personas participantes. Y un 54.17% de las personas participantes presentaron sobrepeso y un 22.92% obesidad. Esta dificultad en referir a las personas a los respectivos centros de salud se debió a la saturación del sistema de salud por la pandemia de COVID-19, y al enfoque único en la mitigación de la pandemia, lo que afectaba el tratamiento de las enfermedades crónicas. Como soluciones a esto, contactamos a responsables de enfermedades crónicas del distrito para facilitar el proceso de referencia. Además, los profesionales de la salud que participan en el proyecto dieron seguimiento al proceso de referencia y resolvieron las dudas de los participantes.

Conclusiones

Si bien la realización de la encuesta piloto en el contexto de la pandemia por COVID-19 tuvo grandes dificultades y retos, también hubo muchos aprendizajes que han permitido que pueda desarrollarse posteriormente de la mejor manera posible. Las adaptaciones realizadas en el contexto de la pandemia permitieron proteger tanto al equipo de encuestadoras como a las personas participantes. Sin embargo, las mismas pudieron haber afectado la participación en la encuesta. A parte de las dificultades derivadas por la pandemia, se lograron identificar y proponer soluciones a otras barreras detectadas.

La encuesta poblacional debió suspenderse debido a la situación epidemiológica en la ciudad entre enero y mediados de marzo del 2021. Al retomar el trabajo, las recomendaciones y cambios realizados durante el piloto fueron esenciales para el correcto funcionamiento del proyecto.

Material suplementario

Manual protocolo de la entrevista.

Contribución de autoría

Todos los autores y autoras han hecho contribuciones sustanciales al manuscrito. LP, ALT, IB, EC y JV participaron en la concepción y el diseño del estudio. TR, JP, MGG, AA y MH realizaron el trabajo de campo y recolección de datos. IB y AP realizaron el análisis inicial e interpretación de los datos. TR, JP, MGG, AA, MH, IB y AP participaron en la escritura del manuscrito original; ALT, LP y EC realizaron la revisión crítica del mismo. El manuscrito final fue aprobado por todas las personas participantes. AP, en calidad de autor de correspondencia, garantiza que todas las partes que integran el manuscrito han sido revisadas y discutidas entre los y las autoras con la finalidad de que sean expuestas con la mayor precisión e integridad.

Nombre de la medida	Descripción	Ventajas / Desventajas
Encuestas en lugares abiertos	Se optó por aplicar la encuesta, los exámenes de laboratorio y antropometría en lugares abiertos como: calles/aceras, patios o afueras del lugar donde vivía la persona participante.	**Ventaja**: Mayor sensación de seguridad de participantes y encuestadoras. **Desventaja**: Menor participación en días lluviosos / fríos.
Pregunta síntomas / diagnóstico antes de ingresar a hogar	Antes de ingresar al hogar, las encuestadoras preguntaban si en la casa había alguna persona con síntomas o diagnóstico de COVID-19. Si la respuesta era afirmativa, se agradece y se intenta reprogramar la visita para el siguiente mes.	**Ventaja**: Protección del equipo de encuestadoras. **Desventaja**: Aumentan las pérdidas.
Búsqueda activa de síntomas dentro del hogar	Una vez dentro del hogar, las encuestadoras mantienen distanciamiento y medidas de bioseguridad, pero también observan si hay síntomas (respiratorios sobre todo). De encontrar estos síntomas, se agradece a la persona participante, se le sugiere contactar a los canales oficiales de manejo de COVID o a su profesional de la salud de confianza. Se intenta reprogramar la visita y se abandona el hogar.	**Ventaja:** Protección equipo encuestadoras. Colaboración con sistema de vigilancia epidemiológica. **Desventaja:** Mayores pérdidas o encuestas inconclusas.

Tabla 1. Medidas Adoptadas para la realización del estudio piloto de la encuesta poblacional ante la Situación de COVID-19.

Financiamiento

Esta investigación fue financiada por H2020 European Research Council 2018 Starting Grant, grant number 804761—CEAD.

Declaración de la Junta de Revisión Institucional

El estudio se realizó de acuerdo a los lineamientos de la Declaración de Helsinki, y fue aprobado por el comité evaluador de proyectos de la Universidad Miguel Hernández (UMH) (número de registro 2018.291.E.OEP) y el comité ético acreditado a nivel nacional de la Universidad Central del Ecuador (UCE). , referencia 00022-UMHE-E-2019), y la autorización ética ha sido proporcionada por la Agencia Ejecutiva del Consejo Europeo de Investigación (ERCEA, Ref. Ares (2018)5827042-14/11/2018).

Declaración de consentimiento informado

Se obtuvo el consentimiento informado de todos los sujetos involucrados en el estudio.

Conflictos de interés

Los autores declaran no tener conflicto de interés.

Referencias bibliográficas

1. International Diabetes Foundation. The IDF Diabetes Atlas; International Diabetes Foundation: Brussels, Belgium, 2015.
2. Registro estadístico de defunciones generales [Internet]. [citado 25 de diciembre de 2023]. Disponible en: https://public.tableau.com/views/Registroestadsticodedefuncionesgenerales_15907230182570/Men?%3Adisplay_static_image=y&%3AbootstrapWhenNotified=true&%3Aembed=true&%3Alanguage=es-ES&:embed=y&:showVizHome=n&:apiID=host0#navType=0&navSrc=Parse
3. Chilet-Rosell E, Piay N, Hernández-Aguado I, et al. Contextualizing Evidence for Action on Diabetes in Low-Resource Settings-Project CEAD Part I: A Mixed-Methods Study Protocol. Int J Environ Res Public Health. 2020;17(2):E569. DOI: 10.3390/ijerph17020569
4. Bernal-Soriano MC, Barrera-Guarderas F, Alonso-Jaquete A, et al. Contextualizing Evidence for Action on Diabetes in Low-Resource Settings-Project CEAD Part-II, Strengthening the Health System: A Mixed-Methods Study Protocol. Int J Environ Res Public Health. 2021;18(7):3391. DOI: 10.3390/ijerph18073391
5. Cevallos-Valdiviezo H, Vergara-Montesdeoca A, Zambrano-Zambrano G. Measuring the impact of the COVID-19 outbreak in Ecuador using preliminary estimates of excess mortality, March 17–October 22, 2020. Int J Infect Dis. 2021;104:297-9.

REVIEW / ARTÍCULO DE REVISIÓN

Oral Nano-Delivery Systems for Colon-Targeted Drug Delivery of Traditional Chinese Medicine in Ulcerative Colitis

Mohammad Javed Ansari[1]*, Suhad J. Hadi[2], Hamzah H. Kzar[2], Moaed E. Al-Gazally[3], Thulfeqar Ahmed Hamza[4], Mohammed Khudair Hasan[5], Aiman Mohammed Baqir Al-Dhalimy[6], Reza Akhavan-Sigari[7,8]
DOI. 10.21931/RB/2023.08.02.17

[1] Department of Pharmaceutics, College of Pharmacy, Prince Sattam Bin Abdulaziz University, Al-kharj, Saudi Arabia.
[2] Veterinary Medicine Collage, Al-Qasim Green University, Al-Qasim, Iraq.
[3] College of Medicine, University of Al-Ameed, Karbala, Iraq.
[4] Medical Laboratory Techniques Department, Al-Mustaqbal University College, Babylon, Iraq.
[5] Al-Manara College of Medical sciences, Department of Pharmacy, Missan, Iraq.
[6] College of Nursing, Altoosi University College, Najaf, Iraq and The Islamic University, Najaf, Iraq.
[7] Department of Neurosurgery, University Medical Center Tuebingen, Germany.
[8] Department of Health Care Management and Clinical Research, Collegium Humanum Warsaw Management University Warsaw, Poland.
Corresponding author: javedpharma@gmail.com

Abstract: Ulcerative colitis (UC) is a type of inflammatory bowel disease with a high recurrence rate. In this regard, sulfasalazine and immunosuppressive medications are often used for an extended period in clinical practice, but their effectiveness is limited, and they are prone to side effects. Modern research has shown that herbal active ingredients of Traditional Chinese Medicine (TCM), such as polyphenols, alkaloids, quinones, and terpenes, have a promising impact on treating UC via a multi-target mechanism and with low side effects. Poor water solubility and low bioavailability of these agents in the gastrointestinal tract are the most challenging issues in delivering these agents to the target tissues. Researchers have created a variety of oral colon-targeted nano-systems of TCM active ingredients in response to the above formulation issues, which significantly improve the treatment of UC by avoiding gastrointestinal damage, prolonging intestinal retention, and achieving controlled drug release at the lesion site. In order to provide ideas for the oral-targeted treatment of UC with active ingredients from TCM, the research progress of an oral colon-targeted nano-system for the treatment of UC is reviewed in the current study, as well as the research progress of an oral colon-targeted nano-system for the treatment of UC.

Key words: Medicine, Chinese Traditional, Colitis, Ulcerative, Nanoparticle Drug Delivery System.

Introduction

Ulcerative colitis (UC) is a non-specific inflammatory bowel disease with a long course and is difficult to cure. The diseased area can reach the submucosa of the rectum, involving the rectum, sigmoid colon, and even the entire colon area[1]. Its clinical manifestations include abdominal pain, diarrhea, weight loss, and blood in the stool, which can be repeated. The World Health Organization has listed it as one of the modern refractory diseases. Its pathogenesis is complicated and related to increased mucosal permeability, imbalance of microbial levels, and tumor necrosis. Factor-α (tumor necrosis factor-α, TNF-α), interleukin-6 (interleukin-6, IL-6), interleukin-10 (interleukin-10, IL-10), and other factors related to the imbalance of the level of inflammatory factors[2]. Currently, the commonly used drugs for treating UC include 5-aminosalicylic acid, cortisol, and immunosuppressive drugs, but long-term use of these drugs can cause serious adverse reactions. According to the symptoms of the disease, UC belongs to the categories of "rest dysentery," "long dysentery," and "intestinal addiction" in Chinese medicine[3]. Based on the concept of syndrome differentiation and treatment, traditional Chinese medicine has a long history of preventing and treating UC, with significant clinical effects and minor adverse reactions. The treatment of UC with traditional Chinese medicine has the advantages of multiple components, multiple targets, and improvement of the internal environment. However, when the active ingredients of traditional Chinese medicine are treated orally, there are disadvantages, such as poor water solubility, low gastrointestinal stability, and poor oral bioavailability. How to achieve high-efficiency delivery of active ingredients of traditional Chinese medicine in colon lesions is a problem that needs to be solved urgently. This article summarizes the representative active ingredients of traditional Chinese medicines with the prevention and treatment effects on UC and their mechanism of action, as well as the research progress of oral colon-targeted nano-system for treating UC by consulting the Chinese and English literature in recent years.

Active ingredients of traditional Chinese medicine with UC prevention and treatment effects and their effects

Traditional Chinese medicine has a long history in treating UC, and its curative effect is noticeable. In particular, traditional Chinese medicine's active ingredients, such as polyphenols, alkaloids, quinones, and terpenoids, have shown therapeutic potential for UC.

Citation: Oral Nano-Delivery Systems for Colon-Targeted Drug Delivery of Traditional Chinese Medicine in Ulcerative Colitis. Ansari M J, Hadi S J,. Kzar H H,Al-Gazally M E, Ahmed HamzaT, Khudair Hasan M, Baqir Al-Dhalimy A M, Akhavan□Sigari R. Revis Bionatura 2023;8 (2) 17. http://dx.doi.org/10.21931/RB/2023.08.02.17
Received: 2 January 2023 / **Accepted:** 19 April 2023 / **Published:** 15 June 2023
Publisher's Note: Bionatura stays neutral with regard to jurisdictional claims in published maps and institutional affiliations.

Polyphenols

Polyphenols are compounds with multiple phenolic hydroxyl groups found in many traditional Chinese medicines. Among them, resveratrol, rutin, silymarin, curcumin and other compounds have been reported to have the effect of treating UC. Resveratrol is often found in common Chinese medicines such as *Cassia, Veratrum, Polygonum cuspidatum*, etc., and plays an essential role in treating and preventing various diseases. Rauf *et al.*[4], and Marques *et al.*[5] found that resveratrol can treat inflammation by down-regulating inflammatory biomarkers such as TNF-α, cyclooxygenase 2, C-reactive protein, and interferon. Rutin, also known as rutin, is found in Chinese medicine such as Sophora japonica, buckwheat leaves, dandelion, etc. It is mainly used for anti-inflammatory, anti-viral, and anti-oxidants[6]. Nones *et al.*[7], and Habtemariam *et al.*[8] found that rutin can inhibit TNF-α and nuclear factor κB (nuclear factor kappa-B, NF-κB). The flavonoid lignan compound silymarin extracted from milk thistle has anti-cancer and anti-inflammatory effects. Silymarin can scavenge free radicals and reactive oxygen species and reduce the release of histamine and TNF-α, IL-6, and IL-8. The expression of UC can effectively improve the inflammatory symptoms of UC[9,10]. Curcumin is derived from the ginger family plant turmeric. It is often used as a food additive and has many functions, such as anti-inflammatory, anti-oxidant, anti-tumor, liver protection, and anti-angiogenesis. Therefore, curcumin has a good effect on the treatment of UC[11].

Alkaloids

Alkaloids are a kind of basic organic compounds containing nitrogen. In recent years, the alkaloids in some Chinese medicines have shown sound UC treatment effects. Berberine, an isoquinoline alkaloid extracted from the Ranunculaceae plant Coptidis, is often used to treat bacterial-related diarrhea.

It can be used clinically for anti-inflammatory, anti-tumor and immune regulation. Studies have shown that berberine can improve UC by inhibiting the expression of certain inflammatory factors[12]. Sinomenine is an alkaloid component extracted from the Chinese vine's roots, a fang chi family plant, and is often used to treat rheumatoid arthritis. Researchers have recently found that sinomenine also has a specific role in treating chronic inflammation[13]. Tang *et al.*[14] and Zhou *et al.*[15] found that sinomenine can reduce inflammation in UC mice induced by dextran sulfate sodium (DSS) by regulating the Nrf2/NQO-1 signaling pathway. Oxymatrine is an active ingredient isolated from the legume Sophora flavescens. Studies have confirmed that oxymatrine has anti-hepatitis virus and anti-tumor effects. Xiong Yongai *et al.*[16] conducted experiments to prove that oxymatrine clearly affects trinitrobenzene sulfonic acid (TNBS)-induced UC in SD rats. Piperine extracted from black pepper and tetrandrine extracted from tetrandrine has also been confirmed to have certain anti-UC effects[17,18].

Quinones

The quinones that have the therapeutic effect of UC are mainly emodin and rhein. Emodin is an anthraquinone derivative contained in most Chinese medicines. It has anti-tumor, antibacterial, diuretic and vasodilator effects. Studies have found that emodin can treat UC by reducing the level of anti-flagellin antibodies in the blood and down-regulating the expression of Toll like receptor 5 (TLR5) and NF-κB p65 pathway[19,20]. Rhein is an anthraquinone compound often used to treat gastrointestinal diseases, which can reduce the level of pro-inflammatory factors induced by lipopolysaccharide in macrophages RAW264.7[21]. Studies have also found that cylindroquinone extracted from the vine fruit of centipede can also reduce the expression of inducible nitric oxide synthase (iNOS), TNF-α, IL-1β, and IL-6 to alleviate inflammation[22].

Terpenes

Terpenoids are the general term for isoprene polymers and their derivatives. Studies have found that certain sesquiterpenes, diterpenoids, and triterpenoids can treat UC. Tripterygium wilfordii, a pentacyclic triterpene component extracted from Tripterygium wilfordii, has potential therapeutic effects on inflammation, cancer and arthritis[23]. Jia *et al.*[24] found that tripterygium can inhibit necroptosis and relieve DSS-induced inflammation in UC mice. Parthenolide is a sesquiterpene lactone compound and an essential effective component of Asteraceae plants. It has biological activities such as anti-oxidative stress, anti-inflammatory, and inhibiting cell apoptosis. Studies have found that parthenolide can be used as an inhibitor of the NF-κB pathway to relieve DSS-induced UC in mice[25]. The diterpene component ester andrographolide is an important component in Andrographis paniculata, which can affect the Th1/Th2/Th17 reaction in patients with UC[26]. In addition, Zhu *et al.*[27] found that andrographolide had a good therapeutic effect on the UC mouse model induced by TNBS. The diterpenoid component dihydrotanshinone has also been reported to have the potential effect of treating UC[28].

Others ingredients

Other ingredients contained in traditional Chinese medicine, such as crocetin, shikimic acid, arctigenin, brucein, and polysaccharide components pectin, cellulose, chitosan, plantago seed gum, etc., have been reported to be therapeutic effect on UC[29-34]. Some Chinese medicine extracts, such as ginger extract, have also been shown to have anti-inflammatory effects. Studies have found that the ingredients 6-gingerol and 6-gingerol in ginger extract can inhibit the expression of inflammation-related genes, thereby improving inflammation[35-37].

Table 1 represents the active ingredients of traditional Chinese medicines that have potential effects on preventing/treating UC.

The therapeutic effect of oral colon-targeted nano-DDS in UC

Although the active ingredients of traditional Chinese medicine have the advantages of multiple pathways, multiple effective targets, and low level of adverse reactions in the treatment of UC, however, they have some shortcomings, such as strong hydrophobicity, poor permeability, and poor oral stability limit their use in the treatment of UC. To make the active ingredients of traditional Chinese medicine treat UC more effectively, some oral colon-targeting nano-systems based on particle size dependence, pH dependence, enzyme response, and active targeting have been developed. Compared with traditional oral formulations, oral colon-targeted nanoformulations have more advantages. First, it can improve the water solubility and stability of the drug, avoid damage of the intestinal environment and certain enzymes to the drug, reduce physical or chemical degradation, delay the release time of the drug, and achieve

Chinese herbal medicine		UC Model	Animal	Dose	Mechanism	Ref
Group	Name					
Polyphenols	**Rutin**	5% DSS	Male ICR mice	Contains 0.1% of diet	Inhibit the production of IL-1β, IL-6, etc., reduce oxidative stress in the colon	38
	Quercetin	7.5% acetic acid solution	Male Swiss mice	10, 100 $mg \cdot kg^{-1}$	Inhibit the activity of MPO, reduce the production of pro-inflammatory factors such as IL-1β, increase the production of anti-inflammatory factors such as IL-10, scavenge free radicals, regulate the endogenous anti-oxidant glutathione, etc.	39
	Silymarin	4% acetic acid	Male C57BL/6 mice	5$mg \cdot kg^{-1} \cdot d^{-1}$	Scavenge free radicals and reactive oxygen species; reduce histamine release, reduce the expression of TNF-α, IL-6, IL-8 mRNA; block the nuclear transcription of NF-κB	9
	Baicalein	TNBS	Female BALB/c mice	20$mg \cdot kg^{-1} \cdot d^{-1}$	Inhibits inflammatory activity by targeting the caudal homeotype receptor 2/pregnane X receptor pathway; inhibits PPARγ pathway expression	40
	Baicalin	2% DSS	Male C57BL/6 mice	50, 100, 150 $mg \cdot kg^{-1}$	Inhibits IL-33 expression, attenuates NF-κB expression	41
	Icariin	2.5% DSS	Female C57BL/6 mice	3, 10 $mg \cdot kg^{-1}$	Inhibits expression of p65, STAT1 and STAT3 pathways	42
	Mullein Isoflavones	2.5% DSS	Male BALB/c mice	25, 50 $mg \cdot kg^{-1}$	Anti-oxidant, scavenging free radicals, neuroprotective	43
	Naringenin	4% acetic acid solution	Wister albino rats	25, 50, 100 $mg \cdot kg^{-1} \cdot d^{-1}$	Reduce lipid peroxidation and scavenge free radicals	44
	Alpine	5% DSS	Female BALB/c mice	25, 50, 100 $mg \cdot kg^{-1} \cdot d^{-1}$	Inhibits the production of pro-inflammatory factors and blocks the activation of NF-κB signaling	45
	Curcumin	3% DSS	Male Swiss albino rat	100 $mg \cdot kg^{-1}$	Anti-inflammatory, anti-oxidant, anti-tumor, inhibits inflammatory pathways; scavenges free radicals; prevents mucosal damage	46, 47
	Resveratrol	Enema with 7.5 mg·mL−1 oxazolone solution	Wister albino rats	10 $mg \cdot kg^{-1}$	Downregulation of TNF-α, COX-2, iNOS, C-reactive protein, interferons and several interleukins	48
	Picclitaxel	Enema with 50% ethanol solution of TNBS	Male SD rats	10 $mg \cdot kg^{-1}$	Regulates the activity of NF-κB, Nrf2, hypoxia-inducible factor-1	49
	Ellagic acid	5% DSS acute UC; 1% DSS chronic UC	Female BALB/c mice; C57BL/6 mice	Contains 1%, 2% diet	Decrease IL-6, TNF-α, IFN-γ, COX-2 and iNOS activity; down	50
	Magnolol	5% DSS	C57BL/6 mice	25, 50, 100 $mg \cdot kg^{-1}$	Regulate signaling pathways p38MAPK, NF-κB, block STAT3 pathway Inhibit TNF-α, IL-1β, IL-12 by regulating NF-κB and PPARγ pathways	51

Table 1. Representative active components of Chinese medicine with prevention and treatment effect of UC and its mechanisms.

Alkaloid	**Berberine**	5% DSS	Male Wistar rats	10, 30, 50 $mg \cdot kg^{-1}$	Activates AMPK enzymes, inhibits the expression of IL-1, IL-1β, IL-6, IL-12, TNF-α, TGF-β and IFN-γ; upregulates the expression of IL-4 and IL-10; increases the expression of SIgA , decreased the expression of iNOS, MPO and malondialdehyde	12
	Tetrandrine	5% DSS	Female BALB/c mice	40 $mg \cdot kg^{-1} \cdot d^{-1}$	Anti-inflammatory, inhibit the activation of NF-κB pathway	18
	Sinomenine	3% DSS	Female C57BL/6 mice	100 $mg \cdot kg^{-1}$	Reduce TNF-α, IL-6, iNOS, SOD levels; activate Nrf2 and its downstream genes, heme oxidase-1 and NADP(H)quinone oxidoreductase-1	14, 15
	Piperine	5% DSS	Male BALB/c mice	2 $mg \cdot kg^{-1}$	Inhibits the activity of metabolic enzymes, regulates the release of p-glycoprotein efflux pump and NF-κB, and provides protection against oxidative damage sites	17
Quinones	**Emodin**	3% DSS	Male C57BL/6 mice	5, 10, 20 $mg \cdot kg^{-1}$	Decreases the level of anti-flagellin antibodies in serum and reduces the expression of TLR5 and NF-κBp65	20
	Rhein	Tail docking-induced inflammation	Transgenic Zebrafish	1, 2, 20 $\mu g \cdot mL^{-1}$	Decrease the activity of MPO in the colonic mucosa and reduce diarrhea due to ulcers	21
	Quinone	3% aqueous acetic acid enema	Male Wistar rats	25, 50 $mg \cdot kg^{-1}$	Has anti-inflammatory, analgesic, anti-oxidant, and healing-promoting effects; inhibits NF-κB signaling pathway	22
Terpenes	**Triptolide**	5% DSS	Female C57BL/6 mice	1 $mg \cdot kg^{-1}$	Has immunomodulatory, anti-inflammatory and anti-tumor activities; inhibits RIP3/MLKL apoptosis pathway	24, 52
	Parthenolide	5% DSS	Male BALB/c mice	10 $mg \cdot kg^{-1}$	Inhibit the activation of NF-κB pathway and inhibit the expression of pro-inflammatory factors	25
	Dihydrotanshinone	5% DSS	Male C57BL/6 mice	10, 25 $mg \cdot kg^{-1}$	Inhibits MPO activity; reduces levels of inflammatory factors TNF-α, IL-1β, IL-6 and high mobility group box protein	28
	Andrographolide	2.5% TNBS, enema	C57BL/6 mice	0.1 $g \cdot kg^{-1} \cdot d^{-1}$	Reduce blood levels of pro-inflammatory factors TNF-α, IL-1β, IL-6 and IL-17A, and reduce levels of IFN-γ	27
Others	**Shikimic acid**	2.5% TNBS, enema	Male BALB/c mice	200 $mg \cdot kg^{-1}$	Anti-inflammatory, affects the metabolism of arachidonic acid, inhibits platelet aggregation, inhibits arterial and venous thrombosis	1, 33
	Arctigenin	DSS	Male BALB/c mice	25, 50 $mg \cdot kg^{-1}$	Inhibit the expression of several genes related to inflammation in the colon such as TNF-α, IL-6, macrophage inflammatory protein 2, monocyte chemoattractant protein 1, immunoglobulin adhesion molecule 1 and vascular adhesion factor 1	32

Table 1. Representative active components of Chinese medicine with prevention and treatment effect of UC and its mechanisms.

	Crocus acid	TNBS/ethanol. enema	SD rats	25, 50 $mg \cdot kg^{-1}$	Inhibit NF-κB inflammatory pathway	29
	Brucein	3% DSS	Male BALB/c mice	0.5, 1, 2 $g \cdot kg^{-1}$	Regulation of TLR4-linked NF-κB signaling	34

MPO-myeloperoxidase PPARγ-peroxisome proliferator-activated receptor γ STAT-signal transducer and activator of transcription
COX-2- cyclooxygenase 2 IFN-γ-interferon γ TGF-β-transforming growth factor β Nrf2-nuelear factor E2-related factor 2

Table 1. Representative active components of Chinese medicine with prevention and treatment effect of UC and its mechanisms.

the purpose of sustained release; second, when the drug is prepared for oral administration in colon-targeting nanoformulations, nano-level particles have better targeting in the colon and can effectively alleviate system adverse reactions[53-54]. Finally, due to the small particle size of the nano-preparation, the drug is more likely to accumulate in the inflammation site of the colon, and a lower drug concentration can achieve a good therapeutic effect[55].

Particle size-dependent type

Studies have shown that the intestinal mucosal layer in the affected area of UC is destroyed,

Inflammation-related cells such as macrophages increase, destroying the original intestinal environment. Macrophages can preferentially absorb nano-scale particles. At the same time, active drugs can be delivered to colon inflammatory tissues through colonic epithelial high permeability and retention effect (enhanced permeability and retention effect, EPR) effects[56]. Lamprecht *et al.*[58] prepared 3 kinds of nanoparticles with fluorescent pigments (with a particle size of 0.1, 1, and 10 μm, respectively), and observed the distribution of various particles after ig 3 d in UC rats induced by TNBS. The distribution index of the size of the nanoparticles in the colon is (5.2%±3.8), (9.1%±4.2) and (14.5%±6.3), respectively. Therefore, in the diseased area of UC, when the particle size is small enough, the drug particles can penetrate into the cell, thereby promoting its rapid passage through the mucosal barrier, interacting with the immune system, and improving the uptake, absorption, distribution and metabolism of the drug[58,59]. Ma *et al.*[60] used the emulsification solvent evaporation method to prepare curcumin-loaded particles (with a particle size of 1.7 μm) and nanoparticles (with a particle size of 270 nm). Compared with the particles, the nanoparticles have a higher release rate; Curcumin nanoparticles are easier to alleviate DSS-induced UC inflammation in mice.

pH-dependent

The pH of the gastrointestinal tract gradually rises from the stomach to the colon. According to the characteristics of colon pH 7-8, a pH-dependent nano-delivery system can be designed, and the nano-system can be targeted for release in the colon[54,61,62]. A pH-dependent drug delivery system can be designed by wrapping pH-sensitive biodegradable polymer materials on the surface of the drug. Methacrylic acid polymer Eudragit® is a common pH-sensitive material. It can be dissolved in different pH by changing its side chain. Raj *et al.*[63] prepared a pH-sensitive curcumin nanoformulation, first prepared a chitosan-encapsulated nano-core structure by the particle gel method, and then prepared the Eudragit FS 30D shell by the emulsification solvent evaporation method to obtain the core-shell structure. This nanoparticle has the ability of controlled the release of drugs and colon targeting. In the release experiment, the cumulative release rate of chitosan nanoparticles coated with pH-sensitive materials in the simulated colon fluid (pH 7.4) reached 84.7%, and the drug was continuously released within 24 hours. Beloqui *et al.*[11] also dissolved curcumin, pH sensitizer Eudragit® S100, poly (lactic-co-glycolic acid) [PLGA] in the organic phase and then dropped it into the organic phase. The pH-sensitive nano-preparation was prepared by stirring in the aqueous solution. The nano-preparation system hardly released curcumin in the pH 1.5 gastric simulation solution and pH 4.5 small intestine simulation solution, and the curcumin release rate after 1 h in the pH 7.2 colon simulation solution reached 90%. In cell uptake experiments, curcumin nanoparticles can penetrate the epithelial barrier more easily than curcumin free solution, and increase the absorption of curcumin by colon cancer Caco-2 cells. In *in vivo* experiments, pH-sensitive curcumin nanoparticle preparations significantly reduced DSS-induced infiltration of mouse neutrophils and TNF-α secretion, lowered the level of MPO, alleviated DSS-induced body weight decline in mice, and inhibited colon shortening; In HE staining, the pH-sensitive nano-preparation group significantly alleviated the inflammation in the colon. Rutin[64], ellagic acid[65], sinomenine[66], etc. have also been reported to have pH-sensitive nanoformulations for the treatment of UC.

Enzyme-responsive

Studies have shown that the colon contains a large number of beneficial microorganisms, which can produce highly active proteases and peptide enzymes, which can be used to make colon enzyme-sensitive nano preparations. After the preparation reaches the colon, the enzyme-sensitive material degrades to release the drug, which improves the bioavailability of the drug[67-69]. Castangia *et al.*[70] used the ultrasonic reaction method to prepare enzyme-sensitive quercetin liposomes to treat UC. Nutriose is a soluble maize dextrin that uses Nutriose's enzymatic degradability to prepare enzyme-sensitive composite liposomes. *In vivo* distribution experiments showed that the liposomes without

Name	Carrier	Preparation	Delivery principle	Formulation characteristics	Therapeutic effect on UC	Ref
Curcumin	PLGA, ABC	Double emulsification solvent evaporation	Porous Nano	The cumulative release at 96 h is about 76%, which is 58% higher than that of nonporous PLGA-encapsulated nanoparticles (58%).	Significantly higher UC mice body weight, colon length↓; spleen body mass ratio↓; inflammatory response↓	78
	PLGA, HA, CS	Double Emulsion Solvent Evaporation Technology	Active targeting	The cumulative release of siCD98 and CUR at 72 h was 68.8% and 89.7%, respectively; increased Colon-26 cells	Fecal Lcn-2, MPO levels↓; CD98 and TNF-α expression levels↓	74
	PLGA, PF127, ABC	Improved double emulsification solvent evaporation technology	Porous Nano	The cumulative release rate at 48 h was 58.3%; there was more accumulation in colon tissue	MPO, spleen mass↓; IL-6, IL-12, TNF-α expression levels↓; IL-10 expression levels↑	76
	SF, CS	Solvent-free self-assembly	Active targeting	Enhanced cellular uptake of Raw264.7	MPO, DAI↓; TNF-α↓, IL-10↑	72
	Eudragit® S100, PLGA	Improved spontaneous emulsification solvent dispersion method	pH-dependent	Curcumin does not release at pH 1.5, 4.5, but is rapidly released at neutral pH 7.2	MPO↓; TNF-α protein expression in blank nano group↓; In tissue staining, inflammatory reaction↓	11
	Eudragit® S100, PLGA	Emulsifying solvent evaporation method	pH-dependent	There is no burst release in the release test, more curcumin can be released in neutral pH, and the release can be controlled	Body mass↓; MPO↓; Spleen mass↑, colon length↓; In HE staining, inflammatory response↓	79
Bruceine	HS-15、PG	Self-assembly nano-emulsification method	Other	The optimized particle size is (18.03±0.59) nm and the potential is (−15.76±0.42) mV	DAI↓; IL-10, TGF-β and other anti-inflammatory factors↑; IL-1β, IL-6, IL-8 and other pro-inflammatory factors↓; iNOS, COX-2 mRNA expression levels↓; TLR4, MyD88, TRAF6, NF-κBp65	77
Silymarin	Eudragit® FS30D Eudragit® RLPO	Emulsifying solvent evaporation method	pH-dependent	The cumulative release rate after 24 h in simulated colonic fluid (pH 7.2) was (40.8±5.5%)	Mucosal injury↓; MPO, IL-6, TNF-α↓	80
Quercetin	Nutriose FM06	Ultrasonic reaction method	Enzyme sensitive	About 20% of quercetin was detected in the jejunum and ileum and about 30% in the colon 3 hours after dosing	Reduced colonic body mass ratio more than unencapsulated Nutriose formulation; MPO↓; MPO I percentage↑↑	70
Icariin	CS	Internal Emulsion Gel Technology	Enzyme sensitive	The cumulative release rate was 10% in simulated gastric and small intestinal fluid, and 65.6% in simulated colonic fluid	Colonic mucosa PGE2↓; TNF-α↓; iNOS, COX-2 71 mRNA levels↓	71
Sinomenine	Eudragit®, CS	Emulsification Crosslinking and Emulsification Solvent Evaporation	Other	The release rate was (8.91±0.39) % at pH 6.8, (59.52±1.23) % at pH 7.4, and (72.54±1.33) % in simulated colonic fluid	DAI↓; expression levels of MyD88, NF-κBp65↓; TLR/NF-κB pathway↓; IFN-γ, IL-1β and other pro-inflammatory factors↓	66
Andrographolide	α-tocopherol	High pressure homogenization self-emulsifying method	Other	The optimized nanoemulsion droplet size is (122±11) nm	Ulcer index↓; tissue damage score↓; small intestinal mucosal damage	81
Quinone	SBO/VCO	Ultrasound after homogenization		The particle size ranges from (196.1±3.57) to (269.2±1.05) nm; the potential ranges from −36.6 to −62.0 mV	CAS↓; colonic mucosal edema, necrosis and inflammatory cell infiltration↓; promote MPO, LPO, GSH, LDH back to normal levels	82

Table 2. Colon-targeted nano drug delivery systems of active components of Chinese medicine in the treatment of UC.

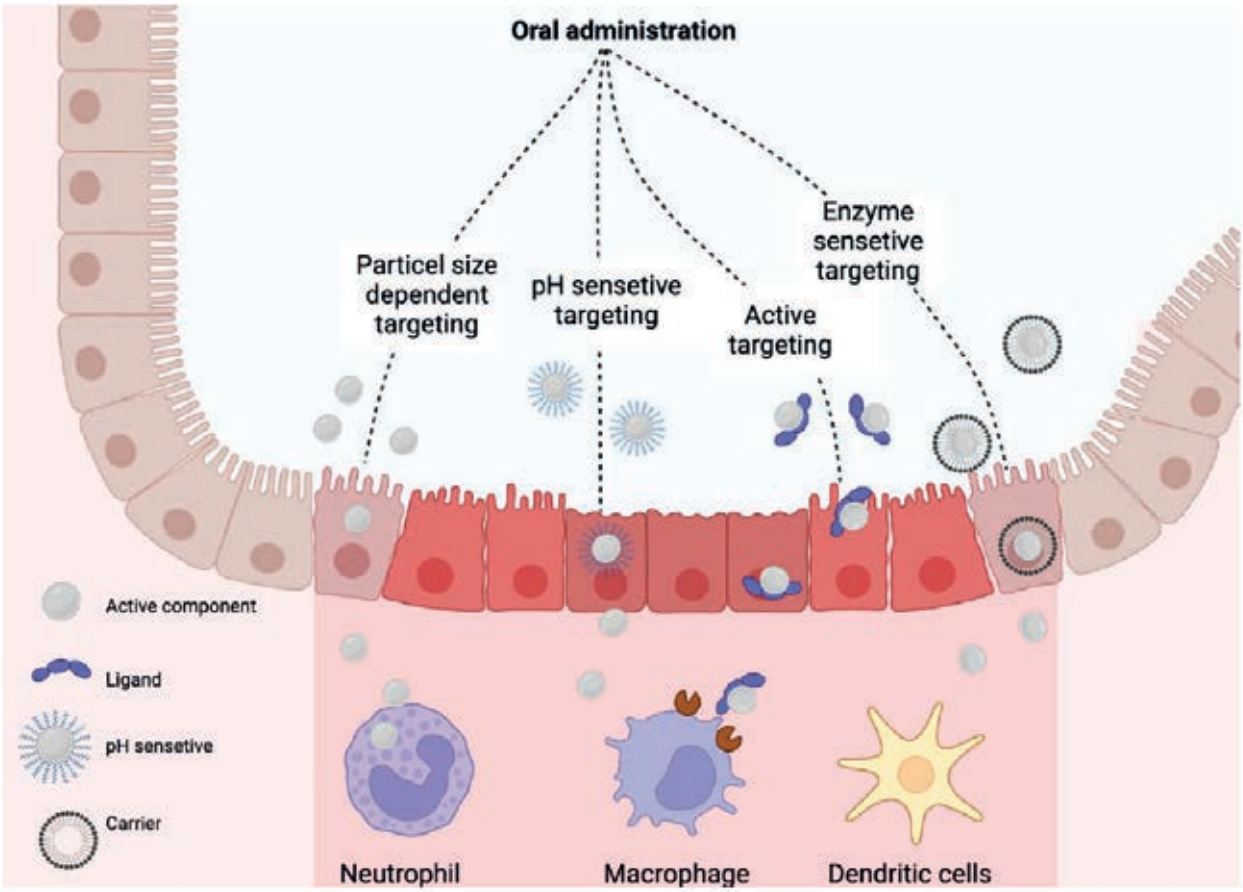

Figure 1. Delivery principles of colon-targeted nano drug delivery systems for UC.

Nutriose ig 4 h showed strong fluorescence in the ileum and cecum, but only weak fluorescence in the colon; the liposomes without Nutriose ig 4 h showed obvious fluorescence in the colon. In addition, the nano-delivery system can delay drug release. In the release experiment, the cumulative release rate of Nutriose-encapsulated liposomes in the colon simulant at pH 7.0 for 8 hours is 15% lower than that of unencapsulated liposomes. In the in vivo efficacy experiment, the nano-preparation group significantly reduced bleeding and ulcers in the colon area, lowered the colonic edema tissue (CAS) index, and decreased the activity of MPO. Chitosan-coated calcium alginate microspheres loaded with icariin can also target drug delivery to the colon through an enzyme response[71].

Active targeting

Studies have found that there are a large number of inflammation-related proteins in the inflammation part of the colon. When a substance that can specifically bind to the nanoparticle is connected, colon targeting can be achieved through the ligand-receptor effect. Chondroitin sulfate (CS) is a glycosaminoglycan substance that binds to the CD44 receptor. CD44 is a transmembrane transport glycoprotein on the surface of activated macrophages. Gou *et al.*[72] used silk fibroin to prepare curcumin nanoparticles and then attached CS to their surface to target colonic macrophages. In the macrophage uptake experiment, the fluorescence of chondroitin sulfate nanoparticles (CS-NPS) was significantly stronger than that of curcumin nanoparticles after 4 hours of treatment. After CS-NPS ig, it significantly inhibited mice's body weight decline, down-regulated TNF-α and IL-6, and upregulated the levels of IL-10; in the HE staining experiment, the accumulation of immune cells was reduced. After CS-NPS ig, the survival rate of mice after 15 d DSS treatment reached 50%. Studies have found that the up-regulation of CD98 in colonic epithelial cells in mice with colon inflammation can be used to treat UC by interfering with its synthesis[73]. Xiao *et al.*[74] prepared curcumin hydrogels containing CD98 synthetic interfering RNA (CD98 siRNA, siCD98) for targeted treatment of UC. Use PLGA to wrap curcumin and siCD98 to form nanoparticles, then wrap chitosan and connect with hyaluronic acid, and finally crosslink into a hydrogel in the presence of chitosan and sodium alginate. In the cell uptake experiment, the fluorescence of the hyaluronic acid nanoparticle group was more potent than that of the curcumin nanoparticle group, which proved that the surface modification of hyaluronic acid (HA) could increase the cell's uptake of nanoparticles. Further cell experiments showed that the nano-preparation system reduces the expression of CD98 in Colon-26 colon cancer cells, down-regulating the levels of MPO and apolipoprotein 2 (Lcn-2) in feces, reduces colon ulcers, and promotes colon tissue returns to normal. Some researchers have also loaded targeted siRNA into ginger-derived natural nanoparticles for targeted therapy of UC[75].

Other ingredients

In addition to the targeted nano-systems mentioned above, there are also some porous nanoformulations and self-assembled nano-delivery systems for colon-targeted delivery of active ingredients of traditional Chinese medicine. Chen *et al.*[76] used dual emulsification solvent eva-

poration technology to use PLGA/PF127 to encapsulate curcumin and ammonium bicarbonate (ABC) as a porogen to produce porous nanoparticles. In macrophage uptake experiments, porous nanoparticles, the fluorescence of the preparation is stronger than that of the non-porous nanoparticle preparation. *In vivo* experiments show that porous nanoparticles have more accumulation in colon tissue. Dou *et al.*[77] constructed bruceine nanoparticles by self-assembly nano-emulsification method and dissolved bruceine D (BD) in (polyethylene glycol-15-hydroxystearate)-propylene glycol- In the chain triacylglycerol (4:2:1) solution, the self-assembled nanoparticles can be obtained by stirring. Compared with BD-free solution, BD self-assembled nano-system has a better inhibitory effect on pro-inflammatory factors and can significantly alleviate the damage of UC tissue.

The delivery principle of the oral colon-targeted nano-system is shown in Figure 1, and the oral colon-targeted nano-system for treating UC with active ingredients of traditional Chinese medicine is shown in Table 2.

Conclusions

Traditional Chinese medicine has the characteristics of multiple components and multiple targets and has significant advantages in treating chronic and complex diseases represented by UC. With the deepening of research, the effective ingredients of traditional Chinese medicine intervention in UC have been discovered. The mechanism has gradually become clear, such as curcumin, triptolide, resveratrol, etc. However, in the formulation development process, problems such as water insolubility, low bioavailability, and poor colon targeting have restricted its use. Therefore, how to effectively deliver drugs to the diseased part of the colon through oral administration to release the drugs to achieve the therapeutic effect is a problem to be solved urgently. The construction of an oral colon-targeted drug delivery system can solve this problem. Nanoformulations for treating UC can be designed according to particle size dependence, pH dependence, enzyme response, and ligand-receptor-specific pairing. Some nanoformulations pass through the colon. The permeability of mucosal cells is not high, and there are problems such as inflammation or low uptake of immune-related cells. These problems will further limit the use of colon-targeted nanoformulations in clinical applications. However, in recent years, with the application of new materials, the discovery of colon-specific receptors, and the research on the pathogenesis of UC, the colon targeting and specificity of oral preparations will be further improved.

Author Contributions

Conceptualization and writing original draft preparation: Mohammad Javed Ansari. Methodology: Suhad J. Hadi and Hamzah H. Kzar. Validation: Moaed E. Al-Gazally. Resource: Thulfeqar Ahmed Hamza. Data collection: Mohammed Khudair Hasan. Data analysis: Aiman Mohammed Baqir Al-Dhalimy, Writing review editing: Reza Akhavan-Sigari.

Funding

This research received no external funding.

Acknowledgments

There is no acknowledgments.

Conflicts of Interest

There are no conflicts of interest.

Bibliographic references

1. Forootan M, Darvishi M. Solitary rectal ulcer syndrome: A systematic review. Medicine (Baltimore). 2018;97(18):e0565.
2. Xavier RJ, Thomas HJ. Gastrointestinal Diseases. Hunter's Tropical Medicine and Emerging Infectious Disease. 2013:18–27.
3. Chen, Y., Wang, P., Zhang, Y. et al. Comparison of effects of aminosalicylic acid, glucocorticoids and immunosuppressive agents on the expression of multidrug-resistant genes in ulcerative colitis. Sci Rep 2022;12:20656.
4. Rauf A, Imran M, Suleria H A R, et al. A comprehensive review of the health perspectives of resveratrol. Food Funct, 2017, 8(12): 4284-4305.
5. Marques F Z, Markus M A, Morris B J. Resveratrol: Cellular actions of a potent natural chemical that confers diverse health benefits. Int J Biochem Cell Biol, 2009, 41(11): 2125-2128.
6. Chua L S. A review on plant-based rutin extraction methods and its pharmacological activities. J Ethnopharmacol, 2013, 150(3): 805-817.
7. Nones K, Dommels Y E, Martell S, et al. The effects of dietary curcumin and rutin on colonic inflammation and gene expression in multidrug resistance gene-deficient (mdr1a-/-) mice, a model of inflammatory bowel diseases. Br J Nutr, 2009, 101(2): 169-181.
8. Habtemariam S, Belai A. Natural therapies of the inflammatory bowel disease: The case of rutin and its aglycone, quercetin [J]. Mini Rev Med Chem, 2018, 18(3): 234-243.
9. Park J W, Shin N R, Shin I S, et al. Silibinin inhibits neutrophilic inflammation and mucus secretion induced by cigarette smoke via suppression of ERK-SP1 pathway. Phytother Res, 2016, 30(12): 1926-1936.
10. Kim B R, Seo H S, Ku J M, et al. Silibinin inhibits the production of pro-inflammatory cytokines through inhibition of NF-κB signaling pathway in HMC-1 human mast cells. Inflamm Res, 2013, 62(11): 941-950.
11. Beloqui A, Coco R, Memvanga P B, et al. pH-sensitive nanoparticles for colonic delivery of curcumin in inflammatory bowel disease. Int J Pharm, 2014, 473(1/2): 203-212.
12. Zhu L, Gu P, Shen H. Protective effects of berberine hydrochloride on DSS-induced ulcerative colitis in rats. Int Immunopharmacol, 2019, 68: 242-251.
13. Li S, Han J, Wang D S, et al. Sinomenine attenuates chronic inflammatory pain in mice. Metab Brain Dis, 2017, 32(1): 211-219.
14. Tang J, Raza A, Chen J, et al. A systematic review on the sinomenine derivatives. Mini Rev Med Chem, 2018, 18(11): 906-917.
15. Zhou Y, Liu H Y, Song J, et al. Sinomenine alleviates dextran sulfate sodium-induced colitis via the Nrf2/ NQO-1 signaling pathway. Mol Med Rep, 2018, 18(4): 3691-3698.
16. Zhou, J., Tan, L., Xie, J., Lai, Z., Huang, Y., Qu, C., Luo, D., Lin, Z., Huang, P., Su, Z. and Xie, Y., 2017. Characterization of brusatol self-microemulsifying drug delivery system and its therapeutic effect against dextran sodium sulfate-induced ulcerative colitis in mice. Drug delivery, 24(1), pp.1667-1679.
17. Li Q P, Zhai W W, Jiang Q L, et al. Curcumin-piperine mixtures in self-microemulsifying drug delivery system for ulcerative colitis therapy. Int J Pharm, 2015, 490(1/2): 22-31.
18. Zhang D K, Cheng L N, Huang X L, et al. Tetrandrine ameliorates dextran-sulfate-sodium-induced colitis in mice through inhibition of nuclear factor-kappaB activation. Int J Colorectal Dis, 2009, 24(1): 5-12.
19. Monisha B A, Kumar N, Tiku A B. Emodin and its role in chronic diseases. Adv Exp Med Biol, 2016, 928: 47-73.
20. Luo S, Deng X L, Liu Q, et al. Emodin ameliorates ulcerative colitis by the flagellin-TLR5 dependent pathway in mice. Int Immunopharmacol, 2018, 59: 269-275.

21. Ge H, Tang H, Liang Y B, et al. Rhein attenuates inflammation through inhibition of NF-κB and NALP3inflammasome in vivo and in vitro. Drug Des Devel Ther, 2017, 11: 1663-1671.
22. Thippeswamy B S, Mahendran S, Biradar M I, et al. Protective effect of embelin against acetic acid induced ulcerative colitis in rats. Eur J Pharmacol, 2011, 654(1): 100-105.
23. Zhao J, Luo D, Zhang Z, et al. Celastrol-loaded PEG-PCL nanomicelles ameliorate inflammation, lipid accumulation, insulin resistance and gastrointestinal injury in diet- induced obese mice. J Control Release, 2019, 310: 188-197.
24. Jia Z Y, Xu C F, Shen J Q, et al. The natural compound celastrol inhibits necroptosis and alleviates ulcerative colitis in mice [J]. Int Immunopharmacol, 2015, 29(2): 552-559.
25. Zhao Z J, Xiang J Y, Liu L, et al. Parthenolide, an inhibitor of the nuclear factor-κB pathway, ameliorates dextran sulfate sodium-induced colitis in mice. Int Immunopharmacol, 2012, 12(1): 169-174.
26. Zhu Q, Zheng P F, Zhou J Y, et al. Andrographolide affects Th1/Th2/Th17 responses of peripheral blood mononuclear cells from ulcerative colitis patients [J]. Mol Med Rep, 2018, 18(1): 622-626.
27. Zhu Q, Zheng P F, Chen X Y, et al. Andrographolide presents therapeutic effect on ulcerative colitis through the inhibition of IL-23/IL-17 axis. Am J Transl Res, 2018, 10(2): 465-473.
28. Guo Y, Wu X, Wu Q, et al. Dihydrotanshinone I, a natural product, ameliorates DSS-induced experimental ulcerative colitis in mice [J]. Toxicol Appl Pharmacol, 2018, 344: 35-45.
29. Si-Yu, C.A.O., Sheng-Jie, Y.E., Wei-Wei, W.A.N.G., Bing, W.A.N.G., Zhang, T. and Yi-Qiong, P.U., 2019. Progress in active compounds effective on ulcerative colitis from Chinese medicines. Chinese journal of natural medicines, 17(2), pp.81-102.
30. Singh B. Psyllium as therapeutic and drug delivery agent. Int J Pharm, 2007, 334(1/2): 1-14.
31. Laroui H, Dalmasso G, Nguyen H T, et al. Drug-loaded nanoparticles targeted to the colon with polysaccharide hydrogel reduce colitis in a mouse model. Gastroenterology, 2010, 138(3): 843-853.
32. Wu X, Dou Y N, Yang Y, et al. Arctigenin exerts anti-colitis efficacy through inhibiting the differentiation of Th1 and Th17 cells via an mTORC1-dependent pathway. Biochem Pharmacol, 2015, 96(4): 323-336.
33. Dong K, Zeng A G, Wang M L, et al. In vitro and in vivo study of a colon-targeting resin microcapsule loading a novel prodrug, 3,4,5-tributyryl shikimic acid. RSC Adv, 2016, 6(20): 16882-16890.
34. Huang Y F, Zhou J T, Qu C, et al. Anti-inflammatory effects of Brucea javanica oil emulsion by suppressing NF-κB activation on dextran sulfate sodium-induced ulcerative colitis in mice. J Ethnopharmacol, 2017, 198: 389-398.
35. Grzanna R, Lindmark L, Frondoza C G. Ginger: An herbal medicinal product with broad anti-inflammatory actions. J Med Food, 2005, 8(2): 125-132.
36. Zhang M, Viennois E, Prasad M, et al. Edible ginger-derived nanoparticles: A novel therapeutic approach for the prevention and treatment of inflammatory bowel disease and colitis-associated cancer. Biomaterials, 2016, 101: 321-340.
37. Brown A C, Shah C, Liu J, et al. Ginger's (Zingiber officinale Roscoe) inhibition of rat colonic adenocarcinoma cells proliferation and angiogenesis in vitro [J]. Phytother Res, 2009, 23(5): 640-645.
38. Kwon K H, Murakami A, Tanaka T, et al. Dietary rutin, but not its aglycone quercetin, ameliorates dextran sulfate sodium-induced experimental colitis in mice: Attenuation of pro-inflammatory gene expression. Biochem Pharmacol, 2005, 69(3): 395-406.
39. Guazelli C F, Fattori V, Colombo B B, et al. Quercetin-loaded microcapsules ameliorate experimental colitis in mice by anti-inflammatory and anti-oxidant mechanisms. J Nat Prod, 2013, 76(2): 200-208.
40. Luo X P, Yu Z L, Deng C, et al. Baicalein ameliorates TNBS-induced colitis by suppressing TLR4/MyD88 signaling cascade and NLRP3 inflammasome activation in mice. Sci Rep, 2017, 7: 16374.
41. Zhang C L, Zhang S, He W X, et al. Baicalin may alleviate inflammatory infiltration in dextran sodium sulfate-induced chronic ulcerative colitis via inhibiting IL-33 expression. Life Sci, 2017, 186: 125-132.
42. Tao F F, Qian C, Guo W J, et al. Inhibition of Th1/Th17 responses via suppression of STAT1 and STAT3 activation contributes to the amelioration of murine experimental colitis by a natural flavonoid glucoside icariin. Biochem Pharmacol, 2013, 85(6): 798-807.
43. Chao L, Zheng P Y, Xia L, et al. Calycosin attenuates dextran sulfate sodium (DSS)-induced experimental colitis. Iran J Basic Med Sci, 2017, 20(9): 1056-1062.
44. Al-Rejaie S S, Abuohashish H M, Al-Enazi M M, et al. Protective effect of naringenin on acetic acid-induced ulcerative colitis in rats. World J Gastroenterol, 2013, 19(34): 5633-5644.
45. He X X, Wei Z K, Wang J J, et al. Alpinetin attenuates inflammatory responses by suppressing TLR4 and NLRP3 signaling pathways in DSS-induced acute colitis. Sci Rep, 2016, 6: 28370.
46. Arafa H M, Hemeida R A, El-Bahrawy A I, et al. Prophylactic role of curcumin in dextran sulfate sodium (DSS)-induced ulcerative colitis murine model. Food Chem Toxicol, 2009, 47(6): 1311-1317.
47. Yadav V R, Suresh S, Devi K, et al. Novel formulation of solid lipid microparticles of curcumin for anti-angiogenic and anti-inflammatory activity for optimization of therapy of inflammatory bowel disease [J]. J Pharm Pharmacol, 2009, 61(3): 311-321.
48. Abdin A A. Targeting sphingosine kinase 1 (SphK1) and apoptosis by colon-specific delivery formula of resveratrol in treatment of experimental ulcerative colitis in rats. Eur J Pharmacol, 2013, 718(1/2/3): 145-153.
49. Yum S, Jeong S, Lee S, et al. Colon-targeted delivery of piceatannol enhances anti-colitic effects of the natural product: Potential molecular mechanisms for therapeutic enhancement. Drug Des Devel Ther, 2015, 9: 4247- 4258.
50. Marín M, María Giner R, Ríos J L, et al. Intestinal anti-inflammatory activity of ellagic acid in the acute and chronic dextrane sulfate sodium models of mice colitis. J Ethnopharmacol, 2013, 150(3): 925-934.
51. Shen P, Zhang Z C, He Y, et al. Magnolol treatment attenuates dextran sulphate sodium-induced murine experimental colitis by regulating inflammation and mucosal damage. Life Sci, 2018, 196: 69-76.
52. Shaker M E, Ashamallah S A, Houssen M E. Celastrol ameliorates murine colitis via modulating oxidative stress, inflammatory cytokines and intestinal homeostasis. Chem Biol Interact, 2014, 210: 26-33.
53. Xiao B, Merlin D. Oral colon-specific therapeutic approaches toward treatment of inflammatory bowel disease. Expert Opin Drug Deliv, 2012, 9(11): 1393- 1407.
54. Collnot E M, Ali H, Lehr C M. Nano- and microparticulate drug carriers for targeting of the inflamed intestinal mucosa. J Control Release, 2012, 161(2): 235-246.
55. Hua S S, Marks E, Schneider J J, et al. Advances in oral nano-delivery systems for colon targeted drug delivery in inflammatory bowel disease: Selective targeting to diseased versus healthy tissue. Nanomed-Nanotechnol Biol Med, 2015, 11(5): 1117-1132.
56. Lamprecht A, Yamamoto H, Takeuchi H, et al. Nanoparticles enhance therapeutic efficiency by selectively increased local drug dose in experimental colitis in rats. J Pharmacol Exp Ther, 2005, 315(1): 196-202.
57. Lamprecht A, Schäfer U, Lehr C M. Size -dependent bioadhesion of micro- and nanoparticulate carriers to the inflamed colonic mucosa [J]. Pharm Res, 2001, 18(6): 788-793.
58. de Jong W H, Borm P J. Drug delivery and nanoparticles: Applications and hazards. Int J Nanomedicine, 2008, 3(2): 133-149.
59. Powell J J, Faria N, Thomas-McKay E, et al. Origin and fate of dietary nanoparticles and microparticles in the gastrointestinal tract. J Autoimmun, 2010, 34(3): J226- J233.

60. Ma P P, Si X Y, Chen Q B, et al. Oral drug delivery systems for ulcerative colitis therapy: A comparative study with microparticles and nanoparticles. Curr Cancer Drug Targets, 2019, 19(4): 304-311.
61. Zhang M Z, Merlin D. Nanoparticle-based oral drug delivery systems targeting the colon for treatment of ulcerative colitis. Inflamm Bowel Dis, 2018, 24(7): 1401-1415.
62. Nugent S G, Kumar D, Rampton D S, et al. Intestinal luminal pH in inflammatory bowel disease: Possible determinants and implications for therapy with aminosalicylates and other drugs. Gut, 2001, 48(4): 571-577.
63. Raj P M, Raj R, Kaul A, et al. Biodistribution and targeting potential assessment of mucoadhesive chitosan nanoparticles designed for ulcerative colitis via scintigraphy. RSC Adv, 2018, 8(37): 20809-20821.
64. Abdel Ghaffar A M, Radwan R R, Ali H E. Radiation synthesis of poly (starch/acrylic acid) pH sensitive hydrogel for rutin controlled release. Int J Biol Macromol, 2016, 92: 957-964.
65. Jeong Y I, Yŏ R P, Ohno T, et al. Application of Eudragit P-4135F for the delivery of ellagic acid to the rat lower small intestine. J Pharm Pharmacol, 2001, 53(8): 1079-1085.
66. Xiong H, Tian L, Zhao Z, et al. The sinomenine enteric-coated microspheres suppressed the TLR/NF-κB signaling in DSS-induced experimental colitis. Int Immunopharmacol, 2017, 50: 251-262.
67. Chourasia M K, Jain S K. Polysaccharides for colon targeted drug delivery. Drug Deliv, 2004, 11(2): 129-148.
68. Basit A W, Short M D, McConnell E L. Microbiota- triggered colonic delivery: Robustness of the polysaccharide approach in the fed state in man. J Drug Target, 2009, 17(1): 64-71.
69. Pinto J F. Site-specific drug delivery systems within the gastrointestinal tract: From the mouth to the colon. Int J Pharm, 2010, 395(1/2): 44-52.
70. Castangia I, Nácher A, Caddeo C, et al. Therapeutic efficacy of quercetin enzyme-responsive nanovesicles for the treatment of experimental colitis in rats. Acta Biomater, 2015, 13: 216-227.
71. Wang Q S, Wang G F, Zhou J, et al. Colon targeted oral drug delivery system based on alginate-chitosan microspheres loaded with icariin in the treatment of ulcerative colitis. Int J Pharm, 2016, 515(1/2): 176-185.
72. Gou S Q, Huang Y M, Wan Y, et al. Multi-bioresponsive silk fibroin-based nanoparticles with on-demand cytoplasmic drug release capacity for CD44-targeted alleviation of ulcerative colitis. Biomaterials, 2019, 212: 39-54.
73. Kucharzik T, Lugering A, Yan Y T, et al. Activation of epithelial CD98 glycoprotein perpetuates colonic inflammation. Lab Invest, 2005, 85(7): 932-941.
74. Xiao B, Zhang Z, Viennois E, et al. Combination therapy for ulcerative colitis: Orally targeted nanoparticles prevent mucosal damage and relieve inflammation. Theranostics, 2016, 6(12): 2250-2266.
75. Zhang M Z, Wang X Y, Han M K, et al. Oral administration of ginger-derived nanolipids loaded with siRNA as a novel approach for efficient siRNA drug delivery to treat ulcerative colitis. Nanomedicine (Lond), 2017, 12(16): 1927-1943.
76. Chen Q B, Gou S Q, Ma P P, et al. Oral administration of colitis tissue-accumulating porous nanoparticles for ulcerative colitis therapy. Int J Pharm, 2019, 557: 135-144.
77. Dou Y X, Zhou J T, Wang T T, et al. Self- nanoemulsifying drug delivery system of bruceine D: A new approach for anti-ulcerative colitis. Int J Nanomedicine, 2018, 13: 5887-5907.
78. Chen Q B, Si X Y, Ma L J, et al. Oral delivery of curcumin via porous polymeric nanoparticles for effective ulcerative colitis therapy. J Mater Chem B, 2017, 5(29): 5881-5891.
79. Xiao B, Si X Y, Zhang M Z, et al. Oral administration of pH-sensitive curcumin-loaded microparticles for ulcerative colitis therapy. Colloids Surf B Biointerfaces, 2015, 135: 379-385.
80. Varshosaz J, Minaiyan M, Khaleghi N. Eudragit nanoparticles loaded with silybin: A detailed study of preparation, freeze-drying condition and in vitro/in vivo evaluation. J Microencapsul, 2015, 32(3): 211-223.
81. Yen C C, Chen Y C, Wu M T, et al. Nanoemulsion as a strategy for improving the oral bioavailability and anti-inflammatory activity of andrographolide. Int J Nanomedicine, 2018, 13: 669-680.
82. Badamaranahalli S S, Kopparam M, Bhagawati S T, et al. Embelin lipid nanospheres for enhanced treatment of ulcerative colitis-Preparation, characterization and in vivo evaluation. Eur J Pharm Sci, 2015, 76: 73-82.

ARTICLE / INVESTIGACIÓN

Coordination compounds of carbonyl oxygen polychelate ligand; synthesis, physicochemical characterization and biological evaluation

Duaa S. Abaas and Mohamad J. Al-Jeboori*

DOI. 10.21931/RB/2023.08.02.18

Department of Chemistry, College of Education for Pure Science (Ibn Al-Haitham), University of Baghdad, Adhamiyah, Baghdad, Iraq.
Corresponding author: mohamad.al-jeboori@ihcoedu.uobaghdad.edu.iq

Abstract: The work covers the formation of the bisaldehyde ligand 2,2'-[ethane-1,2diylbis(oxy)] dibenzaldehyde (M) and its metal complexes. The synthesis of M was achieved via two steps in which two equivalents of the salicylaldehyde were reacted with KOH in an ethanolic medium. Subsequently, the resulting compound dissolved in DMF and one equivalent of 1,2-dibromoethane was added. Adding an ethanolic solution of metal chloride of a range of metal ions to the ligand in a 1:1 (M:L) mole ratio resulted in preparing a new five monomeric complexes. The entity of the isolated structure for the prepared compounds was confirmed using physicochemical methods (FT-IR, electronic spectroscopy, mass and ^{1}H, ^{13}C-NMR spectra, elemental microanalysis, magnetic susceptibility and molar conductance). The characterization data indicated the isolation of six and four-coordinate monomeric complexes with the general formula; $[Cr(M)(Cl)_2(H_2O)_2]Cl$, $[M(M)(Cl)_2].H_2O$ (where M= $Fe^{(II)}$, $Co^{(II)}$ and $Cu^{(II)}$) and $[Ni(M)]Cl_2.H_2O$. The anti-microbiological activity of the title compounds (ligand and complexes) was tested against various bacterial and fungal microorganisms. The acquired data revealed that the metal complexes became potentially more active than the M.

Key words: Bisaldehyde ligand, Novel monomeric metal complexes, Structural study, Antimicrobial activity.

Introduction

The current interests in forming bis-functionalized compounds are due to their wide range of uses in organic and inorganic chemistry, biology and industry[1,2]. These materials are fascinating precursors employed as building blocks in supramolecule and nanotechnology[2,3]. Aromatic aldehydes are natural product species classified as essential compounds due to their uses in the fragrance and cosmetics industries, food technology, medicine, and pharmaceuticals[4,5]. Further, the condensation reaction of these species, the bisaldehyde compounds, with a primary amine segment resulted in the preparation of the Schiff base. Compounds that are derived from bis-functionalized starting materials, in particular, 2,2'-[ethane-1,2diylbis(oxy)]dibenzaldehyde (EDD) precursor, are interesting organic species that are used in the formation of Schiff-bases. The formation of the EDD is based on the reaction of the dibromoalkyl with the salicylaldehyde in the presence of an alkali medium. Several condition reactions were implemented to form the EDD precursor to optimize yield, solvent and other reaction factors; schiff bases derived from the EDD were used as complexation agents and a range of metal complexes were reported[6]. Recently, we reported the isolation of complexes derived from Mannich bases in which carbonyl oxygen moiety of the cyclohexanone segment is involved in coordinating with the metal centers[7,8]. However, to our knowledge, there are no published reports on using EDD as a complexation agent. Therefore, the current work intends to explore the potential ability of EDD as a complexation agent in which carbonyl oxygen of the bisaldehyde moieties is involved in the coordination with the metal center. The preparation of 2,2'-[ethane-1,2diylbis(oxy)]dibenzaldehyde (EDD) with a modification procedure to that reported previously[9] and the formation of a range of monomeric complexes derived from EDD are reported. Further, this study explores the complexation effect on the antimicrobial activity on the free bisaldehyde ligand upon coordination with the mental center.

Materials and methods

The organic and inorganic materials used in this work were commercially available and were used as received. The FTIR spectra of compounds were recorded using KBr and CsI discs from 4000–250 cm^{-1} on a Shimadzu Fourier Transform Infrared Spectrometer (FTIR-600). The mass spectrum for the ligand was determined using the electrospray method (positive mode) with the Agilent mass spectrometer Sciex ESI mass analysis. The ligand's 1H- and 13C-NMR spectra were recorded in DMSO-d_6 with a Brucker-500 MHz. For the ^{1}H-NMR study, tetramethylsilane (TMS) was used as an internal standard to measure chemical shifts. A Shimadzu UV-160 spectrophotometer was used to analyze the electronic spectra of compounds from 200–1000 nm for 10^{-3} M solutions in DMSO at ambient temperature. An electrothermal Stuart apparatus, model SMP_{40}, was used to determine melting points. Elemental analyses (CHN) for the ligand and their metal complexes were performed using EuroEA 3000 machine. A Shimadzu (AA) 680G atomic absorption spectrophotometer and a potentiometric titration technique on a 686-nitro processor-665 Dosimat-Metrom Swiss were used to determine metal and chloride percentages for compounds, respectively. The

Citation: Abaas, D. S.; Al-Jeboori, M. J. Coordination Compounds of Carbonyl Oxygen Polychelate Ligand; Synthesis, Physicochemical Characterisation and Biological Evaluation. Revis Bionatura 2023;8 (2) 18. http://dx.doi.org/10.21931/RB/2023.08.02.18
Received: 2 January 2023/ / **Accepted:** 19 April 2023 / **Published:** 15 June 2023

Publisher's Note: Bionatura stays neutral with regard to jurisdictional claims in published maps and institutional affiliations.

magnetic moments were performed on a Sherwood Scientific Devised at 308 K. A Eutech Instruments Cyberscan con 510 digital conductivity meter was used to measure molar conductance for complexes.

Synthesis

Synthesis of 2,2'-(Ethane-1,2-diylbis(oxy))dibenzaldehyde (M)

The formation of M was based on a published method[9] with a modification and as follows: To an ethanolic solution of KOH (0.56g, 10mmol) in 15ml of absolute EtOH was added with stirring a mixture of salicylaldehyde (1.22g, 10mmol) in EtOH (5ml). The reaction mixture was allowed to reflux until a clear solution was obtained, and then the solvent was removed under reduced pressure to give a pale green solid. 10ml of DMF was added to the solid, and the mixture was heated at 100°C for 10min. Subsequently, a mixture of 1,2-dibromoethane (0.94g, 5 mmol) in DMF (5 ml) was added with stirring. The resulting mixture was allowed to reflux for 30min and stirred at room temperature, then distilled water was added. The mixture was allowed to stir for 2h, and the formed brown solid was collected by filtration and washed with a copious amount of water. The compound was recrystallized from hot ethanol, and bright brown crystals were collected by filtration that was kept in the air to dry. Yield: 2.4g (88%), m.p = 118 - 120°C. M.wt=270 amu. FT-IR (KBr) cm^{-1}; 1685 and 1666 v(C=O)ald, 1242 v(C-O-C) and 1597 v(C=C)cm^{-1}.

Synthesis of complexes

The metal complexes were prepared following an analog procedure. Therefore, the formation of $[Cr(M)(Cl)_2(H_2O)_2]Cl$ is reported as a model for the preparation of complexes and as follows: To a stirring solution of the bisaldehyde ligand (0.10g, 0.37mmol) in 10ml of a hot mixture of DMF and ethanol with an 8:2 (v:v) ratio has added a solution of chromium(III) chloride hexahydrate (0.10g, 0.37mmol) dropwise in 10ml of ethanol. The resulting mixture was heated by stirring at 70°C for 4h. The brownish-red solid that formed was collected by filtration, washed with diethyl ether (5ml) and dried in air. Yield: 0.122g (76%), m.p = 250-248°C. Table 1 includes elemental analytical data, colors, and products of complexes. Tables 2 and 3 show the FT-IR and electronic data of complexes, respectively.

Biological activity measurement

The evaluation of ligand and its metal complexes against four bacterial species (*Escherichia coli, Pseudomonas aeruginosa, Staphylococcus aureus* and *Bacillus subtilis*) and two types of fungi (*Candida albicaus* and *Rhizopus sporium*) were performed using agar-well diffusion[10]. In this method, the wells were dug in the media with the help of a sterile metallic borer with centers of a diameter of at least 6 mm. The recommended concentration (100 µL) of the 1 mg/mL test sample in DMSO was introduced in the respective wells. The plates were incubated immediately at 37°C for 24h. The activity was evaluated by measuring the diameter of inhibition zones (mm). The samples were performed at the Central Service Laboratory / Ministry of Science and Technology / Baghdad / Iraq.

Results and discussion

The synthesis of the ligand (M), 2,2'-[ethane-1,2diylbis(oxy)] dibenzaldehyde, and its metal complexes are reported. The ligand was prepared with modification in a two-step. These include the reaction of salicylaldehyde with KOH in an ethanolic medium. After removing the solvent under vacuum, 1,2-dibromoethane in DMF medium was added and allowed to heat at reflux for 2h. The reaction mixture was allowed to stir at RT, and a precipitate was formed by adding distilled water. The title compound was collected by filtration and then recrystallized from EtOH to give M an excellent yield, Figure 1. The ligand (M) is a potentially tetradentate species that consist of two carbonyl oxygen-aldehydes and two oxygen-ether donor atoms. The reaction of M with metal chlorides of $Cr^{(III)}$, $Fe^{(II)}$, $Co^{(II)}$, $Ni^{(II)}$ and $Cu^{(II)}$ in a 1:1 (L:M) mole ratio using a mixture of EtOH/DMF in a 2:8 ratio at reflux gave the required complexes, Figure 2. The complexation reaction is solvent and temperature-dependent, and unidentified residues were obtained upon using different solvents or temperatures. The obtained data indicated the formation of six-coordinate monomeric complexes (bar $[Ni(M)]Cl_2.H_2O$ that gave a four-coordinate monomeric complex). A variety of physicochemical tools were used to characterize the isolated compounds (ligand and complexes). These include; ^1H, ^{13}C-NMR and mass spectroscopy (for ligand), micro-elemental studies and metal and chloride ratio (Table 1), FT-IR (Table 2) and UV-Vis spectroscopy (Table 3). The isolation of electrolyte complexes ($[Cr(M)(Cl)_2(H_2O)_2]Cl$ and $[Ni(M)]Cl_2.H_2O$) and nonelectrolyte complexes of the general formula $[M(M)(Cl)_2].H_2O$ (where M= $Fe^{(II)}$, $Co^{(II)}$ and $Cu^{(II)}$) was determined by measuring their conductance in DMSO solutions, Table 3.

FT-IR data of bisaldehyde

The FT-IR spectrum of M, Figure 3, indicated two bands at 1685 and 1666 cm^{-1}, which are due to the v(C=O) group, compared with that at 1695 cm^{-1} for the v(C=O) group of the salicylaldehyde. The appearance of two peaks indicates the two carbonyl groups are non-equivalent. The spectrum showed no peak around ca. 3200 and 600 cm^{-1} may be attributed to the v(OH) and v(C-Br) groups[11] indicating the involvement of the O-H and the C-Br in the formation of the ether group. This was confirmed by the appearance of a band at 1242.16 cm^{-1} assigned to v(C-O-C) stretching of the ether group[11,12].

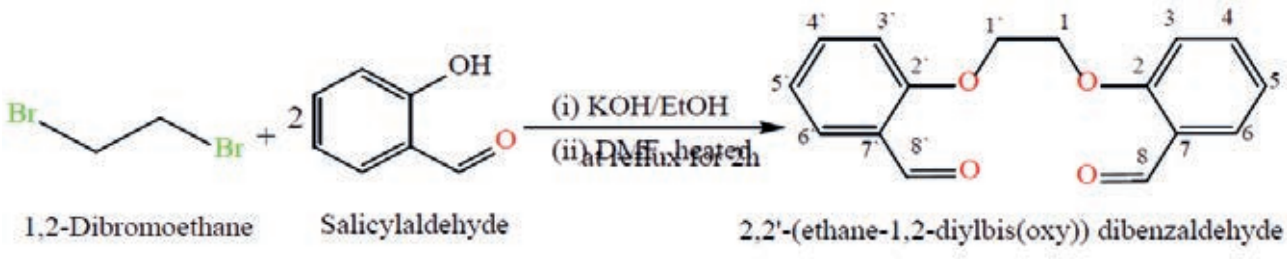

Figure 1. Preparation route and reaction conditions of the bisaldehyde ligand (M).

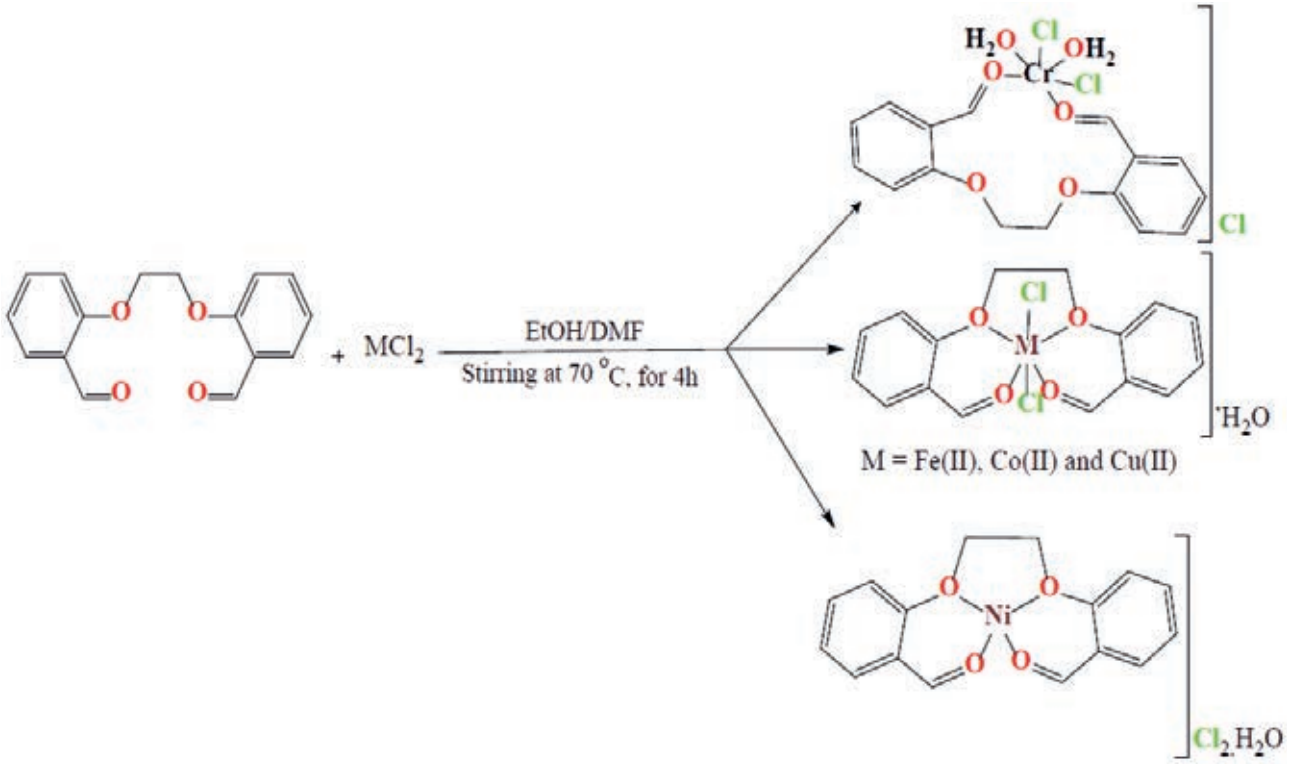

Figure 2. Synthesis route of monomeric complexes.

Complex	MW	Color	m.p °C	Y. %	Micro-analysis; (calculated) & found %found %			
					C	H	M	Cl
$Cr(M)(Cl)_2(H_2O)_2]Cl$	$C_{14}H_{20}Cl_2CrO_6$	Brown-red	250	76	(44.71) 44.77	(4.19) 4.23	(12.16) 12.11	(16.61) 16.52
$[Fe(M)(Cl)_2].H_2O$	$C_{14}H_{20}Cl_2FeO_6$	Brown	190	88	(48.37) 48.40	(3.51) 3.55	(14.11) 14.07	(18.02) 17.86
$[Co(M)(Cl)_2].H_2O$	$C_{14}H_{20}Cl_2CoO_6$	Deep blue	207	81	(47.98) 48.03	(3.47) 3.53	(14.77) 14.73	(17.16) 17.72
$[Ni(M)]Cl_2.H_2O$	$C_{14}H_{20}Cl_2NiO_6$	Deep green	203	85	(58.37) 58.42	(4.25) 4.29	17.88) 17.84	(79.77) 79.74
$[Cu(M)(Cl)_2].H_2O$	$C_{14}H_{20}Cl_2CuO_6$	Green	230	54	(47.45) 47.48	(3.44) 3.49	(15.76) 15.70	(17.58) 17.52

Table 1. The physical properties and elemental analyses of M and its complexes.

NMR and mass spectra of the bisaldehyde ligand

The ^{1}H- and ^{13}C-NMR of M were acquired in DMSO-d_6 on a Brucker-500 MHz machine. The assignment of peaks is based on the numbering fashion reported in Figure 1). The ^{1}H NMR spectrum of 2,2'-(ethane-1,2diylbis(oxy))dibenzaldehyde with an expansion of the aromatic region is shown in Figure 4. The spectrum showed several signals between 10.29-7.08 ppm in the aromatic region. The singlet peak at 10.29 ppm, equivalent to two protons, is related to (2H, s, $C_{8,8}$`-H). The multiple chemical shift at 7.68-7.65 ppm is equivalent to four protons attributed to (4H, m, $C_{6,6}$; $_{4,4}$`-H). A doublet peak at 7.34-7.32 ppm is equivalent to two protons attributed to (2H, d, $C_{3,3}$,-H J = 8.2 Hz). The triplet peak at 7.11-7.08 ppm that equivalent to two protons assigned to (2H, t, $C_{5,5}$`-H `, J = 7.45, 7.50 Hz). The chemical shift related to the ethylene group was detected as a singlet at 4.58 ppm (4H, s, $H_{1,1}$`). The spectrum recorded signals at ca. 2.50 and 3.33 ppm related to the DMSO-d6 and the traces of water in the NMR solvent, respectively. The ^{13}C NMR spectrum of M in the DMSO-d_6 solution is placed in Figure 5. The spectrum indicated the correct resonances for the compound. Resonance related to the carbonyl group assigned to $C_{8,8}$- appeared as a two signal at δ_c = 188.70 and 188.68 ppm. The appearance of two signals indicated that the two C=O groups are slightly inequivalent in solution. This follows the FT-IR data, Figure 3, in which the two carbonyl groups are also inequivalent in the solid state. Signal related to $C_{2,2}$` appeared at $\delta_c$ = 160.39 ppm. Resonances correlated to $C_{4,4}$`, $C_{6,6}$- $C_{5,5}$- $C_{7,7}$- and $C_{3,3}$- were observed at 135.94, 127.13, 124.11, 120.70 and 113.76 ppm, respec-

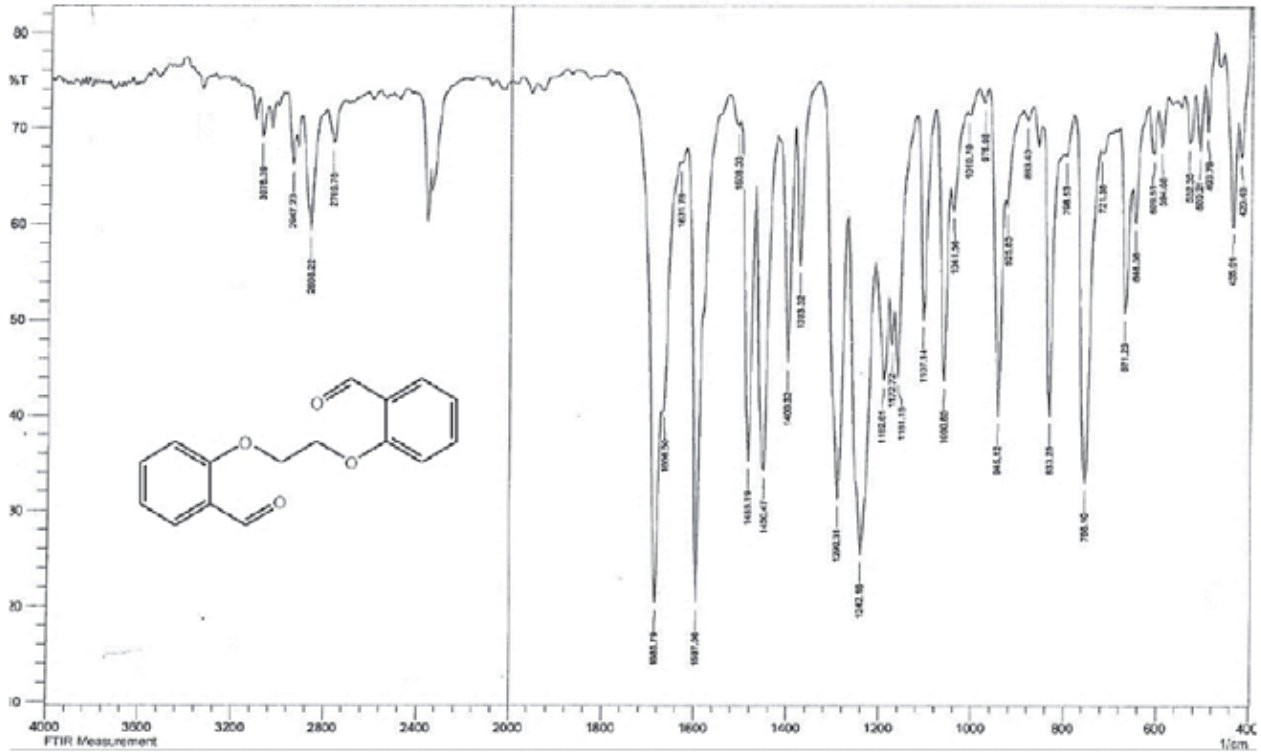

Figure 3. The FT-IR spectrum of the bisaldehyde ligand (M).

tively. The two methylene groups, O-$C_{1,1}$-, appeared to be equivalent and were detected at 67.00 ppm.

The electrospray (+) mass spectrum of M, Figure 6, reveals the parent ion peak at m/z=270.1 amu (18.22%). This peak is related to $(M)^+$, calculated at 270.09 amu for C16H14O4. Peaks detected at m/z = 240.2 (4.52%), 197.1 (7.56%), 149.2 (70.55%),121.2 (100.0%), 105.1 (16.20%), 77.2 (48.10%) and 65.2 (40.56%) related to $[M-(C_{15}H_{12}O_3)]+$, $[M-(C_{13}H_9O_2)]+$, $[M-(C_9H_9O_2)]+$, $[M-(C_7H_5O_2)]+$, $[M-(C_7H_5O)]+$, $[M-(C_6H_5)]+$ and $[M-(C_5H_5)]+$, respectively. The assignment of the successive fragmentation ions of the compound, along with their relative abundance, is shown in Figure 7.

FT- IR spectra of complexes

The FT-IR spectral data of the distinct bands for 1, 2, 3, 4, and 5 are placed in Table 2. The spectra of complexes were compared with the spectrum of the ligand (M) which indicated the involvement of the oxygen moieties, carbonyl oxygen-aldehydes and/or oxygen-ethers in coordination with the metal center. Bands related to the v(C=O) of the carbonyl have suffered a higher shift in complex 4 and appeared at 1687 and 1670 cm^{-1}, compared with that of M at 1685 and 1666 cm^{-1}. However, this band was shifted by 4-47 cm^{-1} to a lower frequency in complexes 1, 2, 3, 4 and 5 and appeared at 1680;1654, 1651;1612, 1685;1662, 1687;1670 and 1643 cm^{-1}, respectively. The shift of the carbonyl bands is related to the involvement of these moieties in the coordination with the metal center[12,13]. Further, the spectra showed the two coordinated carbonyl groups are non-equivalent (except that for the Cu(II)-complex). The v(C-O-C) ether of the M that was detected at 1242 cm^{-1} has shifted to a higher wavenumber by 4-54 cm^{-1} and appeared at 1253, 1253 and 1249 cm^{-1} in complexes 2, 4 and 5, respectively[11,14]. However, in complex 3, the ether band was moved to a lower wavenumber and appeared at 1238 cm^{-1}. More, in complex 1 there was no change in the frequency of the v(C-O-C) ether group, which confirms the chromium(III) ion was not bound to oxygen ether. The shifting of the oxygen ether segment may contribute to the oxygen atoms' involvement in the coordination with the metal center[11,14]. The spectra of metal complexes revealed additional bands between 600-200 cm^{-1} that were not presented in the M spectrum. Bands that are related to v(M-O) carbonyl were detected at 532, 520, 509, 532 and 509 cm^{-1} for v(Cr-O), v(Fe-O), v(Co-O), v(Ni-O) and v(Cu-O), respectively 15,19,20. The v(M-O) for the oxygen ether bands related to v(Fe-O), v(Co-O), v(Ni-O) and v(Cu-O) were detected at 574, 532, 582 and 578 cm^{-1}, respectively[11,15]. The FT-IR spectra revealed bands that belong to v(Cr-Cl), v(Fe-Cl), v(Co-Cl) and v(Cu-Cl) at 243;252, 241;248, 262;283 and 235;246 cm^{-1}, respectively[16]. Finally, peaks were detected at 3321, 3491, 3444, 3329 and 3471 cm^{-1} in the complexes of $Cr^{(III)}$, $Fe^{(II)}$, $Co^{(II)}$, $Ni^{(II)}$ and $Cu^{(II)}$, respectively, were correlated to aqua water molecules. In complex 1, a band that was detected at 756 cm^{-1} is related to v(Cr-O)[17].

Electronic spectra and magnetic moment measurements

The electronic absorption spectra of M, Figure 8, and its complexes were determined in DMSO solutions (con. = 1 x 10^{-3} M). The UV-Vis spectra of $Cr^{(III)}$, $Fe^{(II)}$, $Co^{(II)}$, $Ni^{(II)}$ and $Cu^{(II)}$ complexes indicated peaks around 263-265 nm related to $\pi\rightarrow\pi^*$ and $n\rightarrow\pi^*$ (ligand field transitions), Table 3. The spectra of 1, 2, 3, 4 and 5 showed an extra peak of about ca.315 nm assigned to charge transfer (CT) 16-18. In the d-d region of the Cr(III) complex (Figure 9), bands at 435 and 633 nm correlated to $^4A_2g(F)\rightarrow{}^4T_1g$ and $^4A_2g(F)\rightarrow{}^4T_2g(F)$, respectively indicating a distorted octahedral geometry about the metal center[19]. The $Fe^{(II)}$ complex revealed peaks, at 833, 889 and 977 nm correlated to $^5T_2g\rightarrow{}^2Eg$, indicating an octahedral shape around the core atom[20]. Peaks at 615 and 677 nm in the spectrum of $Co^{(II)}$ are referred to $^4T_1g(F)\rightarrow{}^4A_2g(F)$ and $^4T_1g(F)\rightarrow{}^4A_2g(F)$, respectively confirming a distorted octahedral geometry around the metal center[21,22]. In the $Ni^{(II)}$complex (Figure 10), peaks at 619, 652

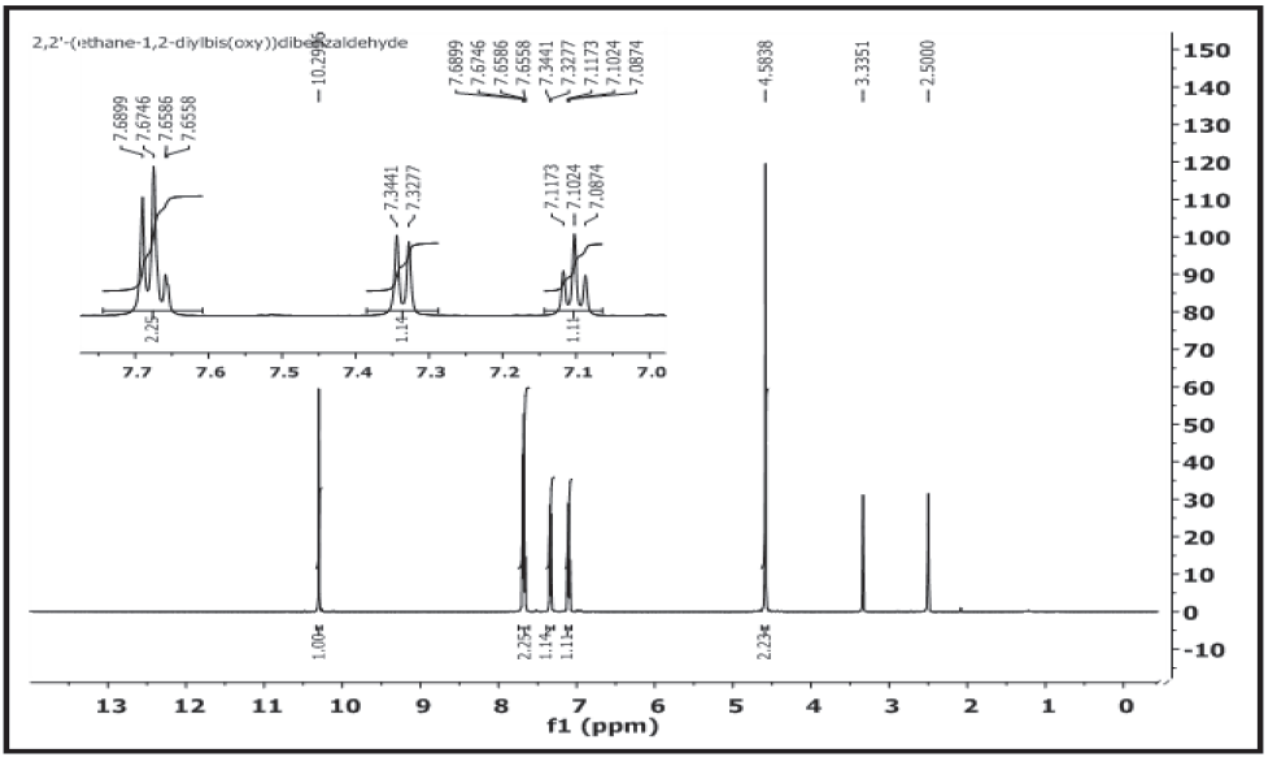

Figure 4. ^{1}H-NMR spectrum of M in DMSO-d_6.

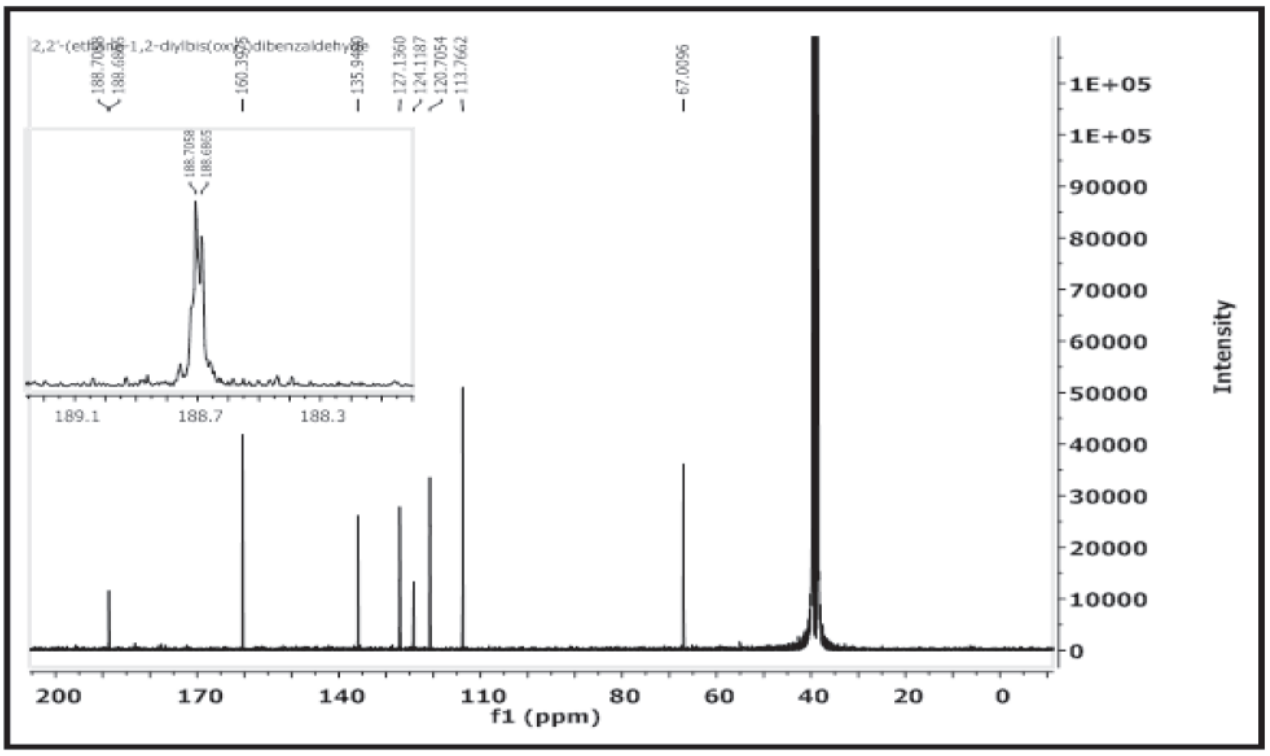

Figure 5. ^{13}C-NMR spectrum of M in DMSO-d_6 solution.

and 692 nm attributed to $^{3}T_{1}(F) \rightarrow {}^{3}A_{2}(F)$, $^{3}T_{1}(F) \rightarrow {}^{3}A_{2}(F)$ and $^{3}T_{1}(F) \rightarrow {}^{3}T_{1}(P)$ that supported a distorted tetrahedral geometry around the metal center[23]. The broad peak at 645 nm in the spectrum of $Cu^{(II)}$ is referred to $^{2}B_{1}g \rightarrow {}^{2}B_{2}g$ confirming a distorted octahedral geometry around the metal center[24]. The magnetic value is an essential factor for the characterisation of complexes, as it may be linked to the shape adopted by ligands around the metal center. For $Cr^{(III)}$, $Fe^{(II)}$, $Co^{(II)}$, $Ni^{(II)}$ and $Cu^{(II)}$ complexes, the obtained magnetic moment was determined to be 3.74, 4.22, 4.35, 4.55 and 2.16 BM, respectively. These values matched the total of the spin's moment, indicating a weak field with sp^3d^2 and sp^3 hybridization of complexes. Therefore, $Cr^{(III)}$, $Fe^{(II)}$, $Co^{(II)}$ and $Cu^{(II)}$ complexes adopted a distorted octahedral geometry. However, the $Ni^{(II)}$ complex adopts a tetrahedral[24].

Biological activity

The prepared ligand and its metal complexes with $Cr^{(III)}$,

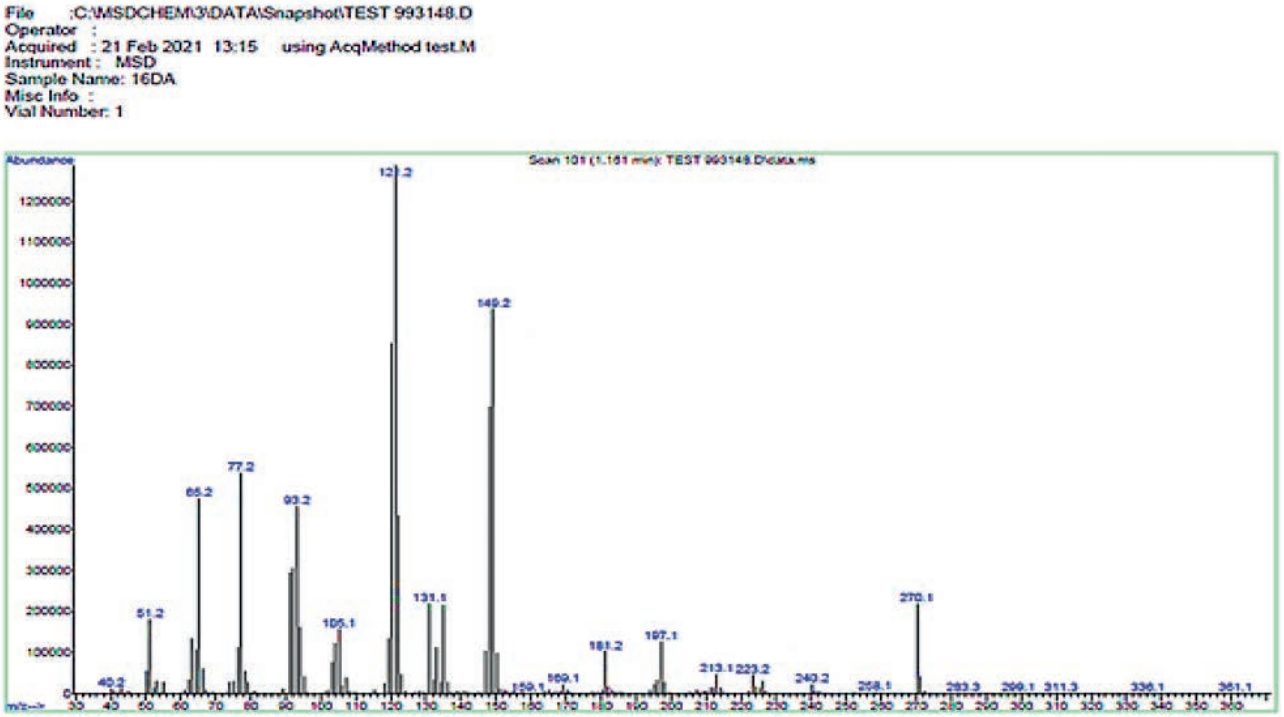

Figure 6. The electrospray (+) mass spectrum of M.

Fe(II), Co(II), Ni(II) and Cu(II) ions were tested against two microbial strains; G-positive (*Staphylococcus aureus, Bacillus subtilis*), as well as G-negative (*Escherichia coli, Pseudomonas auroginosa*). The examined bacteria in this study infect humans' urinary and respiratory tracts, and they are among the most dangerous and lethal pathogens discovered in surgical operating rooms. Further, two types of fungus that affect humans were investigated (*Candida albicans* and *Rhizopus sporium*)[8,17]. The collected data is presented in Figure 11 and Table 4. According to the obtained results, the title compounds exhibit varied antibacterial action against microorganisms. The zone of inhibition ability of compounds was compared with Cefotaxime (100 µg/mL) used as an antibacterial standard. The following essential points are drawn from the gathered data that is given in the Tables:

1- All complexes showed activity against positive and negative bacteria.

2- Experimental data indicated the complexes became more active compared with M. Further, the prepared compounds indicated higher activity compared with cefotaxime.

3- Based on the experimental information, iron and cobalt complexes show higher microbiological activity against strains of (*Escherichia coli*) bacterial, whereas the nickel complex is less effective against (*Escherichia coli*). This may attribute to the influence of the cationic nature and the tetrahedral geometry of the nickel complex, compared with the neutral six-coordinate ion and cobalt complexes.

The antifungal activity of M and its metal complexes were tested against two types of fungi. The role of DMSO in the biological screening was concluded separately using the solutions of DMSO alone, which showed no activity towards fungal species[8,17]. Fungi activity data against tested compounds are shown in Figure 12 and Table 4 and placed in. The following conclusions have been pointed out;

1- The M and its complexes generally showed good results against the rhizopus sporium, compared with fungi *Candida albicans*.

2- The Cr(III), Co(II) and Ni(II) -complex indicated the highest inhibition activity against *Rhizopus sporium*.

3- 3- Complexes of Cr(III) and Cu(II)) showed the lowest anti-fungal activity against *Candida albicans*.

Conclusions

The synthesis and characterization of a bisaldehyde ligand (M) and its new metal complexes are reported. The tetradentate ligand, which consists of two carbonyl-oxygen and two ether-oxygen donor atoms, was prepared in a two-step. The reaction of the ligand with Cr(III), Fe(II), Co(II), Ni(II) and Cu(II) metal ions in a 1:1 (L:M) mole ratio resulted in the isolation of monomeric complexes. The chemical structure of compounds and the overall bonding behavior of the complexes was confirmed through physicochemical techniques. The characterization data confirmed the isolation of six-coordinate monomeric complexes of the general formula; $[Cr(M)(Cl)_2(H_2O)_2]Cl$, $[M(M)(Cl)_2].H_2O$ (where M= Fe(II), Co(II) and Cu(II)) and four-coordinate complex of the general formula $[Ni(M)]Cl_2.H_2O$. The biological activity of the ligand and its complexes against bacterial species and fungi pathogens were also tested. Generally, the bisaldehyd complexes showed more activity compared with the free ligand

Author Contributions

Duaa S. Abaas: Performed All Experiments, Data Curation, and manuscript Writing. Mohamad J. Al-Jeboori: Supervision, Methodology, Project Administration, Conceived the Experimental Plan, Analysed the Data, Writing- Original draft, Writing- Reviewing and Editing.

Acknowledgments

The authors are grateful to the University of Baghdad, College of Education for Pure Science (Ibn Al-Haitham) and Department of Chemistry for providing Ms DSA with the MSc studentship and labs facilities.

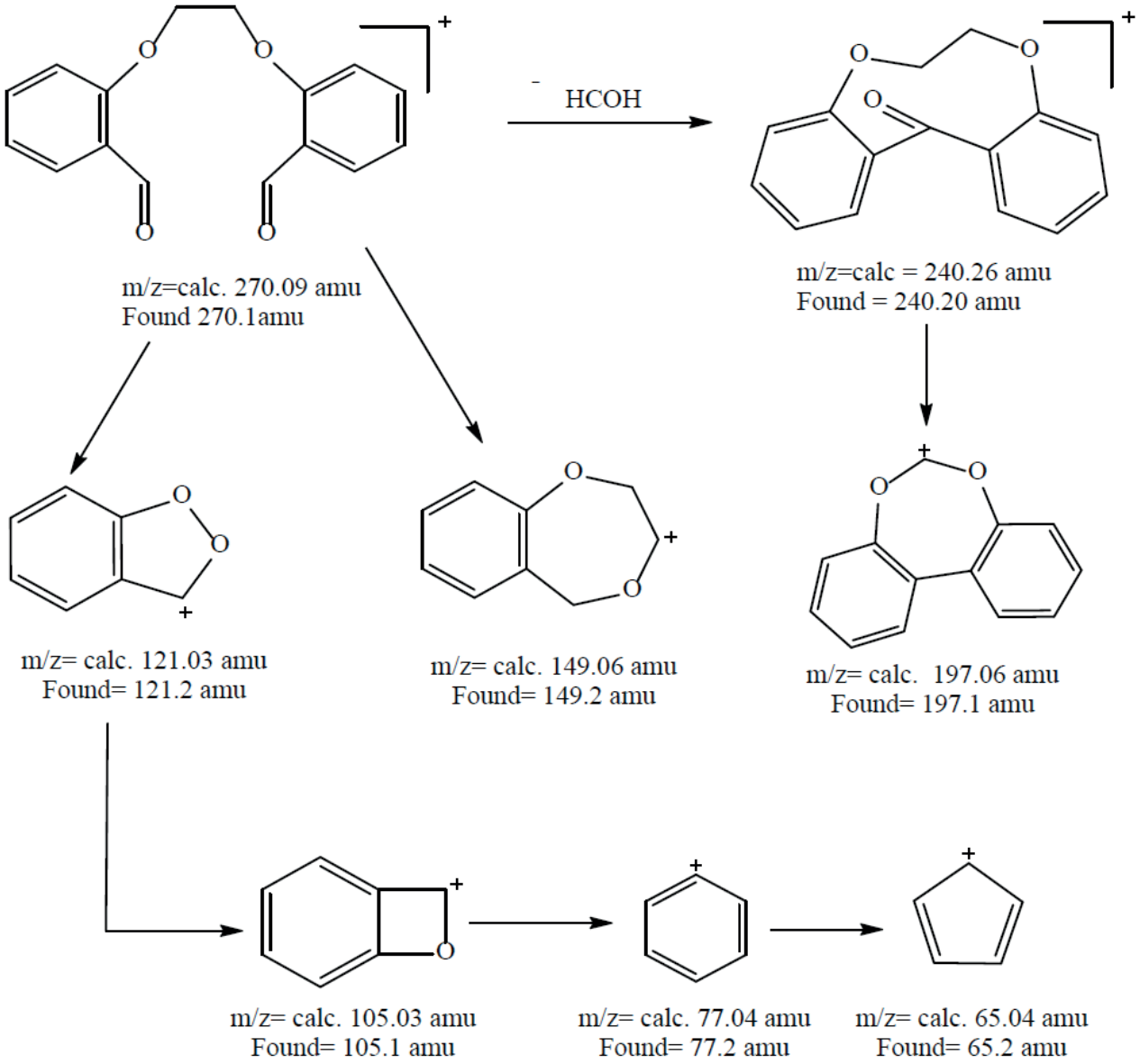

Figure 7. The fragmentation pattern and relative abundance of M.

Complex	$\nu(C=O)_{ald}$	$\nu(C-O-C)$	$\nu(C=C)_{aro}$	$\nu(M-O)$	$\nu(M-O)_{eth}$	$\nu(M-OH_2)$	$\nu(M-Cl)$
M	1685 1666	1242	1597				
$[Cr(M)(Cl)_2(H_2O)_2]Cl$	1680 1654	--	1597	----	532	3321 756	243;252
$[Fe(M)(Cl)_2].H_2O$	1651 1612	1253	1496	574	520	3491	241;248
$[Co(M)(Cl)_2].H_2O$	1685 1662	1238	1597	532	509	3444	262;283
$[Ni(M)]Cl_2.H_2O$	1687 1670	1253	1597	582	532	3329	---
$[Cu(M)(Cl)_2].H_2O$	1732 1643	1249	1558	578	509	3471	235;246

ald=aldehyde, aro=aromatic

Table 2. The Infrared spectrum of the complexes prepared from (M).

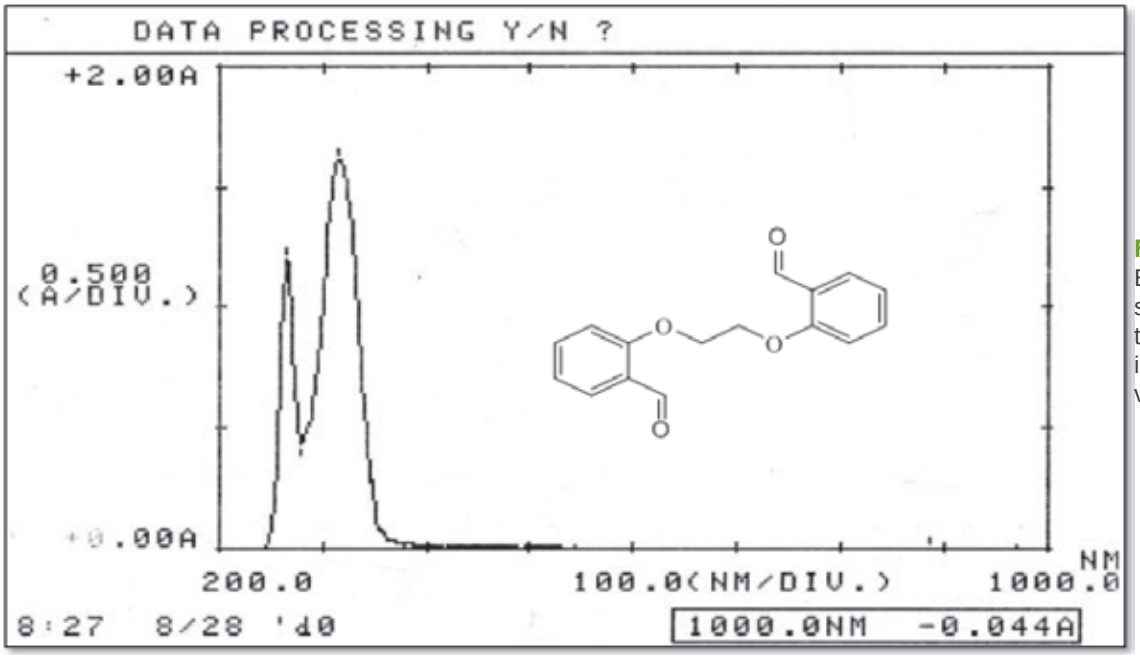

Figure 8. Electronic spectrum of the ligand (M) in DMSO solvent.

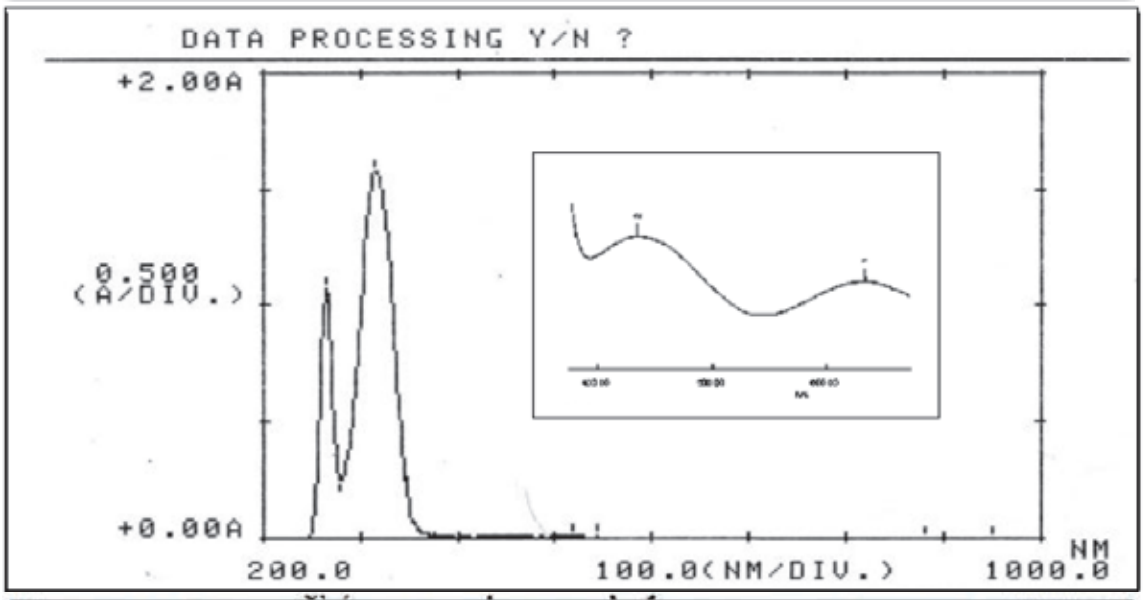

Figure 9. Electronic spectrum of $[Cr(M)(Cl)_2(H_2O)_2]Cl$ in DMSO solvent.

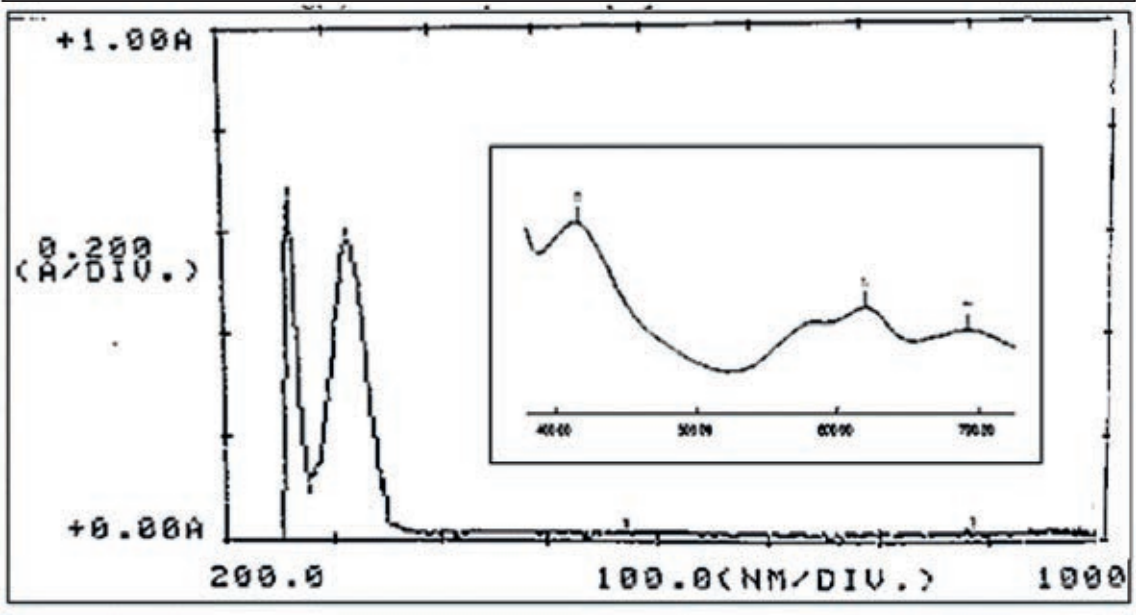

Figure 10. Electronic spectrum of $[Ni(M)]Cl_2.H_2O$ in DMSO solvent.

Comp.	λnm	ῡ(cm^{-1})	ε max (dm^3. mol^{-1}.cm^{-1})	Assignment	Λ_m S.cm^2.mole^{-1}
[Cr(M)(Cl)$_2$(H$_2$O)$_2$]Cl	265	37735	1071	L.F	36.00
	315	31746	1576	C.T	
	435	22988	135	$^4A_2g^{(F)} \rightarrow {}^4T_1g^{(F)}$	
	633	15797	89	$^4A_2g^{(F)} \rightarrow {}^4T_2g^{(F)}$	
[Fe(M)(Cl)$_2$].H$_2$O	250	31446	1059	LF	9.04
	318	40000	1345	CT	
	698	14326	18	$^5T_2g \rightarrow {}^2Eg$	
	993	10070	13	$^5A_2g \rightarrow T_2g$	
[Co(M)(Cl)$_2$].H$_2$O	265	37735	1110	LF	11.0
	316	31645	1453	CT	
	615	16260	101	$^4T_1g^{(F)} \rightarrow {}^4A_2g^{(F)}$	
	677	14771	161	$^4T_1g^{(F)} \rightarrow {}^4A_2g^{(F)}$	
[Ni(M)]Cl$_2$.H$_2$O	263	38022	661	LF	55.00
	318	31446	583	CT	
	415	24096	157	CT	
	619	16155	87	$^3T_1{}^{(F)} \rightarrow {}^3A_2{}^{(F)}$	
	652	15325	59	$^3T_1{}^{(F)} \rightarrow {}^3A_2{}^{(F)}$	
	692	14450	68	$^3T_1{}^{(F)} \rightarrow {}^3T_1{}^{(P)}$	
[Cu(M)(Cl)$_2$].H$_2$O	265	37735	1172	LF	15.65
	314	31847	1497	CT	
	645	15503	19	$^2B_1g \rightarrow {}^2B_2g$	

*L.F=ligand field, C.F=charge transfer

Table 3. Electronic spectral data and molar conductance for M complexes.

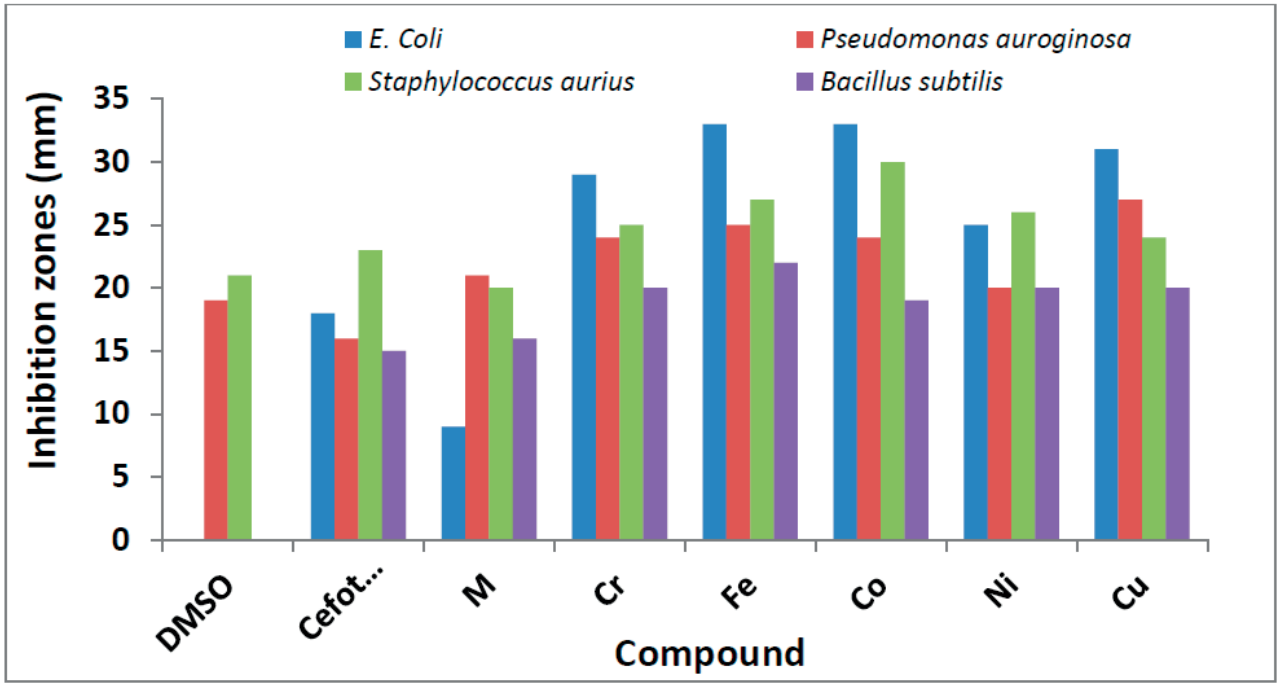

Figure 11. The inhibition zone diameter (mm) against bacterial species for M ligand and its complexes.

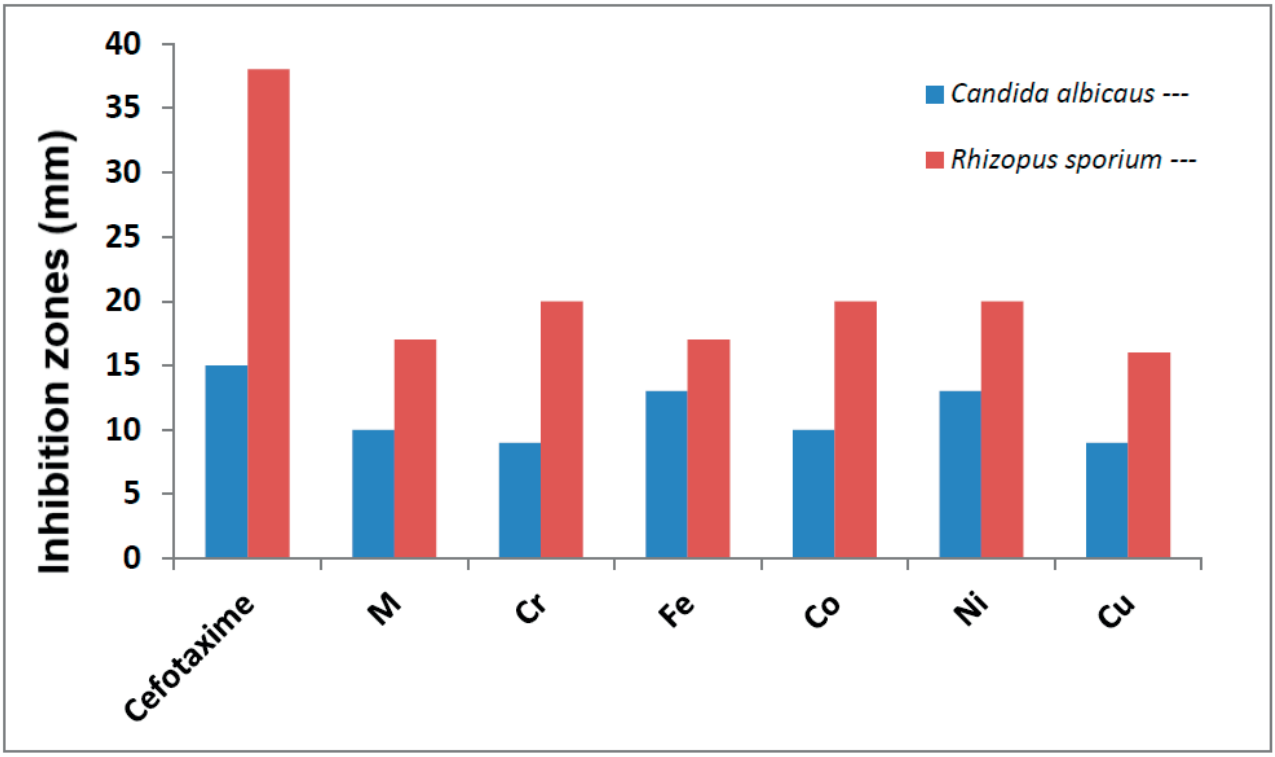

Figure 12. The inhibition zone diameter (mm) against fungi for M ligand and its complexes.

Compound	Bacteria				Fungi	
	Gram-negative		Gram-positive			
	E. Coli	*Pseudomonas auroginosa*	*Staphylococcus aurius*	*Bacillus subtilis*	*Candida albicans*	*Rhizopus sporium*
DMSO	---	19	21	---	---	---
Cefotaxime	18	16	23	15	-	-
M	9	21	20	16	10	17
$[Cr(M)(Cl)_2(H_2O)_2]Cl$	29	24	25	20	9	20
$[Fe(M)(Cl)_2].H_2O$	33	25	27	22	13	17
$[Co(M)(Cl)_2].H_2O$	33	24	30	19	10	20
$[Ni(M)]Cl_2.H_2O$	25	20	26	20	13	20
$[Cu(M)(Cl)_2].H_2O$	31	27	24	20	9	16

Table 4. Electronic spectral data and molar conductance for M complexes.

Conflicts of Interest

The authors declare there are no conflicts of interest.

Bibliographic references

1. Holland, J. P.; Hickin, J. A.; Grenville-Mathers, E.; Nguyen, T.; Peach, J. M. Rapid decomplexation of bis (thiosemicarbazonato) zinc (ll) complexes using citric acid. Journal of Chemical Research, 2008, 12, 702-703.
2. Genta, M. T.; Villa, C.; Mariani, E.; Loupy, A.; Petit, A.; Rizzetto, R.; Morini, F.; Ferro, M. Microwave-assisted preparation of cyclic ketals from a cineole ketone as potential cosmetic ingredients: solvent-free synthesis, odour evaluation, in vitro cytotoxicity and antimicrobial assays. International Journal of Pharmaceutics, 2002, 231(1), 11-20.
3. Mounika, K.; Pragathi, A.; Gyanakumari, C. Synthesis characterization and biological activity of a Schiff base derived from 3-ethoxy salicylaldehyde and 2-amino benzoic acid and its transition metal complexes. Journal of Scientific Research, 2010, 2(3), 513-523.

4. Freeman, A.; Woodley, J. M.; Lilly, M. D. In situ product removal as a tool for bioprocessing. Bio/technology, 1993, 11(9), 1007-1012.
5. Ali, S. M. H.; Yan, Y. K.; Lee, P. P.; Khong, K. Z. X.; Sk, M. A.; Lim, K. H.; Klejevskaja, B.; Vilar, R. Copper (II) complexes of substituted salicylaldehyde dibenzylsemicarbazones: synthesis, cytotoxicity and interaction with quadruplex DNA. Dalton Transactions, 2014, 43(3), 1449-1459.
6. Hasan, S.; Salleh, S.; Hamdan, S.; Yamin, B. Unsaturated 15 and 16 Membered Appended Naphthalene Macrocyclic Molecules for The Development of Fluorometric Chemosensors. Conference Series: Materials Science and Engineering, 2017, 172, 1-11.
7. Hussain, S. A.; Al-Jeboori, M. J. New metal complexes derived from Mannich-base ligand; Synthesis, spectral characterisation and biological activity. Journal of Global Pharma Technology, 2019, 11(2), 548–560.
8. Al-Qazzaz, A. H.; and Al-Jeboori, M. J. New metal complexes derived from Mannich ligands; synthesis, spectral investigation and biological. Biochemical and Cellular Archives, 2020, 02(20), 4207-4216.
9. Akkurt, M.; Mohamed, S. K.; Horton, P. N.; Abdel-Raheem, E. M.; Albayati, M. R. 2, 2′-[Ethane-1,2-diylbis(oxy)]dibenzaldehyde. Acta Crystallographica Section E, 2013, 69(8), o1260-o1260.
10. Ali, A.; Merza, J. Synthesis and Characterization of Novel Dialdehydes based on SN2 Reaction of Aromatic Aldehyde. Inorg Chem Ind J.,2017, 2(1), 111-119.
11. Ilhan, S.; Temel, H. Synthesis and spectral studies of macrocyclic Cu (II), Ni (II) and Co (II) complexes by template reaction of 1,4-bis (3-aminopropoxy) butane with metal (II) nitrate and salicylaldehyde derivatives. Journal of Molecular Structure, 2008, 891(1-3), 157-166.
12. Nair, M. S.; Arish, D.; Johnson, J. Synthesis, characterization and biological studies on some metal complexes with Schiff base ligand containing pyrazolone moiety. Journal of Saudi Chemical Society, 2016, 20, S591-S598.
13. Al-Jeboori, M. J.; Abdul-Ghani, A. J.; Al-Karawi, A. J. Synthesis and structural studies of new Mannich base ligands and their metal complexes. Transition Metal Chemistry, 2008, 33(7), 925-930.
14. Zayed, E. M.; Zayed, M. A.; Fahim, A. M.; El□Samahy, F. A. Synthesis of novel macrocyclic Schiff's□base and its complexes having N2O2 group of donor atoms. Characterization and anticancer screening are studied. Applied Organometallic Chemistry, 2017, 31(9), 1-7.
15. Abdul-Ghani, A. J.; Al-Jeboori, M. J.; Al-Karawi, A. J. Synthesis and characterisation of new N2S2 and N2O2 Mannich base ligands derived from phosphinic acid and their metal complexes. Journal of Coordination Chemistry, 2009, 62(6), 2736-2744.
16. Al-Rubaye, B. K.; Brink, A.; Miller, G. J.; Potgieter, H.; Al-Jeboori, M. J. Crystal structure of (E)-4-benzylidene-6-phenyl-1,2,3,4,7,8,9,10-octahydrophenanthridine. Acta Crystallographica Section E: Crystallographic Communications, 2017, 73(7), 1092-1096.
17. Muat, T, H.; Al-Jeboori, M. J. Phenoxo- and azido-bridged complexes with N2OS2 Schiff-base ligand; synthesis, spectral investigation and bacterial activity, ChemXpress. 2016, 9(2), 156-171.
18. Yousif, E. I.; Ahmed, R. M.; Hasan, A. H.; Al-Fahdawi, A. S.; Al-Jeboori, M. J. Metal Complexes of Heterocyclic Hydrazone Schiff-bases; Preparation, Spectral Characterisation and Biological Study, Iranian Journal for Science and Technology, Trans. A, 2017, 41, 103–109.
19. Ye, Y.; Jiang, Z.; Xu, Z., Zhang.; X., Wang, D.; Lv, L.; Pan, B. Efficient removal of Cr (III)-organic complexes from water using UV/Fe (III) system: negligible Cr (VI) accumulation and mechanism. Water Research, 2017, 126, 172-178.
20. Lever, A. Electronic spectra of dn ions. Inorganic Electronic Spectroscopy. 2nd Edt., Elsevier, Amsterdam, 1984; pp. 376-611.
21. Munde, A. S.; Jagdale, A. N.; Jadhav, S. M.; Chondhekar, T. K. Synthesis, characterization and thermal study of some transition metal complexes of an asymmetrical tetradentate Schiff base ligand. Journal of the Serbian Chemical Society, 2010, 75(3), 349-359.
22. Al-Shaalan, N. H. Synthesis, characterization and biological activities of Cu (II), Co (II), Mn (II), Fe (II), and UO2 (VI) complexes with a new Schiff base hydrazone: O-Hydroxyacetophenone-7-chloro-4-quinoline hydrazone. Molecules, 2011, 16(10), 8629-8645.
23. Al-Jeboori, M. J.; Al-Jebouri,. F. A.; Al-Azzawi, M. A. Metal complexes of a new class of polydentate Mannich bases; synthesis and spectroscopic Characterisation, Inorganica Chimica Acta, 2011, 379, 163–170.
24. Ahmed, R. M.; Yousif, E. I.; Al-Jeboori, M. J. Co(II) and Cd(II) complexes derived from heterocyclic Schiff-bases: synthesis, structural characterisation, and biological activity. The Scientific World Journal, 2013, 2013, 1-6.

REVIEW / ARTÍCULO DE REVISIÓN

Aplicación de un abono foliar líquido en el cultivo de cacao nacional fino de aroma en Morona Santiago, Ecuador

Changes in phytic acid concentration, free phosphorus and soluble iron during fermentation of white cabbage and Chinese cabbage

Marcos Vera-Morales[1]*, Daynet Sosa[1,2], Carlos Arias-Vega[1], Fernando Espinoza-Lozano[1], Simón Pérez- Martínez[3], María F. Ratti[1,2]

DOI. 10.21931/RB/2023.08.02.19

[1] Escuela Superior Politécnica del Litoral, ESPOL, Centro de Investigaciones Biotecnológicas del Ecuador, Guayaquil, Ecuador.
[2] Escuela Superior Politécnica del Litoral, ESPOL, Facultad de Ciencias de la Vida, Guayaquil, Ecuador.
[3] Universidad Estatal de Milagro (UNEMI), Facultad de Ciencias e Ingeniería, Guayas, Ecuador.
Corresponding author: mxvera@espol.edu.ec

Resumen: La descomposición anaeróbica del estiércol de ganado podría generar subproductos que sean empleados en la agricultura como abonos orgánicos. Por lo que la fertilización de la superficie foliar producido a partir de nutrientes orgánicos y microorganismos constituye una fuente en la nutrición y producción de los cultivos. El objetivo de este estudio fue evaluar el efecto de un abono liquido procedente de la descomposición anaeróbica de estiércol de ganado sobre la superficie foliar del cultivo *in situ* del cacao nacional fino de aroma (*Theobroma cacao*) en Morona Santiago, Ecuador. Con este propósito, se tomaron muestras de hojas antes y después de la aplicación del abono foliar. Además, se realizó un experimento completo de bloques al azar con cinco tratamientos. Los tratamientos fueron: T1 y T3 con aplicaciones del abono foliar cada 30 días y concentraciones de 50 y 100% respectivamente, T2 y T4 con aplicaciones cada 60 días y concentraciones de 50 y 100% respectivamente y T5 con manejo convencional (Control). Los resultaron mostraron evidencias estadísticamente significativas antes y después de la aplicación del abono liquido orgánico en el aumento de los macronutrientes de fosforo y potasio, así como al micronutriente de cobre. Por otro lado, la aplicación del abono foliar evidencio efectos positivos en el control *in situ* de *Moniliophthora roreri* y *M. perniciosa* con el tratamiento de 30 días diluido al 50%. Se sugiere que la aplicación del abono foliar procedente de la descomposición de estiércol puede contribuir a aumentar los macro y micronutrientes de las hojas del cultivo de cacao, así como también su potencial efecto en el biocontrol de patógenos fúngicos que afectan al cultivo de cacao nacional fino de aroma.

Palabras clave: Abono líquido, Biocontrol, Cacao nacional, Microorganismos, Nutrientes.

Abstract: The anaerobic decomposition of livestock manure could generate useful agricultural subproducts as organic fertilizers. Thus, fertilization of leaf surface produced from organic nutrients and microorganisms constitutes a source for the nutrition and production of crops. This study aimed to evaluate the effect of a liquid amendment made from the anaerobic decomposition of cow manure on the foliar surface of *in situ* fine aroma cacao (*Theobroma cacao*) in Morona Santiago, Ecuador. For this purpose, we took leaf samples before and after applying the foliar amendment. Furthermore, we performed a complete randomized block experiment with five treatments. Treatments were as follows: T1 and T3 with applications of liquid amendment every 30 days and concentrations of 50 and 100%, respectively; T2 and T4 with applications every 60 days and concentrations of 50 and 100%, respectively and T5 with conventional management (Control). Results showed statistically significant differences before and after applying the liquid organic amendment on the increase of macronutrient phosphorus, potassium, and the micronutrient copper. In addition, the application of foliar fertilizer, evidenced positive effects on the *in situ* control of *Moniliophthora roreri* and *M. perniciosa* with the treatment of 30 days and a 50% concentration. We suggest that applying foliar amendment from cow manure decomposition contributes to the increase of macro and micronutrients of the leaves in cacao crops, also as a potential biocontrol for fungal pathogens that affect fine aroma national cacao.

Key words: Liquid fertilizer, Biocontrol, National cocoa, Microorganisms, Nutrients.

Introducción

El aumento de la población mundial y las demandas que trae consigo, han puesto en riesgo la producción de alimentos y la seguridad alimentaria, de ahí que las prácticas agrícolas sean cada vez más intensivas[1], lo que resulta en un impacto negativo en el funcionamiento de los ecosistemas[2].

La intensificación de los cultivos agrícolas, hace uso de enormes cantidades de fertilizantes químicos que influyen directamente en el equilibrio de las interacciones bióticas y abióticas, lo que altera la biodiversidad y el funcionamiento natural de los sistemas[3]. Por lo tanto, el desarrollo de nue-

Citation: Vera-Morales M, Sosa D, Arias-Vega C, Espinoza-Lozano F, Pérez- Martínez S, Ratti M F. Aplicación de un abono foliar líquido en el cultivo de cacao nacional fino de aroma en Morona Santiago, Ecuador. Revis Bionatura 2023;8 (2) 19. http://dx.doi.org/10.21931/RB/2023.08.02.19
Received: 2 January 2023 / **Accepted:** 19 April 2023 / **Published:** 15 June 2023
Publisher's Note: Bionatura stays neutral with regard to jurisdictional claims in published maps and institutional affiliations.

vos fertilizantes, formulaciones y tecnologías inocuas con el entorno y la salud humana se constituyen en un desafío que van de la mano con la capacitación a productores para el correcto uso y aplicación, cuestiones que interesan a los agricultores e investigadores[4].

Los nutrientes son importantes para el desarrollo de las plantas y las interacciones con fitopatógenos. Cada nutriente juega un papel fundamental en las funciones fisiológicas de las plantas[5]. A pesar de que la adsorción de nutrientes se realiza principalmente por las raíces, estos nutrientes también pueden ser asimilados por las hojas[6,7]; describiéndose los beneficios asociados como resistencia a las enfermedades, tolerancia al estrés y mayor productividad[8].

El abono orgánico liquido procedente de la descomposición anaeróbica de ganado es un subproducto rico en materia orgánica y nutrientes que pueden ser empleado como fertilizantes para la agricultura[9]. El abono orgánico liquido en sistemas agrícolas puede minimizar el uso de fertilizantes minerales[10] con efectos significativos en aplicaciones al suelo y el follaje[11]. La aplicación foliar del abono liquido se ha empleado para corregir deficiencias de micronutrientes que influyen en la producción[12].

Ante este escenario, es necesario investigar alternativas ecológicas que pueden potenciar la producción de cultivos, especialmente los que son de importancia en la economía de los países en vías de desarrollo[13]. Por ejemplo, *Theobroma cacao L.*, es un cultivo que se demanda a nivel mundial y el Ecuador, es el segundo país de mayor producción en América después de Brasil[14]. Por lo tanto, el uso de grandes aplicaciones de fertilizantes químicos aumenta los costos de producción y altera el equilibrio del entorno. Por lo que el objetivo de este estudio fue evaluar el efecto de un abono líquido sobre la superficie foliar del cultivo in situ del cacao nacional fino de aroma (*Theobroma cacao*) en Morona Santiago, Ecuador.

Materiales y métodos

Lugar de estudio

La presente investigación se llevó a cabo en tres localidades del cantón Taisha en la provincia de Morona Santiago, Ecuador; dos localidades en la parroquia Tuuitinentsa (Pampants 2°24′8″S 77°32′35″O y Dos Ríos 2°23′1″S 77°30′23″O) y una en la parroquia Macuma (Amazonas 2°20′50″S 78°20′3″O). El estudio se llevó entre los meses de febrero a diciembre del 2017 en parcelas demostrativas de las tres localidades; mismas que contenían cultivos establecidos de cacao nacional fino de aroma de aproximadamente 5 años. Las características y las condiciones de manejo de las tres fincas se describen en la tabla 1.

Condiciones climáticas

La precipitación total anual en el año 2017 fue de 2423,4 mm, mientras que la precipitación total promedio durante el desarrollo del muestreo en campo (febrero-diciembre) fue de 205,6 mm. La temperatura media en el período de febrero a diciembre fue de 22,1°C (Figura 1). Los datos fueron proporcionados por la estación científica del Instituto Nacional de Meteorología e Hidrología del Ecuador (INAMHI).

Materiales, diseño experimental y evaluación de variables agronómicas

El abono foliar liquido se elaboró en dos fases. La primera una solución madre donde se capturaron microorganismos de suelos aledaños a las parcelas demostrativas. Los microorganismos se capturaron en tarrinas con 250g de arroz precocido y 50 mL de melaza para cubrir el arroz. Las tarrinas con los materiales se colocaron en el suelo a una profundidad de 20 cm cubiertas con tela de toldo. Lue-

Características	Pampants	Dos Ríos	Amazonas
Área del cultivo de cacao	50.0	48.0	50.0
Edad del cultivo	5 años	5 años	5 años
Altura	2 -3 m	2 -3 m	2 -3 m
Distancia de siembra	2 x 2 m^2	2 x 2 m^2	2 x 2 m^2
Material genético	Cacao nacional	Cacao nacional	Cacao nacional
Tipo de sombra	Sin sombra	Sin sombra	Sin sombra
Densidad de siembra	2500 plantas/Ha	2500 plantas/Ha	2500 plantas/Ha
Tipo de poda	Poda de formación	Poda de formación	Poda de formación
Frecuencia de poda	Anual	Anual	Anual
Control de malezas	Manual	Manual	Manual
Otras practicas	Poda fitosanitaria	Poda fitosanitaria	Poda fitosanitaria

Tabla 1. Condiciones de manejo de las plantaciones de cacao en las tres fincas evaluadas.

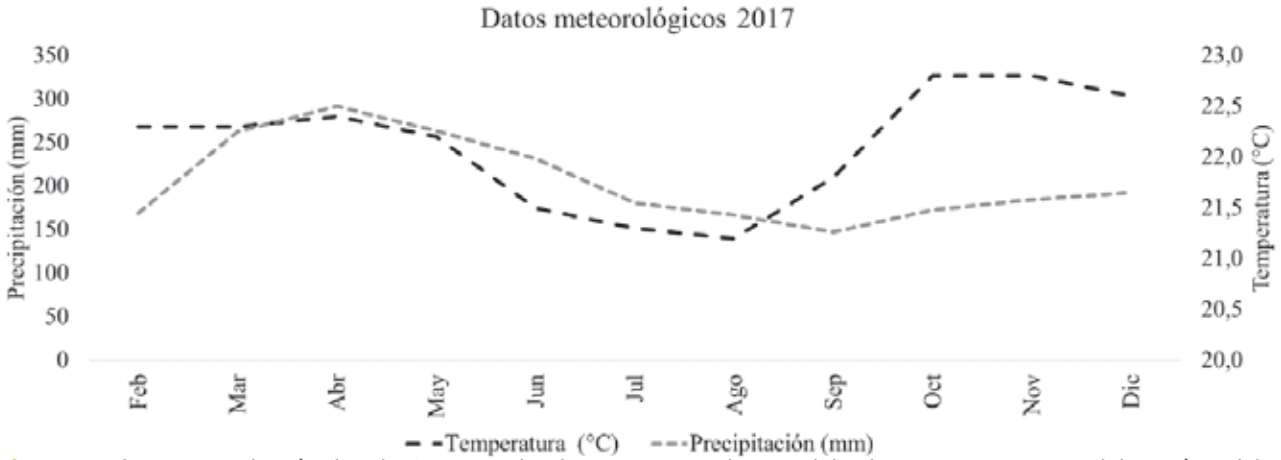

Figura 1. Diagrama ombrotérmico de Gaussen donde se muestran las precipitaciones y temperatura del cantón Taisha en la provincia de Morona Santiago, Ecuador en el año 2017. Datos proporcionados por la estación científica del Instituto Nacional de Meteorología e Hidrología del Ecuador (INAMHI).

go de 21 días se procedió a recolectar los microorganismos y se los colocó en un tanque de 500 mL junto con melaza, sal en grano, de harina de pescado, roca fosfórica y agua hasta completar 300 L, durante 30 días en condiciones anaeróbicas. En la segunda fase se emplearon tanques de 600 L donde se mezclaron estiércol de ganado, roca fosfórica, sulfato de potasio y magnesio, ceniza, leche, melaza y agua hasta completar 400 L. el tanque de la segunda fase se dejó reposar durante 120 días, con reactivaciones de la solución madre a los 30, 60 y 90 días. Adicional se evaluaron parámetros físicos-químicos en cada una de las reactivaciones de abono foliar orgánico (tabla 2)

Se realizaron aplicaciones foliares del abono foliar empleando una motobomba con boquilla electrostática de la marca Nuvola Cifarelli. Las aplicaciones en campo se realizaron con la ayuda de un solo asistente para minimizar el

Fincas	Inicial	React 1	React 2	React 3	Final
Conductividad eléctrica (mS/cm)					
Pampants	14,70 ± 0,46 A*	16,76 ± 0,04 A	17,39 ± 0,09 AB	18,58 ± 0,11 A	19,75 ± 0,33 A
Dos Ríos	14,57 ± 0,39 A	16,68 ± 0,23 A	17,28 ± 0,15 B	18,17 ± 0,48 A	19,83 ± 0,53 A
Amazonas	14,58 ± 0,63 A	16,70 ± 0,36 A	17,58 ± 0,24 A	18,5 ± 0,16 A	19,82 ± 0,25 A
Solutos totales (g/L)					
Pampants	6,68 ± 0,17 A	7,28 ± 0,06 A	7,54 ± 0,06 A	7,68 ± 0,09 A	8,92 ± 0,08 A
Dos Ríos	6,37 ± 0,80 A	7,09 ± 0,34 A	7,51 ± 0,13 A	7,76 ± 0,08 A	9,10 ± 0,42 A
Amazonas	6,38 ± 0,34 A	7,19 ± 0,33 A	7,55 ± 0,08 A	7,74 ± 0,07 A	8,85 ± 0,44 A
Salinidad (ppt)					
Pampants	7,91 ± 0,06 A	9,61 ± 0,22 A	10,27 ± 0,04 A	10,39 ± 0,01 B	10,71 ± 0,12 A
Dos Ríos	8,08 ± 0,25 A	9,61 ± 0,18 A	10,29 ± 0,14 A	10,66 ± 0,14 A	10,93 ± 0,22 A
Amazonas	7,83 ± 0,38 A	9,32 ± 0,42 A	10,26 ± 0,09 A	10,54 ± 0,08 A	10,56 ± 0,47 A
Temperatura (°C)					
Pampants	28,96 ± 0,70 A	27,82 ± 2,18 A	28,32 ± 0,33 A	27,68 ± 0,38 A	28,28 ± 0,08 B
Dos Ríos	28,66 ± 0,57 A	28,30 ± 1,77 A	27,80 ± 1,06 A	28,00 ± 0,43 A	28,52 ± 0,19 A
Amazonas	27,63 ± 2,26 A	27,57 ± 1,79 A	27,16 ± 1,98 A	27,17 ± 1,21 A	28,35 ± 0,19 AB
pH					
Pampants	4,78 ± 0,04 A	4,52 ± 0,14 A	4,27 ± 0,08 A	4,14 ± 0,03 A	3,71 ± 0,17 A
Dos Ríos	4,84 ± 0,03 B	4,61 ± 0,36 A	4,34 ± 0,25 A	4,14 ± 0,14 A	3,93 ± 0,07 A
Amazonas	4,83 ± 0,03 AB	4,33 ± 0,55 A	4,22 ± 0,37 A	4,02 ± 0,29 A	3,81 ± 0,22 A

* Valores promedios de cinco repeticiones ± desviación estándar de los datos correspondientes a los parámetros físicos y químicos del abono liquido orgánico. Las letras diferentes en las mismas filas corresponden a diferencias significativas según la prueba de Duncan $p<0.05$.

Tabla 2. Promedio de los análisis físicos y químicos de las reactivaciones realizadas al abono liquido orgánico.

error de la aplicación. Así mismo, se estandarizó la cantidad de 8 litros por parcela, según estandarizaciones de Corrales y Maldonado, (2019)[15]. Finalmente, antes de la aplicación del abono líquido, se procedió a homogenizar y a tamizar el mismo para separar el líquido de otras sustancias sólidas según protocolo de uso y aplicación del CIBE-ESPOL.

En el presente estudio se evaluaron cinco tratamientos en parcelas demostrativas. Se utilizó un diseño de bloques completamente al azar con cinco tratamientos en cada una de las tres parcelas demostrativas. Las aplicaciones foliares fueron a los 30 y 60 días con abono orgánico al 100% y diluido con agua al 50%. Los tratamientos fueron: T1: 30 días-50%; T2: 60 días-50%; T3: 30 días-100%; T4: 60 días-100% y T5: manejo convencional (Control). El manejo convencional consistió en labores culturales tales como el control mecánico de malezas, podas de mantenimiento (marca Husqvarna) y eliminación de mazorcas enfermas.

Cada una de las parcelas se estableció como un bloque y se dividió en 15 lotes con seis plantas cada uno, por lo que cada tratamiento se repitió tres veces dentro de cada bloque. Cada planta dentro de los tratamientos constituyó una unidad de observación, en la que se evaluaron las variables agronómicas.

Las variables agronómicas evaluadas fueron el número de mazorcas enfermas asociadas al patógeno *Moniliophthora roreri* (moniliasis), incidencia de *M. perniciosa* (escoba de bruja vegetativa) y nutrientes foliares tales como fosforo, calcio, potasio, magnesio, hierro, manganeso, cobre y zinc. Las evaluaciones se de los nutrientes se realizaron antes y después de la aplicación del abono líquido orgánico.

Evaluación in situ de enfermedades asociadas a *Moniliophthora roreri* y *M. perniciosa*

Para la evaluación in situ de la enfermedad asociada al patógeno fúngico de *M. roreri* se procedió a contabilizar las mazorcas que presentaron los síntomas de la enfermedad en cada una de las unidades de observación. Mientras que para evaluar a *M. perniciosa* se contabilizaron las escobas vegetativas presentes en cada unidad de análisis.

Evaluación de nutrientes foliares

En cada una de las parcelas se tomaron muestras foliares antes y después de la aplicación de los tratamientos para realizar el análisis de macro y micronutrientes en tejidos mediante ICP-OES. Para los análisis se tomaron muestras frescas de tejidos de hojas y se procedió a emplear el método de digestión con HNO3. Los macronutrientes evaluados fueron fósforo, potasio, calcio y magnesio y los micronutrientes fueron hierro, manganeso, cobre y zinc. Los análisis se realizaron en el Laboratorio de suelos y nutrición vegetal de la Escuela Superior Politécnica del Litoral.

Análisis de datos

Se analizaron los datos empleando el análisis de varianza mediante el programa estadístico InfoStat versión 2020. Los datos relacionados con la evaluación de las enfermedades fúngicas se transformaron mediante logaritmo de base 10 (x+1). Cuando los datos presentaron diferencias significativas se procedió a aplicar la prueba de rangos múltiples de Duncan con un nivel de significancia estadística de $p<0.05$.

Resultados y discusión

Evaluación in situ de *M. perniciosa* y *M. roreri*

Los resultados en relación a la evaluación de las enfermedades asociadas a *M. perniciosa* demostraron efectos significativos en los tratamientos antes y después de la aplicación del abono liquido foliar. De entre las parcelas evaluadas, los mejores resultados se presentaron en Pampants en los tratamientos T1 y T2 quienes mostraron diferencias significativas con una reducción del 100% de escobas de brujas vegetativas (Fig. 2). Tanto el T1 y el T2 mostraron una reducción del 17,14% más efectiva con relación al control.

Con relación a los resultados de la evaluación de *M. roreri* el mejor tratamiento se presentó en el T1 quien mostró diferencias significativas después de la aplicación del abono liquido orgánico con una reducción de la enfermedad del 50% (Fig. 3). Sin embargo, los resultados evidenciaron resultados no significativos en el resto de tratamientos con relación al control.

La aplicación foliar de abonos líquidos orgánicos puede ser beneficiosas en la planta. Es posible que rociar las hojas con biofertilizantes elaborados con bacterias tengan una acción positiva en la superficie foliar, debido a la colonización de microorganismos beneficiosos[16]. La aplicación de bacterias del género *Bacillus sp.* en combinación con podas

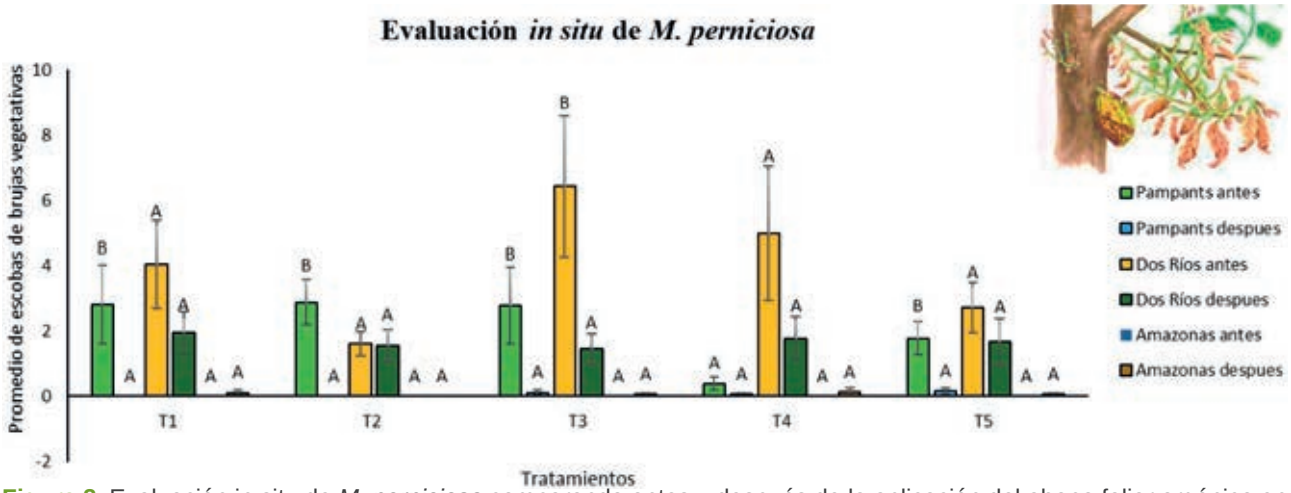

Figura 2. Evaluación in situ de *M. perniciosa* comparando antes y después de la aplicación del abono foliar orgánico en cada uno de los tratamientos y parcelas demostrativas. Letras diferentes encima de las barras indican diferencias estadísticamente significativas, según el test de Duncan ($p<0.05$).

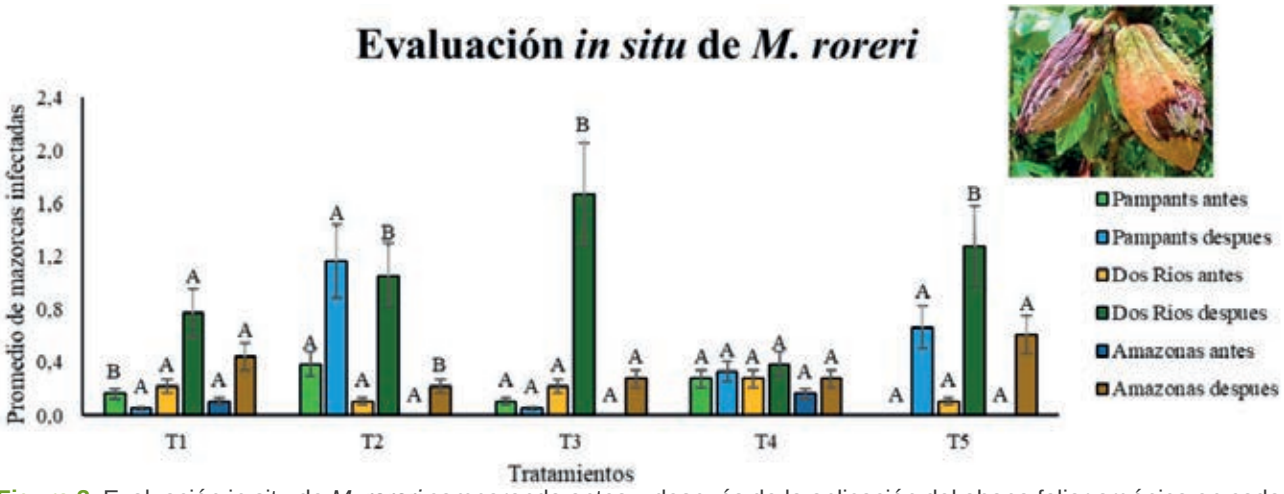

Figura 3. Evaluación in situ de *M. roreri* comparando antes y después de la aplicación del abono foliar orgánico en cada uno de los tratamientos y parcelas demostrativas. Letras diferentes encima de las barras indican diferencias estadísticamente significativas, según el test de Duncan ($p<0.05$).

adecuadas reduce significativamente la incidencia de *M. roreri* en cultivo de cacao[17], por lo que el uso de productos biológicos es una alternativa alentadora en el control de enfermedades tales como la moniliasis[18]. Tales aseveraciones han sido evaluadas en condiciones de campo demostrando la efectividad de los antagonistas microbianos contra los patógenos fúngicos de *Theobroma cacao* L[19,20].

En general, las evaluaciones *in situ* evidenciaron diferencias significativas positivas en el control biológico relacionada con *M. roreri* y *M. perniciosa* aplicando el tratamiento de aplicaciones de 30 días diluido al 50% frente al control convencional. En un estudio experimental en campo, se ha informado que la aplicación de abonos líquidos en la hoja, afecta positivamente la nutrición y biocontrol, sin comprometer la calidad de los frutos[21,22]. Sin embargo, el control biológico puede verse afectado por componentes inherentes al cultivo de cacao tales como la edad de las plantas, presencia de plagas, fertilidad de los suelos y factores climáticos[23]. Por lo que investigadores mencionan la importancia de la respuesta del cultivo de cacao a la dosificación, numero de aplicaciones y frecuencia de aplicación de los abonos líquidos foliares[15].

Las estrategias de manejo integrado combinando productos químicos y biológicos puede aumentar la producción[24], por lo que es importante desarrollar nuevas formulaciones biológicas que tomen en cuenta la efectividad de los microorganismos y los tiempos de aplicación[25]. La superficie foliar de las plantas es un ambiente heterogéneo para las interacciones de diversas comunidades de microorganismos[26]. Esta microbiota foliar contiene organismos que le brindan protección contra los patógenos[27], por lo que bacterias, hongos y virus han sido empleados con éxito como bioestimulantes y agentes de control biológico en la agricultura[28].

Macronutrientes

En base a la evaluación de los macronutrientes en la hoja del cultivo de cacao fino de aroma, es posible indicar que existe un efecto positivo después de la aplicación del abono liquido orgánico en los elementos de fosforo y potasio. El promedio ponderado del fosforo incrementó de 0,17 a 0,21 mg/kg, mientras que el potasio pasó de 1,49 a 2,22 cmol/kg. Sin embargo, los resultados para el calcio evidencian diferencias significativas en contra a la aplicación del abono líquido, con promedios de 1,67 a 1,07. Mientras que en el magnesio no se visualizan diferencias significativas antes y después de la aplicación (Figura 4).

Micronutrientes

Los resultados en micronutrientes demuestran que la aplicación del abono líquido afectó significativamente al cobre, con promedios que fueron de 9,39 a 14,86 mg/kg. Mientras que el hierro presentó resultados que evidencian disminución en las hojas después de la aplicación, con promedios que fueron de 74,62 a 44,59 mg/kg. Finalmente, el uso del abono líquido no afectó significativamente a los elementos de manganeso y zinc (Figura 5).

Las investigaciones en el campo nutricional agrícola, reportan el efecto positivo de la fertilización foliar en la traslocación de los macro y micronutrientes (6). Los resultados de este estudio evidenciaron el efecto positivo de la aplicación del abono líquido sobre el aumento de las concentraciones foliares de macro y micronutrientes, tales como fósforo, potasio y cobre. Estos resultados se relacionan con un estudio desarrollado en *Brassica napus*, donde la aplicación foliar de una combinación de cepas de *Pseudomonas* y *Azospirillum* se correlacionaban positivamente con el aumento de los elementos de potasio y fósforo[29]. Por otro lado, los resultados de esta investigación no evidencian aumentos significativos en otros nutrientes como hierro, calcio y magnesio. Esto puede atribuirse a las condiciones ambientales y efectos del cambio climático[30], tal como lo indican estudios sobre la aplicación de biofertilizantes en el crecimiento y contenido de nutrientes en plantas bajo condiciones ambientales diversas[31].

Las investigaciones sugieren que la aplicación del abonos foliares promueven el crecimiento[32], incluyendo la producción de ácido indol -3 acético, fosfato orgánico, sideróforos, exopolisacáridos y actividad nitrogenasa[33]. Así mismo los productos derivados de los microorganismos tales como los sideróforos pueden ayudar a captar y distribuir los nutrientes en la superficie foliar de la planta[34,35], capaces de mejorar la adquisición de nutrientes[36].

Conclusiones

Por los resultados en este estudio, es posible concluir que la aplicación de un abono líquido orgánico aplicado en el cultivo *in situ* de cacao nacional fino de aroma puede

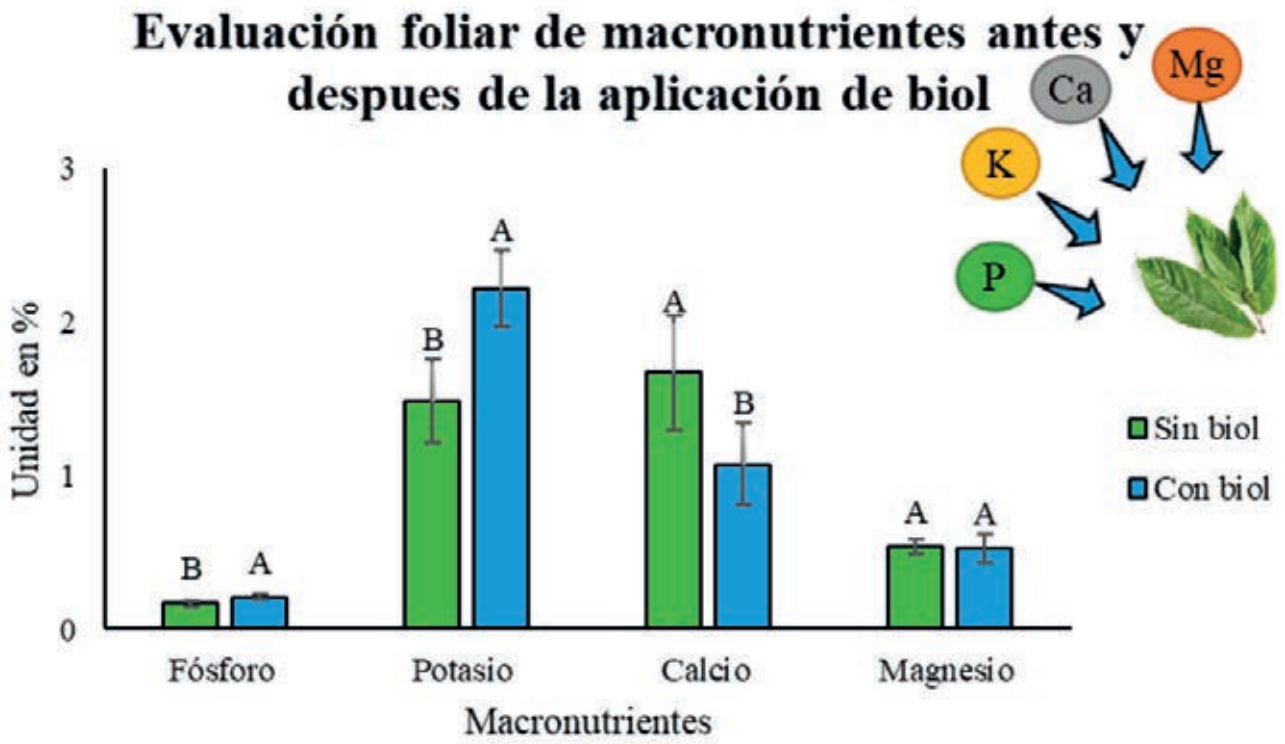

Figura 4. Comparación de medias ± desviación estándar de los macronutrientes en la parte foliar de las plantas de cacao fino de aroma en las parcelas demostrativas antes y después de la aplicación de los tratamientos con el abono líquido orgánico. Letras diferentes encima de las columnas indican diferencias estadísticamente significativas, según el test de Duncan ($p<0.05$).

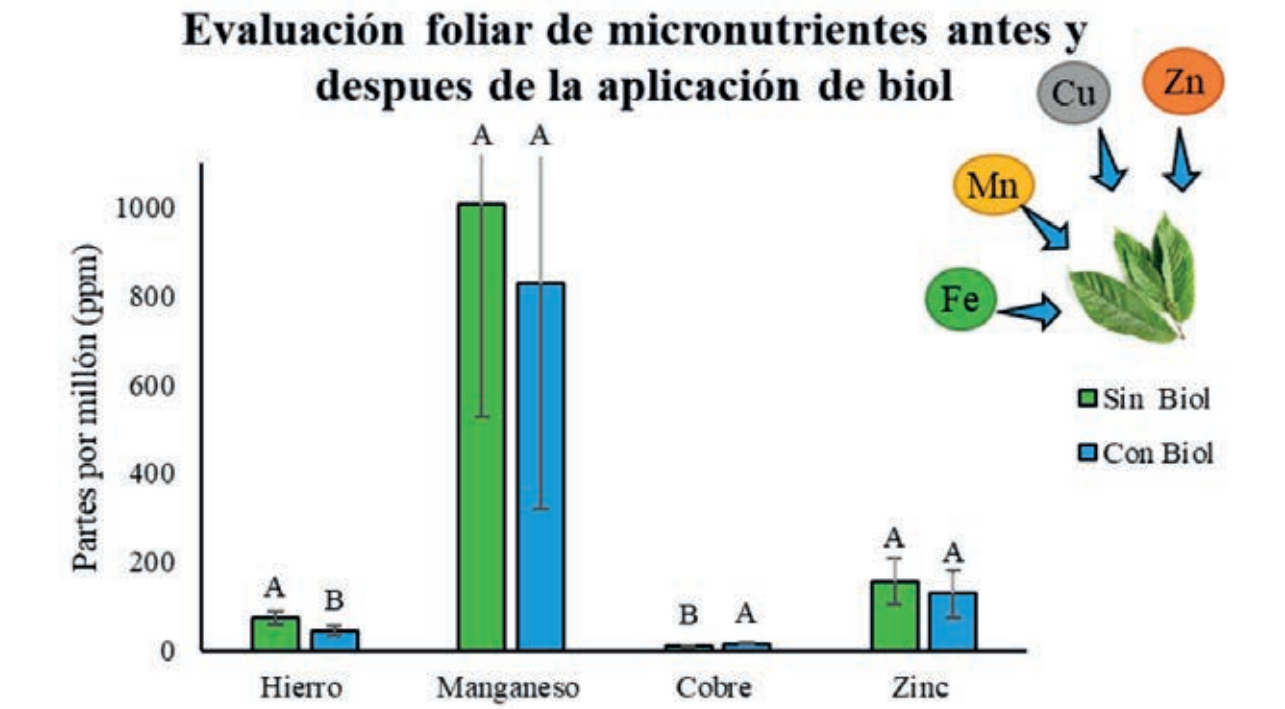

Figura 5. Comparación de medias ± desviación estándar de los micronutrientes en la parte foliar de las plantas de cacao fino de aroma en las parcelas demostrativas antes y después de la aplicación de los tratamientos con el abono líquido orgánico. Letras diferentes encima de las columnas indican diferencias estadísticamente significativas, según el test de Duncan ($p<0.05$).

favorecer la nutrición de las plantas, así como el control de patógenos fúngicos. Por lo que las preparaciones líquidas podrían emplearse como parte de un plan de manejo integrado, reduciendo la dependencia excesiva de químicos.

El desarrollo de nuevas formulaciones biológicas aplicados en la superficie foliar, así como el uso de herramientas genómicas para potenciar cepas microbiológicas están abriendo nuevas posibilidades para una agricultura más equilibrada[37]. Por lo que las futuras investigaciones deben ser más holísticas y relacionar aspectos que son claves

para una producción más sostenible y sustentable, relacionando los microorganismos, la agricultura, el cambio climático y la nutrición[38].

Agradecimientos

Los autores desean expresar sus agradecimientos a Jhonny España, David Catagua, Leonardo León, Byron Moyano, Ronald León y Víctor Hernández por su arduo trabajo en la recolección de datos de campo. La presente investigación se encuentra en el contrato marco MAE-DNB-CM-2017-077 del proyecto "Aislamiento, identificación y caracterización de microorganismos benéficos asociados al cultivo del cacao y su potencial como agentes de control biológico".

Referencias bibliográficas

1. Burritt DJ. Crop plant adaption to climate change and extreme environments. In: Melton L, Shahidi F, Varelis P, editors. Encyclopedia of Food Chemistry. Oxford: Academic Press; 2019. p. 196–201.
2. Rasmussen LV, Coolsaet B, Martin A, Mertz O, Pascual U, Corbera E, et al. Social-ecological outcomes of agricultural intensification. Nat Sustain. 2018 Jun;1(6):275–82.
3. de Graaff MA, Hornslein N, Throop HL, Kardol P, van Diepen LTA. Chapter One - Effects of agricultural intensification on soil biodiversity and implications for ecosystem functioning: A meta-analysis. In: Sparks DL, editor. Advances in Agronomy. Academic Press; 2019. p. 1–44.
4. Quevedo A, Magdama F, Castro J, Vera-Morales M. Interacciones ecológicas de los hongos nematófagos y su potencial uso en cultivos tropicales. Scientia Agropecuaria. 2022 Mar 28;13(1):97–108.
5. Karthika KS, Rashmi I, Parvathi MS. Biological functions, uptake and transport of essential nutrients in relation to plant growth. In: Hasanuzzaman M, Fujita M, Oku H, Nahar K, Hawrylak-Nowak B, editors. Plant Nutrients and Abiotic Stress Tolerance [Internet]. Singapore: Springer; 2018 [cited 2022 Aug 6]. p. 1–49. Available from: https://doi.org/10.1007/978-981-10-9044-8_1
6. Moreira A, Moraes LAC. Yield, nutritional status and soil fertility cultivated with common bean in response to amino-acids foliar application. Journal of Plant Nutrition. 2017 Feb 7;40(3):344–51.
7. Fernández V, Brown PH. From plant surface to plant metabolism: the uncertain fate of foliar-applied nutrients. Front Plant Sci. 2013 Jul 31;4:289.
8. Noreen S, Fatima Z, Ahmad S, Athar H ur R, Ashraf M. Foliar application of micronutrients in mitigating abiotic stress in crop plants. In: Hasanuzzaman M, Fujita M, Oku H, Nahar K, Hawrylak-Nowak B, editors. Plant Nutrients and Abiotic Stress Tolerance [Internet]. Singapore: Springer; 2018 [cited 2022 Aug 6]. p. 95–117. Available from: https://doi.org/10.1007/978-981-10-9044-8_3
9. Zubair M, Wang S, Zhang P, Ye J, Liang J, Nabi M, et al. Biological nutrient removal and recovery from solid and liquid livestock manure: Recent advance and perspective. Bioresource Technology. 2020 Apr 1;301:122823.
10. Martínez-Alcántara B, Martínez-Cuenca MR, Fernández C, Legaz F, Quiñones A. Production of 15N-Labelled liquid organic fertilisers based on manure and crop residue for use in fertigation studies. PLOS ONE. 2016 Mar 16;11(3):e0150851.
11. Fahrurrozi F, Muktamar Z, Setyowati N, Sudjatmiko S, Chozin M. Comparative effects of soil and foliar applications of tithonia-enriched liquid organic fertilizer on yields of sweet corn in closed agriculture production system. AGRIVITA, Journal of Agricultural Science. 2019 May 28;41(2):238–45.
12. Kannan S. Foliar Fertilization for Sustainable Crop Production. In: Lichtfouse E, editor. Genetic Engineering, Biofertilisation, Soil Quality and Organic Farming [Internet]. Dordrecht: Springer Netherlands; 2010 [cited 2022 Sep 28]. p. 371–402. (de Reseñas de Agricultura Sostenible). Available from: https://doi.org/10.1007/978-90-481-8741-6_13
13. Muñoz D, Cuenca C, Banchón CL, Pazos G. Valoración de desechos de banano (Musa acuminata Cavendish Subgroup) y cacao (Theobroma cacao) mediante producción de compost y biol. 3c Tecnología: glosas de innovación aplicadas a la pyme. 2020;9(1):17–29.
14. ICCO. Production of cocoa beans. ICCO Quarterly Bulletin of Cocoa Statistics [Internet]. 2021 [cited 2021 Apr 5];47(1). Available from: https://www.icco.org/statistics/
15. Corrales DO, Maldonado C. Aplicación de biofertilizantes en plantines de cacao (Theobroma cacao L.) en Sapecho - Alto Beni. Apthapi. 2019 Dec 25;5(3):1646–51.
16. Wang D, Deng X, Wang B, Zhang N, Zhu C, Jiao Z, et al. Effects of foliar application of amino acid liquid fertilizers, with or without Bacillus amyloliquefaciens SQR9, on cowpea yield and leaf microbiota. PLoS One. 2019 Sep 4;14(9):e0222048.
17. Pilaloa W, Alvarado A, Pérez D, Torres S. Manejo agroecológico de la Moniliasis en el cultivo de cacao (Theobroma cacao) mediante la utilización de biofungicidas y podas fitosanitarias en el cantón La Troncal. Revista Alfa. 2021 Dec 13;5(15):453–68.
18. Anzules V, Borjas R, Alvarado L, Castro-Cepero V, Julca-Otiniano A. Control cultural, biológico y químico de Moniliophthora roreri y Phytophthora spp en Theobroma cacao 'CCN-51.' Scientia Agropecuaria. 2019 Oct;10(4):511–20.
19. Villamil JE, Viteri SE, Villegas WL. Aplicación de antagonistas microbianos para el control biológico de Moniliophthora roreri Cif & Par en Theobroma cacao L. bajo condiciones de campo. Revista Facultad Nacional de Agronomía - Medellín. 2015 Jan 1;68(1):7441–4750.
20. Ferraz P, Cássio F, Lucas C. Potential of yeasts as biocontrol agents of the phytopathogen causing cacao witches' broom disease: is microbial warfare a solution? Frontiers in Microbiology. 2019;10.
21. Naidu Y, Meon S, Siddiqui Y. Foliar application of microbial-enriched compost tea enhances growth, yield and quality of muskmelon (Cucumis melo L.) cultivated under fertigation system. Scientia Horticulturae. 2013 Jul 30;159:33–40.
22. Naidu Y, Meon S, Siddiqui Y. In vitro and in vivo evaluation of microbial-enriched compost tea on the development of powdery mildew on melon. BioControl. 2012;57(6):827–36.
23. Fuentes CM. Efecto del manejo en la reducción de incidencia de enfermedades (Moniliasis, Escoba de Bruja y Mazorca Negra) en el cultivo de Cacao (Theobroma cacao l.) en la Estación Experimental de Sapecho. Apthapi. 2015;1(1).
24. Anzules-Toala V, Pazmiño-Bonilla E, Alvarado-Huamán L, Borjas-Ventura R, Castro-Cepero V, Julca-Otiniano A. Control of cacao (Theobroma cacao) diseases in Santo Domingo de los Tsachilas, Ecuador. Agronomía Mesoamericana. 2022;33(1):1–12.
25. Krauss U, Hidalgo E, Bateman R, Adonijah V, Arroyo C, García J, et al. Improving the formulation and timing of application of endophytic biocontrol and chemical agents against frosty pod rot (Moniliophthora roreri) in cocoa (Theobroma cacao). Biological Control. 2010 Sep 1;54(3):230–40.
26. Aragón W, Reina-Pinto JJ, Serrano M. The intimate talk between plants and microorganisms at the leaf surface. Journal of Experimental Botany. 2017 Nov 9;68(19):5339–50.
27. Bulgarelli D, Schlaeppi K, Spaepen S, van Themaat EVL, Schulze-Lefert P. Structure and functions of the bacterial microbiota of plants. Annual Review of Plant Biology. 2013;64(1):807–38.
28. Preininger C, Sauer U, Bejarano A, Berninger T. Concepts and applications of foliar spray for microbial inoculants. Appl Microbiol Biotechnol. 2018 Sep 1;102(17):7265–82.
29. Farhangi-Abriz S, Tavasolee A, Ghassemi-Golezani K, Torabian S, Monirifar H, Rahmani HA. Growth-promoting bacteria and natural regulators mitigate salt toxicity and improve rapeseed plant performance. Protoplasma. 2020 Jul 1;257(4):1035–47.

30. Soares JC, Santos CS, Carvalho SMP, Pintado MM, Vasconcelos MW. Preserving the nutritional quality of crop plants under a changing climate: importance and strategies. Plant Soil. 2019 Oct 1;443(1):1–26.
31. Hu Y, Burucs Z, Schmidhalter U. Effect of foliar fertilization application on the growth and mineral nutrient content of maize seedlings under drought and salinity. Soil Science and Plant Nutrition. 2008 Feb 1;54(1):133–41.
32. Olivares FL, Aguiar NO, Rosa RCC, Canellas LP. Substrate biofortification in combination with foliar sprays of plant growth promoting bacteria and humic substances boosts production of organic tomatoes. Scientia Horticulturae. 2015 Feb 12;183:100–8.
33. Abadi VAJM, Sepehri M, Rahmani HA, Zarei M, Ronaghi A, Taghavi SM, et al. Role of dominant phyllosphere bacteria with plant growth–promoting characteristics on growth and nutrition of maize (Zea mays L.). J Soil Sci Plant Nutr. 2020 Dec 1;20(4):2348–63.
34. Fernàndez V, Ebert G, Winkelmann G. The use of microbial siderophores for foliar iron application studies. Plant Soil. 2005 May 1;272(1):245–52.
35. Sharma S, Chandra S, Kumar A, Bindraban P, Saxena AK, Pande V, et al. Foliar application of iron fortified bacteriosiderophore improves growth and grain Fe concentration in wheat and soybean. Indian J Microbiol. 2019 Sep;59(3):344–50.
36. Hafezi MM, Azari A, Rahimi A, Maddah-Hosseini S, Ahmadi-Lahijani MJ. Bacterial siderophore improves nutrient uptake, leaf physiochemical characteristics, and grain yield of cumin (Cuminum cyminum L.) ecotypes. Journal of Plant Nutrition. 2021 Jul 21;44(12):1794–806.
37. Glare TR, O'Callaghan M. Microbial biopesticides for control of invertebrates: Progress from New Zealand. Journal of Invertebrate Pathology. 2019 Jul 1;165:82–8.
38. Fanzo J, Davis C, McLaren R, Choufani J. The effect of climate change across food systems: Implications for nutrition outcomes. Global Food Security. 2018 Sep 1;18:12–9.

ARTICLE / INVESTIGACIÓN

Effect of push-out bond strength of a conventional and a bulk-fill composite resin as a biotechnological technique to root dentin of primary anterior teeth

Shahram Mosharrafian[1], Pegah Khazaei[2], Pegah Rahbar[3], Zahra Hosseini[4*]

DOI. 10.21931/RB/2023.08.02.21

[1] Assistant professor, Department of Pediatric Dentistry, Tehran University of Medical Sciences, Tehran, Iran.
[2] Dentist, University of California, Los Angeles, School of Dentistry.
[3] Assistant professor, Department of Pediatric Dentistry, Ahvaz Jundishapur University of Medical Sciences, Khuzestan, Iran.
[4] Corresponding author, Assistant Professor, Department of Pediatric Dentistry, Faculty of Dentistry, Kermanshah University of Medical Sciences, Kermanshah, Iran.
Corresponding author: zahrahosseini69@gmail.com.

Abstract: This study aimed to compare the push-out bond strength of a bulk-fill and a conventional composite resin to root dentin of primary anterior teeth using a 7th-generation dentin bonding agent. This in vitro study evaluated 24 primary anterior teeth randomly divided into two groups: Filtek P60 conventional and Filtek bulk-fill composite resins. Single Bond Universal adhesive was used for bonding. After filling the coronal part of the canal with composite resin, the teeth were mounted in acrylic resin and sliced to obtain a 1-mm-thick section of each root. Next, the sections underwent the push-out bond strength test. After determining the push-out bond strength, the failure mode was determined under a light microscope at ×40 magnification. The data were analyzed with two-way ANOVA and t-test. The mean push-out bond strength was 13.37±4.40 MPa in the conventional and 5.40±2.91 MPa in the bulk-fill composite resin groups. This difference was statistically significant (P=0.001). In the conventional group, 50% of failures were cohesive in the traditional combined resin group, while in the bulk-fill composite resin group, 75% of losses were mixed. Filtek P60 conventional composite resin and Single Bond Universal 7th-generation bonding agent were determined as appropriate for fabricating intracanal composite posts in primary anterior teeth.

Key words: Push-out, Bond strength, Bulk-fill composite resin, Root dentin, Primary anterior teeth.

Introduction

Preserving primary teeth is of utmost importance[1-5]. Early childhood caries (ECC) is a common cause of early primary tooth loss, which refers to the presence of one or more carious (cavitated or non-cavitated), lost or restored tooth surfaces in any of the primary teeth of a 71-month-old child or younger[6,7]. Severe ECC refers to any sign of caries in smooth surfaces of the teeth in children under the age of 3. ECC often results in losing a significant portion of tooth structure and pulpal involvement[8]. Therefore, restoration of teeth with ECC remains a challenge in pediatric dentistry. Stainless steel crowns used to be the treatment of choice for such teeth. However, many parents no longer accept them due to their unesthetic appearance[9].

A suitable restoration for such teeth should restore the primary function while providing favorable esthetics[10]. Open-face crowns, polycarbonate crowns, and composite resin restorations have been suggested to treat carious primary teeth[11]. Composite resin restoration of severely damaged teeth often requires pulpectomy and placement of intracanal post to serve as a retainer[12]. In addition, the fabrication of a post and core is imperative to retain and stabilize the composite resin crown and resist masticatory forces[13]. In cases where a small amount of coronal tooth structure remains, restorations with posts often result in a better function than those without a post[14]. Several posts can be used for this purpose, such as prefabricated metal posts, fiber-reinforced posts, orthodontic wires, cast posts with retentive grooves, short composite resin posts, and biologic posts[15,16]. Considering the physiological root resorption in primary teeth, only the coronal 3 mm of the root should be used to obtain adequate retention and resistance in severely damaged teeth[17]. Due to increased demand for esthetics, composite resin and fiber posts are increasingly used for the anterior teeth due to advantages such as optimal corrosion resistance, biocompatibility, mechanical strength[18], reinforcement of composite resin crown, improved translucency, optimal esthetics, higher flexibility compared with metal posts, and easy application[19,20]. Also, these posts have a modulus of elasticity close to dentin, which decreases stress accumulation and root fracture[21]. Many attempts have been made to enhance the efficacy of dentin-bonding agents while reducing their procedural steps. Thus, some progress was made in multi-step dentin bonding agents, which were difficult for children due to their technique sensitivity and time-consuming nature[22].

In this respect, 7th-generation dentin bonding agents were introduced to simplify the bonding procedure. In this system, acid, primer, and bonding agent are all supplied in one bottle, which facilitates the application of this bonding agent in non-cooperative children[23]. Conventional methacrylate-based composite resins have long been used to restore primary anterior teeth. However, limited curing depth and the possibility of an inadequate degree of conversion of monomers to polymer in deep areas are among

Citation: Mosharrafian S, Khazaei P, Rahbar P, Hosseini Z. Effect of push-out bond strength of a conventional and a bulk-fill composite resin as a biotechnological technique to root dentin of primary anterior teeth. Revis Bionatura 2023;8 (2) 21. http://dx.doi.org/10.21931/RB/2023.08.02.21
Received: 2 January 2023 / **Accepted:** 19 April 2023 / **Published:** 15 June 2023
Publisher's Note: Bionatura stays neutral with regard to jurisdictional claims in published maps and institutional affiliations.

the drawbacks of conventional composite resins[24], which can deteriorate their physical, mechanical, and biological properties[25,26]. They can be applied in bulk to decrease the application steps and save time[27,28]. Also, they can be applied in 4-mm-thick increments (versus 2 mm in conventional composite resins)[29] with lower polymerization shrinkage compared with conventional composite resins[30].

Since severe destruction of primary anterior teeth often necessitates pulpectomy, the reconstruction of such teeth requires efficient dentin bonding agents, and retention should be obtained from the root dentin. Thus, this study assessed the push-out bond strength of a bulk-fill and a conventional composite resin to root dentin of primary anterior teeth using a 7th-generation dentin bonding agent.

Materials and methods

Study design

This in vitro study evaluated 24 primary anterior teeth extracted due to severe coronal caries within the previous six months. The ethics committee of Tehran University of Medical Sciences approved the study.

Teeth preparation

The collected teeth were immersed in 0.5% chloramine T solution for one week and stored in distilled water. The teeth were then decoronated at 1 mm above the cementoenamel junction using diamond discs perpendicular to the long axis of the tooth.

Sample size measuring

The sample size was calculated at 12 in each group according to a previous study by Torres *et al.*[30], assuming alpha=0.5, beta=0.2, a mean difference of 3.3, and a standard deviation of 3.16 using Minitab software.

Inclusion Criteria and Groups

Inclusion criteria were the absence of dental caries and fractures. The teeth were randomly assigned to two groups. The root canals were instrumented with three sizes of k-files (Mani Inc., Japan) and rinsed with saline solution. They were then dried with paper points (PT Dent, USA). After completion of filing, the root canals were not filled with zinc-oxide eugenol to prevent the possible effect on pulpal dentin. Instead, 1 mm of zinc phosphate paste was applied to create an apical seal for composite resin packing. Next, the coronal 3 mm root canal was filled with composite resin to serve as an intracanal post. Patients with COVID-19, dental infections, and neoplastic lesions of the oral cavity have been excluded from the study. Table 1 presents the composition of this study's bonding agent and composite resins.

Single Bond Universal 7th-generation bonding agent was used for bonding composite resins in both groups. In group 1, Filtek P60 conventional composite resin was incrementally applied according to the manufacturer's instructions and packed into the root canal with a condenser. Each layer was light-cured for 20 seconds. In group 2, Filtek bulk-fill composite resin was applied in the root canal in bulk in one step according to the manufacturer's instructions and light-cured for 40 seconds. All the samples in both groups were light-cured using an LED light-curing unit (WoodPecker, China) at a light intensity of 800–1000 mW/cm2. The tip of the light-curing unit was placed 2 mm away from the tooth surface. The samples were incubated in distilled water at 37°C for 24 hours (Kavoosh Mega, Iran) and then underwent 2000 thermal cycles at 5/55°C with a dwell time of 30 seconds and a transfer time of 10 seconds (TC300; Vafaie Industrial, Iran). Next, the samples were mounted in transparent acrylic resin. A section was made at the midpoint of the prepared root of each tooth with 1-mm thickness using a water-cooled diamond blade on a Labcut 250B cutting machine (Extec, corp, Enfield, CT). The push-out bond strength test was then performed using a universal testing machine (2050; Zwick/Roell, Ulm, Germany). Using a stainless steel cylindrical plunger with a diameter matching the root canal, the load was applied to the bonding interface in an apicocervical direction at a 0.5 mm/min crosshead speed. Maximum load causing debonding was recorded in Newtons (N). The load in Newtons was divided by the surface area in square millimeters (mm2) to determine the bond strength in megapascals (MPa). Prior to the push-out test, both sides of the sliced section were photographed by a digital camera (DSC-HX100v CyberShot, Sony, Japan), and the photographs were fed into AutoCAD 2013 software. The cross-sectional area was calculated using the formula A=H((A1+A2)/2) where A1 is the circumference on one side, A2 is the circumference on the other side, and H is the height (thickness) of the root slice in millimeters. The AutoCAD software measured A1 and A2, and H was measured by a digital caliper (Mitutoyo, Japan). After the push-out test, the samples were inspected under a light microscope (SZX2-2b16; Olympus, Japan) at ×40 magnification to determine the mode of failure, categorized as mixed, cohesive, and adhesive.

Materials	Components	Mode/steps of the application	Manufacturer
Single bond universal Self-etch 1-step	MDP phosphate monomer, dimethacrylate resins, HEMA, Vitrebond™ copolymer, filler, Ethanol, water, initiators, silane	The adhesive was rubbed on the tooth surface for 20 s, gently air-dried for 5 s, and cured for 10 s.	3M, St. Paul, MN, USA
Filtek P60 %fillers/wt: 83.0	BIS-GMA, UDMA, BIS-EMA	Each increment was applied with 2 mm thickness and cured for 20 s.	3M, St. Paul, MN, USA
Filtek bulk-fill %fillers/wt: 64.5	ERGP-DMA, diurethane-DMA, 1,12-dodecane-DMA	Each layer was applied with 4 mm thickness and cured for 40 s.	3M, St. Paul, MN, USA

Table 1. Composition of bonding agent and composite resins used in this study.

Data analysis

The data were analyzed with SPSS 22 via t-test at an 0.05 level of significance[31-37].

Results

Push-out bond strength

Table 2 shows the mean push-out bond strength of the two groups. The t-test showed a significant difference in bond strength between the two groups, such that the conventional composite resin yielded a significantly higher bond strength (P<0.001).

Frequency of different modes of failure

Table 3 shows the frequency of different failure modes in the two groups. In the conventional group, 50% of failures were cohesive in the composite resin, while 75% of failures were mixed in the bulk-fill group.

Discussion

Dental sciences have been considered an important part of medical research on human health[38-40]. This study compared the push-out bond strength of a bulk-fill and a conventional composite resin to root dentin of primary anterior teeth using a 7th-generation dentin bonding agent. The mean push-out bond strength of the conventional composite was significantly higher than that of the bulk-fill composite resin. Afshar *et al.*[23] assessed the push-out bond strength of 5th, 6th-, and 7th-generation bonding agents to root dentin of primary anterior teeth and found no significant difference between them. However, the mean value reported for the 7th-generation bonding agent in their study (12.28 MPa) was lower than that in the present study (13.37 MPa) when a conventional composite resin was used. Differences in age and morphology of the teeth, storage media, and operators' expertise may be responsible for the difference in the results. Also, thermocycling was performed in the present study, which was not conducted in the study above.

Some other studies assessed the shear or tensile bond strength of different composite resins and bonding agents to primary tooth crowns. Yaseen and Reddy[22] reported a shear bond strength of 17.39 MPa for the Clearfil S3 Bond 7th-generation bonding agent, which was higher than the value in the present study. This difference might be attributed to using different bonding agents to assess shear bond strength to dentin far from the pulp chamber (dentin close to dentinoenamel junction). Dentin close to the dentinoenamel junction contains fewer dentinal tubules with smaller diameters than dentin around the pulp chamber. Thus, dentin far from the pulp chamber has a higher amount of calcified tissue, which is the main substrate for etching and bonding and can yield higher bond strength. Thus, the difference between the study above and the present study might be attributed to the difference in the histology of bonded dentin in the crown (far from pulp) and root (close to the pulp) and the difference in the cross-sectional area to which the load was applied.

Ilie *et al.*[41] assessed the shear bond strength of two bulk-fill composite resins and two self-etch adhesive systems to primary dentin and reported higher values than the present study. The bulk-fill composite resin used in the present study differed from the bulk-fill composite resins used by Ilie *et al.*[41], which might explain the differences between the results. Pasdar *et al.*[42] compared the mean push-out bond strengths of three intracanal posts, including short composite post (SCP), glass fiber posts (GFPs) cemented with flowable composite resin, and GFP with glass ionomer cement (GFP + GIC), in anterior deciduous teeth, reporting that the mean push-out bond strengths of SCP was 14.74±6.04 Mpa, which was higher than the other groups. This finding was slightly higher than the present study results concerning conventional composite resins. The differences might be attributed to differences in the techniques used and the morphology of the teeth.

The present study indicated higher bond strength of conventional composite resin to primary dentin using a 7th-generation bonding agent than a bulk-fill composite resin. No similar study was found in the literature to compare the present study results. However, bulk-fill composite resins seem not well-compatible with 7th-generation bonding agents. Although limited studies are available on deciduous teeth, many studies have assessed the push-out bond strength of root dentin in permanent teeth with highly controversial results. Oskoee *et al.*[43] evaluated the push-out bond strength of fiber-reinforced composite resin posts to root dentin of permanent teeth using different adhesive systems. They reported that the push-out bond strength values following a one-step self-etch procedure (27.56 MPa) were higher than those in the present study. This finding might be attributed to differences in primary and permanent dentin. The diameter and number of dentinal tubules in pri-

Composite resin	Minimum	Maximum	Mean	Std. deviation	P-value
Bulk-fill	2.81	12.54	5.40	2.91	0.041
Conventional	7.03	21.94	13.37	4.40	

Table 2. Mean push-out bond strength (MPa) of the two groups.

Composite resin		Cohesive in composite	Cohesive in dentin	Adhesive	Mixed
Conventional	Number	6	2	0	4
	Percentage	50%	16.7%	0%	33.3%
Bulk-fill	Number	0	0	3	9
	Percentage	0%	0%	25%	75%

Table 3. Frequency of different modes of failure in the two groups.

mary dentin are higher than those in permanent dentin. This would decrease the dentin substrate available for bonding to adhesives (reduction of inter-tubular dentin)[44]. On the other hand, the peritubular dentin, which is demineralized faster during the etching process, is thicker in primary dentin than permanent dentin, further reducing the substrate available for bonding[45]. These histological differences are responsible for lower bond strength to primary dentin than permanent dentin.

Dumami *et al.* (2016)[46], consistent with the present study, showed that the push-out bond strength of a bulk-fill composite resin (SonicFill) was lower than that of conventional composite resins. They attributed the differences in the results to factors that affected the integrity of the bond between the root dentin and the restorative materials. In addition, factors such as polymerization shrinkage, the C-factor, application method, and polymerization of the composite resin were considered significant. The authors suggested further studies. Concerning the mode of failure, in the conventional combined resin group in the present study, 50% of losses were cohesive within the composite resin. In contrast, 75% of failures were mixed in the bulk-fill composite resin group, consistent with a previous study on primary dentin[47]. In the conventional composite resin samples, two-thirds of the failures were cohesive, and one-third were mixed. No case of adhesive failure was noted in this group. This result was in agreement with the bond strength test results in this group. Evidence shows that the fracture mode in primary enamel and dentin is mainly of adhesive and mixed types[17].

However, some authors believe that cohesive failure requires a >14-MPa load to occur[47,48]. On the other hand, it has been reported that cohesive failures are not rare in primary dentin and might be due to the low micro-hardness of deep dentin, while some others claim that there is a weak correlation between the failure mode and bond strength in primary dentin[47]. Considering the advantages of self-etch one-step bonding agents, their application with conventional composite resin is recommended for composite resin post-fabrication in primary anterior teeth. However, the Single Bond Universal 7th-generation bonding agent did not seem compatible with Filtek bulk-fill composite. Therefore, future studies with a larger sample size on the push-out bond strength of other composite resins and bonding agents to primary dentin are required to obtain more accurate results in this respect. Also, the efficacy of bulk-fill and conventional composite resins for reconstructing severely damaged primary anterior teeth with fiber posts should be evaluated. Last but not least, in vivo studies are required to assess the efficacy of bulk-fill composite resins with different bonding agents for composite resin post-fabrication in primary anterior teeth in the clinical setting.

The present study was limited to a low number of samples and also experimental groups. However, the main strong point of this survey is the first using push-out bond strength of a conventional and a bulk-fill composite resin technique to root dentin of primary anterior teeth.

Conclusions

Filtek P60 conventional composite resin and Single Bond Universal 7th-generation bonding agent can be a proper choice for fabricating intracanal composite posts in primary anterior teeth.

Acknowledgments

Tehran University of Medical Sciences financially supported this study. There was no conflict of interest to declare.

Bibliographic references

1. Anil S, Anand PS. Early Childhood Caries: Prevalence, Risk Factors, and Prevention. Front Pediatr. 2017;5:157.
2. Rad M., Shahravan A., Haghdoost AA. Effective Factors on Oral Health Behaviors of 12-year-old Children in Cities and Villages of Iran: a Path Analysis. J Dent Shiraz Univ Med Sci., 2018 ; 19(3): 225-231.
3. Monajem Zade SM, Elyaskhil M, Fathi A, Asadinejad SM. Evaluate risk markers for periodontal disease in children with type 1 diabetes: a systematic review and meta-analysis. Turk Online J Qualitative Inq. 2021;12:5715-5722.
4. Motisuki C, Santos□Pinto L, Giro EM. Restoration of severely decayed primary incisors using indirect composite resin restoration technique. International journal of paediatric dentistry. 2005 ;15(4):282-6.
5. Khamisi N, Fathi A, Yari A. Antimicrobial resistance of Staphylococcus aureus isolated from dental plaques. Academic Journal of Health Sciences. 2022;37(1):136-140.
6. Chunawalla YK, Zingade SS, Bijle MN, Thanawalla EA. Glass Fibre Reinforced Composite Resin Post & Core In Decayed Primary Anterior Teeth–A Case Report. International Journal of Clinical Dental Science. 2011 4;2(1).
7. Malekafzali B, Beheshti M, Mirkarimi M, Ahmadi R. Treatment of early childhood caries: A literature review. Journal of Islamic Dental Association of Iran. 2010;21(4):297-306.
8. Colak H, Dülgergil CT, Dalli M, Hamidi MM. Early childhood caries update: A review of causes, diagnoses, and treatments. J Nat Sci Biol Med. 2013;4(1):29-38.
9. Hamrah MH, Mokhtari S, Hosseini Z, Khosrozadeh M, Hosseini S, Somaya Ghafary E, et al. Evaluation of the Clinical, Child, and Parental Satisfaction with Zirconia Crowns in Maxillary Primary Incisors: A Systematic Review", International Journal of Dentistry. 2021; 2021:7877728.
10. Maalekipour M, Safari M, Barekatain M, Fathi A. Effect of Adhesive Resin as a Modeling Liquid on Elution of Resin Composite Restorations. International Journal of Dentistry. 2021;2021:1-9.
11. Vafaei A, Ranjkesh B, Løvschall H, Erfanparast L, Jafarabadi MA, Oskouei SG, Isidor F. Survival of Composite Resin Restorations of severely Decayed Primary Anterior Teeth retained by Glass Fiber Posts or Reversed-orientated Metal Posts. Int J Clin Pediatr Dent 2016;9(2):109-113.
12. Schwartz RS, James W. Post Placement and Restoration of Endodontically Treated Teeth: A Literature Review Journal of endodontics 2004; 30(5):289-301.
13. Bijelic J, Garoushi S, Vallittu PK, Lassila LV. Short fiber reinforced composite in restoring severely damaged incisors. Acta Odontologica Scandinavica. 2013 ;71(5):1221-31.
14. Bonchev A, Radeva E, Tsvetanova N. Fiber Reinforced Composite Posts - A Review of Literature. Int J Sci Res 2017;6(10):1887–1893.
15. Faria AC, Rodrigues RC, de Almeida Antunes RP, de Mattos MD, Ribeiro RF. Endodontically treated teeth: characteristics and considerations to restore them. J Prosthodon Res. 2011;55(2):69-74.
16. Shah S, Bargale S, Anuradha KVR, Patel N. Posts in Primary Teeth-A Sile for Better Smile. J Adv Med Dent Scie Res 2016;4(1):58-64.(14-18)
17. Mosharrafian S, Sharifi Z. Comparison of Push-Out Bond Strength of Two Bulk-Fill and One Conventional Composite to Intracanal Dentin in Severely Damaged Primary Anterior Teeth. J Dent (Tehran). 2016;13(3):207-214

18. Mosharraf R, Molaei P, Fathi A, Isler S. Investigating the Effect of Nonrigid Connectors on the Success of Tooth-and-Implant-Supported Fixed Partial Prostheses in Maxillary Anterior Region: A Finite Element Analysis (FEA). International Journal of Dentistry. 2021;2021:1-12.
19. Demiryürek EÖ, Külünk Ş, Saraç D, Yüksel G, Bulucu B. Effect of different surface treatments on the push-out bond strength of fiber post to root canal dentin. Oral Surgery, Oral Medicine, Oral Pathology, Oral Radiology, and Endodontology. 2009 ;108(2):e74-80.
20. Bayrak S, Tunc ES, Tuloglu N. Polyethylene fiber–reinforced composite resin used as a short post in severely decayed primary anterior teeth: A case report. Oral Surgery, Oral Medicine, Oral Pathology, Oral Radiology, and Endodontology. 2009 ;107(5):e60-4.
21. Falakaloğlu S, Adıgüzel Ö, Özdemir G. Root canal reconstruction using biological dentin posts: A 3D finite element analysis. J Dent Res Dent Clin Dent Prospects. 2019;13(4):274-280.
22. Yaseen SM, Reddy VS. Comparative evaluation of shear bond strength of two self-etching adhesives (sixth and seventh generation) on dentin of primary and permanent teeth: An in vitro study. Journal of Indian Society of Pedodontics and Preventive Dentistry. 2009 ;27(1):33.
23. Afshar H, Baradaran Nakhjavani Y, Rahro Taban S, Baniameri Z, Nahvi A. Bond Strength of 5(th), 6(th) and 7(th) Generation Bonding Agents to Intracanal Dentin of Primary Teeth. J Dent (Tehran). 2015;12(2):90-98.
24. Maalekipour M, Safari M, Barekatain M, Fathi A. Effect of Adhesive Resin as a Modeling Liquid on Elution of Resin Composite Restorations. International Journal of Dentistry. 2021;2021:1-9.
25. Ghasemi E, Fathi AH, Parvizinia S. Effect of three disinfectants on dimensional changes of different impression materials. Journal of Iranian Dental Association. 2019;31(3):169-76.
26. Ashtiani AH, Mardasi N, Fathi A. Effect of multiple firings on the shear bond strength of presintered cobalt-chromium alloy and veneering ceramic. The Journal of Prosthetic Dentistry. 2021;126(6):803-e1.
27. Jafari Navimipour E, Pournaghi Azar F, Keshipour S, Nadervand S. Thermal Stability and Monomer Elution of Bulk Fill Composite Resins Cured from Different Irradiation Distances. Front Dent. 2021:18:9.
28. Pongprueksa P, De Munck J, Duca RC, Poels K, Covaci A, Hoet P, et al. Monomer elution in relation to degree of conversion for different types of composite. J Dent. 2015 ;43(12):1448-55.
29. Bucuta S, Ilie N. Light transmittance and micro-mechanical properties of bulk fill vs. conventional resin based composites. Clinical oral investigations. 2014 ;18(8):1991-2000.
30. Ilie N, Hickel R. Investigations on a methacrylate-based flowable composite based on the SDR™ technology. Dental Materials. 2011 ;27(4):348-55.
31. Fathi A, Salehi A. Antimicrobial resistance properties of Helicobacter pylori strains isolated from dental plaque and saliva samples. Academic Journal of Health Sciences. 2021;36 (4):51-55.
32. Ghorbani F, Gheisari E, Dehkordi FS. Genotyping of vacA alleles of Helicobacter pylori strains recovered from some Iranian food items. Trop J Pharm Res. 2016;15(8):1631-6.
33. Dehkordi FS. Prevalence study of Bovine viral diarrhea virus by evaluation of antigen capture ELISA and RT-PCR assay in Bovine, Ovine, Caprine, Buffalo and Camel aborted fetuses in Iran. AMB Express. 2011;1(1):1-6.
34. Dehkordi FS, Parsaei P, Saberian S, Moshkelani S, Hajshafiei P, Hoseini SR, Babaei M, Ghorbani MN. Prevalence study of Theileria annulata by comparison of four diagnostic Techniques in shouthwest Iran. Bulgar J Vet Med. 2012;15(2): 123-130.
35. Dehkordi FS, Haghighi Borujeni MR, Rahimi E, Abdizadeh R. Detection of Toxoplasma gondii in raw caprine, ovine, buffalo, bovine, and camel milk using cell cultivation, cat bioassay, capture ELISA, and PCR methods in Iran. Foodborne Pathog Dis. 2013;10(2):120-5.
36. Dehkordi FS, Khamesipour F, Momeni M. Brucella abortus and Brucella melitensis in Iranian bovine and buffalo semen samples: The first clinical trial on seasonal, Senile and geographical distribution using culture, conventional and real-time polymerase chain reaction assays. Kafkas Univ Vet Fak Derg. 2014;20(6):821-8.
37. Dehkordi FS, Valizadeh Y, Birgani TA, Dehkordi KG. Prevalence study of Brucella melitensis and Brucella abortus in cow's milk using dot enzyme linked immuno sorbent assay and duplex polymerase chain reaction. J Pure Appl Microbiol. 2014;8(2):1065-9.
38. Ebadian B, Fathi A, Savoj M. In Vitro Evaluation of the Effect of Different Luting Cements and Tooth Preparation Angle on the Microleakage of Zirconia Crowns. International Journal of Dentistry. 2021;2021:1-7.
39. Barakati B, Khodadadi R, Asadi P, Fathi A. Evaluate The Effect Of Various Titanium Abutment Modifications On The Behavior Of Peri-Implant Soft Tissue Healing, Inflammation, And Maintenance: A Systematic Review And Meta-Analysis. Turkish Onilne Journal of Qualitative Inquiry. 2021; 12:11401-11410.
40. Abolhasani M, Ghasemi E, Fathi AH, Hayatizadeh MJ. Color Change of Ceramill Zolid FX Following Abrasion with/ without Toothpaste. Journal of Iranian Dental Association. 2021;33(3):51-7.
41. Ilie N, Schöner C, Bücher K, Hickel R. An in-vitro assessment of the shear bond strength of bulk-fill resin composites to permanent and deciduous teeth. Journal of dentistry. 2014 ;42(7):850-5.
42. Pasdar N, Seraj B, Fatemi M, Taravati S. Push-out bond strength of different intracanal posts in the anterior primary teeth according to root canal filling materials. Dent Res J (Isfahan). 2017 ; 14(5): 336–343.32-Dent Res J (Isfahan). 2017 ; 14(5): 336–343.
43. Oskoee PA, Navimipour EJ, Oskoee SS, Bahari M, Pournaghiazar F. Effect of different adhesion strategies on push-out bond strength of fiber reinforced composite posts. African journal of Biotechnology. 2011;10(76):17593-8.
44. Sardella TN, de Castro FL, Sanabe ME, Hebling J. Shortening of primary dentin etching time and its implication on bond strength. Journal of dentistry. 2005 ;33(5):355-62.
45. Uekusa S, Yamaguchi K, Miyazaki M, Tsubota K, Kurokawa H, Hosoya Y. Bonding efficacy of single-step self-etch systems to sound primary and permanent tooth dentin. Operative dentistry. 2006 ;31(5):569-76.
46. Dumami A, Yilmaz S, Ozbilen G, Gurbuz CC, Yoldas O. Comparative Evaluation of Push-Out Bond Strength of Bulk-Fill versus DualCure Resin Composites in Root Canals. Oral Health and Dental Management. 2016;15(4)212-216.
47. Bolaños-Carmona V, González-López S, Briones-Luján T, De Haro-Muñoz C, José C. Effects of etching time of primary dentin on interface morphology and microtensile bond strength. Dental Materials. 2006 ;22(12):1121-9.
48. Burke FJ, McCaughey AD. The four generations of dentin bonding. American Journal of Dentistry. 1995 ;8(2):88-92.

ARTICLE / INVESTIGACIÓN

Biosynthetic of Green Zinc Oxide Nanoparticles with Effect on Cancer Cell Line Hela

Mohanad W. Mahdi Alzubaidy*, Mohammed Nazar Hussain

DOI. 10.21931/RB/2023.08.02.22

Biology Department, College of Education for Pure Science, University of Diyala, Iraq.
Corresponding author: mohanad@uodiyala.edu.iq

Abstract: The cytotoxic impact of biosynthetic zinc oxide nanoparticles (ZnONPs) was investigated using Vitex agnus-castus, which has been shown to have Effective compounds that suppress cancer cell proliferation. Zinc oxide nanoparticles were biosynthesized in the laboratories of the Biology department /College of Education for the Pure Sciences /University of Diyala. The phenotypic and structural characteristics of biosynthetic nanoparticles were identified using scanning electron microscopy (SEM). The majority of ZnONPs are dense and spherical in shape, with diameters ranging from (20-61) nm, and were discovered on the cervical cancer cell line Hela and compared to the normal line Human Foreskin Fibroblast cells (HFF) using the MTT stain test (3-(4,5-dimethylthiazol-2-yl)-2,5-diphenyltetrazolium). Cytotoxicity experiments were conducted at the Iraqi Center for Cancer Research / Al-Mustansiriya University. This study showed inhibitory activity on Hela cervical cancer cells, where the highest inhibition rate reached 93.6% at a concentration of 200 µg/ml. This raises the prospect of finding a viable therapy for cervical cancer (Hela) or any other malignancy using nanoparticle manufacturing technologies.

Key words: Biosynthetic, Green nanoparticles, Cancer cell, Hela, GC-MS.

Introduction

Cervical cancer is the fourth most frequent disease and the top cause of death among women worldwide, despite being highly preventable. Cervical cancer is frequently the primary cause of cancer-related sickness and mortality in low-income nations[1,2].

Green nanoparticle synthesis using biological systems, mainly plant extracts, is an emerging subject in nanotechnology. Biosynthetic nanoparticles have piqued attention owing to intrinsic benefits such as speed, environmental friendliness, and cost-effectiveness[3]. Nanobiotechnology represents the integration of biotechnology and nanotechnology to develop green, synthetic and environmentally friendly technology for nanomaterials formulations[4,5]. Advances in using metal oxide nanoparticles in environmental applications have stimulated the need to synthesize them using green chemistry techniques across ecologically sensitive biological systems[6,7].

Synthesis of ZnONPs nanoparticles from biological pathways is preferred due to the natural bio-reducing property that reduces the use of toxic chemicals and their exposure to the environment when compared with physical and chemical methods[8]. Among the various inorganic nanoparticles, ZnONPs are attracting more and more attention due to their large bandwidth, high excitation binding energy, simplicity, easy manufacturing, biologically safe, non-toxic, biocompatible, eco-friendly and eco-friendly. Zinc oxide nanoparticles are readily soluble in biological fluids and assemble quickly under different physiological conditions[9].

The effectiveness of biosynthesized ZnONPs as an anticancer agent is dose-dependent, which means that increasing the concentration of ZnONPs increases its efficacy against cancer cells it does not affect normal cells. Using nanoparticles for targeted drug delivery has been an exciting research opportunity for effective cancer treatment. Targeted drug delivery to cancer cells will reduce drug dose for treatment and its other side effects[10]. Nanotechnology in this field aims to develop the therapeutic effect of drug molecules, where drug delivery methods are of great importance in medicine because it achieves more significant success in influencing the biological activity of the cell and the genetic material as well as gene expression[11-13].

Materials and methods

Extract preparation

Vitex agnus-castus was prepared from Krayat nurseries in Baghdad governorate and planted in the house garden. The species was confirmed by classifying it by the botanical herbarium at the College of Science / University of Baghdad, based on the book Flora of Iraq. The leaves were collected and washed with distilled water to remove particulate matter, then dried at room temperature for a week. The dried leaves were ground into a fine powder, and the extract was prepared by boiling 25 g of the powder in 250 ml of distilled water for 15 minutes. Then the extract was filtered using NO: 0.1 filter paper. The filtered extract was stored in a refrigerator at 4°C for later use in the biosynthesis of ZnONPs. Also, an alcoholic extract of the plant was prepared for the detection of the active compounds by using a gas chromatography-integrated mass spectrometer (GC-MS)

Citation: Mohanad W. Mahdi Alzubaidy, Mohammed Nazar Hussain. Biosynthetic of Green Zinc Oxide Nanoparticles with Effect on Cancer Cell Line Hela. Revis Bionatura 2023;8 (2) 22. http://dx.doi.org/10.21931/RB/2023.08.02.22
Received: 2 January 2023 / **Accepted:** 19 April 2023 / **Published:** 15 June 2023

Publisher's Note: Bionatura stays neutral with regard to jurisdictional claims in published maps and institutional affiliations.

device for the alcoholic extract of leaves. The leaves were extracted using the saxolith system and using hexane and methanol as solvents, respectively, according to method[14] with some modifications. 100 g of leaf powder was placed in a filter paper made in the form of a funnel and closed to avoid the exit of the vegetable powder. Then it is placed in a saxolithic apparatus, and 500 ml of solvent is placed on it for 24 hours. Then the solution was concentrated by a rotary evaporator, and the solvent was separated, as a dark brown oil was produced.

Biosynthesis of (ZnONPs)

According to a method described by Pillai et al. (2020), modifications were made to 100 ml of the previously prepared plant extract heated to 60-70°C on a magnetic stirrer. When the temperature reaches 60 degrees Celsius, 10 grams of zinc nitrate Zn(NO3)2 is added. It is boiled until it turns into a creamy white paste. After that, the dough is washed with distilled water and placed in a hot oven at 400 ° C for two hours. Then a white powder will be formed from ZnONPs loaded with active compounds from the plant extract[15], as shown in Figure (1).

Scanning Electron Microscope (SEM)

The biosynthetic ZnONPs assays were carried out to show the phenotypic and structural properties of the biosynthetic particles using scanning electron microscopy (SEM) at Kashan University - Iran. The device works on imaging samples with a magnification of 25-250000 times and scans samples with very high accuracy. The focused beam interacts with the samples by means of electrons that collide with the sample atoms and transmit signals that evaluate the topography. The detectors turn the electron intensity into a digital voltage that is stored. Three-dimensional images are composed of a size that can measure 1 to 5 nanometers[17].

Cytotoxicity Assays

The cell lines were placed in a tissue culture vessel of 25 cm3 in size. The container includes Roswell Park Memorial Institute (RPMI-1640) culture medium and 10% calf fetal serum. The container was placed on the cell suspension and culture medium in a 5% CO2 incubator at 37 °C for 24 hours. After that, the container with the cell suspension is taken out of the incubation, and it is confirmed that there is no contamination in the cell culture through an inverted microscope. Secondary cultures are formed and left in the incubator for 24 hours, after which they are examined again with an inverted microscope to ensure their growth and the absence of contamination in the medium. Then the cells were transferred to the growth cabin, the used culture medium was emptied, and the cells were washed using Phosphate Buffer Saline. The washing process was repeated twice for 10 minutes each time. A sufficient amount of Trypsin/Versine enzyme was added to cover the cells and placed in the incubator for 30-60 seconds at a temperature of 37°C. Then it is noticed that it has transformed from a group of cells compact in one layer to single cells that are not compact after disengaging them with the tissue culture vessel. The action of the Trypsin/Versine enzyme is stopped by adding a fresh culture medium containing 10% serum. The test was performed by 3-(4,5-dimethylthiazol-2-yl)-2,5-diphenyltetrazolium bromide (MTT) dye[18]. using 96-hole Cell culture plates, each line was cultured at 10,000 cells/pit using an automatic Micotiter plat for tissue culture.

After 24 hours, the monolayer cells were confirmed. Biosynthetic ZnONPs nanoparticles were added at various concentrations for 72 hours. After exposure, the cells were washed three times with phosphate buffer saline after the culture medium was taken out. The culture plate was then incubated at 37 °C after 30 l of MTT dye was added at a concentration of 2 mg/ml. For 3 hours, then 25 µl of DMSO (Dimethyl Sulphoxide) solution was added to each pit for 10 minutes. The culture plate was incubated again at 37°C, after which the absorbance was measured on a microplate reader (ELISA) at 492 nm. Then the percentage of cytotoxicity was calculated after that, the rate of cytotoxicity was calculated using the following equation.

Cytotoxicity killing % = CO.O mean – txO.Omean / CO.O mean x 100

where :

CO.O mean: Optical density of cells that are not treated with nanomaterial

txO.Omean: Optical density of cells which are treated with nanomaterial

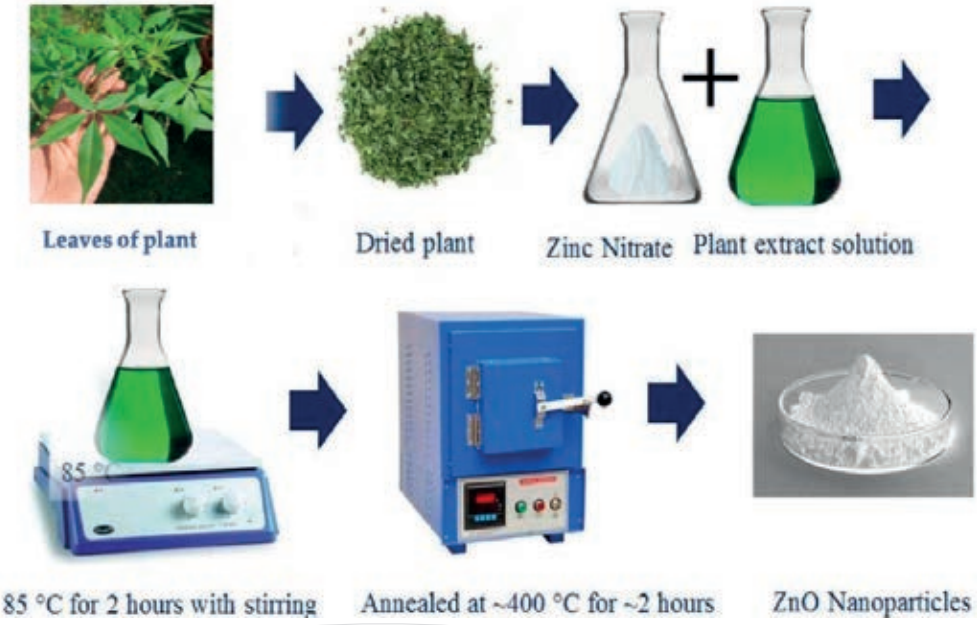

Figure 1. Biosynthesis of zinc oxide nanoparticles[16].

Statistical Analysis

The data attained by using the unpaired t-test were analyzed using the statistical software (Graphpad Prism 6). The values were estimated as (arithmetic mean ± standard error) for the three replicates with a significant difference at the significance level $P < 0.05$ according to the statistical package used in[19].

Results

GC-Mass assay results for essential oils

The individual components of the leaf extract were identified by computer matching with the commercial Wiley GC/MS mass spectral libraries, the Mass Finder 3 library, and the Baser library for the essential oil components which includes more than 3,200 authentic compounds with mass spectra and retention data of pure oil. The results appeared in the presence of active compounds in the extract as shown in Table (1).

(SEM) Scanning Electron Microscope

The surface morphology of the biosynthesized ZnONPs was characterized using (SEM) as in Fig. (2). The image has a magnification power (150 KX). It can be seen that most of the ZnONPs are dense and spherical in shape, their sizes range between (20-61) nm.

No	Compound	Chemical formula	Structural formula
1	Phytol	C20H40O	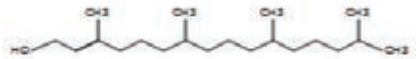
2	Phenol, 2-hexadecy	C22H38O	
3	Vitamin E	C29H50O2	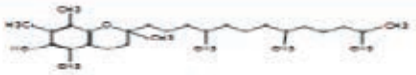
4	Kolavelool	C20H34O	
5	6-Octen-1-ol, 3,7-dimethyl-, propanoate	C13H24O2	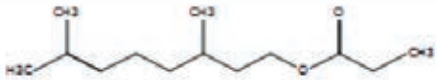

Table 1. Shows the active compounds of Vitex agnus-castus leaf extract in the GC-Mass system.

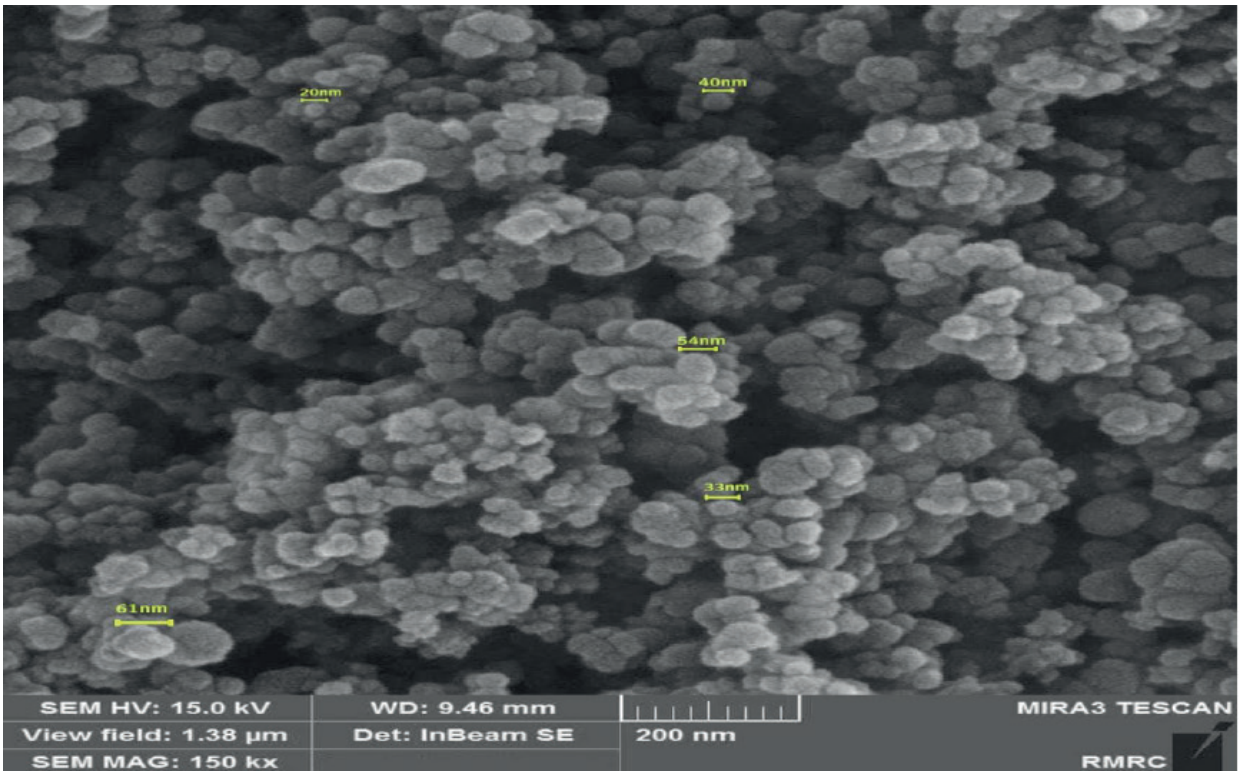

Figure 2. SEM image showing biosynthesized ZnONPs.

Cytotoxicity Experiments

The cytotoxicity of cervical cancer Hela was investigated by comparison with the normal cell line HFF using various concentrations of biosynthetic zinc oxide nanoparticles. The cytotoxicity was investigated by reading the intensity of cell uptake using an ELISA device at wavelength 492 nm and calculating the percentage change in cell growth according to the following equation:

$$\text{Percentage change in growth} = \frac{\text{Optical density of drilling parameter} - \text{Optical density of drilling } control}{\text{Optical density for drilling control}} \text{ x100}$$

Percentage change in growth = x 100

The toxicological effect of various concentrations of biosynthetic ZnONPs on the growth of cervical cancer Hela cells was investigated and compared with the normal HFF line by calculating the optical density (0.D) values of cell growth after an exposure period of 72 hours and at a temperature of 37 °C in three replicates with eight various concentrations: (6.25), (12.5), (25), (50), (100), (200), (400), and (800) µg/ml. Cytotoxicity test was performed using MTT stain. Depending on the results of the average percentage inhibition as well as the percentage of cell vitality as shown in Figure (3), the inhibition in the vitality of cervical Hela cells increases as the percentage of inhibition increases with the increase in the concentration of biosynthetic ZnONPs. The results are shown in Figure (4), indicating shallow inhibition values for the viability of HFF cells when treated with biosynthetic ZnONPs. Table (2) shows the percentage of cell viability inhibition at each cervical cancer Hela cell concentration and its comparison with the regular HFF line.

The IC50 half-lethal dose of biosynthetic ZnONPs on cervical cancer cells was 35.74 µg/ml as shown in Figure (5). In the cells of the normal line, half of the lethal dose IC50 was 655.7 µg/ml as shown in Figure (6).

Discussion

GC-Mass assay results for essential oils were *Vitex agnus* - castus possesses a wide range of active chemical ingredients, including essential oils, flavonoids, iridoid glycosides, diterpenoids and phenolic compounds[20].

The results of (the SEM) Scanning Electron Microscope are most of the ZnONPs are dense and spherical in shape ranging in size from (20-61) nanometers; in another study, ZnO nanoparticles were synthesized using plant extracts, the researchers observed that the SEM images at room temperature and 90 °C had 50 nm and 40 nm size and spherical morphology[21,22].

The results in Table (2) showed a decrease in the vitality of the cells, and this decrease is inversely related to the concentration. The higher the engagement, the lower the vitality of the cells. The first decrease in the viability of cancer cells started at a concentration of 6.25 µg/ml on cervical cancer cells. Cell viability decreased to 92.86% in cervical cancer. Cell viability continues to decline as the concentration of biosynthetic ZnONPs increases. As the cell viability reaches 10.99% in cervical cancer cells at a concentration of 800 µg/ml. In normal cells, the cell viability reached 92.22% at a concentration of 800 µg/ml. This confirms that the biosynthetic zinc oxide nanoparticles have a toxic effect on cancer cells with low impact on normal cells. This is identical to what was stated in the results of the research by Latif and Alzubaidy (2021)[23]. Nanoparticles are used in nanomedicine that contribute to diagnosing and treating various diseases including cancer. The unique property of nanomedicine, that is, their high surface-to-volume ratio enables them to bind, absorb and transport small biomolecule such as DNA, RNA, drugs, proteins, and other molecules. to the target site, thus enhancing the efficacy of therapeutic agents[24].

The results proved that the biosynthesized ZnONPs can cause phenotypic changes in the shape, size and number of cancer cells. Still, these changes occurred at concentrations lower than the concentrations used for the physically prepared ZnONPs, as well as a higher rate of inhibition in using the biosynthetic ZnONPs. Cells after exposure to biosynthetic ZnONPs became non-adherent single cells after they were compact cells. The differentiation of these cells is due to the death of many cells and their loss of adhesion to each other, which leads to the death of many cancer cells, as shown in Figure (7). These results prove that the biosynthetic ZnONPs are more effective and inhibiting on cancer cell lines and safer, less expensive and easier to prepare than other methods (physical or chemical). These results are consistent with the findings of studies[22-26]. The cytotoxicity of biosynthetic ZnONPs may be due to the release of dissolved zinc ions within cells and the induction of reactive oxygen species (ROS). The increase in zinc ions also led to an imbalance in the activity of proteins and oxidative stress, thus killing the cell[27]. The cytotoxicity of biosynthetic ZnONPs is also due to the ability of these particles to slip into the nucleus, bind to the genetic material, and cause a disruption in cell functions, leading to cell death[28].

No	Concentrations	Decrease in cell viability	
		Cervical cancer (Hela)	Normal line HFF
1	µg/ml6.25	% 92.86	% 100 +
2	µg/ml12.5	% 86.85	% 100 +
3	µg/ml25	% 69.18	% 100 +
4	µg/ml50	% 19.18	% 49
5	µg/ml100	% 10.53	% 44.48
6	µg/ml200	% 6.4	% 46.24
7	µg/ml400	% 6.4	% 62.07
8	µg/ml800	% 10.99	% 92.22

Table 2. Shows the percentage of decrease in cell viability in each cell line at different concentrations of biosynthetic ZnONPs.

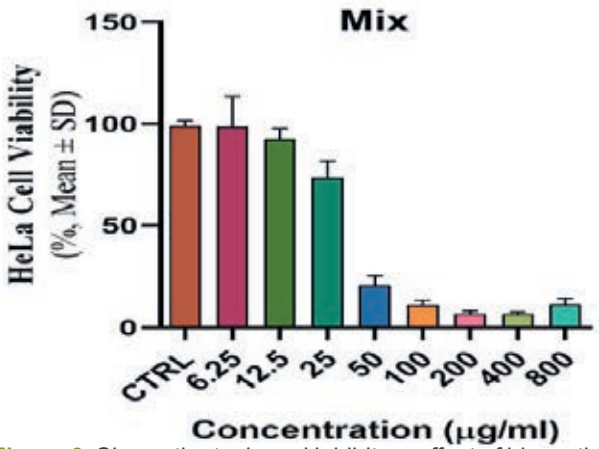

Figure 3. Shows the toxic and inhibitory effect of biosynthetic ZnONPs on cervical cancer Hela cells.

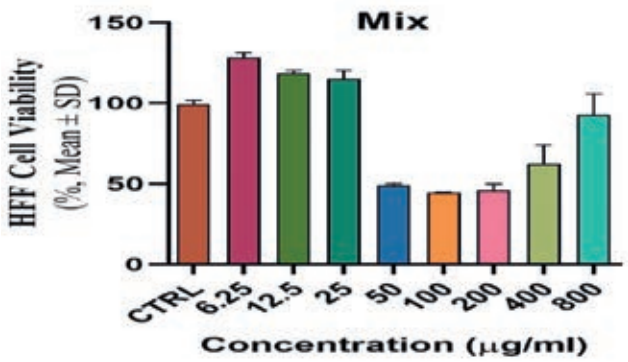

Figure 4. Shows the toxic and inhibitory effect of biosynthetic ZnONPs on HFF normal line cells.

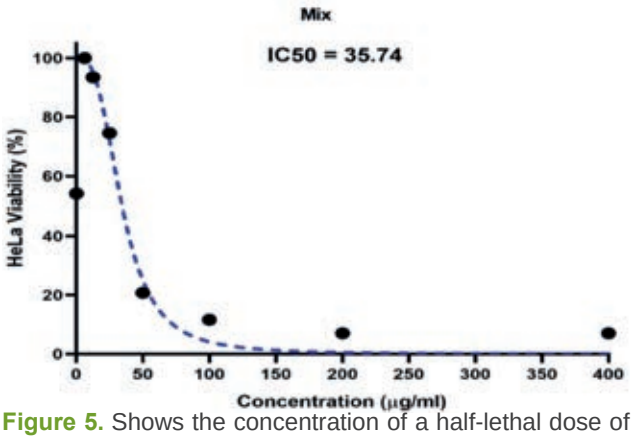

Figure 5. Shows the concentration of a half-lethal dose of biosynthetic ZnONPs on cervical cancer Hela cells.

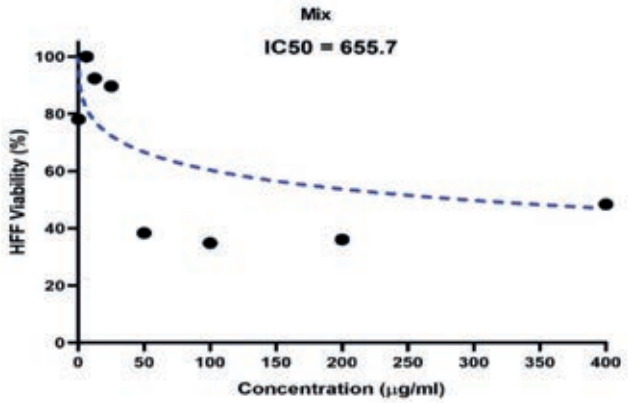

Figure 6. Shows the concentration of half the lethal dose of biosynthetic ZnONPs on normal HFF cells.

Conclusions

The process of using plant extracts in the biosynthesis of nanoparticles had high activity in inhibiting cancer cells because of its unique properties represented by considering the active substances in the plant as a reducing agent. It can be considered as one of the most environmentally friendly methods. Biosynthesis is safer for normal, uninfected cells. This gives hope to discover a successful treatment to eliminate the most common types of cancer, including cervical cancer (Hela).

Acknowledgments

Thanks and appreciation to the Deanship of the College of Education for Pure Sciences and the Deanship of the Iraqi Institute for Cancer Research and Medical Genetics / Al-Mustansiriya University. For their help and for facilitating all the requirements for conducting the study.

Bibliographic references

1. Castle, P. E., Einstein, M. H., and Sahasrabuddhe, V. V. Cervical cancer prevention and control in women living with human immunodeficiency virus. CA: a cancer journal for clinicians (2021). https://acsjournals.onlinelibrary.wiley.com/doi/full/10.3322/caac.21696
2. Preciado, C., & Janeta, P. V. Bionatura Conference Series Vol 2. No 1. 2019; https://www.revistabionatura.com/files/CS-2019.02.01.25---Bionatura.pdf
3. Jadoun, S., Arif, R., Jangid, N. K., and Meena, R. K. . Green synthesis of nanoparticles using plant extracts: A review. Environmental Chemistry Letters(2021) , 19(1), 355-374;https://link.springer.com/article/10.1007/s10311-020-01074-x
4. Buazar, F., Baghlani□Nejazd, M. H., Badri, M., Kashisaz, M., Khaledi□Nasab, A., & Kroushawi, F. Facile one□pot phytosynthesis of magnetic nanoparticles using potato extract and their catalytic activity. Starch□Stärke, (2016), 68(7-8), 796-804. https://onlinelibrary.wiley.com/doi/abs/10.1002/star.201500347
5. Mohanad W. Mahdi Alzubaidy. Evaluation the Breast Cancer Cell Line DNA Damage by Biosynthetic Silver-Green Nanoparticles. Texas Journal of Agriculture and Biological Sciences, (2022), 3, 14–19. https://zienjournals.com/index.php/tjabs/article/view/1254
6. Selim, Y. A., Azb, M. A., Ragab, I., & Abd El-Azim, M. H. Green synthesis of zinc oxide nanoparticles using aqueous extract of Deverra tortuosa and their cytotoxic activities. Scientific reports, (2020), 10 (1), 1-9.https://nature.com/articles/s41598-020-60541-1
7. Dahoumane, S. A., Mechouet, M., Alvarez, F. J., Agathos, S. N., & Jeffryes, C. (2016). Microalgae: An outstanding tool in nanotechnology. Bionatura, 1(4), 196-201; http://revistabionatura.com/files/7-Microalgae--An-outstanding-tool-in-nanotechnology.pdf
8. Aldalbahi, A., Alterary, S., Ali Abdullrahman Almoghim, R., Awad, M. A., Aldosari, N. S., Fahad Alghannam, S., ... & Abdulrahman Alrashed, R. Greener synthesis of zinc oxide nanoparticles: Characterization and multifaceted applications. Molecules, (2020), 25 (18), 4198;https://mdpi.com/1420-3049/25/18/4198

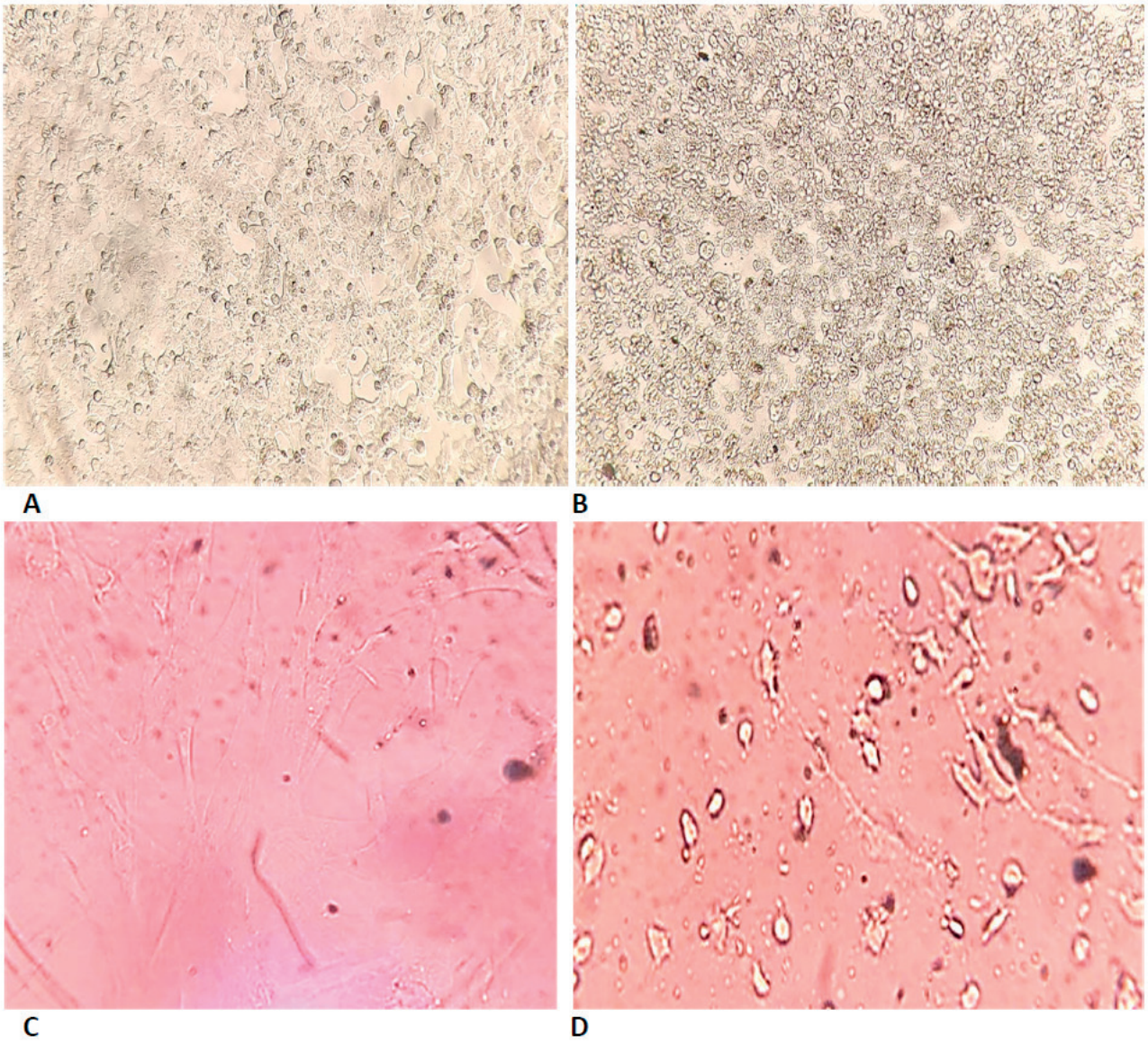

Figure 7. Shows the cytotoxicity of biosynthesized ZnONPs on cell lines using MTT dye for 72 hours at 37°C. (A) represents cervical cancer Hela cells which are not treated with biosynthetic ZnONPs. (B) represents cervical cancer Hela cells treated with biosynthetic ZnONPs at a 50 µg/ml concentration. (C) represents normal HFF cells untreated with biosynthetic ZnONPs. (D) Represents normal HFF cells treated with biosynthetic ZnONPs at a 25 µg/mL concentration.

9. Hamrayev, H., Shameli, K., and Yusefi, M. Preparation of zinc oxide nanoparticles and its cancer treatment effects: A review paper. Journal of Advanced Research in Micro and Nano Engineering, (2020), 2 (1), 1-11 https://akademiabaru.com/submit/index.php/armne/article/view/2962
10. Wu, H. and J. Zhang. "Chitosan-Based Zinc Oxide Nanoparticle for Enhanced Anticancer Effect in Cervical Cancer: A Physico-chemical and Biological Perspective." Saudi Pharm J 26, (2018) no: 205-10. http://dx.doi.org/10.1016/j.jsps.2017.12.010
11. Ziad T. Khodair, Mohanad W. Mahdi Alzubaidy, Asmaa M. Salih Almohaidi, Ammar Ahmed Sultan, Sana M. H. AL-Shimmary, and Sarah S. Albusultan. Synthesis of copper oxide nanoparticles (CuO-NPs) and its evaluation of antibacterial activity against P. aeruginosa biofilm gene's. Technologies and Materials for Renewable Energy, Environment and Sustainability AIP Conf. Proc. 2190, 020006-1–020006-7; https://doi.org/10.1063/1.5138492 Published by AIP Publishing. (2019), 978-0-7354-1937-7/.
12. Mohanad W. Mahdi Alzubaidy, Asmaa M. Salih Almohaidi, Ammar Ahmed Sultan, and Sana M. H. ALShimmary. Virulence gene of Pseudomonas aeruginosa with nanoparticle. AIP Conf. Proc. 2123, 020039-1–020039-9; https://doi.org/10.1063/1.5116966 Published by AIP Publishing. (2019), 978-0-7354-1863-9/.
13. Mohanad W. Mahdi Alzubaidy. SILVER NANOPARTICLES PREPARED BY SOL-GEL METHOD EFFECT ON ESCHERICHIA COLI AS ANTIMICROBIAL. International Scientific Research Journal (WoS) Vol. 3 (2022), No. 3 https://doi.org/10.17605/OSF.IO/UCTVJ.
14. Uddin, S., Alnsour, L., Segun, P., Servi, H., Celik, S., Göktürk, R. S., ... & Sarker, S. D. Flavonoids from two Turkish Centaurea species and their chemotaxonomic implications. Trends in Phytochemical Research, 1,(2017),(4), 243-248. http://tpr.iaushahrood.ac.ir/article_535458_4bd1d338c5035fbec3291473fba50bdc.pdf
15. Pillai, A. M., Sivasankarapillai, V. S., Rahdar, A., Joseph, J., Sadeghfar, F., Rajesh, K., & Kyzas, G. Z. Green synthesis and characterization of zinc oxide nanoparticles with antibacterial and antifungal activity. Journal of Molecular Structure, (2020), 1211, 128107. https://sciencedirect.com/science/article/abs/pii/S0022286020304324
16. Barzinjy, A. A Characterization of ZnO Nanoparticles Prepared from Green Synthesis Using Euphorbia Petiolata Leaves. Eurasian Journal of Science & Engineering, (2019), 4(3), 74-83. http://eprints.tiu.edu.iq/645/

17. Řiháček, T., Horák, M., Schachinger, T., Mika, F., Matějka, M., Krátký, S., ... & Müllerová, I. Beam shaping and probe characterization in the scanning electron microscope. Ultramicroscopy, 225, (2021), 113268. https://sciencedirect.com/science/article/abs/pii/S0304399121000589
18. Wu, S., & Shah, D. K.. Determination of ADC cytotoxicity in immortalized human cell lines. In Antibody-Drug Conjugates (2020) , (pp. 329-340). Humana, New York, NY. https://link.springer.com/protocol/10.1007/978-1-4939-9929-3_23
19. Mitteer, D. R., & Greer, B. D. Using GraphPad Prism's Heat Maps for Efficient, Fine-Grained Analyses of Single-Case Data. Behavior Analysis in Practice, (2022), 1-10.https://link.springer.com/article/10.1007/s40617-021-00664-7.
20. Ababutain, I. M., & Alghamdi, A. I. In vitro anticandidal activity and gas chromatography-mass spectrometry (GC-MS) screening of Vitex agnus-castus leaf extracts. PeerJ, 9, (2021), e10561 .https://peerj.com/articles/10561/
21. Gur, T., Meydan, I., Seckin, H., Bekmezci, M., & Sen, F. Green synthesis, characterization and bioactivity of biogenic zinc oxide nanoparticles. Environmental (2022), Research, 204, 111897. https://sciencedirect.com/science/article/abs/pii/S0013935121011920
22. Alzubadiy, M. W. M., Almohaidi, A. M. S., Sultan, A. A., & Abdulhameed, L. Q. Evaluation of E-selectin rs 5367 C/T Polymorphism in Iraqi Diabetic Foot patients. Paper presented at the Journal of Physics: Conference Series(2019). https://iopscience.iop.org/article/10.1088/1742-6596/1294/6/062021/meta
23. Latif, B. M. A., & Alzubaidy, M. W. M. Effect of Zinc Oxide Nanoparticles On Activity of Cell Line (B16) Causes Skin Cancer. NVEO-NATURAL VOLATILES & ESSENTIAL OILS Journal| NVEO, (2021), 472-478. https://nveo.org/index.php/journal/article/view/3645.
24. Chaturvedi, V. K., Singh, A., Singh, V. K., & Singh, M. P. Cancer nanotechnology: a new revolution for cancer diagnosis and therapy. Current drug metabolism, (2019). 20(6), 416-429.
25. Vijayakumar, S., Chen, J., González-Sánchez, Z. I., Durán-Lara, E. F., Divya, M., Shreema, K., ... & Vaseeharan, B. Anti-Colon Cancer and Antibiofilm Activities of Green Synthesized ZnO Nanoparticles Using Natural Polysaccharide Almond Gum (Prunus dulcis). Journal of Cluster Science, (2021) , 1-12. https://link.springer.com/article/10.1007/s10876-021-02205-2
26. Abdelhakim, H. K., El□Sayed, E. R., & Rashidi, F. B.. Biosynthesis of zinc oxide nanoparticles with antimicrobial, anticancer, antioxidant and photocatalytic activities by the endophytic Alternaria tenuissima. Journal of Applied Microbiology, (2020), 128(6) 1634-1646. https://sfamjournals.onlinelibrary.wiley.com/doi/abs/10.1111/jam.14581.
27. Hamrayev, H., Shameli, K., & Korpayev, S.. Green Synthesis of Zinc Oxide Nanoparticles and Its Biomedical Applications: A Review. Journal of Research in Nanoscience and Nanotechnology, 1 ,(2021), (1) 62-74. https://akademiabaru.com/submit/index.php/jrnn/article/view/3595
28. Wang, J., Lee, J. S., Kim, D., & Zhu, L.. Exploration of zinc oxide nanoparticles as a multitarget and multifunctional anticancer nanomedicine. ACS applied materials & interfaces, (2017), 9(46) 39971-39984. https://pubs.acs.org/doi/abs/10.1021/acsami.7b11219.

ARTICLE / INVESTIGACIÓN

Molecular identification and Phylogenetic-Tree Analysis of Hard Ticks from wild and domestic cat *Felidae* in Iraq

Afkar Muslim Hadi, Hind Dyia Hadi*, Suhad Yasin Jassim

DOI. 10.21931/RB/2023.08.02.23

Iraq Natural History Research Center and Museum, University of Baghdad, Iraq.
Corresponding author: hinddhiaa86@gmail.com

Abstract: A total of 13 samples of domestic cat *Felis cattus* (Linnaeus, 1758) and 9 samples of wild cat *Felis chaus furax* (de Winton, 1898) of the Felidae Family were trapped and examined to detect the hard ticks. The areas of the collection were: Baghdad, Al-Rashidiya, Tharthar, Nahrawan, AL-Mahmoudiya (middle of Iraq) and AL-Haretha (south of Iraq), Mosul (north of Iraq). The results of the current study revealed that four species belong to two genera of hard ticks: *Haemaphysalis sp*. (Koch, 1844), *Rhipicephalus turanicus* (Morel, 1969), *Rhipicephalus sanguineus* (Neumann, 1904) and *Rhipicephalus appendiculatus* (Santos, 1955). The rates and the density of infestation were discussed. The current study aimed to clarify the infestation difference between domestic and wild cats with hard ticks (3, 14.88) because domestic cats enjoy human attention, as they live close to him. The current study identified the *Rhipicephalus appendiculatus* for the first time in Iraq from domestic cat *Felis cattus*.

Key words: Felidae, *Haemaphysalis*, Ixodidae, *Rhipicephalus*, wild cat.

Introduction

Hard ticks were belonging to the Family Ixodidae consisting of 700 species. They have scutum or "hard shield" in the dorsal side of the body; therefore, they are called hard ticks[1] Tick usually carry many pathogenic microorganisms and parasites that cause diseases for both humans and animals[2] These may be bacteria, helminths, protozoa and viruses[3,4] In Iraq, (5) revealed to the endemic area of Theileriosis and Babesiosis which transmitted by ticks. The current study aims to investigate a phenotypic description of the species of ticks that infest the domestic and wild cat (Family: Felidae). Second: look at tick biodiversity and complete an ecological map for the prevalence of tick species in domestic and wild animals.

Materials and methods

Collection of samples

A total of 13 samples of domestic cat *Felis cattus* (Linnaeus, 1758) and 9 samples of wild cat *Felis chaus furax* (de Winton, 1898) of the Felidae Family were trapped and examined to detect the hard ticks. The areas of the collection were: Baghdad, Al-Rashidiya, Tharthar, Nahrawan, AL-Mahmoudiya (middle of Iraq) and AL-Haretha (south of Iraq), Mosul (north of Iraq). The infestation of hard ticks was in the animals' dorsal, femoral and udder. All the collected ticks samples were kept in sterile tubes containing 70% alcohol, and the place of collection and the females and males were recorded on it. Ticks sampled were transported to the Iraq Natural History Research Center and Museum (INHM) for examining, diagnosing and photographed with a digital camera.

Results and discussion

33 (17 female &16 male) hard ticks samples were isolated from 13 domestic cats, and 134 (44 female & 90 male) hard ticks samples were isolated from 9 wild cats. The infestation rates were 84.61% and 100% in domestic and feral cats, respectively. The infestation density was 3, 14.88 in domestic and wild cats, respectively. (Table 1).

The results of the current study revealed that four species belong to two genera of hard ticks: *Haemaphysalis sp.* (Koch, 1844), *Rhipicephalus turanicus* (Morel, 1969), *Rhipicephalus sanguineus* (Neumann, 1904) and *Rhipicephalus appendiculatus* (Santos, 1955), as in table 2 and figures (1-4).

The biodiversity of ticks in domestic and wild animals is an important topic to study that highlights to the reservoir hosts which play a role in distribution of ticks and disease. The current study revealed a clear difference in the infestation density between domestic and wild cats with hard ticks (3, 14.88); domestic cats enjoy human attention, as they live close to him. Rhipicephalus turanicus appeared in both domestic and wild cats; this result agrees with (6,7). They revealed domestic cats infested with Rhipicephalus turanicus. Previously,(8) Recorded *Rhipicephalus turanicus* in wild cats. Rhipicephalus sanguineus was recorded in the Canidae previously in Iraq by (8,6), while (9) recorded it in dogs and humans in Daiwania city; so this recording in wild cat *Felis chaus furax* in the current study consider a new host for *R. sanguineus*. The present study identified the *Rhipicephalus appendiculatus* for the first time in Iraq from domestic cat *Felis cattus*; this result agrees with 10 who revealed to *R. appendiculatus* in feline (Sable). The current results recorded the *Haemaphysalis sp.* in wild cat *Felis chaus furax.* While (8,6) isolated *Haemaphysalis Adler* from the Wild jungle cat.

Citation: Muslim Hadi A, Dyia Hadi H, Yasin Jassim S. Molecular identification and Phylogenetic-Tree Analysis of Hard Ticks from wild and domestic cat Felidae in Iraq. Revis Bionatura 2023;8 (2) 24. http://dx.doi.org/10.21931/RB/2023.08.02.24
Received: 2 January 2023 / **Accepted:** 19 April 2023 / **Published:** 15 June 2023

Host	No. of exam samples	No. of infest samples	%	No. of ticks	Infestation density
Domestic cat	13	11	84.61	33	3
Wild cat	9	9	100	134	14.88

Table 1. Total rates and the density of infestation hard ticks for Felidae in Iraq.

Host	*R. turanicus*	*R. sanguineus*	*R. appendiculatus*	*Haemaphysalis*
Domestic cat	11♀, 13♂	.....	5♀, 4♂	.....
Wild cat	31♀, 29♂	8♀, 15♂	.....	7♀, 46♂

Table 2. Distribution of complex ticks species in domestic and wild cats in Iraq.

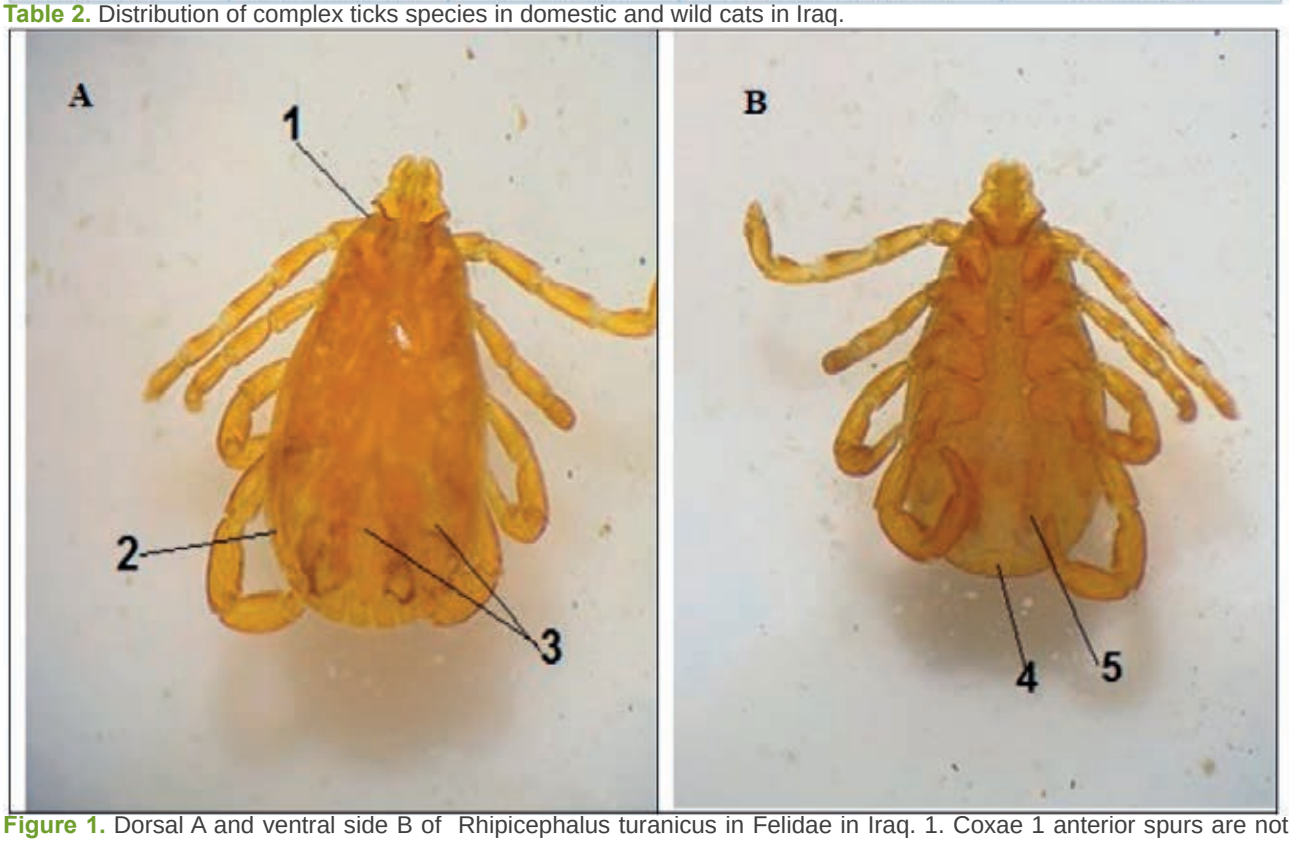

Figure 1. Dorsal A and ventral side B of Rhipicephalus turanicus in Felidae in Iraq. 1. Coxae 1 anterior spurs are not visible dorsally. 2. Lateral groove type is a distinct groove. 3. Posterior grooves are distinct grooves. 4. Caudal appendage is broad in fed males. 5. Adanal plate shape is narrow and trapezoid.

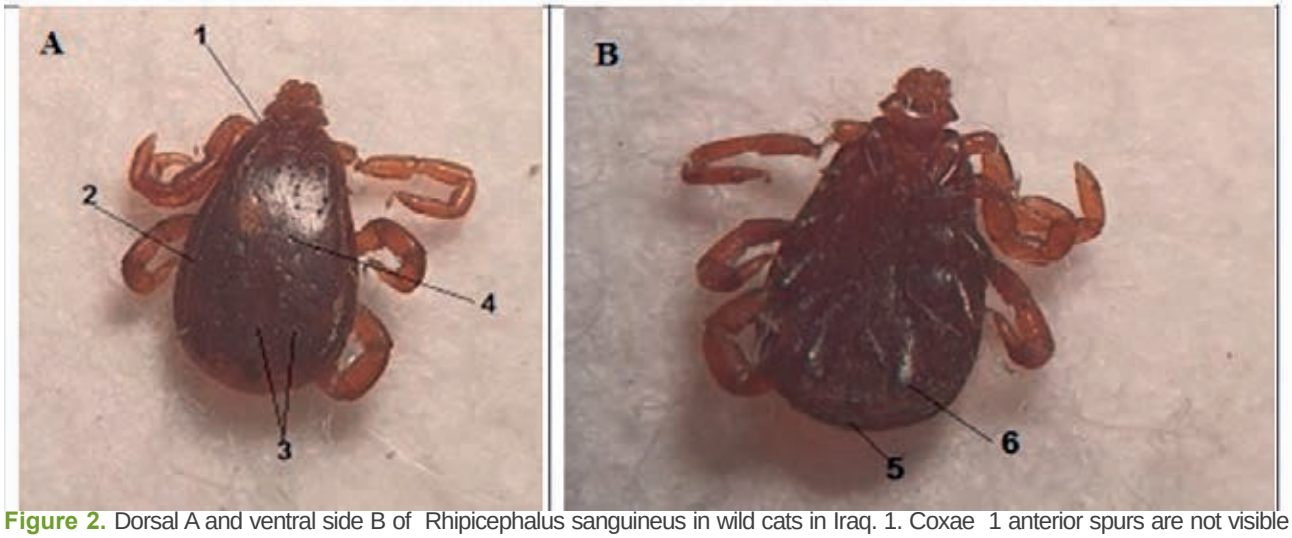

Figure 2. Dorsal A and ventral side B of Rhipicephalus sanguineus in wild cats in Iraq. 1. Coxae 1 anterior spurs are not visible dorsally. 2. Lateral groove type is a distinct groove. 3. Posterior grooves are distinct grooves (deep and wide with wrinkled texture). 4. Conscutum color is dark. 5.Caudal appendage is broad in fed males. 6.Adanal plates shape are abroad and curved appearance.

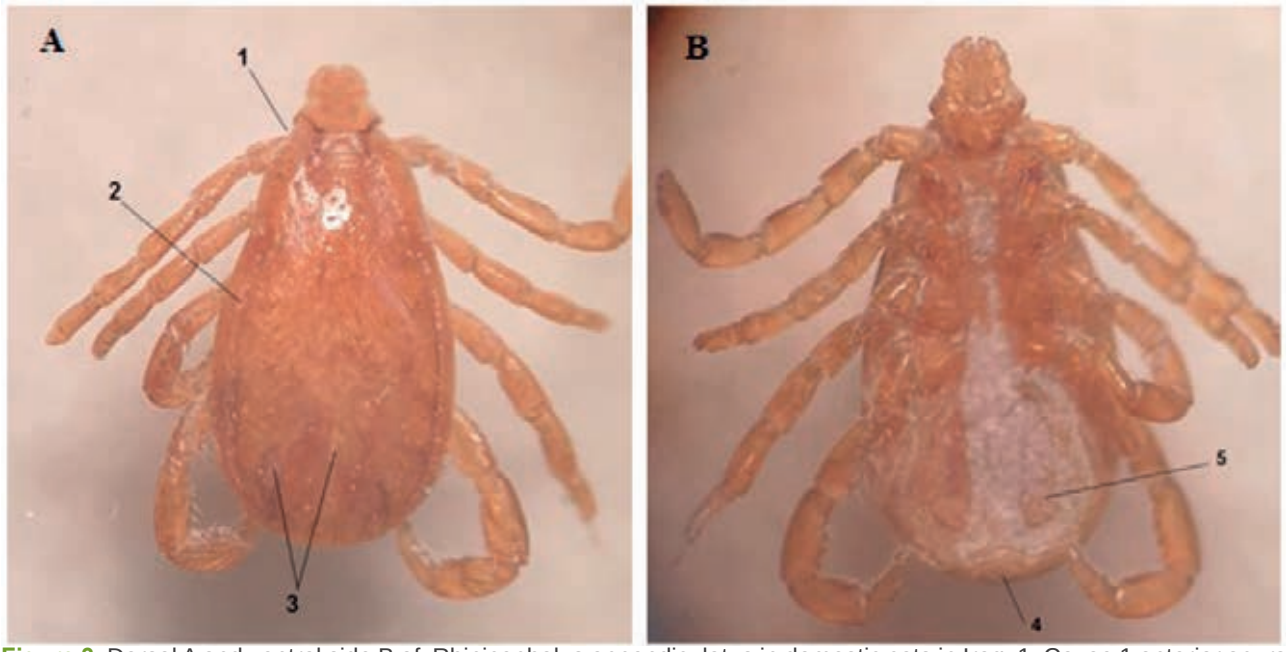

Figure 3. Dorsal A and ventral side B of Rhipicephalus appendiculatus in domestic cats in Iraq. 1. Coxae 1 anterior spurs are visible dorsally. 2. Lateral groove type is a distinct groove. 3. Posterior grooves are distinct grooves (shallow with wrinkled texture). 4. Caudal appendage is narrow in fed males. 5. Adanal plates shape is narrow and trapezoid.

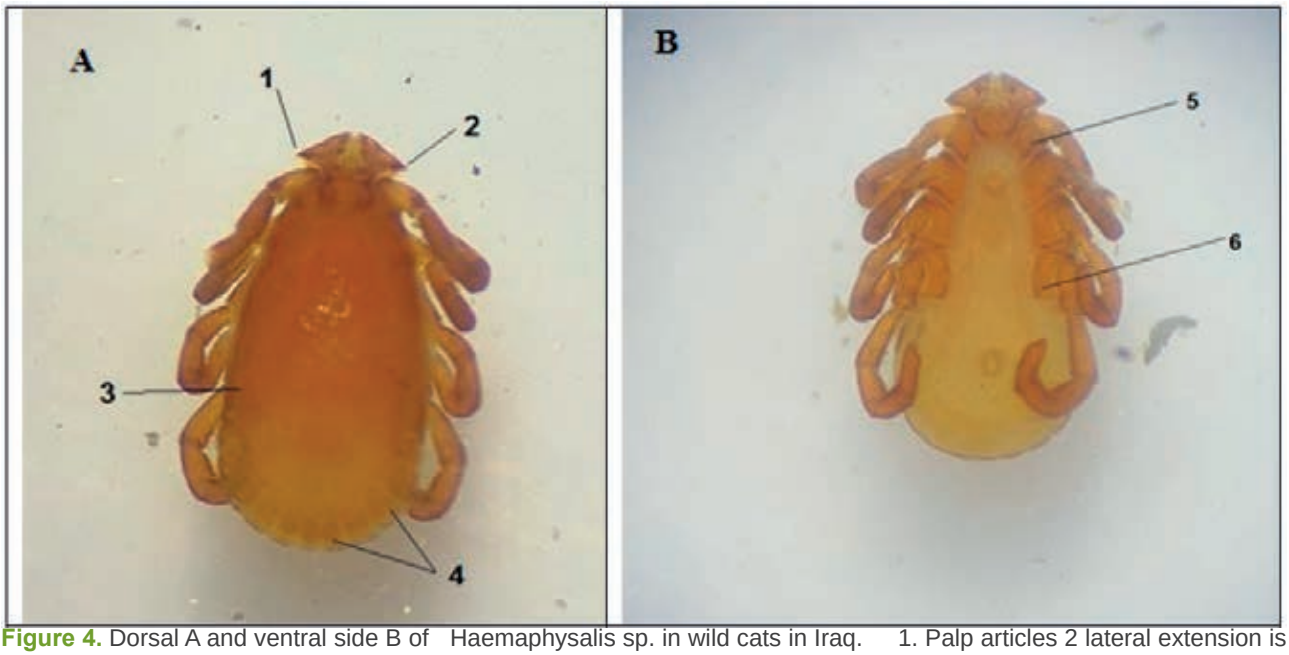

Figure 4. Dorsal A and ventral side B of Haemaphysalis sp. in wild cats in Iraq. 1. Palp articles 2 lateral extension is large (the palps form a distinctly conical shape). 2. Palp articles 2 dorsal spur is present. 3. Festoons enclosed by each lateral groove. 4. Festoons numbers = eleven.

Review for Molecular Identification and Phylogenetic-Tree Analysis of Hard Ticks

The sequencing of the genus *Rhipicephalus* was reported as follows: *Rhipicephalus turanicus*, Seq1 (MN999872), Seq2 (MN999873), Seq3 (MN999874) and Seq4 (MN999875) by (11) In Iraq. *R. appendiculatus* (MK551199) was reported by (12) In South Africa. *Rhipicephalus sanguineus* (MG386819) was reported by (13) in Portugal. The sequencing of the genus *Haemaphysalis sp*. is not represented in Iraq, while, in China *Haemaphysalis parva* (FN296280), *Haemaphysalis punctata* (FN296264) by (14) And *Haemaphysalis flava* (JQ737122), *Haemaphysalis doenitzi* (JQ346685) by (15). Morethan, *Haemaphysalis longicornis* (MF490294) and (MF490308) by (16) In South Africa, (17) revealed to the *Haemaphysalis leachi* (MN661151). *Haemaphysalis adleri* was not reported in NCBI till now.

Conclusions

The biodiversity of ticks in domestic and wild cats alike is an important topic to study that highlights the reservoir hosts who play a role in the distribution of ticks and, therefore, diseases. The current study revealed apparent differences in the infestation density between domestic and wild cats with hard ticks. *Rhipicephalus turanicus* appeared in both domestic and feral cats. The present study recorded *Rhipicephalus sanguineus* in wild cat *Felis chaus furax*; this

recording was considered a new host for *R. sanguineus*. The current study identified the *Rhipicephalus appendiculatus* for the first time in Iraq from domestic cat *Felis cattus*. The present results recorded the *Haemaphysalis sp*. in wild cat *Felis chaus furax*.

Supplementary Materials

The following are available in this PDF, Table S1: Composition culture medium, Sheet 1 S2: Total cost, Sheet 2 S2: Stages of production, Sheet 3 S2: Direct and indirect labor, Sheet 4 S2: Culture medium, Sheet 5 S2: IMC, Sheet 6 S2: 6. Assumptions.

Author Contributions

Conceptualization, Ana María Henao Ramírez and Aura Inés Urrea Trujillo; methodology and software, Hernando David Palacio Hajduck and Ana María Henao Ramírez; validation anf formal analysis, Ana María Henao Ramírez; investigation, resources, data curation, writing—original draft prepara-tion, Ana María Henao Ramírez; writing—review and editing and supervision, Aura Inés Urrea Trujillo. All authors have read and agreed to the published version of the manuscript.

Funding

This research was funded by General Royalties System - Science, Technology, and Innovation Fund with the Center of Agrobiotechnological Development and Innovation– CE-DAIT- BPIN 2016000100060, National Planning Department, Office of the Governor of Antioquia, Universidad de Antioquia, Universidad Católica de Oriente and Compañía Nacional de Chocolates.

Acknowledgments

We would like to thank Laboratory of Plant Physiology and Plant Tissue Culture of the Universidad de Antioquia. A special acknowledgment to Universidad de Antioquia's Research Development Committee (CODI) and Granja Yariguíes – Compañia Nacional de Chocolates.

Conflicts of Interest

The authors declare no conflict of interest.

Bibliographic references

1. Burger ,T. D., Shao, R., Beati, L., Miller. H. and Barker, S.C., Phylogenetic analysis of ticks (Acari: Ixodida) using mitochondrial genomes and nuclear rRNA genes indicates that the genus Amblyomma is polyphyletic. Mol Phylogenet Evol ,2006 ; 64 :45-55.
2. Hajdušek, O., Šima, R., Ayllon, N., Jalovecka, M., Perner, J., Fuente, J. and Kopaček, P., Interaction of the tick immune system with transmitted pathogens. Front Cell Infect Microbiol , 2013; 3: 26- 41.
3. Greay , T. L., Oskam, C. L., Gofton, A.W., Rees, R. L., Ryan, U.M. and Irwin Peter, J . A survey of ticks (Acari: Ixodidae) of companion animals in Australia. Parasit . Vectors , 2016 ; 9: 207.
4. Silaghi, C., Beck, R ., Oteo , J. A., Pfeffer, M. and Sprong, H. Neoehrlichiosis: an emergingtick-borne zoonosis caused by Candidatus Neoehrlichia mikurensis . Exp Appl Acarol , 2016; 68: 279-297.
5. Hadi, A. M., and Al- Amery, A. M. ISOLATION of Theileria and Babesia from gut and overy of Hard Ticks: Hyalomma A. Anatolicum In Baghdad. Diyala Agricultural Sciences Journal, 2012; 4: 1 - 8.
6. Shubber, H. W. K., Al-Hassani, N. A.W. and Mohammad, M. K. Ixodid ticks diversity in the middle and south of Iraq. IJRSR , 2014 ; 5:1518-1523.
7. Mohammad , K. M. Distribution of Ixodid ticks among domestic and wild animals in Central Iraq. Bull. Iraq Nat. Hist. Mus, 2015; 13: 23-30.
8. Mohammad, M. K. A bio-taxonomic study on the hard ticks (Acari: Ixodidae) of some domestic and wild animal from Iraq. Ph. D. thesis, College of Science, University of Baghdad , Page RD (1996) TREEVIEW: an application to display phylogenetic trees on personal computers. Comput Appl Biosci , 1996; 12: 357-358.
9. Al-Mhana, T. I. A survey of some ixodid tick species in Diwaniya province and possibility of using garlik water extract and cypermethrin in tick control. M. Sc. thesis, College of Vet. Med., Al-Qadisiya University, 2010; 81.
10. Walker, A. R. A., Bouattour, J. L., Camicas, A., Estrada-Peña, I.G., Horak, A. A., Latif, R .G. and Pegram, P. M. Ticks of Domestic Animals in Africa: a Guide to Identification of Species. Copyright: The University of Edinburgh, 2014; 227.
11. Hadi, H. D., Hadi, A. M . and Jassim, S. Y., Molecular Diagnosis Of Ixodidae From Canidae In Iraq . Plant Archives , 2020; 20: 353-357.
12. Mahlobo, S. I. C., Zishiri, O.T. and Thekisoe, O. M. M. Phylogenetic analysis of tick species naturally infesting livestock in South Africa using the cytochrome c oxidase subunit I mitochondrial gene marker , 2019. https://www.ncbi.nlm.nih.gov/nuccore/MK551199
13. Sanches, G.S., Couto, J., Pedrosa,A. R., Ferrolho,J., Santos,A. S., Santos-Silva, M. M., Antunes,S. and Domingos, A. Molecular heterogeneity of Rhipicephalus sanguineus sensu lato and screening for Ehrlichia canis in mainland Portugal , 2017. https://www.ncbi.nlm.nih.gov/nuccore/MG386819.1
14. Chitimia, L., Lin, R.Q., Cosoroaba, I., Braila, P., Song, H.Q. and Zhu, X.Q. Molecular characterization of hard and soft ticks from Romania by sequences of the internal transcribed spacers of ribosomal DNA, Parasitol. Res, 2009 ; 105 : 907-911.
15. Chen, X., Xu, S., Yu, Z., Guo,L., Yang,S., Liu, L., Yang, X. and Liu, J. Multiple lines of evidence on the genetic relatedness of the parthenogenetic and bisexual Haemaphysalis longicornis (Acari: Ixodidae) . Infect. Genet. Evol, 2014; 21: 308-314.
16. Zhong-Bo, L., Hua Liu, G. and Yin Cheng, T., Molecular characterization of hard tick Haemaphysalis longicornis from China by sequences of the internal transcribed spacers of ribosomal DNA . Exp Appl Acarol , 2018; 74: 171-176.
17. Thompson Alec, T., Kristen Dominguez, 1., Christopher, A., Cleveland, 1., Shaun, J., Dergousoff 3. , Kandai Doi 4 ., Richard, C. Falco5, Telleasha Greay 6., Peter Irwin6, L., Robbin Lindsay 7., Jingze Liu8., Thomas, N., Mather 9., Charlotte, L., Oskam6., Roger, I., Rodriguez-Vivas 10., Mark G. Ruder 1., David Shaw1., Stacey, L., Vigil 1., Seth White1,11. and Michael, J. Y. Molecular Characterization of Haemaphysalis Species and a Molecular Genetic Key for the Identification of Haemaphysalis of North America. Frontiers for Veterinary Science, 2020; 7: 1-11.

ARTICLE / INVESTIGACIÓN

16SrRNA sequencing analysis for identification of *Klebsiella pneumoniae* isolated from the extreme kitchen environment

Ikhlas Ramadan Matter, Aisha W.AL-Omari, Alaa Hussein Almola

DOI. 10.21931/RB/2023.08.02.24

Department of Biology, College of Science, Mosul University, Mosul, Iraq.
Corresponding author: iklasbio120@uomosul.edu.iq

Abstract: Swabs from dishwasher samples were collected and cultured on different media, and then a gram stain was conducted on pure colonies to find whether they were Gram-positive or negative. 32-gram negative Isolates were obtained from the dishwasher; then, we chose isolates under study depending on morphological features on previous media for further investigation. 32 Gram-negative isolates were obtained from a dishwasher, and three isolates of *Klebsiella pneumoniae* were diagnosed by some phenotypic characteristics and approved by using 16 SrRNA partial sequencing analyses. The 3 isolates deposited in the NCBI database under accession number OK 254156.1 for *K.pneumoniae* strain NPK 323, OK 247423.1 for *K. pneumonia* as strain CUMB SAM-61, and OK245427.1 for *K. pneumonia* strain PD17. The phylogenetic tree for 3 isolates was done by using MEGA II software. Many experiments have been conducted on two isolates (OK 247423.1 and OK245427.1) because the OK 254156.1 strain was lost during laboratory work and repeated cultures. A hemolysis test on blood agar and a lipase test on egg–yolk agar were done; both isolates showed negative results for hemolysis blood and producing lipase enzyme, while both isolates showed their ability to produce lecithinase enzyme. The two isolates gave an excellent result in the tube method for the biofilm formation test. Also, a good candidate production test was obtained for these two isolates using L.B. acetate agar medium. Conclusion: Bacterial species differ according to the environments in which they live, as the species that are isolated from clinical sources and possess many virulence factors that make them more dangerous and pathogenic to humans differ about the same species if isolated from a variety of external environments, which makes them virulent or have new characteristics that make them adapted to live in the environments from which they are isolated.

Key words: *Klebsiella pneumonia*, virulence factor, extreme conditions, phylogenetic tree.

Introduction

Scientists are always trying in their microbial biological research and studies to search for species that can withstand harsh environmental conditions, whether in water, air or soil. Europe finally discovered several hardy bacteria and fungi lurking on the rubber seals of dishwasher doors, some of which are opportunistic pathogens. These microbes must withstand high temperatures, high NacL Concentration, acidity, cleaning products, and the shear force of water during washing cycles to establish a home there[1].

Studying bacterial diversity that has survived in complex environments has contributed to understanding how life has developed. Despite their limited worldwide distribution, severe environments are home to many microorganisms important to science and technology[2], such as bacteria producing antibiotics[3] and those involved in pollution biodegradation[4]. Many taxa are represented in these habitats, giving a wealth of knowledge on microbial physiology and biodiversity.

Gram-negative bacilli are characterized by several characteristics, including that they are widespread in environmental systems, where they are found in air, water, and soil, in addition to their presence in sewage systems and wet places. What also distinguishes them is that they need few nutrients for growth, unlike other species, and they are characterized by resistance to chemical antibiotics[5-7].

Klebsiella bacteria are characterized by causing many respiratory system diseases, infecting the blood circulation of the heart, and causing severe infections in hospitals. This pathogen is also one of the most commonly isolated bugs in community-acquired illnesses.. The gastrointestinal system may be the primary pathogenic reservoir for transmitting these dangerous diseases, with the majority of cases coming from the hands of hospital staff or healthcare workers. *Klebsiella pneumoniae* is an opportunistic pathogen that targets individuals whose immune has been weakened by an underlying disease such as diabetes mellitus, persistent lung obstruction, or major surgery; also often detected in inhalation; in addition, their clinical relevance in individuals whose immune is weakened by underlying disease is challenging to determine[8-12].

Materials and methods

Isolation

Swabs from dishwasher samples were collected by passing sterile swabs on the specific area in 6 dishwashers. The swabs were cultured on different media such as Nutrient agar, MacConkey agar, Blood agar and methylene

Citation: Matter I R, AL-Omari A W, Almola A H. 16SrRNA sequencing analysis for identification of Klebsiella pneumoniae isolated from the extreme kitchen environment. Revis Bionatura 2023;8 (2) 24. http://dx.doi.org/10.21931/RB/2023.08.02.24
Received: 2 January 2023 / **Accepted:** 19 April 2023 / **Published:** 15 June 2023

blue agar and incubated at 37C for 24 hours, when isolated and cultured continually until they were obtained pure colonies. Then gram stain was conducted on pure colonies to find whereas Gram-positive or negative. 32-gram negative Isolates were obtained from the dishwasher; then, we chose isolates under study depending on morphological features on previous media for further investigation.

Identification by 16SrRNA sequencing

Three isolates of Klebsiella were selected for identification by 16SrRNA.In the first step of identification, the total DNA of isolates is extracted depending on the instruction of a specific kit (G-spin DNA kit, intron biotechnology). The primers of the PCR reaction included forward primer (5'-AGAGTTTGATCCTGGCTCAG- 3') and reverse primer(5'-GGTTACCTTGTTACGACTT- 3'), the final volume of the reaction was done as 25 ML that is composed of 5ML of pre mix,1ML from each forward primer and reverse primer, and then added 1.5 ML of total DNA.finally the total volume of reaction completed by 16.5 ML of D.W into 25ML. The condition of the reaction is in Table 1.

Detection of Virulence Factors of K. pneumoniae Isolates

Hemolysin test

A hemolysin test was carried out to determine the hemolytic activity of Klebsiella pneumoniae isolates; two Test isolates were inoculated in a blood agar plate that contained 5%(vol\vol) of human blood after activated in nutrient broth for incubation at 37°C, for 24 hours. The presence or absence of hemolysis in the surrounding colonies was recorded[13].

Production of lecithinase and lipase enzyme:

By using egg–yolk agar medium, the ability of the isolates was tested for the production of lecithinase and lipase enzyme; the medium contained 85 ml of nutrient agar and 15 ml of egg-yolk, sterilized the nutrient agar and then cool to 55c added egg –yolk and mixed then poured in plates.

The isolates were inoculated in the plate and incubated at 37C for 24h. The plates were filled with a saturated copper sulfate aqueous solution and let to stand for 20 minutes before the surplus solution was drained. The results were read after a few minutes of drying. The green-blue color of opalesces showed lipolysis synthesis, and the area of clearing surrounding the colony was declared positive for lecithinase production[14-16].

Biofilm formation

The two bacterial isolates were screened for the ability of biofilm(method) formation by using the test tube method. In the test tube method, the isolates were grown in the test tube containing tryptic soy broth and 1% glucose and incubated for 24h at 37C; then, the media was discarded. The lines were gently rinsed with phosphate buffer saline and left to dry, then 1ml of 1% w/v crystal violet solution was added to the tube to stain the cells attached to the walls, Crystal violet solution was discarded after 3 min. The tubes were washed with deionized water and left to dry inverted. The staining of the walls of tube 17 indicated biofilm synthesis.

Investigation of the ability of Klebsiella pneumonia to produce calcite

Klebsiella pneumonia isolates were grown on Luria-Bertani acetate agar medium (Tryptophane 1g, Yeast extract 0.5g. Nacl 0.05g, Calcium acetate 1g, Agar 1.5g, D.W 100ml)the Ph adjusted at (8) and incubated at 37C for a week. After the incubation period was over, the formation of calcite crystals was investigated[18].

Chemical diagnosis of calcite crystals

A chemical examination of the crystals was carried out by adding drops of HCL 10% solution to the calcifications to observe the formation of bubbles as a result of the formation of carbon dioxide gas as a product of the reaction, and the result was recorded[19].

Results

The isolates under study showed coccobacilli gram-negative cells, and the morphological features on McConkey agar showed 3 high mucus strains with pink mucoid colonies, while on Eosin methylene blue agar are appear pink to purple colonies finally, colonies on blood agar are smooth raised mucoid colonies. figure (1).

The 3 mucus strains were selected for 16SrRNA sequencing analysis by amplifying 16S rRNA genes and analysis by electrophoresis on 1% agarose gel, as shown in Figure (2).

The result of 16SrRNA sequencing compared with NSBI database, through NSBI blast with similarity 99%of standard K.pneumoniae isolates as (*K. pneumoniae* NPK 323, *K. pneumoniae* CUMB SAM-61 and *K. pneumonia* PD17).

The use of 16SrRNA analysis is regarded as an appropriate tool for the specific identification of isolates under study and gives a proven method for molecular analysis. The 3 isolates of *K. pneumoniae* were deposited in NSBI with accession numbers OK 254156.1 for *K.pneumoniae* strain NPK 323, OK 247423.1 for *K. pneumoniae* as strain CUMB SAM-61, and OK245427.1 for *K. pneumonia* strain PD17.

Stage	Cycle	Temperature	Time
Denaturation 1	1	95c	5 min.
Denaturation 2	35	95 c	45 sec.
Annealing	35	58 c	45 sec.
Extension 1	35	72 c	45 sec.
Extension 2	1	72 c	7 min

Table 1. The reaction of PCR.

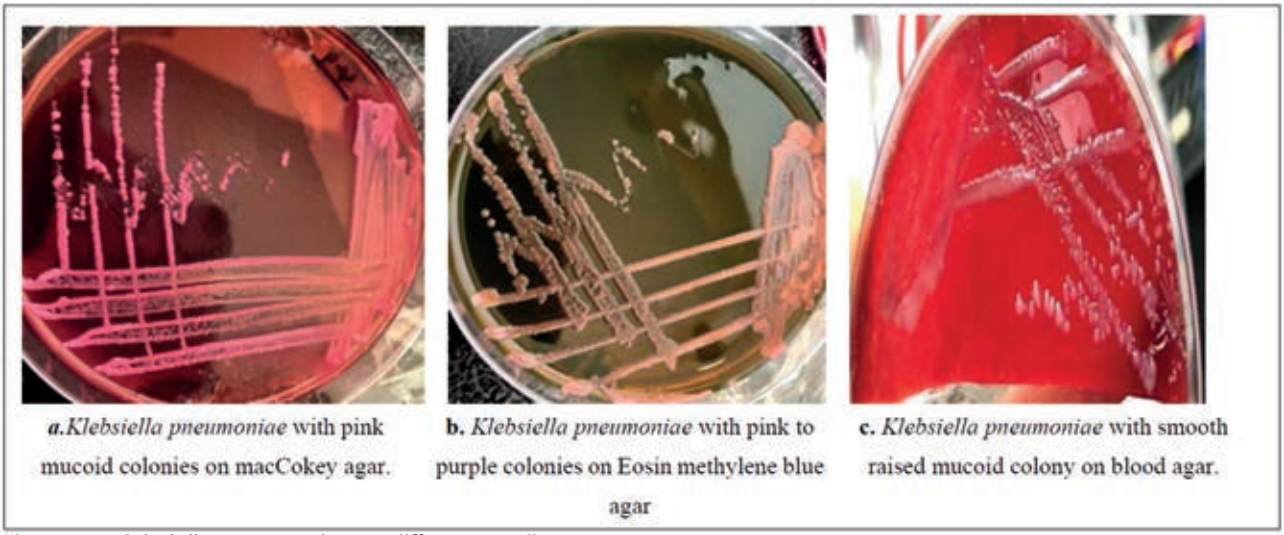

a.Klebsiella pneumoniae with pink mucoid colonies on macCokey agar.

b. Klebsiella pneumoniae with pink to purple colonies on Eosin methylene blue agar

c. Klebsiella pneumoniae with smooth raised mucoid colony on blood agar.

Figure 1. *Klebsiella pneumoniae* on different media.

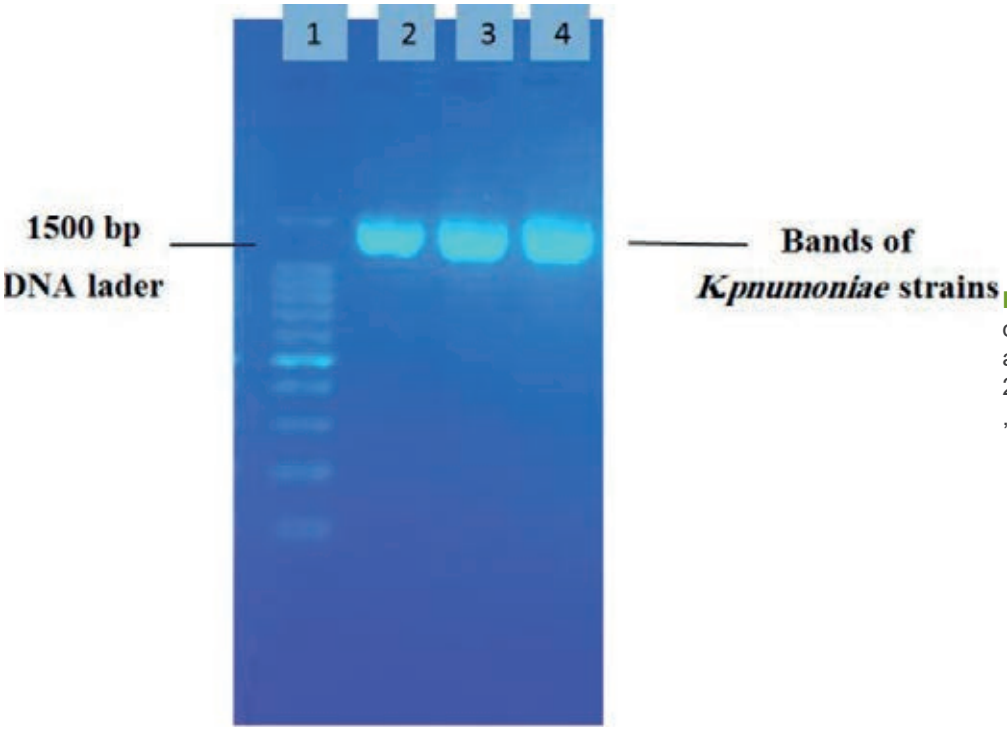

Figure 2. Electrophoresis of 16SrRNA products by agarose gel 1:DNA ladder , 2:OK247423, 3:OK254156 , 4:OK254156

The phylogenetic analysis done by the Neighbor-Joining tree showed a relationship between OK 247423.1 CUMB SAM—61 and OK254156.1 NPK 323 with other K.pneumoniae strains recently deposited in NSBI database (The OK247423.1 and OK254156.1 strains) showed related to MH938261.1 strain. Still, the relationship between OK247423.1 and MH938261.1 was more closely. the strain OK245427 was closely related to the KU711913 strain (figure 3).

Klebsiella pneumoniae isolates and their ability for hemolysis blood, production of lecithinase and lipase enzymes, biofilm and calcite formation:

The two isolates of *Klebsiella pneumonia* ((OK 247423.1 and OK245427.1)) give a negative result for hemolytic activity on blood agar plates, and the same two isolates of *Klebsiella pneumoniae* showed their ability for lecithinase production by formation a clear zone around the bacterial colonies, as shown in (figure 4). In contrast, it gives a negative result with lipase enzymes.

Our findings refer to the two isolates of *Klebsiella pneumonia*((OK 247423.1 and OK245427.1)) which showed the ability for biofilm formation on the inner walls and down of tubes in the form of a violet color, as shown in (figure 5). While L. B. acetate agar showed calcite formation through the calcifications on the surface of the growing colonies, as shown in (figure 6).

Discussion

Life evolution produced new chances for microbial development, resulting in a shift in the microorganisms we encounter[20].

Microorganisms enter dwellings with air, soil, water, live plants, various food products, other pets, and humans[21,22]. Most available overviews of indoor microbiomes focus on air-borne, dust-associated microbes[23]. Compared with few published research on microbes in humid household environments such as bathrooms, kitchens, and appliances that need water in their work.

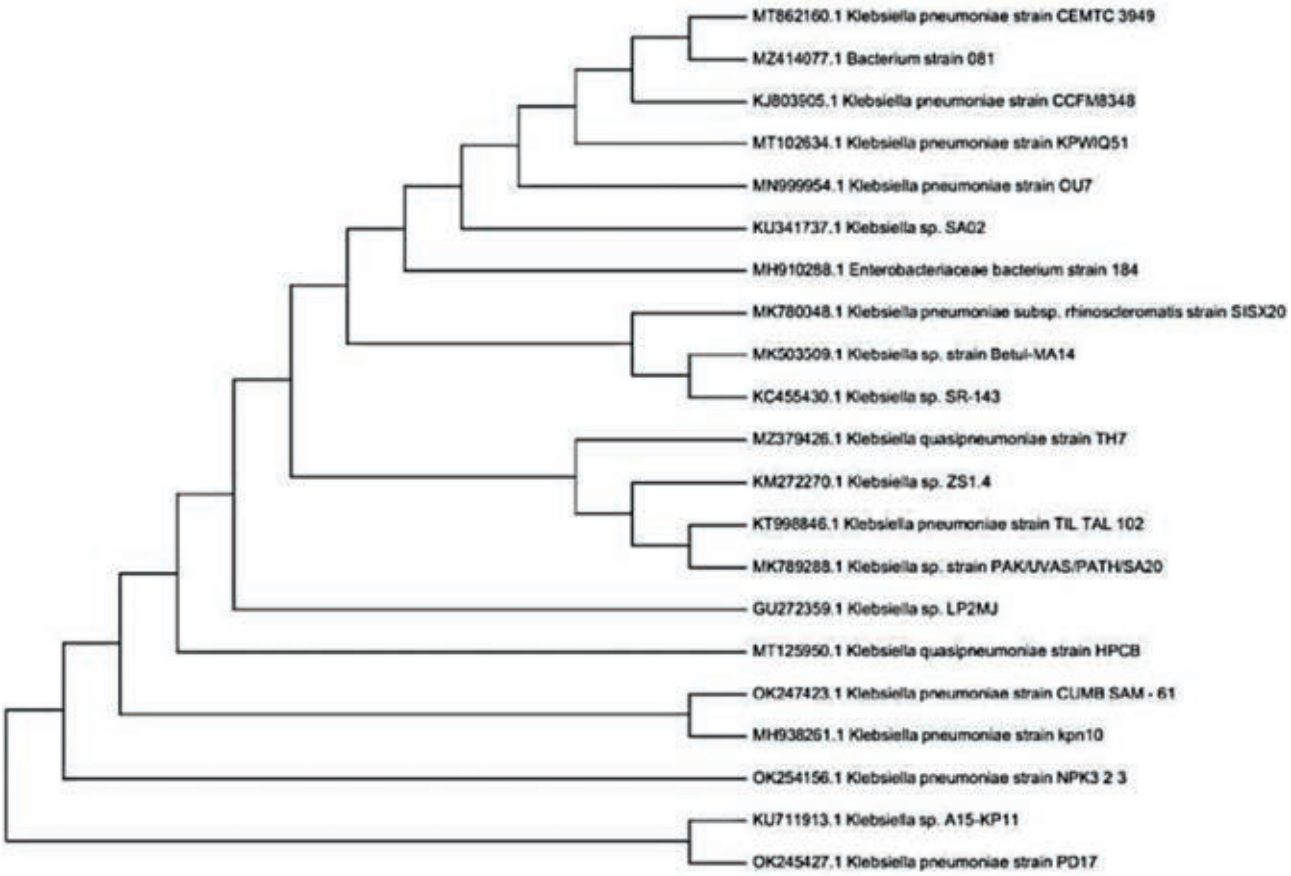

Figure 3. Phylogenetic tree.

The isolates of *Klebsiella pneumoniae* obtained from extreme environments differ in their possession of virulence factors. Our isolates could not cause hemolysis of blood, and this result agrees with Pereira and Vanetti[24] may be due to the absence of activators for gene expression that code for this enzyme[25]. In recent research, none of the 54 strains isolated had blood hemolysis or possessed the hlyA and cnf-1 genes, which code for this activity. Although hemolytic activity has been documented, few studies show the genotypic and phenotypic existence of hemolysis in Klebsiella[25,26]. At the same time, our result differs from Kalaivani and his group[27], who reported that the *Klebsiella pneumonia* isolates had a high percentage of hemolytic activity.

The two isolates of *Klebsiella pneumoniae* showed their ability for lecithinase production by forming a large zone of opalescence around the colonies. At the same time, give a negative result with the production of lipase enzyme. Studies have varied concerning the output of lecithinase enzyme. This research by Singh[28], with 208 *Klebsiella pneumoniae isolates* (7.69%), produced lecithinase activity. And a research study by Kalaivani,55.7% (64) *Klebsiella pneumoniae isolates* observed Lecithinase production, which might predict more pathogenic ability among this isolates[27] Our result differs from other study[29] which referred that *Klebsiella pneumoniae* isolates, cannot produce lecithinase enzyme. At the same time, the development of our study agrees with the same study in the inability of *Klebsiella pneumoniae* isolates to produce lipase enzyme (figure 4).

Microbial biofilms are colonies of clustered microbial cells immersed in an extracellular polymeric material matrix that they generate by themselves (EPS). Biofilms can protect bacteria against ultraviolet (U.V.) radiation,, high pH, severe temperature salt stress, high pressure, inadequate nutrition, antibiotics, and other factors by functioning as "protective clothing."[30].

Our finding refer the two isolates of *Klebsiella pneumoniae* that showed good ability for biofilm formation, and this agreement with (31) which they found that 93.6% of *K. pneumoniae* isolates formed biofilms. These strains were divided into four categories as strains that generate a moderate biofilm, completely established biofilms, insignificant biofilms, and non-biofilm providers.

Also, our result was similar to 27, found among the several virulence strategies investigated, mainly of *Klebsiella pneumoniae* isolates (79%) demonstrated biofilm methods. In another recent study, 100 % biofilm production was documented for *Klebsiella pneumoniae* isolates[32]., while the study of Abbas in 2020 33 showed that only 4 out of 73 isolates of *Klebsiella pneumoniae* were able to form biofilms (figure 5).

Microbially induced calcite precipitation (MICP) is the generation of calcium carbonate from a saturated solution caused by microbial cells and metabolic activity 24. During MICP, organisms can emit one or more metabolic products (CO3 2), which react with ions (Ca2+) in the environment, resulting in mineral precipitation.

The MICP process is an eco-friendly and effective technology that may be used to solve a variety of environmental concerns, including radionuclide cleanup, heavy metal remediation, consolidation, CO2 sequestration, bio cement,, and other uses[35].

The results of two *Klebsiella pneumonia* isolates on L. B. acetate agar showed calcite formation by creating calcifications on the surface of the growing colonies on the

Figure 4. *Klebsiella pneumoniae* on egg yolk agar with clear zone around colonies.

Figure 5. Formation of biofilm by *Klebsiella pneumoniae*.

L.B. acetate agar. This was indicated by the researchers[36], which explained the bacterial role in calcite formation due to its metabolic activity that increases the pH and deposition of calcite on its surface (figure 6).

Monte Carlo Simulation Analysis (MCS)

After structuring costs, the most influential cost component was direct labor, representing 53% of the total cost. The cost of culture media was 12% of the total, IMC represented 5%, and operating expenses, including administrative expenses and infrastructure, were 30% (Figure 2).

Conclusions

Bacterial species differ according to the environments in which they live, as the species that are isolated from clinical sources and possess many virulence factors that make them more dangerous and pathogenic to humans differ about the same species if separated from a variety of external environments, which makes them virulent or have new characteristics that make them adapted to live in the domains from which they are isolated

Funding

This research received no external funding

Acknowledgments

The author would like to thank Biology depart. , University of Mosul for supporting this study.

Conflicts of Interest

The authors declare no conflict of interest.

Bibliographic references

1. Halford B., Mighty microbes lurking in the kitchen, Extreme environments: Dishwasher edition,2018, Volume 96, Issue 12.
2. Malik, A.; Grohmann, E.; Alves, M. Management of Microbial Resources in the Environment, 1st ed.; Springer: Amsterdam, The Netherlands, 2013. [CrossRef]

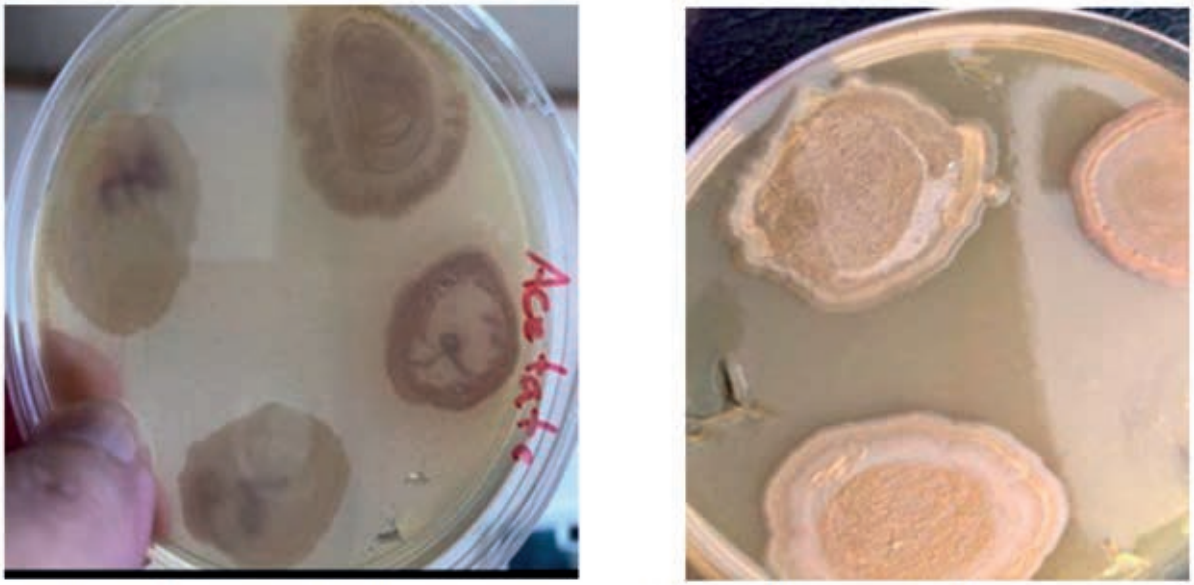

a. Calicate production by *Klebsiella pneuomoniae* b.Chemical diagnosis of calcite crystals

Figure 6. *Klebsiella pneuomoniae* on L.B. acetate agar.

3. Patel, K.; Amaresan, N. Antimicrobial Compounds from Extreme Environment Rhizosphere Organisms for Plant Growth. Int. J. Curr. Microbiol. Appl. Sci. 2014, 3, 651–664.
4. Yong, Y.C.; Zhong, J.J. Recent Advances in Biodegradation in China: New Microorganisms and Pathways, Biodegradation Engineering, and Bioenergy from Pollutant Biodegradation. Process Biochem. 2010, 45, 1937–1943. [CrossRef]
5. Sikkema R., Koopmans M. One Health training and research activities in Western Europe. Infection Ecology and Epidemiology. 2016; (6):1-9. doi:10.3402 / iee.v6.33703.
6. World Organization for Animal Health (OIE). Animal Production Food Safety. 2016.: http://www.oie.int/en/foodsafe...
7. Cray J.A., Bell A.N.W., Bhaganna P., Mswaka A.Y. et al. The biology of habitat dominance; can microbes behave as weeds?. Microb. Biotechnol. 2013; (6):453492.
8. Williams, P., and J. M. Tomas. The pathogenicity of Klebsiella pneumoniae. Rev Med Microbiol 1990;1:196–204.
9. Montgomerie, J. Z. Epidemiology of Klebsiella and hospitalassociated infections. Rev Infect Dis 1979;1:736–53.
10. Podschun, R., and U. Ullmann. Klebsiella spp. as nosocomial pathogens: epidemiology, taxonomy, typing methods, and pathogenicity factors. Clin Microbiol Rev 1998;11:589–603.
11. Kaul S, Brahmadathan KN, Jagananati M, Sudarsanam TD, Pitchamuthu K, Abraham OC, John G. One Year Trends in the Gram Negative Bacteria antibiotic susceptibility patterns in a Medical Intensive care unit in South India. Indian J Med Microbiol 2007;25:230-5.
12. Podschun R, Pietsch S, Holler C, Ullmann U. Incidence of Klebsiella species in surface waters and their expression of virulence factors. Appl Environ Microbio 2001;67(7):3325- 3327.
13. Russell, F. M., Biribo, S. S. N., Selvaraj, G., Oppedisano, F., Warren, S., Seduadua, A.,... & Carapetis, J. R.. As a bacterial culture medium, citrated sheep blood agar is a practical alternative to citrated human blood agar in laboratories of developing countries. Journal of clinical microbiology,2006; 44(9), 3346-3351.
14. Esselmann TM, Liu PV. Lecithinase production by Gram negative bacteria. J Bacteriol 1961;81(6):939-45.
15. Cappuccino JG, Sherman N. Microbiology - A laboratory manual 1996;159-201.
16. Panus. E, Chifiriuc M. B., Bucur M. Virulence, pathogenicity, antibiotic resistance and plasmid profile of Escherichia coli strains isolated from drinking and recreational waters, in 17th European Congress of Clinical Microbiology and Infectious Diseases and 25th International Congress of Chemotherapy, 2008.
17. Hassan A,Usman J, Kaleem F,et al. Evalution of different detection methods of biofilm formation in the clinical isolates. Braz J Infect Dis,2011; 15(4) 305-311.
18. Lee NY. Calcite Production by Bacillus amyloliquefaciens CMB01, J. Microbiol., 2003; 41(4): 345-348.
19. Hamilton,W.R. ; Woolley,A. R. and Bishop, A. C..Minerals Rocks and Fossils.The Hamlyn Publishing Group Limited,1986; Italy.
20. Babič, M. N., Gostinčar, C., & Gunde-Cimerman, N.. Microorganisms populating the water-related indoor biome. Applied Microbiology and Biotechnology, 2020;104(15), 6443-6462
21. Weikl F, Tischer C, Probst AJ, Heinrich J, Markevych I, Jochner S, Pritsch K. Fungal and bacterial communities in indoor dust follow different environmental determinants. PLoS One.2016; 11: e0154131. https://doi.org/10.1371/journal.pone.0154131.
22. Jayaprakash B, Adams RI, Kirjavainen P, Karvonen A, Vepsäläinen A, Valkonen M, Järvi K, Sulyok M, Pekkanen J, Hyvärinen A, Täubel M. Indoor microbiota in severely moisture damaged homes and the impact of interventions. Microbiome.2017; 5(1):138. https://doi. org/10.1186/s40168-017-0356-5.
23. Shan Y, Wu W, Fan W, Haahtela T, Zhang G . House dust microbiome and human health risks. Int Microbiol.2019; 22(3):297–304. https://doi.org/10.1007/s10123-019-00057-5.
24. Pereira, S. C. L., & Vanetti, M. C. D. . Potential virulence of Klebsiella sp. isolates from enteral diets. Brazilian Journal of Medical and Biological Research,2015; 48, 782-789.
25. Albesa, I. Klebsiella pneumoniae haemolysin adsorption to red blood cells. Journal of applied bacteriology,1989; 67(3), 263-266.
26. Gundogan N, Citak S, Yalcin E. Virulence properties of extended spectrum beta-lactamase-producing Klebsiella species in meat samples. J Food Prot 2011; 74: 559-564, doi: 10.4315/0362-028X.JFP-10-315.
27. Kalaivani et al.,. Clinical isolates of Klebsiella pneumoniae and its virulence factors from a tertiary care hospital. Original Research Article,2019;023.
28. Singh, B. R., Sharma, V. D., & Chandra, R.. Detection, prevalence, purification and characterization of lecithinase of Klebsiella pnemoniae.1999.
29. Ali, M. J., & Al-Rikabi, R. H. December). Antibiotic and virulence profile of UTIs associated bacteria. In AIP Conference Proceedings.2020; (Vol. 2290, No. 1, p. 020008). AIP Publishing LLC. 15.
30. Yin, W., Wang, Y., Liu, L., & He, J. Biofilms: the microbial “protective clothing” in extreme environments. International journal of molecular sciences, 2019;20(14), 3423.

31. Seifi, K., Kazemian, H., Heidari, H., Rezagholizadeh, F., Saee, Y., Shirvani, F., & Houri, H. Evaluation of biofilm formation among Klebsiella pneumoniae isolates and molecular characterization by ERIC-PCR. Jundishapur journal of microbiology, 2016;9(1).
32. Aljanaby, A. A. J., & Alhasani, A. H. A.. Virulence factors and antibiotic susceptibility patterns of multidrug resistance Klebsiella pneumoniae isolated from different clinical infections. African Journal of Microbiology Research, 2016;10(22), 829-843.
33. Abbas, O. N., Mhawesh, A. A., & Al-Shaibani, A. B. Molecular Identification of Pathogenic Klebsiella pneumoniae Strains Producing Biofilm. Medico Legal Update,2020; 20(3), 1068-1074.
34. Bosak T. Calcite precipitation, microbially induced. In: Reitner J, Thiel V (eds) Encyclopedia of earth sciences series. Springer, Netherlands, 2011;pp 223–227.
35. De Muynck W, De Belie N, Verstraete W. Microbial carbonate precipitation in construction materials: a review. Ecol Eng.2010; 36:118–136.
36. Chahal, N., Rajor, A., & Siddique, R. Calcium carbonate precipitation by different bacterial strains. African Journal of Biotechnology, 2011;10(42), 8359-

ARTICLE / INVESTIGACIÓN

Response genotypes of sunflower (*Helianthus annuus* L.) and amount of nitrogen fertilizer on growth characteristics, oil yield, and its percentage

Khalid Najim Abdullah[1]*, Waleed A. Jabail[2] and Kefah Abdel-Reda Jassim[3]

DOI. 10.21931/RB/2023.08.02.25

[1] Department of Field Crops Science, College of Agriculture, University of Basrah, Iraq.
[2] College of Education, Qurna, University of Basrah, Iraq.
[3] College of Agriculture, University of Basrah, Iraq.
Corresponding author: khaldnjmbdallhfrj@gmail.com

Abstract: The field experiment was conducted during the spring and autumn seasons of 2021 in the Al-Haritha area, AL-Basra Governorate, to study the response of six genotypes of sunflower (Local, Aqmar, Ishaqi 1, Ishaqi 2, Turki Tarzan and Shmoos) and four levels of nitrogen fertilizer control treatment N0, N1 = (N100 kg. ha^{-1}), N2 = (N200 kg.ha^{-1}) and N3 = (N300 kg.ha^{-1}) according to the complete randomized block design RCBD with three replications in the order of the split-plot design (the levels of nitrogen fertilization were distributed in the main plot and the varieties in the secondary Sub-plot). Results showed the superiority of the Shmoos genotype with the highest average number of leaves that, reached (27.05 and 29.41) leaves. plant^{-1}. while the nitrogen fertilizer effect showed a superior fertilizer level of N3, which gave (26.32 and 29.94) leaves. plant^{-1}. As for characteristic of fertility percentage, there were no significant differences between the genotypes (Local, Aqmar, and Tarzan) for the spring season; it appears the superiority of fertilizer level N3, which gave (93.79 and 91.79), Shmoos genotype was superior with the highest average yield of an individual plant (78.50 and 84.73) gm.plant^{-1} compared to the local genotype, which gave the lowest average of (44.80, and 51.23) gm.plant^{-1} for the two seasons, respectively, and N3 level of fertilizer, which gave average (77.82 and 88.88) gm.plant^{-1} and local composition outperformed the proportion of oil (39.55 and 41.13%) and the Shmoos genotype in the total oil yield (1161.4 and 1461.3) kg.ha^{-1}, while this study showed the superiority of the fertilizer level N0 with the oil percentage, which gave (39.63 and 43.65%). As for the total oil yield, the composition was superior to Shamus by giving the highest mean of oil yield (1161.4 and 1461.3) kg.ha^{-1} for two seasons, respectively, and the superiority of the fertilizer level N3, which gave the highest oil yield (1,247.6 and 1673.6) kg.ha^{-1}, for two seasons, respectively.

Key words: Sunflower, genetic structures, nitrogen fertilizer.

Introduction

Due to its short growth period and high economic returns, the sunflower crop *Helianthus annuus L* is one of the most important oil crops in the world. Its seeds contain a high percentage of oil, reaching up to 55 percent in some varieties. It is healthy oil because it contains Omega-3 fatty acids and unsaturated fatty acids like Oleic. Linoleic acid has low oxidation sensitivity during the packing and storage process[1].

Vitamins A, D, E, and K are found in sunflower seeds. They also contain about 27% protein and 60% polyunsaturated fatty acids, ideal for heart patients who want to lower their blood cholesterol levels[2]. For the 2019 sunflower crop, the estimated cultivated area in Iraq is 450 ha, with an average yield of 2333. 2 tons in hiktar[3]. Sunflower oil was the first to be used in Iraq, and its productivity is still limited due to a failure to follow proper scientific methods in serving the soil and crop, as it is determined by genetic structures and environmental conditions, as well as their interaction. Many factors, including genetic systems, environmental factors, and pre-and post-cultivation processes like plowing and fertilization, particularly nitrogen fertilization, have been shown to affect sunflower growth and productivity[4].

According to studies, phenotypic traits in general, and yield components in particular, are good criteria for selecting plants from various genotypes, whether to improve quality or yield, and its components represented in disc diameter, seeds number in the disc, and seed weight[5]. Schoeman[6] demonstrated in his study that the stability of genotype productivity in different environments has become increasingly important to plant breeders, as stable varieties are one of the most important aspects of modern agriculture. After all, knowing their behavior and response to various environmental conditions leads to understanding environmental and genetic interference. Different levels of nitrogen fertilizer had a significant impact on yield and components[7]. Due to a lack of high-yield seed varieties and a reliance on the cultivation of local cultivars, it is necessary to investigate compositions with high yield and good quality under southern conditions.

As a result, this study was conducted to assess the performance of various sunflower genotypes under Basra region conditions, determine the level of nitrogen fertilizer that yields the highest yield, and investigate the interaction between genotypes and nitrogen fertilizer levels.

Citation: Abdullah K N, Jabail W A, Reda Jassim K A. Response genotypes of sunflower (Helianthus annuus L.) and amount of nitrogen fertilizer on growth characteristics, oil yield, and its percentage.Revista Bionatura 2023;8 (2) 25. http://dx.doi.org/10.21931/RB/2023.08.02.25
Received: 2 January 2023 / **Accepted:** 19 April 2023 / **Published:** 15 June 2023

Publisher's Note: Bionatura stays neutral with regard to jurisdictional claims in published maps and institutional affiliations.

Materials and methods

The experimental unit consisted of four harrows, with a distance of 75 cm between each plow and 25 cm between each plant. On the meadow side, planting was done using a complete random block design and splintered plots to achieve a plant density of 53,333 plants/ ha (RCBD). The experiment had two components: the first was a set of six Sunflower genotypes (Local, Aqmar, Ishaqi 1, Ishaqi 2, Tarzan, and Shmoos). Baghdad's Agricultural Research Department is the source of the seeds. The second factor was the amount of nitrogen fertilizer in urea (46 percent N) added in two batches (0,100, 200, 300 kg N/ha). The first was the appearance of four true leaves, and the second was the appearance of four true leaves batches at the beginning of the emergence of flower buds[8]. Phosphorous and potassium fertilization operations were carried out according to the fertilizer recommendation. Phosphate fertilizer was added in the form of P2O5) 110 kg/ ha, and potassium sulfate, 120 kg/ha, in the form of K_2SO_4. Add it all at once when planting.

Before planting seeds, some properties of the study soil were screened as pH, EC, minute volume analysis and soil texture. The experimental field was produced in the spring season on 16.02.2021 and the fall season on 27.07.2021[8] by placing 3-4 seeds in one hole at a depth of 3-5 cm. After two weeks of planting, the plants are thinned to one per hole. Weed control, hoeing, and weeding were done manually as needed.

Studied Traits

The number of leaves: according to the total number of leaves per plant, which starts from the first leaf on the soil's surface until the last leaf on the plant[9].

Fertility ratio (%): A random seed sample was taken at a rate of 50 gm from each experimental unit and according to the number of empty and filled seeds. Then the fertility rate was calculated according to the following equation[10]:

$$\text{Fertility percentage} = \frac{\text{number of full seeds}}{\text{number of empty seeds} + \text{number of full seeds})} * 100$$

The yield of the individual plant (gm/ plant) was calculated from the average result of one plant after extracting the seeds from the flowering disc of ten plants randomly selected from the two middle lines, separating their seeds, and weighing each plant separately.

Oil percentage: The oil percentage was measured by taking a sample of 5 gm of ground sunflower seeds with their husks and using Soxhlet apparatus with Petroleum Ether solvent, the boiling point of 60-80 C°, then it was dried in the oven at 90 C°[11] then weighed the oil that produced from the extraction process

(weight of oil = weight of the beaker with oil - the weight of empty beaker) and its percentage was calculated.

Oil yield (kg.h^{-1}): According to the following equation:-

Oil yield = % oil percentage x total seed yield.

The data were analyzed using the GenStat procedure Library release PL 18.2 software and an analysis of variance (ANOVA) spreadsheet.

Results

The experimental unit consisted of four harrows, with a distance of 75 cm between each plow and 25 cm between each plant. On the meadow side, planting was done using a complete random.

Results presented in Table 1 showed the soil characteristics for the two planted seasons.

Results in Table 2 showed a significant difference between the genotypes among it for the characteristic of leaves number per plant, as between the Table the superiority of the genotype is Shmoos with the highest average number of leaves that reached (27.05 and 29.41) leaves. Plant-1 for two seasons, respectively, compared to the local genetic structure, which gave the lowest number of leaves per plant, with an average of (21.89 and 25.02) for two seasons, respectively. The local genotypes, Ishaqi 1 and Tarzan, did not differ significantly in this trait for the spring season. In contrast, the local genotypes Ishaqi 1 and Tarzan did not vary greatly in the autumn season. The same Table showed the superiority of the fertilizer level N3, which gave (26.32 and 29.94) for two seasons, respectively, compared to level N0, which gave the lowest average (21.68 and 24.05) leaves—plant^{-1} with a significant difference from the other groups. As for the interaction, the Shmoos genotype and N3 fertilizer level showed the highest mean (31.52 and 33.85) leaf. plant^{-1} compared with the fertilizer level N0 and the local genotype, which gave the lowest mean (20.26 and 22.63) leaf.plant^{-1} for two seasons.

Results in Table 3 referred to no significant difference between the genotypes (Local, Aqmar, and Tarzan) for the percentage fertility characteristic in the spring season, and it differed significantly with the Shmoos genotype. In contrast, the two genotypes (Ishaqi 1 and Ishaqi 2) did not differ between it, respectively and differed substantially with the Shmoos genotype. In contrast, in autumn, there were no significant differences between the genotypes (Local, Ishaqi 2 and Tarzan), while Aqmar and Ishaqi 1 did not differ. All genotypes differed significantly from the Shmoos genotype.

The results of the same Table show the superiority of fertilizer level N3 which gave (93.79 and 91.79)% for two seasons, respectively, compared with control treatment N0, which gave the lowest average (91.56 and 88.83) % for the two levels, respectively and with a significant difference from the other levels. As for interaction, it was not substantial for the spring season. During the autumn season, the genetic structure of Aqmar and fertilizer level N1 outperformed them with an average of 92.96%.

Results in Table 4 indicated that significant difference between the genotypes among it for the trait of individual plant yield; the Table showed the superiority of the Shmoos genotype with the highest average unique plant yield amounted to (78.50 and 84.73) gm.plant^{-1} for two seasons, respectively, compared to the local genotype which gave the lowest average (44.80 and 51.23) gm. plant^{-1} for two seasons. The results of the same Table show the superiority of fertilizer level N3, which gave (77.82 and 88.88) gm. plant^{-1} for two seasons, respectively, compared to control treatment N0, which gave the lowest average (44.07 and 43.78) gm. plant^{-1} with a significant difference from other treatments, As for the interaction, Shmoos genotype and the fertilizer level N3 showed the highest average (103.07 and 108.33 gm) compared with the fertilizer control level N0 and the local genotype, which gave the lowest average

Adjective	Quantity			Unit
PH	spring season		Autumn season	–
	7.24		7.80	
EC	6.6		6.3	dSm $^{-1}$
Minute volume analysis	sand	46.50	44.30	gm Km $^{-1}$ soil
	silt	535.80	537.70	
	clay	417.70	418.00	
soil texture	Silty clay loam			

Table 1. Properties of the study soil before planting *Helianthus annuus* L seeds.

Spring season					
genetics	Nitrogen fertilization levels kg ha^{-1}				
	0	100	200	300	average
Local	20.26	21.59	22.18	23.52	21.89
Aqmar	21.85	23.59	25.92	28.59	25.32
Ishaqi 1	19.92	21.92	23.26	24.18	22.32
Ishaqi2	25.59	23.92	24.59	26.59	24.42
Tarzan	20.18	22.52	22.78	23.52	22.25
Shmoos	22.26	24.26	27.18	31.52	27.05
average	21.68	23.13	24.32	26.32	
Lsd $_{0.05}$	0.427= N		0.544= V		1.050=N*V
Autumn season					
genetics	Nitrogen fertilization levels kg ha^{-1}				average
Local	22.63	24.66	25.59	27.18	25.02
Aqmar	24.96	26.66	31.26	33.00	28.97
Ishaqi 1	22.66	24.52	26.26	27.18	25.16
Ishaqi2	25.77	26.59	29.00	31.59	28.24
Tarzan	23.00	25.00	26.00	26.85	25.21
Shmoos	25.26	26.66	31.85	33.85	29.41
average	24.05	25.68	28.32	29.94	
Lsd $_{0.05}$	0.7398= N		0.6477= V		1.3277=N*V

Table 2. The effect of sunflower genotypes and nitrogen fertilizer levels and their interaction on the number of leaves in plants for the spring and autumn seasons 2021.

spring season					
genetics	Nitrogen fertilization levels kg ha^{-1}				
	0	100	200	300	average
Local	92.68	93.55	93.71	93.88	93.45
Aqmar	90.39	91.86	92.65	93.70	92.15
Ishaqi 1	91.20	92.11	93.49	93.65	92.61
Ishaqi2	92.05	93.27	93.64	93.97	93.23
Tarzan	92.24	93.59	93.96	94.32	93.53
Shmoos	90.78	90.58	91.36	93.24	91.49
average	91.56	92.49	93.14	93.79	
Lsd 0.05	0.5194= N		0.5237= V		=N*V S. N
Autumn season					
genetics	Nitrogen fertilization levels kg ha^{-1}				average
Local	90.16	92.96	91.69	91.55	91.59
Aqmar	89.39	89.55	90.46	92.01	90.35
Ishaqi 1	88.76	90.91	92.04	91.65	90.84
Ishaqi2	87.83	91.78	92.03	92.55	91.05
Tarzan	90.11	92.02	91.49	91.68	91.33
Shmoos	86.76	87.89	88.17	91.29	88.53
average	88.83	90.85	90.98	91.79	
LSD 0.05	0.7149= N		0.4574= V		1.0286=N*V

Table 3. The effect of sunflower genotypes and nitrogen fertilizer levels and their interaction on the fertility percentage% characteristic of the spring and autumn seasons 2021.

(37.47 and 33.33) gm. plant^{-1} for two seasons, respectively.

The data in Table 5 indicated that there is a significant difference between the genotypes among it for the characteristic of oil percentage, the Table showed the superiority of the local structure which its seeds containing the highest average rate of oil amounted to (39.55) and (41.13%) compared to the Shmoos genotypes and Tarzan, whose seeds had the lowest percentage oil averaged (36.69%, 37.46% and 37.50%, 38.30%) respectively for two structure and two seasons, and the reason for the superiority of the compositions in the oil percentage may be because the quality of the sunflower seeds.

From the results of the same Table, it appears that the fertilizer level N0, which gave (41.47، 43.87%) for two seasons, respectively, compared with the group N3, which gave the lowest percentage of oil with an average(36.36) and (37.46%), with a significant difference from the other levels.

Results in Table 6 indicated that there is a significant difference between the genotypes in the total oil yield trait; Shmoos composition outperformed by giving the highest mean of oil yield (1161.4 and 1461.3 kg.ha^{-1}) compared to the local genotype, which showed the lowest average (906.8 and 1185) kg.ha^{-1} for two seasons respectively. From the results of the same Table, it appears that the fertilizer level N3, which gave the highest oil yield (1,247.6 and 1673.6) kg.ha^{-1}, compared with the control N0, which gave the lowest oil yield with an average (619.6 and 885.3) kg.ha^{-1} for two seasons, respectively, with a significant difference from the other levels. And the reason for the superiority of fertilizer N3 is due to the abundance of the total seed yield ton.ha^{-1} in addition to the percentage of oil.

The Shmoos genotype and the fertilizer level N3 gave the highest mean of oil yield, which reached (1350.5 and 1778.7) compared with the local genotype and fertilizer level N0 with the lowest average (558.0 and 758.0) kg.ha^{-1} for two seasons, respectively.

Discussion

The reason for the superiority of the local genotypes, Ishaqi 1 and Tarzan, might be due to the nature of the ge-

spring season					
genetics	Nitrogen fertilization levels kg ha^{-1}				
	0	100	200	300	average
Local	37.47	41.20	46.93	53.60	44.80
Aqmar	52.93	57.42	64.63	92.60	66.90
Ishaqi 1	35.13	46.87	50.93	61.00	48.48
Ishaqi2	43.13	51.07	63.47	85.53	60.80
Tarzan	41.33	54.27	59.60	71.13	56.58
Shmoos	54.43	70.47	86.03	103.07	78.50
average	44.07	53.55	61.93	77.82	
Lsd 0.05	2. 684= N		3.348= V		6.477=N*V
Autumn season					
genetics	Nitrogen fertilization levels kg ha^{-1}				average
Local	33.33	45.10	57.13	69.37	51.23
Aqmar	45.30	63.37	82.60	91.67	70.73
Ishaqi 1	40.20	58.03	72.87	86.00	64.27
Ishaqi2	45.60	62.67	74.33	88.40	67.75
Tarzan	40.93	56.50	77.70	89.53	66.17
Shmoos	57.30	81.53	91.77	108.33	84.73
average	43.78	61.20	76.07	88.88	
Lsd 0.05	0.800= N		1.619= V		3.021=N*V

Table 4. Effect of genotypes from sunflower and nitrogen fertilizer levels and their interaction on the trait of individual plant yield in grams for the spring and autumn seasons 2021.

notypes for this trait because this trait has a high response in variable to sunflower cultivars[12], and these results are in agreement with the researches[13,15]. Also, the superiority of these genotypes might be due to the increase in the number of leaves for the genetic structure and the increase in the leaf area which the photosynthesis process occurs through it, as well as the nature and extent of its effect on environmental conditions, including the high temperature that accompanies the process of pollination and fertilization[11,16].

The superiority of the fertilizer level N3, which gave (26.32 and 29.94) for two seasons, respectively, compared to the level N0, could be explained by the effect of nitrogen, which is involved in all vital processes that consider as a basis for building proteins and nucleic acids and encouraging rapid growth as well as the process of cell division and thus positively reflected on the height of the plant, which in turn leads to an increase in the number of leaves[13], and this agrees with what was mentioned[11,17,18]. As well as The reason for the superiority of fertilizer level N3 is that nitrogen is considered the main component in building vital processes, including the leaf area, which helps in the activity and increase of pollen production[4,11,19,20].

The reason behind the significant difference between the genotypes among it the trait of individual plant yield might be due to the increase in fertility rate in Table (3), which resulted in mature seeds and thus led to an increase in the work of the individual plant, as well as to the different transformative nature of foodstuffs as a result of the different genetic structures[21]. These results are consistent with (17, 20). The results in Table (2) may be attributed to the increase in the number of leaves and, thus increase in the leaf area, which led to raising the efficiency of the plant, including an increase in the concentration of elements, increasing the concentration of nutrients inside the plant and converting it into carbohydrates and protein materials that transferred to the seeds in the phase of filling the seeds[17,22,23].

The percentage of oil is affected by environmental and genetic conditions because high temperature reduces the rate of oil[19]. These results are consistent with (11,24). They found the difference in the sunflower genotypes in the percentage of oil in the seeds, and these results agree with the findings of (11,19,24).

spring season					
genetics	Nitrogen fertilization levels kg ha^{-1}				
	0	100	200	300	average
Local	41.47	40.26	39.01	37.45	39.55
Aqmar	39.04	38.84	36.86	37.04	37.95
Ishaqi 1	39.24	37.03	36.72	36.39	37.35
Ishaqi2	41.05	39.67	39.33	36.81	39.21
Tarzan	38.23	38.20	37.75	35.81	37.50
Shmoos	36.74	37.04	36.34	34.64	36.69
average	39.63	38.51	37.67	36.36	
Lsd $_{0.05}$	= N0.695		= V0.631		=N*V1.280
Autumn season					
genetics	Nitrogen fertilization levels kg ha^{-1}				average
Local	43.87	41.56	39.73	39.36	41.13
Aqmar	40.38	40.16	39.35	38.29	39.54
Ishaqi 1	41.42	38.45	38.60	37.46	38.98
Ishaqi2	43.65	37.94	39.14	37.92	39.66
Tarzan	41.08	37.80	37.49	36.83	38.30
Shmoos	39.41	38.03	36.24	35.18	37.46
average	41.80	38.99	38.42	37.51	
Lsd $_{0.05}$	1.066 = N		0.588=V		1.417=N*V

Table 5. Effect of sunflower genotypes and nitrogen fertilizer levels and their interaction on the percentage of oil content for the spring and autumn seasons 2021.

Because nitrogen is the main component in building plant tissue units and increasing these tissues at the expense of the percentage of oil in seeds according to the well-known inverse relationship between oil and nitrogen, when the number of sources increases in the plant due to increases in nitrogen, the oil in the seeds will decrease, these results are in agreement with the findings of19. While interaction showed, the local genotype and N0 fertilizer level showed the highest average oil content (41.47 and 43.87%) compared to the N3 level and the Shamoos genotype, which gave the lowest average (34.64) and (35.18%) for two seasons respectively,

Conclusions

In this study, we can conclude the following: The superiority of the genotype of Suns for two seasons in most of the studied traits of the number of leaves per plant and yield of the individual plant, as well as the highest total oil yield, and the superiority of the local genotype in the percentage of fertility and rate of oil %. All the genotypes showed an apparent response to the fertilizer level N3 in most of the studied traits, and this was reflected positively in the increase in the number of leaves in the plant, the yield of the individual plant, the percentage of fertility and the total oil yield.

Bibliographic references

1. Pand, SB and G.C. Srivestance. Influence of cycocel on seed yield and oil content in sunflower Helianthus annuus L. CCF seed. Field Crop Abst. 1988. 41: 858.
2. Ahuja S.S., H.S. Dhingra and B.S. Bhatia. Comparison of various sunflower planting methods in Punjab. Journal of Agricultural Research. 2003. 40 (1): 64-70.
3. Central Statistics Organization., 2019.
4. I-Rawi, Wajih Mezal Hassan . Guidelines for growing a sunflower. Guidance Bulletin No. (8) The General Authority for Agricultural Extension and Cooperation, Ministry of Agriculture - Iraq. 1998.

spring season					
genetics	Nitrogen fertilization levels kg ha^{-1}				
	0	100	200	300	average
Local	558.0	835.4	1032.8	1200.8	906.8
Aqmar	595.6	1036.6	1098.9	1309.3	1010.1
Ishaqi 1	556.5	871.1	989.3	1191.0	902.0
Ishaqi2	605.1	960.6	1186.1	1245.0	999.2
Tarzan	533.9	918.9	1042.4	1189.2	921.1
Shmoos	868.5	1131.9	1294.6	1350.5	1161.4
average	619.6	959.1	1107.3	1247.6	
Lsd 0.05	24.56=N		29.13=V		56.69=N*V
Autumn season					
genetics	Nitrogen fertilization levels kg ha^{-1}				average
Local	758.0	1056.8	1342.3	1584.3	1185.3
Aqmar	832.7	1354.3	1509.1	1743.6	1359.9
Ishaqi 1	835.5	1182.8	1394.5	1640.0	1263.2
Ishaqi2	916.3	1174.3	1418.3	1705.6	1303.6
Tarzan	815.2	1196.0	1365.6	1589.3	1241.5
Shmoos	1153.9	1368.4	1544.3	1778.7	1461.3
average	885.3	1222.1	1429.0	1673.6	
Lsd 0.05	= N 55.63		= V 74.39		= N*V31.41

Table 6. Effect of sunflower genotypes and nitrogen fertilizer levels and the interaction between them on the characteristic of total oil yield kg. ha^{-1} for the spring and autumn seasons 2021.

5. Killi, F. A. T. I. H. Influence of different nitrogen levels on productivity of oilseed and confection sunflowers (Helianthus Annuus L.) under varying plant populations. International Journal of Agriculture and Biology. 2004. 6(4), 594-598.
6. Al-Sahoki, M., and Karima, M. W. Applications in the design and analysis of experiments. Ministry of Education and Scientific Research - University of Baghdad. 1990.
7. Schoeman. L. J. Genotype X environment interaction in sunflower (Helianthus Annuus L.)in South Africa. Master's degree University of The Free State Blown Fountain. Sunflower Hybrids For Grain And , Fertilization Times Effects on New Oil Yields. Adv. Environ. Biol. 2003. 5(7): 1968-1975.
8. Ibraheem M W, AL Mjbel A A, Abdulwahid A S, Mohammed Th. T. Characterization of the influence of diet on Japanese quail. Revis Bionatura. 2022;7(4) 21. http://dx.doi.org/10.21931/RB/2022.07.04.21.
9. Hunt , R. Plant Growth Cures . The Functional Approach to Plant Growth Analysis. London. Edward Arnold 1982. pp 248.
10. Nima, S. I. Response of growth and yield of two sunflower genotypes (Helianthus annus L.) to phosphate and boron foliar feeding. Master Thesis - Department of Field Crops - College of Agriculture - University of Anbar. 2009.
11. Alrseetmiwe, D. S. .; Almayah, A. A. .; Nasser, A. A. .; Alnussairi, M.; Zadeh, H. A.; Mehrzi, F. A. . CLONING AND EXPRESSION OF AN OPTIMIZED INTERFERON ALPHA 2B IN ESCHERICHIA COLI STRAIN BL21 (DE3). Journal of Life Science and Applied Research 2020, 1, 40-44..
12. Aliwi, E. Y. Response of some sunflower genotypes (Helianthus annus L.) to spraying with folic acid (vitamin B9). Master Thesis - Department of Field Crops - College of Agriculture - University of Baghdad. 2020.
13. Hassan, W., and Ahmed, K. H. Evaluation of sunflower genotypes (Helianthus Annuus L.) in the early stages of growth under different nitrogen and potassium fertilizers levels. Al Furat Journal of Agricultural Sciences. 2017. 9 (1): 152-136.
14. Ozturk, E., POLAT, T., & Sezek, M. The effect of sowing date and nitrogen fertilizer form on growth, yield and yield components in sunflower. Turkish Journal of Field Crops. 2017. 22(1), 143-151.
15. Bjaili, A. A., Al-Solaimani, S. G. and EL-Nakhlawy, F. S. Growth and Seed Quality of Sunflower (Helianthus Annuus L.)Cultivars as Affected by Nitrogen Fertilizer and Defoliation Rates. international Journal of Engineering Research and Technology (IJERT). 2019. 08 (1): 161-167.

16. Al-haidary, H. K. M. Splitting of nitrogen application through growth stages in various sunflower cultivars to improve their vegetative growth and seed yield. Asian J Agriculture and Biology. 2018. 6(3), 357-366.
17. Abd EL-Satar, M. A., and Hassan, T. H. A. Response of seed yield and fatty acid compositions for some sunflower genotypes to plant spacing and nitrogen fertilization. Information Processing in Agriculture. 2017. 4(3), 241-252.
18. Akpojotor, E., Olowe, V. I. O., Adejuyigbe, C., and Adigbo, S. O. Appropriate Nitrogen and Phosphorus Fertilizer Regime for Sunflower (Helianthus Annuus L.) In the Humid Tropics. Helia, 2019. 42(70), 111-125.
19. Ahbabi, H. A. Response of growth and yield of two sunflower cultivars (Helianthus annus L.) to different levels of nitrogen fertilizer and application dates. Master's thesis, Al-Qasim Green University - College of Agriculture - Department of Field Crops. 2015.
20. Abbas, H. A., Khudair, H. U., and Hussain, A. J. Effect of Nitrogen Fertilizer and Plant Density on Yield and Growth of Sunflower. Baghdad Science Journal. 2008. 5(2).
21. Abd, S. A., Jassem, K. A., and Mohsen, B. M. Response of Four Sunflower Genotype (Helianthus Annuus L.) to Different Planting Dates. Jornal of Al-Muthanna for Agricultural Sciences. 2019. 7(2).
22. Abd Elrahman, H., Mohamed, I., and Gangi, A. Effects of cultivar, irrigation interval and nitrogen on seed yield, oil content and quality of sunflower (Helianthus annuus L.). Gezira Journal of Agricultural Science. 2014. 12(2).
23. Abro, T. F., Oad, P. K., Sootaher, J. K., Menghwar, K. K., Soomro, T. A., Shaikh, A. A., . and Channa, Z. Genetic variability and character association between grain yield and oil content traits in sunflower (Helianthus annuus L.). International Journal of Biology and Biotechnology. 2020. 17(4), 701-706.
24. Maliki, A. A. A. M. A. Effect Of Gibberellic Acid And Water Stress In Growth, Yield Characteristics And Oil Percentage On Sunflower. Nveo-Natural Volatiles and Essential Oils Journal. 2022. 1837-1847.

ARTICLE / INVESTIGACIÓN

Genetic analysis of milk production and lactation period in Holstein cows according to BTN1A1 Gene Polymorphism

Riyadh Senekal, Hussien Al-Waith, Nasar Al-Anbari, Wafa'a Al-Samarai
DOI. 10.21931/RB/2023.08.02.26
University of Baghdad, Iraq.
Corresponding author: riyadh.senkal@coagri.uobaghdad.edu.iq.

Abstract: The results showed that the Holstein BTN1A1gene has two alleles (A allele) which is superior to the second allele (B allele)in the two values of the substitution effect and the average effect of the allele, and the homo genotype AA over the hetero genotype AB was successful in the breeding value of the two traits. It was also revealed through the new equations that the gene is responsible for the characteristic of milk production of the total output and the amount of 37725 Iraqi dinars of the full value of the milk price, and it also affects by ±7.24 days of the length of the milking season, which is estimated at 3583.8 Iraqi dinars. It is responsible for the inheritance of 70.09 kg of total milk production for 6.35 days/season length, reflecting the product's price value.The possibility of adopting the BTN1A1 gene within the selection programs to improve some productive traits, as well as the possibility of conducting a comparison between genes on the basis of the new equations, determining their contribution to the studied traits, and choosing the most influential gene to be an effective marker in the selection of quantitative traits.

Key words: Genetic analysis, Milk production, length of lactation, Holstein cows, BTN1A1 gene.

Introduction

Heritability is defined as the ratio of the genetic variance to the total variance, which means that it is the product of dividing the part of the variance due to the inheritance (numerator) by the total variance of the trait (denominator). It gives an idea of the extent of the effect of heritage on a specific quantitative quality; for example, the heritability of a milk production trait is 25%. This percentage shows the total impact of the total of genes affecting the feature, meaning that it is a function of the estimation of the increase or decrease in the genetic variation resulting from the selection of parents and mothers that are transmitted to the next generation without knowing the contribution of each gene to this ratio[1,2], which is shown by the new equation (that is, the proportion of each gene's contribution to the variance of the studied quantitative trait.

The most critical traditional methods for calculating the heritability of any characteristic are full-sib, half-sib, regression on one parent, regression on average parents, and third-generation declines over the first generation, and all of these methods require information for at least two generations. Therefore, the environment is different between the two generations, which leaves a certain percentage of error in estimation, and the result of these equations represents the sum of the effect of genes affecting the studied trait entirely without specifying the development of each gene separately, and the new equation dealt with the two previous points[3].

Calculating the heritability of the trait based on the gene's contribution to the total genetic variance does not need information about the ancestors of the current generation (you do not need the knowledge of the previous generation), as the equation is more accurate than its predecessors because it studies the effect of genetics and the environment in one time and not between two different times, which in turn causes the addition of a ratio. It needs to be corrected in heritability, through which it is possible to compare the other genes that affect the studied trait and choose the gene most influencing the selection processes in what is known as marker-assisted selection.

It estimates the value of the quantitative and price effect of the gene (in the studied herd) using the root of the total variance since the variance is the square of the sum of the deviations of the valuesfrom the general average. This value and dividing the result by the number of individuals will dictate the extent of the effect of the studied gene (±) on the studied trait, such as grams of weight or minutes of height and according to the type of the studied trait. The studied gene per kilogram of milk), which is an essential value because the number of units (such as the number of kilograms) differs between individuals, as the general average of the trait represents the contribution of all genes affecting the studied feature without discrimination of the practical value of each gene, which can be identified through the equation It is possible to use the same equations to predict the gene's contribution to the same traits studied in the next generation, and this is done by replacing the genetic variance with the clustering variance since the clustering two is the one that will be inherited to the next generation.

Butyrophyllin (BTN) belongs to the immunoglobulin family of membrane proteins[4]; the bovine Butyrophyllin (BTN) gene is present in the long arm of chromosome 23, consisting of 8 exons and 7 introns[5,6].

Genetic variation in the bovine BTN1A1 gene has been studied as a genetic marker to control milk production and lipid content at the QTL. It affects economically essential traits in milk animals because it is expressed explicitly in

Citation: Senekal R, Al-Waith H, Al-Anbari N, Al-Samarai W. Genetic analysis of milk production and lactation period in Holstein cows according to BTN1A1 Gene Polymorphism. Revis Bionatura 2023;8 (2) 26. http://dx.doi.org/10.21931/RB/2023.08.02.26
Received: 2 January 2023 / **Accepted:** 19 April 2023 / **Published:** 15 June 2023

Publisher's Note: Bionatura stays neutral with regard to jurisdictional claims in published maps and institutional affiliations.

lactating milk tissues, and the BTN1A1 gene product may act in the secretion of milk fat[7].

Therefore, this study aims to devise new equations to analyze the genetic information of the studied gene to facilitate understanding the genetic contribution in quantitative units (grams, centimeters) of the studied traits.

Materials and methods

This study was conducted in Al-Salam station for Dairy cattle /private sector (Al-Latifia district 25 km southern Baghdad) on 50 Holstein cows, genetic analysis of the BTN1A1 gene was carried out according to the characteristics of milk production and the length of lactation to devise modern equations to calculate the genetic equivalent in the broad sense and limited and the amount of the gene's contribution to the amount of total milk produced as well as The contribution of the gene to the length of lactation as well as its final effect on the milking price in days. Based on the genetic information, DNA samples of good quality, purity and concentration were used for further analysis; the polymerase chain reaction (PCR) technique for BTN1A1 typing is based upon the extensive polymorphism that is present in an 893 region of exon 8 of the butyrophyllin gene was amplified by using primers as[8,9].

-Inferred equations:

1- Heritability of a gene effect (in the broad sense):

$H^2G= 2pq\alpha^2 + 4\ p^2\ \ q^2\ d^2\ /б^2$

P: repetition of the dominant allele, q: repetition of the recessive allele, α: the average effect of allele substitution, d: repeat the hybrid composition, б: variance

The numerator in this equation is the sum of the covariance $A=2pq\alpha^2$ and $D=4\ p^2\ \ q^2\ d^2\ \ ^3$; as for the denominator, it represents the total variance of the trait and can be obtained from one of the following two equations:

A- $б^2 = \sum x^2 – (\sum x)^{\ 2} /n$

B- $SST = \sum Yij^2 – CF$

2- Heritability of a gene effect (in the narrow sense):

$h^2G= 2pq\alpha^2 /б^2$

3- Quantitative effect of a gene:

4- The calorific value of the gene effect:

$$\sqrt{(vA+vD/n)}\ \text{X Price} \qquad (1)$$

Since the previous value represents the estimate of the increase and decrease in the units of the quantitative trait, multiplying it by the value of one unit price will represent the price value of the gene effect.

5- The ratio of the quantitative effect of a gene:

$$\sqrt{(vA+vD/n)}\ /\ M \qquad (2)$$

Dividing the quantitative effect value by the average of the trait will show the extent of the gene's contribution to one unit of the quality (for example, the effect of the studied gene in every kilogram of milk), which is an essential value because the number of units (such as the number of kilograms) differs between individuals, as the general average of the trait is It represents the contribution of all genes affecting the studied trait without discrimination of the practical value of each gene, which can be identified through the current equation.

6- The percentage of the gene's economic contribution to the price value of the studied trait.

$$\sqrt{(vA+vD/n)}\ /M\ \text{X price} \qquad (3)$$

It represents the percentage of the gene's contribution to the unit price of the studied quantitative trait.

7- Prediction of the quantitative and price contribution of the fetus in the next generation:

$$\sqrt{(vA/n)} \qquad (4)$$

- Quantitative effect of a gene in the offspring:

The clustering variance is the part inherited from the genetic variance of the individual, which is a fair value because it is part of the variance value, which in turn is a fair value for deviations from the general mean of the trait. In the offspring of the current herd.

a- Calorific value of the quantitative effect of a gene in the offspring:

$$\sqrt{(vA/n)}\ \text{X Price} \qquad (5)$$

Multiplying the previous value (the quantitative effect) by the price of one unit of the quantitative trait indicates the price value of the effect of the gene on the offspring.

b- The percentage of the quantitative effect of a gene in the offspring:

$$\sqrt{(vA/n)}\ /\ M \qquad (6)$$

The division of the value of the quantitative effect of the gene in the offspring by the average of the quantitative trait in the progeny shows the ratio of this effect, which is an essential value because the number of units differs from one individual to another, which gives a specific value for each individual if this value is multiplied by the number of units of the quantitative trait that the individual possesses.

c- The price value of the ratio of the quantitative effect of a gene in the offspring:

$$\sqrt{(vA/n)}\ /M\ \text{X Price} \qquad (7)$$

Multiplying the previous equation with the price of one unit of the studied quantitative trait shows the extent of the gene's contribution to the cost of this unit and its reflection on the price of the animal as a whole.

Results

The AA genotype recorded the highest educational value, and it is consistent with the fact that this combination is the highest in milk production and lactation period, as well as the least deviating dominantly compared to the genotype (AB) (Table 1), that this result indicates that the AA genotype is the best. And because the additive variance (VA) is high compared to the dominant variance (VD), so choosing the best genotype (AA) will be feasible because the clustering effect will be inherited for the following generations[4,10]. It was understanding the variation mechanism in hybrid individuals[11].

The average effect of the A allele of BTN1A1 was the highest compared to that of the B allele, and it is expected that the presence of the allele A added an increase in the

total milk production and lactation period and the average substitution effect of allele A was positive because it contributed to the total milk production and lactation period (Table 2), which shows the value Added or missing as a result of selection for one of the alleles[3], these results give an absolute preference to allele A of the BTN1A1 gene over the mutant B allele, which indicates the importance of selection in favor of this allele

Table2. Average of allele effect and the average of allele substitution for total milk production and lactation period traits.

The equations extracted in this research found that the heritability in its broad and narrow sense amounted to 0.26 and 0.22, respectively, for the milk production trait is within the logical range of the trait[12,13].

Also, the quantitative effect of the gene is 75.45 kg (Table 3) of milk within the total milk production, meaning that the AA genotype adds this amount. Still, the mutant structure causes a loss of the same amount, which gives clear pictures of the quantitative contribution of this gene within the total quantitative effect of all genes affecting the production trait. Milk is a quantitative trait that is affected by a large number of genes[14], and the effect of the gene on each kilogram of milk reached 0.04 kg (Table 3). If we assume that the price of milk is 500 Iraqi dinars, it affects the price value of milk by an amount of 37725 and 200 dinars in the value of Total milk produced and price per kilogram, respectively; on the other hand, the value of what this gene inherits to the next generation in the case of the AA composition is approximately 70 kg of milk per season and 0.037 kg per kilogram of milk per person (Table 3) if these values are calculated based on the cumulative variance of the gene, which is the value that is inherited to the next generation. Suppose the price value of the inherited values is calculated. In that case, it becomes evident that this gene is responsible for the value of 35 thousand and 18.5 dinars of the total milk price and each kilogram in the next generation.

These values are understandable for educators and economists, which enhances their understanding of the importance of marker-assisted selection programs and facilitates comparison between different genes, relying on candidate genes within the selection programs.

The equations extracted in this research found that the genetic equivalent in its broad and narrow sense amounted to 0.11 and 0.09, respectively, for the lactation period (Table 4), which is within the logical range of the trait[15,16].

The gene's quantitative effect on the lactation period's characteristic was 7.24 days (Table 4). It shows that the pure, wild composition of the gene increases the production season by seven days (Table 4), which is very close to the price value of the gene calculated through the total production of milk, which is 37725 (Table 3), which supports the accuracy of the equations that the researcher devised in this research. And it supports the adoption of this method with other genes affecting the characteristic of milk production and lactation period, considering that this characteristic is A quantitative characteristic that is affected by a large number of genes, as it can be seen from the table that the value of the effect of this gene per day ranges from 0.037 per day, meaning its weight of 18 Iraqi dinars (Table 4).

As for the amount of this gene inherited, it increases the number of days of the production season for the offspring by about 6.35 days, with a price value of 3143.25 and 0.03 dinars for the season and one day, respectively.

That the price value of the gene matches when measured by season length and total production indicates the importance of adopting these equations to clarify the percentage of genes participation accurately and naturally in the studied traits as well as facilitate the task for breeders and economists in adopting genetic improvement programs, which enhances the improvement of the studied traits and increases the support of researchers in this field.

Genotype	Traits	Mean	Adjusted average	Breeding value	Dominance deviation	VA	VD	VG
AA	Total milk production	1992.24	1910.874	2347.978	1872.462	245647.91	39025.15	284673.06
AB		1486.07		1567.4358	2108.42			
BB		0		786.894	2418.85			
Genotype	Trait	Mean		Breeding value	Dominance deviation	VA	VD	VG
AA	lactation period	195.35	192.6224	232.274	187.8349	2021.46	606.21	2627.68
AB		158.74		161.46759	217.244			
BB		0		90.6612	255.935			

Table 1. Mean, adjusted average, Breeding value, Dominance deviation and variance components of milk production and lactation period.

Allele	Trait	Average of allele effect	Average of allele substitution
A	Total milk production	218.55176	780.542
B		-561.9902	-780.542
A	lactation period	19.825792	70.8064
B		-50.98061	-70.8064

Table 2. Average of allele effect and the average of allele substitution for total milk production and lactation period traits.

Measurements of the actual and relative values of gene	Values (total milk production)
Heritability (broad)	0.26
Heritability (Narrow) based on VA	0.22
Measurements based on genetic variance (current values)	
The value of the actual (real) effect of a gene (or quantitative effect)	75.45 Kg / total weight
The price effect or total (price value)	37.725 Iraqi dinars *
Percentage of the true effect of the gene(Kg)	0.04 / day
The price effect of the gene (Kg)	200 Iraqi dinars
Measurements based on clustering variance (predicted genetics)	
The actual inherited collective effect (Kg)	70.09 Kg/ weight
Inherited calorific value (total)	35.045 Iraqi dinars
Percentage of the true aggregate effect of inheritance (Kg) [1]	0.037 Kg
The inherited calorific value ratio(Kg)	18.5 Iraqi dinars

[1] 1 Kg of milk = 500 Iraqi dinars

Table 3. Measurements of the actual and relative values of genes for total milk production trait.

Conclusions

We conclude from this study the possibility of adopting these equations in calculating the effect of individual genes affecting the quantitative traits studied, mainly after it was found in this research that the gene obtained the same value after studying its effect using these equations through two characteristics separately. The BTN1A1 gene can be adopted in milk production trait genetic improvement programs (AA genotype).

Bibliographic references

1. Jalal, S.; Karam, H. Animal breeding. Dar Almaraf publication. Cairo, 4th Ed. 2003.
2. Greeff, JM Deconstructing jaco: Genetic heritage of an Afrikaner, Ann Hum. Genetics 2020, 71: 674-688.
3. Falconer, D.S; Mackay T. F.C. Introduction to quantitative genetic. 4th edition, Longman Group Ltd. 1996.
4. Yardibi, H.; Esen Gürsel, F.; Ates, A.; etal. BTN1A1, FABP3 and TG genes polymorphism in East Anatolian red cattle breed and South Anatolian red cattle breed. African J. of Bio. Tech. 2013, 12 (20) :2802-2807.
5. Brunner, R.M.; Guerin, G.; Goldammer, T.; etal. The bovine Butyrophyllin encoding gene. (BTN) maps to chromosome 23. Mammalian Genome 1996. 7, 635.
6. Taylor, C.; Everest, M.; Smith, C. Restriction fragment length polymorphism in amplification products of the bovine Butyrophyllin gene: assignment of bovine butyrophilin to bovine chromosome 23. Anim. Gen. 1996, 27, 183-5.
7. Zegeye, A. Quantitative Trait Loci (QTL) and promoter analysis of the bovine Butyrophilin gene. Ph.D. Thesis. Maryland: Department of Animal and Avian Sciences, University of Maryland. 2003.
8. AL- Shamary, W. A. .; Alkhateb, B. A. A. H. .; Abdel, E. T. . role of perlite quantity and intervals of irrigation on potatoes (solanum tuberosum l.) grown in gypsiferous soil. JLSAR 2020, 1, 31-39.
9. Emad H. H. Alsalmany , TH. T. Mohammed. Effect of adding natural zeolite and vitamin E to diets of laying hens (Lohman Brown) on some physiological traits and productive performance during hot weather. Revis Bionatura .2022;7(4) 12. http://dx.doi.org/10.21931/RB/2022.07.04.12..
10. Al-Waith, H.K. Association between BTN1A1 gene polymorphism and milk production and its contents in Holstein cows. Plant Archives 2019,Vol.19 (2): 1184-1187.
11. Visscher, P.M.; Woolliams, J.A.; Smith. D.; Williams, J.L. Estimation of pedigree errors in the UK dairy population using microsatellite markers and the impact on selection, Journal of Dairy Science 2002, 85:2368-2375.
12. Gebreyohannes, G.; Koonawootrittriron, S.; Elzo, A.; Suwanasopee. T. Variance Components and Genetic Parameters for Milk Production and Lactation Pattern in an Ethiopian Multibreed Dairy Cattle Population. Asian-Australas. J. Anim. Sci. 2013, 26(9): 1237–1246.
13. Canaza-Cayo, A.W.; Lopes, P.S.; Cobuci, J.A.; Martins, M.F.; da Silva, M.V.; Genetic parameters of milk production and reproduction traits of Girolando cattle in Brazil. Italian J. oh Anim. Sci. 2017, 1-9. http://www.tandfonline.com/loi/tjas20
14. Chamberlain, A.J.; McPartlan, H.C.; Goddard. ME The number of loci that affect milk production traits in dairy cattle. Genetics 2007, 177(2): 1117-1123.

Measurements of the actual and relative values of gene	Values (lactation period)
Heritability (broad)	0.11
Heritability (Narrow) based on VA	0.09
Average milk production per day	9.95 Kg [1]
Measurements based on genetic variance (current values)	
The value of the actual (real) effect of a gene (or quantitative effect)	7.24 Kg / total weight
The price effect or total (price value)	35.838 Iraqi dinars [2]
Percentage of the true effect of the gene(Kg)	0.037 / day
The price effect of the gene (Kg)	18.29 Iraqi dinars
Measurements based on clustering variance (predicted genetics)	
The actual inherited collective effect (Kg)	6.35 Kg/ weight
Inherited calorific value (total)	31.432 Iraqi dinars
Percentage of the true aggregate effect of inheritance (Kg)	0.03 Kg
The inherited calorific value ratio(Kg)	14.85 Iraqi dinars

[1] Price (4950 Iraqi dinars)

[2] 1 Kg of milk = 500 Iraqi dinars

Table 4. Measurements of the actual and relative values of the gene for the lactation period trait.

15. Pantelić, V.; Sretenović, L.; Ostojić-Andrić, D.; Trivunović, S.; Petrović, M.M.; Aleksić, S.; Ružić-Muslić, D. Heritability and genetic correlation of production and reproduction traits of Simmental cows. African Journal of Biotechnology 2011, Vol. 10 (36), pp. 7117-7121.
16. Santos, D.J.A.; Peixoto, M.G.; Borquis, R.R.A.; Verneque, R.S.; Panetto, J.C.C.; Tonhati, H. Genetic parameters for test-day milk yield, 305-day milk yield, and lactation length in Guzerat cows. Elsevier B.V. 2013,114-119. Open access under the Elsevier OA license. http://dx.doi.org/10.1016/j.livsci.2012.12.012.

ARTICLE / INVESTIGACIÓN

Epidemiological Study of Prevalence TB in Iraq

Asmaa A. AL-Kaisse[1]*, Amina N.AL-Thwani[1], Ahmed A. Mankhi[2], Zainab H. Abood[1] and Ruqaya Mustafa Ali[3]

DOI. 10.21931/RB/2023.08.02.27

[1] Institute of Genetic Engineering and Biotechnology for Post Graduate Studies, Baghdad University, Iraq.
[2] National Specialized Center for Chest and Respiratory Diseases, Ministry of Health and Environment, Baghdad, Iraq.
[3] Ministry of Agriculture, Veterinary Department, Baghdad, Iraq.
Corresponding author: asmaa.adnanalqaisi@yahoo.com

Abstract: To assess the prevalence of tuberculosis epidemic in Iraq in terms of the age groups most affected by tuberculosis bacteria, for both gender and for all governorates of Iraq, various clinical specimens were obtained from 744 patients attending the Specialized Chest and Respiratory Disease Center / National Reference Laboratory (NRL) for tuberculosis in Baghdad between April 15 and November 14 2021 the diagnosis by direct microscopy using the Zeihl-Nelsen (ZN) stain and followed by culturing on Lowenstein-Jensen medium (LJ), for 744 clinical specimens revealed that 92(12.37%) specimens were positive by direct examination while 111(14.9%) specimens were positive by culturing on LJ medium with sputum specimens accounting for the majority of culture positive specimens 103/111(92.8%) the rate of Pulmonary tuberculosis (PTB) was a higher than (EPTB) extra-pulmonary (94.6%), (5.4%) respectively the most of tuberculosis cases were found in Baghdad city (62.2%) vs other governorates (37.8%) males were more affected (63.0%) than females (37.0%) and the majority of patients were aged 35–44 years (30.6%) but the lowest age group was least than 15 years (1.8%) the data above ** (P≤0.01) showed a statistically significant difference, cultivation dependence most be more sensitive than direct method and require more attention in TB control programs to healing patients.

Key words: Tuberculosis, *Mycobacterium tuberculosis*, Iraq.

Introduction

Infectious tuberculosis, or TB, is a leading cause of death and poor health worldwide; anyone can contract it. Before the coronavirus (COVID-19) pandemic, TB was the most significant cause of death from a single infectious disease. Higher than HIV/AIDS in terms of both treatability and preventability is tuberculosis (TB). A six-month pharmacological regimen effectively treats about 85% of people with TB illness[1]. TB infection can be treated with a regimen lasting one to six months. 1.3 million more people will die from tuberculosis-related causes in 2020 than from HIV/AIDS-related causes combined (0.68 million). The COVID-19 outbreak has impacted TB mortality more than HIV/AIDS in 2020. The number of people who died from HIV/AIDS fell between 2019 and 2020[2], in contrast to those who died from tuberculosis. Most droplets released from the mouth, nose, and throat when someone talks, or coughs transmit tuberculosis, a respiratory disease. However, tuberculosis can also spread to other body regions, such as the lymph nodes, pleura, belly and urogenital tract[3,4], skin and joints[5,6], bones[7,8], and the meninges. Extra-pulmonary tuberculosis is the name given to the following type of illness. Although no signs or symptoms of tuberculosis may be present, a continuing immune response to Mycobacterium tuberculosis (M. tb) antigens is what the World Health Organization (WHO) considers an LTBI. The World Health Organization estimates that approximately one-fourth of the world's population is infected by Mtb and has a latent TB infection (LTBI)[4]. To reduce the risk of poor treatment outcomes, health sequelae, as well as the negative social and economic consequences of tuberculosis, the first goal is to ensure that tuberculosis disease is exposed early and treated promptly; the second goal is to reduce community-level TB disease prevalence, thus preventing the spread of tuberculosis in the future in fetuses and children. There is a connection between these two objectives. Preventative tuberculosis (TB) treatment can be provided to individuals diagnosed with the disease, decreasing the chance of future cases of illness[5]. TB and other kinds of tuberculosis are affected by this (TB). According to WHO research, the frequency of tuberculosis in Iraq will reach 27 cases per 100,000 people by the year 2020, according to WHO. A steady decline in disease prevalence had occurred throughout the prior decade[6]. The goal of this research was to find out how common tuberculosis is among Iraqi patients.

Materials and methods

Collection of Samples To investigate Mycobacterium tuberculosis, a total of 744 diagnostic specimens were collected from patients who went to the “Specialized Chest and Respiratory Diseases Center/National Reference Laboratory for Tuberculosis (NRL) in Baghdad” between April 15 and November 14 2021. There were 429 males, which accounts for 60.0 percent of the total, and 315 females, which accounts for 37.0 percent. The ages of the individuals ranged from a few months to over 65 years. The specimens were divided into two categories: those with pulmonary tu-

Citation: AL-Kaisse A A, AL-Thwani A N, Mankhi A A. Abood Z H, Ali R M. Epidemiological Study of Prevalence TB in Iraq. Revis Bionatura 2023;8 (2) 27. http://dx.doi.org/10.21931/RB/2023.08.02.27
Received: 10 February 2023 / **Accepted:** 15 May 2023 / **Published:** 15 June 2023

berculosis 603 and those with extra-pulmonary tuberculosis 141 (Table 1).

Sample Processing: To digest and disinfect the specimens, standard operating protocols for laboratory manual labor were followed[7]. Ziehl Neelsen (ZN) stain was employed in smear microscopy, which is a form of direct inspection. This was done to examine all clinically decontaminated specimens.

Cultivation: Each decontaminated specimen was injected into LJ media by spreading three to four drops of centrifuged sediment all over the surface of three slops of LJ medium. This was done in order to culture the bacteria. After having each culture sit at an angle for three days at 37 degrees Celsius with the lids only partially closed, the lids were secured, and the cultures were incubated vertically for a total of eight weeks (cultures were examined weekly). After this incubation period, the growth was either observed or dismissed as negative, and the results were recorded according to whether they were positive or negative. It takes anywhere from six to eight weeks for the consequences of solid culture to become visible. The growth rate, colony morphology, and ZN staining of positive cultured isolates were also used to gain further identifications.

Results

Colony morphology and staining

During 8 weeks, the results of culture on LJ media became seen. M. tuberculosis complex colonies on LJ media were big, uneven in form, scratchy, inflexible, and non-pigmented, similar to coli flower colonies. Bacilli were straight or slightly curved red-dotted rods organized singly or in pairs when microscopic culture isolates were inspected with ZN dye.

Coverage of the database

According to the results obtained, pulmonary TB (PTB) specimens accounted for 603(81%) of the total 744 specimens, whereas extra-pulmonary TB (EPTB) specimens accounted for 141(19%), as indicated in Table (2). Smear microscopy (direct examination) revealed that 92(12.37%) specimens were positive, 111(14.9 %) specimens were able to develop on LJ media, and culture examination revealed 633 negative specimens. ** (P≤0.01), a very significant difference between all category specimens. The positive cultivation rate of M. tuberculosis complex from pulmonary tuberculosis (PTB) specimens was more excellent 105/111(94.6%) than extra-pulmonary tuberculosis (EPTB) specimens 6/111(5.4%), with a highly significant difference ** (P≤ 0.01) between them. Sputum specimens 103/111(92.8%) had the highest proportion of bacterial growth out of 111 specimens, whereas PTB specimens 103/105 had a higher rate (98.1%).

Tuberculosis prevalence in Baghdad and neighboring governorates

Table (3) shows that Bagdad City had a more significant percentage of culture-positive specimens than other governorates, with 69/111(62.2%) specimens being positive by cultivation on LJ media, compared to 42/111 (37.8%) in other governorates, with very significant dereference ** (P< 0.01), shows.

Connection of Tuberculosis with Gender and Age

The data presented in Table (4) indicated that males had a significantly higher prevalence of tuberculosis than females; the overall male-to-female attribution was 1.7 (70/41), and the variation was statistically significant. The data also indicated that the ratio of males to females was significantly different (P<0.01). The patients were placed in one of the Table's seven distinct age groups, which were assigned to them following their ages in Table (5). The age groups (35–44 years) exhibited higher frequencies of TB cases (30.6 percent) than any other age group. In comparison, the age groups (15 years) with a percentage (1.8 percent) were revealed to be the least recorded age groups, with highly significant differences between all age groups ** (P< 0.01).

Discussion

The direct smear microscopy method applied frequently in the third world and particularly in Iraq, is one of the methods that can be used to diagnose tuberculosis. Regarding the diagnosis of tuberculosis, the LJ culture medium is usually recognized as the gold standard in underdeveloped nations[8]. In terms of the clinical manifestations that they cause, pulmonary tuberculosis (also known as PTB) and extra-pulmonary tuberculosis (also known as EPTB) are the two most frequent types of tuberculosis (TB). The pleura, lymph nodes, bones, and the meningeal lining of the brain are not the only organs that tuberculosis (TB) can affect; they can also affect other organs (extra-pulmonary tuberculosis, EPTB). Even though pulmonary tuberculosis is the most common form, it is not the only kind of tuberculosis (PTB).

Pulmonary TB (PTB) expands at a quick rate in 94.6 percent of cases, with the remaining incidences of the disease happening outside of the lungs in 5.4 percent of patients (EPTB). This investigation determined that PTB's prevalence was higher than EPTB's, aligning with earlier studies' findings[9-12]. According to a study that was conducted in Iraqi Kurdistan[13], it was found that 63.5% of patients had extra-pulmonary tuberculosis, whereas only 36.5% of patients had pulmonary tuberculosis. Extra-pulmonary tuberculosis is a condition that affects a significant portion of people who have tuberculosis. There are several potential explanations for why the risk of extra-pulmonary tuberculosis varies from person to person; several of these features include the inherent immunity of the host, the pathogenicity of various strains of Mycobacterium tuberculosis, and the mechanism of transmission. According to the findings of yet another Iranian study[14,15], patients diagnosed with extra-pulmonary tuberculosis face a mortality risk of 5.58 times higher than those diagnosed with pulmonary tuberculosis.

On the other hand, the sputum smear test can differentiate between two types of pulmonary tuberculosis, which are referred to as smear-positive and smear-negative pulmonary tuberculosis, respectively. In this experiment, 92.8 percent of the total sputum samples showed positive results for pulmonary tuberculosis on a smear test; the fact that it poses a danger of infecting others by droplet or airborne transmission[16,17] is one reason why it could be considered a source of community contagiousness. In addition, the findings demonstrated that patients with EPTB were more likely to have pleural infections than any other type of infection, which is consistent with (9,18) in Iraq and (19,20) in

No	Specimen type	Number	Percentage (%)
1.	Sputum (Sp.)	546	73.3
2.	Bronchoalveolar lavage -(BAL)-	57	7.7
Total pulmonary TB specimens		603	81.0
3.	42	5.6	5.6
4.	26	3.5	3.5
5.	18	2.4	2.4
6.	11	1.5	1.5
7.	11	1.5	1.5
8.	11	1.5	1.5
9.	8	1.1	1.1
10.	7	1.0	1.0
11.	4	0.5	0.5
12.	2	0.3	0.3
13.	1	0.1	0.1
Total extra pulmonary TB specimens		141	19.0
Total		**744**	**100%**
Chi-square-χ^2		--	**22.075 ****
P-value		--	**0.0001**
** ($P \leq 0.01$)			

Table 1. Specimen numbers and kinds.

Iran and Uzbekistan; further research has found that lymph nodes are to blame for nearly half of the cases of extra-pulmonary tuberculosis (EPTB) in Iraqi Kurdistan[21] and in Turkey[22]. For instance, the genitourinary system and the skin were the two most common sites of infection in Hong Kong[23], but in the United States, bone and joint infections were more prevalent[24].

In this investigation, the M. tuberculosis cultivation ratio in clinical specimens was 14.9%, significantly higher than the percentage that could be determined with a detailed visual examination (12.37 percent). Smear microscopy and Ziehl–Neelsen (ZN) staining are the two methods most commonly used to diagnose tuberculosis in underdeveloped countries (TB). This strategy does not require the utilization of advanced technology[25], among its many appealing features, low expense, great performance, and a high degree of precision. It takes two hours to receive the results of the smear microscopy, but it is less sensitive than other testing procedures since it requires between 5000 and 10,000 bacteria in a milliliter of sputum to achieve a positive result. Consequently, it takes longer to get the results of the smear microscopy. Patients with a positive culture but a negative sputum smear account for 13% of all cases of tuberculosis that are spread from patient to patient. When healthy persons come into close contact with TB suspects with negative sputum cultures, the risk of getting MTB and developing active TB increases for both sets of individuals. The test's sensitivity can be improved by following a routine in which sputum samples are collected on three separate days first thing in the morning. As a result of its lack of sensitivity, sputum smear microscopy cannot differentiate between Mycobacterium tuberculosis and Mycobacterium tuberculosis complex[26].

Consequently, the Lowenstein–Jensen (LJ) medium for the growth of Mycobacterium is utilized in tuberculosis diagnosis. This medium is recognized as the gold standard. This

Specimen		No. of Specimens	Type of Examination				
			Direct		Culture		% of Positive culture
			+Ve	-Ve	+Ve	-Ve	
PTB	Sputum	546	88	458	103	443	92.8%
	Bronchoaveolar Lavage – (BAL)	57	1	56	2	55	1.8%
EPTB	Pleural fluid (Pl.F)	42	2	40	3	39	2.7%
	Aspiration	1	0	1	1	0	0.9%
	Cerebrospinal fluids - CSF	4	0	4	1	3	0.9%
	PUS	7	1	6	1	6	0.9%
	Ascetic fluid (AF)	26	0	26	0	26	0%
	General Biopsy	18	0	18	0	18	0%
	Abscess	11	0	11	0	11	0%
	Urine	11	0	11	0	11	0%
	Swab	11	0	11	0	11	0%
	Body Fluid	8	0	8	0	8	0%
	Gastric fluid (GF)	2	0	2	0	2	0%
Total		744	92	652	111	633	--------
%		---	12.37	87.6	14.9	85.0	100%
Chi-square-χ2		---	421.50 **		366.24 **		46.741 **
P-value		---	0.0001		0.0001		0.0001
** (P≤0.01).							

Table 2. Division of specimens according to the kind of TB and test.

	Governorate	No. of Specimens	Culture		% of positive culture
			+Ve	-Ve	
1	Baghdad	506	69	437	62.2%
2	Wasit	27	9	18	8.1%
3	Dhi Qar	32	6	26	5.4%
4	Nineveh	11	6	5	5.4%
5	Al-Anbar	19	2	17	1.8%
6	Al-Basra	5	2	3	1.8%
7	Al-Najaf	14	2	12	1.8%
8	Babylon	15	2	13	1.8%
9	Diyala	21	2	19	1.8%
10	Karbala	15	2	13	1.8%
11	Salah Al-Dien	15	2	13	1.8%
12	Al-Diwaniyah	2	1	1	0.9%
13	Al-Muthanna	6	1	5	0.9%
14	Al-Sulaymaniyah	8	1	7	0.9%
15	Dohuk	6	1	5	0.9%
16	Erbil	18	1	17	0.9%
17	Kirkuk	13	1	12	0.9%
18	Maysan	11	1	10	0.9%
Total		744	111	633	100%
Chi-square-χ 2		---	---	---	21.583 **
P-value		---	---	---	0.0001
** (P<0.01).					

Table 3. Apportionment of tuberculosis cases in Baghdad and other governorates.

Sex	No. of Specimens	Culture Based Diagnosis	
		+Ve	%
Male	429	70	%
Female	315	41	63.0%
Total	744	111	37.0%
Chi-square-χ 2	---	---	100%
P-value	---	---	9.027 **
** (P<0.01).			

Table 4. Divide TB patients according to gender.

Age group (year)	No. of Specimens	Culture Based Diagnosis	
		+Ve	%
< 15	35	2	1.8
15 – 24	103	11	9.9
25 – 34	126	18	16.2
35 – 44	153	34	30.6
45 – 54	142	21	19.0
55 – 64	101	14	12.6
> 65	84	11	9.9
Total	744	111	100%
Chi-square-χ 2	---	---	11.782**
P-value	---	---	0.0003
** (P<0.01)			

Table 5. Patients diagnosed with tuberculosis are classified according to age group.

technique has high sensitivity, even though it can take many weeks to complete. Cultures of Mycobacterium TB grown in LJ medium can detect the presence of Mycobacterium tuberculosis in sputum samples when there are at least 10 viable bacilli per milliliter of sample[27]. Regardless of the incidence of HIV, sputum induction detected approximately 75% of culture-positive TB cases in children and adults, according to a meta-analysis that included 17 independent research. However, the percentages estimated by individual investigations varied[28]. Researchers came to this conclusion after investigating the sensitivity of the sputum induction process. The generation of sputum was typically successful, with success rates ranging from 76.4 percent to 100 percent, and side effects were uncommon and modest, according to a new comprehensive examination of 23 trials. This review came to the additional conclusion that the majority of adverse effects were controllable. Compared to culture, the range of sensitivity that can be achieved by using microscopy on induced sputum samples is 0% to 100%. When compared to nasopharyngeal aspiration and stomach lavage, sputum induction produced significantly larger yields[29].

Only three extra-pulmonary specimens were found to have ZN stain, whereas six solid culture specimens were found to contain it. This difference is likely because ZN stain is only present in extra-pulmonary models. Even though pulmonary tuberculosis is the most common form of the disease in children, it is rarely tested for because children have trouble coughing up enough phlegm to get a good specimen for bacteriological verification. This is even though pulmonary tuberculosis is the most common disease in children. In children, the risk of contracting pulmonary tuberculosis is significantly higher than other kinds of tuberculosis. In some instances, it has been reported that the organism spreads through the bloodstream. This has been observed most frequently in infants and children under the age of five. The disease, which is often referred to as "military tuberculosis," can be spread through traumatic means and can affect any organ or tissue in the body, including the bones, brain, meninges, and stomach. The most prevalent indications of extra-pulmonary tuberculosis in children are TB adenitis and TB pleural effusion. The extra-pulmonary form of tuberculosis affects approximately 20–30% of all children who get the disease. If children with tuberculosis (TB) are not given the appropriate medication or develop a resistant strain, treatment may become substantially more challenging for these patients[30]. The AFB smear is quite specific for Mycobacterium; nonetheless, it is essential to remember that a positive AFB result might be caused by any non-tuberculous mycobacteria (NTM).

The acid resistance of Nocardia and other actinomycetes is not as high as that of other actinomycetes, although these species are uncommon. In a positive AFB smear, mycobacteria are almost invariably present; however, M. tuberculosis is not a prerequisite for mycobacteria[31]. Mycobacterium culture is, as of the time of this writing, the method that is both the most sensitive and trustworthy in terms of determining whether or not a current case of tuberculosis exists[31-33]. If the smear test returns negative results for tuberculosis, a residual culture must be performed. DNA fingerprinting and DST are two methods that can be utilized to identify culture isolates; these culture isolates can subsequently be used in molecular epidemiology research, culture can be performed on any sample, and sputum is the most usually used material for diagnosing pulmonary tuberculosis[33], but culture can be performed on any sample also Mycobacteria can be found at a density of 10–100 viable cells per milliliter of material when culture procedures are used[34]. Because of the limited sensitivity of the direct smear method, live bacteria may be missed while using this method[35]. There is a higher probability of infection when acid-resistant bacteria are not tested for beforehand.

It is essential to detect pulmonary tuberculosis as early as possible and make an accurate diagnosis to cut down on the disease's transmission rate and the severity of its long-term effects. The sputum smear microscopy test is the most common test used to determine whether a patient has lung tuberculosis. This test is widely available in a variety of countries around the world. According to a recent study[36-38], most tuberculosis patients with a positive smear test have high-quality microscopy of two consecutive sputum specimens. This percentage ranges from 95 to 98 percent. This finding was uncovered by scientists working in the United States. The World Health Organization (WHO) advises that only two sputum specimens should be collected on the same day, and this recommendation can only be obtained through high-grade acid-fast bacilli (AFB) microscopy. Consequently, diagnostic costs can be brought down to a more manageable level by reducing the number of patients who withdraw from the procedure[38].

The more significant number of tuberculosis cases in Baghdad may be attributable to the city's high population density and crowded conditions (close contact with patients), as well as the availability of more diagnostic methods facilities than in other governorates, which allowed for the recording of more tuberculosis cases among suspected TB patients and patients who were unable to travel to Baghdad and who went to the TB center in their governorate. According to the data presented in Table 3, Baghdad has a significantly greater rate of TB patients than the national average. Because it is the only accredited laboratory in Iraq to perform such tests, patients with suspected tuberculosis bring their samples to the National Reference Laboratory (NRL) for identification and culture. This is done because the NRL is the only place in Iraq where such tests can be performed. The high incidence of tuberculosis in Baghdad can be attributed to several different factors. The most important of them are the growing population, the increasing urbanization, and the presence of people in enclosed areas for the majority of the day; all of these factors are contributing to an increase in the number of refugees and displaced persons living there. Because HIV, smoking, diabetes, alcoholism, and malnutrition are all key risk factors and social determinants of tuberculosis (TB), the significance of these factors has come under increased scrutiny over the past several years[39]; the list is rounded out by overcrowding, the challenge of successfully navigating day-to-day life, and a lack of resources. Tuberculosis is the most significant cause of mortality and disability in the developing world and the primary source of HIV infection in the world's poorest countries, according to the World Health Organization (WHO)[40,41].

The findings presented in Table (4) align with those found in studies[42] and research[9,43,44], which indicate that men risk developing tuberculosis three times higher than women. According to the findings of a study that was carried out in Iran, males have a higher risk of developing pulmonary tuberculosis than females[45]. Around the world, the proportion of males to females among newly diagnosed tuberculosis (TB) cases with a positive smear test is approximately two to one. This is not the case, however, in the country of Pakistan. The rate of tuberculosis cases reported by females is 20–30 percent higher than those reported by males, and this difference remains even with increasing age[46]. As a point of interest, the disparity in mortality rates between men and women persists throughout all stages of life. Those who are HIV-positive and have a history of tuberculosis have a greater chance of passing away from the disease than those who are HIV-positive and have an account of tuberculosis but are male. Even more so for women in Africa, where several studies have discovered a fatality rate that is 20% higher for HIV/TB co-infected women than for co-infected men[47]. This is especially true for women in Africa. In nations like South Africa, the rate of HIV-associated tuberculosis fatalities among women with HIV and tuberculosis is also twenty percent greater. It is more common for males to develop tuberculosis than women because men partake in more activities outside the home, such as smoking, consuming alcohol, and engaging in behaviors that are against the law. Among the many different examples, one that has a significant connection to these connections is bottomless pit mining[48].

Comparable to this, the fact that women have connec-

tions with tuberculosis patients who are not members of their immediate family or household can be considered a risk factor[49]. Pregnant women with tuberculosis and HIV infection may have an increased chance of dying from tuberculosis (TB) because of the medical problems that suppress the immune system during pregnancy[50]. Because of these chromosomal and hormonal variances, the host's response to an infection differs in males and females. This is because the immune system is regulated differently. Estradiol seems to be the hormone responsible for maintaining a healthy immune system, in contrast to progesterone and testosterone, which appear to inhibit the body's natural defenses against infectious diseases. Genetic variables, such as those connected with a person's sex chromosomes, can also play a role in determining an individual's vulnerability to infection[51]. Research has shown that characteristics related to a person's line of work and their way of life play a significant part in the risk of contracting an illness and its treatment. When researching tuberculosis, it is customarily a good idea to focus on those who fall into high-risk categories, such as those who are incarcerated; vaccinations against tuberculosis, on the other hand, offer protection to children against the illness[52].

As seen in Table (5), the incidence of tuberculosis in children under 15 is relatively low, which may be attributed to the widespread use of the BCG vaccine beginning in childhood. The effectiveness of immunization is highest in children but declines with increasing age[53]. These occurrences are far more likely to occur during puberty and the early years of young adulthood. There is a marked decrease in cases among children and adolescents between the ages of 10 and 14. For these evaluations, the most extensive tuberculosis surveillance dataset that is currently available was utilized[54]. This dataset includes data from a diverse range of countries, many of which have a high endemicity of tuberculosis, as well as a range of epidemiological and topographical characteristics that are indicative of many different regions across the globe. According to the results of this survey, an overwhelming majority of respondents possess complete knowledge of tuberculosis transmission. Accurate information regarding the spread of tuberculosis is associated with various other factors. These characteristics include being between the ages of 35 and 44, having completed secondary or higher education, coming from a wealthy family, being exposed to all three types of mass media, working in a professional, technical, or managerial capacity, and residing in an urban area. Other characteristics include being born into a family with a high level of education and being exposed to all three types of mass media. The study's findings indicated a significant connection between the self-reported age of individuals in Malawi who received accurate information regarding the spread of tuberculosis and their actual age[55]. Those older than 25, in particular, better understood how tuberculosis was spread. Adults have a higher risk of contracting tuberculosis (TB) than children do. In our most recent study, we found that those between the ages of 25 and 34 had a positivity rate of 16.2 percent, those between the ages of 35 and 44 had a positivity rate of 30.6 percent, and those 55 and older had a positivity rate of 19.0 percent. Although tuberculosis is most frequently found in adult males, people of any age can become infected with the disease[56]. According to a report published by the World Health Organization, the prevalence of tuberculosis in Iraq has been steadily declining across various age groups[6].

Conclusions

Our results suggest that cultivation dependence is more sensitive than the direct method. On the other hand, require more attention in TB control programs to help patients prevent infection and healing.

Funding

Self-funded this research.

Informed Consent Statement

Statement Regarding Informed Consent The Specialized Chest and Respiratory Disease Center / National Reference Laboratory (NRL) in Baghdad has given their announced written agreement for studying tuberculosis.

Acknowledgments

We are pleased to extend our thanks to all the medical staff at “Specialized Chest and Respiratory Disease Center / National Reference Laboratory (NRL) for Tuberculosis” in Baghdad.

Conflicts of Interest

None.

Bibliographic references

1. World Health Organization. Global Tuberculosis Report 2021. https://doi.org/10.1016/j.ijid.2021.02.107
2. World Health Organization . TB Data [website]. Geneva.2021: (https://worldhealthorg.shinyapps.io/tb_pronto/).
3. Sharma, S.K., Mohan, A. and Kohli, M. Extra-pulmonary tuberculosis. Expert Review of Respiratory Medicine, 2021. 15(7), pp.931-948. https://doi.org/10.1080/17476348.2021.1927718
4. Khabibullina, N.F., Kutuzova, D.M., Burmistrova, I.A. and Lyadova, I.V. The biological and clinical aspects of a latent tuberculosis infection. Tropical Medicine and Infectious Disease, 7(3), p.48.Tuberculosis Infection. Trop. Med. Infect. Dis., 2022. 7, 48. https://doi.org/10.3390/tropicalmed7030048
5. World Health Organization,. WHO consolidated guidelines on tuberculosis: module 2: screening: systematic screening for tuberculosis disease. 2021. World Health Organization. https://archive.lstmed.ac.uk/id/eprint/17349
6. World Health Organization. 2020. Global Tuberculosis Report. Incidence of Ttuberculosis (Per 100,000 People).
7. Ahmed, M. M. Tuberculosis Situation in Iraq: A puzzle of Estimates. In. J. Mycobacter, 2013. 2(4): 248-249. https://doi.org/10.1016/j.ijmyco.2013.10.002
8. Shoukrie, A., Alameen, A., Shaban, D., Alamari, M., Aboguttaia, N. and Askar, N. The Yield of Sputum Smear Direct Microscopy Using Ziehl-Neelsen Stain in Comparison with Lowenstein Jensen Culture on the Diagnosis of Pulmonary Tuberculosis in Tripoli-Libya. Mycobact Dis, 2018. 8(1). DOI: 10.4172/2161-1068.1000256.
9. Ahmed, S.T., Ali, R.M. and Shihab, B.A. Prevalence of tuberculosis infection among Iraqi patients. World Journal of Pharmaceutical Research, 2018. 7(1), pp.1383-1394. DOI: 10.20959/wjpr20181-10557.
10. Ali, S.M., Al-Faham, M.A. and Mankhi, A.A. Identification and Discrimination of Mycobacterium tuberculosis Complex with Traditional and Real-Time PCR in Different Specimens in Iraq. Journal of the Faculty of Medicine Baghdad, 2020. 62(3). https://doi.org/10.32007/jfacmedbagdad.6231787 .
11. Alateah, S.M., Othman, M.W., Ahmed, M., Al Amro, M.S., Al Sherbini, N. and Ajlan, H.H. A retrospective study of tuberculosis prevalence amongst patients attending a tertiary hospital in Riyadh, Saudi Arabia. Journal of Clinical Tuberculosis and Other Mycobacterial Diseases, 2020. 21, p.100185. https://doi.org/10.1016/j.jctube.2020.100185

12. Eddabra, R. and Neffa, M. Epidemiological profile among pulmonary and extra-pulmonary tuberculosis patients in Laayoune, Morocco. The Pan African Medical Journal, 2020. 37. https://doi.org/10.11604%2Fpamj.2020.37.56.21111
13. Balaky, S.T.J., Mawlood, A.H. and Shabila, N.P. Survival analysis of patients with tuberculosis in Erbil, Iraqi Kurdistan region. BMC Infectious Diseases, 2019. 19(1), pp.1-8. https://doi.org/10.1186/s12879-019-4544-8
14. García-Rodríguez, J.F., Álvarez-Díaz, H., Lorenzo-García, M.V., Mariño-Callejo, A., Fernández-Rial, Á. and Sesma-Sánchez, P. Extrapulmonary tuberculosis: epidemiology and risk factors. Enfermedades infecciosas y microbiologia clinica, 2011. 29(7), pp.502-509. https://doi.org/10.1016/j.eimc.2011.03.005
15. Rahmanian, V., Rahmanian, K., Rahmanian, N., Rastgoofard, M.A. and Mansoorian, E. Survival rate among tuberculosis patients identified in south of Iran, 2005-2016. Journal of Acute Disease, 2018. 7(5), p.207. DOI: 10.4103/2221-6189.244172
16. WHO. Global Tuberculosis Report World Health Organization: Geneva, Switzerland. Available Online: 2020. https://apps.who.int/iris/bitstream/handle/10665/336069/9789240013131-eng.pdf (Accessed on May 5 2020).
17. WHO. Tuberculosis; World Health Organization: Geneva, Switzerland. Available online: 2020 https://www.who.int/news-room/fact-sheets/detail/tuberculosis (Accessed on May 17 2020).
18. M Jumaah, H. The roles of radiology and ESR in the diagnosis of tuberculosis in young military males in Iraq. Annals of the College of Medicine, Mosul, 2013. 39(2), pp.182-185. http://dx.doi.org/10.33899/mmed.2013.81270
19. Nikonajad, A., Azimi, S.A., Allami, A., Qasemi Bargi, R. and Tabarraei, A. Epidemiology of extrapulmonary tuberculosis in Northeast of Iran. Medical Laboratory Journal, 2021. 15(1), pp.1-7. http://dx.doi.org/10.29252/mlj.15.1.1
20. Abdugapparov, F., Grigoryan, R., Parpieva, N., Massavirov, S., Riskiyev, A., Gadoev, J., Buziashvili, M., Tukvadze, N., Hovhannesyan, A. and Dadu, A. Diagnostic Procedures, Diagnoses, and Treatment Outcomes of Patients with Presumptive Tuberculosis Pleural Effusion in Uzbekistan. International Journal of Environmental Research and Public Health, 2021.18(11), p.5769. https://www.mdpi.com/1660-4601/18/11/5769#
21. Merza, M.A. A 5-year experience characterizing the demographic and clinical profile and directly observed treatment short-course treatment outcome in National Tuberculosis Center of Duhok province, Iraqi Kurdistan. SAGE Open Medicine, 2020. 8, p.2050312120921055. https://doi.org/10.1177%2F2050312120921055
22. Aygün D, Akçakaya N, Çokuğraş H, Camcıoğlu H. Clinical Manifestations and Diagnosis of Extra-pulmonary Tuberculosis in Children. J Pediatr Inf; 2019. 13(2):e74-e79. DOI: 10.5578/ced.201922
23. Noertjojo, K., Tam C, M., Chan S, L. and Chan-Yeung MM, W. Extra-pulmonary and pulmonary tuberculosis in Hong Kong. The International Journal of Tuberculosis and Lung Disease, 2002. 6(10), pp.879-886. 879-886. PMID: 12365574.
24. Yang, Z., Kong, Y., Wilson, F., Foxman, B., Fowler, A.H., Marrs, C.F., Cave, MD and Bates, J.H. Identification of risk factors for extra-pulmonary tuberculosis. Clinical infectious diseases, 2004. 38(2), pp.199-205. https://doi.org/10.1086/380644
25. Riaz, M., Mahmood, Z., Javed, M.T., Javed, I., Shahid, M., Abbas, M. and Ehtisham-ul-Haque, S. Drug resistant strains of Mycobacterium tuberculosis identified through PCR-RFLP from patients of Central Punjab, Pakistan. International journal of immunopathology and pharmacology, 2016. 29(3), pp.443-449. https://doi.org/10.1177%2F0394632016638100
26. Caulfield, A.J. and Wengenack, N.L. Diagnosis of active tuberculosis disease: From microscopy to molecular techniques. Journal of Clinical Tuberculosis and Other Mycobacterial Diseases, 2016. 4, pp.33-43. https://doi.org/10.1016/j.jctube.2016.05.005
27. Munir, M.K., Rehman, S., Aasim, M., Iqbal, R. and Saeed, S. Comparison of Ziehl Neelsen microscopy with GeneXpert for detection of Mycobacterium tuberculosis. IOSR J Dent Med Sci, 2015. 14(11), pp.56-60. DOI: 10.9790/0853-1411105660
28. Gonzalez-Angulo, Y., Wiysonge, C.S., Geldenhuys, H., Hanekom, W., Mahomed, H., Hussey, G. and Hatherill, M. Sputum induction for the diagnosis of pulmonary tuberculosis: a systematic review and meta-analysis. European journal of clinical microbiology & infectious diseases, 2012. 31(7), pp.1619-1630. https://doi.org/10.1007/s10096-011-1485-6
29. Hepple, P., Ford, N. and McNerney, R. Microscopy compared to culture for the diagnosis of tuberculosis in induced sputum samples: a systematic review. The international journal of tuberculosis and lung disease, 2012. 16(5), pp.579-588. https://doi.org/10.5588/ijtld.11.0617
30. WHO. Global Tuberculosis Report. 2018. Vol. 69, Pharmacological Reports. 2017. 683-690 p.
31. Association of Public Health Laboratories. Mycobacterium Tuberculosis: Assessing Your Laboratory. Silver Spring, 2009.MD: APHL.
32. American Thoracic Society and the Centers for Disease Control. Diagnostic Standards and Classification of Tuberculosis in Adults and Children. This Official Statement of the American Thoracic Society and the Centers for Disease Control and Prevention was Adopted by the ATS Board of Directors, July 1999. This Statement was Endorsed by the Council of the Infectious Disease Society of America, September 1999. Am J Respir Crit Care Med; 2000.161(4 Pt 1):1376-95. https://doi.org/10.1164/ajrccm.161.4.16141
33. American Thoracic Society.Diagnostic Standards and Classification of Tuberculosis. Am Rev Respir Dis; 1990. 142(3):725-35. https://doi.org/10.1164/ajrccm/142.3.725
34. El Khechine, A., Henry, M., Raoult, D. and Drancourt, M. Detection of Mycobacterium tuberculosis complex organisms in the stools of patients with pulmonary tuberculosis. Microbiology, 2009. 155(7), pp.2384-2389. https://doi.org/10.1099/mic.0.026484-0
35. Ambreen, A., Jamil, M. and Mustafa, T. Viable Mycobacterium tuberculosis in sputum after pulmonary tuberculosis cure. BMC infectious diseases, 2019. 19(1), pp.1-8. https://doi.org/10.1186/s12879-019-4561-7
36. Davis, J.L., Cattamanchi, A., Cuevas, L.E., Hopewell, P.C. and Steingart, K.R. Diagnostic accuracy of same-day microscopy versus standard microscopy for pulmonary tuberculosis: a systematic review and meta-analysis. The Lancet infectious diseases, 2013. 13(2), pp.147-154. https://doi.org/10.1016/S1473-3099(12)70232-3
37. Ryu YJ . Diagnosis of Pulmonary Tuberculosis: Recent Advances and Diagnostic Algorithms. Tuberc Respir Dis (Seoul); 2015. 78(2):64–71. https://doi.org/10.4046/trd.2015.78.2.64
38. World Health Organization. Same-Day Diagnosis of Tuberculosis by Microscopy: WHO policy Statement. Geneva: World Health Organization; Available from: https://apps.who.int/iris/bitstream/handle/10665/44603/9789241501606_eng.pdf; jsessionid=613A37FA332657028E190531EB53D770?sequence=1. [Accessed January 25 2019] 2011. https://doi.org/10.1016/j.ijid.2019.03.021
39. Creswell, J., Raviglione, M., Ottmani, S., Migliori, G.B., Uplekar, M., Blanc, L., Sotgiu, G. and Lönnroth, K. Tuberculosis and noncommunicable diseases: neglected links and missed opportunities. European Respiratory Journal, 2011. 37(5), pp.1269-1282. DOI: 10.1183/09031936.00084310.
40. Duarte, R., Gomes, M., Oliveira, A., Sousa, P., Franco, I. and Gaio, A.R. Social profile of the highest tuberculosis incidence areas in Portugal. Revista Portuguesa de Pneumología, 2016. 22(1), pp.50-52. https://doi.org/10.1016/j.rppnen.2015.08.006
41. Sousa, P., Oliveira, A., Gomes, M., Gaio, A.R. and Duarte, R. Longitudinal clustering of tuberculosis incidence and predictors for the time profiles: the impact of HIV. The International Journal of Tuberculosis and Lung Disease, 2016.20(8), pp.1027-1032. https://doi.org/10.5588/ijtld.15.0522
42. Amiri, H., Mohammadi, M.J., Alavi, S.M., Salmanzadeh, S., Hematnia, F., Azar, M. and Rahmatiasl, H. Capture-recapture based study on the completeness of smear positive pulmonary tuberculosis reporting in southwest Iran during 2016. BMC Public Health, 2021.21(1), pp.1-10. https://doi.org/10.1186/s12889-021-12398-w

43. Ali, Z.A., Al-Obaidi, M.J., Sameer, F.O., Mankhi, A.A., Misha'al, K.I., Jassim, IA, Taqi, EA and Ad'hiah, A.H. Epidemiological profile of tuberculosis in Iraq during 2011–2018. Indian Journal of Tuberculosis, 2022. 69(1), pp.27-34. https://doi.org/10.1016/j.ijtb.2021.01.003
44. Hamasaeed, P.A. Microscopic and Molecular Diagnosis of Mycobacterium Tuberculosis in Erbil city-Iraq. Journal of University of Babylon for Pure and Applied Sciences, 2019. 27(4), pp.20-29. https://www.journalofbabylon.com/index.php/JUBPAS/article/view/2298
45. Nazar, E., Baghishani, H., Doosti, H., Ghavami, V., Aryan, E., Nasehi, M., Sharafi, S., Esmaily, H. and Yazdani Charati, J. Bayesian Spatial Survival Analysis of Duration to Cure among New Smear-Positive Pulmonary Tuberculosis (PTB) Patients in Iran, during 2011–2018. International Journal of Environmental Research and Public Health, 2021. 18(1), p.54. https://doi.org/10.3390/ijerph18010054
46. Codlin, A.J., Khowaja, S., Chen, Z., Rahbar, M.H., Qadeer, E., Ara, I., McCormick, J.B., Fisher-Hoch, S.P. and Khan, A.J. Gender differences in tuberculosis notification in Pakistan. The American journal of tropical medicine and hygiene, 2011. 85(3), p.514. https://doi.org/10.4269%2Fajtmh.2011.10-0701
47. Getahun, H., Sculier, D., Sismanidis, C., Grzemska, M. and Raviglione, M. Prevention, diagnosis, and treatment of tuberculosis in children and mothers: evidence for action for maternal, neonatal, and child health services. Journal of Infectious Diseases, 2012. 205(suppl_2), pp.S216-S227. https://doi.org/10.1093/infdis/jis009
48. Z. Al-Fayyadh, D. .; Hasson, A. A. .; Hussein, A. K. .; Hassan, R. K. EFFECT OF HUMIC ACID SPRAY ON GROWTH CHARACTERISTICS OF WHEAT VARIETIES. JLSAR 2020, 1, 10-19.
49. Crampin, A.C., Glynn, J.R., Floyd, S., Malema, S.S., Mwinuka, V.K., Ngwira, B.M.M., Mwaungulu, F.D., Warndorff, D.K. and Fine, PEM Tuberculosis and gender: exploring the patterns in a case control study in Malawi. The international journal of tuberculosis and lung disease, 2004. 8(2), pp.194-203.
50. Noaman A I, Khalaf R M, Emad GH, Al-Abbasy, Mohammed Th. T. Effect of flaxseed oil dosing on fertility, growth characteristics and some physical, biochemical, and hormonal blood parameters during the early pregnancy of Awassi ewes. Revis Bionatura. 2022;7(4) 5. http://dx.doi.org/10.21931/RB/2022.07.04.5.
51. Laetitia Gay, Cle´ a Melenotte, Ines Lakbar, Soraya Mezouar, Christian Devaux, Didier Raoult, Marc-Karim Bendiane, Marc Leone, and Jean-Louis Mège. Sexual Dimorphism and Gender in Infectious Diseases. Frontiers in Immunology | 2021.| Volume 12 | Article 698121. https://doi.org/10.3389/fimmu.2021.698121
52. Schito, M., Migliori, G.B., Fletcher, H.A., McNerney, R., Centis, R., D'Ambrosio, L., Bates, M., Kibiki, G., Kapata, N., Corrah, T. and Bomanji, J. Perspectives on advances in tuberculosis diagnostics, drugs, and vaccines. Clinical infectious diseases, 2015. 61(suppl_3), pp.S102-S118. https://doi.org/10.1093/cid/civ609
53. Neyrolles, O. and Quintana-Murci, L. Sexual inequality in tuberculosis. PLoS medicine, 2009. 6(12), p.e1000199. https://doi.org/10.1371/journal.pmed.1000199
54. World Health Organization. Global tuberculosis database. www.who.int/tb/publications/global_report/en/. Date last accessed: 2017 November 13, 2017.
55. Ou, Y., Luo, Z., Mou, J., Ming, H., Wang, X., Yan, S. and Tan, A. Knowledge and determinants regarding tuberculosis among medical students in Hunan, China: a cross-sectional study. BMC Public Health, 2018. 18(1), pp.1-7. https://doi.org/10.1186/s12889-018-5636-x
56. Gaur, P.S., Bhaskar, R., Singh, S., Saxena, P. and Agnihotri, S. Incidence and clinical profiles of pulmonary and extra-pulmonary tuberculosis patients in North Indian population: a hospital based retrospective study. International Journal of Research and Development in Pharmacy & Life Sciences, 2017. 6(5), pp.2773-2778. https://doi.org/10.21276/IJRDPL.2278-0238.2017.6(5).2773-2778

ARTICLE / INVESTIGACIÓN

Relationship between Toll-like Receptors and Pathogenesis of Systemic Lupus Erythematosus

Basma Ahmed Ratib*, Asmaa Mohammed Saud

DOI. 10.21931/RB/2023.08.02.28

Institute of genetic engineering and Biotechnology for postgraduate studies, University of Baghdad, Iraq.
Corresponding author: basima @ige.uobaghdad.edu.iq

Abstract: Systemic Lupus Erythematosus is a chronic inflammatory disease characterized by a loss of self-antigen tolerance and the development of high titers of serum autoantibodies, with a wide range of clinical manifestations and complex etiologies. Its etiology is influenced by various genetic, hormonal, immunologic, and environmental factors. SLE affects around 90% of women of reproductive age. The study aims to evaluate the serum levels of Toll-like receptor 7 (TLR7) in a sample of Iraqi SLE patients and its potential relationship with other clinical and laboratory parameters. The study included 100 female patients and 50 healthy females with an age range of (16-65) years old and healthy individuals with an age range of (16-65) years old and mean ages of (35.72 ±11.66 and 35.72 ±11.66) respectively. The current study is performed to estimate the serum levels of (TLR7, ANA, Urea, creatinine, and Vitamin D3) and a laboratory investigation for ESR, hemoglobin, and white blood cells by using the enzyme-linked immunosorbent assay (ELISA)and automated Fujifilm. Serum levels of TLR7 were increased in the SLE patients compared to the control, and a significant difference has been observed (P≤0.01) among SLE patients compared to the control. Urea, creatinine, and ESR were significantly higher; at the same time, the Vitamin D3, hemoglobin, and white blood cells were significantly lower (p< 0.01) among SLE patients as compared to control. On the other hand, there was no evidence of any correlation between TLR7 serum level and disease laboratory investigation.

Key words: Antinuclear autoantibody, Haemoglobin, Interferon, SLE, Toll-Like Receptor-7, WBC.

Introduction

Systemic lupus erythematosus (SLE) is a systemic autoimmune disease characterized by multisystemic and multi-organ involvement. The presence of numerous autoantibodies that induce the development and deposition of immune complexes as well as other immunological processes is related to the symptoms of SLE[1]. The mechanisms underlying this disease are complicated and unknown, but they are thought to be linked to environmental activation of the body's immunological dysfunction and defective immune regulation[2]. Antinuclear antibody (ANA), anti-double-stranded DNA antibodies, complement 3 protein (C3), complement 4 protein (C4), and leukopenia are among the few indicators that help physicians make decisions on disease diagnosis and prognosis[3]. Human plasmacytoid dendritic cells (pDCs) are thought to be essential contributors to the development of autoimmune disorders, SLE; they can produce cytokines and chemokines in response to autoimmune complexes such as self-DNA and small nuclear ribonucleoprotein particles (snRNPs). TLR7 had a higher expression on human pDCs than the other TLRs. Continuous stimulation of pDCs by endogenous nucleic acids activates SLE's type I IFN system, resulting in prolonged type I IFN production. TLR7 and TLR9 are associated with B cell activation and IFN- production in SLE[4,5]. B cell abnormalities are crucial in developing systemic lupus erythematosus (SLE)[6]. Both central and peripheral tolerance mechanisms inhibit the growth and survival of B lymphocytes that react to self-antigens[7]. When these tolerance mechanisms fail, autoreactive B cells are produced, contributing to SLE's pathogenesis. TLRs, which sense nucleic acids in endosomes, are responsible for the cell-intrinsic loss of B cell tolerance to autoantigens in people with SLE. TLR7 drives the extrafollicular B cell response and the germinal center reaction, which are involved in autoantibody production and disease pathogenesis. Autoreactive B cells identify DNA-associated antigens (such as unmethylated cytosine-phosphate-guanosine (CpG) motifs) and RNA-associated antigens (such as the single-stranded RNA (ssRNA) short nuclear RNA, U11) in systemic lupus erythematosus (SLE). These self-antigens are thought to be released due to dysregulated pathways that cause an increase in neutrophil extracellular traps (NETs), necrotic cells, or apoptotic cells[8]. The B cell receptor (BCR) recognizes these autoantigens on the surface of B cells and triggers their cellular internalization. Once within the endosomes, In B lymphocytes, self-antigens can activate Toll-like receptor 7 (TLR7) and TLR9. TLR7 expression is greater in women than in men because TLR7 is located on X chromosome[9,10]. The TLR7 gene escapes X-chromosome inactivation, resulting in considerably higher amounts of TLR7 protein than in male cells[11]. Genetic or environmental factors contributing to TLR7 overexpression enhance an individual's sensitivity to SLE (such as gender, nutrition, and cytokine media, especially the amount of type I interferons)[8]. In physiological circumstances, TLR9 inhibits TLR7 signaling, and this che-

Citation: Ratib B A, Saud A M. Relationship between Toll-like Receptors and Pathogenesis of Systemic Lupus Erythematosus. Revis Bionatura 2023;8 (2) 28. http://dx.doi.org/10.21931/RB/2023.08.02.28
Received: 10 February 2023 / **Accepted:** 15 May 2023 / **Published:** 15 June 2023

Publisher's Note: Bionatura stays neutral with regard to jurisdictional claims in published maps and institutional affiliations.

mical protects people from developing SLE. TLR9 function disruption, on the other hand, may favor TLR7 signaling and contribute to the development of SLE[8]. This study aims to assess the relationship between serum levels of TLR7 and clinical and laboratory indicators in Iraqi female patients with SLE.

Materials and methods

Subject

After obtaining the approval of the Ethics Committee in the Biotechnology Department, College of the Science , University of Baghdad, the peripheral blood samples were collected from all participants of 100 SLE patients. Informed consent was obtained from all participants before their inclusion in the study. All SLE patients met the American College of Rheumatology 12 classification criteria.

Inclusion and Exclusion criteria

We used available data to apply typical inclusion criteria for SLE, including the age of (16-65) years and a positive SLE EULAR/ACR 12 diagnosis. Patients with other immunological disorders or overlapping autoimmune diseases and patients with juvenile SLE (early-onset) who were less than 16 years old were excluded from the study.

Laboratory Investigations

The laboratory tests were conducted to evaluate the immunological and routine tests. The patients and controls were tested for total serum levels of TLR-7 as well as antinuclear autoantibody (ANA), complete blood count (CBC), Erythrocyte sedimentation rate (ESR), Vitamin D3 (25(OH)D), blood urea and creatinine levels. Blood (3 ml) was withdrawn from each subject (patients and controls), divided into sterile gel tubes, and left for about two hours to clot. The sample was then centrifuged at 3000 rpm for 15 minutes to separate the serum stored at -20°C until assayed. ELISA kits were employed to assess levels of total TLR-7(BioSource Inc, British) and ANA[13]. The blood urea and creatinine levels were measured using an automated Fujifilm. Two milliliters of venous blood were withdrawn from each subject by vein puncture under an aseptic technique with a multi-sample syringe. To estimate the complete blood count, whole blood was placed in EDTA tubes and tested by a Hematology analyzer.

Toll-Like Receptor-7 Measurement

The serum level of TLR-7 titer was measured using the ELISA technique and commitment to the instructional manual provided by manufacturer BioSource Inc, British (Cat. No RDEEH2015).

Statistical analysis

SPSS software (Statistical Package for the Social Sciences) version-13 was used to analyze the subjects' data to determine the effect of different components in research parameters. Parametric results (quantitative) were used to compute TLR7 levels, whereas non-parametric data (qualitative) was calculated using means and standard deviation. Additionally, the Pearson Chi-square test was utilized for comparisons, and the Spearman correlation was used to test the correlation between different study parameters if the P-value is considered significant if it is less than 0.05[14].

Results

The number of Systemic Lupus Erythematosus patients selected for the current study was 100 of SLE patients and 50 healthy control individuals; all participants in this study were female. The age range of SLE patients was between 16 to 65 years, with a mean and standard deviation value equal to (35.72 ± 11.66 years). The age range of the controls was identical to the age range of patients (34.05 ± 11.02 years). The participants were divided into ages 16-29, 30-49 and > 50 years. The percentage of the SLE patient in the same age groups was (36.00%, 54.00%, and 10.00%), respectively. While the rate of healthy subjects for the same age groups was (42.00%, 48.00%, and 10.00%), respectively. as shown in Table 1.

One of the essential parameters in SLE diagnosis is the serum level of total TLR-7. Table 3 shows the average concentration level of total TLR-7 in the serum of SLE patients compared to that of the control. The total TLR-7 mean level of the systemic lupus group (4.68 ±1.65) was higher than that of the control group (1.86 ±0.41), with a highly significant difference (P=0.0001), as shown in Table 2.

All the laboratory tests of the female SLE patients and healthy control enrolled in this study were described in Table 3. There was a significant difference in Urea, creatinine, ANA, and ESR were significantly higher; at the same time, the Vitamin D3, hemoglobin, and white blood cells were significantly lower among SLE patients as compared to control.

Groups		Patients (No.=100)	Controls (No.=50)	*p*-value
Age (mean±S. D.) year		35.72 ±11.66	34.05 ±11.02	0.491
Age Group (No.%)	16-29 years	36(36.00%)	21(42.00%)	0.382
	30-50 years	54(54.00%)	24(48.00%)	0.379
	<50years	10(10.00%)	5(10.00%)	1.00

P-value: probability; No.; Number, S. D.; standard deviation

Table 1. Distribution of subjects according to age and age group.

Groups / (No,)	TLR7 level mean ± SD (ng/ml)	*p*-value
Patients / 100	4.68 ±1.65	0.0001
Control / 50	1.86 ±0.41	

P-value: probability; No.; Number of subjects, S. D.; standard deviation.

Table 2. TLR7 level of systemic lupus erythematosus patients in comparison with controls.

Parameters Mean ±SD or N (%)	Patients (N=100)	Controls (N=50)	*P*-value
ESR (mm/hr.)	27.12 ±15.27	15.40 ±5.66	0.0001
WBC (10^3/mL)	4.21 ±2.04	7.61 ±1.72	0.0001
HB (g/dl)	10.48 ±2.35	13.01 ±1.67	0.0001
V.D 3	24.78 ±9.21	37.53 ±5.93	0.0001
Urea (mg/dl)	51.58 ±25.94	29.12 ±7.82	0.0001
Creatinine (mg/dl)	1.906 ±1.76	0.720 ±0.17	0.0001
ANA positivity	7.15 ±3.34	0.296 ±0.25	0.0001

Table 3. Laboratory investigations in all studied groups.

Values are expressed as N: number in each parameter, %: percentage in each group and mean ± SD. The abbreviations are; WBC: white blood cell, Hb: hemoglobin, S: serum, V.D3: vitamin D3, ANA: antinuclear antibody. Normal ranges: WBCs (109/L), 4.00-10.00; HB (g\dl), 150-450; urea (mg\dl), 15-45; Creatinine (mg\dl), 0.3-0.7, V.D3: (ng/ml), 30-50. *Correlation is significant at the 0.05 level (2-tailed).

Personal correlation between TLR-7 levels and laboratory parameters, including ANA, WBC, Hb, ESR, Urea, creatinine, and Vit.D3, statistically show an insignificant correlation with TLR7 according to laboratory examinations, as shown in Table 4.

Parameters

TLR-7 in SLE patients (N=100)
R
P-value
ANA
-0.003
0.985 NS
WBC
-0.12
0.376 NS
Hb
-0.14
0.339 NS
ESR
0.04
0.769 NS
Urea
-0.21
0.140 NS
Creatinine
-0.14
0.338 NS
Vit. D3
0.12
0.396 NS

*. Correlation is significant at the 0.05 level (2-tailed). **. Correlation is significant at the 0.01 level (2-tailed). R: Pearson's correlation.

Parameters	TLR-7 in SLE patients (N=100)	
	R	*P*-value
ANA	-0.003	0.985 NS
WBC	-0.12	0.376 NS
Hb	-0.14	0.339 NS
ESR	0.04	0.769 NS
Urea	-0.21	0.140 NS
Creatinine	-0.14	0.338 NS
Vit. D3	0.12	0.396 NS

*. Correlation is significant at the 0.05 level (2-tailed). **. Correlation is significant at the 0.01 level (2-tailed). R: Pearson's correlation.

Table 4. Correlations between TLR-7 and laboratory parameters.

Discussion

Systemic lupus erythematosus is a multisystemic autoimmune disease with a wide range of clinical manifestations and a high risk of morbidity and mortality[15]. SLE is characterized by an increased production of autoantibodies directed against self-antigens, a wide range of clinical symptoms, and an entirely unpredictable flare-up course[16]. Due to the low prevalence of the disease in males, all the studied group were females; due to different hormonal secretions between males and females, SLE primarily affects women in their reproductive years and affects any organ in the body[17], estrogen and prolactin (sex hormones associated with female reproduction and development) higher levels of these hormones can allow more B cells to circulate in the body. Next, the increased level of B cells can lead to an immune response and may trigger symptoms of SLE, and this can be attributed to a risk factor for female gender and age in the genesis of SLE. Concerning age, SLE is thought to be a disease that affects middle-aged individuals more than younger or older persons. The recorded age of this study ranged from 16 to 65 years with a mean age of (35.72years). These results correspond with (18) studies documenting SLE Iraqi patients' peak range between <20 to >50. The current study showed that the thirtieth decade is regarded as a critical risk factor; this is in agreement with (19), who showed that The most susceptible age for SLE is 20–39 years for females. Women were more frequently affected than men for every age and ethnic group[20]. The current study applied SLE cases to females of different ages; most studies agree that females are affected at considerably higher rates than males[21]. Sex hormones affect immunological responses and modulate molecular pathways in the innate and adaptive immune systems[22]. Women's higher rates of SLE may be due to endogenous estrogen, X chromosomal inactivation failures, increased Toll-like receptor gene products, and alterations in microRNA activity, among other factors[23].

Human SLE has been associated with TLR7 overexpression[24]. In the current study, there was a significant difference in mean TLR7 serum levels between SLE patients (4.68 ±1.65) and healthy controls (1.86 ±0.41), so (P= 0.0001). This is because TLR7 produces type I interferon and promotes the activation of autoreactive B lymphocytes[25]. This study showed a significant increase in the serum level of TLR7 in SLE patients; this result was supported by (26) who showed that total TLR-7 (p<0.01) levels were significantly increased in lupus patients compared to age-matched controls.

Antinuclear antibodies (ANA) more specific autoantibody testing may be helpful in the diagnosis of suspected SLE or ANA-associated disease[27]. Also, it is discussed as an entrance criterion for SLE, while the number of ANA-negative patients worldwide is small (>5%)[28]. Evidence suggests that ANA responses can deteriorate over time due to disease progression or medication side effects[29]. The current study finds that ANA positivity of 98% in SLE patients, as a result, shows a significant difference in the mean of ANA serum levels between SLE patients and healthy controls, however, these results correspond with (30) studies on Iraqi SLE patients who recorded ANA test:98%. Also, ANA shows an insignificant correlation with TLR7. This disagrees with (31), who reported that TLR7 ligand stimulation in SLE patients resulted in antinuclear autoantibodies (ANA) production.

Evidence suggested that Vitamin D3 could exert some of its immunomodulatory effects in SLE patients by affecting the expression levels of some TLRs[32]. Vitamin D3 in the current study shows an insignificant correlation with TLR7. In contrast, it offers a significant difference in the mean of V.D3 serum levels between SLE patients and controls (P value=0.0001).This is in agreement with Meza-Meza *et al.*, who reported that Vitamin D deficiency is more common in people with systemic lupus erythematosus (SLE) than in healthy people[33].

The laboratory investigations in total (Urea, creatinine, ESR, hemoglobin, and WBC) show an insignificant correlation with TLR7. Studies reported that TLRs, found on both leukocytes and resident renal cells, play a role in the start of glomerulonephritis and the progression of kidney injury by bridging the gap between innate and adaptive immune responses[34,35]. Other studies found a link between B lymphocyte infiltration in the kidneys and glomerulonephritis, more significant activity and chronicity indices, and higher serum creatinine levels, highlighting the prognostic relevance of tubulointerstitial involvement[36].

Conclusions

The results suggested that female gender and age play a role in the etiology of SLE. Increasing TLR7 serum levels in patients compared to control indicate that TLR7 indicates the onset of the disease. There was no evidence of a correlation between TLR7 serum levels and any clinical signs or (laboratory investigations) in this study.

Acknowledgments

The authors acknowledge the contribution of the medical staff in the Rheumatology Clinic of Baghdad Teaching Hospital and appreciate the facilities introduced by the University of Baghdad\ College of Science and Department of Biotechnology.

Bibliographic references

1. Basta F, Fasola F, Triantafyllias K, Schwarting A. Systemic Lupus Erythematosus (SLE) Therapy: The Old and the New. Rheumatol Ther. 2020 Sep 1 [cited 2022 Apr 17];7(3):433–46.
2. She Z, Li C, Wu F, Mao J, Xie M, Hun M, et al. The Role of B1 Cells in Systemic Lupus Erythematosus. Front Immunol. 2022 Mar 28 [cited 2022 Apr 17];13.
3. González LA, Ugarte-Gil MF, Alarcón GS. Systemic lupus erythematosus: The search for the ideal biomarker. Lupus. 2021 Feb 1 [cited 2022 Apr 17];30(2):181–203.
4. Chen JQ, Szodoray P, Zeher M. Toll-Like Receptor Pathways in Autoimmune Diseases. Clin Rev Allergy Immunol. 2016 Feb 1;50(1):1–17.
5. Bengtsson AA, Rönnblom L. Role of interferons in SLE. Best Pract Res Clin Rheumatol. 2017 Jun 1;31(3):415–28.
6. Yap DYH, Chan TM. B Cell Abnormalities in Systemic Lupus Erythematosus and Lupus Nephritis—Role in Pathogenesis and Effect of Immunosuppressive Treatments. Int J Mol Sci 2019, Vol 20, Page 6231 [Internet]. 2019 Dec 10 [cited 2022 Apr 17];20(24):6231.
7. Karrar S, Cunninghame Graham DS. Abnormal B Cell Development in Systemic Lupus Erythematosus: What the Genetics Tell Us. Arthritis Rheumatol (Hoboken, NJ) [Internet]. 2018 Apr 1 [cited 2022 Apr 17];70(4):496–507.
8. Fillatreau S, Manfroi B, Dörner T. Toll-like receptor signalling in B cells during systemic lupus erythematosus. Nat Rev Rheumatol [Internet]. 2021 Feb 1 [cited 2022 Apr 17];17(2):98–108.

9. Souyris M, Cenac C, Azar P, Daviaud D, Canivet A, Grunenwald S, et al. TLR7 escapes X chromosome inactivation in immune cells. Sci Immunol [Internet]. 2018 [cited 2022 Apr 17];3(19).
10. Mustafa R. et al. Impact of Gene Expression of TLR4 TLR7 and TLR9 in Children with Acute Lymphocytic Leukemia in Basrah - Iranian Journal of War and Public Health. 2022. [cited 2022 Jul 24].
11. Salwan M. Abdulateef, Ahmad A. Majid, Mohammed A. Al-Bayer, Srwd S. Shawkat, Ahmad Tatar, Thafer T. Mohammed, Firas M. Abdulateef, Mohammed Q. Al-Ani. Effect of aromatase inhibitors on sex differentiation and embryonic development in chicks. Veterinary Medicine and Sciencethis.2021, 7(6), pp. 2362–2373.
12. Aringer M, Leuchten N, Johnson SR. New Criteria for Lupus. Curr Rheumatol Rep [Internet]. 2020 Jun 1 [cited 2022 Apr 17];22(6):1–8.
13. Maguire GA, Ginawi A, Lee J, Lim AYN, Wood G, Houghton S, et al. Clinical utility of ANA measured by ELISA compared with ANA measured by immunofluorescence. Rheumatology. 2009;48(8):1013–4.
14. McLeod, S. A. (2019). What a p-Value Tells You about Statistical Significance. Simply Psychology. - References - Scientific Research Publishing [Internet]. [cited 2022 Jun 11].
15. Narváez J. Systemic lupus erythematosus 2020. Med Clin (Barc) [Internet]. 2020 Dec 11 [cited 2022 Apr 23];155(11):494–501.
16. Morawski PA, Bolland S. Expanding the B Cell-Centric View of Systemic Lupus Erythematosus. Trends Immunol. 2017 May 1;38(5):373–82.
17. Moulton VR, Suarez-Fueyo A, Meidan E, Li H, Mizui M, Tsokos GC. Pathogenesis of Human Systemic Lupus Erythematosus: A Cellular Perspective. Trends Mol Med [Internet]. 2017 Jul 1 [cited 2022 Apr 23];23(7):615–35.
18. Al-Sarray ZA, Izzat ;, Al-Rayahi A, Al-Hafidh AH, Dwayyikh AT. Serum Protein Electrophoresis in Iraqi Systemic lupus Erythematous Patient. J Med Sci. 2(1):2020.
19. Ohta A, Nagai M, Nishina M, Tomimitsu H, Kohsaka H. Age at onset and gender distribution of systemic lupus erythematosus, polymyositis/dermatomyositis, and systemic sclerosis in Japan. Mod Rheumatol [Internet]. 2013 Jul [cited 2022 Apr 24];23(4):759–64.
20. Rees F, Doherty M, Grainge MJ, Lanyon P, Zhang W. The worldwide incidence and prevalence of systemic lupus erythematosus: a systematic review of epidemiological studies. Rheumatology [Internet]. 2017 Nov 1 [cited 2022 Jun 10];56(11):1945–61.
21. Schwartzman-Morris J, Putterman C. Gender differences in the pathogenesis and outcome of lupus and of lupus nephritis. Clin Dev Immunol. 2012;2012.
22. M. Ajeel, A.; A. Mehdi, L. . EFFECT OF ERUCA SATIVA SEEDS POWDER AS FEED SUPPLEMENTATION ON SOME PHYSIOLOGICAL TRAITS OF MALE LAMBS. JLSAR 2020, 1, 20-30..
23. Nusbaum JS, Mirza I, Shum J, Freilich RW, Cohen RE, Pillinger MH, et al. Sex Differences in Systemic Lupus Erythematosus: Epidemiology, Clinical Considerations, and Disease Pathogenesis. Mayo Clin Proc [Internet]. 2020 Feb 1 [cited 2022 Apr 24];95(2):384–94.
24. Celhar T, Lu HK, Benso L, Rakhilina L, Lee HY, Tripathi S, et al. TLR7 protein expression in mild and severe lupus-prone models is regulated in a leukocyte, genetic, and IRAK4 dependent manner. Front Immunol [Internet]. 2019 [cited 2022 Apr 26];10(JULY).
25. Wang T, Marken J, Chen J, Tran VB, Li QZ, Li M, et al. High TLR7 expression drives the expansion of CD19+CD24HiCD38hi transitional B cells and autoantibody production in SLE patients. Front Immunol. 2019;10(JUN):1243.
26. Lyn-Cook BD, Xie C, Oates J, Treadwell E, Word B, Hammons G, et al. Increased expression of Toll-like receptors (TLRs) 7 and 9 and other cytokines in systemic lupus erythematosus (SLE) patients: ethnic differences and potential new targets for therapeutic drugs. Mol Immunol [Internet]. 2014 [cited 2022 Apr 27];61(1):38–43.
27. Nashi RA, Shmerling RH. Antinuclear Antibody Testing for the Diagnosis of Systemic Lupus Erythematosus. Med Clin North Am [Internet]. 2021 Mar 1 [cited 2022 Jun 19];105(2):387–96.
28. Aringer M, Johnson SR. Systemic Lupus Erythematosus Classification and Diagnosis. Rheum Dis Clin North Am [Internet]. 2021 Aug 1 [cited 2022 Apr 25];47(3):501–11.
29. Pisetsky DS, Lipsky PE. New insights into the role of antinuclear antibodies in systemic lupus erythematosus. Nat Rev Rheumatol [Internet]. 2020 Oct 1 [cited 2022 May 28];16(10):565.
30. Noori A, M. Jawad A, A.Jassim N, I. Gorial F. Prevalence of Antiphospholipid Antibodies in Sample of Iraqi Patients with Systemic Lupus Erythematosus: A Cross Sectional Study. Am J Clin Med Res. 2013 Oct 3;1(4):61–4.
31. Wang T, Marken J, Chen J, Tran VB, Li QZ, Li M, et al. High TLR7 expression drives the expansion of CD19+CD24HiCD38hi transitional B cells and autoantibody production in SLE patients. Front Immunol [Internet]. 2019 [cited 2022 Apr 28];10(JUN):1243.
32. F. T. Al-Rawi, Y. T. Abdul-Rahaman , Abdullah I.Noaman , Th. T. Mohammed, S. M Abdulateef, Nadia Jebril and KI. Mahmud. Role of ascorbic acid and appetite stimulants on a few blood serum biochemical characteristics in pregnant Iraqi ewes under heat stress. Revis Bionatura. 2022;7(4) 6. http://dx.doi.org/10.21931/RB/2022.07.04.6.
33. Meza-Meza MR, Muñoz-Valle JF, Ruiz-Ballesteros AI, Vizmanos-Lamotte B, Parra-Rojas I, Martínez-López E, et al. Association of High Calcitriol Serum Levels and Its Hydroxylation Efficiency Ratio with Disease Risk in SLE Patients with Vitamin D Deficiency. J Immunol Res. 2021;2021.
34. Conti F, Spinelli FR, Truglia S, Miranda F, Alessandri C, Ceccarelli F, et al. Kidney Expression of Toll Like Receptors in Lupus Nephritis: Quantification and Clinicopathological Correlations. Mediators Inflamm [Internet]. 2016 [cited 2022 Apr 29];2016.
35. =Meza-Meza MR, Muñoz-Valle JF, Ruiz-Ballesteros AI, Vizmanos-Lamotte B, Parra-Rojas I, Martínez-López E, et al. Association of High Calcitriol Serum Levels and Its Hydroxylation Efficiency Ratio with Disease Risk in SLE Patients with Vitamin D Deficiency. J Immunol Res [Internet]. 2021 [cited 2022 Apr 29];2021.
36. Chang A, Henderson SG, Brandt D, Liu N, Guttikonda R, Hsieh C, et al. In situ B cell-mediated immune responses and tubulointerstitial inflammation in human lupus nephritis. J Immunol [Internet]. 2011 Feb 1 [cited 2022 Apr 29];186(3):1849–60.

ARTICLE / INVESTIGACIÓN

Comparative study of the effect of adding different levels of *Chenopodium quinoa* seed powder to the diet and vitamin C to drinking water on some biochemical traits of blood serum to broilers Ross 308

Evan Najah Abdulhadi and Nihad Abdul-Lateef Ali*
DOI. 10.21931/RB/2023.08.02.29
Department of Animal Production, College of Agriculture, Al-Qasim Green University, Iraq.
Corresponding author: amaria.henao@udea.edu.co

Abstract: This experiment was conducted in the poultry" field "of the" Department of "Animal Production, College of Agriculture, Al-Qasim Green University for" the period "1/10"/2021 until 4/11/2021. The study aimed to add different levels of *Chenopodium quinoa* seed "powder to the diet and" vitamin C "to" the "drinking water" to know "the" best levels of quinoa seed powder to the diet that can be used in poultry diets. "In the experiment, 225 unsexed broiler chicks (Ross 308") were used, distributed randomly to 15 (cages) with 5 experimental treatments for "each treatment" of "45 birds, and each treatment" included "three replicates" for "each replicate of 15 birds. The "experimental treatments were as follows: The first treatment: control treatment" (basic diet "free of" any addition, whether in feed or drinking water). The second treatment: add 12 g of quinoa seeds/kg of feed; the third treatment: add 14 g of quinoa seeds/kg of feed; the fourth treatment: add 16 g of quinoa seeds/kg of feed; the fifth treatment: add 300 mg of vitamin C/liter of drinking water. The results of the experiment showed a significantly excelled (P≤0.05) for the "third, fourth, and fifth treatments" in total protein "concentration compared to the first treatment" (control). As for "the concentration of" albumin and globulin, no significant differences were recorded among all treatments. "As for the concentration of" cholesterol and low-"density lipoproteins, the second, third," fourth, and fifth "treatments" showed "a significant decrease (P≤0.05") compared to "the" first treatment (control) "and a significant increase (P≤0.05) in the concentration" of high-density lipoproteins.

Key words: *Chenopodium quinoa* seed, vitamin C, biochemical traits, broilers Ross 308.

Introduction

One of the most critical challenges facing the poultry industry is the search for natural additives to water and feed to improve the productive efficiency of poultry, especially when the European Union in 2006 banned the use of antibiotics that stimulate the growth of the diseases afflict him[1].

This led researchers to produce derivatives of some plants and use them in treatments. In contrast, others turned to use medicinal plants because they contain natural chemicals that have proven their ability to improve productivity and physiological and immune traits in broilers, such as lemongrass leaves[2] and Bay leaves[3], as well as many medicinal plants that were used as growth stimulants in animal diets[4].

So, the seeds of Chenopodium quinoa were selected as one of the medicinal plants for its strong antioxidant activities and nutritional properties as a vital precursor that promotes growth and improves the health status because it contains many effective compounds such as phytoecdysteroids, phytosterols and saponins and phytic acid[5] and essential fatty acids such as linoleic oleic and palmitic acid[6]. As well as containing amino acids such as tyrosine and arginine and mineral elements such as iron, calcium phosphorous and zinc[7]. In addition to its role in improving the coefficient of digestion[8].

Quinoa is a food crop similar to grain and has a higher nutritional value than other grains and is an excellent source of fiber 10% which is much higher than wheat 27%, maize 17% and rice 04%[9]. Vitamin C, or ascorbic acid, is a water-soluble vitamin with negligible solubility in organic solvents. It is relatively stable in its dry crystalline form In natural conditions, poultry does not need to add it due to the ability of their bodies to form it from glucose sugar, but it was observed that the level of vitamin C decreases in the blood intestines and liver when birds are exposed to stress but it is an antioxidant where vitamin C increases the birds' resistance to some bacterial and viral diseases and thus reduces the percentage of fatalities[10]. Research has shown that vitamin C acts as an antioxidant and is involved in many vital processes in the body, especially for broilers.

This may be due to the role of vitamin C in the manufacture and regulation of the secretion of corticosteroid hormones from the adrenal cortex[11] and because the synthesis of vitamin C is insufficient in newly hatched chicks. As well as birds bred under stress conditions it was necessary to add it to drinking water to provide the required needs of it to reduce the negative impact of its deficiency in the body[12] and because quinoa is an important nutrient and there is no local study on its use in poultry feeding.

This plant was chosen to know the effect of adding it at different levels to the broiler's diet as a natural antioxidant and comparing it with the synthetic antioxidant Vitamin C on production performance and knowing the best concentration Which we can recommend to poultry breeders.

Citation: Abdulhadi, E.N; Ali, N A.Comparative study of the effect of adding different levels of Chenopodium quinoa seed powder to the diet and vitamin C to drinking water on some biochemical traits of blood serum to broilers Ross 308. Revis Bionatura 2023;8 (2) 29. http://dx.doi.org/10.21931/RB/2023.08.02.29

Received: 10 February 2023 / **Accepted:** 15 May 2023 / **Published:** 15 June 2023

Publisher's Note: Bionatura stays neutral with regard to jurisdictional claims in published maps and institutional affiliations.

Materials and methods

This study was conducted in the poultry field of the Department of Animal Production College of Agriculture/ Al-Qasim Green University from 1/10/2021 to 4/11/2021. In the experiment, 225 unsexed Ross 308 broiler chicks were used and randomly distributed to 15 cages with 5 experimental treatments for each treatment of 45 birds; each treatment included three replicates for each replicate of 15 birds. The chicks were raised in the nests on a bed of white sawdust with a thickness of 7 cm.

The feed was provided to the birds freely as it was provided as a starter diet from the age of 1-11 days on the growth diet from the age of 12-22 days, and on a final diet from the age of 23-35 days at the end of the experiment as shown in Table 1 where the experiment parameters were as follows:

In the first treatment, the control treatment essential diet is free of any addition, whether in feed or drinking water Second treatment, add 12 g of quinoa seeds/kg of the third feed treatment, add 14 g of quinoa seeds/kg in the fourth feed treatment add 16 grams of quinoa seeds/kg of fifth feed treatment add 300 mg of vitamin C/L of drinking water.

The experiment included studying the following characteristics average live body weight gain, feed consumption, food conversion factor, and mortality rate. The averages of these traits were estimated for each week of the experiment, which amounted to five weeks, Use a Completely Randomized Design CRD to study the effect of different treatments on the studied traits the differences between the means were compared using Duncan's polynomial test[13] and the readymade statistical program SAS[14] was used to analyze the data.

Figure 1. The quinoa seeds used in the experiment.

Results

Table 2 shows the effect of adding different levels of quinoa seeds to the diet and vitamin C to drinking water on the biochemical traits of the blood serum of broilers at 35 days of age. Where the results of the analysis concerning the concentration of total protein (g/100 ml) showed a significant improvement (P≤0.05) for the birds of the third, fourth and fifth treatments, which recorded the highest concentration of total protein, while the first treatment" (control) "recorded the lowest concentration of total protein."

However, the second treatment did not record any significant differences between it and the other treatments, where there are no significant differences between all treatments for albumin concentration (gm/100ml) and globulin concentration (gm/100ml), we notice.

Table 3 shows the effect of adding different levels of" quinoa seeds "to the" diet "and" vitamin C "to drinking water in the serum lipid profile of broilers at" 35 days of "age, where the first treatment (control) recorded the highest" cholesterol "concentration" and reached 215.51 mg / 100 ml, while the treatments recorded.

The third, fourth and fifth lowest cholesterol concentrations, "As for the second treatment, no significant" difference was recorded "between" it "and the" rest of "the" treatments. We also note that there are no significant differences in the concentration of triglycerides (mg / 100 ml) among all the treatments of the experiment.

From the same table, the birds "of the" second, "third). fourth, and fifth" treatments recorded a significant (P≤0.05) superiority (P≤0.05) "over the birds of the first treatment (control) in the trait "of high-density" lipoproteins ("HDL).

While the first treatment recorded the" highest "concentration of" LDL, "with a significant difference (P≤0.05") compared to "the" (second, "third, fourth and fifth") addition treatments, "which recorded the lowest" concentration "of" LDL, which "recorded the lowest concentration of" LDL. As for the" "very low-density lipoproteins" (VLDL), "the results of the" statistical analysis indicate "that there" are no "significant differences between" all "the" experimental "treatments" "at the age of 35 days.

Discussion

The significant improvement of the treatments of quinoa seeds (third and fourth) in total protein concentration compared to the first treatment (control) may be because they contain some biologically active compounds such as saponins and glycosides by increasing the secretion of digestive enzymes, improving the immune response, and protecting gut tissue[16]. In addition to the high protein content of quinoa seeds by 23%, it became an essential source of protein and used as a partial substitute for protein in broiler diets[17].

Thus, this leads "to an increase in the concentration of total protein", as the high concentration of total protein in the blood serum is a good indicator of the bird's good health. The quinoa plant "plays an important role in the" health status "of the" organism "by" containing many active compounds and many minerals in addition to vitamins and fatty acids and a high percentage of amino acids[18]. As for the significant improvement of vitamin C treatment (the fifth treatment) in the concentration of total protein, it may be due to The role "of vitamin C" in reducing "the secretion of corticosterone" is through inhibiting "the" two enzymes - 21 hydroxylase and 11-penta-hydroxylase, which dominate the synthesis of this hormone from the adrenal cortex[19] which leads to a decrease in the effectiveness of protein catabolism to benefit from sugar and then maintaining High level of protein in blood plasma[20]. The reason for the" reduction in the "concentration of cholesterol and low-density lipoproteins and" the rise of "high-density lipoproteins in" quinoa seed addition "treatments compared to the first treatment (control) may be due to the" quinoa seeds containing many active chemical substances and compounds such as vola-

Components	diets types		
	Starter 1-10 days	Growth 11-22 days	Final 23-35 days
yellow corn	42	47	48.54
Wheat	15	15	15
protein concentrate*	5	5	5
Soybean meal 48%**	32.5	28	25
Sun flower oil	3	3	4.5
dicalcium and phosphorous	0.7	0.5	0.5
Limestone	1.2	1.14	1.1
Methionine	0.25	0.13	0.13
Lysine	0.25	0.13	0.13
table salt	0.1	0.1	0.1
Total	100	100	100
Calculated Chemical Analysis ***			
Represented energy (kilo calories / kg of feed)	3043.35	3101.05	3214.44
Crude protein (%)	23.05	21.31	20.00
Methionine + Cysteine (%)	1.12	0.96	0.92
Lysine (%)	1.51	1.29	1.21
Calcium (%)	0.98	0.90	0.87
Fat	5.5	5.7	7.2
Available phosphorous (%)	0.48	0.44	0.44
Crude fiber (%)	2.8	2.7	2.6

*The protein concentrate used is animal produced by a Dutch company; imported Brocon contains 40% raw protein 2017 kilocalories/kg protein energy represented by 5% crude fat, 220% crude fiber 5% Calcium, 468% phosphorous, 385% lysine 412% methioline 412% methionine + cysteine 042% tryptophan 170% threonine, and it contains a mixture of rare vitamins and minerals that provide the bird's need of these elements

** The soybean meal used is from an Argentine source; the percentage of crude protein is 48%, and 2440 kcal / kg is a representative energy

*** According to the chemical composition based on the NRC[15]

Table 2. Formulas and variables for calculating the components of the productive process' cost.

Treatments	studied traits		
	total protein concentration g/100 ml	albumin concentration g/100 ml	Globulin concentration g/100 ml
first treatment	3.90 ± 0.06 B	2.37 ± 0.03	1.53 ± 0.28
second treatment	3.97 ± 0.17 ab	2.47 ± 0.11	1.50 ± 0.37
Third treatment	4.15 ± 0.03 a	2.48 ± 0.12	1.67 ± 0.17
Fourth treatment	4.39 ± 0.06 a	2.56 ± 0.07	1.83 ± 0.30
Fifth treatment	4.18 ± 0.05 a	2.49 ± 0.04	1.69 ± 0.12
significant level	*	NS	NS

Table 2. "Effect of adding different levels of" quinoa seeds" to" the diet "and" vitamin C "to drinking water on the" biochemical traits "of" serum "of" broilers "at 35 days of" age ("arithmetic mean ± standard error").

Treatments	studied traits				
	Cholesterol concentration mg /100 ml	Triglyceride concentration mg/100 ml	high density lipoprotein concentration HDL mg/100 ml	Low-density lipoprotein concentration LDL mg/100 ml	Very low-density lipoprotein concentration VLDL mg/100 ml
first treatment	215.51 ± 12.43 a	138.84 ± 20.60	70.53 ± 2.41 b	117.22 ± 14.08 a	27.76 ± 4.12
second treatment	192.27 ±12.53 Ab	112.03 ± 12.88	88.64 ± 8.20 a	81.23 ± 6.18 b	22.40 ± 2.57
Third treatment	186.56 ± 3.71 b	108.09 ± 19.66	89.06 ± 2.59 a	75.89 ± 5.23 b	21.61 ± 4.93
Fourth treatment	184.46 ± 4.42 b	107.77 ± 11.89	95.72 ± 4.81 a	67.19 ± 6.47 b	21.55 ± 2.37
Fifth treatment	188.56 ± 0.82 b	117.70 ± 31.22	93.38 ± 6.09 a	71.64 ± 7.22 b	23.54 ± 3.40
significant level	*	NS	*	*	NS

* "The averages with different letters within the same column differ significantly between them (P≤0.05")
No significant: NS , The "first treatment (control) without addition. The second treatment": adding quinoa seeds = (12 g / g feed) The third treatment: adding quinoa seeds = (14 g / g of feed) Fourth treatment: adding quinoa seeds = (16g/gm of feed) "Fifth treatment, adding vitamin" C "at a concentration" (300 mg/L "of water")

Table 3. Effect of adding different levels of" quinoa seeds "to the diet" and vitamin C "to drinking water" as lipids for serum of broilers "at 35 days of" age ("arithmetic mean ± standard error").

tile oils, saponins, tannins, glycosides and phenols, which are in its insoluble form, it forms a complex with cholesterol, which prevents its absorption by the intestines, thus lowering the level of cholesterol and low-density lipoproteins[21,22] another explanation for the low cholesterol level is due to the role of quinoa seeds in reducing cholesterol synthesis by decreasing the activity of the enzyme HMG-CoA reductase, which has an important role in the cholesterol formation pathway[23]. Also, the high level of HDL includes inhibiting the oxidation of low-density protein. It thus protects the endothelial cells from the toxic effect of the oxidation of low-density lipoprotein[24,25].

Conclusions

Quinoa seeds significantly improved total protein concentration in the study treatment, making it an important protein source and used as a partial substitute for protein in broiler diets. Similarly, vitamin C's role in resisting stress is controlling the secretion of corticosterone, which is secreted by the adrenal cortex. As vitamin C has an essential role in synthesizing corticosterone hormone, this hormone works to increase glucose utilization by breaking it down. Protein to produce energy. In contrast, there were no significant differences were recorded among all treatments in the concentration of'' albumin and globulin.

Bibliographic references

1. Fugh-Berman, A. Clinical trials of herbs. Complementary and Alternative therapies in primary care. 1997. 24: 889-908.
2. Al-Awadi, D. H. Yasir and Al- Nadawi, N. A. Ali . “Effect of adding different levels of lemon grass leaves (Cymbopogon citratus) to the diet or its extract into drinking water on some blood parameters for broiler chickens (Ross 308). “ Journal of Physics: Conference Series. 1st International Virtual Conference on Pure Science. 2020. 1-8.
3. Ali, N. A. and Al-Shuhaib M. B. S. Highly effective dietary inclusion of laurel (Laurus nobilis) leaves on productive traits of broiler chicken. Acta Scientiarum. Animal Sciences. 2021. (43): 1-6.
4. Sarinivasan, K. Spices as influencers of body metabolism: An overview of three decades of research. Food Res. Int. 2005.38:77-86.
5. Al-Anbari, I. H. and Sudad K. Al-Taweel. "Nutritional values, medicinal and phytochemical profiling of white Quinoa (Chenopodium quinoa Willd.) Seeds and leaves planted in Iraq." Fayoum J. Agric. Res, & Dev. 2019. 33 (1):179 – 191.
6. Altuna, JL; Silvam M.; Álvarz M.; Quinteros M.F; Morales D. and Carrillo W. "Ecuadorian quinoa (Chenopodium quinoa willd) fatty acids profile" Asian J. Pharm Clin. Res. 2018. 11(11): 1-3.
7. Safiullah P.; Frieda E.; Babu V.; Kamalendu P.; Grato N. and Kerry C. "Nutritional Composition of the Green Leaves of Quinoa (Chenopodium quinoa Willd)" Journal of Food Research. 2019. 8(6): 55-65.
8. Silva José Antonio da; Dávia Guimarães Pompeu; Olavo Flores da Costa; Daniel Bonoto Gonçalves; Carlos Roberto Spehar; Sérgio Marangoni and Paulo Afonso Granjeiro. "The importance of heat against antinutritional factors from Chenopodium quinoa seeds." Food Sci. Technol, Campinas, 2015. 35(1): 74-82.
9. Muhammad A. A.; Mahmoud A.; Muhammad S.; Muhammad U. and Mohamed E. A. Importance of Quinoa (Chenopodium Quinoa) in Poultry Nutrition. In book: Natural Feed Additives Used in the Poultry Industry Edition: 2021. Chapter: 6.
10. Sokolowicz, Z.; E. Herbut and M. Pietras. “Effect of the heat stress onthyroid and adrenal gland functions of broiler chicks, “Anim. Prod. Rev., 1993. 8(suppl.), p. 31.
11. Jaffar, G.H., and Blaha, J. “Effect of ascorbic acid supplementation in drinking water on growth rate, feed efficiency of broiler chickens maintained under acute heat stress conditions.,” Zivocisna – vyroba – UZPI. 1996. 41(11): 485.
12. M. Ajeel, A.; A. Mehdi, L. . Effect Of Eruca Sativa Seeds Powder As Feed Supplementation On Some Physiological Traits Of Male Lambs. Journal of Life Science and Applied Research. 2020, 1, 20-30..
13. Duncan, D.B . Multiple range multiple F-test-Biometeics. 1955. 11:1 – 42.
14. SAS. Statistical Analysis System, User's Guide. Statistical. Version 9.1th ed. SAS. Inst. Inc. Cary. 2012. NC USA .
15. NRC National Research council . Nutrient Requirement of Poultry. (9th rev. ed.). National Research Council. Nat. Academy Press, Washington, 1994. DS, USA.
16. Zeyneb, H.; Pei, H.; Cao, X.; Wang, Y.; Win, Y., and Gong, L. In vitro study of the effect of quinoa and quinoa polysaccharides on human gut microbiota. Food Science & Nutrition, 2021. 00, 1–11.
17. Mustafa S.; Zainab T.; Ayesha R.; Muhammad S.; Muhammad A.; MadihaI.; Sadaf N.; Anwar I. and Zahida S. Laboratory scale study on the effect of feeding quinoa (Chenopodium quinoa) as meal on serum biochemistry of broiler. Pure Appl. Biol., 2019. 8(4): 2326- 2332.
18. Farhan, S. M., Abdulateef, S. M. Al-Enzy, A. F. M, Mohammed, Th. T., Saeid, Z. J. M., Al-Khalani, F. M. H. & Abdulateef, F. M. Effect of heat stress on blood alkalinity of broiler chicks and its reflection in improving the productive performance. Indian Journal of Ecology. 2020, 47: 107-109.
19. Pardue, S. L. Relationship of ascorbic acid to physiological stress in the domestic fowl ph.D.dissertation, Thesis North Caroline State University. Raleigh, NC World. Poultry Science, 1983. 107-123.
20. Coles, E. H. Veterinary clinical pathology. 4th ed. W.B. Saunders. Philadelphia, London, 1986. Hong Kong.
21. Rao, A.V. and Gurfinkel, D.M. The Bioactivity of Saponins: Triterpenoid and Steroidal Glycosides. Drug Metabolism and Drug Interactions. 2000. 17(1-4):211-35.
22. Nickel, J. L. P.; Spanier, F. T.; Botlho, M.; Arocha Gularte and E. Helbig. Effect of different types of processing on the total phenolic compound content, antioxidant capacity, and saponin content of Chenopodium quinoa Willd grains. Food chemistry. 2016. 139-143
23. Takao T.; Nakamichi W.; Kana Y.; Syoko I.; Saori.; Yukari T.; Kenichi N. and Yotaro K. Hypocholesterolemic Effect of Protein Isolated from Quinoa (Chenopodium quinoa Willd.) Seeds. Food Sci. Technol. Res., 2005. 11 (2): 161 – 167.
24. Navarro-Perez D.; Radcliffe J.; Tierney A. and Jois M. Quinoa Seed Lowers Serum Triglycerides in Overweight and Obese Subjects: A Dose-Response Randomized Controlled Clinical Trial. Curr Dev Nutr. 2017. 1(9): 1-9.
25. Farhan, S. M., Abdulateef, S. M. Al-Enzy, A. F. M, Mohammed, Th. T., Saeid, Z. J. M., Al-Khalani, F. M. H. & Abdulateef, F. M. Effect of heat stress on blood alkalinity of broiler chicks and its reflection in improving the productive performance. Indian Journal of Ecology, 2020. 47: 107-109

SHORT ARTICLES / INVESTIGACIÓN

Evaluation of the efficacy of *Beauveria bassiana* filtrate in controlling the beetle *Everts Tragoderma granarium* (Coleoptera: Dermestidae) *in vitro*

Farah Hadi Abdul Hussain and Yousef Dakhil Rashid
DOI. 10.21931/RB/2023.08.02.30
Al-Musayyib Technical College, Al-Furat Al-Awsat University, Iraq.
Corresponding author: farahhadi8789@gmail.com

Abstract: The present study was performed to test the impacts of the fungus *B. bassiana* filtrate, at 25, 50, and 75% concentrations, on the larvae of the second and fourth instars of *T. granarium*. The study showed the superiority of the fungus filtrate at the concentration of 75% when treating the larvae of the second and fourth instars, with mortality rate values of 45.0% and 33.3%, respectively, after 7 days of treatment and diagnosis of several chemical compounds of different chemical groups for the filtrate fungus *B .bassiana* using the GC mass.

Key words: *Tragoderma ganarium*, *Beauveria bassiana*, GC mass.

Introduction

Stored materials, particularly those composed of cereal grains and their products, are of major importance to the food security of the entire global population, providing the necessary calories for daily consumption. Stored materials are among the main protein sources essential for human nutrition[1]. The wheat species *Triticum aestivum* L. is among these crops, constituting one-third of the world's grain production. The importance of wheat lies in its nutritional value, being the main source of carbohydrates, including starch. One of the problems facing cultivating different crops in developing countries is the losses that occur after the harvest and during the storage period. These crops are exposed to damage due to infections with various warehouse pests[2]. One of the most important pests that attack crops are the hairy grain beetle *T. granarium Everts* (Khabra), considered one of the most dangerous and pesticide-resistant insects[3]. It attacks the stored grains and their products, which suffered tremendous damage due to their usage as food by the larvae. The infection is usually determined by the presence of the pest, whether adults or larvae and molting skins[4]. To reduce the damages caused by this insect, several means were used, the chemical pesticides were the most common. But several problems have been encountered upon applying these pesticides, including the threats resulting from the residuals of pesticides or used chemicals and their economic cost. Therefore, Researchers have developed Modern methods, the latest of which was nano pesticides, to control stored pests[5]. And among the other ways, biological control by entomopathogenic, one of the best alternatives to chemical pesticides, is safe, environmentally friendly, and has equal efficacy. The fungus *Beauveria bassiana* is a biological control agent used on a large scale to control insect stored such as *Sitophilus granarius*[6]. This study aims to test the effects of crude filtrate of *B. bassiana* on some aspects of the biological performance of *T. granarium* beetle *in vitro* and to detect the active compounds in the filtrate by using the GC-mass technique.

Materials and methods

Collection and breeding of *T. granarium*

The hairy grain beetles were obtained from the laboratories of the Ministry of Science and Technology, Baghdad, Iraq. Healthy wheat grains were cleaned of impurities and placed in the freezer for 72 hours at -20 ºC to ensure they were internally free from other insect infections. Ten adult beetle pairs of males and females were placed on 1 kg of healthy wheat grains with 5 g of dry yeast in plastic bottles of 100 ml volume and 10 cm diameter. The bottle opening was covered with organza fabric and sealed with a rubber band to prevent adults' escape. The renewal of the culture was occasionally ensured[7]. The insect was identified by an expert in the Natural History Research Center and Museum / the University of Baghdad.

Preparation of Fungal Filtrates

The entomopathogenic fungus *B. bassiana* was obtained from the Laboratory of Insects, Department of biological control, Al-Furat Al-Awsat University; the funges were cultured on potato dextrose agar at 25 ± 1°C for 15 days before the initiation of the experiment. Two discs (7 mm diameter) were cut from the growing pathogen, placed in a sterile flask containing 500 mL of potato dextrose broth, and incubated at 27°C for 21 days. The filtrates were sterilized using the Millipore sterile filter (Millipore 0.45 µm syringe filter). The filtrate was considered a stock solution (100%) and then diluted to other concentrations by sterile distilled water. The control treatment was sterile distilled water only.

Gas Chromatography-Mass Spectrometry (GC-MS) Analysis

To identify compounds of the filtrate of B.bassiana This analysis was performed by Instrument of Gas Chromatography-Mass spectrometry Shimadzu's in laboratories of the Ministry of Science and Technology – Baghdad.

Citation: Hussain, F.H.A.; Rashid, Y.D. Evaluation of the efficacy of Beauveria bassiana filtrate in controlling the beetle Everts Tragoderma granarium (Coleoptera: Dermestidae) in vitro. Revis Bionatura 2023;8 (2) 30. http://dx.doi.org/10.21931/RB/2023.08.02.30
Received: 10 February 2023 / **Accepted:** 15 May 2023 / **Published:** 15 June 2023

Effects of *B. bassiana* filtrate on the mortality rate of the second and fourth larval instars

Three concentrations of the filtrate (25, 50, and 75%) were prepared by withdrawing a fixed volume of the filtrate through a sterile medical syringe and diluting it with different volumes of sterile distilled water. Twenty larvae from each stage were tested for each concentration, with three replicates, and compared to distilled water as control. For each replicate, 5 larvae were placed in a Petri dish, treated with the filtrate, and sprayed from a distance of 5 cm to ensure complete coverage. After spraying, the larvae were supplied with feeding, a wheat powder and a yeast mixture, as prepared previously. The dishes were incubated at a temperature of 30 ± 2 °C. The mortality rate was calculated after 1, 3, 5, and 7 days.

Statistical analysis

The results of the laboratory experiments were analyzed by applying the Complete Randomizd Design (CRD) according to the factorial experiments. The Less Significant Difference (LSD) test was used under the probability level of 0.05 to test the significance of the differences[8].

Results

Figure 1 shows the most important active compounds separated from the filtrate of the fungus B. bassiana using the GC mass technique. Abdel-Wareth The results presented in this study are consistent with the findings of Abdel-Wareth[9,10], who indicated that the filtrate of B. bassiana contains the compounds 9- octadecenoic acid, nonacosane, nonanedioic acid, and dibutyl ester, as identified by using the GC mass technique.

Table 2 shows the superiority of *B. bassiana* filtrate at the concentration of 75%, which exerted the highest mortality rate of 45.0% for the second larval stage. In contrast, the lowest was 15.0% at the lowest concentration25%. The most increased mortality of the fourth larval stage was 33.3% at the concentration of 75%, whereas the lowest was 13.2% at the lowest concentration25%. It is noticed that the longer the period after the treatment with the filtrate, the higher the mortality rate, which reached values of 5.8, 15.0, 25.8, and 36.6% after 1, 3, 5, and 7 days, respectively. It was also noticed that the higher the concentration, the higher the mortality rate, which reached 30.0, 18.3, and 45.0% at concentrations of 25, 50, and 75%, respectively, for the second larval instar. For the fourth instar, the mortality rate values reached 13.2, 26.7, and 33.3% at 25, 50, and 75% concentrations, respectively. As for the concentration/period interaction treatment, the highest mortality rate for the second larval instar (66.7%) was recorded at the concentration of 75%, showing highly significant differences with the remainder of the treatments, where the lowest was 33.3% at the concentration of 25% concentration. As for the fourth larval instar, the highest mortality rate was 53.3% at 75% concentration, and the lowest was 26.7% at 25% concentration. However, the control treatment did not record any mortality. These results agree with the reported effectiveness of the fungal filtrate of *B. bassiana*, which is conferred by the active compounds shown in Figure 1 and Table 1.

Discussion

These compounds are like those found in manufactured pesticides but with no effects on the environment. The cause of death is also attributed to the fact that the secondary metabolites of the fungus can interfere with the immune system, thus causing changes in the host's behavior. These changes include for example, reduced feeding, reduced activity, and paralysis of the insect, as well as changes in tissue structures and, thus, the rapid death of the host[11]. Al-Shuwaili[12] utilized the filtrate of B. bassiana against the black bean aphid *Aphis fabae*, where the concentration of 100% of the filtrate caused mortality rates of 52.17 and 54.10% of nymphs and adults, respectively. These results agree with the study of Ghaylan[13], where the filtrate of *B. bassiana* caused the highest mortality rate. The mortality rate of *Spodoptera litura* larvae was 73.33% at 100% concentration. (14,15), used *Trichoderma harzianum* filtrate against Aphis fabae nymphs, which showed the highest mortality rate of 71.81% at 100% concentration.

Figure 1. Identification of the active compounds in the crude filtrate of the fungus *B. bassiana* using the GG mass technique.

Peak number	Name of compound	Area	Detention number
1	1-Butanol	0.77	5.310
2	Acetic acid, propyl ester	11.10	6.059
3	Acetic acid, 2-methyl propyl ester	5.52	7.374
4	Nonanedioic acid, dibutyl ester	3.80	8.505
5	Heptadecane	2.70	46.889
6	Hexanedioic acid, bis (2-ethylhexyl)	38.25	52.582
7	Z-5-Nonadecane	5.15	53.073
8	Nonacosane	16.92	53.942
9	n- Hexadecanoic acid	2.53	55.937
10	Eicosane	1.61	57.194
11	Heneicosane	8.11	60.332
12	9-Octadecenoic acid	1.76	61.498
13	9-Tricosene	1.78	61.658

Table 1. Effects of *B. bassiana* filtrate on the second and fourth instar larvae of *T. granarium.*

Larval instar	Period (days) Conc. (%)	1	3	5	7	Mean mortality rate for concentrations.
Second larval instar	0	0.0	0.0	0.0	0.0	0.0
	25	0.0	6.7	20.0	33.3	15.0
	50	6.7	26.7	33.3	53.3	30.0
	75	20.0	40.0	53.3	66.7	45.0
Fourth larval instar	0	0.0	0.0	0.0	0.0	0.0
	25	0.0	0.0	20.0	26.7	13.2
	50	6.7	20.0	33.3	46.7	26.7
	75	13.3	26.7	40.0	53.3	33.3
Mean mortality rate for period		5.8	15.0	25.0	36.6	
LSD (0.05) for concentration					2.83	
LSD (0.05) for period					3.22	
LSD (0.05) for conc./period interaction					5.88	

Table 2. Effects of *B. bassiana* filtrate concentration on the mortality rate of the second and fourth larval instars of *T. granarium*.

Conclusions

The results of the laboratory experiments were analyzed by applying the Complete Randomizd Design (CRD) according to the factorial experiments. The Less Significant Difference (LSD) test was used under the probability level of 0.05 to test the significance of the differences.

Bibliographic references

1. Sherry, P.R.and Halford, N.G. Cereal seed storage proteins; structures, properties and role in grain utilization. Journal of Experimental Botany, 2007; 539(370);947-958.
2. Ismail, Iyad Youssef. Pests of stored materials. Mosul University, 2014;156 p.
3. Lowe,S.; Browne M.; Boudjelas S. and DePoorter, M. 100 of the word Invesive Alien Species:A Selection from the Global Invasive Species Database.Invesive Species Specialist Group,World Conservation Union(IUCN) . 2000.
4. Hagstrum, D.W. and Subramanyam B. Stored-Product Insect Resource. AACC International, St. Paul, Minnesota, USA, 2009; 509 pp.
5. Hilal, S. M.; Mohmed, A. S. ; Barry ,N. M. and Ibrahim, M. H. Entomotoxicity of TiO2 and ZnO Nanoparticles Against Adults Tribolium Castaneum (Herbest) (Coleoptera: Tenebrionidae). IOP Conf. Series: Earth and Environmental Science 910, doi:10.1088/1755-1315/910/1/012088. 2021.
6. Mantzoukas, S.; Lagogiannis, I.; Mpekiri, M.; Pettas, I.and Eliopoulos, P.A. Insecticidal Action of Several Isolates of Entomopathogenic Fungi against The Granary Weevil Sitophilus granarius. Agriculture , 2019; 9, 222. https://doi.org/10.3390/agriculture9100222
7. Al-Nuaimi, M. AT The effect of the fungus Metarhizium anisopliae and silver nanoparticles manufactured by it on the development of the hairy beetle Trogoderma granarium. PhD thesis. College of Women for Sciences, University of Baghdad. 2018; page 28.
8. Al-Rawi, K. M. and Khalaf Allah, A.M. Design and Analysis of Agricultural Experiments. Dar Al-Kutub for Printing and Publishing. University of Mosul, 488 pages. College of Education, Department of Biology. 1980.
9. Abdel-Wareth, Marwa T.A, Mosad A. Ghareeb ,Mohamed S. Abdel-Aziz and Ali M. El-Hagrassi. Snailicidal, antimicrobial, antioxidant and anticancer activities of Beauveria bassiana, Metarhizium anisopliae and Paecilomyces lilacinus fungal extracts . Egyptian Journal of Aquatic Biology & Fisheries . 2019; 23(2): 195 - 212
10. Abedalhammed, H. S., Naser, A. S., Al-Maathedy, M. H., Mohammed, Th. T., Jaber, B. T. & Al-Asha'ab, M. H. The effect of vitamin e as an antioxidant with different levels of dried tomato pomace supplementation on diets of common carp (cyprinus carpio l) on blood indices. Biochemical and Cellular Archives, 2020; 20(2): 5173-5176.
11. Charnley, A . K . Fungal Pathogens of Insects: Cuticle Degrading Enzymes and Toxins. Advances in Botanical Research. 2003;40: 241-321.
12. Al-Shuwaili, T. S. J. Evaluation of the efficiency of some biological and chemical factors in controlling the black bean aphid, Aphis phapae (Aphididae..Homoptera). Master's thesis. 2010; 73 pages.
13. Ghaylan, A. H. Y. and Al Masoudi, A. D. Biological resistance of Spodoptera litura (Fab.) using the filtrate of the fungus Beauveria bassiana. Babylon University Journal , Pure and Applied Sciences, 2013; 1(2).
14. Ohmayed, K. H. .; Sharqi, . M. M. .; Rashid, H. M. . Comparison Of The Physical And Chemical Changes In Local Organic Waste After Cultivation Of The Ganoderma Lucidum Mushroom And Composting By Common Methods. Journal of Life Science and Applied Research. 2020, 1, 1-9..
15. Al-Maathedy, M. H., Mohammed, Th. T. & Al-Asha'ab, M. H. The effect of vitamin e supplementation and different levels of dried tomato pomace on common carp diets (cyprinus carpio l.) on productive performance. Biochemical and Cellular Archives, 2020; 20(2): 5371-5377.
16. RELYEA, RA A cocktail of contaminants: how mixtures of Pesticides at low concentrations affect aquatic communities. Oecologia, 2009 ; 159: 363 – 376.

La Universidad Nacional Autónoma de Honduras

SE ENCUENTRA DENTRO DEL RANKING SCIMAGO Y RANKING QS

UNAH RANKING MUNDIAL 2023

RANKING MUNDIAL SCIMAGO UNAH 2022

"AGRADECEMOS A LOS INVESTIGADORES QUE LO HAN HECHO POSIBLE"

FRANCISCO JOSÉ HERRERA ALVARADO
Rector UNAH

DICIHT
DIRECCIÓN DE INVESTIGACIÓN CIENTÍFICA, HUMANÍSTICA Y TECNOLÓGICA

UNAH
UNIVERSIDAD NACIONAL AUTÓNOMA DE HONDURAS

UNAH RANKING MUNDIAL 2023

RANKING MUNDIAL SCIMAGO UNAH 2022

LA UNAH CUENTA CON

162 Instancias de investigación:

72 Grupos de investigación científica

67 Unidades de gestión de la investigación

10 Institutos de investigación científica

7 Observatorios universitarios de investigación

6 Centros experimentales y/o de innovación

DICIHT
DIRECCIÓN DE INVESTIGACIÓN CIENTÍFICA, HUMANÍSTICA Y TECNOLÓGICA

UNAH
UNIVERSIDAD NACIONAL AUTÓNOMA DE HONDURAS

Docencia, investigación, extensión y proyección social al servicio del territorio

UCO
Universidad Católica de Oriente
Vigilada Mineducación

Fortalezas **institucionales**

- Biotecnología
- Limnología
- Derechos Humanos – Posconflicto
- Internacionalización
- Inclusión Social
  - SER Servicio Educativo Rural
  - Educación de Alfabetización
- MIS – Instituto de formación para el trabajo y el desarrollo humano
- Formación humanística "Ruta Humanística en el currículo - Cátedra abierta Madre de la Sabiduría"
- Investigación y desarrollo tecnológico
- Comprometida con la calidad
- Centro de Estudios Territoriales
- Biodiversidad
  - Herbario
  - Ictiología
  - Litoteca

Áreas del **conocimiento**

- Ciencias Agropecuarias
- Ciencias de la Educación
- Ciencias de la Salud
- Ciencias Económicas y Administrativas
- Ciencias Sociales
- Derecho
- Ingenierías
- Teología y Humanidades

- 26 programas de pregrado
- 16 programas de posgrado
  - 1 doctorado
  - 8 maestrías
  - 7 especializaciones

www.uco.edu.co Universidad catolicadeoriente @uconia

Contacto institucional Universidad Católica de Oriente
Sector 3, Cra. 46 No. 40B 50 - **PBX:** (57)(4) 569 90 90. Ext. 694
Fax: (57)(4) 531 09 72 - **Email:** uco@uco.edu.co